LEABHARLANN CHOLÁISTE NA TRÍONÓIDE, BAILE ÁTHA CLIATH | TRINITY COLLEGE LIBRARY DUBLIN
Ollscoil Átha Cliath | The University of Dublin

Terms and Conditions of Use of Digitised Theses from Trinity College Library Dublin

Copyright statement

All material supplied by Trinity College Library is protected by copyright (under the Copyright and Related Rights Act, 2000 as amended) and other relevant Intellectual Property Rights. By accessing and using a Digitised Thesis from Trinity College Library you acknowledge that all Intellectual Property Rights in any Works supplied are the sole and exclusive property of the copyright and/or other IPR holder. Specific copyright holders may not be explicitly identified. Use of materials from other sources within a thesis should not be construed as a claim over them.

A non-exclusive, non-transferable licence is hereby granted to those using or reproducing, in whole or in part, the material for valid purposes, providing the copyright owners are acknowledged using the normal conventions. Where specific permission to use material is required, this is identified and such permission must be sought from the copyright holder or agency cited.

Liability statement

By using a Digitised Thesis, I accept that Trinity College Dublin bears no legal responsibility for the accuracy, legality or comprehensiveness of materials contained within the thesis, and that Trinity College Dublin accepts no liability for indirect, consequential, or incidental, damages or losses arising from use of the thesis for whatever reason. Information located in a thesis may be subject to specific use constraints, details of which may not be explicitly described. It is the responsibility of potential and actual users to be aware of such constraints and to abide by them. By making use of material from a digitised thesis, you accept these copyright and disclaimer provisions. Where it is brought to the attention of Trinity College Library that there may be a breach of copyright or other restraint, it is the policy to withdraw or take down access to a thesis while the issue is being resolved.

Access Agreement

By using a Digitised Thesis from Trinity College Library you are bound by the following Terms & Conditions. Please read them carefully.

I have read and I understand the following statement: All material supplied via a Digitised Thesis from Trinity College Library is protected by copyright and other intellectual property rights, and duplication or sale of all or part of any of a thesis is not permitted, except that material may be duplicated by you for your research use or for educational purposes in electronic or print form providing the copyright owners are acknowledged using the normal conventions. You must obtain permission for any other use. Electronic or print copies may not be offered, whether for sale or otherwise to anyone. This copy has been supplied on the understanding that it is copyright material and that no quotation from the thesis may be published without proper acknowledgement.

TRINITY COLLEGE
- 4 MAR 2014
LIBRARY DUBLIN

Thesis 10252

Declaration

This thesis has not been submitted as an exercise for a degree at this or any other University. The work described is entirely my own work except where duly acknowledged. I agree that the library of University of Dublin, Trinity College may lend or copy this thesis on request.

Gary Stack



Summary

The principal objective of the work described in this thesis was the synthesis of a series of novel tubulin inhibitors, with defined stereochemistry and diverse functionality, suitable for the formation of molecular conjugates and designed multiple ligands. It was envisaged that these compounds would permit the synthesis of molecular conjugates *via* a wide variety of coupling methodologies, while retaining the tubulin inhibitor activity of the core structure. Furthermore, the design, synthesis and evaluation of a designed multiple ligand possessing both tubulin polymerisation and aminopeptidase N inhibition activity was proposed.

Chapter one presents a comprehensive review of strategies used to optimise the delivery of tubulin targeting agents through molecular conjugation. The advantages and disadvantages of this approach are discussed and an exhaustive overview of the various molecular conjugate types and their biological activity is discussed.

Chapter two introduces the novel tubulin inhibitors which were the lead molecules for the work undertaken in this thesis. The original synthesis of these conformationally restricted biaryl combretastatin-like molecules is outlined. The significant difficulties associated with the challenging and ultimately poor yielding synthesis of these compounds are described. A revised and improved synthetic strategy involving a Wittig reaction chain extension and an alternative oxidation strategy for the C-7 alcohol is subsequently presented. The synthesis of a water soluble phosphate ester prodrug is also described.

The synthesis of a novel aniline containing tubulin inhibitor, offering additional opportunities for molecular conjugation, is then recounted. The use of Suzuki coupling methodology to link the boronic acid C-ring component to the AB-ring enol triflate is described.

Chapter three begins with a discussion of the importance of enantiomeric purity in pharmacologically active molecules. The proposal to synthesise both the (*R*) and (*S*)-enantiomers of **the alcohol containing lead compound** is framed accordingly. A review of the diverse strategies exploited to achieve enantioselective synthesis is then summarised. The use of non-fermenting yeast to achieve the stereoselective reduction of an achiral ketone intermediate in the synthesis of the (*S*)-enantiomer is detailed. The procedures undertaken to confirm the enantiomeric purity and absolute configuration of the resultant molecules is described. The complications

encountered in achieving the desired inversion of configuration necessary for the synthesis of **the (*R*)-enantiomer** are detailed, together with the ultimately successful approach involving the use of the MOM ether protection strategy and the displacement of a mesylate with cesium acetate. The asymmetry in the biological activity of the (*S*) and (*R*)-enantiomers serves to emphasise the importance of defined stereochemistry in these compounds.

Chapter four outlines the successful synthesis of a series of novel tubulin inhibitors containing diverse functionality at the C-7 position. These compounds offer the potential for diverse molecular conjugation strategies to be employed due to the wide range of functional groups they contain. The synthesis of enantiomerically pure amine, alcohol and carboxylic acid containing tubulin inhibitors is described, together with an account of their antiproliferative activity *in vitro*.

Chapter five focuses on the synthesis of a small molecule designed multiple ligand possessing both tubulin polymerisation and aminopeptidase N inhibition activity. It is suggested that this dual acting compound would offer an attractive alternative to the high molecular weight conjugates described in chapter 1. The adversity associated with the introduction of the hydroxamic acid functional group at the C-7 position is discussed. The challenging thirty-one step synthesis of the dual acting compound is ultimately described.

Chapter six outlines the protocols employed for the biological evaluation of the novel compounds synthesised.

Chapter seven describes all of the experimental procedures involved in the synthesis of the molecules in this thesis, together with their full characterisation.

This thesis is dedicated to the memory of my mother, Noreen Stack

Acknowledgements

Firstly, I would like to offer my sincere gratitude to my supervisor Dr. John Walsh. His ingenuity and imagination were invaluable in accomplishing our shared goals. But more importantly, his patience and good nature throughout the last four years is greatly appreciated.

I wish to extend my appreciation to IRSET and enterprise Ireland for providing the funding for this project. I would like to thank Dr. John O'Brien and Dr. Manuel Reuther for the time and expertise given to my NMR samples. I am also very grateful to Brian Talbot for all the mass spectral data. I wish to acknowledge Dr. Helen Sheridan for generously allowing me to "borrow" her polarimeter cell for the last three years. I would also like to offer a big thank you to the technical staff in the School of Pharmacy and to Pauline, Maureen, Marcus, Ray and Joe in particular for always responding to my endless requests with a smile and a helping hand.

I would like to thank, in a special way, Brian, Elaine, Adrian, Orla, Tao, Paul and Deirdre for sharing the lab with me at various stages over the last four years and to Katerina in particular for her help in the biological evaluation of my compounds. I would also like to thank all the other postgraduates of the School of Pharmacy, past and present, for all the happy memories, nights out and fun days that we shared.

I would like to reserve a special thank you for Eddie, Jason, Claire, Brian and Emma for proof-reading the contents of this thesis. Your efforts are greatly appreciated.

To my darling Claire, you've been my sunshine throughout the wintery final furlong. Thank you from the bottom of my heart for listening to my gripes and for your support and encouragement.

To my father, Eamonn and sister, Shauna, I would not have been able to write this thesis without you. Your constant belief, encouragement and support will never be forgotten. I genuinely cannot thank you enough.

And finally to my mother, Noreen, your love and kindness has always been a source of strength, conviction and determination for me. I would not be the person I am without your influence. This thesis is dedicated to your memory.

Table of contents

1 Chapter 1 1

1.0 Introduction 1

1.0.1 Microtubules as a target for cancer chemotherapy 1

1.0.2 Tubulin targeting agents 2

1.1 Antibody-drug Conjugates 3

1.1.1 Drug characteristics 6

1.1.2 Antibody characteristics 7

1.1.3 Linker unit selection 9

1.1.3.1 Acid-labile linkers 10

1.1.3.2 Disulfide-containing linkers 10

1.1.3.3 Peptide linker units 14

1.1.3.4 Alternative linker units 16

1.1.4 Antibody-drug conjugates in preclinical development 18

1.1.5 Antibody-drug conjugates undergoing clinical evaluation 21

1.2 Vitamin-drug conjugates 25

1.3 Polyunsaturated fatty acid conjugates 33

1.4 Hormone receptor ligand conjugates 36

1.5 Peptide-drug conjugates 40

1.6 Macromolecular Conjugates 47

1.6.1 EPR effect-dependent macromolecular conjugates 48

1.6.2 Macromolecular conjugates with a tumour targeting moiety 62

1.6.3 Macromolecular conjugates with novel tumour-specific release mechanisms 71

1.7 Miscellaneous conjugates 74

1.8 Conclusions 80

1.9 Aims of the project 81

2 Chapter 2 83

2.0 Introduction 83

2.1 Aims and objectives 84

2.2 Original synthesis of lead compounds **(2.02)** and **(2.03)** 85

2.2.1 Malonic acid coupling and reduction 85

2.2.2 Meldrum's acid coupling and methanolysis 85

2.2.3 Reduction of ketone **(2.07)** and protection of alcohol **(2.08)** 86
2.2.4 Hydrolysis of methyl ester **(2.09)** and intramolecular cyclisation 86
2.2.5 Synthesis of C-ring **(2.14)** 87
2.2.6 Organolithium coupling of **(2.11)** and **(2.14)** 87
2.2.7 Removal of silyl protecting groups of **(2.15)** and oxidation 88
2.3 Improved synthesis of lead compounds **(2.02)** and **(2.03)** 88
2.3.1 Synthetic strategy 88
2.3.2 Alternative synthesis of **(2.10)** utilising the Wittig reaction 89
2.3.2.1 Synthesis of ylide **(2.16)** 89
2.3.2.2 Reduction of **(2.16)** 90
2.3.2.3 Characterisation of β-keto ester **(2.17)** 91
2.3.2.4 Characterisation of β-hydroxy ester **(2.18)** 93
2.3.2.5 Optimising the Wittig reaction 94
2.3.2.6 Synthesis of carboxylic acid **(2.10)** from β-keto ester **(2.17)** 95
2.3.3 Alternative oxidation of C-7 alcohol using Dess-Martin periodinane 96
2.3.4 Oxidation of secondary alcohol in the presence of protected phenol 97
2.3.4.1 Synthesis of coupled compound with protected phenol 97
2.3.4.2 Oxidation and removal of phenolic silyl protecting group 98
2.4 Synthesis of phosphate ester prodrug of **(2.03)** 99
2.4.1 Phosphate ester prodrugs 99
2.4.2 Synthesis of phosphate ester prodrug **(2.24)** 100
2.4.3 Characterisation of phosphate disodium salt **(2.24)** 101
2.5 Synthesis of aniline analogue of **(2.03)** 104
2.5.1 Synthetic strategy 104
2.5.2 Preparation of enol-triflate **(2.26)** 104
2.5.3 Synthesis of aniline containing C-ring 105
2.5.4 Suzuki coupling of enol triflate **(2.26)** and boronic acid **(2.31)** 108
2.5.5 Synthesis and coupling of boronate ester 108
2.5.6 Removal of protecting groups and oxidation of C-7 alcohol 111
2.5.7 Characterisation of aniline **(2.25)** 113
2.5.8 Synthesis of aniline hydrochloride salt **(2.36)** 115
2.6 Biological evaluation 116
2.6.1 Cell proliferation inhibition assays 116
2.6.2 Immunofluorescence staining of the microtubules 116
2.6.3 Cell cycle analysis 117

2.6.4 Endothelial cell morphology analysis 118
2.6.5 Angiogenesis inhibition assay 120
2.6.6 Aortic ring: angiogenesis assay 121
2.6.7 Aortic ring: anti-vascular assay 123
2.6.8 *In vivo* evaluation of phosphate ester prodrug **(2.24)** 125
2.7 Conclusions 127
3 Chapter 3 128
3.0 Introduction 128
3.1 Aims and Objectives 129
3.2 Homochiral drug substances 129
3.3 Asymmetric reduction of ketones 131
3.4 Yeast reduction of β-keto ester **(2.07)** 133
3.5 Determination of enantiomeric purity of **(3.07)** by NMR 134
3.6 Confirmation of absolute configuration of bioreduced alcohol by NMR 138
3.7 Synthesis of enantiomerically pure **(3.01)** 142
3.7.1 Silyl protection of **(3.07)** and hydrolysis of ester **(3.15)** 143
3.7.2 Cyclisation of **(3.16)** and removal of silyl protecting group of **(3.17)** 143
3.7.3 Coupling of **(2.14)** and **(3.18)** and removal of silyl groups 144
3.8 Introducing (*R*)-configuration at the C-7 position 145
3.8.1 Synthetic strategy 145
3.8.2 Use of CBS reagents to reduce **(2.07)** 145
3.8.3 Attempted inversion of configuration using the Mitsunobu reaction 147
3.8.4 Removing the source of conjugation: Reduction of the C-7 position carbonyl and protection of the resultant alcohol 148
3.8.5 The acetate protecting group 149
3.8.5.1 Reduction of ketone **(3.17)** and synthesis of acetate ester 149
3.8.5.2 Mitsunobu reaction on acetate protected alcohol **(3.26)** 150
3.8.6 The 2-methoxyethoxymethyl ether protecting group 151
3.8.6.1 Synthesis of MEM ether containing compound **(3.28)** 151
3.8.7 The tetrahydropyranyl ether protecting group 153
3.8.8 The methoxymethyl ether protecting group 154
3.8.8.1 MOM ether synthesis 154
3.8.8.2 Characterisation of MOM ether **(3.30)** 155
3.8.8.3 Removal of MOM protecting group 158

3.8.9 Attempted inversion of configuration using the Mitsunobu reaction on MOM protected alcohol **(3.30)** 161
3.8.9.1 Synthesis of derivative suitable for esterification with Mosher's acid 163
3.8.9.2 Determination of stereoselectivity of Mitsunobu reaction 165
3.8.10 Mesylate formation and acetate substitution 167
3.8.10.1 Synthesis of derivative of **(3.47)** suitable for esterification with Mosher's acid 169
3.8.10.2 Determination of stereoselectivity of mesylate displacement reaction 170
3.9 Synthesis of (*R*)-enantiomer alcohol **(3.02)** 171
3.10 Biological evaluation 172
3.11 Conclusions 173
4 Chapter 4 175
4.0 Introduction 175
4.1 Aims and objectives 175
4.2 Synthesis of the enantiomerically pure acetamide **(4.01)** 175
4.2.1 Synthetic strategy 176
4.2.2 Synthesis of enol triflate **(4.07)** 176
4.2.2.1 Mesylation of **(3.26)** and subsequent azide displacement 176
4.2.2.2 Acetate deprotection 177
4.2.2.3 Azide reduction and BOC protection of amine 178
4.2.2.4 Formation of enol triflate **(4.07)** 178
4.2.3 Synthesis of boronic acid **(4.08)** 179
4.2.4 Suzuki coupling and synthesis of **(4.01)** 179
4.2.4.1 Suzuki coupling of enol triflate **(4.07)** and boronic acid **(4.08)** 179
4.2.4.2 Removal of BOC and silyl protecting groups 180
4.2.4.3 Acetylation and hydrolysis of phenolic ester 181
4.3 Synthesis of C-7 methylene acetamide analogue **(4.12)** 182
4.3.1 Synthetic strategy 182
4.3.2 Synthesis of enol triflate containing additional methylene unit 182
4.3.2.1 Mesylation and cyanide displacement 183
4.3.2.2 Reduction of nitrile **(4.14)** 184
4.3.2.3 BOC protection of primary amine **(4.15)** 184
4.3.2.4 MOM deprotection and oxidation of benzylic alcohol 185
4.3.2.5 Synthesis of enol triflate **(4.19)** 186
4.3.3 Suzuki coupling and synthesis of **(4.12)** 187
4.3.3.1 Suzuki coupling of enol triflate **(4.19)** and boronic acid **(4.08)** 187

4.3.3.2 Removal of BOC protecting group of **(4.20)** 187
4.3.3.3 Acetylation of **(4.21)** 188
4.3.3.4 Removal of phenolic silyl protecting group of **(4.22)** 189
4.3.3.5 Characterisation of compound **(4.12)** 189
4.4 Synthesis of C-7 methylene alcohol analogues 192
4.4.1 Synthetic strategy 192
4.4.2 Synthesis of (*R*)-enantiomer methylene alcohol 193
4.4.2.1 Nitrile reduction 193
4.4.2.2 Silyl protection of alcohol **(4.26)** 194
4.4.2.3 MOM deprotection and alcohol oxidation 194
4.4.2.4 Formation of enol triflate **(4.31)** 195
4.4.2.5 Suzuki coupling of enol triflate **(4.31)** and boronic acid **(4.08)** 196
4.4.2.6 Simultaneous removal of both silyl protecting groups of **(4.32)** 197
4.4.2.7 Increased stability of **(4.23)** 197
4.4.2.8 Characterisation of **(4.23)** 198
4.4.3 Synthesis of (*S*)-enantiomer methylene alcohol **(4.24)** 200
4.4.3.1 Synthesis of mesylate **(4.35)** and displacement with cyanide 200
4.4.3.2 Two-step reduction of nitrile **(4.35)** to alcohol **(4.37)** 201
4.4.3.3 Silyl protection of the alcohol **(4.37)** 201
4.4.3.4 Removal of the MOM group of **(4.38)** and oxidation of alcohol **(4.39)** 202
4.4.3.5 Removal of silyl protecting group of **(4.40)** 202
4.4.3.6 Coupling of the ketone **(4.41)** with the C-ring bromide **(2.14)** 203
4.4.3.7 Removal of the phenolic silyl group of compound **(4.42)** 204
4.5 Synthesis of C-7 carboxylic acid tubulin inhibitors 204
4.5.1 Synthetic strategy 205
4.5.2 Synthesis of (*R*)-enantiomer carboxylic acid **(4.43)** 205
4.5.2.1 Silyl deprotection of **(4.29)** 205
4.5.2.2 Organolithium coupling of ketone **(4.45)** and C-ring bromide **(2.14)** 206
4.5.2.3 Direct oxidation of alcohol **(4.46)** to carboxylic acid **(4.47)** 206
4.5.2.4 Attempted PDC oxidation of **(4.46)** 207
4.5.2.5 Attempted DMP/NHS oxidation of **(4.46)** 207
4.5.2.6 Oxidation of alcohol **(4.46)** to aldehyde **(4.48)** 208
4.5.2.7 Characterisation of aldehyde **(4.48)** 209
4.5.2.8 Attempted PDC oxidation of aldehyde **(4.48)** 211

4.5.2.9 Attempted oxidation of aldehyde **(4.48)** using sodium chlorite and hydrogen peroxide 212
4.5.2.10 Attempted oxidation of **(4.48)** using sodium chlorite and DMSO 214
4.5.2.11 Oxone oxidation of aldehyde **(4.48)** 214
4.5.2.12 Removal of the silyl protecting group of **(4.47)** 216
4.5.2.13 Characterisation of compound **(4.43)** 216
4.5.3 Synthesis of (*S*)-enantiomer carboxylic acid **(4.44)** 218
4.5.3.1 Two-step oxidation of alcohol **(4.42)** to carboxylic acid **(4.50)** 218
4.5.3.2 Silyl deprotection of compound **(4.50)** 219
4.6 Biological Evaluation 220
4.6.1 MTT assay results for **(4.01)** and **(4.12)** 220
4.6.2 MTT assay results for **(4.23)** and **(4.24)** 220
4.6.3 MTT assay results for **(4.43)** and **(4.44)** 221
4.7 Conclusions 223
5 Chapter 5 225
5.0 Introduction 225
5.0.1 Conjugates containing a homing moiety 225
5.0.2 Conjugates containing a complimentary pharmacophore 225
5.0.3 Aminopeptidase N inhibition as complimentary target for dual acting compounds 226
5.0.4 Disadvantages of the molecular conjugation drug design paradigm 228
5.0.5 Hydroxamic acid containing APN inhibitors 229
5.0.6 Designed multiple ligands 230
5.1 Aims and objectives 231
5.2 Attempted synthesis of **(5.05)** 231
5.2.1 Synthetic strategy 231
5.2.2 Synthesis of pentafluorophenyl ester of **(4.47)** 232
5.2.3 Displacement of PFP ester of **(5.06)** with hydroxylamine 232
5.3 Attempted synthesis of ether containing hydroxamic acid compound 234
5.3.1 Synthetic strategy 235
5.3.2 Suzuki coupling of enol triflate **(4.31)** and boronic ester **(2.33)** 235
5.3.3 Removal of silyl protecting group on **(5.09)** 236
5.3.4 Attempted O-alkylation of compound **(5.10)** 236
5.3.4.1 Characterisation of compound **(5.12)** 237
5.4 Synthesis of methylene containing hydroxamic acid compound **(5.13)** 240
5.4.1 Synthetic strategy 241

5.4.2 Synthesis of mesylate **(5.14)** and displacement with cyanide 241
5.4.3 Two step reduction of nitrile **(5.15)** 242
5.4.4 Silyl protection of alcohol **(5.17)** 243
5.4.5 Removal of MOM protecting group of **(5.18)** and oxidation of alcohol **(5.19)** 244
5.4.6 Removal of the silyl protecting group of **(5.20)** 244
5.4.7 Organolithium coupling of AB-ring ketone **(5.20)** and C-ring bromide **(2.14)** 245
5.4.8 Removal of phenolic silyl protecting group of **(5.21)** 245
5.4.8.1 Characterisation of compound **(5.22)** 246
5.4.9 Two step oxidation of alcohol **(5.21)** to carboxylic acid **(5.24)** 249
5.4.10 Removal of silyl protecting group of **(5.24)** 249
5.4.10.1 Characterisation of **(5.25)** 250
5.4.11 Formation of PFP ester of compound **(5.24)** 253
5.4.12 Displacement of PFP ester **(5.26)** with hydroxylamine 254
5.4.13 Removal of silyl group on compound **(5.27)** 255
5.4.13.1 Characterisation of **(5.13)** 256
5.5 Biological evaluation 259
5.5.1 MTT assay results for **(5.22)**, **(5.25)** and **(5.13)** 260
5.5.2 Aminopeptidase N UV spectrophotometric assay results 261
5.6 Conclusions 262
6 Biological Experimental 263
6.0 Introduction 263
6.1 MTT Cell proliferation assay 263
6.1.1 Materials 263
6.1.2 Equipment 263
6.1.3 Test compounds 264
6.1.4 Cell line 264
6.1.5 Cell maintenance and sub-culture 264
6.1.6 Cell count 265
6.1.7 Assay protocol 265
6.1.8 Plate reader settings 266
6.1.9 Interpretation of data 266
6.2 Aminopeptidase N UV Spectrophotometric Assay 266
6.2.1 Materials 266
6.2.2 Equipment 267
6.2.3 Buffers and Solutions 267

6.2.4 Assay protocol 267
6.2.5 Plate reader settings 268
6.2.6 Interpretation of data 268
7 Chemistry Experimental 269
8 References 412
9 Appendix A 436

Table of Figures

Figure 1.1 Schematic of an antibody-drug conjugate 6
Figure 1.2 mAb-SPDB-DM4 11
Figure 1.3 mAb-SMCC-DM1 12
Figure 1.4 huC242-SPP-DM1 13
Figure 1.5 mAb-Val-Cit-MMAE and mAb-Phe-Lys-MMAE 15
Figure 1.6 mAb-AEBV 15
Figure 1.7 mAb–mcMMAF 16
Figure 1.8 mAb–PEG_4Mal–DM1 17
Figure 1.9 MMAE/MMAF-glucuronic acid linker-antibody conjugate 18
Figure 1.10 SB-T-12136-mAb conjugates 19
Figure 1.11 Colchicine-cobalamin conjugate **(1.01)** 26
Figure 1.12 Biotin-linker-SB-T-1214 conjugate **(1.02)** 27
Figure 1.13 Paclitaxel-folic acid conjugate **(1.03)** 28
Figure 1.14 EC140 **(1.04)** 29
Figure 1.15 EC145 (folate-S-S-deacetylvinblastine monohydrazide) **(1.05)** 30
Figure 1.16 EC0305 **(1.06)** 31
Figure 1.17 EC131 **(1.07)** 32
Figure 1.18 Vitamin E-paclitaxel glycinate ester conjugate **(1.08)** 32
Figure 1.19 DHA-paclitaxel **(1.09)** 34
Figure 1.20 Conjugated linoleic acid-paclitaxel **(1.10)** 35
Figure 1.21 Paclitaxel-lipoamino acid conjugates 36
Figure 1.22 Colchicine-cyanonilutamide conjugate **(1.13)** 37
Figure 1.23 Estradiol-paclitaxel conjugate **(1.14)** 38
Figure 1.24 Deslorelin-docetaxel conjugate **(1.15)** 39
Figure 1.25 Luteinising hormone-releasing hormone analogue-paclitaxel conjugate **(1.16)** . 40
Figure 1.26 2'-[Mu-Ser-Ser-Lys-Tyr-Gln--NH-$(CH_2)_2$-$N(CH_3)$]-Paclitaxel **(1.17)** 41
Figure 1.27 ANG1005 **(1.19)** 42
Figure 1.28 Paclitaxel-7-AcGPLGIAGQ **(1.20)** 43
Figure 1.29 Paclitaxel-EC1 conjugate **(1.21)** 43
Figure 1.30 Paclitaxel-E[c(RGDyK)]$_2$ conjugate **(1.22)** 44
Figure 1.31 E-[c$(RGDfK)_2$]-paclitaxel **(1.23)** 45

Figure 1.32 Paclitaxel–H2009.1 peptide conjugate **(1.24)** 46
Figure 1.33 Paclitaxel–HSA–PEG **(1.25)** 49
Figure 1.34 Schematic representation of Paclitaxel poliglumex **(1.26)** 51
Figure 1.35 PGG-PTX **(1.27)** 52
Figure 1.36 P(LGG-paclitaxel)-PEG-P(LGG-paclitaxel) conjugate **(1.28)** 53
Figure 1.37 PHEA-2'-O-Succinylpaclitaxel conjugate **(1.29)** 54
Figure 1.38 PVA–SPTX Conjugate **(1.30)** 54
Figure 1.39 Paclitaxel–carboxymethyl dextran conjugates 56
Figure 1.40 LMWC-paclitaxel **(1.31)** 57
Figure 1.41 LMWC-docetaxel **(1.32)** 58
Figure 1.42 Cyclotriphosphazene–paclitaxel conjugate **(1.33)** 58
Figure 1.43 Paclitaxel-triazine dendrimer prodrug 1 **(1.34)** 59
Figure 1.44 Paclitaxel-triazene dendrimer prodrug 2 **(1.35)** 60
Figure 1.45 Tubulysin analogue-dendrimer conjugate **(1.36)** 61
Figure 1.46 HPMA Copolymer-PTX-ALN Conjugate **(1.37)** 63
Figure 1.47 PTX-PEG-ALN **(1.38)** 64
Figure 1.48 HYTAD1-p20 **(1.39)** 65
Figure 1.49 HA-amino acid-paclitaxel 67
Figure 1.50 PGA-PTX-E-[c(RGDfK)$_2$] **(1.40)** 68
Figure 1.51 PHEA–PEG2000-succinyl-oxytocin–succinyl-paclitaxel conjugate **(1.41)** 69
Figure 1.52 Glycopeptide dendrimer colchicine conjugate J1C **(1.42)** 70
Figure 1.53 SynB1-ELP1-PTX **(1.43)** 72
Figure 1.54 HPMA-AB3-(PTX)$_3$ **(1.44)** 73
Figure 1.55 FA-AD-Suc-PTX **(1.45)** 75
Figure 1.56 FA-Ad-ICG02-Glu-PTX **(1.46)** 75
Figure 1.57 Glucuronic acid containing paclitaxel conjugate **(1.47)** 76
Figure 1.58 Paclitaxel-glucose conjugate **(1.48)** 77
Figure 1.59 Thymidine-paclitaxel conjugate **(1.49)** 78
Figure 1.60 Phototaxel **(1.50)** 78
Figure 2.1 Combretastatin A-4 83
Figure 2.2 Core structure of lead tubulin polymerisation inhibitors 83
Figure 2.3 Lead molecules **(2.02)** and **(2.03)** 84
Figure 2.4 ^{1}H NMR spectrum of **(2.27)** 92
Figure 2.5 ^{13}C, DEPT 135 and DEPT 90 spectra of **(2.17)** 92
Figure 2.6 ^{1}H spectrum of **(2.18)** 93

Figure 2.7 ^{13}C, DEPT 135 and 90 NMR spectra of **(2.18)** 94
Figure 2.8 ^{1}H NMR spectrum of **(2.24)** 102
Figure 2.9 ^{13}C, DEPT 135 and DEPT 90 spectrum of **(2.24)** 102
Figure 2.10 HSQC NMR spectrum of **(2.24)** 103
Figure 2.11 HMBC NMR spectrum of **(2.24)** 103
Figure 2.12 Proposed aniline containing tubulin inhibitor **(2.25)** 104
Figure 2.13 ^{11}B NMR of impure boronic acid **(2.31)** 107
Figure 2.14 ^{1}H NMR spectrum of **(2.25)** 114
Figure 2.15 ^{13} C, DEPT 135 and DEPT 90 NMR spectra of **(2.25)** 114
Figure 2.16 HSQC spectrum of **(2.25)** 115
Figure 2.17 HMBC spectrum of **(2.25)** 115
Figure 2.18 Microtubule disruption of endothelial cells. 117
Figure 2.19 Percentage of G2/M phase cell count of **(2.03)**, **(2.36)** and CA-4. 118
Figure 2.20 The effect of **(2.03)** and CA-4 on endothelial cells' morphology 119
Figure 2.21 The effect of **(2.36)** on endothelial cells' morphology 119
Figure 2.22 Angiokit angiogenesis assay 120
Figure 2.23 The effect of **(2.03)** on microvessel formation 121
Figure 2.24 Effect of treatment with **(2.03)** on growth of new blood vessel capillaries 121
Figure 2.25 The effect of **(2.03)** on new blood vessel capillary formation 122
Figure 2.26 Effect of treatment with **(2.36)** in an *ex vivo* aortic ring assay 122
Figure 2.27 The effect of **(2.36)** on new blood vessel capillary formation 123
Figure 2.28 Anti-vascular effect of **(2.03)** 124
Figure 2.29 Anti-vascular effect of **(2.03)** 124
Figure 2.30 Evaluation of the efficacy **(2.24)** and CA-4P in PC-3 tumour xenograft model . 125
Figure 2.31. The effect of **(2.24)** treatment on tumour vasculature 126
Figure 3.1 Schematic of tubulin inhibitory pharmacophore 128
Figure 3.2 (*S*) and (*R*)-enantiomers of racemic lead compound **(2.02)** 128
Figure 3.3 Structure of (*S*)-omeprazole **(3.03)** and racemic omeprazole **(3.04)** 130
Figure 3.4 (*S*)-ofloxacin (Levofloxacin) **(3.05)** and racemic ofloxacin **(3.06)** 131
Figure 3.5 (*R*)-Mosher's acid) **(3.09)** 135
Figure 3.6 ^{19}F NMR spectrum of racemic alcohol (R)-Mosher's ester **(3.10)** 137
Figure 3.7 ^{19}F NMR spectrum of bio reduced alcohol R-Mosher's ester **(3.11)** 137
Figure 3.8 Ohtani's Model for determination of absolute configuration by NMR 139
Figure 3.9 ^{1}H NMR of (*R*)-Mosher's ester **(3.11)** 140
Figure 3.10 ^{1}H NMR of (*S*)-Mosher' s ester **(3.12)** 140

Figure 3.11 a) Model A re-drawn illustrating the (*S*)-stereochemistry of the alcohol **(3.07)** 142
Figure 3.12 (*S*) and (*R*)-Mosher's esters of ethyl ester **(3.08)** 142
Figure 3.13 ^{19}F NMR spectrum of (*R*)-Mosher's ester **(3.21)** 147
Figure 3.14 ^{1}H NMR spectrum of **(3.30)** 156
Figure 3.15 ^{13}C, DEPT 135 and DEPT 90 spectra of **(3.30)** 157
Figure 3.16 HH COSY spectrum of **(3.30)** 157
Figure 3.17 HSQC spectrum of **(3.30)** 158
Figure 3.18 Selected expansion of HSQC of **(3.30)** 158
Figure 3.19 ^{19}F NMR of **(3.43)** 165
Figure 3.20 ^{19}F NMR of **(3.44)** 166
Figure 3.21 ^{19}F NMR spectrum of **(3.50)** 171
Figure 4.1 (*R*)-enantiomer acetamide **(4.01)** 176
Figure 4.2 Methylene containing acetamide analogue **(4.12)** 182
Figure 4.3 ^{1}H NMR spectrum of **(4.12)** 190
Figure 4.4 ^{13}C, DEPT 135 and DEPT 90 spectra of **(4.12)** 191
Figure 4.5 HSQC spectrum of **(4.12)** 191
Figure 4.6 (*R*) and (*S*)-enantiomers of methylene containing **(2.02)** analogues 192
Figure 4.7 ^{1}H NMR spectrum of **(4.23)** 199
Figure 4.8 ^{13}C, DEPT 135 and DEPT 90 spectra of **(4.23)** 199
Figure 4.9 HSQC NMR spectrum of **(4.23)** 200
Figure 4.10 (*R*) and (*S*) carboxylic acid containing tubulin inhibitors **(4.43)** and **(4.44)** 205
Figure 4.11 ^{1}H NMR spectrum of **(4.48)** 210
Figure 4.12 ^{13}C, DEPT 135 and DEPT 90 NMR spectra of **(4.48)** 210
Figure 4.13 HSQC NMR spectrum of **(4.48)** 211
Figure 4.14 ^{1}H NMR spectrum of **(4.43)** 217
Figure 4.15 ^{13}C, DEPT 135 and DEPT 90 spectra of **(4.43)** 217
Figure 4.16 HSQC NMR spectrum of **(4.43)** 218
Figure 5.1 Compound **(5.01)** 226
Figure 5.2 Structure of bestatin **(5.02)** 227
Figure 5.3 APN inhibitor **(5.03)** synthesised by Wang *et al.* 229
Figure 5.4 APN inhibitor **(5.04)** evaluated by Inagaki *et al.* 230
Figure 5.5 Structure of proposed DML compound **(5.05)** 231
Figure 5.6 Proposed mechanisms for the instability of **(5.07)** 234
Figure 5.7 Proposed ether containing hydroxamic acid compound **(5.08)** 235
Figure 5.8 ^{1}H NMR spectrum of **(5.12)** 239

Figure 5.9 ^{13}C and DEPT 135 NMR spectrum of **(5.12)** 239
Figure 5.10 Expansion of ^{13}C spectrum of **(5.12)** from 76-78 ppm 240
Figure 5.11 HSQC NMR spectrum of **(5.12)** 240
Figure 5.12 Methylene-containing hydroxamic acid compound **(5.13)** 241
Figure 5.13 ^{1}H NMR spectrum of **(5.22)** 247
Figure 5.14 ^{13}C, DEPT 135 and DEPT 90 NMR spectra of **(5.22)** 247
Figure 5.15 HSQC NMR spectrum of **(5.22)** 248
Figure 5.16 HSQC NMR spectrum expansion of **(5.22)** 248
Figure 5.17 ^{1}H NMR spectrum of **(5.25)** 251
Figure 5.18 ^{13}C, DEPT 135 and DEPT 90 NMR spectra of **(5.25)** 251
Figure 5.19 Expansion of aliphatic region of HSQC NMR spectrum of **(5.25)** 252
Figure 5.20 Expansion of HSQC of **(5.25)** illustrating methoxy carbon and proton signals .. 252
Figure 5.21 Expansion of aromatic region of HSQC NMR spectrum of **(5.25)** 253
Figure 5.22 ^{1}H NMR spectrum of **(5.13)** 257
Figure 5.23 ^{13}C, DEPT 135 and DEPT 90 NMR spectra of **(5.13)** 257
Figure 5.24 Expansion of ^{13}C NMR spectrum of **(5.13)** from 160-165 ppm 258
Figure 5.25 HSQC NMR spectrum of **(5.13)** 258
Figure 5.26 Expansion of aliphatic region of HSQC NMR spectrum of **(5.13)** 259

Abbreviations

2,6-DCBCl	2,6-dichlorobenzoyl chloride
ADC	antibody-drug conjugate
ALN	alendronate
APN	aminopeptidase N
aq.	aqueous
BINAP	2,2'-bis(diphenylphosphino)-1,1'-binaphthyl
BMPEO	*bis*-maleimido-trioxyethylene glycol
Boc_2O	di-*tert*-butyl dicarbonate
BOC	*N*-*tert*-butoxycarbonyl
br	broad
CA-4	combretastatin A-4
CA-4P	combretastatin A-4 phosphate
CAR	coxsackie adenovirus receptors
COSY	correlation spectroscopy
CMDex	carboxymethyldextran
d	doublet
DCC	*N,N'*-dicyclohexylcarbodiimide
DCM	dichloromethane
dd	double doublet
DEPT	distortionless enhancement by polarisation transfer
DHA	docosahexaenoic acid
DIAD	diethylazodicarboxylate
DIBAL-H	diisobutylaluminium hydride
DIPA	diisopropylamine
DIPEA	*N,N*-diisopropylethylamine
DM	drug maytansinoid
DMAP	4-dimethylaminopyridine
DMF	*N,N*-dimethylformamide
DML	designed multiple ligand
DMP	Dess-Martin periodinane
DMPU	*N,N'*-dimethylproyleneurea

DMSO	dimethyl sulfoxide
EDTA	ethylenediaminetetraacetic acid
EGFR	epidermal growth factor receptor
ELP	Elastin-like polypeptide
EPR	enhanced penetration and retention
EtOAc	ethyl acetate
EtOH	ethanol
FA	folic acid
FBS	foetal bovine serum
FR	folate receptor
GRP	gastrin-releasing peptide
HA	hyaluronic acid
HER2	human epidermal growth factor receptor 2
HEPES	4-(2-Hydroxyethyl)piperazine-1-ethanesulfonic acid
HMBC	heteronculear multiple bond correlation
HPMA	*N*-(2-hydroxypropyl) methacrylamide
HRMS	high resolution mass spectrometry
HSA	human serum albumin
HSQC	heteronuclear single quantum coherence
HUVECs	human umbilical vein endothelial cells
Hz	hertz
IC_{50}	concentration required for 50% inhibition
IBX	1-hydroxy-1,2-benziodoxole-3(1H)-one-1-oxide
IR	infrared
i.p.	intraperitoneal
IPA	isopropyl alcohol
i.v.	intravenous
KHMDS	potassium bis(trimethyl-silyl)amide
LA	linoleic acid
LD_{50}	concentration required for 50% lethality
LDA	lithium diisopropylamide
LNA	linolenic acid
LRP	lipoprotein receptor related protein
m	multiplet

mAb	monoclonal antibody
MC	maleimido-caproyl
mCPBA	*meta*-chloroperoxybenzoic acid
MDR-1	multidrug resistance protein 1
MEM	2-methoxyethoxymethyl
MeOH	methanol
MMAE	monomethyl auristatin E
MMAF	monomethyl auristatin F
MMP	matrix metalloproteinase
MOM	methoxymethyl
MsCl	methanesulfonyl chloride
MTD	maximum tolerated dose
MTT	thiazolyl blue tetrazolium bromide
nBuLi	*n*-butyllithium
NHS	*N*-hydroxysuccinimide
NMR	nuclear magnetic resonance
PAB	para-amino-benzyloxy carbonyl
PABC	*p*-aminobenzyl carbonyl
PAMAM	polyamidoamine
PBS	phosphate buffered saline
PDC	pyridinium dichromate
Pd/C	palladium on carbon
$Pd(dppf)Cl_2$	[1,1-bis(diphenylphosphino)ferrocene]dichloropalladium(II)
$Pd(PPh_3)_4$	(tetrakis(triphenyl)phosphine) palladium
PEG	polyethylene glycol
PFP	pentafluorophenol
PGA	poly (L-glutamic acid)
PGG	poly (L-γ-glutamyl-glutamine)
PPh_3	triphenylphosphine
PHEA	poly (hydroxyethylaspartamide)
PI	propidium iodide
ppm	parts per million
PPX	paclitaxel poliglumex
PTX	paclitaxel

PVA	poly (vinyl alcohol)
q	quartet
QC	quaternary carbon
R_f	retention factor
RHAMM	receptor for hyaluronic acid mediated motility
rpm	revolutions per minute
RT	room temperature
s	singlet
SCCHN	squamous cell carcinomas of the head and neck
SMCC	succinimidyl trans-4-(maleimidylmethyl) cyclohexane-1- carboxylate
SPDB	*N*-Succinimidyl-3-(2-Pyridylthio) propionate
SPP	*N*-succinimidyl 4-(2-pyridyldithio) pentanoate
TBAF	tetrabutylammonium fluoride
TBDMSCl	*tert*-butyldimethylsilyl chloride
TBDPSCl	*tert*-butyldiphenylsilyl chloride
THF	tetrahydrofuran
THP	tetrahydropyranyl
TIP-1	tax-interacting protein-1
TLC	thin layer chromatography
TF	tissue factor
TFA	trifluoroacetic acid
UV	ultraviolet
vc	valine-citrulline
VTA	vascular-targeting agent

1 Chapter 1

1.0 Introduction

Cancer patients with metastasises typically present with approximately 10^{12} tumour cells. In order to achieve clinical remission it has been established that greater than 99% of these need to be killed [1]. Despite the emergence of novel treatments for malignancy, conventional chemotherapeutics and tubulin targeting agents in particular remain a cornerstone in many anticancer regimens. The major difficulty with these chemotherapeutic agents is that in order to reach that target of 99% cancer cell death, unacceptable toxicities are inevitable. In this respect significant challenges remain in developing new therapies that are suitably toxic to cancer cells while leaving normal cells relatively unscathed.

Molecular conjugation is an approach that has been extensively explored to achieve enhanced delivery of existing cytotoxics to the tumour site. The rationale behind this approach is two-fold. Firstly, by masking the toxicity of the drug until it reaches the active site, a lower incidence of side effects is expected. Secondly, by enhancing the specificity of the cytotoxic agent for the desired target cells, greater efficacy may be attainable.

1.0.1 Microtubules as a target for cancer chemotherapy

Microtubules, which are the target of tubulin binding agents, consist of α and β tubulin heterodimers. They are hollow tubes approximately 25 nm in diameter that are involved in various cellular functions, most notably cell movement, intracellular transport and cell division [2]. Microtubule dynamics are very tightly regulated both spatially and temporally. At the onset of mitosis in particular there are dramatic changes in the microtubule network in which the disassembly of microtubules is followed by the formation of a new network of spindle microtubules. Tubulin targeting agents are known to bind to one of four main binding sites on the β-tubulin subunit: the vinca domain, the colchicine binding site, the paclitaxel site and the laulimalide site. Once bound, these agents act as either microtubule-stabilising or microtubule-destabilising agents, interfering with mitosis and leading to cell death. One reason that cancer cells are particularly sensitive to these drugs compared with normal cells is that many cancer cells divide much more rapidly than normal cells offering many more opportunities for tubulin binding agents to disrupt mitosis and cause cell death. Hundreds of compounds have been observed to

arrest mitosis by interacting with microtubules. It has been shown without exception, that they act by potently suppressing microtubule dynamics [3].

1.0.2 Tubulin targeting agents

Tubulin binding agents are principally natural product or natural product derived small molecule inhibitors that have diverse structural classes and origins. Lead compounds for these agents include substances derived from bacteria, plants, marine sponges and molluscs [2].

Two of the most clinically pertinent classes of tubulin binding agents are the taxanes and the vinca alkaloids. The vinca alkaloids were first identified greater than 50 years ago while the taxanes where first identified greater than 40 years ago, yet both classes of agents still find significant utility in the first line treatment of many solid tumours and haematological malignancies [3].

Other tubulin targeting agents that have been evaluated for anticancer activity include the colchinoids and the epothilones. In more recent years, tubulin binding agents that demonstrate cytotoxicities many orders of magnitude greater than clinically used agents, have been evaluated. Synthetic taxoids that exhibit approximately 100-fold greater cytotoxicity than the parent compounds have been developed [4]. The tubulysins, isolated from various myxobacterial species, have also demonstrated IC_{50} values 20- to 1000-fold lower than many clinically used tubulin binding agents [5]. The maytansinoids are another such class of compound. The lead molecule of this class, maytansine, is an ansa macrolide first isolated from the Ethiopian shrub *Maytenus ovatus* by Kupchan *et al.* [6]. Maytansine causes depolymerisation of microtubules and displays almost 100-fold higher cytotoxicity than the vinca alkaloids [7]. Synthetic analogues of maytansine, referred to as drug maytansinoids (DMs), have subsequently been developed which possess 100- to 1000-fold greater cytotoxicity than existing agents in the clinic [8-9]. DM1 (*N*-methyl-*N*-[3-mercapto-1-oxopropyl]-L-alanine ester of maytansinol) is an example of one such maytansinoid which has been shown to be effective against a wide range of tumour cells with IC_{50} values in the range of 10-100 pM [10].

Dolastatin-10 is another highly potent inhibitor of microtubule dynamics and is a non-competitive inhibitor of the binding of vinblastine to tubulin. Synthetic analogues of dolastain-10, known as auristatins, are potent tubulin inhibitors with cytotoxicities 50- to 200-fold greater than the vinca alkaloids [4].

As well as their ability to interfere with mitosis, tubulin targeting agents have been shown to exert an effect on immature endothelial cells. These agents act by disrupting the tubulin cytoskeleton which these rapidly dividing cells rely upon to maintain their structural integrity. The endothelium of solid tumour vasculature is particularly sensitive to these effects. Destruction of the endothelium of solid tumours by vascular targeting agents (VTAs) causes the death of tumour cells due to a lack of oxygen and nutrients with consequent necrosis of established tumours [11]. Most tubulin targeting agents only demonstrate antivascular activity close to the maximum tolerated dose (MTD), with direct tumour cell killing *via* mitotic arrest being the dominant mechanism of action. This partly explains why the early tubulin-binding agents studied, such as colchicine, vincristine, and vinblastine, have a narrow therapeutic window [6, 8]. Combretastatin A-4 was the first small molecule VTA shown to have antivascular effects at doses below the maximum tolerated dose and is currently undergoing clinical trials for use in various angiogenesis dependent cancers [11].

Despite the promise of tubulin binding agents as cancer therapeutic agents, there are a number of significant disadvantages to their use. Paclitaxel for example, while remaining one of the most clinically important agents currently in use, suffers from dose-limiting toxicity and multidrug resistance. The action of efflux pumps such as multidrug resistance protein-1 (MDR-1), which actively pumps paclitaxel out of resistant cells, is known to cause subtherapeutic intracellular drug concentrations. Resistance is also known to occur due to changes in β-tubulin or apoptotic and mitosis checkpoint proteins [12]. In order to overcome these difficulties various attempts have been made to specifically target tumour cells through the molecular conjugation of tumour delivery enhancing moieties to existing tubulin targeting agents. By selectively delivering existing cytotoxic agents to tumour cells, the ambition is that more potent cytotoxicity to target cells may be achieved while simultaneously reducing the systemic toxicity associated with these agents.

In the remainder of this chapter, a review of the disparate methodologies utilised to optimise the delivery of tubulin targeting agents to the tumour site which have been published throughout the last ten years has been undertaken. The merits of each approach will be critically appraised in terms of efficacy, therapeutic window and ability to overcome drug resistance.

1.1 Antibody-drug Conjugates

In early antibody evaluation, a number of antibodies were produced that bound very specifically to various tumour cell surface antigens. However, in many cases such binding was insufficient to

affect tumour growth *in vitro*. Two of the most effective monoclonal antibodies for the treatment of cancer currently licensed by the FDA are trastuzumab for breast cancer and cetuximab for colorectal tumours and squamous cell carcinoma of the head and neck. However, both these drugs offer only modest single agent activity [4, 13]. One way to take advantage of the selectivity of monoclonal antibodies for various cell specific antigens is to utilise molecular conjugation to attach a non-selective cytotoxic agent to a monoclonal antibody selective for tumour specific antigens. Various concepts along this theme have been explored but the most common approach involves the monoclonal antibody acting as a vector to the tumour cell, facilitating internalisation and downstream processing to liberate the cytotoxic effector molecule within the cell. This has led some commentators to refer to drug-antibody conjugates as tumour-activated prodrugs [4].

Antibody conjugation is considered to be one of the most promising approaches to increasing the anti-tumour activity of antibodies, while simultaneously reducing the systemic toxicity of existing cytotoxics such as tubulin targeting agents [14]. The various advantages and disadvantages of antibody-drug conjugates (ADCs) are summarised in Table 1.1.

Despite early promise, the emergence of clinically successful drug-antibody conjugates has been somewhat slow due to the difficulties involved in successfully formulating these agents in presentations that can overcome the pharmacokinetic and pharmacodynamic impediments of these relatively large molecules. Durcy *et al.* framed the characteristics of an ideal antibody-drug conjugate along five distinct headings [18]:

1. *Circulation:* The antibody should be stable in circulation and should not have cytotoxic activity until intracellular release of the active drug.
2. *Antigen binding:* The monoclonal antibody should retain its high binding affinity for its intended target despite molecular conjugation to the cytotoxic agent.
3. *Internalisation:* A sufficient intracellular concentration of the ADC should be obtained to cause cell death. This can be challenging if the antigen is expressed only in limited numbers.
4. *Drug release:* Once internalisation has occurred, release of the cytotoxic agent should be timely and efficient.
5. *Drug action:* The drugs utilised in the ADC should be capable of causing cell death at subnanomolar concentrations.

Table 1.1 Advantages and disadvantages of antibody-drug conjugates

Advantages	Disadvantages
Targeted binding specific for tumour antigen	Requires that tumour be tested for expression of target antigen
Highly potent agents can be selectively delivered to target cells	Molecular target may have some normal tissue expression
Wide therapeutic index	Linker may not be stable leading to premature cytotoxic agent release
Prolonged circulation half-life	Antibody may not reach target in sufficient concentration to be lethal
Stable in circulation	Antigen expression could be heterogeneous especially in solid tumours [15]
Decreased adverse effects	ADC must cross the vascular endothelium and circumvent the interstitial pressure within the solid tumour [16]
Bystander killing effect of endothelial cells and stromal cells essential to tumour growth	Antibody may itself be immunogenic
Reduced MDR-1 mediated resistance compared to systemic administration of the respective drug [14]	Masking of the target antigen with monoclonal antibody devoid of its cytotoxic payload in ADCs with poor stability [17]

The three constituent parts of an ADC are the antibody, the cytotoxic drug molecule and the linker connecting them as illustrated schematically in Figure 1.1.

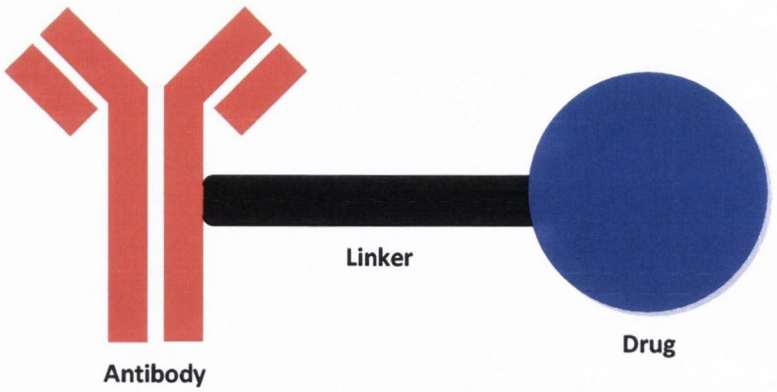

Figure 1.1 Schematic of an antibody-drug conjugate

It has been suggested that early ADCs failed because of inappropriate drug selection, non-specific antibody selection and use of linkers that were not stable [19]. Another difficulty with ADCs is that only a tiny fraction of administered ADC reaches the tumour site. Consequently, the cytotoxic agent used needs to be much more potent than currently used clinical agents. Thus, it became apparent that optimisation of each of these three variables was required in order to maximise the potential of ADCs.

1.1.1 Drug characteristics

Although antibodies often display high specificity for the tumour, most of them are not potent enough to be clinically efficacious. Imaging studies with radiolabelled antibodies have shown that the peak concentration of antibodies deposited at the tumour site was of the order of 0.01% of the injected dose per gram of tumour at 24 h [20]. Therefore, the cytotoxicity of the drug in an ADC must be several-fold higher than conventional anticancer drugs [4]. It has been suggested that the cytotoxicity of the drug used in an ADC must possess an IC_{50} of the order of 10-100 pM. Since paclitaxel displays an IC_{50} of approximately 10 nM in a number of cell lines it has been suggested that it is not suitable for this approach [21].

The *in vitro* cytotoxicity (IC_{50} values) of the maytansinoids and auristatins are even lower than the concentration of antibodies found to accumulate at the tumour site, making them suitable candidates for ADC synthesis. For this reason the maytansinoid DM1 [$N^{2'}$-deacetyl-$N^{2'}$-(3-

mercapto-1-oxopropyl)-maytansine] has become one of the most widely utilised tubulin targeting agents in the synthesis of ADCs [22].

To exploit the long plasma half life of intact IgG antibodies necessary to achieve maximal deposition at tumour sites the drug must be non-toxic in conjugated form, a requirement which both the maytansinoids and auristatins possess. Furthermore, these cytotoxic agents are readily linkable to an appropriate antibody, sufficiently water soluble and stable on storage [8].

Drug loading is another critical factor which determines the therapeutic characteristics of an ADC. A series of conjugates of the anti-CD30 monoclonal antibody cAC10 linked to either 2, 4 or 8 monomethyl auristatin E (MMAE) molecules were synthesised. Although the *in vitro* toxicity of the resultant conjugates was directly dependent on the drug loading, *in vivo,* the antitumour activity of the 4 MMAE antibody was comparable with the 8 MMAE containing conjugate. However, the maximum tolerated dose of the 4 MMAE containing conjugate was found to be double that of the 8 MMAE containing conjugate [23]. It has also been demonstrated for other conjugates that the *in vivo* activity drops off significantly when less than three cytotoxic drug molecules per antibody are used while an upper limit is often imposed by the solubility characteristics of the resulting conjugate [10].

1.1.2 Antibody characteristics

The cell surface antigen which the antibody recognises is typically a glycoprotein, a carbohydrate, an oncoprotein, a growth factor receptor or a hormone receptor. The factors that need be considered in selecting an appropriate antibody target for the synthesis of an ADC include [1]:

1. Degree of target expression on tumour cells compared to normal tissues.
2. Affinity of antibody for target.
3. Efficiency of internalisation following antibody binding.
4. Homogeneity of target expression on all target cells.
5. Degree of target shedding into circulation.

Many early monoclonal antibodies investigated as potential drugs lacked specificity. Some of these agents bound to antigens expressed on a wide variety of normal cells that were merely upregulated in various tumours. Cross-reactivity of the chosen antibody with normal tissues is thus of utmost concern when designing any ADC [1]. Bivatuzumab mertansine illustrates the potential pitfalls associated with poor target antigen selection. This conjugate consists of the

monoclonal antibody bivatuzumab covalently conjugated to the maytansinoid DM1. Bivatuzumab is a humanised monoclonal antibody (BIWA 4) that binds selectively to CD44v6. This cell surface antigen is highly and homogenously expressed on squamous cell carcinoma of the head and neck, oesophagus, lung, cervix and vulva. Its expression was also found in some normal tissues such as skin keratinocytes, squamous epithelium of the cervix, epithelium of the cornea and epithelium of the tonsils. Tijink *et al.* evaluated this agent in patients with incurable squamous cell carcinoma of the head, neck or oesophagus. Seven patients received a total of 23 weekly doses of bivatuzumab mertansine [24]. One patient at 100 mg/m^2 and another at 120 mg/m^2 experienced stable disease during the treatment phase but also experienced severe skin toxicity in the form of desquamation. At the highest dose level achieved, 140 mg/m^2, one patient developed toxic epidermal necrolysis after two infusions and died. It was concluded that expression of CD44v6 was not specific enough for tumour cells to allow the formulation of a safe antibody-based therapy. Development of this agent was discontinued.

Immunogenicity of antibodies is another issue which must be considered. Antibodies that are used in the construction of ADCs need to be humanised in order to avoid the potential of generating an immune response in the patient upon administration. This further complicates the synthesis of these agents [25].

As large molecular weight biomolecules, antibodies display certain physicochemical properties that are unfavourable to the crossing of biological barriers, thereby somewhat limiting their scope for *in vivo* applications [26]. To affect solid tumours, ADCs must cross the vascular endothelium and circumvent the interstitial pressure within the solid tumour. Also, expression of target antigens can be heterogeneous throughout the tumour. Therefore, the pharmacodynamics of the large immunoglobulin containing ADC may impede its ability to penetrate deep into solid tumours which are often poorly vascularised [25]. Smaller, recombinant monoclonal antibody structures such as single chain antibodies and diabodies have been shown to penetrate into the tumour with greater efficiency than the parent antibodies [27]. However, these smaller molecules are more rapidly cleared from the plasma resulting in shorter half-lives [28]. In fact, overall tumour accumulation of diabodies is found to be more than two-fold less than that achieved for corresponding IgG [29].

Modification of the structure of the monoclonal antibodies used in ADCs has also been attempted. An engineered thio-trastuzumab-DM1 conjugate has been developed which possesses two free cysteine residues to facilitate the attachment of two molecules of DM1 to each thio-

trastuzumab molecule *via* a non-reducible *bis*-maleimido-trioxyethylene glycol (BMPEO) linker [30]. Trastuzumab is a recombinant human anti-epidermal growth factor receptor 2 (HER2) monoclonal antibody. HER2 is a receptor tyrosine kinase found to be overexpressed on the surface of breast cancer cells in ~30% of newly diagnosed patients and is found to be associated with a poor prognosis. Furthermore, 60-70% of breast cancer cell bone metastases overexpress HER2 [31]. The conjugate retained similar *in vitro* cell proliferation inhibitory activity and HER2 binding properties to the conventional trastuzumab-succinimidyl trans-4-(maleimidylmethyl) cyclohexane-1-carboxylate-DM1 (trastuzumab-SMCC-DM1). Furthermore, the conjugate showed improved efficacy over the conventional trastuzumab-DM1 at DM1 equivalent doses and retained efficacy at equivalent antibody doses. The thio-trastuzumab conjugate also displayed a greater than two-fold reduction in toxicity in a safety study in rats compared with the conventional ADC. It is thought that this was due to the lower drug loading per antibody and the improved stability of the linker unit in circulation [30].

Previous experiments utilising these thio-mAbs led to the development of thio-anti-MUC16-maleimidocaproyl-valine-citrulline-*p*-aminobenzyl-carbonate-MMAE (thio-anti-MUC16-MC-vc-PABC-MMAE) [32]. This conjugate contained a derivatised humanised anti-MUC16 monoclonal antibody engineered to contain two free thiol groups to which MMAE was conjugated *via* a MC-vc-PABC linker. The conjugate synthesised was found to be as efficacious as a conventional conjugate in a MUC16 ovarian cancer xenograft model in mice. Moreover, it was tolerated at higher doses in rats and cynomolgus monkeys than the same conjugate prepared by conventional approaches suggesting the potential of this strategy in the synthesis of more therapeutically favourable ADCs [32].

1.1.3 Linker unit selection

For an ADC to be effective, the chemotherapeutic agent should remain non-toxic as part of the conjugate while in circulation but should be readily liberated on internalisation into the target cell [17]. Thus, the choice of linker is of paramount importance in the synthesis of an ADC with a favourable therapeutic index. Several strategies have been employed to maximise the stability of ADCs in circulation while allowing for selective release of the tubulin binding agent at the desired target. Acid labile hydrazone linkers were among the early linkers to be considered. However, in more recent times, conjugates containing disulfide linkages, peptide based linkages and thioester linker units have found favour due to their greater stability in circulation. The advantages and

disadvantages of each of these conjugate types, along with other methodologies, will thus be discussed in turn, together with examples of how these technologies have been utilised to facilitate the selective delivery of the parent ADC to the tumour site.

1.1.3.1 Acid-labile linkers

Early linkers evaluated include various acid-labile hydrazone linkers that utilised the acidic environment of endosomes for cleavage. Linkages such as those containing hydrazones have relatively short half-lives that can be significantly less than the expected circulating half life of the ADC. This can present toxicity issues, especially in the case of high potency cytotoxics such as MMAE [17].

Drugs linked to monoclonal antibodies *via* acid-labile linkers have been found to undergo approximately 50% drug release within 2 days upon incubation in human serum [17]. Peptide and disulfide containing linkers were subsequently adjudged to be superior to these acid sensitive linkers due to the selective cleavage of these linker types within the tumour intracellular environment [33].

1.1.3.2 Disulfide-containing linkers

Disulfide containing linkers are extremely common in the synthesis of ADCs due to their stability at physiological pH. While the disulfide bond is thermodynamically very stable, it is kinetically labile in the presence of sulfhydryl groups. It has been shown that the concentration of the tripeptide glutathione, which cleaves disulfide bonds, is 1000-fold higher within cells than in the circulation resulting in preferential drug release within target cells [8, 22].

The relative strength of the disulfide bond in various maytansinoid-antibody conjugates can be manipulated to achieve maximum stability in circulation, while allowing for efficient cleavage inside the target cell [22]. This is achieved by the introduction of methyl substituents on the carbon atoms geminal to the disulfide link conferring varying degrees of steric hindrance [22]. The location of the methyl groups was also found to be of vital importance. Those conjugates where the methyl groups were located on the maytansinoid side of the disulfide bond were found to have superior activity *in vivo* than those with the methyl groups located on the antibody side of the disulfide bridge, despite the fact that both conjugates have identical stability in terms of the fate of the disulfide bridge [10].

The humanised monoclonal antibody, huC242, has been used in a series of experiments to synthesise conjugates with maytansinoids in order to explore the effect of the linker group on the activity of resultant conjugates. huC242 binds to the CanAg antigen expressed on colorectal, pancreatic and certain non-small cell lung cancer cells. Conjugates of huC242 and the maytansinoids DM4 and DM1 containing a cleavable disulfide linkage huC242-*N*-succinimidyl-3-(2-pyridylthio) propionate-DM4 (huC242-SPDB-DM4) (Figure 1.2) and a non-cleavable thioether linkage (huC242-SMCC-DM1) (Figure 1.3) were synthesised and evaluated *in vitro* and *in vivo* [34]. It was found that both conjugates displayed comparable activity *in vitro* though huC242-SPDB-DM4 was significantly more active in multiple xenograft tumour models. It was concluded that both conjugates are efficiently degraded in lysosomes to release the free maytansinoid molecule together with a number of cytotoxic metabolites. It has been suggested that the enhanced activity of the disulfide containing conjugate is related to the formation of the potent S-methyl-DM4 metabolite following lysosomal reduction of the disulfide bond. Lopus *et al.* demonstrated that such maytansine derivatives are themselves potent microtubule poisons, interacting with microtubules as effectively as, or more effectively than, the parent molecules [35].

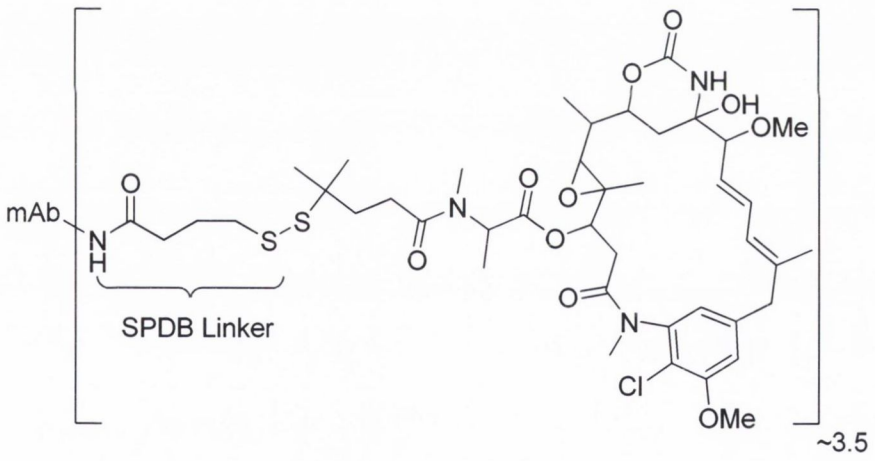

Figure 1.2 mAb-SPDB-DM4

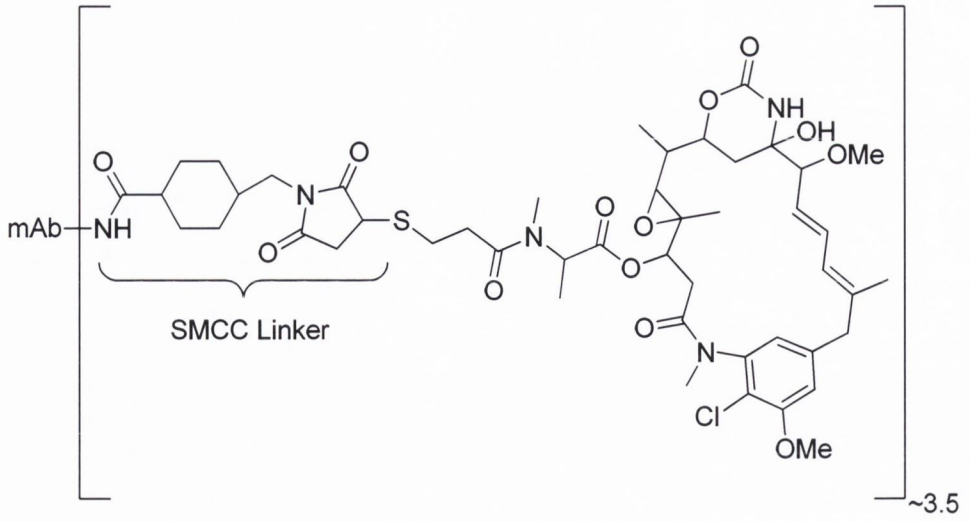

Figure 1.3 mAb-SMCC-DM1

In further experiments conducted by Kovtun *et al.*, it was observed that huC242-DM1 conjugates with non-cleavable linkers such as SMCC (Figure 1.3) had similar *in vitro* activity to disulfide containing *N*-succinimidyl 4-(2-pyridyldithio) pentanoate (SPP) linked conjugates (Figure 1.4) but were not as active *in vivo* [36-37]. Considerable evidence suggests that a bystander killing of neighbouring cells is responsible for this disparity [36]. It was found that conjugates linked *via* a reducible disulfide bond were capable of this effect, while equally potent conjugates linked *via* a non-reducible thioether bond were not. It has been suggested that this mechanism may overcome various barriers to the even distribution of maytansinoid effector molecules to all cells within a tumour. However, it should be noted that in the case of a number of other maytansinoid-antibody conjugates such as trastuzumab linked to DM1, it was the SMCC linked conjugate which was the most effective [10] (Figure 1.3).

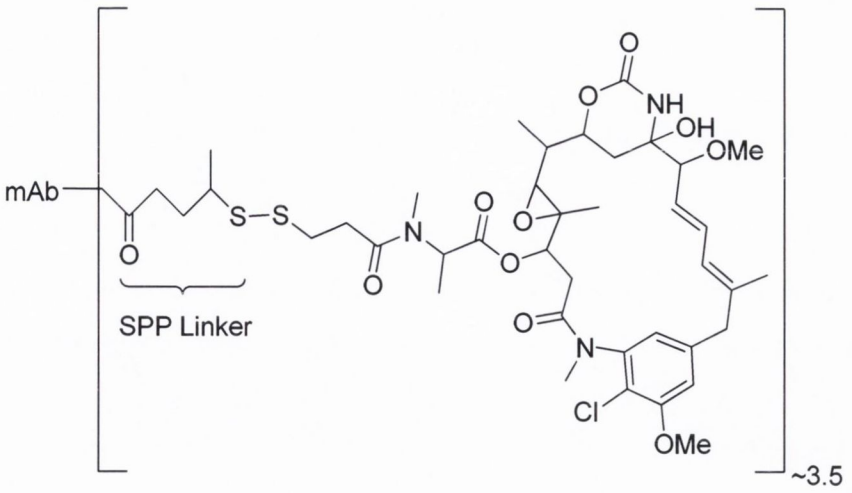

Figure 1.4 huC242-SPP-DM1

In preclinical studies, the monoclonal antibody nBT062 was conjugated to DM1 and DM4 using different linker technologies. nBT062-SMCC-DM1, nBT062-SPP-DM1 and nBT062-SPDB-DM4 were then evaluated *in vitro* and *in vivo* against multiple myeloma cell lines [38]. It was found that the nBT062-SPDB-DM4 was the most efficacious of the conjugates *in vivo*, demonstrating target dependent antitumour activity. Bystander killing in the presence of CD138-positive cells observed *in vitro* was hypothesised to be vitally important for BT062 activity *in vivo*, causing the death of tumour cells that heterogeneously express CD138 and disrupting the tumour microenvironment [39]. The structure of nBT062-SPDB-DM4, designated BT062 consists of a murine/human IgG4 chimeric form of B-B4 (nBT062) targeting CD138 conjugated to DM4 *via* a disulfide linkage (Figure 1.2). Phase I clinical trials are currently underway evaluating the safety, tolerability, pharmacokinetics and efficacy of BT062 in patients with CD138-positive multiple myeloma. BT062 is also at an advanced stage of preclinical development for the treatment of a number of CD138-positive solid tumours [40].

Polson *et al.* systematically examined potential antigenic targets and drug linker combinations in an attempt to develop the most clinically relevant ADC for the treatment of non-Hodgkin's lymphoma [41]. The antibodies used targeted the antigens CD19, CD20, CD21, CD22, CD72, CD79b, and CD180, all of which are found to be highly expressed on non-Hodgkin's lymphoma cells. The disulfide linker containing maytansinoid derivative SPP-DM1 (Fig. 1.4) and the non-cleavable thioether derivative SMCC-DM1 (Figure 1.3) were variously conjugated to the different antibodies. Similarly the cathepsin B substrate containing MC-vc-PABC-MMAE and the non-cleavable MC-MMAE were also conjugated to the various antibodies. It was found that the ADCs

with cleavable linkers mediated efficacy *via* all these targets whereas the ADCs with non-cleavable linkers were only effective when conjugated with anti-CD22 and anti-CD79b. It was also found that those conjugates containing uncleavable linkers showed reduced toxicity *in vivo*. It was suggested that the reason for the broad applicability of the cleavable disulfide linker containing ADCs is that extracellular cleavage to release the cytotoxic agent occurs following antigen binding and it is the free drug that crosses the cell membrane to exert its effect passively, whereas internalisation and intracellular metabolism is necessary to enable release of the cytotoxic agent in the case of ADCs with a non-cleavable linker.

1.1.3.3 Peptide linker units

Ma *et al.* synthesised a conjugate by combining a prostate specific membrane antigen (PSMA) monoclonal antibody and MMAE *via* a valine-citrulline linkage (Figure 1.5) [42]. This linkage was designed to maintain serum stability while maximising intracellular drug release by human cathepsin B [42]. Cathepsin B is a lysosomal exocarboxydipeptidase which is often found to be upregulated in tumour cells particularly during tumour progression [43]. *In vitro*, the conjugate potently eliminated all PSMA-positive cell lines at IC_{50} values of 65 pM to 210 pM whereas these concentrations had no effect on PSMA-negative cells. In fact, the conjugates demonstrated nearly 1000-fold selectivity compared with an isotype control conjugate. *In vivo* efficacy was demonstrated in a mouse xenograft model of androgen independent prostate cancer cell line, C4-2. Each of the two regimens tested were effective in increasing median survival and decreasing serum PSMA in a dose dependent fashion. Overall a 40% cure rate was observed in animals with established tumours following treatment with a 6 mg/kg regimen. Moreover, no apparent toxicity was observed with this regimen which may permit the use of even more intense regimens resulting in further improvements in antitumour activity [42].

Auristatin E and the related compound MMAE were conjugated to the chimeric monoclonal antibodies cBR96 (specific for the Lewis Y antigen on carcinomas) and cAC10 (specific to CD30 on haematological malignancies) using three distinct linker methodologies [44]. CD30 has limited expression in normal tissues but is widely expressed in Hodgkin's disease, non-Hodgkin's lymphoma, multiple myeloma and cutaneous T-cell lymphoma [45]. Firstly, conjugates containing the 5-benzoylvaleric acid ester of auristatin E were synthesised (Figure 1.6).

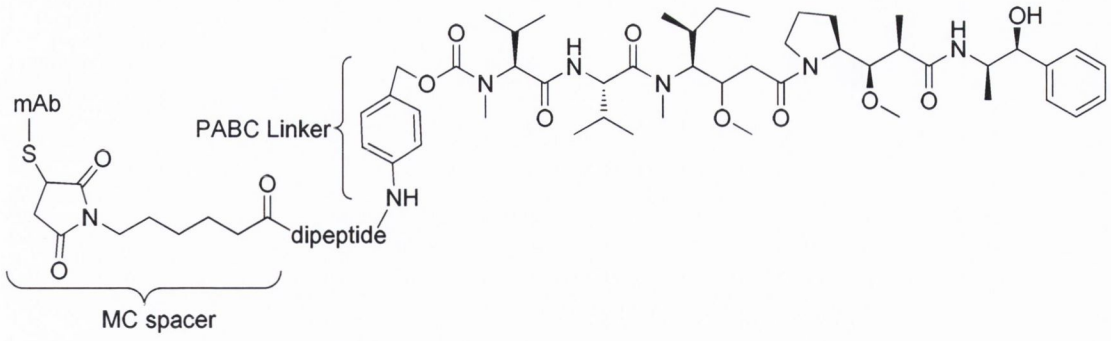

Figure 1.5 mAb-Val-Cit-MMAE and mAb-Phe-Lys-MMAE (where dipeptide=valine-citrulline and phenylalanine and lysine respectively)

Secondly, conjugates consisting of the dipeptide valine-citrulline attached to MMAE *via* the self-immolative *p*-aminobenzyl carbonyl (PABC) spacer unit were synthesised. Finally conjugates consisting of the dipeptide lysine-phenylalanine attached to MMAE *via* the same *p*-aminobenzyl carbonyl spacer were synthesised (Figure 1.5). All three conjugates also contained a maleimidocaproyl (MC) spacer group. It was found that the peptide linker containing conjugates were much more stable in buffers and plasma than the hydrazone linker conjugates. The mAb-val-cit-MMAE conjugates also demonstrated greater *in vitro* specificity and lower *in vivo* toxicity than corresponding hydrazone containing conjugates. In tumour xenograft models, the peptide linked conjugates induced tumour regression and cures with therapeutic indices as high as 60-fold (*i.e.* 1/60th of the maximum tolerated dose of cAC10-Val-Cit-MMAE was shown to achieve therapeutic efficacy in a CD30 positive anaplastic large cell lymphoma (ALCL) tumour model).

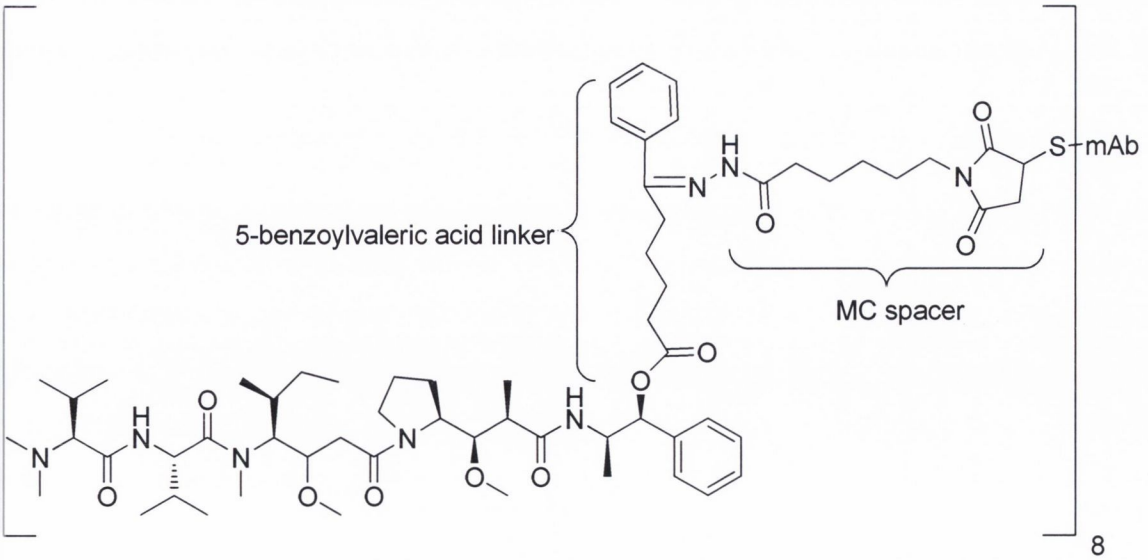

Figure 1.6 mAb-AEBV

1.1.3.4 Alternative linker units

In an attempt to further increase the therapeutic window of cAC10-maleimidocaproyl-valine-citrulline-*p*-aminobenzyloxycarbonyl-monomethyl auristatin F conjugate (cAC10-MC-vc-PABC-MMAF), a series of alternate linker units underwent preclinical evaluation [46]. One conjugate containing a noncleavable maleimidocaproyl linker unit (Figure 1.7) was shown to have roughly equivalent activity *in vitro* and *in vivo* but with a maximum tolerated dose greater than 3-fold higher than AC10-MC-vc-PABC-MMAF.

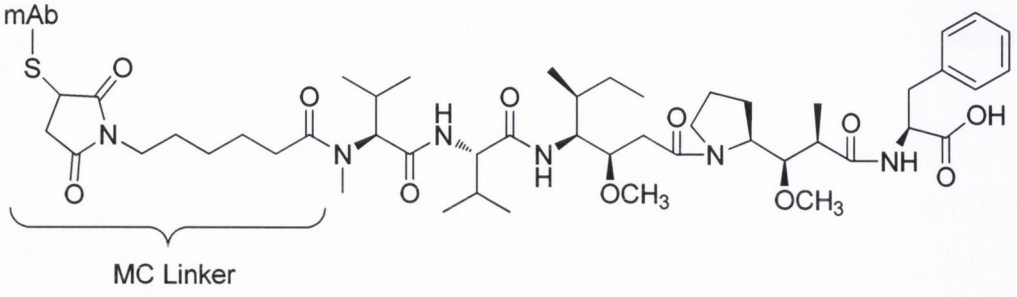

Figure 1.7 mAb–mcMMAF

Novel linker mechanisms have also been utilised in order to synthesise ADCs which may be able to evade multidrug resistance strategies such as overexpression of the transporter MDR-1. In one study conducted by Kovtun *et al.* a DM1-antibody conjugate using a maleimidyl-based hydrophilic linker, PEG_4Mal, was shown to overcome MDR-1 mediated multidrug resistance *in vitro* and eradicate human MDR-1 xenograft tumours *in vivo* [47]. Following uptake into cells, it was found that conjugates with the PEG_4Mal linker (Figure 1.8) were transformed to cytotoxic conjugates that were better retained by MDR-1 expressing cells than metabolites of similar conjugates with a SMCC linker (Figure 1.3).

Even with relatively hydrophilic cytotoxic agents such as DM1 and DM4 conjugated to antibodies *via* the somewhat hydrophobic linkers SPDB and SMCC, only conjugates with 4-5 drug molecules per antibody could be synthesised. When conjugates with higher maytansinoid loads were attempted, the resultant conjugates tended to aggregate and precipitate [48]. In an attempt to increase the drug antibody ratio without causing aggregation or affecting the binding affinity of the resultant conjugate, a number of different hydrophilic linkers containing either a negatively charged sulfonate group or a hydrophilic, uncharged PEG group were synthesised [48]. An important advantage of the conjugates containing these more hydrophilic linkers is their potential to overcome multidrug resistance. Incorporation of the sulfonate group both in cleavable and

non-cleavable linkers was found to be associated with enhanced activity of B38.1-DM1 conjugates against MDR cell lines. B38.1-DM1 conjugates consisting of a PEG_4 linker were also observed to display enhanced activity *in vitro* against MDR cell lines. Incorporation of the sulfonate group or the PEG_4 group into non-reducible linkers in DM1 and DM4 conjugates of huC242 also resulted in approximately 100-fold greater cytotoxicity against both COLO 205 and COLO 205 / MDR cells. *In vivo,* the B38.1-DM1 and B38.1-DM4 conjugates prepared with sulfonate or PEG containing linkers demonstrated enhanced antitumour activity against the COLO205MDR xenograft model in mice.

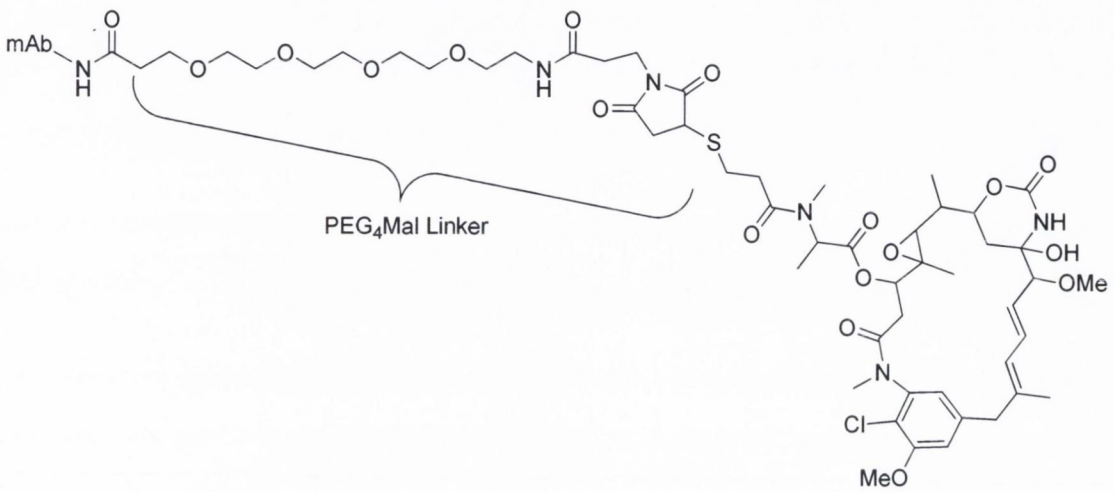

Figure 1.8 mAb–PEG_4Mal–DM1

A β-glucuronic acid based linker was also utilised for the synthesis of a number of maytansinoid conjugates in which hydrolysis by the lysosomal enzyme β-glucuronidase releases the active drug. MMAE and MMAF were conjugated to the monoclonal antibodies c1F6 (anti-CD70) and cAC10 (anti-CD30) *via* a novel glucuronic acid linker (Figure 1.9) [49]. It has been shown that β-glucuronidase is abundantly present within lysosomes and is overexpressed in some tumour types, while extracellular enzyme activity is low [50]. The resulting conjugates were found to be highly stable in plasma, well tolerated at high doses and efficacious both *in vitro* and *in vivo*.

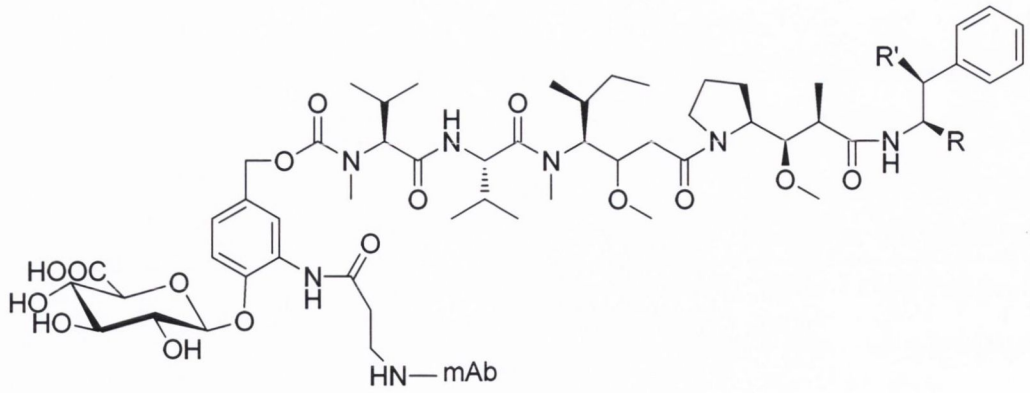

Figure 1.9 MMAE/MMAF-glucuronic acid linker-antibody conjugate (where R=Me and R'=OH for MMAE while R=COOH and R'=H for MMAF)

Trastuzumab was chemically linked to paclitaxel *via* a novel A-Z-CINN linker resulting in an ADC with the potential for light accelerated release of paclitaxel at the tumour site. *In vivo,* in HER2 positive BT-474 mammary tumour cells in mice, the conjugate showed enhanced antitumour activity following 5 min light exposure (light from a halogen bulb delivered through a fiber optic probe) adjacent to the tumour. The conjugate was also found to cause more rapid and extensive reduction in tumour volume than a 10-fold higher concentration of free paclitaxel and free trastuzumab administered to the mice [51].

1.1.4 Antibody-drug conjugates in preclinical development

The novel taxoid SB-T-12136 was variously linked to three murine monoclonal antibodies against the human epidermal growth factor receptor (EGFR) [21, 52]. The antibodies KS-61, KS-77 and KS-78 were linked to SB-T-12136 *via* a 4-thiopentanoyl linker (Figure 1.10). These conjugates were shown to possess remarkable target-specific antitumour activity *in vivo* against EGFR-expressing A431 tumour xenografts in mice, resulting in complete inhibition of tumour growth without any noticeable toxicity.

Anti-CD22-SMCC-DM1 is another ADC in preclinical development. It consists of DM1 conjugated to a humanised antibody that targets CD22, a siglec (sialic acid binding Ig-like lectins) family lectin expressed predominantly on mature B-cells. It was found that most non-Hodgkin's lymphoma patients express CD22 and this conjugate was shown to inhibit the proliferation of several non-Hodgkin's lymphoma cell lines *in vitro* and also induced complete regression of tumours in xenograft mouse models. It was well tolerated in cynomolgus monkeys and substantially

decreased circulating B-cells as well as follicle size and germinal centre formation in lymphoid organs. It has been suggested that the low levels of expression of CD22 should not limit the scope of this conjugate as some cell lines with very low levels of CD22 expression were sensitive to these agents [53].

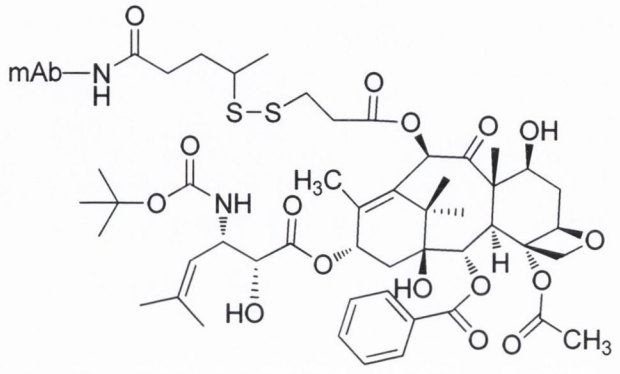

Figure 1.10 SB-T-12136-mAb conjugates

Chimeric anti-CD20 antibody, rituximab, has already found use in the clinic in the treatment of certain B-cell lymphomas, most notably Hodgkin's lymphoma. The specific binding of rituximab and the anti-CD20 antibody IF5 for CD20 positive B-lymphoma cells both offer the potential for the synthesis of an effective ADC [54]. Conjugates of these antibodies linked to MMAE *via* a valine-citrulline linker were synthesised by Law *et al.* [54]. These conjugates were shown to be selectively toxic to CD20 positive B-cell lymphoma cell lines *in vitro* with IC_{50} values of between 50 ng/ml and 1 μg/ml. Furthermore, rituximab-vc-MMAE showed antitumour efficacy in human lymphoma CD20 positive tumour xenograft models in mice at doses where rituximab was ineffective.

While CD20 immunotherapy effectively depletes mature B-cells, it does not deplete pre-B cells or immature B cells, some B cell subpopulations, plasma cells or their malignant counterparts [55]. Because CD19 is expressed earlier in B cell development it offers the potential to target lymphoblastic leukaemias and lymphomas. Therefore, a humanised anti-CD19 antibody (hBU12) was conjugated to MMAE via a valine-citrulline linker to yield hBu12-vc-MMAE [56]. This conjugate was shown to exhibit potent cell killing against rituximab sensitive and resistant non-Hodgkin's lymphoma cell lines *in vitro*. Furthermore high rates of durable tumour growth suppression were observed in mice implanted with these tumours. Further examples of ADCs containing tubulin targeting agents currently in preclinical development are shown in Table 1.2.

Table 1.2 Antibody-drug conjugates in preclinical development

Antibody-drug conjugate	***Target antigen***	***Cytotoxic agent***	***Linker used***	***Anticancer activity/ Stage of development***	***References***
Anti-CD79b-SMCC-DM1	Anti-CD79b	DM1	SMCC	*In vitro* activity against non-Hodgkin's lymphoma cell lines. Effective *in vivo* in follicular, mantle cell and Burkitt's lymphoma	[57]
Anti-CD79b-MC-MMAF	Anti-CD79b	DM1	MC	*In vitro* activity against non-Hodgkin's lymphoma cell lines. Effective *in vivo* in follicular, mantle cell and Burkitt's lymphoma	[57]
Anti-CD79b-vc-MMAE	Anti-CD79b thiomab	MMAE	Vc	*In vitro* and *in vivo* activity against non-Hodgkin's lymphoma cell lines	[58]
Anti-huCD79b (SN8)-MCC-DM1	Humanised anti-CD79b antibody	DM1	SMCC	Caused complete regression of Burkitt's, follicular, and mantle cell lymphoma xenograft tumours	[59]

IMGN853	Anti-folate antibody M9346A	DM4	sulfo-SPDM	Selective cytotoxicity *in vitro* and *in vivo* for FR+ cells, efficacy in MDR-1-positve tumours	[60]

1.1.5 Antibody-drug conjugates undergoing clinical evaluation

Brentuximab vedotin is now approved for the treatment of CD30-positive haematological malignancies while trastuzumab emtansine is in Phase III for HER2-positive breast cancer [19, 61]. A number of other promising ADCs are undergoing Phase I/II evaluation at present (Table 1.3). Of these, C242-DM1 was among the first maytansinoid-antibody conjugates synthesised. C242 recognises CanAg (MUC1), a mucin type glycoprotein expressed on the surface of human colorectal cancer cells. It was shown to be effective in mice xenograft models in which complete tumour regression was observed [62]. This agent subsequently progressed to clinical evaluation as cantuzumab mertansine (huC242-DM1) in which the antibody was humanised. Cantuzumab mertansine consists of up to four molecules of mertansine conjugated to each antibody. The drug showed considerable tumour localisation without inducing severe haematological toxicity in patients with pancreatic and colorectal cancers [63].

Another agent that has shown great potential in preclinical testing is huC242-DM4. Treatment of mice with a single dose of huC242-DM4 resulted in complete regression of tumour xenografts at a dose well below the maximum tolerated dose while equivalent doses of free maytansinoid and a DM4 conjugate with a non-binding antibody had no effect on tumour growth in this model [10]. *In vivo* distribution experiments in mice have shown that greater than 1000-fold higher accumulation of maytansinoid at the tumour site can be achieved compared with non-conjugated maytansinoids after 24-28 h. This conjugate contains a disulfide linkage and has an increased stability under physiological conditions. It was found to have a half-life of 7.7 days in mice versus ~2 days for cantuzumab mertansine, and is now undergoing phase I clinical evaluation [4].

CD37 also represents an attractive target for an antibody-maytansinoid ADC due to its high expression in B-cell malignancies such as non-Hodgkin's lymphoma and chronic lymphocytic leukaemia and its limited expression in normal tissues. Furthermore, anti-CD37 antibodies have been shown to possess intrinsic anti-tumour activity and therefore offer the potential for the

synthesis of a dual acting ADC [64]. The humanised anti-CD37 monoclonal antibody K7153A was thus conjugated to DM1 using either the hindered disulfide containing SPP linker or the non-cleavable SMCC linker. It was found that K17153A-SMCC-DM1 (designated IMGN529) was more active against lymphoma cells both *in vitro* and *in vivo* against SU-DHL-4 subcutaneous xenograft tumours. This agent is currently undergoing phase I clinical trials in patients with relapsed or refractory non-Hodgkin's lymphoma [65].

The conjugate MEDI-547 (1C1-mcMMAF) consists of a fully human monoclonal antibody against murine and human EphA2 (1C1) attached to MMAF *via* a stable maleimidocaproyl linker (Figure 1.7). The EphA2 receptor is a subtype of the erythropoietin producing hepatoma receptor that is overexpressed in tumours of the breast, prostate, lung, colon and in glioblastoma multiforme [66]. It has also been reported that the EphA2 receptor is upregulated in the neovasculature of tumours, which may contribute to the activity associated with agents targeting this receptor [67]. *In vivo* experiments in mouse orthotopic xenograft models resulted in 86% to 88% growth inhibition in the orthotopic Hec-1A and Ishikawa models following treatment with this agent. The mice treated with this ADC also had a lower incidence of metastasis than controls and this effect was observed without overt signs of toxicity [68]. This agent was subsequently evaluated in phase I clinical trials however the outcome of these studies have yet to be reported.

Trastuzumab emtansine is currently undergoing a number of phase III clinical trials in patients with HER-positive metastatic breast cancer [19]. It consists of the anti-HER2 monoclonal antibody trastuzumab conjugated to an average of 3.5 molecules of the maytansinoid DM1 *via* a nonreducible SMCC thioether linkage (Figure 1.3). It has been shown that trastuzumab emtansine retains the mechanism of action of unconjugated trastuzumab and is active against lapatinib resistant cell lines and tumours [69]. It was also effective in patients for whom trastuzumab alone was found to be inadequate [10]. Trastuzumab emtansine's systemic side effects are significantly minimised due to its targeted delivery to HER2 positive cells. Two phase II studies comparing trastuzumab-DM1 with trastuzumab plus docetaxel showed improved tolerability and at least equivalent efficacy. Two phase III randomised trials are currently underway for refractory and HER2-positive breast cancer [70].

In August 2011, brentuximab vedotin (cAC10-vc-MMAE, SGN-35) was approved by the FDA for the treatment of patients with Hodgkin's lymphoma and systemic ALCL [71]. To date, the only other ADC to have made it to the clinic is Wyeth's Mylotarg (gentuzumab ozogamicin) which received FDA approval in 2000 for the treatment of acute myeloid leukaemia. However, it was voluntarily

withdrawn after follow up studies raised concern about its safety and clinical efficacy [19]. Brentuximab vedotin is a conjugate of the chimeric monoclonal antibody cAC10, directed against CD30, covalently coupled to MMAE. The valine-citrulline peptide linker unit connecting the two components is subject to cleavage by lysosomal enzymes following internalisation into target cells (Figure 1.5). The tumour necrosis factor receptor family member CD30 is highly expressed on the cell surfaces of Hodgkin's disease, ALCL and a subset of non-Hodgkin's lymphomas, but has only limited expression on healthy tissues. Brentuximab vedotin potently interferes with the growth of CD30-positive haematological tumours including Hodgkin's lymphoma and ALCL [72]. It has been suggested that the *in vivo* efficacy of brentuximab vedotin might be mediated, in part, by the diffusion of free MMAE from the target cells resulting in a bystander effect that kills the normal supporting cells in close proximity to malignant cells [61].

Table 1.3 Antibody-drug conjugates under clinical investigation

Antibody-drug Conjugate	Target; Indications	Clinical Stage	References
Brentuximab vedotin (SGN-35; Brentuximab-MC-VC-MMAE)	CD30; hematologic malignancies, Hodgkin's lymphoma	FDA approved	[71]
Trastuzumab emtansine (Trastuzumab-SMCC-DM1)	HER2-positive breast cancer	Phase III	[19]
Lorvotuzumab mertansine (IMGN901; HuN901-SPP-DM1)	CD56; Merkel cell cancer, small cell lung cancer, multiple myeloma ovarian cancer	Phase II	[8]
Glembatumumab vedotin (CDX-011; CDX-011-MC-	Glycoprotein NMB; melanoma,	Phase II	[19]

VC-MMAE)	Breast cancer		
SAR3419 (huB4-SPDB-DM4)	CD19; B cell lymphoma	Phase I and II	[73-74]
IMGN388 (Antibody-SPDB-DM4)	Integrin; antivascular/ solid tumours	Phase I	[15]
BIIB-015 (Antibody-SPDB-DM4)	Cripto; solid tumours	Phase I	[15]
BT-062 (Anti-CD138-SPDB-DM4)	CD138; multiple myeloma	Phase I and II	[39]
BAY 79-4620 (3ee9-MMAE)	CAIX (MN); solid tumours	Phase I	[15]
MEDI-547 (1C1-MC-MMAF)	EphA2; ovarian cancer, solid tumours	Phase I	[75]
SGN-75 (SGN-70-MC-VC-MMAF)	CD70; renal cell carcinoma, non-Hodgkin's lymphoma	Phase I	[76]
SAR566658 (huDS6-DM4)	CA6; ovarian, cervical, breast cancers	Phase I	[15]
PSMA-ADC (anti-PSMA-MMAE)	PSMA; prostate cancer	Phase I	[77]

MLN2704 (MLN591-DM1)	PSMA; prostate cancer	Phase II	[4]
IMGN529 (Antibody-SMCC-DM1)	Anti-CD37	Phase I	[65]
AVE9633 (Antibody-DM4)	Anti-CD33 antibody (huMy9); acute myeloid leukaemia	Phase I	[8]

1.2 Vitamin-drug conjugates

At the molecular level cancer cells possess a number of characteristics that differentiates them from normal cells. Due to their high rate of proliferation, they rapidly consume primary metabolites and require large amounts of certain vitamins to sustain their growth. Consequently, receptors for vitamins in particular are often overexpressed on the surface of cancer cells. These differences can be exploited by covalently attaching ligands for these cell surface receptors to cytotoxic agents with a view to enhancing delivery of the cytotoxic agents to the tumour.

Bagnato *et al.* have described the synthesis and evaluation of a conjugate **(1.01)** consisting of a colchicine derivative conjugated to cobalamin (vitamin B_{12}) through an acid labile hydrazone linker [78]. Rapidly dividing cells such as tumour cells require large quantities of cobalamin for the synthesis of the DNA base thymidine to permit DNA replication prior to cell division. Furthermore, cobalamin can be covalently modified to facilitate its conjugation without disrupting the corrin ring pharmacophore necessary for recognition and transport *via* the B_{12} transport proteins [78]. The cobalamin moiety causes the conjugate to be preferentially taken in by cancer cells. Once internalised, the hydrazone linker is hypothesised to undergo hydrolysis in the low pH environment of the lysosome to liberate the cytotoxic moiety. The bioconjugate exhibits stability in cell culture media and at neutral pH but undergoes hydrolysis with a half-life of 138 min at pH 4.5. *In vitro*, the conjugate was shown to have nanomolar LC_{50} values against breast, brain and melanoma cancer cell lines. Despite the encouraging *in vitro* data, according to the literature, only a finite amount of cobalamin can be transported into the cell before all of the cellular receptors have been saturated which may limit the usefulness of this approach [78].

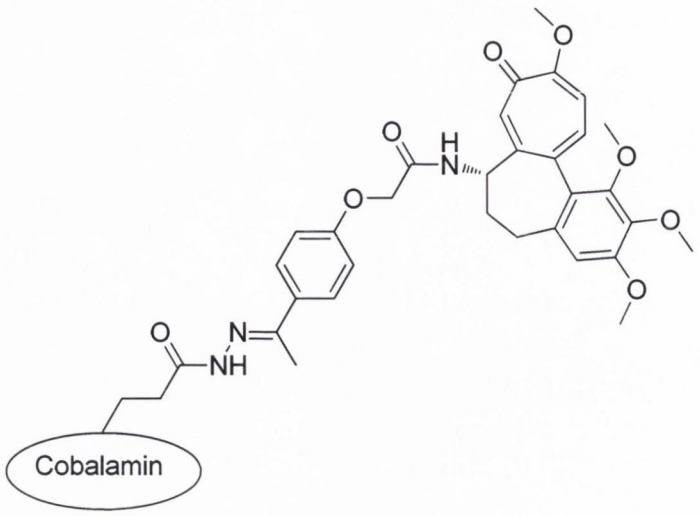

Figure 1.11 Colchicine-cobalamin conjugate **(1.01)**

Biotin (vitamin-H or B-7) is another vitamin essential for cell development. Cell surface receptors for biotin have been shown to be overexpressed on the surface of a number of cancer cell lines to a greater degree than both folate and vitamin B_{12} receptors [79]. Chen *et al.* have synthesised conjugate **(1.02)** consisting of biotin and the second generation taxoid, SB-T-1214, in an attempt to target the cytotoxic agent to cells overexpressing the biotin receptor (Figure 1.12) [80]. The conjugate consisted of a disulfide linker unit in order to readily release the cytotoxic agent following biotin receptor mediated endocytosis within target cells. A 60-fold selectivity was observed for L1210FR cells which overexpress biotin receptors (IC_{50} of 8.8 nM) over non-target cell lines. Data was not presented on the efficacy of this conjugate in vivo.

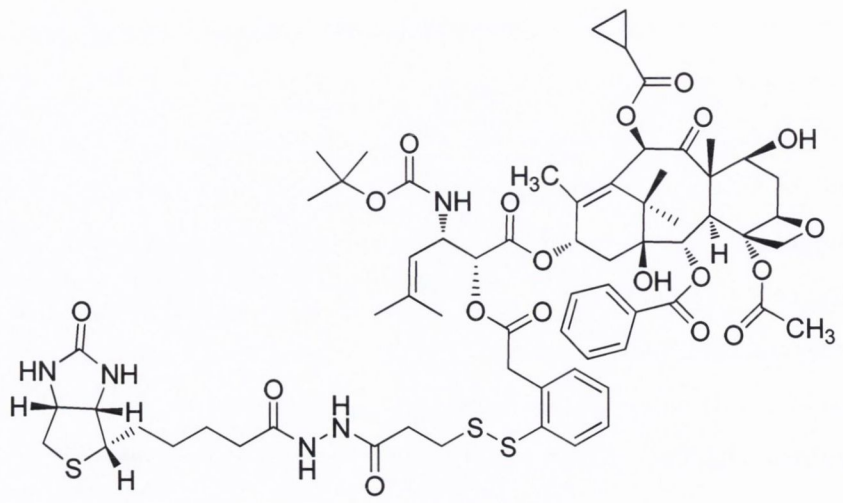

Figure 1.12 Biotin-linker-SB-T-1214 conjugate **(1.02)**

The folate receptor (FR) is expressed at relatively high levels in human epithelial cancers but has limited expression on normal tissues. Folic acid (FA) binds with high affinity ($K_D < 10^{-9}$ M) to the cell-surface glycoprotein folate receptor. Folic acid is then transported into the cell by folate receptor mediated endocytosis. Furthermore, conjugation to biologically active compounds such as tubulin targeting agents, does not significantly affect folate receptor binding making folate receptor mediated endocytosis ideal for exploitation as a selective tumour delivery strategy [81].

Lee *et al.* synthesised a series of paclitaxel-folic acid conjugates using a number of different linkage methodologies and evaluated the resultant conjugates *in vitro* [82]. One of the conjugates, **(1.03)**, was chosen for further *in vivo* evaluation (Figure 1.13). However, despite its lack of toxicity in tumour xenograft models, it failed to demonstrate selective toxicity for FR-positive cells *in vitro* and failed to demonstrate a superior therapeutic response to paclitaxel *in vivo*.

Folic acid was also conjugated *via* a PEG linker to a paclitaxel-human serum albumin conjugate and evaluated *in vitro* [83]. Binding and *in vitro* cytotoxicity evaluation demonstrated increased selectivity for FR-positive cell lines and enhanced antitumour activity compared to free paclitaxel.

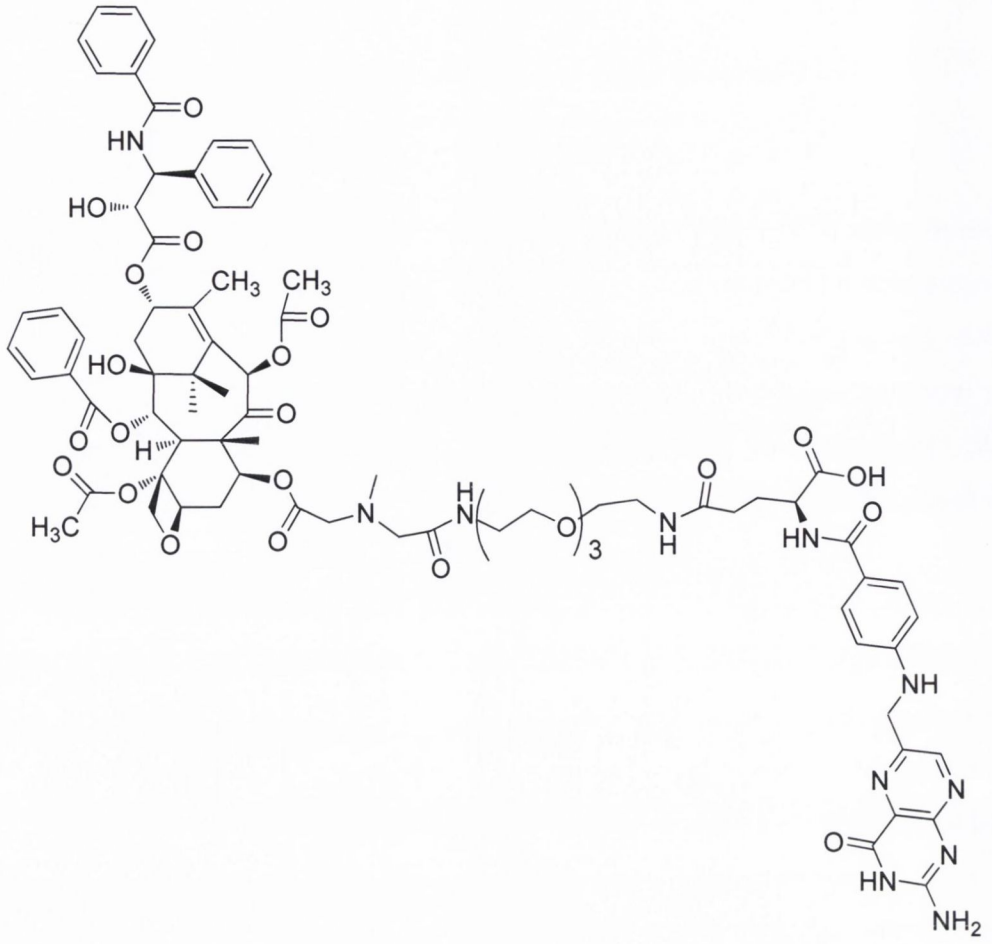

Figure 1.13 Paclitaxel-folic acid conjugate **(1.03)**

Vlahov *et al.* synthesised various epothilone-folic acid conjugates utilising a reducible disulfide bond [81]. The conjugates were designed to have a peptide spacer incorporated into their structure containing both acidic and basic amino acids to provide solubility to the drug conjugate under physiological conditions. It was demonstrated *in vitro* that release of free drug within the reductive environment of the endosome was complete within 45 min. The clinical potential of these agents is now being evaluated, with one of the conjugates, Epofolate (BMS-753493), currently undergoing phase I clinical evaluation.

Folic acid was also conjugated to deacetylvinblastine monohydrazide *via* a hydrazone linker unit with a view to selective release in the acidic environment of the endosome [84]. This compound designated EC140 (folate-deacetylvinblastine monohydrazide) **(1.04)**, exhibited impressive *in vitro* activity against FR-positive cell lines and also induced tumour regression in numerous FR-positive tumour xenografts in mice. The conjugate **(1.04)** caused complete remission of tumour xenografts in mice. However, the treatment regimen was not without side effects. The treated animals

experienced weight loss periodically during the treatment schedule. It was suggested that this was possibly due to systemic release of free drug due to the labile nature of the acyl hydrazone linker. Thus, other linker approaches were explored.

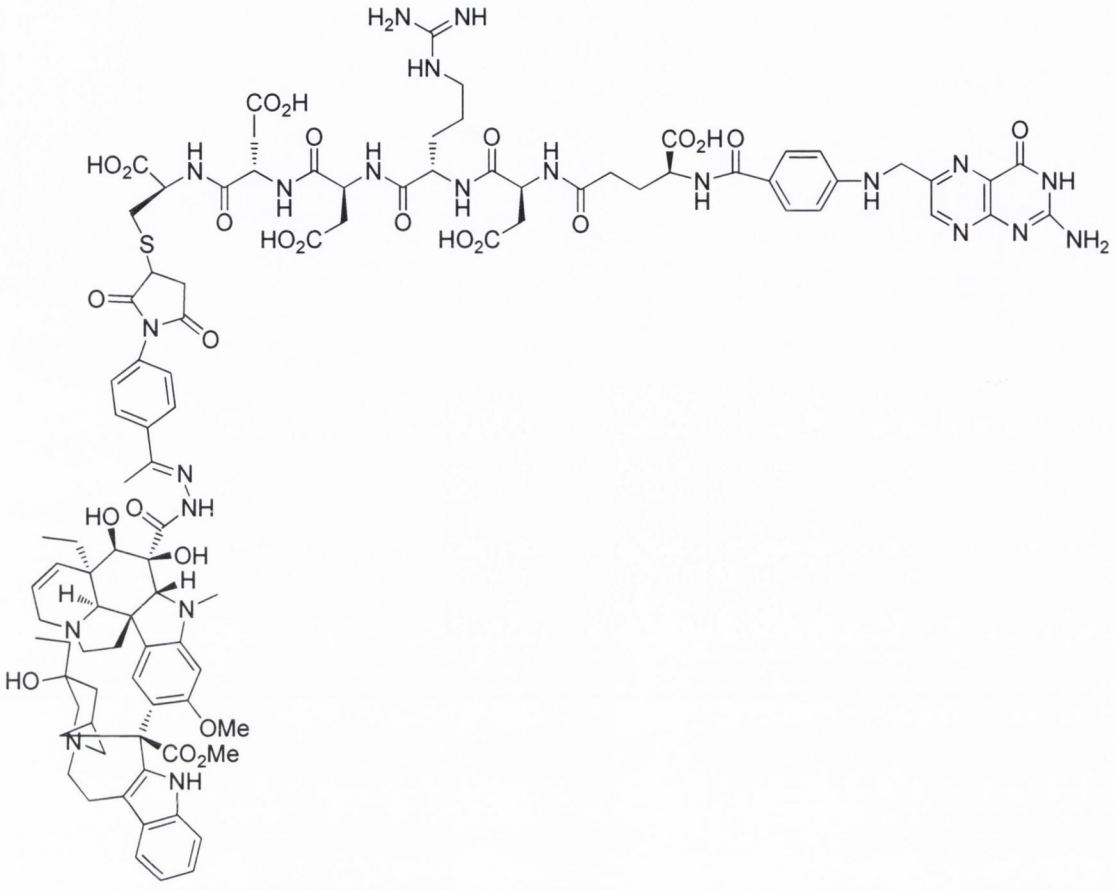

Figure 1.14 EC140 **(1.04)**

In a continuation of this theme, conjugate **(1.05)**, consisting of deacetylvinblastine monohydrazide tethered to folic acid *via* a reducible disulfide containing linker, was synthesised by Vlahov *et al.* [85]. Following positive *in vitro* and *in vivo* results, the conjugate, designated EC145 (folate-S-S-deacetylvinblastine monohydrazide) was selected for clinical evaluation.

In a further extension of this work, a related conjugate, consisting of folic acid linked to two different biologically active agents, deacetylvinblastine monohydrazide and the alkylating agent mitomycin C, *via* two disulfide based release systems was investigated [86]. This conjugate demonstrated impressive activity *in vitro* and *in vivo* and in fact, showed superior activity to its monodrug folate conjugate counterpart at equimolar concentrations in mice xenograft models. This compound was subsequently chosen for phase I clinical trials.

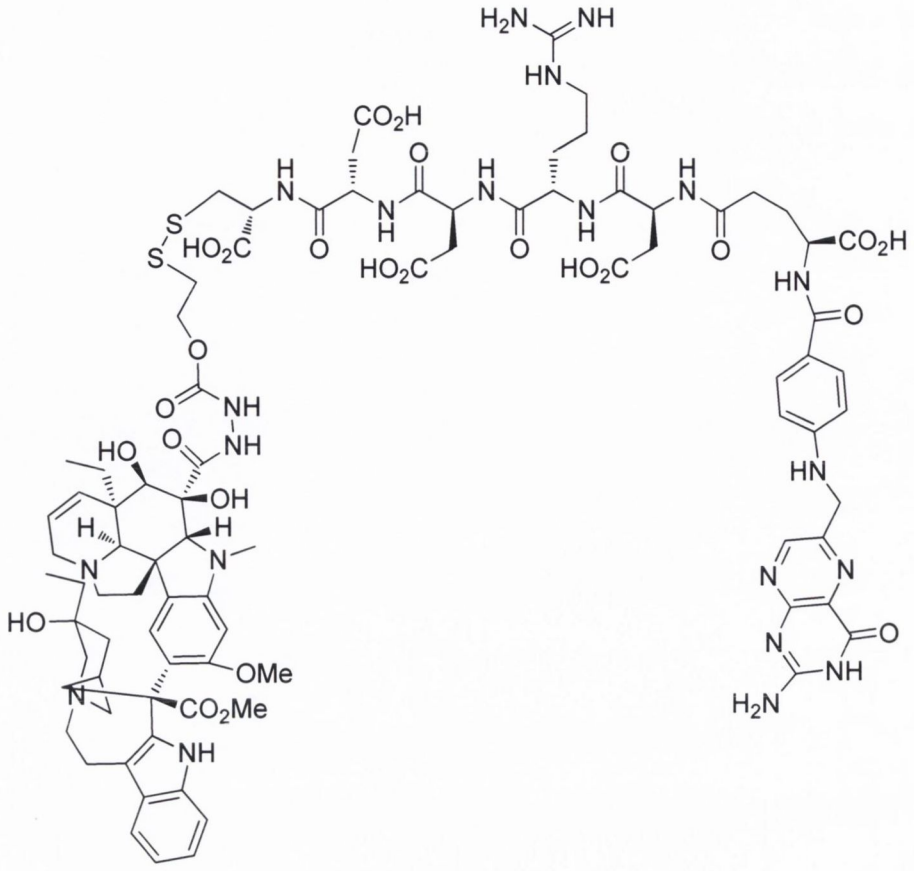

Figure 1.15 EC145 (folate-S-S-deacetylvinblastine monohydrazide) **(1.05)**

Folate-tubulysin conjugates were similarly synthesised and have undergone preclinical evaluation. The FA-tubulysin B hydrazide conjugate **(1.06)**, referred to as EC0305, in particular, demonstrated favourable characteristics both *in vitro* and *in vivo* [87]. EC0305 was found to specifically inhibit the growth of a number of FR-positive cell lines (IC_{50} range = 1-10 nM) while FR-negative cell lines were unaffected. EC0305 was also found to inhibit KB (nasopharyngeal) cells with an IC_{50} value 3-fold lower than any previously reported folate drug conjugate. *In vivo,* the conjugate demonstrated impressive antitumour activity in a human KB xenograft model in mice resulting in complete tumour regression without causing significant weight loss or damage to major organ tissue.

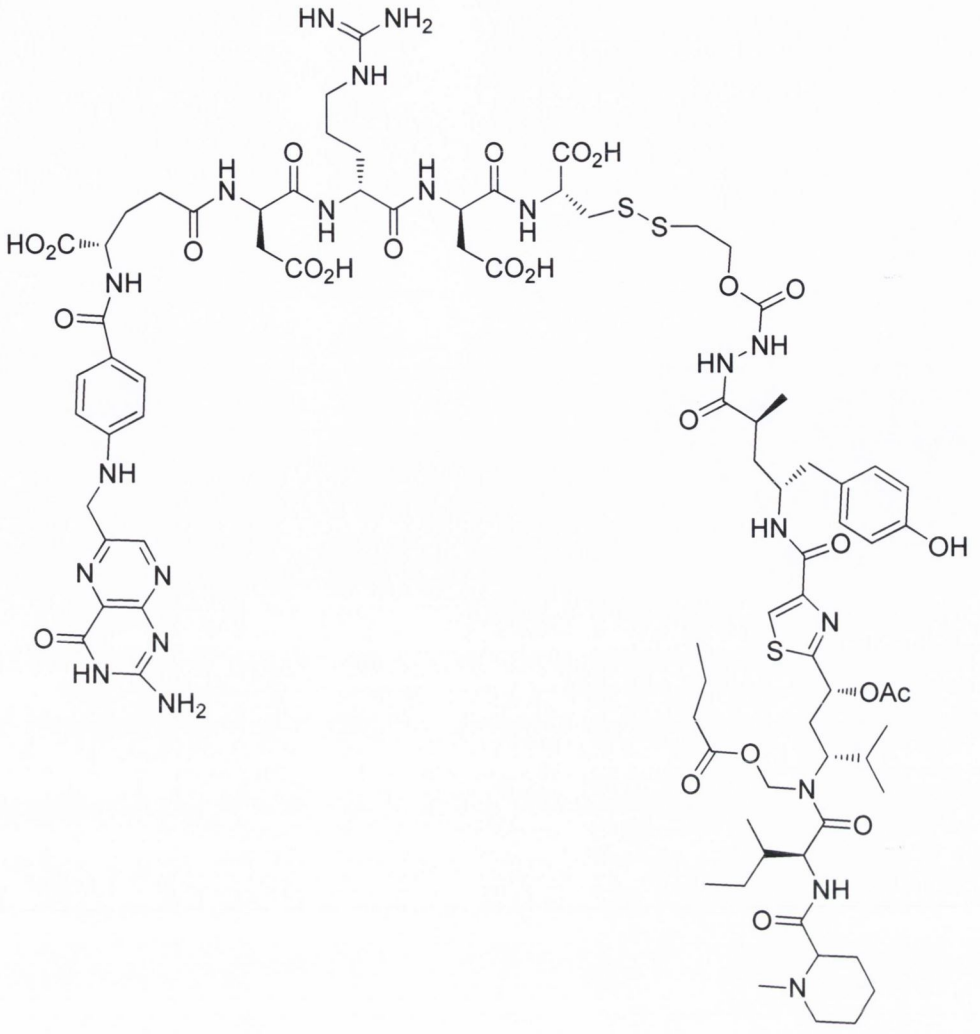

Figure 1.16 EC0305 **(1.06)**

A conjugate consisting of the maytansinoid DM1 linked *via* a disulfide bond to folic acid was synthesised and evaluated *in vitro* and *in vivo* [88]. The conjugate **(1.07)**, designated EC131, was found to be cytotoxic to FR-positive cell lines with an IC_{50} value in the low nanomolar range but possessed no activity against FR-negative cell lines. *In vivo* EC131 was found to be effective against FR positive M109 and KB human cancer tumour xenografts in mice but not against FR-negative A549 tumours. This agent also showed no evidence of systemic cytotoxicity in either case.

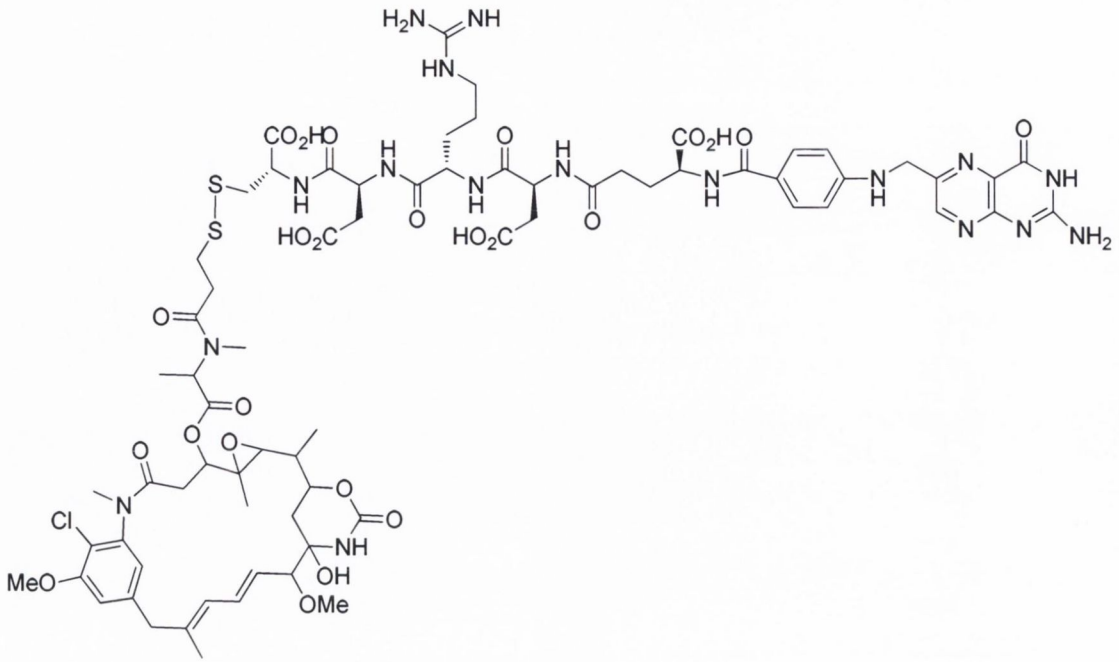

Figure 1.17 EC131 **(1.07)**

Nakagawa-Goto *et al.* synthesised a series of conjugates consisting of the 2'-hydroxy esters of paclitaxel and a series of dietary antioxidants such as Vitamins A, C and E and various flavanoids [89]. It was found that most conjugates selectively inhibited the growth of 1A9 (ovarian) and KB cancer cells without activity on other cell lines. A conjugate of Vitamin E and paclitaxel, compound **(1.08)**, however showed the most promise. This conjugate strongly and selectively inhibited the growth of Panc-1 (pancreatic cancer) cells with less effect on the related E6E7 (normal) cell line. However, no *in vivo* data demonstrating an improved therapeutic profile was presented for this conjugate.

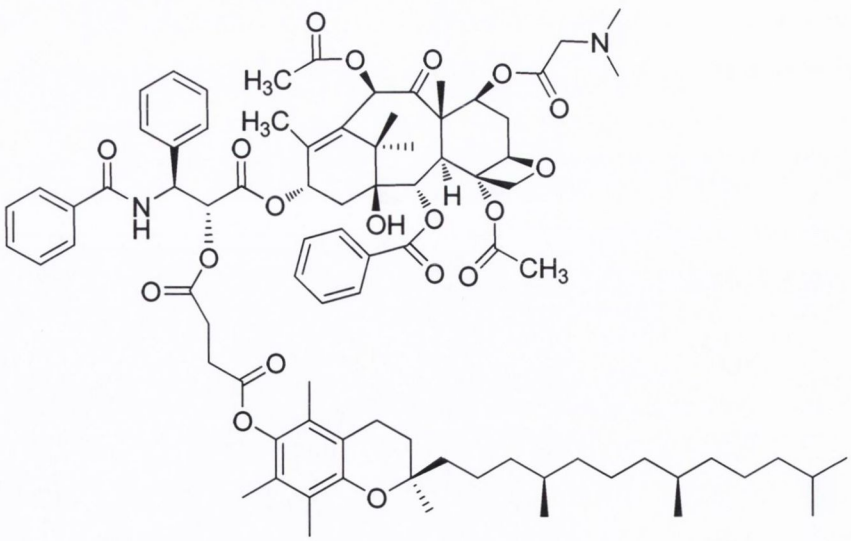

Figure 1.18 Vitamin E-paclitaxel glycinate ester conjugate **(1.08)**

1.3 Polyunsaturated fatty acid conjugates

Fatty acids are essential for the development of malignancy and are rapidly extracted from the circulation by tumour cells [90-91]. To exploit this phenomenon for selective cytotoxic drug delivery, a number of different polyunsaturated fatty acids have been conjugated to various tubulin binding agents. The natural fatty acid docosahexaenoic acid (DHA) was conjugated to the 2'-hydroxyl position of paclitaxel to afford DHA-paclitaxel **(1.09)** [92]. The intention behind the synthesis of this conjugate was to increase the efficacy and widen the therapeutic index of paclitaxel by selectively targeting tumour cells. It has been widely reported in the literature that a free 2'-hydroxyl functionality is necessary for tubulin binding. Thus, the conjugate was found to be largely devoid of *in vitro* cytotoxicity. The conjugate exhibited superior *in vivo* antitumour activity in M109 lung tumour mouse models compared with free paclitaxel. The conjugate also demonstrated a lower incidence of undesirable toxicity. In further pharmacokinetic studies, carried out by Bradley *et al.* on mice bearing M109 tumours, an 8-fold higher tumour uptake of DHA-paclitaxel was found compared with equimolar doses of free paclitaxel [92]. Phase I clinical trials conducted on DHA-paclitaxel revealed that no alopecia, nausea, vomiting or significant peripheral neuropathy was observed in participants even at a dose equivalent to 4.6 times the maximum approved dose of paclitaxel. Furthermore, 50% of the patients treated with the conjugate attained stable disease [92]. A further phase I clinical trial of DHA-paclitaxel, conducted by Wolff *et al.* demonstrated that DHA-paclitaxel administration resulted in a dramatically altered pharmacokinetic profile to that of paclitaxel with approximately 10-fold lower C_{max} values and a 5-fold increase in plasma half life [93]. In this study DHA-paclitaxel demonstrated a favourable toxicity profile with no evidence of significant alopecia, arthralgia, myalgia, mucositis or peripheral neuropathy. In a phase II trial conducted by Jones *et al.,* DHA-paclitaxel was shown to have only modest activity in patients with oesophago-gastric cancer with haematological toxicity comparable to that of paclitaxel and docetaxel [94]. A further phase III study comparing the activity of DHA-paclitaxel to decarbazine in patients with metastatic melanoma found that DHA-paclitaxel was superior to decarbazine [95]. While there were no significant differences in overall survival, response rate, duration of response, time to progression and time to treatment failure between the two drugs, myelosuppression was more common with DHA-paclitaxel compared to free paclitaxel. Further clinical evaluation of DHA-paclitaxel for this patient population was therefore not advocated.

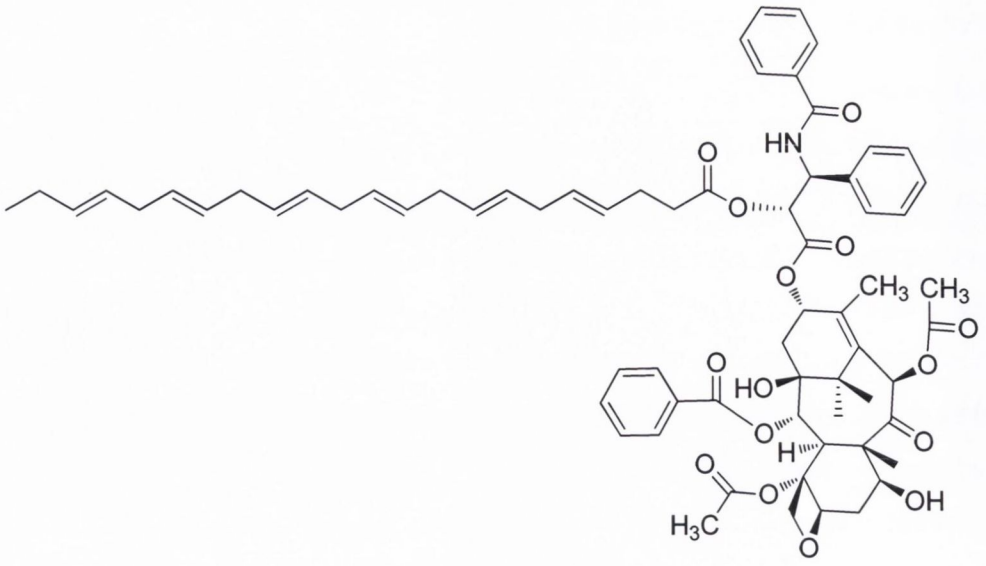

Figure 1.19 DHA-paclitaxel **(1.09)**

Other polyunsaturated fatty acids have also been utilised to achieve selective delivery of tubulin binding agents to their target cells. Ke *et al.* synthesised a conjugated linoleic acid-paclitaxel conjugate **(1.10)** in an attempt to enhance the delivery of paclitaxel across the blood brain barrier to effectively target brain tumour cells [96]. The stability of the conjugate was examined in phosphate buffered saline (PBS) and rat plasma. No free paclitaxel was observed in the PBS buffer after 48 h while only 4.7% free paclitaxel was observed in the rat plasma study after 48 h. *In vitro*, the conjugate demonstrated 4-fold increased up-take into C6 glioma cells after 6 h, in comparison to paclitaxel. Furthermore, the conjugate was found to have an IC_{50} of 3.47 μM compared to an IC_{50} of 2.13 μM for free paclitaxel. Pharmacokinetic analysis of the conjugate demonstrated that the AUC and half-life of the conjugate were much higher than that of free paclitaxel, indicating prolonged circulation of the conjugate. Analysis of the biodistribution of the conjugate demonstrated that it was still detectable in brain tissue 360 h post administration. At a dose of 40 mg/kg in C6 glioma tumour-bearing rats, the conjugate demonstrated significant antitumour activity whereas the paclitaxel treatment group showed no difference from control animals. Although it remains to be seen if the conjugate can elicit a therapeutic response in the clinic, the results of the *in vivo* work carried out to date are encouraging.

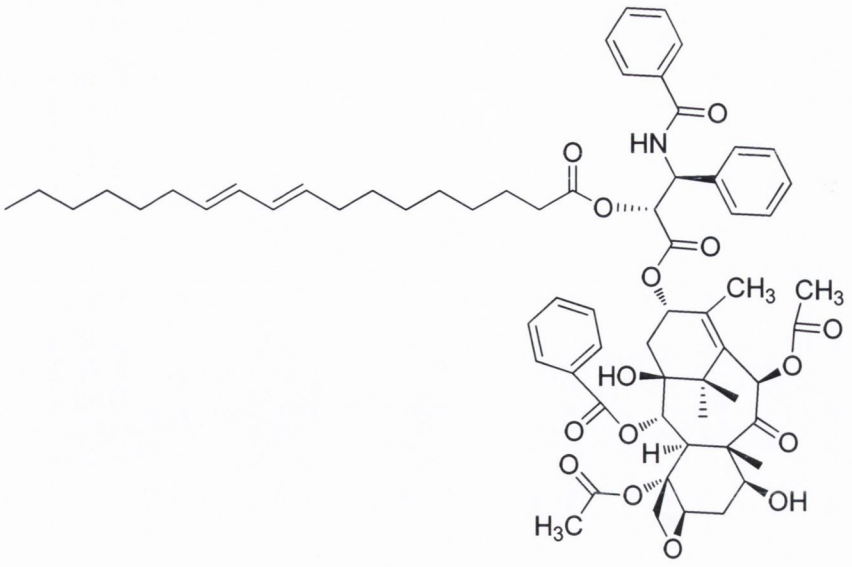

Figure 1.20 Conjugated linoleic acid-paclitaxel **(1.10)**

P-glycoprotein efflux is one of the principal mechanisms of paclitaxel treatment failure in drug-resistant tumours [97]. DHA-paclitaxel **(1.09)** has not been reported to be a good substrate for P-glycoprotein. However, once paclitaxel is released intracellularly it is likely to become susceptible to efflux *via* P-glycoprotein. In an attempt to circumvent this mechanism of resistance, Kuznetsova *et al.* conjugated a number of second generation taxoids to docosahexaenoic acid, linolenic acid, and linoleic acid [97]. These second generation taxoids, bearing different substituents at the C-2, C-10 and C-3' positions, exhibited 2-3 orders of magnitude greater cytotoxicity than paclitaxel against multidrug resistant tumour cell lines. *In vivo* studies with these conjugates, using both drug sensitive human ovarian tumour xenograft (Pgp-) A121 and the drug resistant human colon tumour xenograft (Pgp+) DLD-1 in mice, showed favourable outcomes. One of the conjugates designated DHA–SB-T-1214 achieved complete regression of the DLD-1 tumour whereas paclitaxel and DHA-paclitaxel were found to be completely ineffective. DHA–SB-T-1213 and DHA–SB-T-1216 also exhibited impressive results *in vivo*. Following on from this work, Kuznetsova *et al.* evaluated conjugates of SB-T-1213 with linoleic acid (LA) and linolenic acid (LNA). While LNA-SB-T-1213 demonstrated superior efficacy to DHA-SB-T-1213, it also exhibited greater toxicity to the animals, while LA-SB-T-1213 did not display meaningful activity *in vivo*.

Lipoamino acid residues have also been utilised to synthesise tumour targeting conjugates. Pignatello *et al.* synthesised two conjugates of paclitaxel linked *via* a succinate linker at the 2'-hydroxyl position to the lipoamino acids norleucine (C6) **(1.11)** or 2-aminodecanoic acid (C10) **(1.12)** [98]. The conjugates were more potent in the ARO human anaplastic thyroid cancer cell line

than free paclitaxel. A decrease in drug expulsion due to MDR-1 efflux pumps also suggested that these conjugates may have enhanced activity in multidrug resistant tumour types.

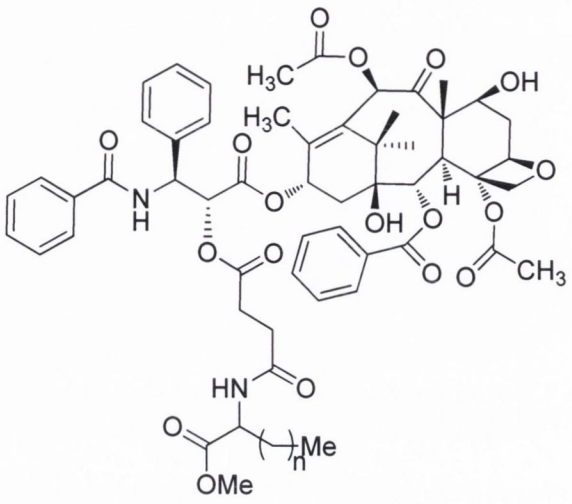

Figure 1.21 Paclitaxel-lipoamino acid conjugates (where n=3 for norleucine conjugate **(1.11)** and n=7 for 2-aminodecanoic acid conjugate **(1.12))**

1.4 Hormone receptor ligand conjugates

Hormone receptors are widely known to be overexpressed in a number of hormone-dependent cancers. Conjugates targeting androgen, oestrogen, somatostatin and luteinising hormone-releasing hormone have all been synthesised in recent years with a view to taking advantage of the selective expression of these receptors in cancer cells to improve drug targeting of tumours.

In an attempt to selectively target cells expressing the androgen receptor, while having minimal impact on normal cells, a colchicine-cyanonilutamide conjugate **(1.13)** was synthesised by Sharifi *et al.* [99]. The conjugate was observed to have a lower IC_{50} value in tubulin polymerisation assays than colchicine itself. The conjugate also demonstrated a greater toxicity against androgen-independent prostate cancer cells than a 1:1 combination of colchicine and nilutamide, suggesting that the enhanced *in vitro* activity was not exclusively related to androgen receptor interaction. The androgen receptor binding affinity of the conjugate was found to be only 10-fold lower than the clinically active androgen receptor antagonist, nilutamide. The conjugate was also found to be more cytotoxic *in vitro* than colchicine. While this conjugate represents a novel mechanism of selective delivery to target tumour cells, the proposed specificity remains to be confirmed in an *in vivo* model.

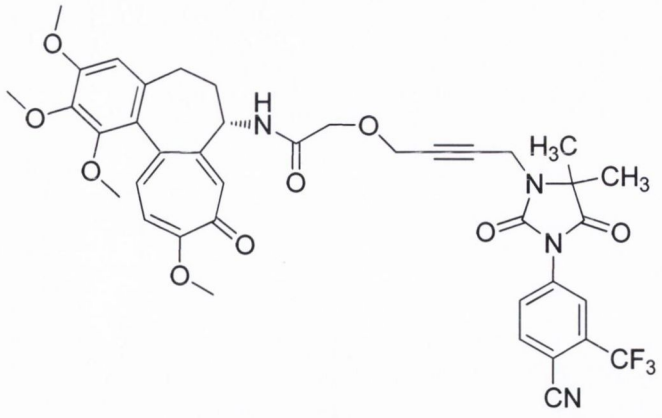

Figure 1.22 Colchicine-cyanonilutamide conjugate **(1.13)**

Many breast cancer cells are hormone dependent. By targeting the oestrogen receptors on their surface, selective delivery of a known cytotoxic agent to the interior of these cells could theoretically be achieved [100]. In an attempt to specifically target breast cancer tumour cells, estradiol-paclitaxel conjugates were synthesised by Liu *et al* through linkages from the 11- or 16-position of estradiol to the 2'-, 7-, or 10-position of paclitaxel [100]. Structure activity relationships conducted on estradiol demonstrated that modification of the 16- and 11- positions could be carried out without adversely affecting oestrogen receptor binding. Structure activity relationship analysis conducted on paclitaxel demonstrated that modifications at the 10- and 7-positions were possible resulting in only slightly diminished tubulin binding activity. Furthermore, ester linkages at the 2'-position have been extensively utilised for the synthesis of conjugates, as this group has been reported to undergo hydrolysis over time *in vivo*. The series of conjugates synthesised by Liu *et al* were found to be cytotoxic to the A2870 ovarian cancer cell line *in vitro* although less so than free paclitaxel [100]. The MCF-7 breast cancer cell line and the MDA-MB-231 breast cancer cell line were also used to evaluate the activity of the conjugates in oestrogen receptor positive and oestrogen receptor negative cell lines respectively. While one conjugate **(1.14)** showed 3-fold greater activity for the oestrogen receptor positive cell line compared with the oestrogen receptor negative cell line, it was found to be less potent than free paclitaxel. Two estradiol-paclitaxel hemisuccinates were also prepared to increase the solubility of the conjugates. The corresponding sodium and triethanolammonium salts were found to be slightly more cytotoxic than the acid forms, but were substantially less cytotoxic than the corresponding estradiol-paclitaxel conjugates. While this work suggests that it is possible to selectively target oestrogen receptor positive cells, the disappointing potency of the resulting conjugates suggests that the clinical usefulness of this approach may be limited.

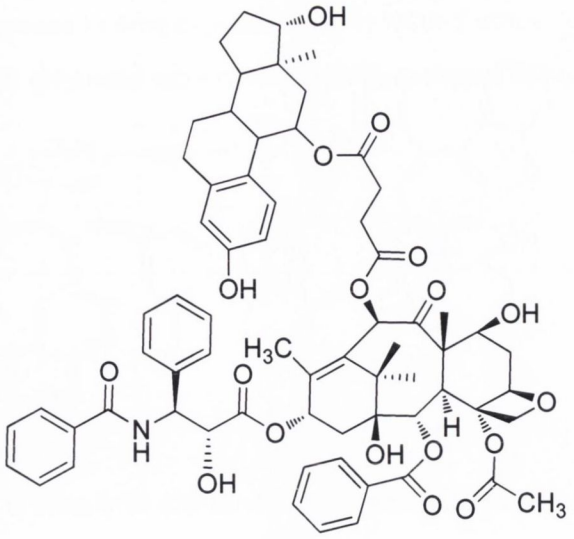

Figure 1.23 Estradiol-paclitaxel conjugate **(1.14)**

Shen *et al.* attempted to exploit the overexpression of somatostatin receptors on the surface of tumour cells by covalently conjugating one or two paclitaxel molecules to an octreotide molecule in order to selectively deliver the cytotoxic agent to the target cells [101]. Octreotide is an octapeptide analogue of endogenous somatostatin that binds with high affinity to somatostatin receptors *in vivo*. A number of different tumour types have been shown to overexpress somatostatin receptors, in particular non-small cell lung cancer cells [102]. *In vivo*, significant tumour growth inhibition was observed in human NSCLC A549 tumour xenografts in mice following administration of the paclitaxel-octreotide-$(paclitaxel)_2$ conjugate, whereas an equivalent dose of paclitaxel was found to be ineffective and more toxic to the test animals. Studies by Sun *et al.* demonstrated that the octreotide-paclitaxel conjugates were particularly effective against the somatostatin receptor positive cell lines A549 and Calu-6 and encouragingly, showed less activity than paclitaxel against somatostatin receptor negative fibroblasts *in vitro* [103].

Sundaram *et al.* synthesised a conjugate of docetaxel and deslorelin **(1.15)** in order to increase the specificity of docetaxel for prostate cancer cells [104]. Docetaxel is an analogue of paclitaxel while deslorelin is a luteinising hormone-releasing hormone superagonist. Luteinising hormone-releasing hormone receptors are overexpressed in a number of human cancers including prostate, ovarian, breast and endometrial cancer, making it a suitable target for the delivery of cytotoxic drugs. The conjugate was superior to docetaxel and deslorelin alone *in vitro* against LNCaP and PC-3 cell lines. *In vivo*, the conjugate was found to cause 5.5 times greater tumour growth

inhibition than docetaxel in PC-3 tumour xenografts in mice. Taken together, these results are encouraging. However, the potential for non-target toxicity should be evaluated *in vivo* before clinical evaluation is commenced.

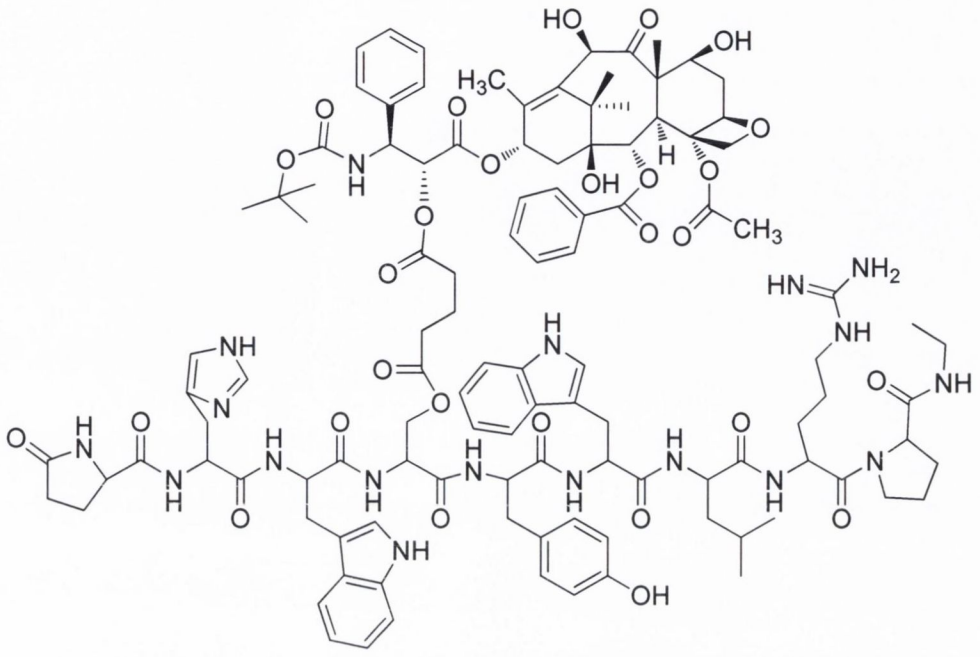

Figure 1.24 Deslorelin-docetaxel conjugate **(1.15)**

Pribylova *et al.* subsequently synthesised a series of conjugates of an analogue of luteinising hormone-releasing hormone and paclitaxel [105]. *In vitro,* one of the conjugates **(1.16)** demonstrated superior activity to free paclitaxel against MCF-7 human cancer cells. Further *in vivo* evaluation of this compound and other analogues is currently underway.

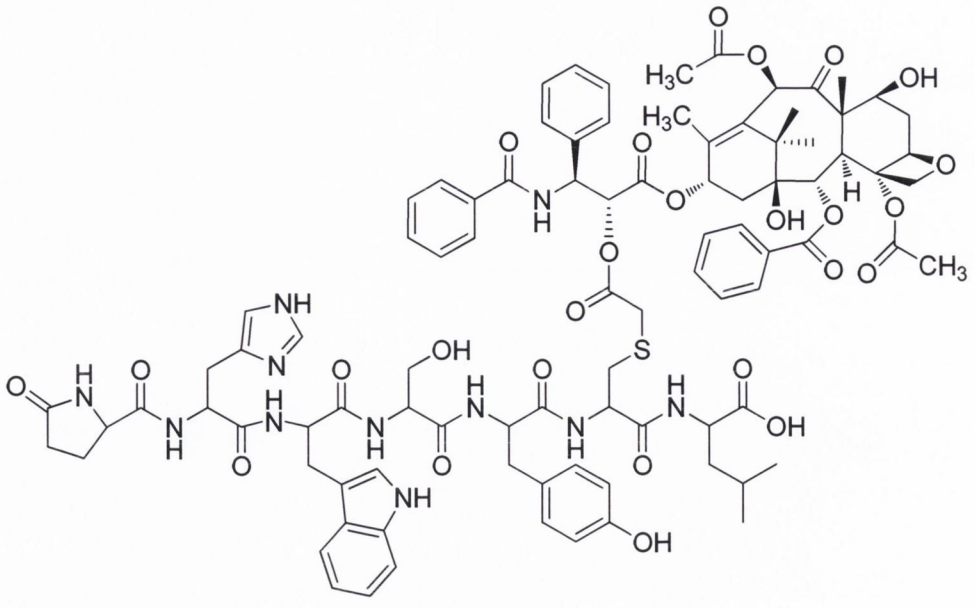

Figure 1.25 Luteinising hormone-releasing hormone analogue-paclitaxel conjugate **(1.16)**

1.5 Peptide-drug conjugates

A number of cell surface receptors and antigens are selectively expressed on tumour cells. Various peptide based ligands for these targets have been conjugated to tubulin binding agents in order to achieve tumour localised delivery. Conjugates targeting prostate specific antigen, lipoprotein receptor related (LRP) protein, matrix metalloproteinase-2 (MMP-2), HER2, integrins $\alpha_v\beta_3$ and $\alpha_v\beta_6$, the radiation inducible tax-interacting protein-1 (TIP-1), gastrin-releasing peptide (GRP) receptor and tissue factor (TF) have each been developed and evaluated.

Kumar *et al.* synthesised a number of conjugates composed of paclitaxel covalently attached to a peptide substrate for prostate-specific antigen [106]. Conjugate **(1.17)**, in particular, was shown to be stable in the presence of serum but selectively released the active cytotoxic agent in the presence of prostate specific antigen.

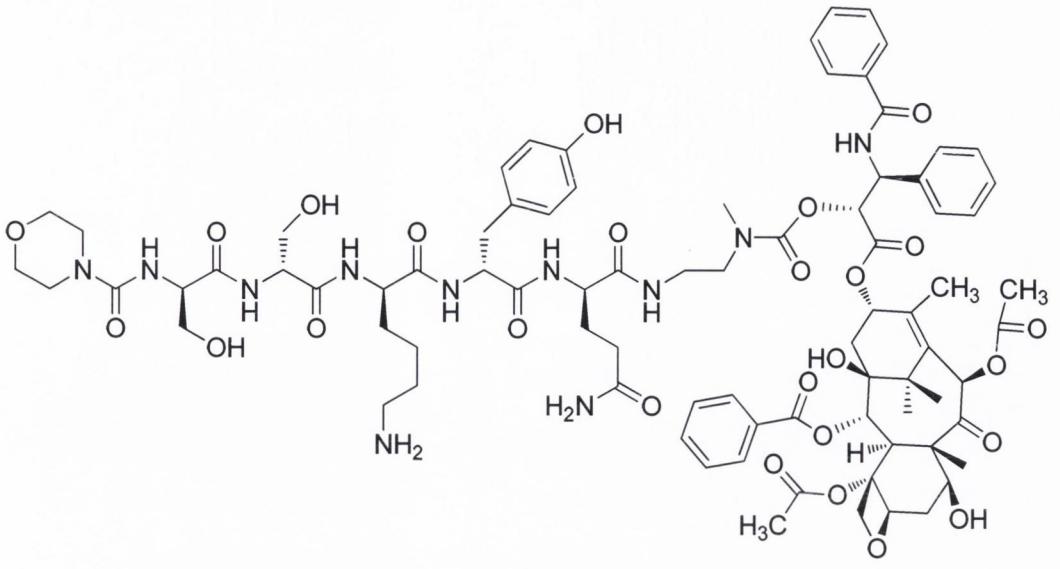

Figure 1.26 2'-[Mu-Ser-Ser-Lys-Tyr-Gln--NH-$(CH_2)_2$-N(CH_3)]-Paclitaxel **(1.17)**

MDR-1 (P-glycoprotein) efflux-mediated resistance to paclitaxel transport across the blood brain barrier represents a considerable obstacle to the treatment of brain malignancy with this agent. In an attempt to overcome this difficulty, Regina *et al.* synthesised ANG1005, **(1.18)**, a novel conjugate of the brain peptide vector angioprep-2 linked to 3 molecules of paclitaxel [107]. Angioprep-2 binds to the low density lipoprotein receptor related protein (LRP) receptors at the blood brain barrier. Therefore, it was hypothesised that this mechanism could be exploited to deliver drugs by receptor-mediated transport [108]. *In situ* brain perfusion studies demonstrated that ANG1005 enters the brain to a greater extent than paclitaxel and is not a substrate for the MDR-1 efflux pump. ANG1005 showed approximately 161-fold greater brain uptake *in vivo* compared with free paclitaxel 30 min post i.v. injection [108]. Furthermore, tumour uptake of ANG1005 was found to be approximately 1.5 times that in the surrounding brain tissue, demonstrating a degree of tumour specific localisation. Increased expression of LRP in many tumour cells has been offered as a possible explanation for this observation [109]. Decreased susceptibility of the conjugate to MDR-1 mediated efflux has also been suggested to contribute to this effect. *In vitro*, efficacy comparable to that observed for paclitaxel has been established in a number of human cancer cell lines. Furthermore, the conjugate was found to be more efficacious *in vivo* than paclitaxel. Increased survival of mice with intracerebral implantation of U87 MG glioblastoma cells or NCI-H460 lung carcinoma cells was observed following ANG1005 administration.

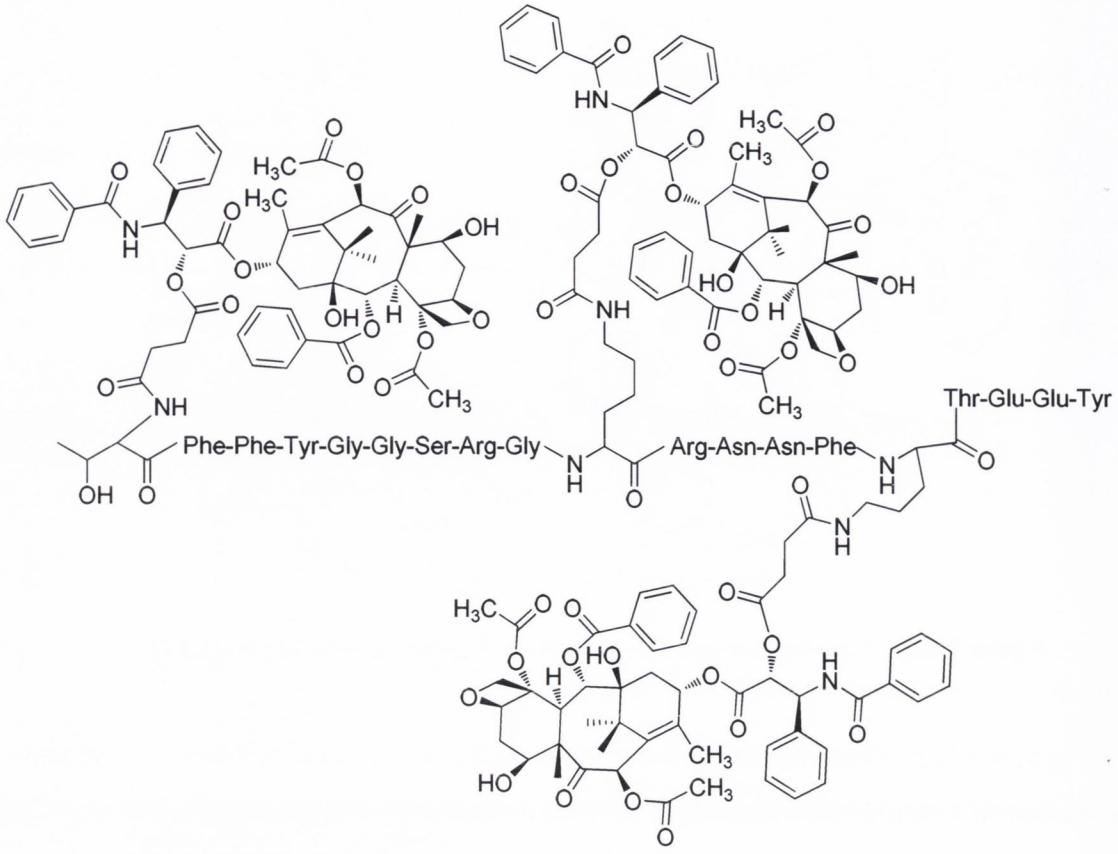

Figure 1.27 ANG1005 **(1.19)**

Yamada *et al.* synthesised conjugates of paclitaxel linked to the MMP-2 substrate octapeptide (AcGPLGIAGQ) *via* either the 2'hydroxy or the 7-hydroxy positions **(1.20)** [110]. The octapeptide was designed to be selectively cleaved at the tumour site due to the overexpression of MMP-2 on target tumour cells. It was hypothesised that this would result in accumulation of paclitaxel at the tumour site. *In vitro* the conjugates were shown to exhibit greater anti-proliferative activity than free paclitaxel in a number of human cancer cell lines. *In vivo*, the conjugates caused extensive areas of necrosis in a human tumour cell xenograft model in mice. Thus, it was suggested that the conjugate may have the potential for selective tumour targeting.

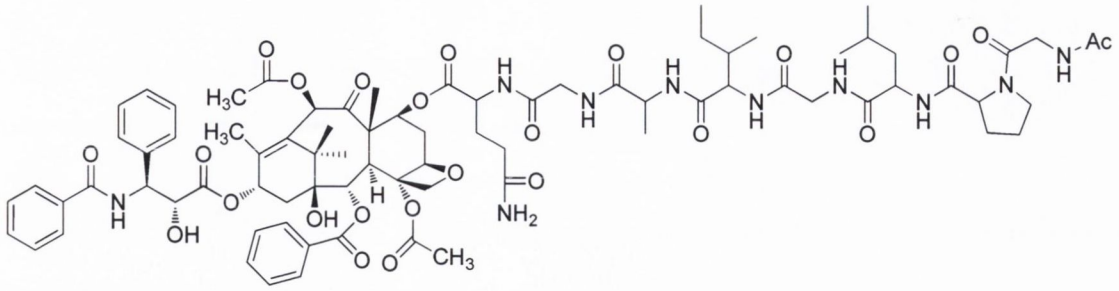

Figure 1.28 Paclitaxel-7-AcGPLGIAGQ **(1.20)**

In an attempt to selectively deliver paclitaxel to HER2 overexpressing cancer cells, Li *et al.* synthesised a novel conjugate of paclitaxel and the cyclic peptide EC-1 **(1.21)** [111]. The cyclic peptide EC-1 has been shown to bind specifically to HER2. Despite the interesting nature of the targeting approach, no *in vitro* or *in vivo* data was presented to demonstrate the efficacy of this agent

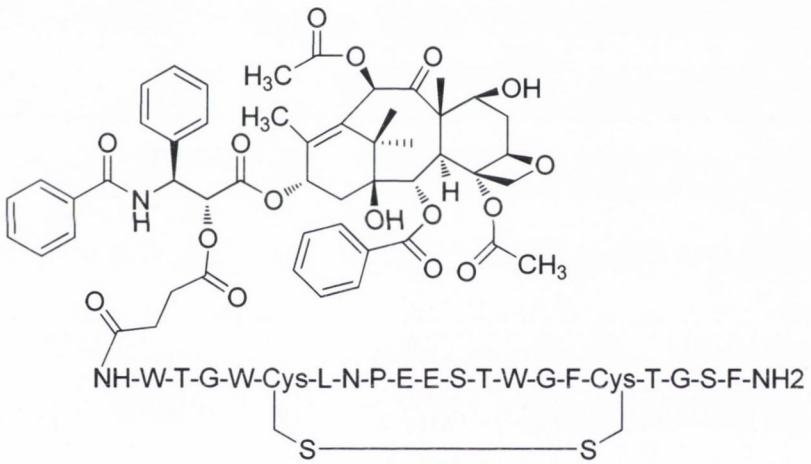

Figure 1.29 Paclitaxel-EC1 conjugate **(1.21)**

In malignant tumours, $\alpha_v\beta_3$ receptors are overexpressed on the surface of sprouting capillaries and also on certain types of tumour cells (e.g. 25% of lung cancers) [26]. Peptide ligands containing the tripeptide, arginine-glycine-aspartate are found to bind with high affinity and selectivity to the $\alpha_v\beta_3$ and $\alpha_v\beta_5$ integrins [112]. Furthermore, cyclic pentapeptide ligands containing the RGD moiety are found to bind to $\alpha_v\beta_3$ integrins with even greater affinity and selectivity. By synthesising a conjugate of paclitaxel with the bicyclic peptide E[c(RGDyK]$_2$ **(1.22)**, Chen *et al.* demonstrated that such an approach can be used to introduce selectivity for tumour tissue to the drug conjugate [113]. *In vitro,* the conjugate inhibited cell proliferation of the MDA-

MB-435 cell line with activity comparable to that observed for free paclitaxel. Despite showing slightly decreased integrin binding affinity compared to the unconjugated peptide, the conjugate also demonstrated integrin specific accumulation in an *in vivo* orthotopic nude mouse breast cancer model. Biodistribution analysis conducted *in vivo*, using tritium labelled conjugate and paclitaxel in human xenograft models in mice, indicated that the conjugate had a higher initial tumour uptake and more prolonged tumour retention than free paclitaxel. However, the absolute tumour uptake still remained low [114].

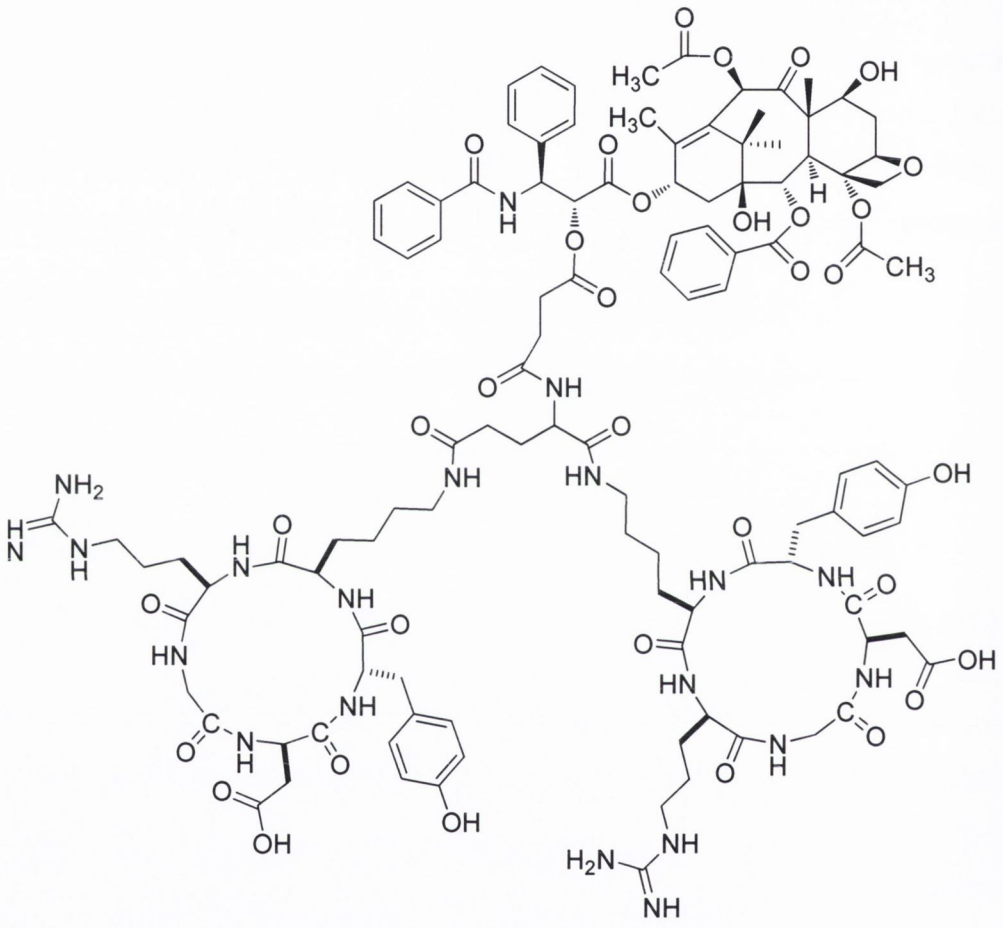

Figure 1.30 Paclitaxel-E[c(RGDyK)]$_2$ conjugate **(1.22)**

The divalent integrin homing peptide E-[c(RGDfK)$_2$] was similarly coupled to paclitaxel by Ryppa *et al.* to yield E-[c(RGDfK)$_2$]-paclitaxel **(1.23)** [115]. The related conjugate c(RADfK)-paclitaxel was also prepared as a non-integrin $\alpha_v\beta_3$ binding control. Using a standard 72 h endothelial cell proliferation assay, both conjugates demonstrated inhibition of human umbilical vein endothelial cells (HUVEC) comparable to free paclitaxel. However the authors reported that the half-life of the paclitaxel ester bond was of the order of 2 h at pH 7. It is therefore plausible that the activity of

the conjugates was largely due to the premature release of paclitaxel. In contrast, following a 30 min incubation of the three agents with the cells, marked differences in the IC_{50} values of the conjugates were observed. IC_{50} values of 10 nM, 25 nM and 60 nM were found for the free paclitaxel, E-[c(RGDfK)$_2$]-paclitaxel and c(RADfK)-paclitaxel respectively. An endothelial cell adhesion assay showed that inhibition of cell attachment was only observed with E-[c(RGDfK)$_2$]-paclitaxel, indicating its potential specificity. Despite the promising *in vitro* results, *in vivo* studies in an OVAR-3 xenograft model demonstrated no increase in antitumour efficacy for either E-[c(RGDfK)$_2$] or E-[c(RGDfK)$_2$]-paclitaxel compared to paclitaxel [115]. Poor stability of the paclitaxel ester bond, resulting in premature release of free paclitaxel and an insufficient density of receptors on target cells, were presumed to be responsible for an insufficiently toxic dose being internalised into the target cells [115].

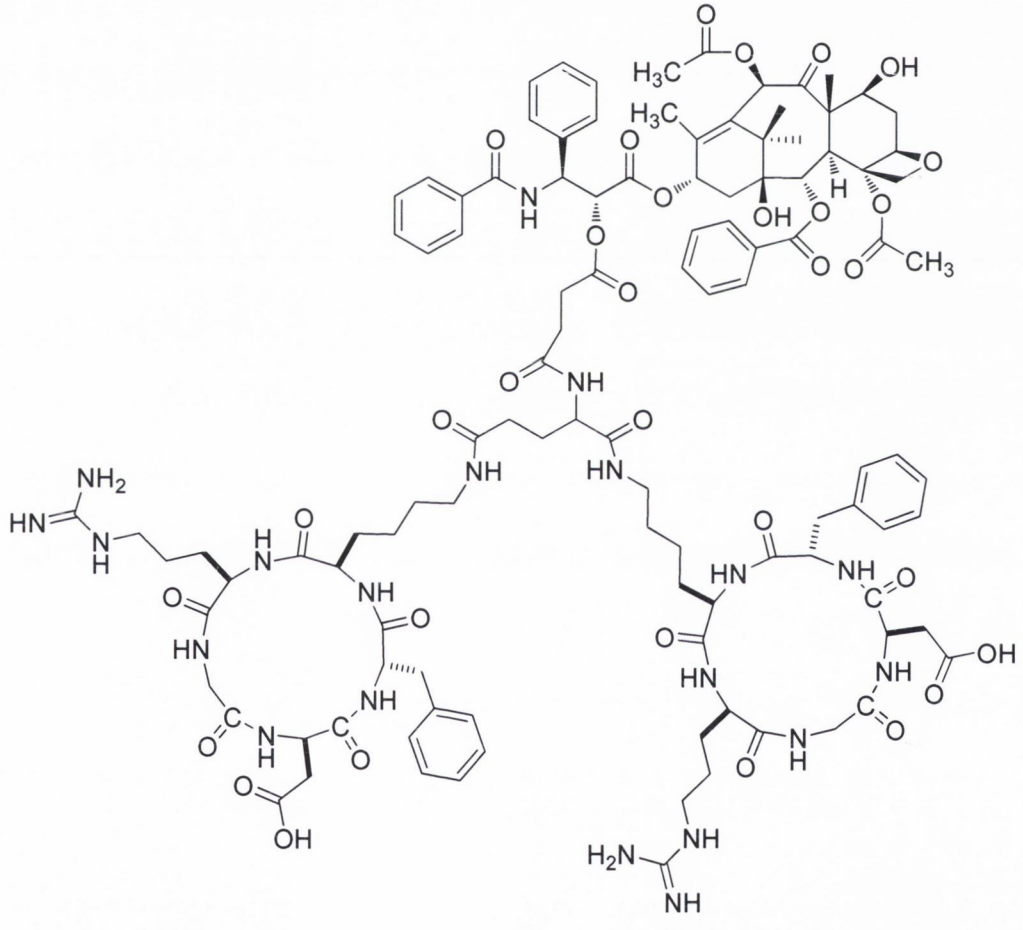

Figure 1.31 E-[c(RGDfK)$_2$]-paclitaxel **(1.23)**

Li *et al.* have synthesised a conjugate consisting of paclitaxel covalently tethered to a tetrameric peptide ligand of integrin $\alpha_v\beta_6$ **(1.24)** [116]. This integrin is widely expressed on early stage non-

small cell lung cancer cells and is associated with poor prognosis. It is also overexpressed in many epithelial carcinomas but is not expressed in normal tissues. The tetrameric peptide based $\alpha_v\beta_6$ ligand, designated H2009.1, binds with high affinity to $\alpha_v\beta_6$ but minimally with other integrin receptors. *In vitro,* the conjugate was found to be selectively cytotoxic to $\alpha_v\beta_6$ positive cell lines and displayed equivalent efficacy to free paclitaxel in tumour xenograft models. However, no statistically significant benefit was observed between the conjugate and free paclitaxel, either in terms of antitumour efficacy or reduced cytotoxicity. It was suggested by Liu *et al.* that the disappointing *in vivo* activity may be due to inefficient cleavage of the linker unit to release paclitaxel intracellularly or perhaps due to poor tumour cell internalisation of the conjugate.

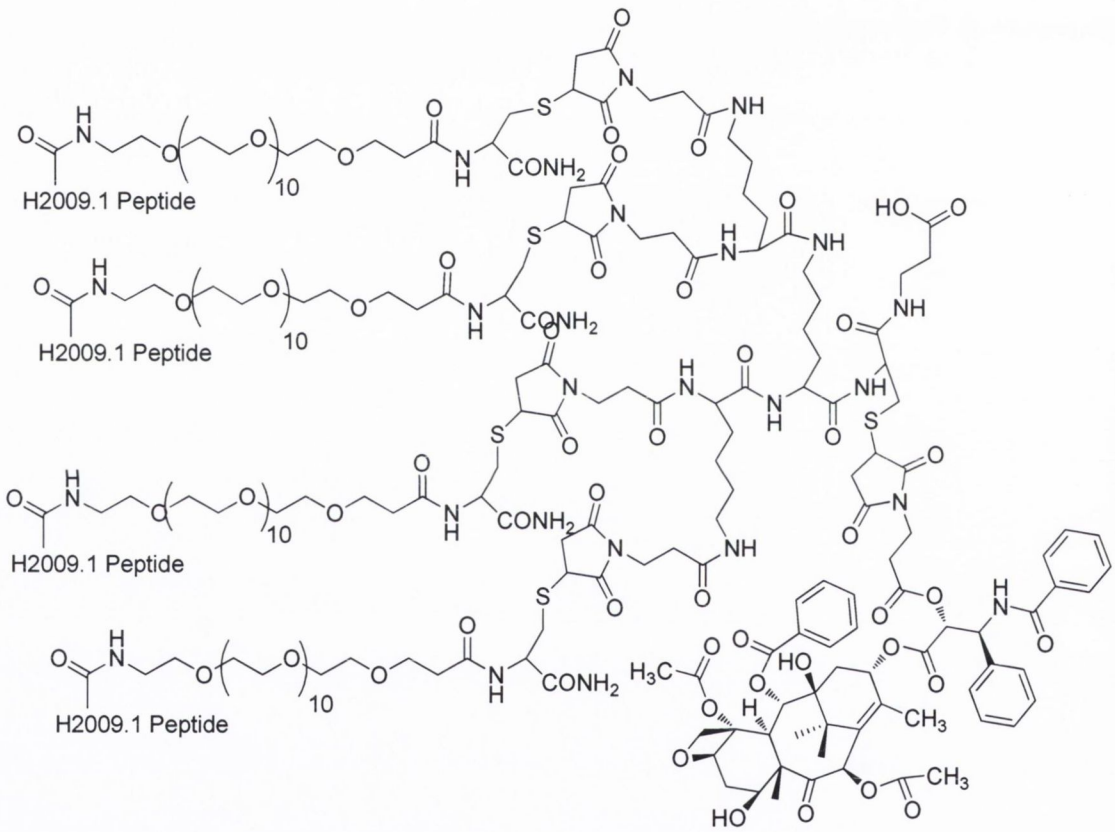

Figure 1.32 Paclitaxel–H2009.1 peptide conjugate **(1.24)**

Radiation has been used to induce the expression of cell surface receptors within the tumour microvasculature [117]. A number of tumour targeting peptides were subsequently developed to bind to these radiation inducible receptors. The HVGGSSV peptide is one such peptide. It was found to selectively bind to the tax-interacting protein-1 (TIP-1) receptor whose expression is induced in the microvasculature of irradiated tumours. Hariri *et al.* synthesised a novel conjugate

of human serum albumin-paclitaxel to which HVGGSSV was covalently tethered [117]. The conjugate was shown to bind specifically to TIP-1 receptors expressed in irradiated tumours. It was found to enhance the bioavailability of paclitaxel and significantly increased tumour growth delay in a human lung cancer xenograft model in mice. In fact, a 5-fold increase in paclitaxel concentrations in irradiated tumours was observed after administration of the conjugate, compared with human serum albumin-paclitaxel.

Safavy *et al.* synthesised a conjugate in which paclitaxel was linked to a dimeric presentation of the peptide YQWAVGHLM [118]. This peptide corresponds to a segment of the amphibian peptide bombesin. The peptide was shown to bind selectively to the gastrin-releasing peptide (GRP) receptor, which is overexpressed in a variety of cancer cells but has limited expression in normal tissues [119]. The conjugate, paclitaxel-glu(YQWAVGHLM)$_2$ was found to be more potent than paclitaxel *in vitro* in GRP receptor-positive cell lines. No data was presented on the efficacy of the conjugate in vivo.

Ndungu *et al.* synthesised a number of conjugates of the endogenous coagulation protein factor VII covalently attached to paclitaxel [120]. The conjugates were designed to take advantage of factor VIIs high affinity for tissue factor (TF) which is selectively overexpressed on tumour associated vascular endothelial cells and on many cancer cells [121]. While the conjugates were found to be cytotoxic against various TF-positive cell lines, *in vivo* evaluation of the conjugates was not reported.

1.6 Macromolecular Conjugates

The targeting of cytotoxic agents to the tumour site can occur *via* passive as well as active processes. While many of the targeting methodologies discussed thus far rely on the selectivity of a targeting moiety for tumour expressed antigens or receptors and the binding-mediated entry of the conjugate into target cells, it is also possible to target tumours passively by exploiting differences in the anatomical structure of the tumour. Macromolecular drugs have high molecular weights, typically greater than 40 kDa, which enables them to overcome renal excretion and attain prolonged plasma or tissue half-lives [122]. Due to their large size however, macromolecules can often have difficulty in crossing the tight endothelial junctions of normal vasculature [122]. Tumour vasculature however, is characterised by a number of pathophysiological alterations such as increased vascular density due to tumour angiogenesis, impaired lymphatic recovery and absence of a basement membrane and associated smooth

muscle. This permits the extravasation of these agents in tumour vasculature and causes them to become trapped in the tumour vicinity [122]. There is also a further amplification of vascular permeability due to the extensive production of vascular mediators locally such as bradykinin, nitric oxide and prostaglandins. Over time, the macromolecules concentration at the tumour site will gradually increase, reaching several-fold the drug concentration in circulation [123]. This concept of macromolecule accumulation and selective retention at the tumour site is referred to as the enhanced penetration and retention (EPR) effect [122]. The EPR effect does not just imply passive delivery of macromolecular anticancer drug conjugates into tumour tissues, but also refers to the prolonged retention of these drugs for weeks or even months in the tumour tissues, permitting effective and prolonged anticancer efficacy [123]. The EPR effect has been observed with biocompatible macromolecules or nanoparticles, with a molecular size of more than 40 kDa and up to 1μm in size, in most experimental solid tumours [124].

In order to exploit this phenomenon for the selective delivery of tubulin targeting agents to tumours, a number of macromolecular drug conjugates have been synthesised and evaluated. These conjugates typically consist of three distinct components, namely a suitable polymeric carrier, a biodegradable linker, and a bioactive antitumor agent. Some of the more complex macromolecular conjugates also contain a more conventional tumour targeting moiety to further increase selectivity for tumour cells and some novel tumour-specific release mechanisms have also been incorporated into these agents.

1.6.1 EPR effect-dependent macromolecular conjugates

For clinical administration, paclitaxel is typically formulated as a polyethylated castor oil based preparation (Cremophor EL) or using ethanol as a co-solvent (Taxol). However, the excipients used in these formulations have been reported to contribute to the toxicity of the preparations and hypersensitivity reactions are common. To address this concern, a co-solvent free formulation has been developed that consists of 130 nm albumin particles to which paclitaxel is non-covalently bound (Abraxane) [125-128]. However, this technology is not the first to employ human serum albumin as a delivery vehicle for paclitaxel. Dosio *et al.* developed a poly(ethylene glycol)–human serum albumin–paclitaxel conjugate **(1.25)** to improve the water solubility and stability of paclitaxel [129]. Paclitaxel was conjugated to the serum albumin *via* a 2'hydroxy succinate linker. Approximately six paclitaxel molecules were conjugated to each human serum albumin molecule, whereas an average of eight monomethoxy poly(ethylene glycol) chains of either 2 or 5 kDa mass were conjugated to each albumin molecule. *In vitro* cytotoxicity assays determined that the

conjugates had activity in each of three human cancer cell lines tested. *In vivo,* a 10-fold increase in half-life compared to the unconjugated paclitaxel was achieved. While the resultant conjugates would be expected to accumulate selectively at the tumour site by virtue of their size, no data was presented to confirm this hypothesis.

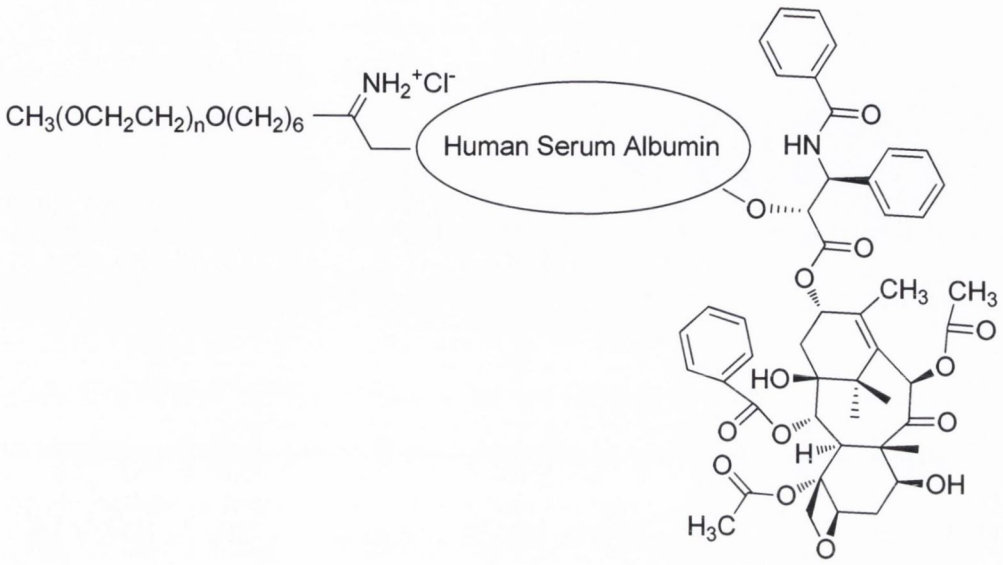

Figure 1.33 Paclitaxel–HSA–PEG **(1.25)**

Paclitaxel poliglumex (PPX, also called Xyotax or CT2103) **(1.26)** is a macromolecular drug conjugate consisting of paclitaxel covalently attached to the biodegradable polymer, poly(L-glutamic acid). The 2′ hydroxy group of paclitaxel is linked to the γ-carboxylic acid side chains of poly-L-glutamic acid. On average there are 10.4 non-conjugated monomer units (a+b) for every monomer conjugated to a paclitaxel molecule (γ). Due to the importance of the 2′ hydroxyl position on paclitaxel for tubulin binding, the conjugate remains biologically inactive in circulation. In stability studies, carried out by Chipman *et al.*, less than 14% of bound paclitaxel had been hydrolysed following 24 h incubation in human plasma at 37 °C [130]. The molecular weight of PPX is approximately 48 kDa. Therefore, enhanced tumour delivery is achieved by taking advantage of the EPR effect. A 10-100-fold increase in tumour drug concentration, compared with an equivalent dose of drug given conventionally, was observed. Once the polymer reaches the tumour, endocytosis of the conjugate occurs. Release of free paclitaxel was found to be at least partially dependent on proteolysis by cathepsin B [131]. As well as selective tumour delivery by virtue of the EPR effect and cathepsin B dependent release, PPX is water soluble without the need for potentially toxic excipients. Preclinical studies in animal tumour models demonstrated that paclitaxel poliglumex was more efficacious than standard paclitaxel treatment and was associated

with prolonged tumour exposure to the active drug while minimising systemic exposure. Phase I and II clinical trials with the conjugate showed encouraging outcomes in comparison with free paclitaxel, with lower incidences of myelosuppression and alopecia. The polymeric presentation also allowed more convenient administration schedules to be adopted without the need for premedication. Human pharmacokinetic data verified the prolonged tumour exposure and limited systemic exposure initially suggested by preclinical studies [132].

Clinically, in comparison with docetaxel, PPX was associated with a favourable haematological toxicity profile with an associated reduction in incidences of severe neutropenia and infection. A phase I and pharmacokinetic study of PPX conducted by Boddy *et al.* demonstrated a prolonged half-life of greater than 100 h for the conjugate and limited volume of distribution compared to that of free paclitaxel [133]. Hypersensitivity reactions were reported to be mild and there was no necessity for premedication. Neutropenia was also relatively mild but neuropathy was found to be comparable with equivalent doses of free paclitaxel. Notably, alopecia was almost absent in patients treated with PPX compared with an incidence of 50% in patients receiving an equivalent regimen consisting of free paclitaxel. In three phase III clinical trials conducted on patients with advanced non-small cell lung cancer, PPX was shown to be as effective as current treatment options [130]. However, in a retrospective analysis of data from two phase III clinical trials, it became apparent that the activity of the conjugate may be regulated by estradiol. Increased survival was observed in the female, but not the male, cohort of patients. It has been shown that cathepsin B activity is induced by estradiol and since cathepsin B was known to be central to paclitaxel release from the conjugate it was suggested that such a connection could be exploited for clinical benefit [130]. Furthermore, in a subsequent phase III trial comparing the conjugate with docetaxel in the second line treatment of non-small cell lung cancer, both agents produced similar survival results but had different toxicity profiles. While the conjugate benefited from less febrile neutropenia and less alopecia (43% versus 14%), shorter infusion times and elimination of the need for premedication to prevent hypersensitivity reactions, it was also associated with a greater incidence of neurotoxicity compared to docetaxel (19% versus 3% incidences of grade 3 neuropathy) and actually resulted in a higher discontinuation rate due to adverse events [134]. Despite early promise, the therapeutic benefits of this agent have yet to be conclusively determined and the product is still awaiting marketing authorisation.

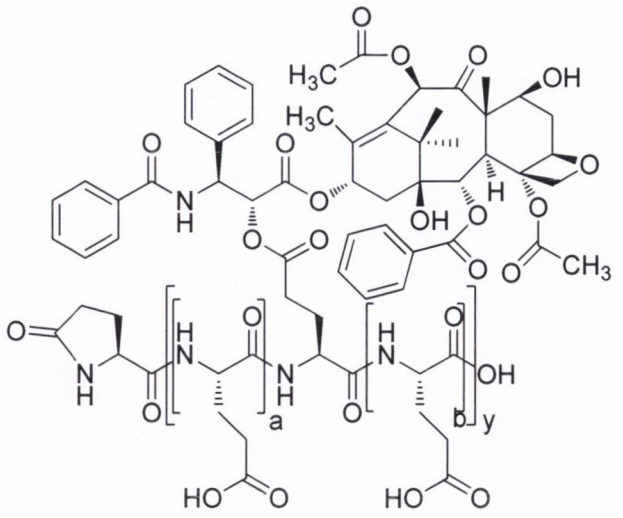

Figure 1.34 Schematic representation of Paclitaxel poliglumex **(1.26)**

The related poly (L-γ-glutamyl-glutamine)-paclitaxel (PGA-PTX) conjugate **(1.27)** was synthesised and evaluated by Van *et al.* [135]. This conjugate consists of poly (L-glutamic acid) in which another glutamic acid has been coupled to each glutamic acid in the polymer backbone. Paclitaxel was then covalently attached to the glutamic acid side chain. There are approximately five non-paclitaxel conjugated monomer units (Y) to each paclitaxel-conjugated monomer unit (X). This conjugate was found to have superior water solubility and a faster dissolution rate than the related PPX conjugate **(1.26)** and was found to have a comparable potency when tested *in vitro* against the human lung cancer cell line H460 [135]. The IC_{50} of PGG-PTX was 2.31 μM compared to 2.25 μM for PPX. It does however, possess a lower toxicity than the PPX conjugate with a 2.2-fold higher maximum tolerated dose demonstrated *in vivo* in mice [135]. Furthermore, the maximum tolerated single dose of PGG-PTX in mice was 350 mg PTX/kg as compared to 160 mg PTX/kg for PPX and 80 mg/kg for paclitaxel in the Cremophor formulation [135]. The authors have also indicated that PGG-PTX has shown superior therapeutic activity to that of Abraxane in multiple tumour models and that the conjugate is less toxic than poly (l-glutamic acid) *in vivo* [135].

Tritium labelled PGG-PTX was used to investigate the tumour targeting effect of the macromolecular conjugate. It was found that a 7.7-fold increase in tumour taxane concentration was obtained following administration of the conjugate, compared to an equivalent dose of free paclitaxel [136]. Furthermore, the conjugate produced significantly greater inhibition of tumour growth in three different cell models following administration of single equitoxic doses of PGG-PTX and Abraxane. PGG-PTX was also found to generate much less weight loss in mice bearing H460 tumours [137].

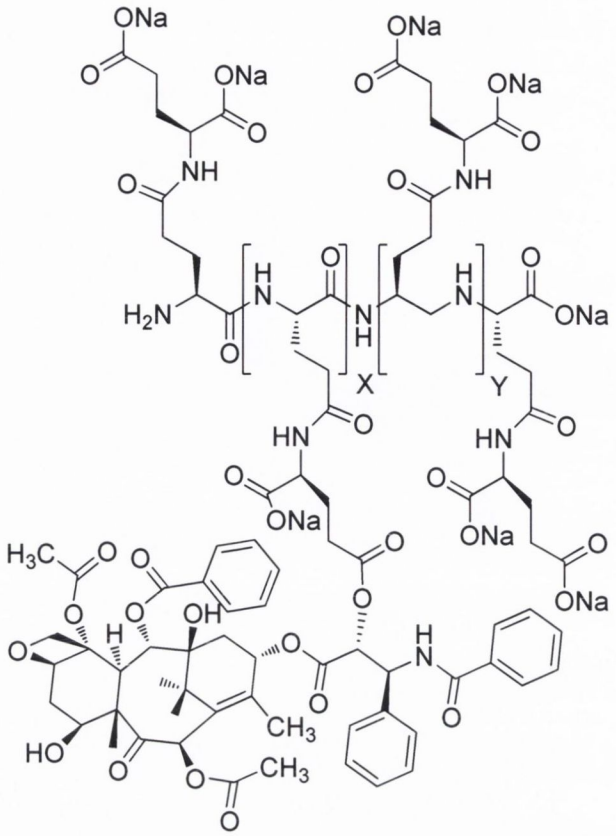

Figure 1.35 PGG-PTX **(1.27)**

Xie *et al.* have synthesised and characterised another paclitaxel-polymer conjugate for the enhanced delivery of paclitaxel to the tumour site [138]. The conjugate is a triblock polymeric construct designated P(LGG-paclitaxel)-PEG-P(LGG-paclitaxel) **(1.28)**. *In vitro* studies indicated that release of paclitaxel from the polymer is pH dependent with release occurring more rapidly at low pH than at neutral pH. This was hypothesised to offer the potential for selective intracellular release following endocytosis due to the lower pH within lysosomes. *In vitro* cytotoxicity assays carried out on the rat brain glioma C6 cell line indicated that the conjugate had comparable activity to free paclitaxel suggesting that the drug would be released *in vivo*. However, no *in vivo* evaluation has been carried out on this conjugate to date.

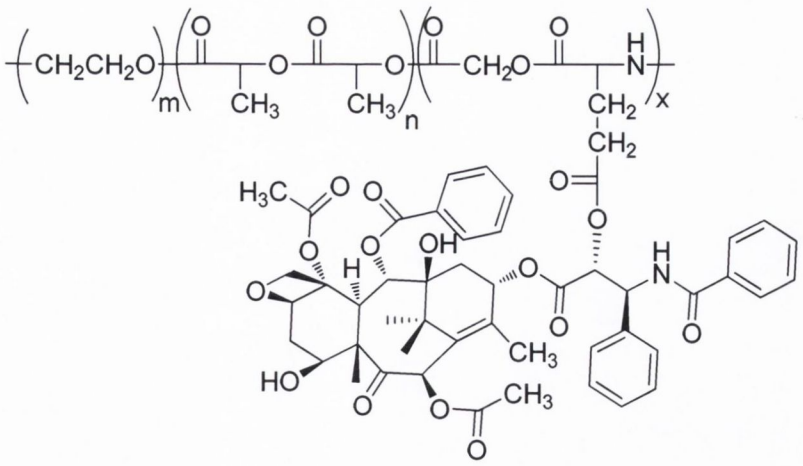

Figure 1.36 P(LGG-paclitaxel)-PEG-P(LGG-paclitaxel) conjugate **(1.28)**

A monomethoxy-poly(ethylene glycol)-b-poly lactide copolymer (MPEG-PLA) was conjugated to paclitaxel *via* an ester linkage by Zhang *et al.* [139]. The conjugate was evaluated *in vitro* using human liver cancer H7402 cells and was subsequently shown to release paclitaxel and exert a cytotoxic effect.

Conjugates of paclitaxel linked *via* an acid sensitive hydrazone linker to bifunctional PEGs (MW 20,000) were also shown to inhibit three human cell lines with low micromolar IC_{50} values [140].

Paclitaxel was also conjugated to poly (hydroxyethylaspartamide) (PHEA) *via* a succinate ester linker **(1.29)** by Cavallaro *et al.* [141]. Paclitaxel release from the resultant conjugate was found to be negligible at pH 7.4 and pH 5 and very slow in plasma. *In vitro,* the conjugate was found to be 40-fold less active than free paclitaxel. Following *in vivo* administration, over 80% of the dose was found to accumulate in the liver within 1 h and a high concentration was found to remain in the liver at 144 h post administration. No significant increase in conjugate uptake was observed in the tumour however.

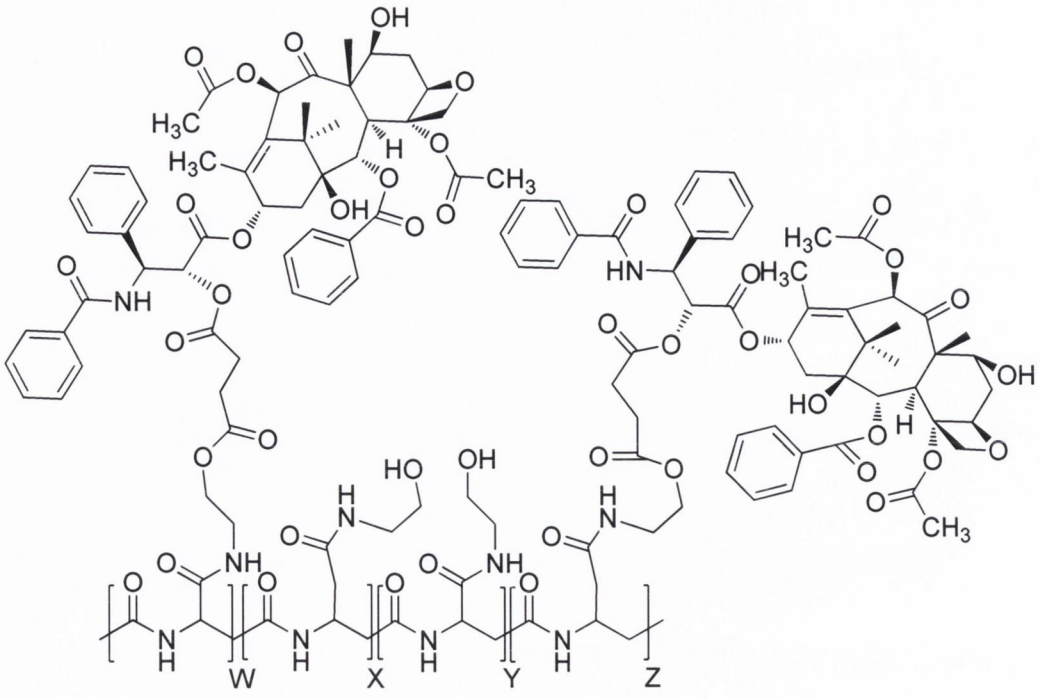

Figure 1.37 PHEA-2'-O-succinylpaclitaxel conjugate **(1.29)**

The poly (vinyl alcohol) based paclitaxel macromolecular conjugate **(1.30)** was synthesised by linking the 2'hydroxy of paclitaxel to the carboxylic acid side chain of poly (vinyl alcohol) *via* a succinyl and ethyldiamine spacer group [142]. This conjugate was reported to possess superior aqueous solubility to paclitaxel with substantially improved pharmacokinetic characteristics. When evaluated *in vivo* using subcutaneous sarcoma 180 tumour xenografts, tumour accumulation and significant antitumour activity was observed.

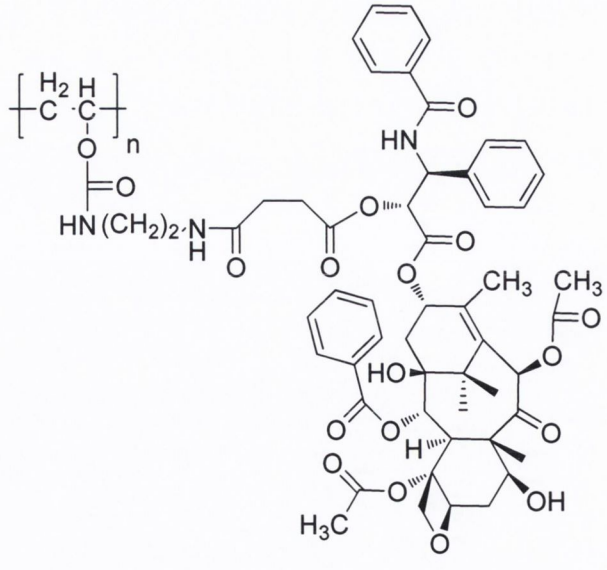

Figure 1.38 PVA–SPTX Conjugate **(1.30)**

The endogenous biopolymer heparin has also been utilised to synthesise a paclitaxel macromolecular conjugate. Wang *et al.* synthesised a series of heparin-paclitaxel conjugates either by a direct ester bond between the heparin backbone and paclitaxel or by incorporating an amino acid spacer [143]. Valine, leucine and phenylalanine were all used as linker groups. It was subsequently shown that these conjugates had better aqueous solubility and faster hydrolysis rates than the directly linked heparin-paclitaxel conjugate. The major difficulty with heparin as a drug delivery vehicle is the increased risk of haemorrhage. This disadvantage can be partially mitigated by using O-acetylated heparin, a derivative with low anti-coagulant activity. The bioconjugates formed from this modified heparin derivative were found to have a greatly decreased anti-coagulant effect. In related work, Wang *et al.* [144] synthesised a series of O-succinylated-heparin-paclitaxel conjugates using similar amino acid spacer groups. The anticoagulant activity of these conjugates was found to be dramatically reduced compared to unconjugated heparin and the conjugates exhibited greater activity *in vitro* against MCF-7 cells than paclitaxel. In a mouse xenograft of human ovarian serous cystocarcinoma cells, the leucine linker containing conjugate was shown to have similar rates of tumour growth inhibition to paclitaxel, with reduced loss in body weight among the treated animals.

Carboxymethyldextran (CMDex) has a number of characteristics which make it suitable for the synthesis of a macromolecular drug delivery agent. It is biocompatible, contains a large number of carboxylic acid residues for convenient drug attachment and the resulting bioconjugates are readily water soluble. A number of such conjugates were synthesised by Sugahara *et al.* utilising glycine, leucine, isoleucine or alanine as linker units between the 2' hydroxy position of paclitaxel and the free carboxyl groups of the CMDex (Figure 1.39) [145]. In a stability study conducted in mouse plasma over 72 h at 37 °C, it was found that the conjugate with the glycine linker released the most paclitaxel. In the accompanying *in vivo* pharmacokinetic studies conducted on colon 26 human colon cancer cell tumour xenograft models in mice, it was found that the glycine containing conjugate resulted in the greatest paclitaxel release. Furthermore, the release of paclitaxel was found to correlate with the activity of the compound *in vivo* for all conjugates. The tumour specific cytotoxicity of this conjugate was not determined *in vivo* however.

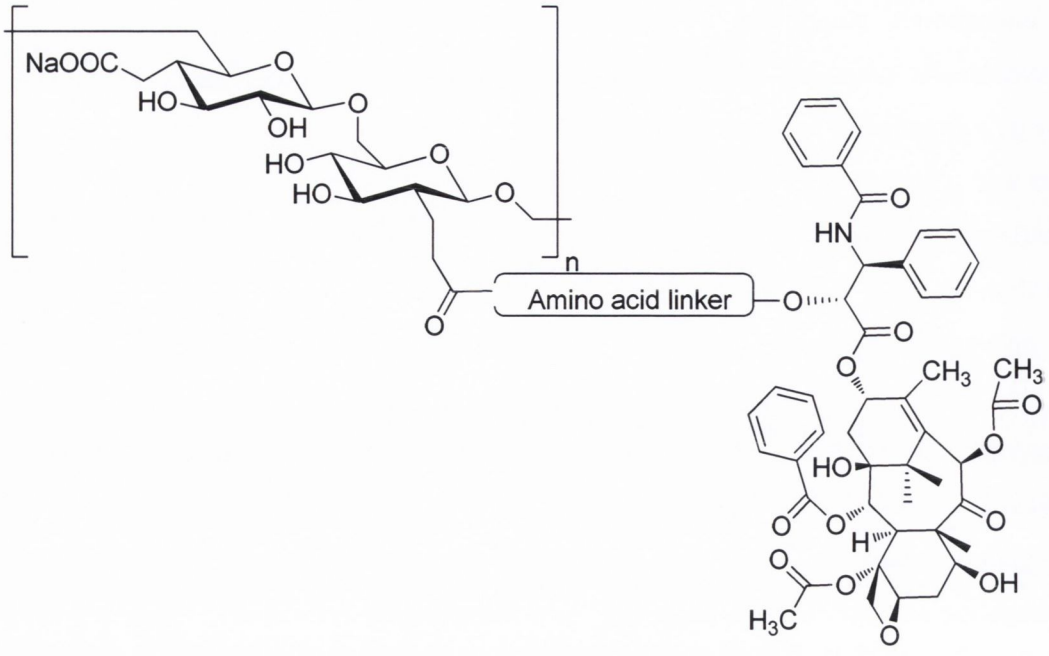

Figure 1.39 Paclitaxel–carboxymethyl dextran conjugates

In closely related work, Sahara *et al.* subsequently synthesised a paclitaxel-CMDex conjugate linked *via* a glycine-glycine-phenylalanine-glycine tetrapeptide spacer (GGFG) which was designated AZ10992 [146]. This conjugate showed no activity *in vitro* but displayed superior activity to free paclitaxel against colon 26, MX-1, LX-1 and HT-29 tumour xenografts in mice. In fact, AZ10992 administration resulted in complete regression of MX-1 mammary carcinoma xenografts *in vivo*. The maximum tolerated dose of AZ10992 was also twice that of free paclitaxel *in vivo*. Pharmacokinetically, AZ10992 also resulted in greater tumour paclitaxel exposure compared to free paclitaxel. In further studies, AZ10992, unlike paclitaxel, was shown not to induce degeneration of myelin or swelling of Schwann cells in sciatic nerves in mice. The conjugate was also shown to display superior therapeutic activity in other human tumour xenograft models [147]. However, any potential benefits of this conjugate over more established paclitaxel-biopolymer conjugates have yet to be determined.

Chitosan is another biopolymer which has been investigated for the tumour targeted delivery of tubulin inhibitors. Chitosan is a natural polysaccharide found in many living organisms [148]. It is widely used pharmaceutically because it is biocompatible, biodegradable, mucoadhesive and non-toxic [148]. Using a CaCo-2 cell model, it was shown that low molecular weight chitosan can reversibly open the tight junctions between intestinal cells [148]. Thus it has been hypothesised that chitosan may find utility as an absorption enhancing agent in pharmaceutical formulations

[148]. A low molecular weight chitosan paclitaxel conjugate (LMWC-paclitaxel) **(1.31)**, containing approximately 12% paclitaxel by weight, was synthesised and evaluated *in vitro* and *in vivo* by Lee *et al.* [149]. The conjugate exhibited comparable activity to free paclitaxel *in vitro* while oral bioavailability was 42%. When the conjugate was administered orally to mice bearing murine melanoma BF16F10 or human non-small cell carcinoma NCI-H358 tumour xenografts, comparable anti-tumour activity was seen to those treated with i.v. free paclitaxel, but with much lower incidences of toxicity.

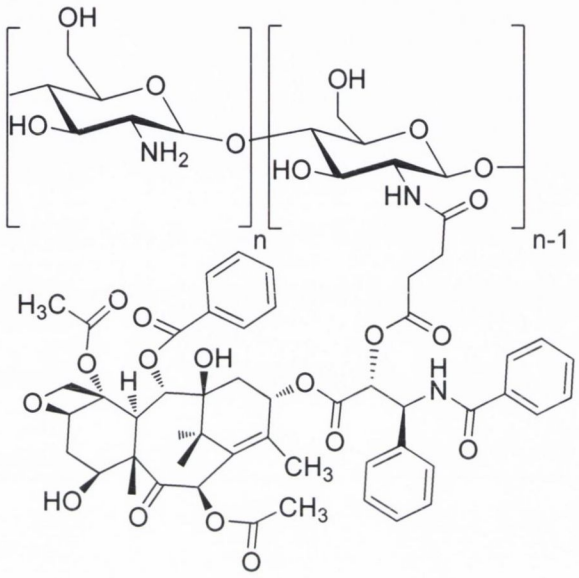

Figure 1.40 LMWC-paclitaxel **(1.31)**

Subsequently, a docetaxel-LMWC conjugate **(1.32)** was synthesised by Lee *et al.* [150]. This conjugate showed equivalent activity to free docetaxel *in vitro* against human non-small cell lung cancer (NCI-H358) and brain glioblastoma (U87MG) cell lines. Pharmacokinetic data following oral administration showed that the half-life of the conjugate was approximately 15-fold greater and the AUC 3.8-6.2 times higher in comparison with i.v. administered docetaxel. The conjugate showed comparable anti-tumour activity to an equivalent i.v. dose of docetaxel when administered orally in two human xenograft tumour models (NCI-H358 and U87MG). However, the conjugate was found to cause less pronounced side effects than docetaxel. Significantly less weight loss and haematological toxicity was observed in the conjugate treated mice [150].

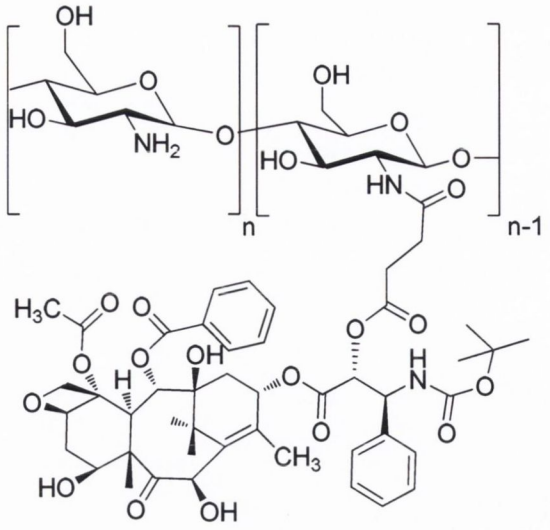

Figure 1.41 LMWC-docetaxel **(1.32)**

Jun *et al.* synthesised a novel water soluble and biodegradable cyclotriphosphazene–paclitaxel conjugate **(1.33)** in order to improve delivery of paclitaxel to the tumour site [151]. The conjugate was synthesised by reacting 2'-succinyl paclitaxel with cyclotriphosphazenes bearing equimolar glycyl-L-lysine and methoxy poly (ethylene glycol) as side groups. It was found to be readily water soluble and was shown to form stable micelles by self-assembly. The conjugate exhibited an IC_{50} value approximately twice that of free paclitaxel in a number of human cancer cell lines. It was shown to undergo hydrolytic cleavage in physiological solution, showing a release of 50% of bound paclitaxel after 72 h incubation at 37 °C.

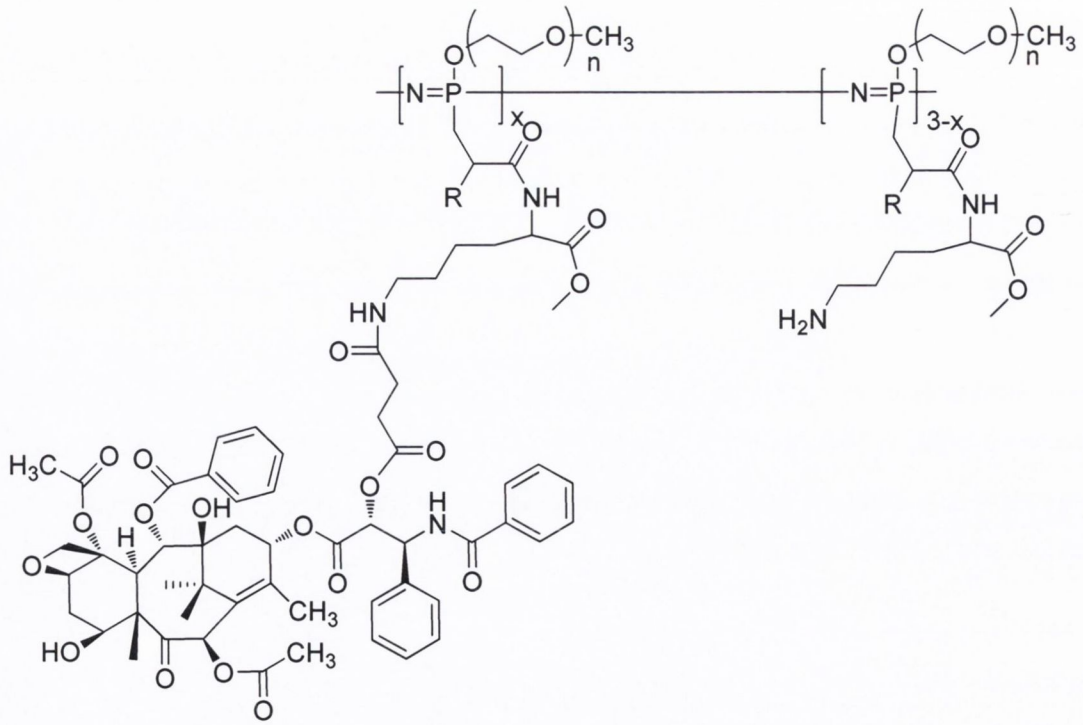

Figure 1.42 Cyclotriphosphazene–paclitaxel conjugate **(1.33)**

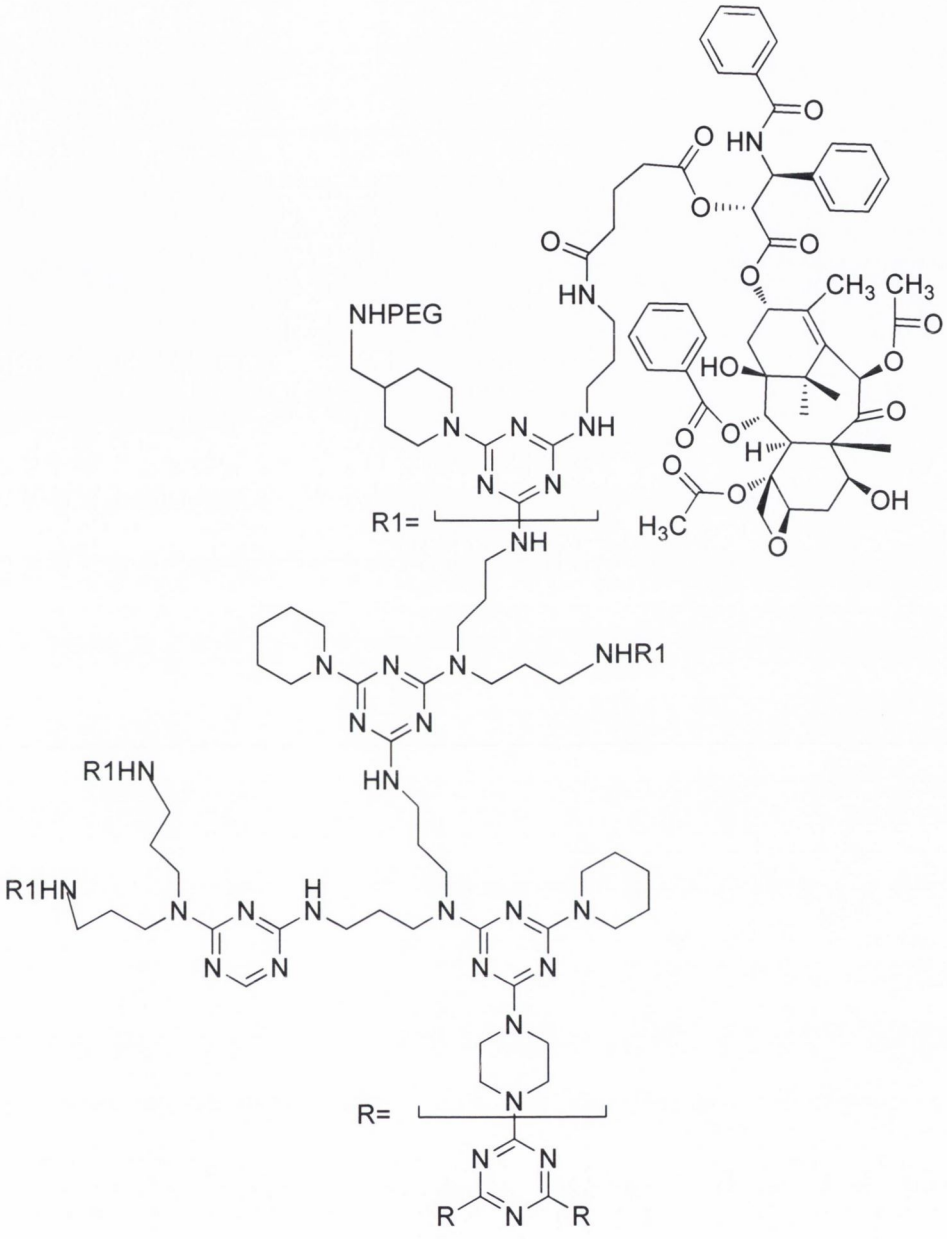

Figure 1.43 Paclitaxel-triazine dendrimer prodrug 1 **(1.34)**

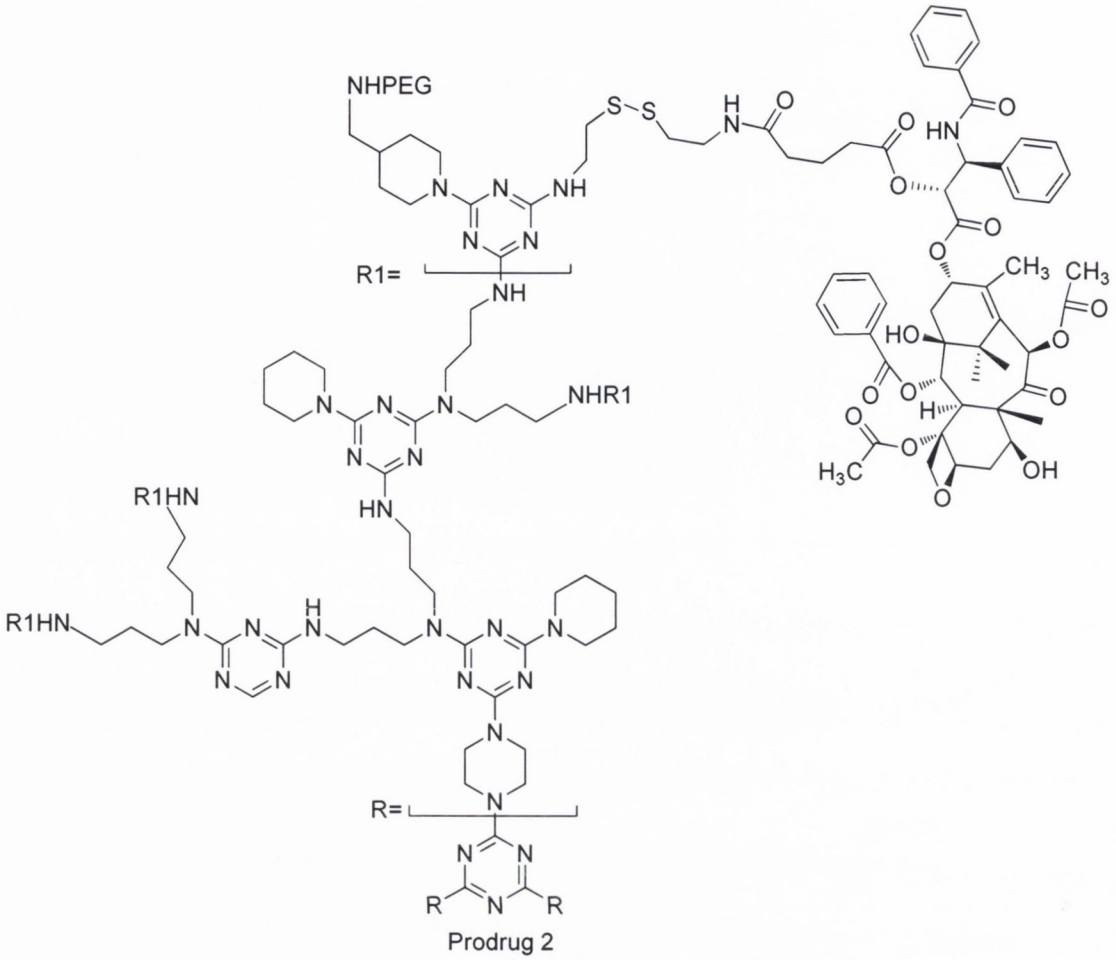

Figure 1.44 Paclitaxel-triazene dendrimer prodrug 2 **(1.35)**

Lim *et al.* recently synthesised paclitaxel-triazine dendrimer macromolecular constructs consisting of a triazine dendrimer conjugated to 12 paclitaxel molecules and an average of 8 to 9 PEG chains [152]. While prodrug 1 **(1.34)** consisted of an ester linkage between the dendrimer and the paclitaxel, prodrug 2 **(1.35)** incorporated an additional disulfide linkage in the linker molecule. Prodrug 2 was evaluated in PC3 human prostate cancer tumour xenografts in mice. It was determined that on average 11% cumulative release of paclitaxel occurred following incubation of prodrug 2 in human plasma for 48 h at 37 °C. The conjugate was found to be 2-3 orders of magnitude less toxic than free paclitaxel against human hepatocarcinoma (HepG2), porcine proximal tubule (LLC-PK1) and human colon carcinoma cells (LS174T), but showed similar cytotoxicity to Abraxane in LS174T cells. *In vivo,* it was found to possess comparable toxicity to Abraxane. The conjugate also showed significant anti-tumour activity in a PC-3 tumour xenograft

in mice [153]. At equivalent doses, prodrug 2 demonstrated greater toxicity than prodrug 1, suggesting that it may have greater activity at lower doses. Both conjugates also demonstrated significant antitumour activity *in vivo*. Lim *et al.* further established that these agents exhibited cytotoxicity in the low nanomolar range against PC-3 cells, with dithiothreitol and glutathione enhancing the toxicity of the disulfide-containing conjugates such as prodrug 2 [154]. A small degree of tumour localisation was also observed *in vivo*.

Floyd *et al.* also synthesised a dendrimer based conjugate **(1.36)** consisting of a 40 kDa PEGylated dendrimer with a polypeptide core to which 16 tubulysin D analogue molecules were conjugated *via* an acyl hydrazone linkage [155]. The conjugate was evaluated in C26 tumour bearing mice. The mice receiving the conjugate showed a 172% tumour growth delay, without significant weight loss, while the mice who received the free tubulysin analogue showed no tumour growth delay compared to controls.

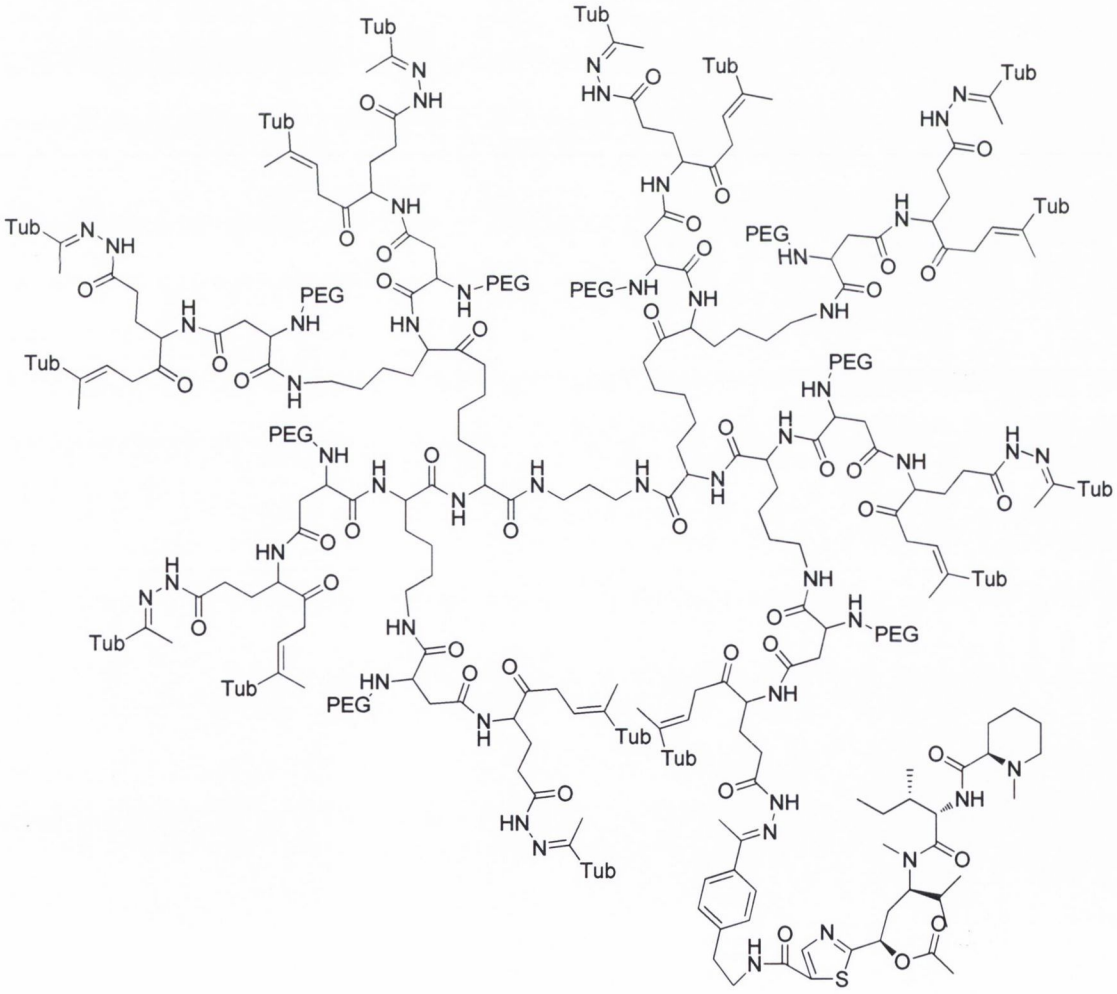

Figure 1.45 Tubulysin analogue-dendrimer conjugate **(1.36)**

Khandare *et al.* also synthesised a number of dendrimer based bioconjugates consisting of a polyamidoamine (PAMAM) G4 hydroxyl-terminated dendrimer covalently coupled to paclitaxel *via* a succinate ester linkage and to bis (carboxymethyl) PEG *via* an equivalent succinic acid bridge [156]. It was found that the linear bis(PEG)-succinic acid-paclitaxel conjugate had an IC_{50} 25 times higher than free paclitaxel against A2780 human carcinoma cells while the PAMAM dendrimer-succinic acid-paclitaxel conjugate was found to be 10 times more active than free paclitaxel.

1.6.2 Macromolecular conjugates with a tumour targeting moiety

The covalent attachment of tumour targeting moieties to macromolecular drug conjugates has been hypothesised to augment the degree of tumour targeting achievable through the EPR effect. To this end, Miller *et al.* synthesised a novel conjugate **(1.37)** consisting of paclitaxel covalently linked *via* a Phe-Lys–p-aminobenzyl carbonate (FK–PABC) spacer to a N-(2-hydroxypropyl) methacrylamide (HPMA) copolymer, to which an alendronate moiety has been incorporated, in order to selectively target bone metastases [157]. The linker unit was designed to be stable in circulation but readily cleaved following tumour cell internalisation by the lysosomal enzyme, cathepsin B. The bisphosphonate alendronate exhibits an exceptionally high affinity for the bone mineral hydroxapatite, which makes it a suitable agent for the targeting of paclitaxel to the bone. The selectivity of the release of paclitaxel for cathepsin B mediated release was confirmed *in vitro*. An analogue of the conjugate with a non-cathepsin B cleavable linker unit demonstrated 100-fold lower activity against human umbilical vein endothelial cells than the HPMA copolymer-PTX-ALN conjugate. The conjugate was also shown to have anti-angiogenic activity equivalent to equimolar doses of free alendronate and paclitaxel. The conjugate demonstrated 10-fold higher IC_{50} values than free paclitaxel against both human MDA-MB-231 and murine 4T1 adenocarcinoma of the mammary cell lines, but demonstrated superior activity to free paclitaxel and a combination of free paclitaxel and alendronate at equivalent doses in mice bearing 4T1-mCherry mammary adenocarcinoma in the tibia. The bone targeted polymeric conjugate was also better tolerated than free paclitaxel and was proposed to have an additional anti-angiogenic effect *in vivo*, suggested by increased levels of apoptotic circulating endothelial cells and decreased microvessel density observed in the treated animals [158].

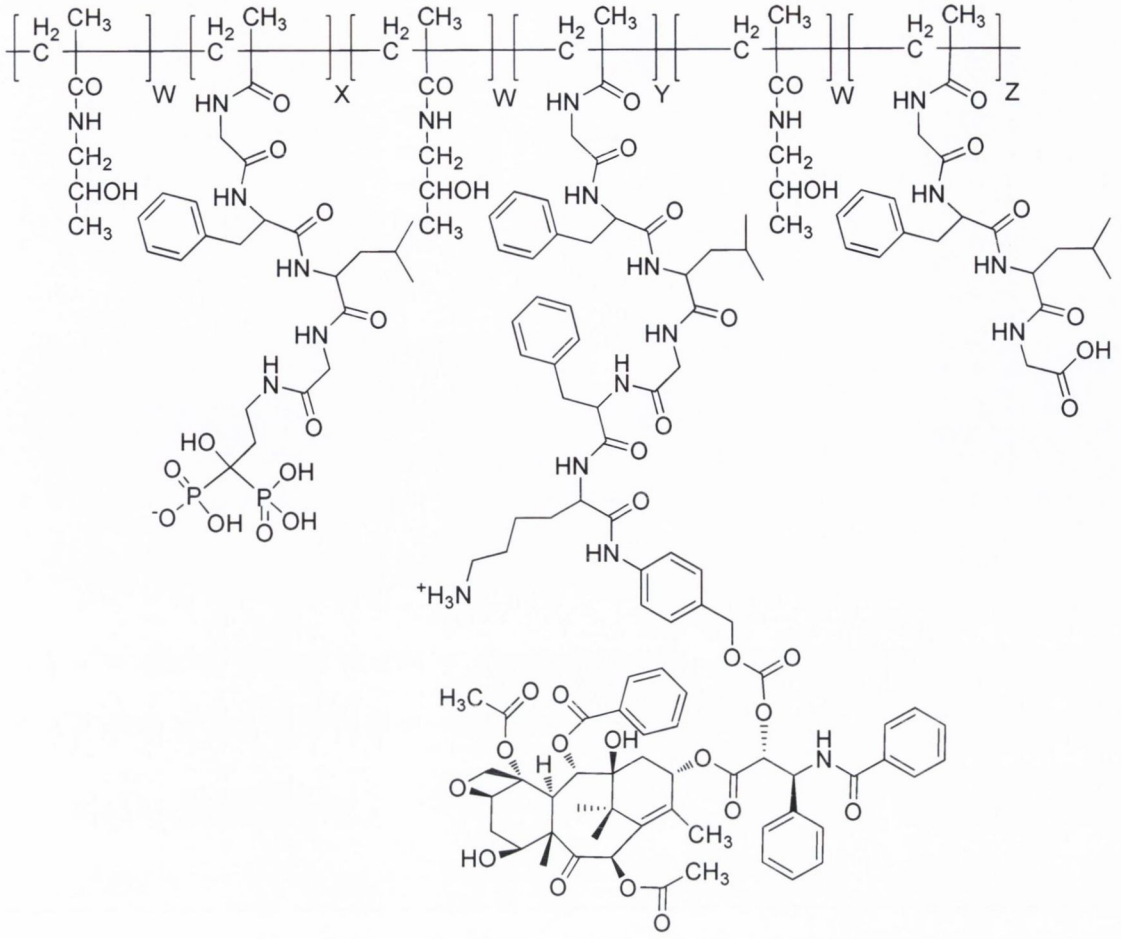

Figure 1.46 HPMA Copolymer-PTX-ALN Conjugate **(1.37).** (W= 90%, X= 2.5%, Y= 4%, Z= 3.5%)

A PEG dendrimer composed of H_2N-PEG-dendrimer-$(COOH)_4$ has also been utilised as a backbone for the attachment of paclitaxel and alendronate with a view to selectively targeting bone neoplasias. This carrier has the advantage of offering four carboxylic acid groups and a free amine functionality for the possible conjugation of five molecules onto the central PEG polymer backbone. Clementi *et al.* have used the polyfunctionalised dendrimer to synthesise conjugate **(1.38)** which targets the succinimidyl linked paclitaxel selectively to bone utilising four alendronate moieties [159]. The rate of release of paclitaxel was equivalent following incubation in buffer at pH 7.4 and in plasma, indicating that paclitaxel is released hydrolytically without a significant contribution from plasma esterases. The conjugate demonstrated a very high affinity for the bone mineral hydroxyapatite *in vitro* and also exhibited an IC_{50} value comparable to the free paclitaxel/alendronate in PC-3 cells. The PTX-PEG-ALN conjugate also exhibited an improved pharmacokinetic profile *in vivo* in mice with an elimination half-life of 85.5 min for the conjugate compared with just 15.1 min for free paclitaxel.

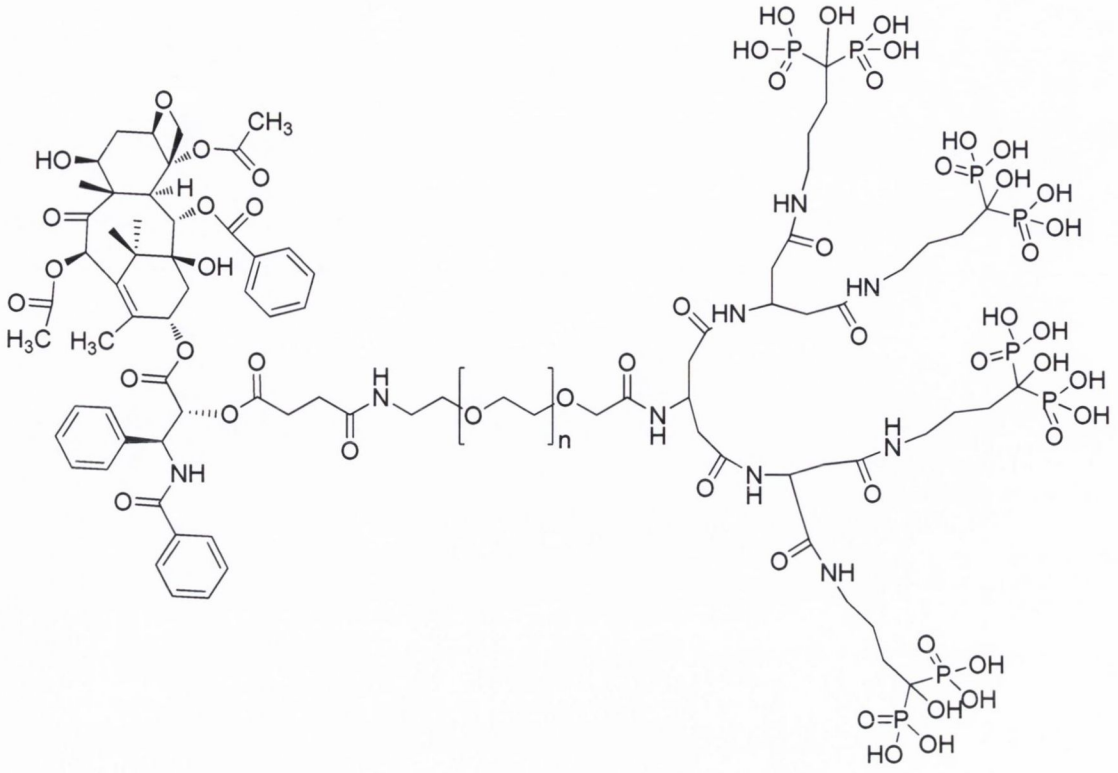

Figure 1.47 PTX-PEG-ALN **(1.38)**

Rosato *et al.* developed a macromolecular conjugate of hyaluronic acid and paclitaxel (HA-PTX) designated HYTAD1-p20 **(1.39)**, for the intravesicular delivery of paclitaxel in superficial bladder cancer [160]. Hyaluronic acid is a linear polysaccharide composed of alternating D-glucuronic acid and *N*-acetyl-D-glucosamine units. Hyaluronic acid is found extensively throughout connective, epithelial and neural tissues and is one of the main constituents of the extracellular matrix [161]. Two receptors for hyaluronic acid are present physiologically, CD44 and receptor for hyaluronic acid mediated motility (RHAMM) [160]. Both of these cell surface receptors are found to be overexpressed in a wide variety of cancers including bladder cancer [160]. *In vitro,* HYTAD1-p20 exerted a much higher dose dependent inhibitory effect against RT-4 and RT-112/84 bladder carcinoma cell lines than free paclitaxel, exhibiting IC_{50} values 800 and 120 times lower than paclitaxel in RT-4 and RT-112/84 respectively. It was suggested that this increased activity was as a result of CD44 receptor mediated endocytosis of the conjugate and subsequent intracellular release of paclitaxel. *In vivo* studies, conducted on RT-122/84 orthotopic tumour containing mice, demonstrated an antitumour efficacy equivalent to that of free paclitaxel.

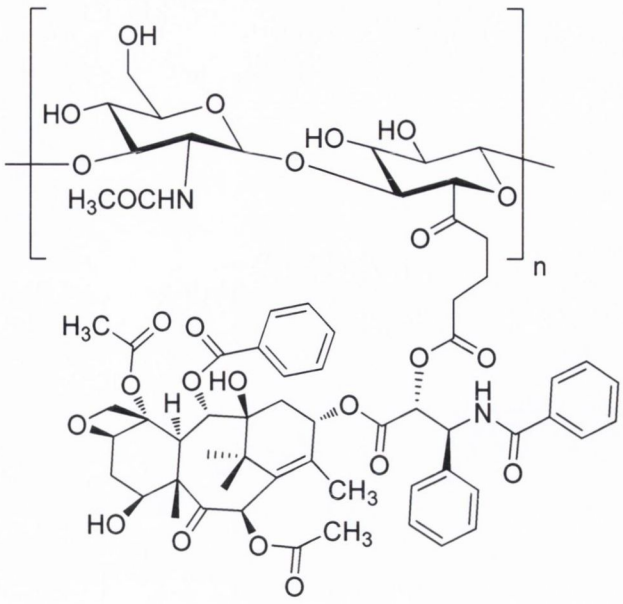

Figure 1.48 HYTAD1-p20 **(1.39)**

A subsequent study carried out by Banzato *et al.* demonstrated the applicability of HYTAD1-p20 to ovarian cancer [162]. Antitumour activity against both IGROV-1 and OVCAR-3 human ovarian cancer xenografts was determined following i.p. administration in mice. It was found that the conjugate interacted with CD44 and entered target cells *via* receptor mediated endocytosis. After i.p. administration, the conjugate was well tolerated, with no histological evidence of toxicity. Pharmacokinetic studies demonstrated that blood levels of paclitaxel were higher and persisted longer following administration of the conjugate than those obtained with free paclitaxel. Overall survival was significantly increased in two *in vivo* models of human ovarian carcinoma when the bioconjugate was compared to free paclitaxel.

The applicability of HYTAD1-p20 to ovarian cancer was also shown in intraperitoneal CD44-positive OVCAR-3 or SKOV-3 human ovarian cancer tumour xenografts [163]. HA-PTX was shown to be less effective *in vitro* against OVCAR-3 or SKOV-3 cells than free paclitaxel. However when administered at their maximum tolerated doses *in vivo* (MTD of i.p. HA-paclitaxel, i.v. paclitaxel and i.p. paclitaxel = 168, 80 and 80 mg/kg respectively) i.p. HA-paclitaxel was shown to be more effective than i.v. and i.p. free paclitaxel in inhibiting intra-abdominal tumour dissemination, abrogating ascites, prolonging survival and curing mice. Paclitaxel i.p. and HA-PTX i.p. were equivalent in terms of myelotoxicity, although the latter was administered at twice the dose.

In a further attempt to map the biodistribution of hyaluronic acid conjugates, a [^{99m}Tc] radiolabelled bioconjugate of paclitaxel linked to hyaluronic acid was administered to mice and the fate of the conjugate followed for 2 h using a small gamma camera [162]. It was shown that over 80% of the conjugate was detected in the liver 10 min after injection and remained there for the remainder of the study. This suggested that this method of delivery may have significant benefits in the treatment of primary or metastatic liver neoplasias. Imaging of the bladder, abdomen and gastrointestinal tract after local administration confirmed that the conjugate remained confined to these cavities, suggesting potential tumour selective delivery to bladder cell carcinomas, ovarian cancers and gastric tumours respectively.

The HA-PTX conjugates were also shown to be efficacious in mice bearing NMP-1 xenografts. Mice administered an i.p. dose of HA-paclitaxel equivalent to 100 mg/kg and 200 mg/kg of paclitaxel survived to day 60 and day 199 respectively, with control mice surviving to day 30 post tumour implantation [164]. Furthermore, it was found that mice receiving a single HA-paclitaxel dose experienced a longer survival time than those treated with multiple paclitaxel doses [164].

Another *in vivo* study on hyaluronic acid-paclitaxel conjugates was conducted by Galer *et al.* [165]. HA-paclitaxel was found to inhibit the growth of human squamous cell carcinomas of the head and neck (SCCHN) cell lines OCS-19 and HN5 with an activity comparable to free paclitaxel. Tumour uptake of the conjugate was found to be significantly impeded by free hyaluronic acid, indicating the dependence of uptake on CD44 interaction. HA-paclitaxel administered i.v. once weekly for three weeks at a dose equivalent to 120 mg/kg exerted superior tumour growth control to that of paclitaxel in both orthotopic OSC-19-luciferase and HN5 xenograft models *in vivo*. Markedly reduced microvessel density was also observed in those treated with the conjugate compared to those treated with free paclitaxel.

A novel series of hyaluronic acid paclitaxel conjugates were synthesised by Xin *et al.* utilising valine, leucine or phenylalanine containing linkages between the hyaluronic polymer backbone and the 2'-hydroxy group of paclitaxel (Figure 1.49) [166]. *In vitro*, HA-leucyl-paclitaxel exhibited the lowest IC_{50} value of the three conjugates (equivalent to 0.253 nM of paclitaxel) against MCF-7 human cancer cells compared to free paclitaxel (IC_{50} = 0.795 nM).

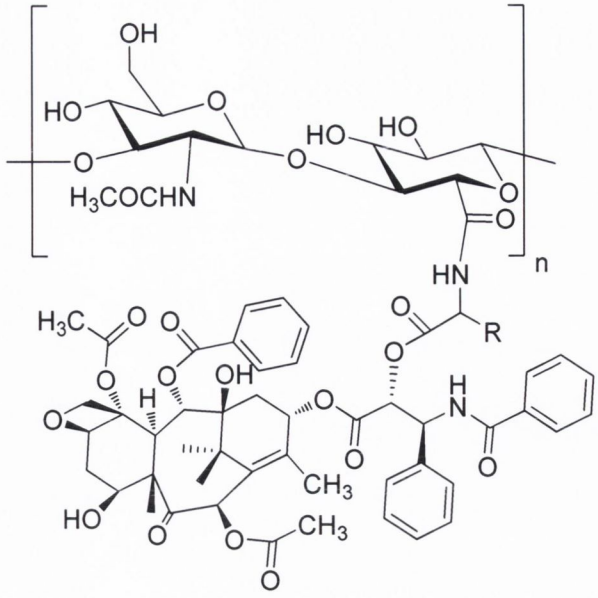

Figure 1.49 HA-amino acid-paclitaxel (where the amino acid is valine, leucine or phenylalanine)

Integrin targeting ligands have also been utilised in the homing of tubulin targeting agents, containing macromolecular constructs, to the tumour site. The tumour vasculature targeting effect of the cyclic pentapeptide c[RGDfK] was integrated into a poly (L-glutamic acid) polymer-paclitaxel conjugate with the synthesis of PGA-PTX-E-[c(RGDfK)$_2$] **(1.40)** [167]. As $\alpha_v\beta_3$ is overexpressed in tumour endothelial cells, it was expected that such a polymeric conjugate could find clinical use in various highly vascularised tumours. Stability studies in plasma indicate negligible paclitaxel release; while it was found that time dependent paclitaxel release occurred following incubation in aqueous buffer containing cathepsin B at acidic pH. PGA-PTX-E-[c(RGDfK)$_2$] inhibited the growth of $\alpha_v\beta_3$ expressing HUVECs and several cancer cell lines *in vitro*. Studies in mice bearing orthotopic 4T1 tumours demonstrated preferential tumour accumulation of the conjugate resulting in enhanced anti-tumour efficacy and a marked decrease in toxicity compared to free paclitaxel and to PGA-paclitaxel. The fact that 4T1 cells do not overexpress $\alpha_v\beta_3$ suggests that the enhanced activity is potentially due to an anti-angiogenic and tumour vasculature homing effect.

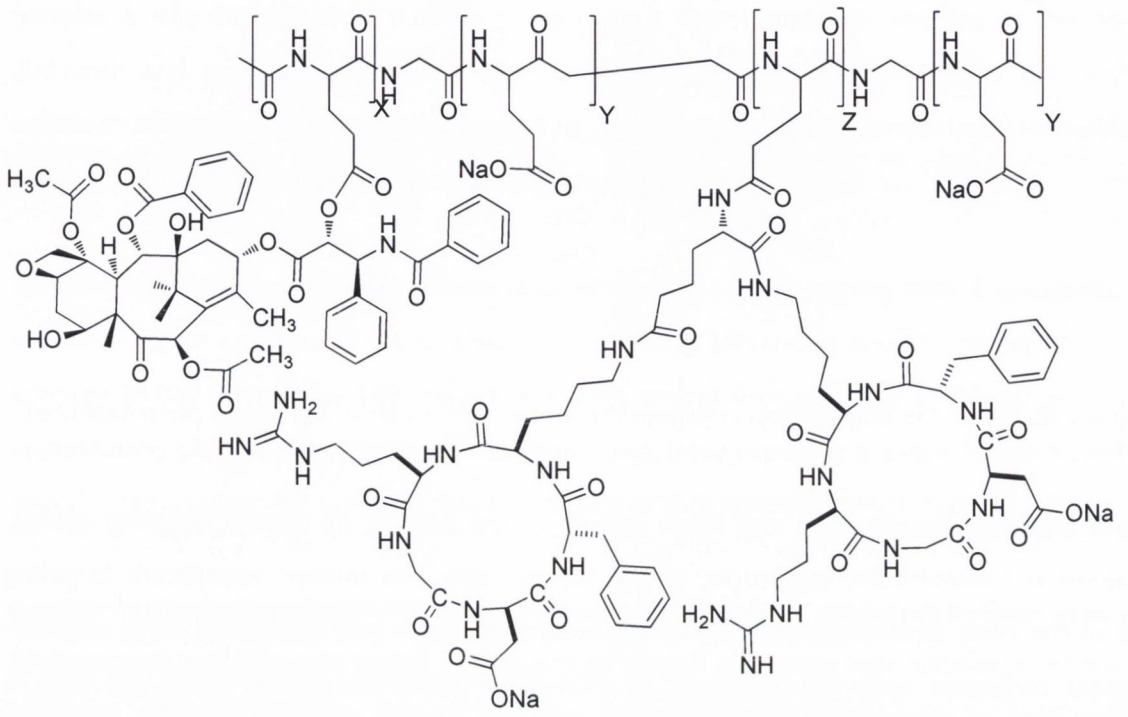

Figure 1.50 PGA-PTX-E-[c(RGDfK)$_2$] **(1.40)** (where X=5, Y=87 and Z=8)

PHEA is another polymer which was utilised in the synthesis of conjugates bearing tumour homing moieties. The PHEA polymer was PEGylated and conjugated at various points along the polymeric backbone to molecules of paclitaxel and oxytocin in order to synthesise polymeric drug delivery conjugate **(1.41)** to selectively target oxytocin receptor expressing tumour cells [168]. Approximately 90% of breast cancer cell lines including MCF-7 cells overexpress oxytocin receptors and oxytocin receptor interaction causes rapid internalisation of the receptor ligand complex. Therefore, molecular conjugation to oxytocin was anticipated to represent a novel tumour targeting approach [168]. Preliminary *in vitro* cytotoxicity assays carried out on the oxytocin receptor expressing cell line MCF-7, demonstrated that the conjugate had equivalent activity to free paclitaxel [169].

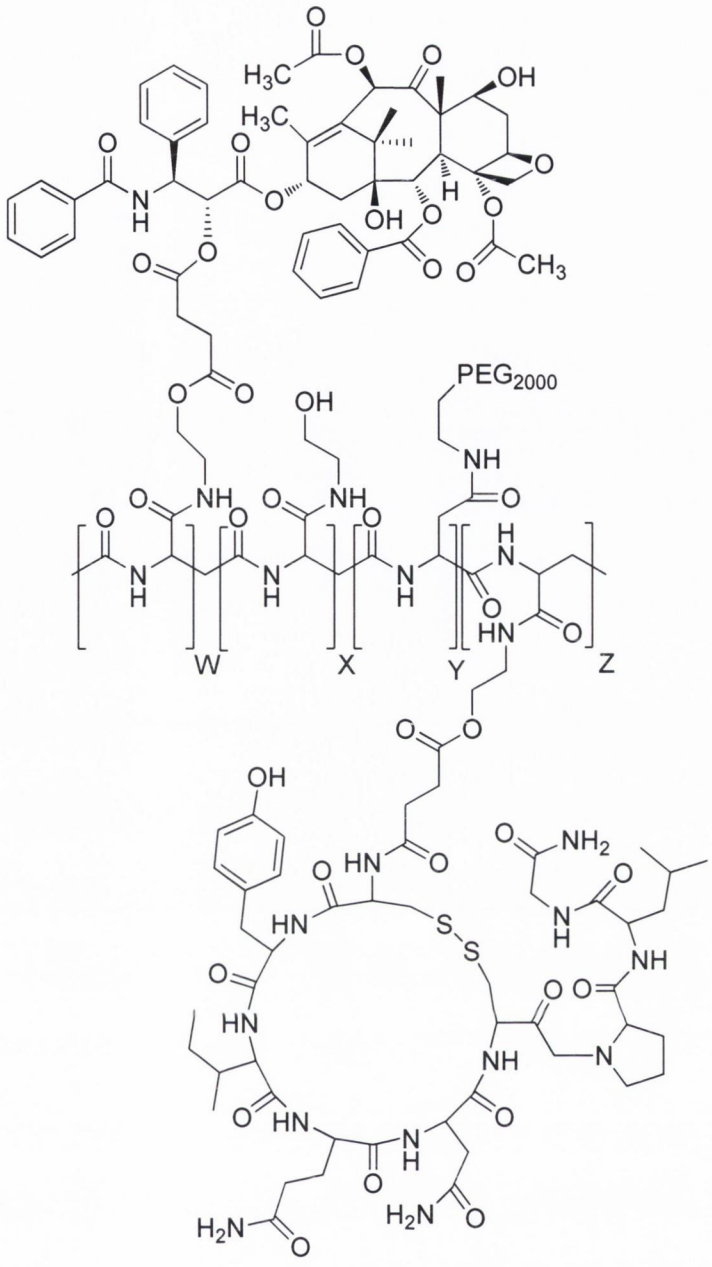

Figure 1.51 PHEA–PEG2000-succinyl-oxytocin–succinyl-paclitaxel conjugate **(1.41)**

Johansson *et al.* have reported a combinatorial study of glycopeptide dendrimers carrying two to five copies of a β-galactoside, as targeting device, with a colchicine molecule at their core [170]. Various glycoprotein receptors occur at cell surfaces where they mediate cell-cell recognition and the uptake of macromolecules, giving credence to this approach [171]. The structure of the most active glycopeptide dendrimer colchicine conjugate in the series designated J1C **(1.42)** is shown in Figure 1.52. The presence of β-galactoside groups was found to be necessary for efficient cell binding. In cytotoxicity assays, only three of the dendrimer colchicine conjugates, each carrying two β-galactoside residues in their branches, showed activity. Dendrimers with different

sequences, including a higher valency of galactose or non-galactosylated dendrimers, were non-cytotoxic. Tubulin polymerisation inhibition assays showed no tubulin binding activity for the complete dendrimers, but weak binding for fragments, suggesting that the inactive glycopeptide dendrimer colchicine conjugates are internalised and degraded to release small fragments whose affinity might be significantly weaker than colchicine itself. This may explain the higher LD_{50} values of the conjugates (LD_{50} = 1.5-5.3 μM) compared to free colchicine (LD_{50} = 0.02 μM). While these dendrimer macromolecules may be selectively internalised in cancer cells *in vitro*, their molecular weight is substantially lower than the accepted threshold for EPR effect mediated tumour targeting. Further *in vivo* evaluation is therefore required to demonstrate their potential for selective tumour targeting of cancer cells.

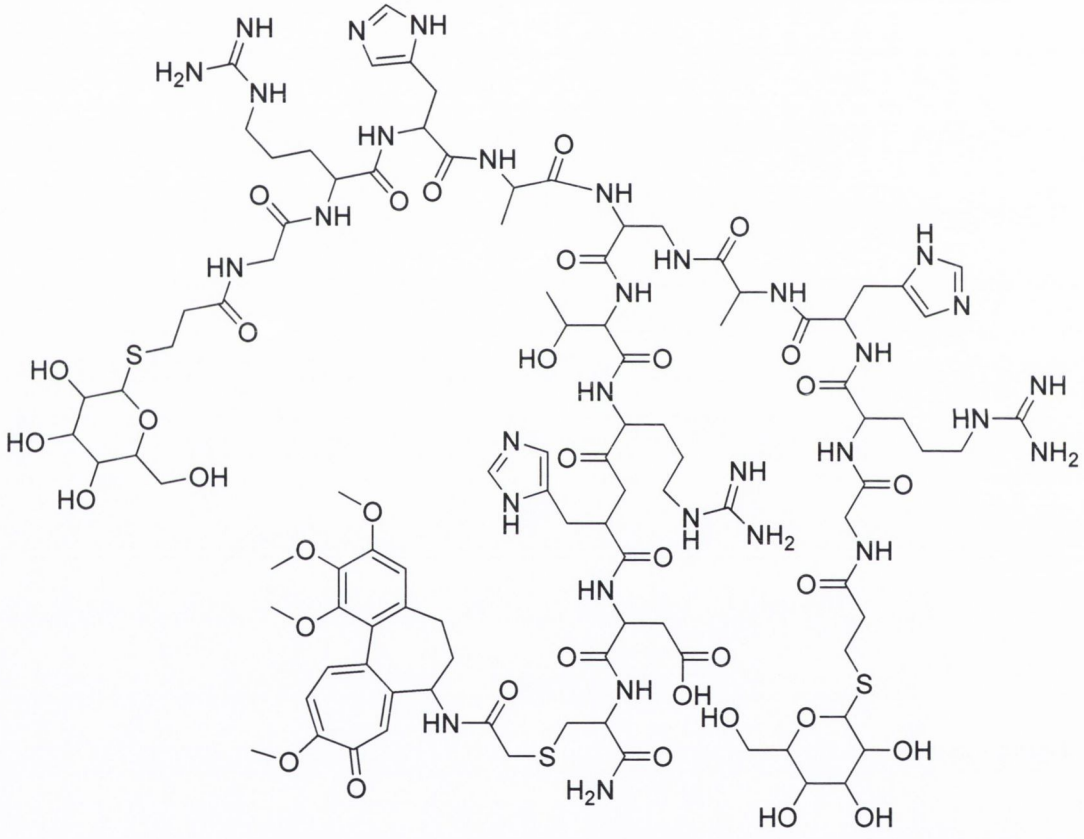

Figure 1.52 Glycopeptide dendrimer colchicine conjugate J1C **(1.42)**

Lagnoux *et al.* also reported the preparation of glycopeptide dendrimer drug conjugates of colchicine equipped with surface glycosides as targeting devices [171]. These dendrimers were shown to inhibit mitosis 20-100 times more potently in HeLa cancer cells (IC_{50} > 1μM) compared to mouse embryonic fibroblasts. Although less potent than free colchicine, these conjugates showed an enhanced selectivity towards cancer cells versus immortalised but non-transformed

cells. In comparison, non-glycosylated dendrimers and colchicine itself show a selectivity of 10-fold or less for HeLa cells. The bioactivity of the glycoprotein dendrimer conjugates is explained in terms of internalisation followed by degradation, with the release of an active colchicine derivative. While this work demonstrates the enhanced selectivity that can be achieved by the use of dendrimers, its applicability to clinically relevant drug development is not readily evident.

1.6.3 Macromolecular conjugates with novel tumour-specific release mechanisms

A number of alternative methodologies have also been explored in order to attain tumour localisation of tubulin binding agent containing macromolecules. Elastin-like polypeptide (ELP) is a thermally responsive biopolymer derived from the hydrophobic domain of tropoelastin [172]. It is composed of repeating pentapeptide units of VPGXaaG, where Xaa is any amino acid except proline. ELP has the interesting property that when heated to a specific temperature it undergoes a phase transition [172]. In an attempt to utilise the unique properties of ELP for focused drug delivery, paclitaxel was bound to an ELP with an inverse phase transition temperature of 40 °C by conjugation with the 6-maleimidocaproyl hydrazone derivative of paclitaxel to afford conjugate **(1.43)** [172]. Focused heating above the phase transition temperature of the ELP at the site of the tumour was found to cause the conjugate to aggregate and thus accumulate selectively at the tumour site. The conjugate also incorporates the cell penetrating peptide, SynB1 at the *N*-terminus of the ELP, in order to cross the cell membrane of tumour cells by adsorptive-mediated endocytosis. *In vitro,* the conjugate displayed 20-fold lower activity against MCF-7 cells when compared with free paclitaxel following a 3 day drug incubation with hyperthermia, whereas the conjugate demonstrated a 2-fold lower activity than free paclitaxel following a 6 day drug incubation. The conjugate also displayed a greater relative activity in MCF-7_{tax} paclitaxel resistant cells compared to unconjugated paclitaxel. The conjugate was found to have a 14-fold lower activity in these cells when compared to sensitive cells, whereas paclitaxel was found to have a 113-fold lower activity against these cells compared to MCF-7 paclitaxel sensitive cells. Therefore, it is suggested that conjugation to ELP may offer a mechanism of delivery of paclitaxel that can over come resistance to paclitaxel. It was acknowledged by the authors of this study that *in vivo* evaluation is necessary to demonstrate the potential of this polymeric conjugate for the enhancement of tumour delivery of paclitaxel.

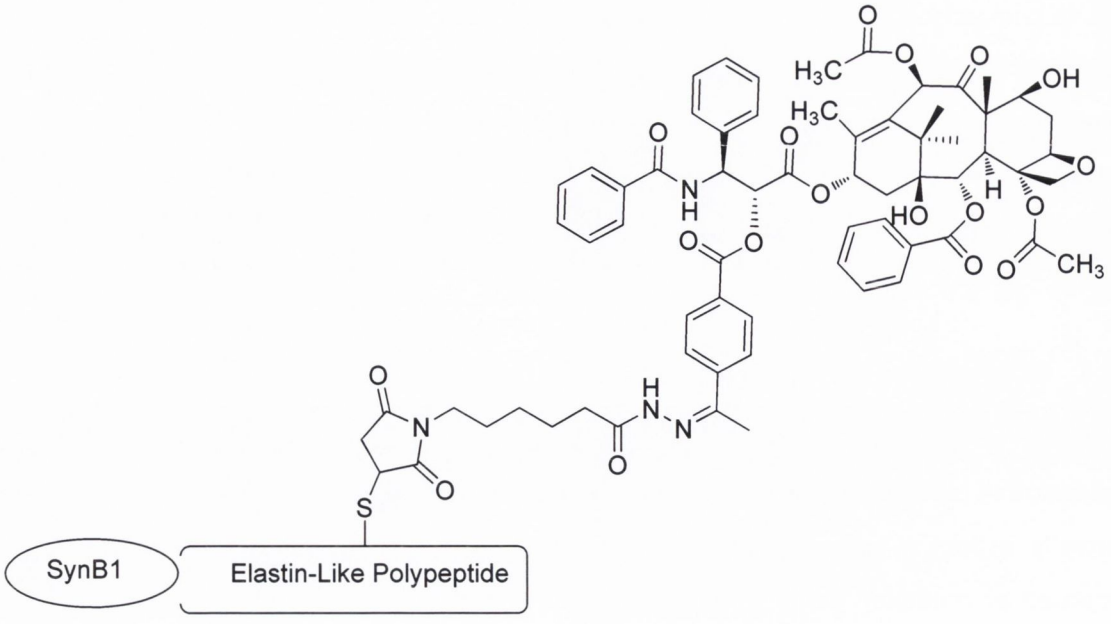

Figure 1.53 SynB1-ELP1-PTX **(1.43)**

Another similar approach, utilising a thermosensitive poly(organophosphazene)-paclitaxel conjugate, was developed by Chun *et al.* [173]. This conjugate was found to be readily soluble in aqueous solution at room temperature but immediately forms a hydrogel once injected into the tumour. *In vitro,* it was shown that the conjugate released paclitaxel over time, with the IC_{50} values of the polymer conjugate 2-6 times lower at 96 h than at 72 h in a number of cancer cell lines. In human gastric cancer (HSC-45M2) cell xenografts in mice, intratumoural injection of the polymer conjugate was found to be more efficacious than the equivalent dose of paclitaxel alone.

Erez *et al.* synthesised a novel macromolecular delivery system for paclitaxel composed of a HPMA copolymer backbone linked *via* a self-immolative dendritic system (designated AB3) to three paclitaxel molecules **(1.44)** [174]. The dipeptide phenylalanine-lysine is a substrate for cathepsin B. Lysosomal cleavage of this dipeptide causes the remainder of the linker to disassemble, liberating the paclitaxel molecules intracellularly. The detail of this enzyme initiated chemical cascade is discussed in detail by Erez *et al.* [174]. While the conjugate exhibited enhanced cytotoxicity on murine prostate carcinoma cells (TRAMP C2) compared to a non-cathepsin cleavable polymer conjugate, an *in vivo* demonstration of enhanced anti-tumour effects is required to fully validate the utility of this mechanism of paclitaxel delivery.

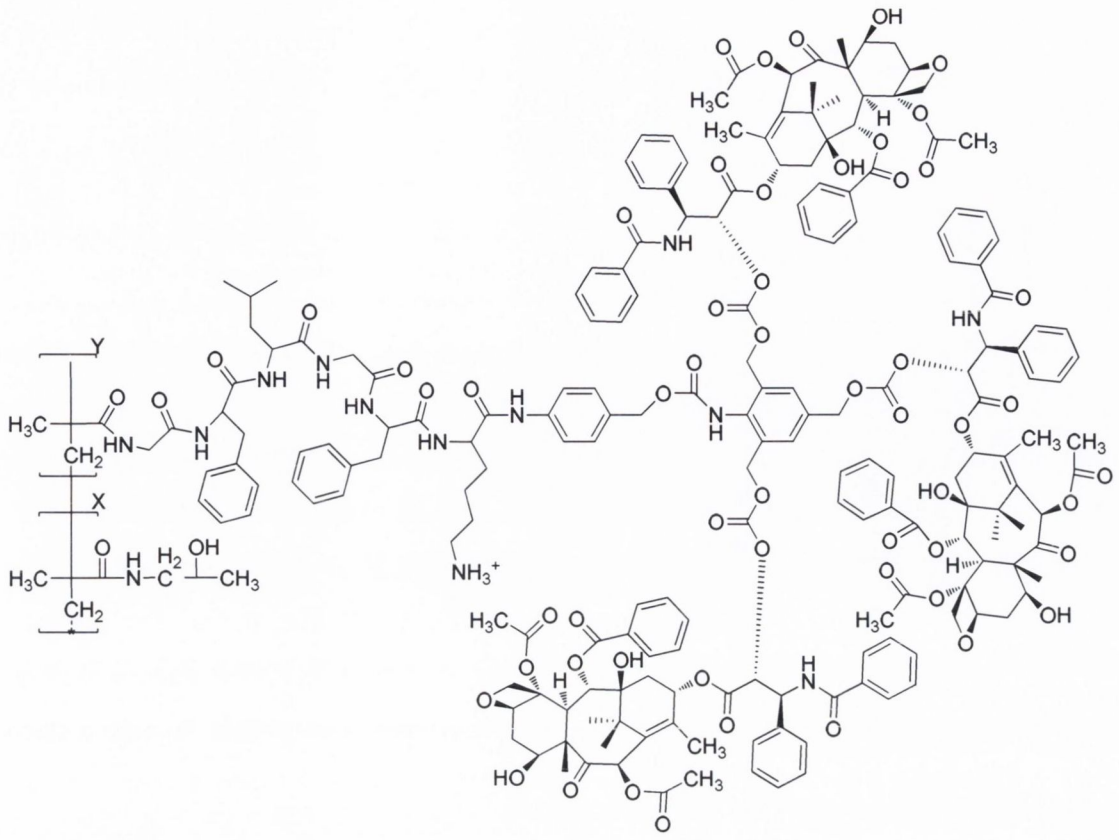

Figure 1.54 HPMA-AB3-(PTX)$_3$ **(1.44)**

A number of HMPA copolymer taxane conjugates were synthesised by Etrych *et al.* utilising different linker units in order to control the pH at which release of the cytotoxic payload occurred [175]. By attaching the conjugates to the polymeric backbone *via* spacers that are stable under physiological conditions (pH 7.4), but hydrolytically degradable in mild acidic environments such as endosomes (pH 5), it was hoped that selective release of the cytotoxic agent could be achieved within tumour cells. It was hypothesised that this would minimise the exposure of normal tissues to the drug. The linker units included levulic acid, 3-acetyl(acrylic acid) and 4-(2-oxopropyl) benzoic acid containing spacer units. Studies indicated much faster release of the cytotoxic agents at pH 5 than at pH 7.4, with the rate dependent on the properties of the linker. Conjugates of paclitaxel containing the levulic acid spacer showed better anti-tumour activity in a 4T1 mouse model of human mammary carcinoma than free paclitaxel, while the docetaxel conjugate containing the levulic acid spacer demonstrated substantial activity in EL4 T cell lymphoma in mice. Both conjugates tested *in vivo* were found to be devoid of toxicity to the animal.

Studies using polylactide-paclitaxel nanoconjugates to which aptamers specific for prostate specific membrane antigen are attached, were also reported to be under development for the selective delivery of paclitaxel to prostate cells [176].

1.7 Miscellaneous conjugates

Several studies have been published investigating the potential of conjugating novel drug delivery entities with tubulin targeting agents. Conjugates containing the adenovirus capsid, glucose and glucose derivatives and thymidine, as well as systems which are activated by light and bioreductive mechanisms in hypoxic tumour tissue, have all been synthesised and evaluated.

Shan *et al.* have recently explored the idea of utilising adenovirus drug delivery vectors for the targeting of existing chemotherapeutic agents, including paclitaxel [177]. The adenovirus capsid conjugated with paclitaxel was designed to be selectively internalised in tumour cells *via* endocytosis following binding of virus fiber protein "knob" domains and cellular Coxsackie adenovirus receptors (CAR). These receptors are variably expressed on human cancer cells and are highly expressed on human hepatocytes potentially leading to liver accumulation [178]. In an effort to broaden the applicability of the adenovirus delivery vector, the viral capsid was covalently conjugated to folic acid in order to make use of folate receptor (FR) mediated endocytosis to further improve the targeted delivery of the paclitaxel payload to target tumour cells. Thus, Shan *et al.* synthesised two folate modified adenovirus nanoparticles-paclitaxel conjugates with two distinct linker units [178]. The first conjugate, folic acid-adenovirus-succinate-paclitaxel (FA-Ad-Suc-PTX) **(1.45)** consisted of a succinate ester containing linker unit while the second conjugate, folic acid-adenovirus-ICG02-Glu-paclitaxel (FA-Ad-ICG02-Glu-PTX) **(1.46)** contained a glutamic acid linker. The dual receptor binding ligands were found to bestow the conjugates with greater selectivity for CAR and FR positive tumour tissue. This was demonstrated by improved cytotoxicity *in vitro* against MDA-MB-231 and SKOV3 human tumour cell lines, compared to free paclitaxel. Both conjugates displayed negligible paclitaxel release following incubation in rat plasma, but were found to release paclitaxel selectively at the tumour site. *In vitro* evaluation indicated that both conjugates inhibited CAR and FR-positive cell lines, with no toxicity observed towards HELF (human embryonic lung fibroblast) cells at equivalent doses. The conjugates were found to be non-hepatotoxic as verified biochemically, by determining levels of AST and ALT, with the FA-AD-Suc-PTX conjugate treatment group showing equivalent levels of these heptaotoxicity markers to control animals. Tumour growth inhibition rates for both conjugates in MDA-MB-231 tumour xenograft models in mice were found to be

superior to free paclitaxel; with inhibition rates of 74.82% reported for FA-AD-Suc-PTX, 45.12% for FA-Ad-ICG02-Glu-PTX and 41.04% for free paclitaxel respectively. Furthermore, the treatment group receiving either conjugate did not experience significant weight loss during the experiment, whereas the paclitaxel treatment group did. Given the extensive *in vitro* and *in vivo* testing of these compounds, they appear to represent a novel and potentially efficacious tumour targeting modality.

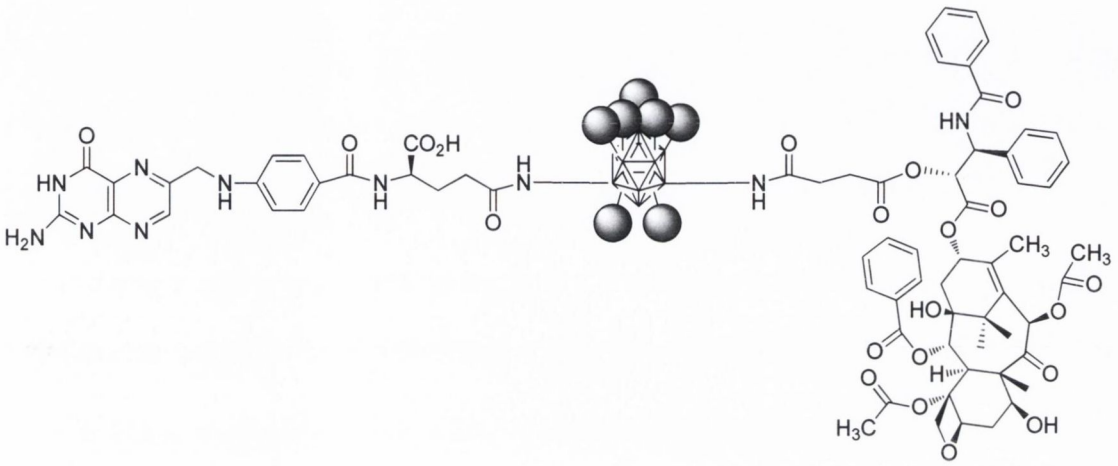

Figure 1.55 FA-AD-Suc-PTX **(1.45)**

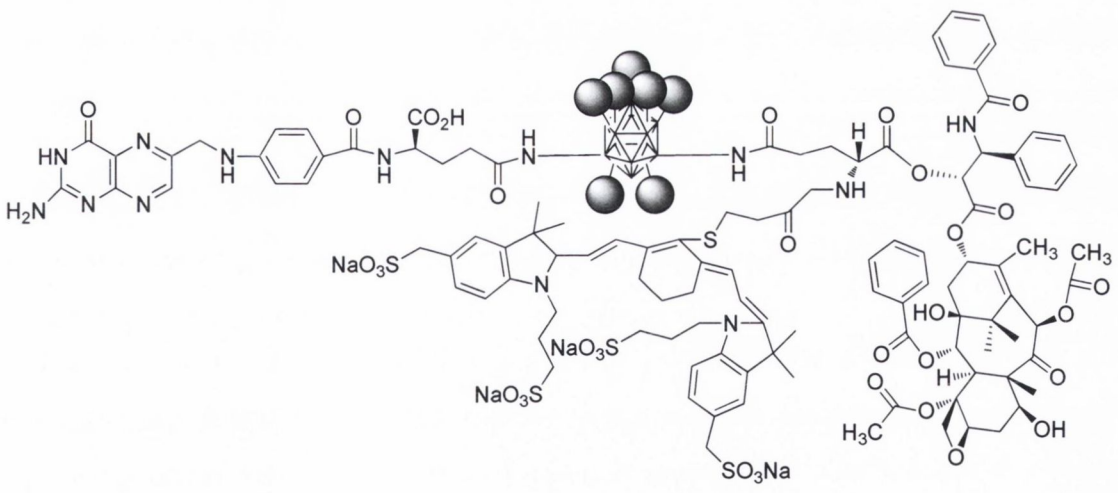

Figure 1.56 FA-Ad-ICG02-Glu-PTX **(1.46)**

Glucose and a number of glucose derivatives have also been conjugated with tubulin binding agents with a view to selectively targeting tumour tissue. Bouvier *et al.* have synthesised a novel glucuronic acid containing conjugate **(1.47)** designed to be activated by human β-glucuronidase

delivered separately to the tumour site [179]. The conjugate consists of glucuronic acid linked covalently to paclitaxel *via* two self-immolative spacer groups. The IC_{50} value of the conjugate in L1210 cells was found to be 1500 nM, while the IC_{50} value of paclitaxel was 9.8 nM. It has also been shown that free paclitaxel can be readily liberated from the prodrug selectively using β-glucuronidase under conditions compatible with *in vivo* experimentation. Nevertheless, it still remains to be proven if this approach will result in clinical benefits, in terms of enhanced efficacy and safety.

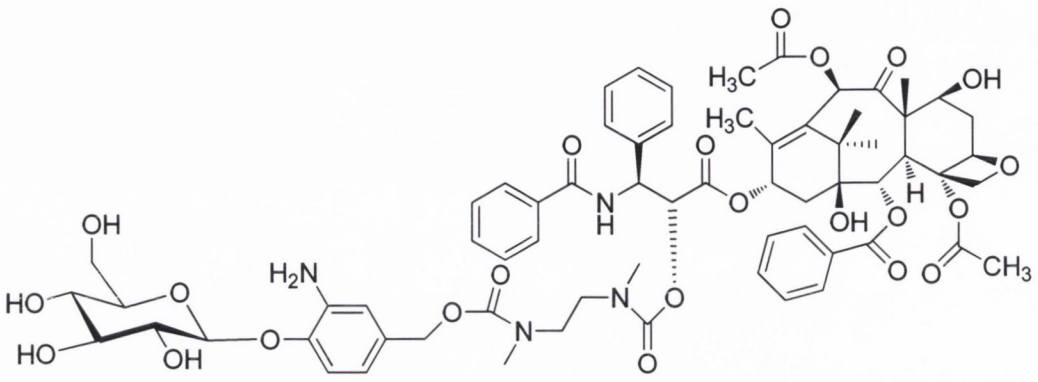

Figure 1.57 Glucuronic acid containing paclitaxel conjugate **(1.47)**

Further work on glucuronic acid containing paclitaxel conjugates was carried out by Alaoui *et al.* [180]. Novel conjugates with different linker units were synthesised and evaluated *in vitro.* These conjugates demonstrated efficient paclitaxel release and comparable IC_{50} values to free paclitaxel in the presence of β-glucuronidase.

In an effort to exploit the increased GLUT expression and β-glucuronidase activity of cancer cells, Lin *et al.* synthesised 2'-paclitaxel methyl 2-glucopyranosyl succinate **(1.48)** [181]. Glucose uptake into cells is mainly mediated by GLUTs (glucose transporters), a family of membrane bound proteins. Cancer cells generally express higher levels of GLUTs than normal cells, due to the increased energy demands of rapid growth and division [182]. The resulting conjugate demonstrated selective cytotoxicity against MCD-7 compared to non-cancer cell lines *in vitro.*

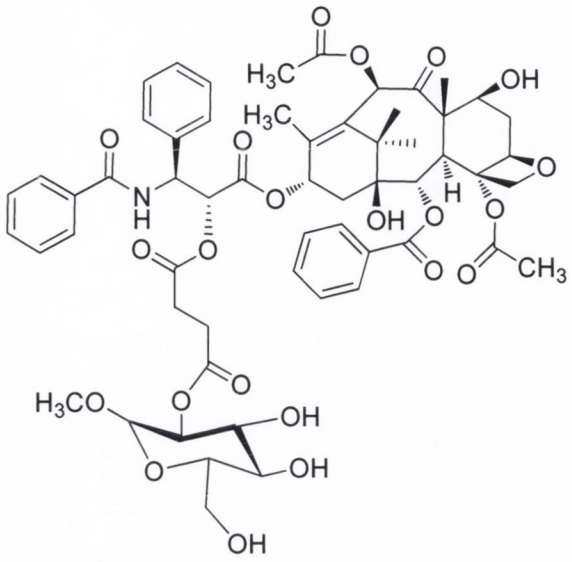

Figure 1.58 Paclitaxel-glucose conjugate **(1.48)**

In related work, Lin *et al.* synthesised two glucose and two glucuronic acid conjugates of paclitaxel [182]. Fluorescent microscopy studies showed that the glucose-paclitaxel conjugates were rapidly transported into cancer cells *via* GLUT mediated transmembrane transport.

A number of kinases, including thymidine kinase 1, are known to be either overexpressed or aberrantly activated in ovarian and colorectal carcinomas, as well as certain leukaemias. By conjugating the tubulin binding agents paclitaxel and vinblastine to thymidine, Aspland *et al.* have suggested that the conjugates become phosphorylated selectively in tumour cells by these overexpressed kinases, essentially trapping the conjugates within the target cells [183]. This proposed mechanism of enhanced selectivity for target cancer cells has been referred to as 'kinase-mediated trapping' of cancer therapeutics. The structure of the thymidine-paclitaxel conjugate **(1.49)** is shown in Figure 1.59. Many of the conjugates synthesised maintained microtubule-binding ability comparable to the parent drug, while several of the chemically phosphorylated conjugates exhibited comparable activity to their non-phosphorylated counterparts. However, phosphorylation rates of 13% to 68% of that of thymidine have been determined. Despite the fact that phosphorylation and tubulin binding of the phosphorylated derivatives has been demonstrated in various biochemical and *in vitro* models, additional *in vivo* experiments are necessary to evaluate any potential gain in selectivity that may be achieved by kinase mediated trapping with these agents.

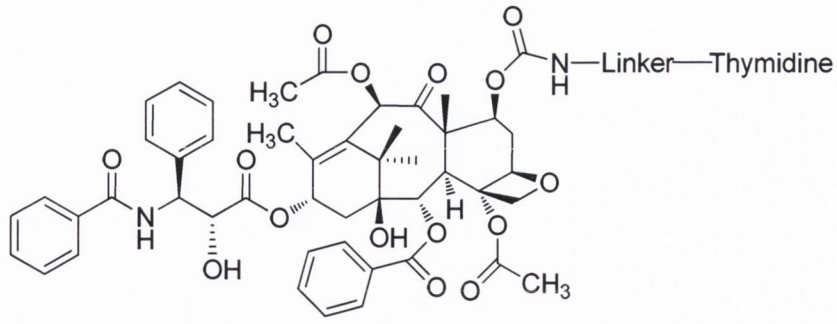

Figure 1.59 Thymidine-paclitaxel conjugate **(1.49)**

A prodrug of paclitaxel that remains biologically inactive until activated by visible light has been designed by Skwarczynski *et al.* [184]. The structure of the conjugate **(1.50)** consists of the O-acyl isoform of paclitaxel to which a coumarin derivative has been conjugated (Figure 1.60). Following exposure to visible light, it was shown that the coumarin is photolytically cleaved and that O-N intramolecular acyl migration yields paclitaxel. Despite the interesting release mechanism of this conjugate, no supporting biological data was presented to demonstrate the validity of this strategy.

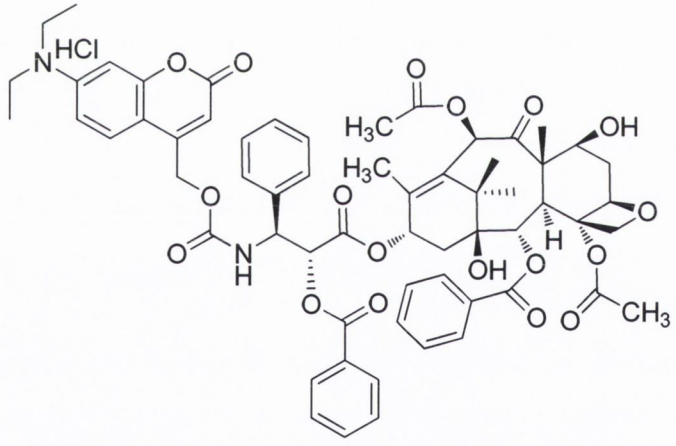

Figure 1.60 Phototaxel **(1.50)**

Attempts to optimise the photoresponsive release of paclitaxel from the conjugate resulted in a further series of so called phototaxels. However, they suffered from poor stability and low rates of paclitaxel release [185].

Paclitaxel prodrugs that undergo bioreductive activation in hypoxic tumour tissue have also been designed and evaluated *in vitro* [186]. Aromatic nitro and azide groups were used as the

bioreductive trigger. While these compounds were found to be stable in buffered solution, a number of the conjugates were not found to have diminished cytotoxicity *in vitro*. Some agents did demonstrate reduced activity in aerobic cell toxicity assays and may represent potentially selective paclitaxel conjugates for *in vivo* evaluation.

1.8 Conclusions

There is currently a vast array of delivery strategies being evaluated for the more selective targeting of tubulin binding agents to the tumour site. Encouragingly, many of these methodologies are resulting in agents with improved tumour cell targeting, enhanced pharmacokinetic characteristics and greater anticancer efficacy. The licensing of brentuximab vedotin in particular marks significant progress towards the synthesis of targeted conjugate molecules and away from non-specific small molecule tubulin inhibitors with their associated toxicities. Macromolecular conjugates are another area where significant progress has been made. Paclitaxel-poliglumex in particular has received considerable attention for its potential to selectively deliver the cytotoxic agent to the tumour site *via* the EPR effect and cathepsin B mediated release. However, recent disappointing phase III clinical trials suggest that further modification of this agent may be required to fully realise its selective tumour targeting potential. A number of the tumour targeting moieties utilised in various macromolecular conjugates appear to have potential to further increase the selectivity of such agents for the tumour site and may offer a solution to the development of clinically useful macromolecular tubulin targeting conjugates.

In the area of non-antibody tumour ligand conjugates, there appears to be great difficulty in the selection of appropriate linkers to connect the tubulin targeting agent and the homing modality. Many of the conjugates are connected to the cytotoxic agents *via* ester based linkers which often results in conjugates with poor stability in circulation leading to premature drug release, poor tumour targeting and increased systemic toxicity. Many of the lessons learned from ADC development in the exploration of appropriate linker technologies could be readily applied to the synthesis of these compounds, potentially leading to much more efficacious conjugates.

A further limitation of the work currently being carried out in the area of non-antibody ligand conjugates of tubulin targeting agents, is the frequent absence of suitable *in vivo* data to confirm the selectivity of a conjugate for tumour cells. In evaluating the tumour specific cytotoxicity of a novel conjugate, *in vivo* demonstration of selective tumour targeting is of paramount importance. While *in vitro* selectivity of a conjugate for one cell line over another is encouraging, *in vivo* evaluation is essential to determine the stability of the conjugate in circulation and the extent of any off-target toxicity. Despite these limitations, many of the conjugates presented are at an advanced stage of clinical evaluation and will undoubtedly contribute to the arsenal of tubulin targeting agent conjugates with improved tumour selectivity.

In conclusion, it would appear that molecular conjugation is most certainly a viable methodology for the synthesis of tubulin targeting agents with improved tumour selectivity, lower incidences of resistance and side effects and superior therapeutic efficacy than currently used clinical agents. Therefore, the work outlined in this thesis, describes the efforts made towards the synthesis of tubulin targeting agents suitable for integration into conjugates of the type described in this chapter.

1.9 Aims of the project

The principal objective of the work described in this thesis was the synthesis of a series of novel tubulin inhibitors with defined stereochemistry and diverse functionality suitable for the formation of molecular conjugates and designed multiple ligands.

The initial aim of the project was to establish a more efficient and high yielding synthetic route to the lead compounds to facilitate further derivatisation and innovation. The synthesis of derivatives of these compounds with superior physicochemical characteristics was then undertaken. The synthesis of an aniline containing tubulin inhibitor was also deemed desirable due to the additional opportunities for further functionalisation which it would afford.

A method of introducing defined stereochemistry into the synthesis of the lead molecules was a major objective of this project. Furthermore, it was hoped to develop a methodology of establishing the enantioselectivity of any stereoselective synthesis and also to determine the absolute configuration of the resultant products.

Once a suitable method of achieving the desired stereochemistry had been established, the synthesis of analogues of the lead molecules with diverse functional groups suitable for further derivatisation and conjugation was to be undertaken. It was hypothesised that the biological evaluation of these novel compounds would enable further optimisation of the tubulin inhibitory pharmacophore.

Building upon the expertise gained from the stereoselective synthesis of the functionalised tubulin inhibitors, the synthesis of a designed multiple ligand (DML) incorporating both tubulin polymerisation and aminopeptidase N inhibition was proposed. It was hypothesised that the purported designed multiple ligand would possess the advantages of the molecular conjugation

approach (tumour site selectivity, dual target activity) but without the inherent disadvantages of this methodology (large molecular size, poor physicochemical characteristics). Therefore, the synthesis of this designed multiple ligand became the ultimate synthetic aim of the work outlined in this thesis.

2 Chapter 2

2.0 Introduction

A series of novel tubulin polymerisation inhibitors was synthesised by Dr. R. Shah as part of the work submitted for his doctoral thesis [187]. These compounds were biaryl, conformationally restricted analogues of the naturally occurring tubulin binding agent combretastatin A-4 **(2.01)**.

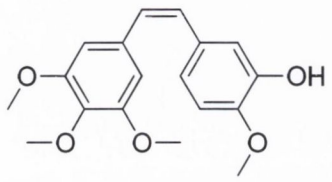

(2.01)

Figure 2.1 Combretastatin A-4

Extensive structure-activity relationship studies carried out on these compounds, by Shah and subsequently by Hudson, revealed a discernable pattern of structural characteristics among the most biologically active compounds (Figure 2.2) [187-188]. The 2,3,4-trimethoxy A-ring was found to be essential for tubulin-binding activity. The most active compounds were also found to contain a 3-hydroxy-4-methoxyphenyl C-ring. The presence of an oxygen containing functional group at the C-7 position was found to confer greatly enhanced activity, while the double bond at C-8 and C-9 was also found to be critical for tubulin-binding activity.

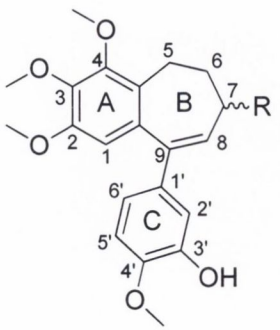

Figure 2.2 Core structure of lead tubulin polymerisation inhibitors

The most active compounds in the series, **(2.02)** and **(2.03)**, were found to possess all the essential characteristics necessary for potent tubulin binding activity (Figure 2.3). Compound **(2.02)** was found to have an IC_{50} value of 1.10 μM in the tubulin polymerisation inhibition assay, while compound **(2.03)** had an IC_{50} value of 1.05 μM. These results compared very favourably with the activity of the model compound combretastatin A-4, which had an IC_{50} value of 1.45 μM. As a result of their encouraging activity, these molecules became the lead compounds for the work described in this thesis.

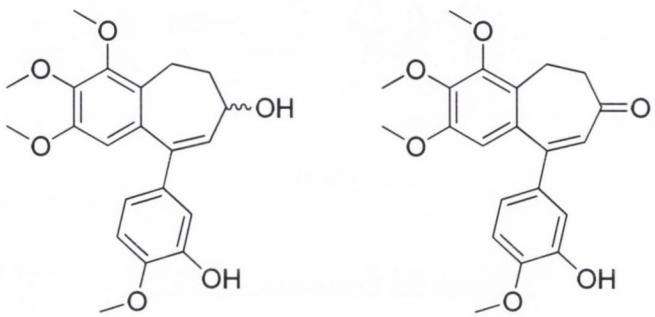

(2.02) **(2.03)**

Figure 2.3 Lead molecules **(2.02)** and **(2.03)**

2.1 Aims and objectives

The synthesis of compounds **(2.02)** and **(2.03)**, as initially described by Shah and subsequently by Hudson, remained challenging and ultimately poor yielding [187-188]. Therefore, the initial aim of the work described in this chapter was to optimise the synthesis of **(2.02)** and **(2.03)**, in particular, in order to obtain sufficient quantities for further *in vitro* and *in vivo* evaluation.

The synthesis of the water soluble phosphate ester prodrug of **(2.02)** was subsequently devised, in order to facilitate its *in vivo* evaluation.

Replacement of the C-ring hydroxyl functionality with an amino group was also investigated. It was proposed that this analogue would offer additional opportunities for the synthesis of molecular conjugates.

2.2 Original synthesis of lead compounds (2.02) and (2.03)

2.2.1 Malonic acid coupling and reduction

2,3,4-Trimethoxybenzaldehyde was coupled to malonic acid using pyridine as solvent and piperidine as base. This afforded compound **(2.04)** and achieved some elongation of the carbon chain. The double bond was then reduced by catalytic hydrogenation using palladium on activated carbon (5% w/w) under an atmosphere of hydrogen to afford **(2.05)** (Scheme 2.1).

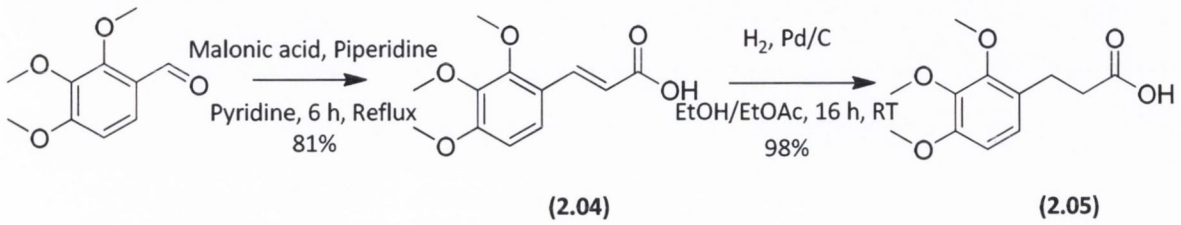

(2.04) **(2.05)**

Scheme 2.1 Coupling of malonic acid and reduction of double bond

2.2.2 Meldrum's acid coupling and methanolysis

Compound **(2.05)** was coupled with Meldrum's acid using DCC (*N,N'*-dicyclohexylcarbodiimide) as coupling reagent and DMAP (4-dimethylaminopyridine) as catalyst. The crude coupled product, compound **(2.06)** was then subject to methanolysis to afford the β-keto ester **(2.07)** (Scheme 2.2).

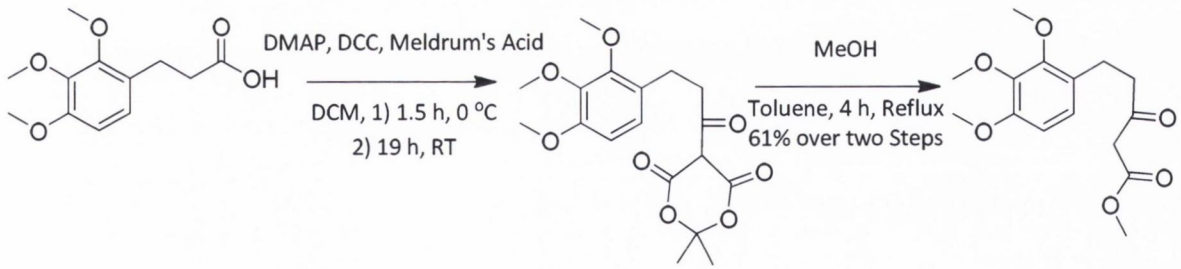

(2.05) **(2.06)** **(2.07)**

Scheme 2.2 Meldrum's acid coupling and methanolysis

2.2.3 Reduction of ketone (2.07) and protection of alcohol (2.08)

The β-ketone functionality of **(2.07)** was reduced by the addition of sodium borohydride at -15 °C to afford alcohol **(2.08)**. The alcohol of compound **(2.08)** was then protected using *tert*-

butyldiphenylsilyl chloride (TBDPSCl), together with imidazole as base and DMF as solvent to afford **(2.09)** (Scheme 2.3).

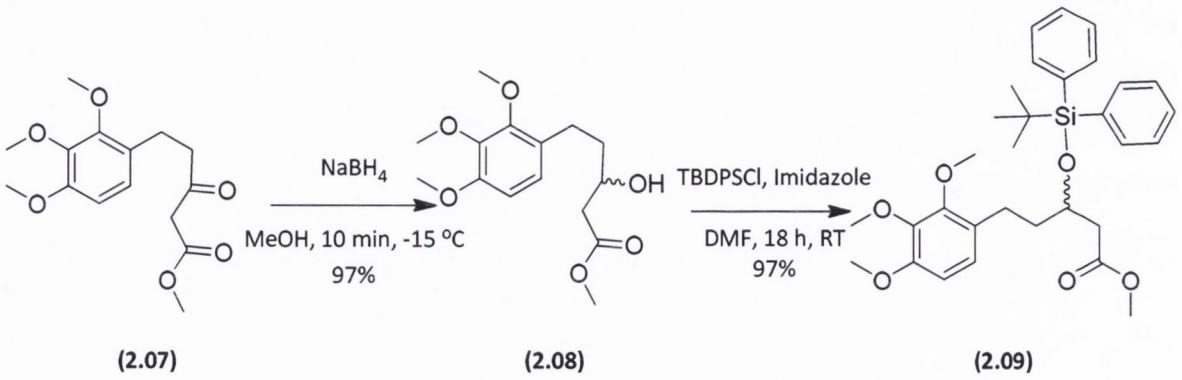

Scheme 2.3 Reduction of ketone **(2.07)** and protection of resulting alcohol **(2.08)**

2.2.4 Hydrolysis of methyl ester (2.09) and intramolecular cyclisation

The methyl ester **(2.09)** was then dissolved in methanol and THF and hydrolysed using sodium hydroxide aqueous solution, to afford the carboxylic acid **(2.10)**. The free carboxylic acid was activated by the formation of an acid chloride. The intramolecular cyclisation reaction catalysed by tin (IV) chloride solution was then carried out to afford **(2.11)** (Scheme 2.4).

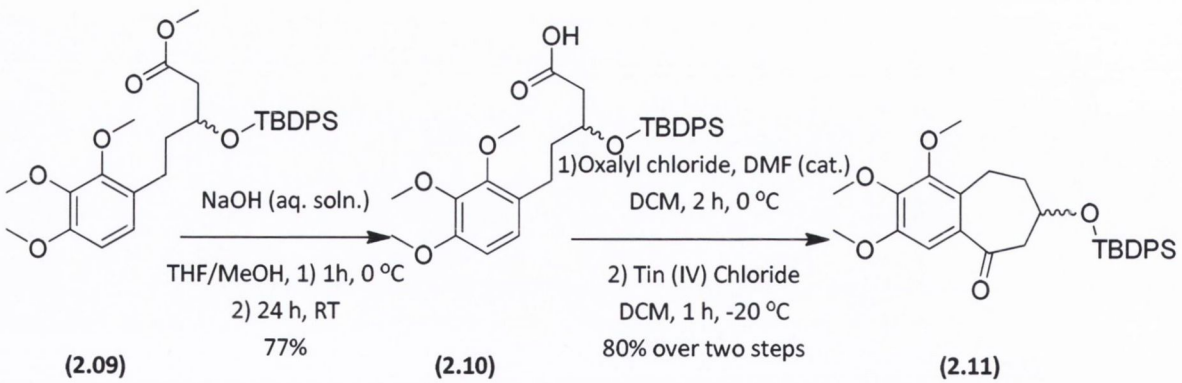

Scheme 2.4 Synthesis of ketone **(2.11)**

2.2.5 Synthesis of C-ring (2.14)

The C-ring component was synthesised in parallel. Commercially available 5-bromo-2-methoxybenzaldehyde was subjected to Baeyer-Villager oxidation to afford the formate ester

(2.12). Hydrolysis of the formate ester to yield 5-bromo-2-methoxy phenol **(2.13)** was then accomplished using sodium hydroxide aqueous solution in methanol/THF. The phenol group of **(2.13)** was then protected by the use of *tert*-butyldimethylsilyl chloride (TBDMSCl), together with the use of imidazole as base to afford **(2.14)** (Scheme 2.5).

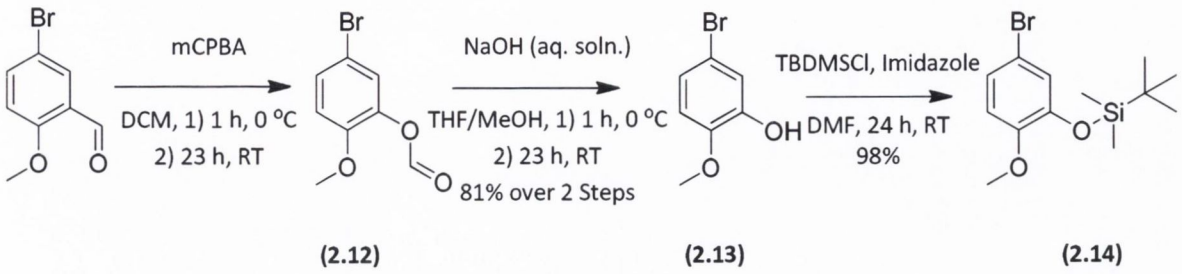

(2.12) **(2.13)** **(2.14)**

Scheme 2.5 Synthesis of phenol containing C-ring **(2.14)**

2.2.6 Organolithium coupling of (2.11) and (2.14)

Compound **(2.11)** was then coupled to compound **(2.14)** using an organolithium coupling reaction. The C-ring bromide **(2.14)** was lithiated with *n*-butyllithium (nBuLi) at -78°C. The AB ring component, **(2.11)**, was then added. Following work-up with HCl aqueous solution, a molecule of water was lost to afford compound **(2.15)** (Scheme 2.6).

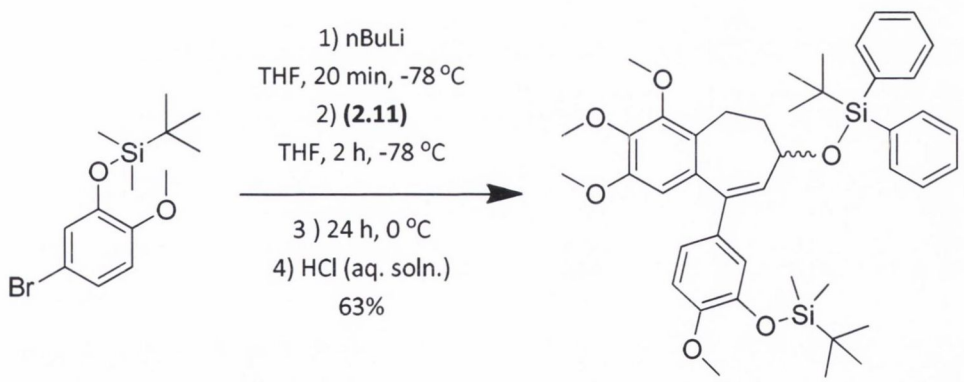

(2.14) **(2.15)**

Scheme 2.6 Organolithium coupling reaction to yield **(2.15)**

2.2.7 Removal of silyl protecting groups of (2.15) and oxidation

The two silyl protecting groups on **(2.15)** were simultaneously removed by the addition of TBAF solution to afford compound **(2.02)**. The C-7 position alcohol was then oxidised using pyridinium dichromate (PDC) to afford compound **(2.03)** in poor yield (13%; Scheme 2.7).

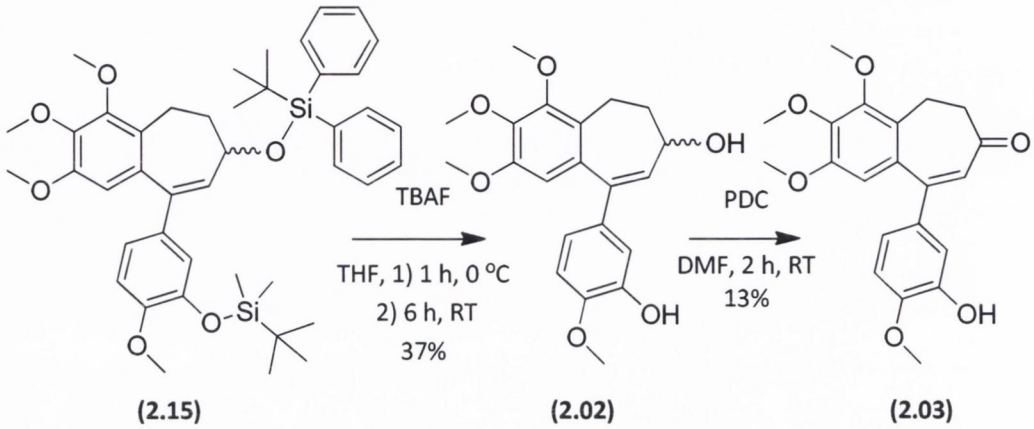

Scheme 2.7 Deprotection and oxidation to afford **(2.02)** and **(2.03)**

2.3 Improved synthesis of lead compounds (2.02) and (2.03)

Due to the long and difficult synthesis of compounds **(2.02)** and **(2.03)**, an alternative synthetic route with fewer steps and a higher yield was deemed extremely desirable. To this end, an alternative synthetic scheme was developed.

2.3.1 Synthetic strategy

In the protocol employed by Hudson, furnishing the key intermediate **(2.07)** necessitated a four-step synthetic scheme. Furthermore, the synthetic route involved two steps requiring refluxing conditions. A Wittig reaction was thus explored as the pivotal step in a potential alternative path to this intermediate. It was suggested that if the appropriate Wittig reagent could be identified, then it could be possible to synthesise an analogue of compound **(2.07)** in only 2 steps from 2,3,4-trimethoxybenzaldehyde.

Furthermore, the oxidation of the secondary alcohol **(2.02)** using PDC was identified as a significant obstacle to the synthesis of compound **(2.03)** in acceptable yield. Depending on the scale of the reaction, yields as low as 13% had been reported for this transformation. It was

hypothesised that oxidation of the C-ring phenol was occurring, resulting in the formation of an undesired quinone type structure [189]. It was proposed that a suitable protection strategy for the phenolic alcohol group combined with the use of Dess-Martin periodinane (DMP) could accomplish the desired oxidation in significantly improved yield, without the use of the toxic, chromium based reagent PDC.

2.3.2 Alternative synthesis of (2.10) utilising the Wittig reaction

The Wittig reaction is an olefination reaction between an aldehyde or ketone and a species known as a phosphonium ylide (also known as a Wittig reagent) [190]. The proposed mechanism for this reaction is illustrated in Scheme 2.8.

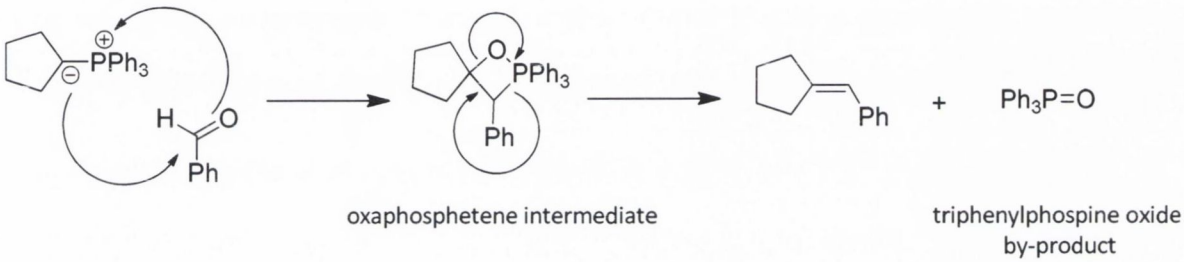

Scheme 2.8 Proposed mechanism of the Wittig reaction [190]

The four-membered oxaphosphetene intermediate is particularly unstable and affords the desired alkene *via* elimination. The strength of the oxygen-phosphorous bond formed in the triphenylphosphine oxide by-product acts as the driving force for the reaction [190].

2.3.2.1 Synthesis of ylide (2.16)

Ylides are formed from phosphonium salts by deprotonating them with a strong base. Using a procedure reported by Carter, the commercially available phosphonium salt, [3-(ethoxycarbonyl)-2-oxypropyl]triphenyl-phosphonium chloride was reduced to its corresponding ylide using sodium hydride [191]. The ylide was then reacted *in situ* with 2,3,4-trimethoxybenzaldehyde to afford compound **(2.16)** (Scheme 2.9).

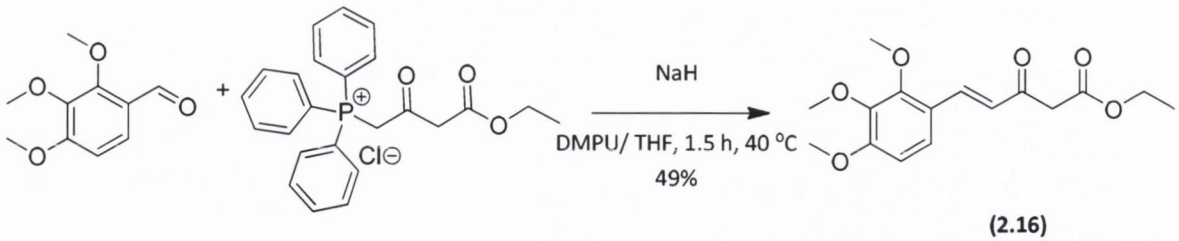

(2.16)

Scheme 2.9 Formation of ylide and reaction with 2,3,4-trimethoxybenzaldehyde *in situ*

N,N'-dimethylproyleneurea (DMPU) was used as a co-solvent. The presence of the ketone group adjacent to the phosphorous-carbon bond on the reactant ylide acted as a conjugating or anion-stabilising substituent for the negative charge. Therefore, the ylide was said to be stabilised [190]. An elevated temperature and long reaction time was thus required to push the reaction to completion. It would be expected that the stabilised ylide would lead to the formation of predominantly the (*E*)-alkene [190]. However, this was not considered significant because the resulting olefin intermediate was subsequently reduced without characterisation. Monitoring the progress of the reaction was complicated by the fact that both the product and the aldehyde starting material had the same R_f value on TLC. Therefore, potassium permanganate solution was used to visualise the unsaturated product as it formed. Once the reaction was deemed to have gone to completion, the mixture of aldehyde starting material and product was purified by flash column chromatography. Due to the complexity of the resulting NMR spectrum, the resultant mixture containing **(2.16)** was carried forward without further characterisation.

2.3.2.2 Reduction of (2.16)

The enone **(2.16)** was then reduced using palladium on activated carbon (5% w/w) in a mixture of ethyl acetate and ethanol (1:1) under an atmosphere of hydrogen. After 24 h, two principal products were observed. Following purification and characterisation the products were identified as the desired β-keto ester **(2.17)** and the further reduced β-hydroxy ester **(2.18)** (Scheme 2.10).

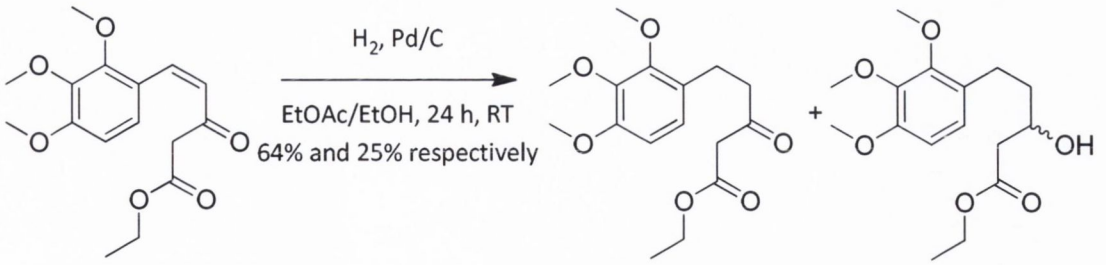

(2.16) **(2.17)** **(2.18)**

Scheme 2.10 Reduction of **(2.16)**

2.3.2.3 Characterisation of β-keto ester (2.17)

The β-keto ester **(2.17)** was observed to have the same R_f on TLC as the starting material **(2.16)**. However, the desired β-keto ester was readily identified by NMR analysis. Eight CH_2 protons were clearly apparent in the ^1H spectrum at 2.74 ppm (2 x CH_2), 3.36 ppm and 4.08 ppm (Figure 2.4). The ester methyl group was found to resonate as a triplet (J = 7.27 Hz) at 1.17 ppm. The three remaining methoxy group proton signals were identified as singlets at 3.73 ppm, 3.76 ppm and 3.79 ppm (Figure 2.4). The two aromatic CH protons were found to resonate as two doublets (J = 8.7 Hz) at 6.50 ppm and 7.73 ppm (Figure 2.4).

In the DEPT 135 NMR spectrum, four CH_2 signals were present at 23.54 ppm, 43.22 ppm, 48.71 ppm and 60.66 ppm (Figure 2.5). The ester methyl group was assigned to the furthest upfield signal at 13.52 ppm while the remaining methoxy CH_3 signals were found at 55.34 ppm, 60.06 ppm and 60.21 ppm. Finally, the two carbonyl carbons were found to resonate furthest downfield at 166.64 ppm and 201.80 ppm, while the four remaining quaternary carbons were found at 125.80 ppm, 141.64 ppm, 151.25 ppm, and 151.85 ppm (Figure 2.5).

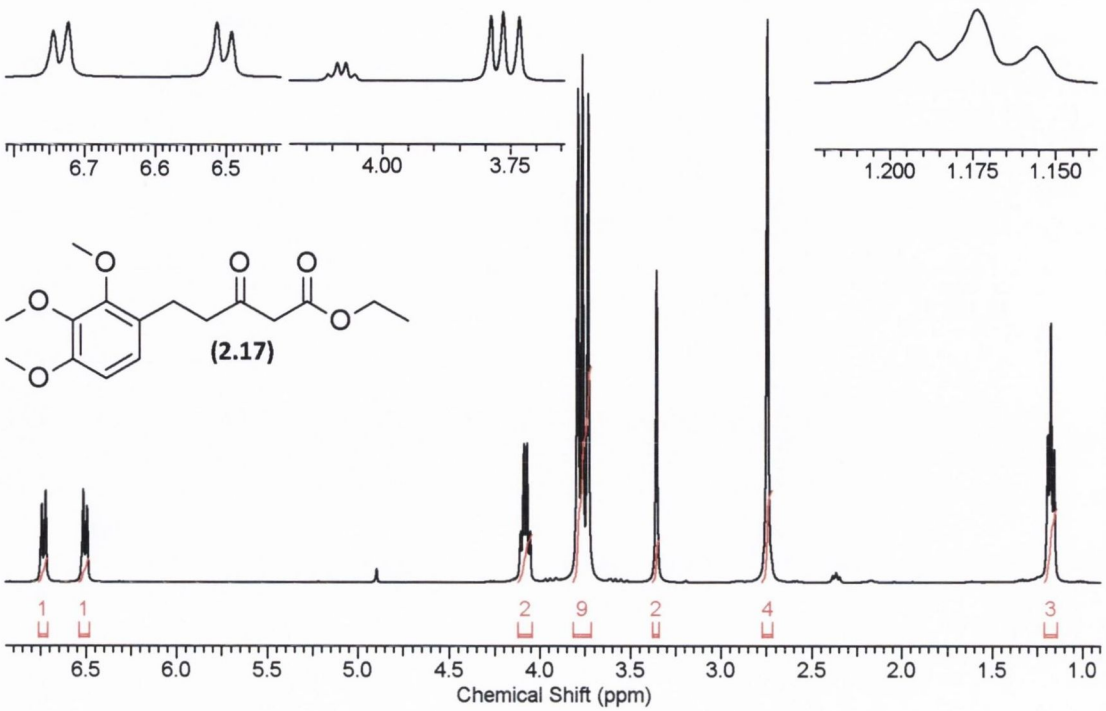

Figure 2.4 ^{1}H NMR spectrum of **(2.27)**

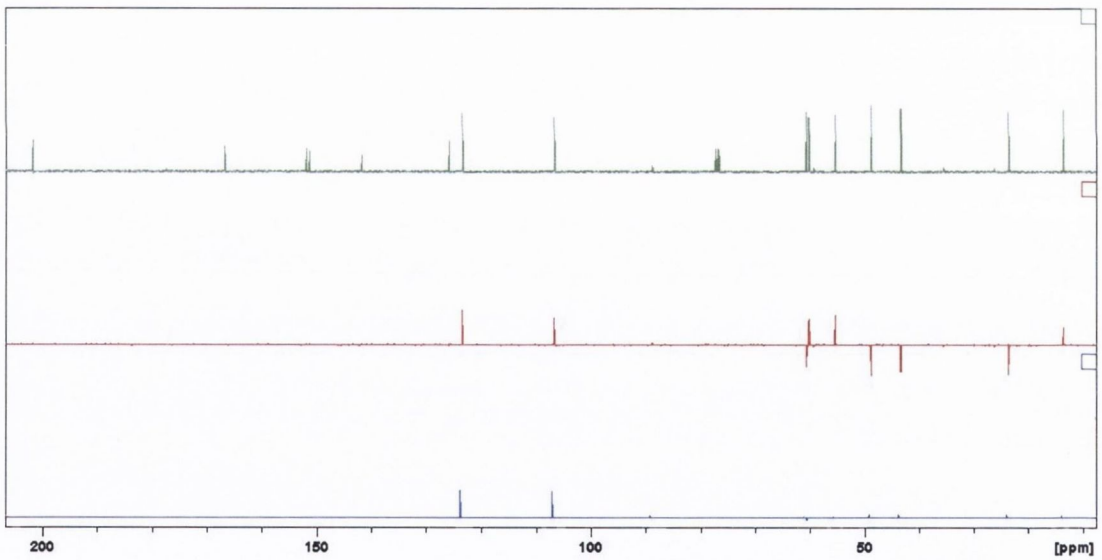

Figure 2.5 ^{13}C, DEPT 135 and DEPT 90 spectra of **(2.17)**

Further confirmation of identity was derived from the mass spectrometry data. The molecular ion peak $[M+Na]^+$ was observed to have a mass of 333.1320, closely correlating with the calculated value of 333.1314. The presence of two distinct carbonyl stretching absorption bands in the IR spectrum at 1743.98 cm^{-1} and 1716.23 cm^{-1} further indicated the presence of the two carbonyl functionalities within the molecule.

2.3.2.4 Characterisation of β-hydroxy ester (2.18)

The β-hydroxy ester **(2.18)** was found to have a lower R_f on TLC than the enone starting material **(2.16)** or β-keto ester product **(2.17)**. The identity of **(2.18)** was confirmed by NMR analysis. The ester CH_3 group resonated furthest upfield as a triplet (J = 7.42 Hz) at 1.25 ppm (Figure 2.6). A broad alcohol proton signal at 3.23 ppm was observed in the ^1H NMR spectrum. A multiplet at 3.98 ppm corresponding to the alcohol carbon's lone proton was also observed. Eight CH_2 proton signals were apparent as four discrete multiplets at 1.72 ppm, 2.47 ppm, 2.69 ppm and 4.15 ppm. The two neighbouring aromatic protons on the A-ring resonated as two doublets (J = 8.5 Hz) at 6.60 ppm and 6.84 ppm (Figure 2.6). The presence of only one carbonyl signal in the ^{13}C NMR spectrum at 172.39 ppm also indicated that the β-ketone functionality had been reduced (Figure 2.7). Four CH_2 carbon signals were apparent at 25.14 ppm, 37.20 ppm, 40.95 ppm and 60.15 ppm from the DEPT 135 NMR spectrum. The four methoxy carbons resonated at 13.70 ppm, 55.51 ppm, 60.27 ppm and 60.51 ppm respectively. The carbon attached to the alcohol group was found to resonate at 66.78 ppm. The four remaining quaternary carbons were assigned to peaks at 123.51 ppm, 127.00 ppm, 141.70 ppm and 151.31 ppm respectively.

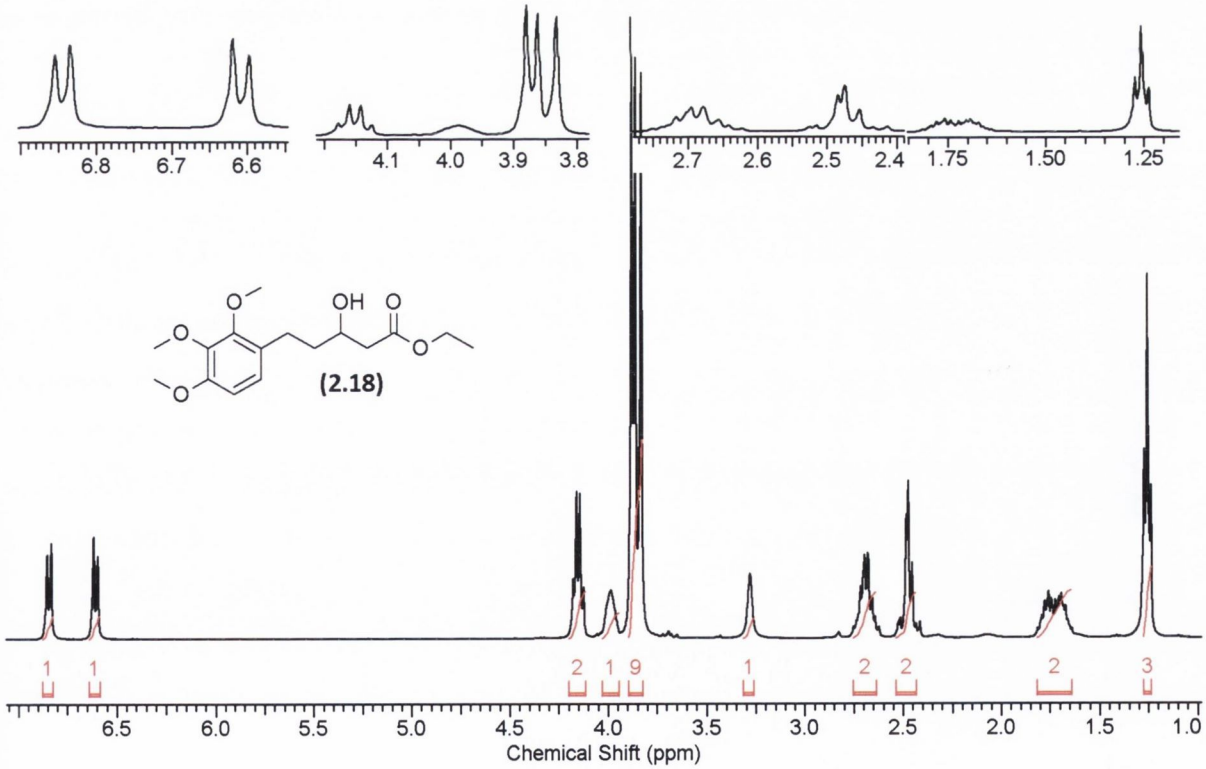

Figure 2.6 ^1H spectrum of **(2.18)**

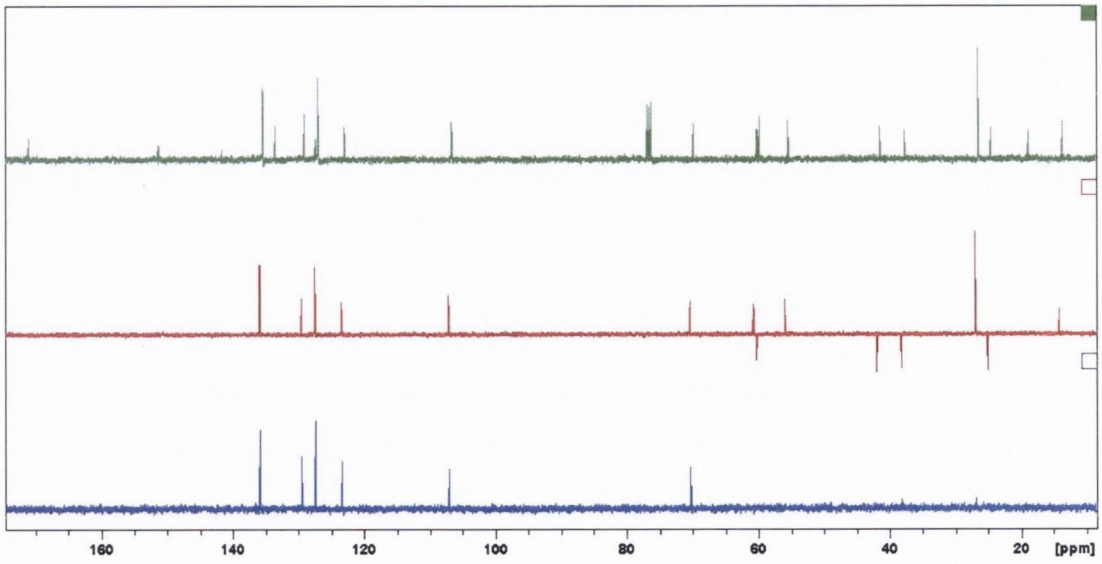

Figure 2.7 ^{13}C, DEPT 135 and 90 NMR spectra of **(2.18)**

Mass spectrometry was also used to further confirm the identity of **(2.18)**. The mass of the molecular ion peak $[M+Na]^+$ was found to be in very close agreement with the calculated value (found = 335.1474, observed = 335.1471). The presence of a single absorption band in the carbonyl region of the IR spectrum at 1726.08 cm^{-1} also indicated the presence of the ester functional group within in the structure of **(2.18)**.

2.3.2.5 Optimising the Wittig reaction

A commercially available source of the ylide **(2.16)** was obtained and a variety of reaction conditions were investigated in order to establish the optimal conditions for the reaction (Table 2.1). The Wittig reactions were all carried out using 1 equivalent of 2,3,4-trimethoxybenzaldehyde and 1.2 equivalents of ylide and were conducted at room temperature. The reductions were carried out in ethyl acetate and ethanol (1:1) using palladium on activated carbon (5% w/w) under an atmosphere of hydrogen overnight. From the comparative study, it was found that methanol was the most suitable solvent and that a longer reaction time resulted in a higher yield.

Reaction Conditions	Solvent	Wittig Reaction Time (h)	Hydrogenation Reaction Time (h)	Ketone Yield (%)	Alcohol Yield (%)
A	THF	2	19	11	n/a
B	Methanol	4	19	27	8
C*	Methanol	4	19	23	15
D	Methanol	24	19	62	21
E	DCM	24	19	n/a	n/a
F	Methanol	60	19	57	23
G	THF	60	19	6.3	8

Table 2.1 Comparison of reaction conditions and yields for the Wittig reaction. The ketone and alcohol yields for each hydrogenation reaction are given since both products were formed in each case. *Aldehyde was added in two aliquots, 2 h apart.

2.3.2.6 Synthesis of carboxylic acid (2.10) from β-keto ester (2.17)

Once the optimal set of reaction conditions had been established, the synthesis was scaled up appropriately. The ketone **(2.17)**, obtained from reduction of the Wittig reaction product, was further reduced using sodium borohydride to afford **(2.18)**.

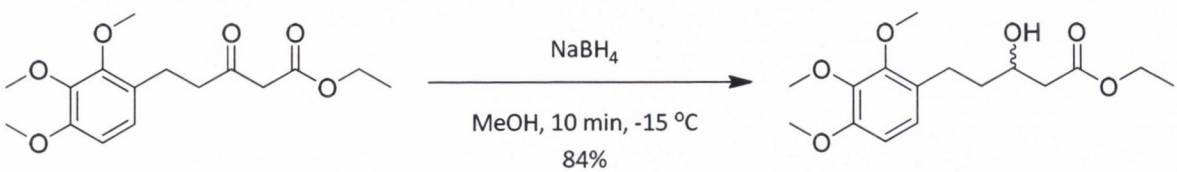

(2.17) **(2.18)**

Scheme 2.11 Reduction of β-keto ester **(2.17)**

The alcohol **(2.18)** was then protected using *tert*-butyldiphenylsilyl chloride together with imidazole as base, to afford **(2.19)** in moderate yield (71%). Finally, the resulting protected compound **(2.19)** was hydrolysed readily, using sodium hydroxide aqueous solution, to afford the carboxylic acid **(2.10)** in excellent yield (91%; Scheme 2.12).

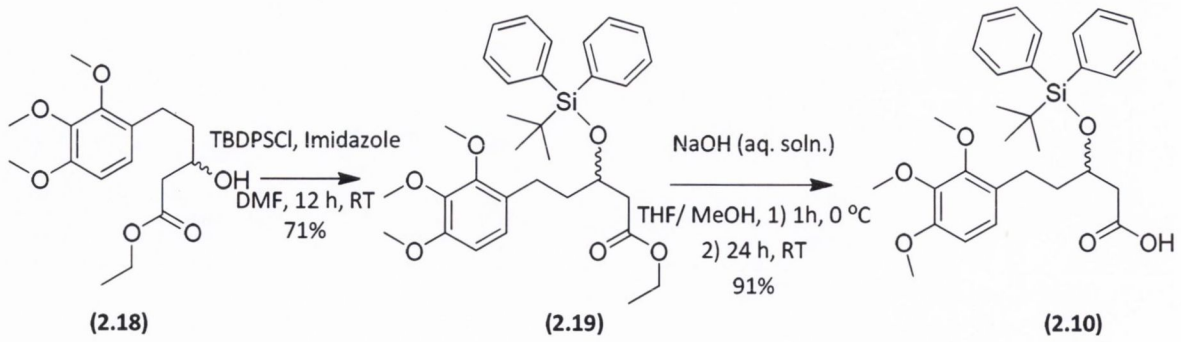

Scheme 2.12 Protection of alcohol **(2.18)** and hydrolysis of ester **(2.19)**

Overall, the revised synthetic sequence employing the Wittig reaction, resulted in a yield of **(2.10)** comparable to that obtained for the original synthetic scheme devised by Hudson (33% v 36%). However, more significantly, it accomplished this in two fewer synthetic steps (5 v 7). It was proposed that the revised synthesis of **(2.10)** was also significantly more energy and time efficient as it avoids the large scale reflux and anhydrous reactions required in the original synthesis.

2.3.3 Alternative oxidation of C-7 alcohol using Dess-Martin periodinane

Dess-Martin periodinane (DMP or 1,1,1-triacetoxy-1,1-dihydro-1,2-benziodoxol-3(L*H*)-one) is a pentavalent, iodine based oxidising reagent [192]. It is currently gaining increasing favour in organic synthesis, with a reputation as one of the mildest and most convenient reagents available for the oxidation of alcohols [193]. Dess-Martin periodinane was therefore explored as an alternative oxidising reagent in the regioselective oxidation of the secondary alcohol **(2.02)**. The alcohol **(2.02)** was dissolved in DCM and DMP was added (Scheme 2.13).

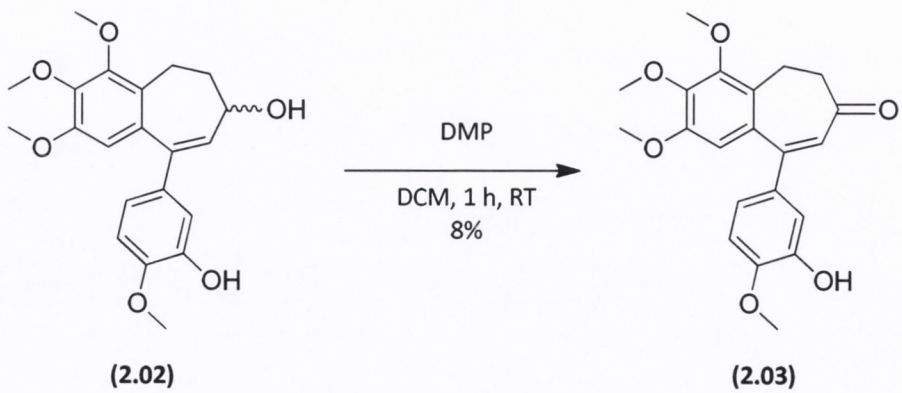

Scheme 2.13 DMP oxidation of **(2.02)**

Disappointingly, the change in oxidising reagent did little to affect the outcome of the reaction, with a yield as low as 8% recorded for this transformation. It was hypothesised that oxidation of the C-ring phenol was again responsible for the poor performance of this reaction. A review of the literature revealed additional evidence for the oxidation of phenol containing systems to quinones under conditions analogous to those employed here [194]. Therefore, an alternative approach involving the protection of the phenol prior to oxidation was explored.

2.3.4 Oxidation of secondary alcohol in the presence of protected phenol

In the original synthesis of **(2.03)** developed by Shah, the organolithium coupling reaction was carried out using an AB-ring system with a free alcohol group [187]. This was undertaken as it was envisaged that the steric hindrance, caused by the bulk of the *tert*-butyldiphenylsilyl protecting group, would compromise the success of the reaction. This methodology was thus employed in order to facilitate an oxidation reaction in which the phenol group was suitably protected.

2.3.4.1 Synthesis of coupled compound with protected phenol

The silyl protecting group on the cyclised compound **(2.11)** was removed using TBAF solution to afford **(2.20)** in moderate yield (54%) as a yellow oil (Scheme 2.14).

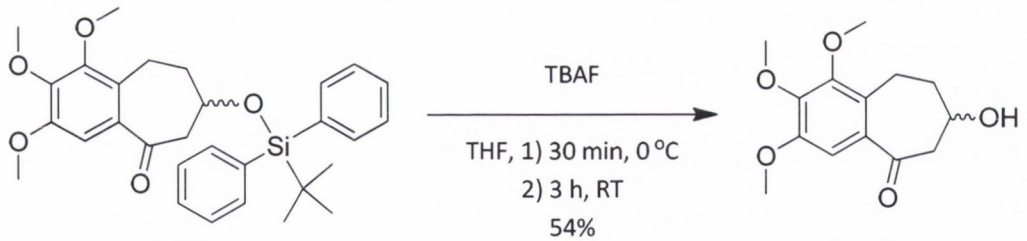

(2.11) **(2.20)**

Scheme 2.14 Silyl deprotection of **(2.11)**

The organolithium coupling reaction was then carried out, in an analogous fashion to that used for the protected alcohol **(2.11)**, to yield the tricyclic compound **(2.21)** in 70% yield (Scheme 2.15).

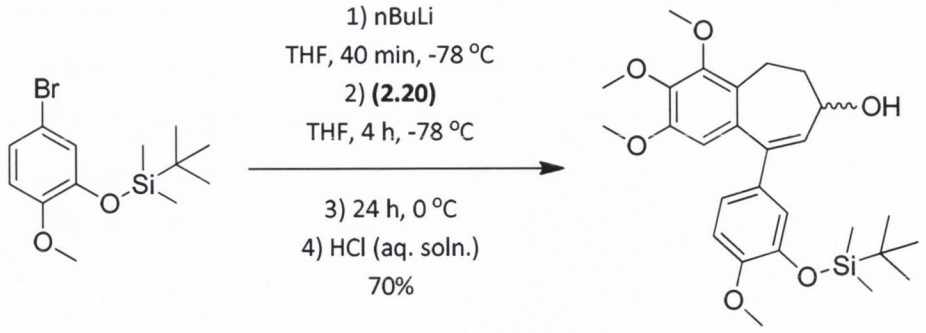

(2.14) **(2.21)**

Scheme 2.15 Revised organolithium reaction to afford **(2.21)**

It was found that the elimination reaction involving the formation of the double bond occurred much more readily during acid work-up in this case compared with the protected compound **(2.15)**. This resulted in a cleaner and more convenient work-up and purification of the product.

2.3.4.2 Oxidation and removal of phenolic silyl protecting group

The allylic hydroxyl group of **(2.21)** subsequently underwent facile oxidation in the presence of DMP in DCM to afford **(2.22)** (Scheme 2.16). The outcome of this reaction represented a dramatic increase in yield compared with the analogous reaction carried out in the presence of the free phenol group (87% v 8%).

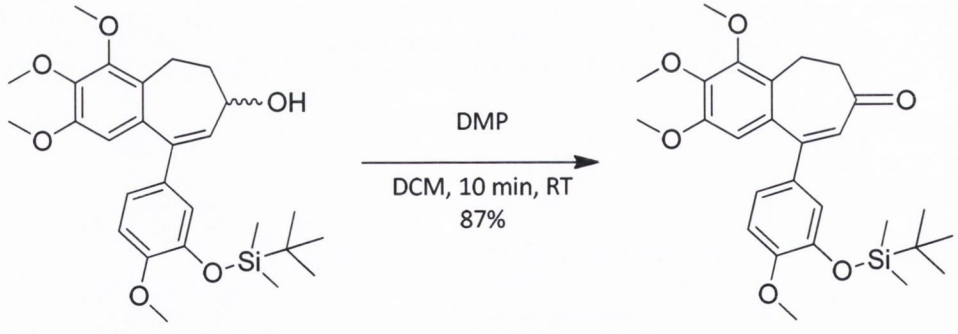

(2.21) **(2.22)**

Scheme 2.16 Oxidation of allylic hydroxyl of **(2.21)**

The silyl protecting group on the phenol was then conveniently removed using TBAF to afford **(2.03)** as a white solid in excellent yield (94%; Scheme 2.17).

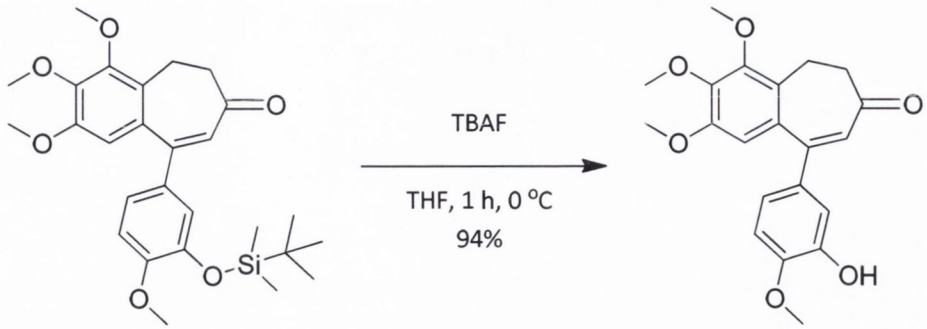

(2.22) **(2.03)**

Scheme 2.17 Removal of phenol protecting group on **(2.22)**

Despite the extra synthetic step required, a significant increase in yield was obtained following this strategy for oxidation of the C-7 alcohol compared with the equivalent oxidation carried out in the presence of the free phenol.

2.4 Synthesis of phosphate ester prodrug of (2.03)

Once a suitable scheme had been developed in order to allow the convenient synthesis of sufficient quantities of **(2.03)**, the compound was evaluated *in vitro* for antiproliferative activity against human umbilical vein endothelial cells (HUVECs) and human prostate cancer (PC-3) cell lines. The encouraging activity of the compound suggested that it was an ideal candidate for *in vivo* evaluation. However, due to the largely lipophilic nature of the compound it was found to be poorly water soluble. It thus became desirable to synthesise an analogue of **(2.03)** which would possess greater water solubility, while retaining the biological activity of the parent compound.

2.4.1 Phosphate ester prodrugs

Phosphate ester prodrugs are a common solution to the formulation of poorly water soluble compounds. The dianionic phosphate moiety typically increases the aqueous solubility of the parent compound dramatically [195]. The resultant phosphate prodrugs also tend to exhibit excellent stability [195]. Alkaline phosphatase, an enzyme expressed abundantly in the intestinal brush border, plasma and liver, is found to be responsible for the rapid hydrolysis and release of the parent drug from these compounds *in vivo* [196-197]. Phosphate ester prodrugs of the anticancer agents estramustine [198], etoposide [199], taxol [200] and combretastatin A-4 [201]

have all been reported to confer the parent drugs with enhanced water solubility. It was thus decided to synthesise a phosphate ester prodrug of **(2.03)** and to evaluate the activity of this compound *in vivo*.

2.4.2 Synthesis of phosphate ester prodrug (2.24)

The dibenzyl phosphate ester of **(2.03)** was synthesised using a procedure developed by Pettit *et al.* [202]. The reaction was carried out in an acetonitrile/carbon tetrachloride solvent system under an atmosphere of nitrogen at -10 °C. DIPEA was utilised as base. DMAP was employed as acylation catalyst. After 30 min, the temperature of the reaction was allowed to increase to 0 °C and dibenzyl phosphite was added. After a further 12 h, the dibenzyl phosphate **(2.23)** was obtained in a modest yield (40%) as a green oil, following purification (Scheme 2.18).

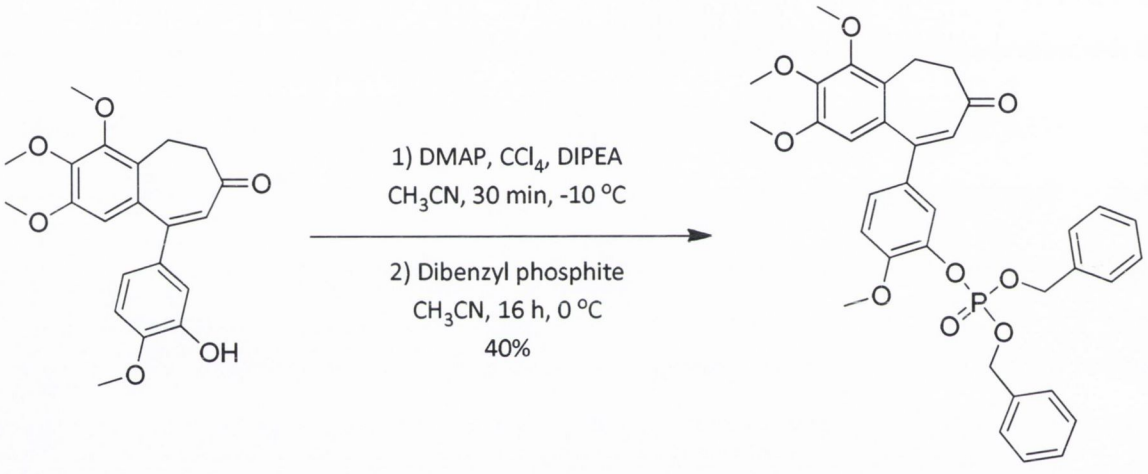

(2.03) **(2.23)**

Scheme 2.18 Synthesis of dibenzyl phosphate ester **(2.23)**

Due to the presence of the enone double bond in compound **(2.03)**, the benzyl groups could not be removed reductively using palladium on activated carbon under an atmosphere of hydrogen. Consequently, bromotrimethylsilane was used to remove the benzyl groups to afford the free phosphate. This reaction occurred readily and in good yield. Following purification, the phosphate was dissolved in methanol and a stoichiometric amount of sodium methoxide was added to afford the disodium phosphate salt **(2.24)** as a yellow solid in excellent yield (90%; Scheme 2.19).

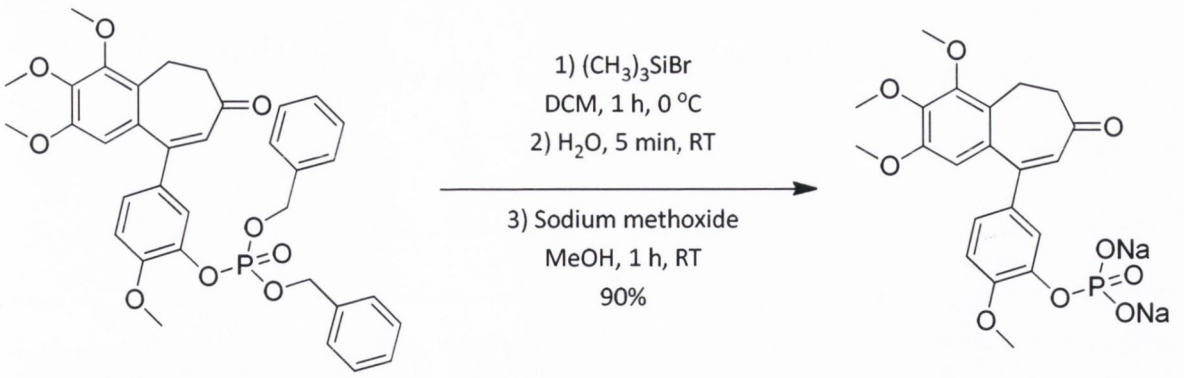

(2.23) **(2.24)**

Scheme 2.19 Removal of benzyl groups and formation of disodium salt **(2.24)**

2.4.3 Characterisation of phosphate disodium salt (2.24)

The ^1H NMR of **(2.24)** was assigned with the aid of the HSQC and HMBC NMR spectra (Figures 2.8-11). The four CH_2 protons were found to resonate as two distinct multiplets at 2.85 ppm and 3.28 ppm, by reference to the HSQC spectrum. The four methoxy group protons were found to resonate as three distinct singlets at 3.64 ppm, 3.90 ppm (2 x OCH_3) and 3.91 ppm. The singlet at 6.43 ppm was found to correlate with a CH_2 carbon according to the HMBC spectrum, indicating that it represented the signal of the vinylic proton (Figure 2.11). The four aromatic protons were found to resonate at 6.51 ppm, 7 ppm, 7.03 ppm and 7.54 ppm respectively.

Utilising the data available from the DEPT 135 and DEPT 90 spectra, the two CH_2 carbons were assigned to the peaks at 19.72 ppm and 45.17 ppm (Figure 2.9). The four methoxy carbons were found to resonate at 55.03 ppm, 55.10 ppm, 59.86 ppm and 60.50 ppm. Utilising the HSQC spectrum, the vinylic CH carbon was identified as corresponding to the signal at 127.12 ppm (Figure 2.10). The enone carbonyl carbon was found to resonate furthest downfield at 205.01 ppm, while the nine remaining quaternary carbons were found to resonate at 128.92 ppm, 132.38 ppm, 134.68 ppm, 142.63 ppm, 143.32 ppm, 149.83 ppm, 151.24 ppm, 152.06 ppm and 152.81 ppm.

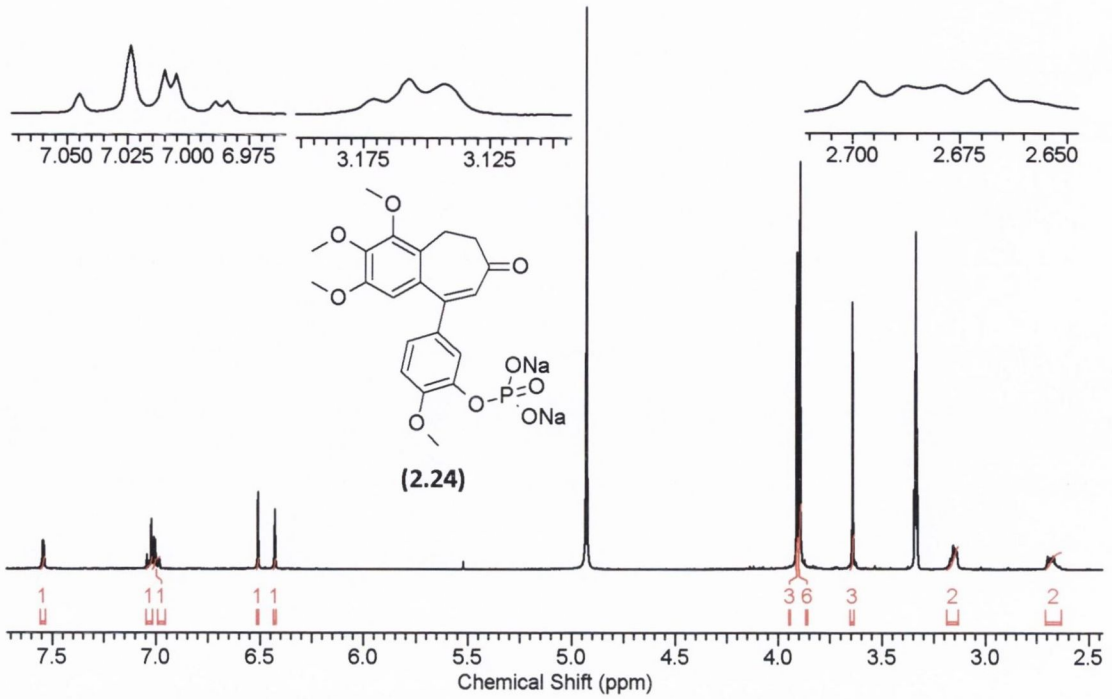

Figure 2.8 ^{1}H NMR spectrum of **(2.24)**

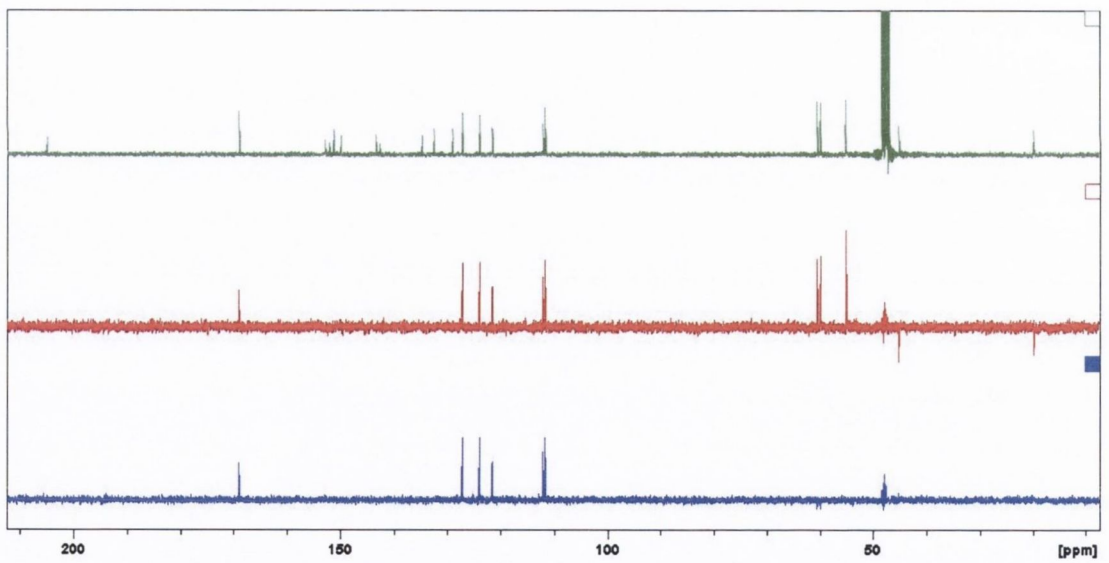

Figure 2.9 ^{13}C, DEPT 135 and DEPT 90 spectrum of **(2.24)**

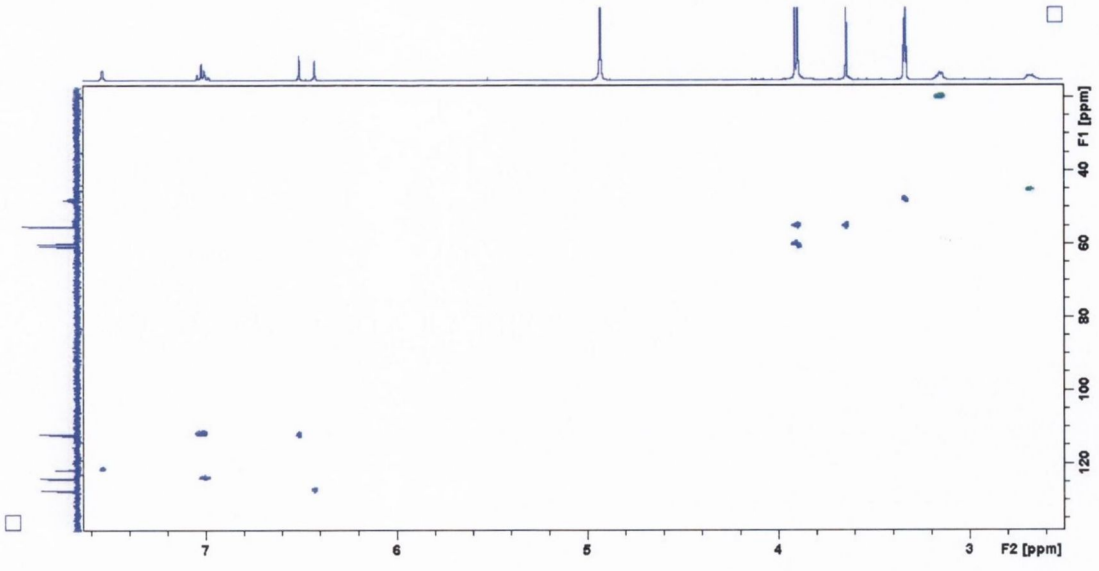

Figure 2.10 HSQC NMR spectrum of **(2.24)**

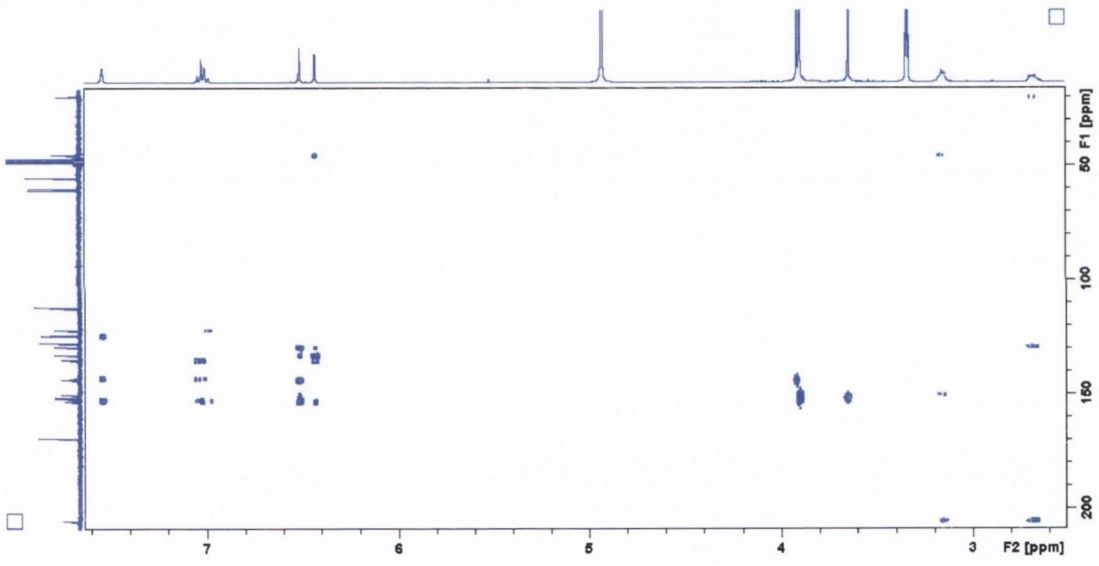

Figure 2.11 HMBC NMR spectrum of **(2.24)**

Mass spectrometry further confirmed the identity of **(2.24)**. The mass of the molecular ion peak M+H] of 449.1022 was in close agreement with the calculated value of 449.1007.

2.5 Synthesis of aniline analogue of (2.03)

Replacement of the C-ring hydroxy of compound **(2.03)** with an amine was subsequently investigated. It was proposed that the aniline analogue **(2.25)** would offer additional conjugation opportunities for the synthesis of molecular conjugates (Figure 2.12).

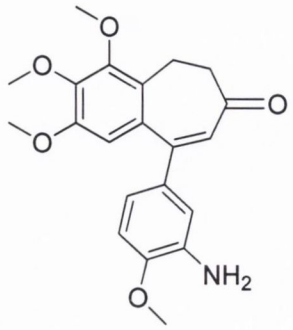

(2.25)

Figure 2.12 Proposed aniline containing tubulin inhibitor **(2.25)**

2.5.1 Synthetic strategy

The palladium catalyzed Suzuki-Miyaura cross-coupling reaction of organoboron reagents with organic triflates and related electrophiles is among the most widely utilised approaches for the formation of new carbon-carbon bonds. The reaction proceeds under relatively mild conditions, typically uses water as a co-solvent, tolerates a wide variety of functional groups and yields non-toxic by-products [203]. It was decided to utilise this methodology to construct the biaryl structure envisioned for **(2.25)**. It was therefore proposed to synthesise the enol triflate of compound **(2.11)**, together with an aniline containing boronic acid C-ring and to couple them together using standard Suzuki coupling methodology.

2.5.2 Preparation of enol-triflate (2.26)

Using the procedure outlined by Hudson, the AB-ring ketone **(2.11)** was reacted with freshly prepared lithium diisopropylamide (LDA) to yield the ketone enolate [188]. This was then reacted with 2-[*N,N*-bis(trifluoromethylsulfonyl)amino]-5-chloropyridine to form the triflate **(2.26)** in modest yield (45%; Scheme 2.20)

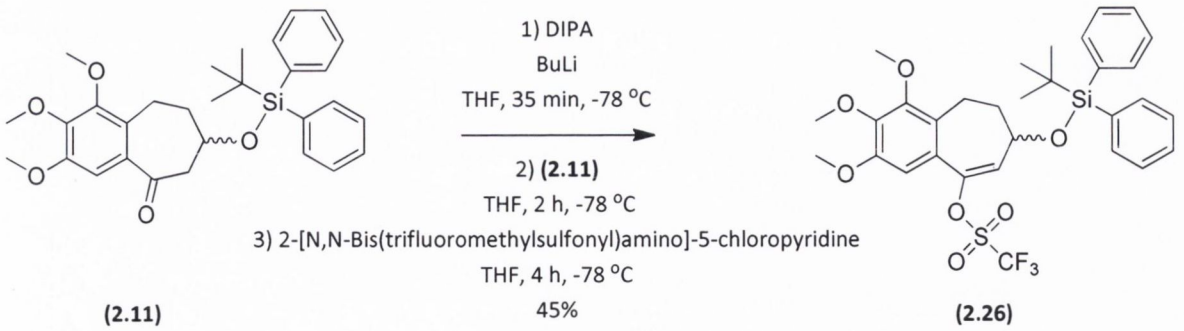

Scheme 2.20 Synthesis of triflate **(2.26)**

It was proposed that the omission of THF, to solvate the reagents in the formation of the LDA, and the relatively low number of equivalents of reagents used in the procedure were responsible for the disappointing yield. Therefore, the reaction conditions were amended accordingly. The reaction was repeated ensuring that the diisopropylamine was solvated in a suitable amount of THF and 1.5 equivalents of LDA was used. Furthermore, 2 equivalents of the triflating reagent were also used. These modifications to the initial reaction conditions resulted in a significant increase in the yield of enol triflate isolated (72%).

2.5.3 Synthesis of aniline containing C-ring

The starting material for the synthesis of the C-ring was the commercially available 4-bromo-2-nitrophenol. The phenol was methylated using iodomethane together with potassium carbonate as base, following a procedure described Shah, to afford **(2.27)** as an off-white solid in excellent yield (99%; Scheme 2.21) [187].

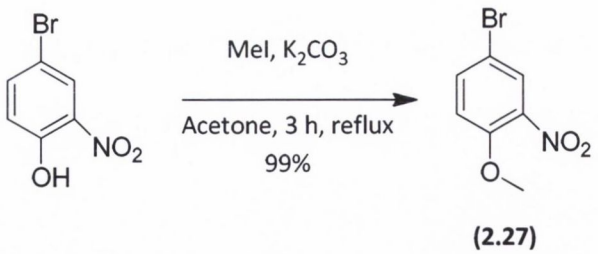

Scheme 2.21 Methylation of 4-bromo-2-nitrophenol

An attempt was then made to synthesise the boronic acid of **(2.27)**. Lithiation with *n*-butyllithium at -78 °C was followed by reaction with excess triisopropyl borate. A complex mixture of products,

presenting as a thick black oil, was obtained following work-up of the reaction. As a result, this approach was not pursued.

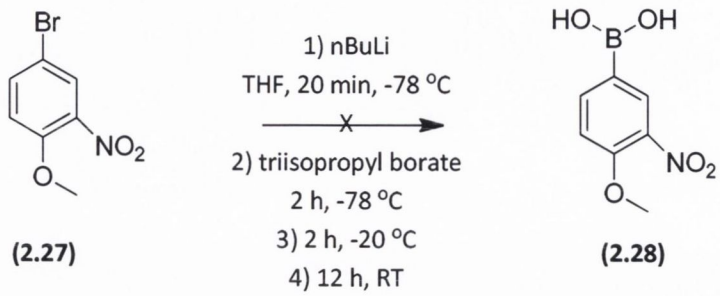

Scheme 2.22 Attempted synthesis of boronic acid **(2.28)**

The nitro group of **(2.27)** was instead reduced, using tin powder and concentrated HCl solution, to afford the aniline **(2.29)** as a brown solid in excellent yield (100%). The aniline **(2.29)** was then protected as a *N-tert*-butoxycarbonyl (BOC) group by heating to 80 °C with di-*tert*-butyl dicarbonate solution in THF to afford **(2.30)** as a yellow oil in excellent yield (98%; Scheme 2.23).

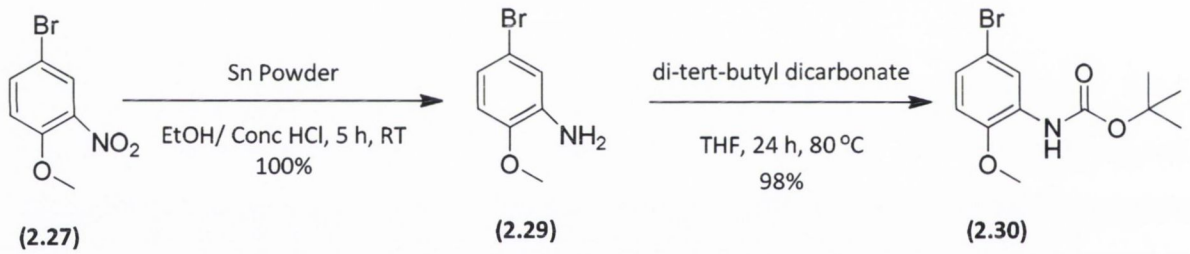

Scheme 2.23 Reduction of nitro group of **(2.27)** and BOC protection of aniline

According to the literature, BOC groups are labile in the presence of *n*-butyllithium [204]. Therefore, an alternative procedure for the synthesis of boronic acids from halogenated aromatic compounds was required.

A procedure utilising an organomagnesium intermediate was thus explored. Firstly, a magnesium-ate complex (nBu$_3$MgLi) was generated by combining butylmagnesium chloride with *n*-butyllithium at -5 °C in THF, utilising a procedure described by Kitagawa [205]. The bromide containing C-ring **(2.30)** was then added and halogen-magnesium exchange furnished the organomagnesium intermediate. Following a procedure outlined by Song *et al.*, this intermediate

was subsequently reacted *in situ* with excess trimethyl borate (11 eq.) to afford the desired boronic acid **(2.31)** as a crude mixture (Scheme 2.24) [206].

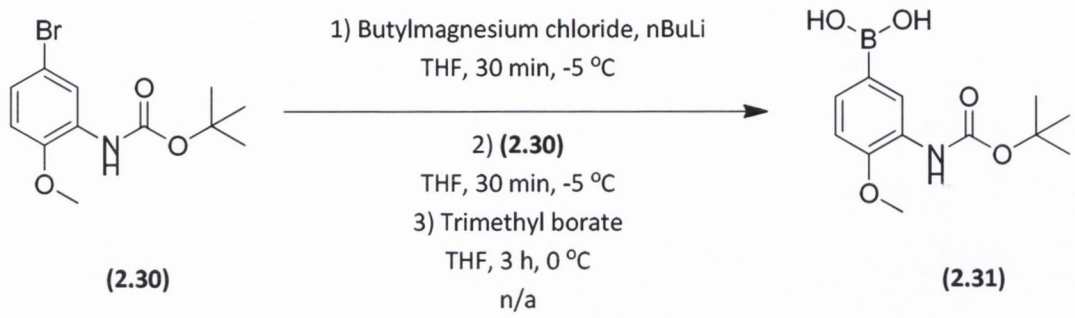

Scheme 2.24 Synthesis of Boronic Acid **(2.31)**

Significant difficulties were encountered in the purification of the boronic acid. It was not stable and appeared to be air-sensitive. It was also partially degraded during purification by flash column chromatography. ^{11}B NMR of the crude product confirmed the presence of boron within the molecule (Figure 2.13). The purported boronic acid **(2.31)** was thus carried forward to the next reaction without further purification.

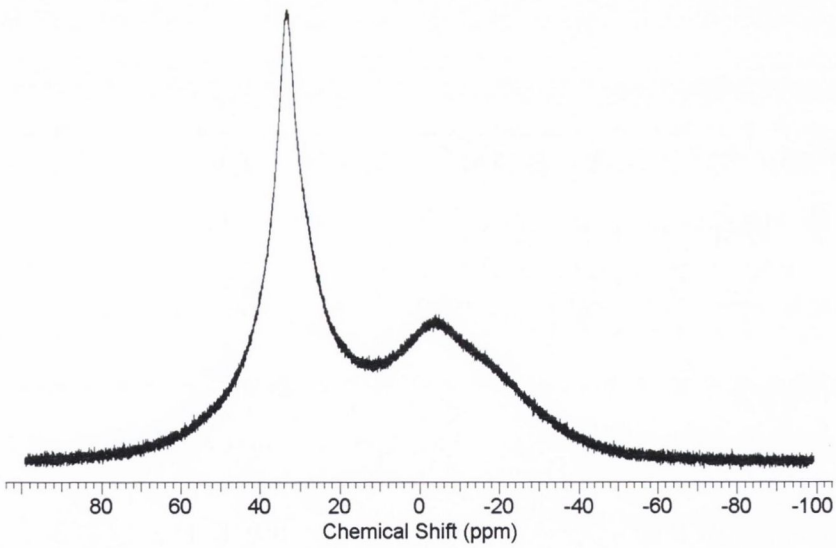

Figure 2.13 ^{11}B NMR of impure boronic acid **(2.31)**

2.5.4 Suzuki coupling of enol triflate (2.26) and boronic acid (2.31)

Utilising the Suzuki reaction conditions employed by Hudson, the crude boronic acid **(2.31)** was coupled to the enol triflate **(2.26)** [188]. The reaction conditions employed involved the use of the palladium catalyst tetrakis(triphenylphosphine)palladium(0) ($Pd(PPh_3)_4$), potassium carbonate as base and a mixture of toluene, ethanol and water (3:1:1) as solvent. The reaction proceeded smoothly under reflux. Following consumption of the boronic acid after 30 min, the reaction was quenched and the coupled product **(2.32)** was isolated by flash column chromatography in excellent yield (83%; Scheme 2.25).

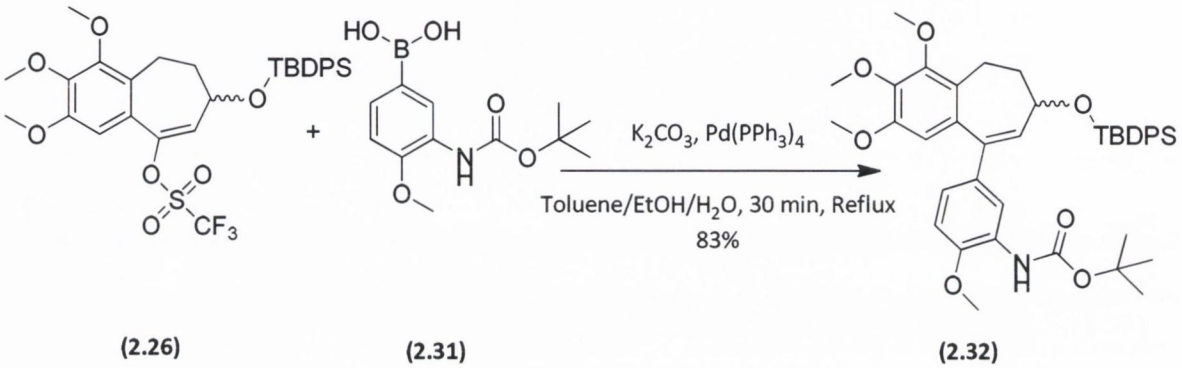

(2.26) **(2.31)** **(2.32)**

Scheme 2.25 Suzuki coupling of boronic acid **(2.31)** and triflate **(2.26)**

Despite the relative success of the Suzuki coupling reaction, significant difficulties were still associated with both the preparation and storage of the boronic acid **(2.31)**. Therefore, an alternative coupling methodology, employing the use of a boronate ester, was explored.

2.5.5 Synthesis and coupling of boronate ester

The use of boronic acid esters or boronate esters has become quite a common theme in Suzuki coupling in recent years [207]. Unlike boronic acids, boronate esters are known to be stable to moisture and silica gel chromatography, making their preparation, isolation and storage much more convenient [208].

The transition-metal-catalysed cross-coupling reaction of boron nucleophiles and aryl electrophiles has become very common in the synthesis of boronate esters [207]. The pinacol ester of diboron, tetraalkoxydiboron, when reacted with aryl halides, provides a convenient one step method of generating the corresponding aryl pinacolboronate [207]. This reaction was

carried out on the aniline-protected bromide compound **(2.30)** according to a procedure developed by Ishiyama *et al* [207]. Bis(pinacolato)diboron was added to a solution of **(2.30)** in dry DMSO under an atmosphere of nitrogen. The palladium catalyst used in the reaction was [1,1'-bis(diphenylphosphino)ferrocene]dichloropalladium(II) or $Pd(dppf)Cl_2$ and the base used was potassium acetate. The reaction was heated at 80 °C and was deemed to have gone to completion after 4 h. The product was then purified by flash column chromatography to afford the desired pinacolboronate **(2.33)** in an acceptable yield (40%; Scheme 2.26). The resulting white solid was subsequently found to be extremely stable under normal storage conditions.

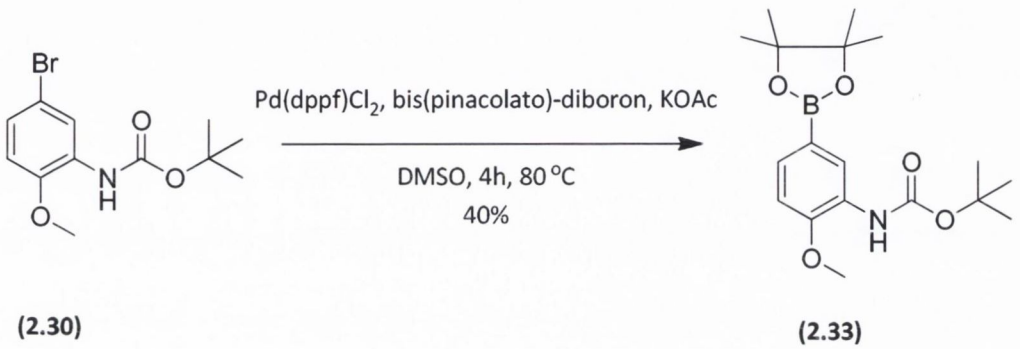

(2.30) **(2.33)**

Scheme 2.26 Synthesis of pinacolboronate **(2.33)**

The pinacolboronate ester **(2.33)** was then coupled to the enol triflate **(2.26)**, using the same conditions employed for the coupling of the boronic acid **(2.31)**, using $Pd(PPh_3)_4$ as catalyst. After 1 h heating under reflux, the reaction was adjudged to have gone to completion by TLC analysis. Following purification, the coupled compound **(2.32)** was isolated in satisfactory yield (75%; Scheme 2.27).

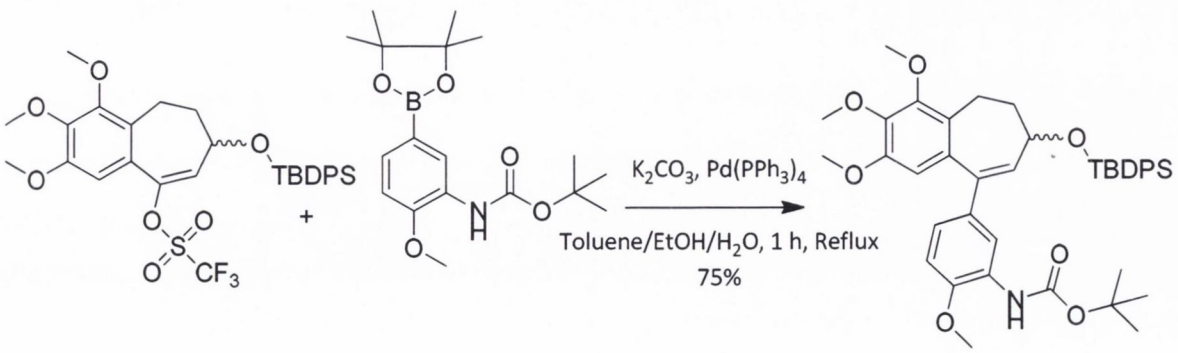

(2.26) **(2.33)** **(2.32)**

Scheme 2.27 Alternative Suzuki coupling of **(2.26)** and **(2.33)**

Overall, this method was much more efficient than the use of the boronic acid **(2.31)**, considering the ease of formation, the almost equivalent yield (75% v 83%) and the increased stability on storage of the pinacolboronate ester **(2.33)**.

In an attempt to further improve the synthetic route to the coupled product **(2.32)**, a one pot biaryl synthesis, via *in situ* boronate formation, was attempted [209]. The formation of the aryl pinacolboronate **(2.33)** was first conducted. Compound **(2.31)** was dissolved in DMF together with bis(pinacolato)-diboron, $Pd(dppf)Cl_2$ as catalyst and potassium acetate as base. The reaction was then heated under reflux at 80 °C. The reaction was monitored by TLC. Following exhaustion of the bromide **(2.31)**, the enol-triflate **(2.26)** was added together with sodium carbonate aqueous solution and an additional quantity of catalyst. After an additional 30 min heating at 80 °C under reflux, the reaction was deemed to have gone to completion. The product **(2.32)** was isolated by flash column chromatography in modest yield (43%; Scheme 2.28).

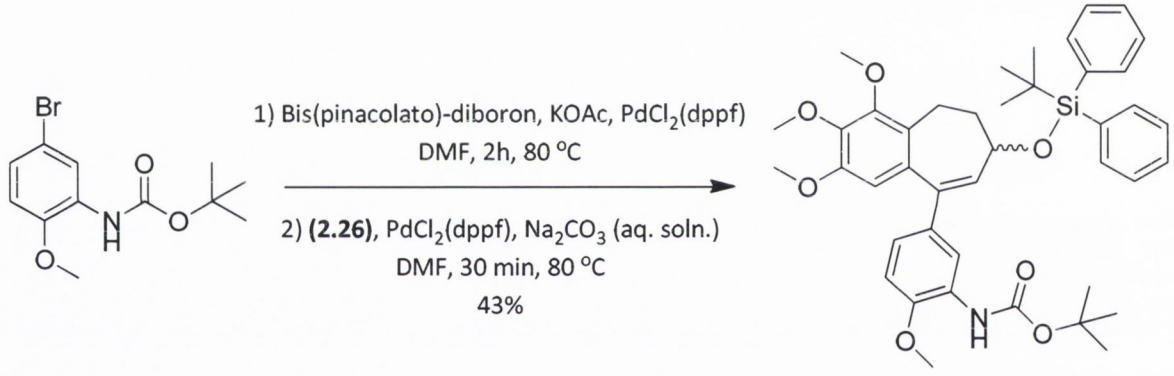

(2.31) **(2.32)**

Scheme 2.28 Preparation of pinacolboronate **(2.33)** followed by *in situ* Suzuki coupling with enol-triflate **(2.26)**

Although the yield following the two contiguous reactions represented a slight improvement over the total yield after the two discrete steps (43 v 33%), the one pot reaction was found to be somewhat inflexible. Depending on the yield of the initial step, significant waste could potentially occur. Therefore, it was decided not to pursue this approach further.

2.5.6 Removal of protecting groups and oxidation of C-7 alcohol

Removal of the silyl protecting group of **(2.32)** was carried out using TBAF in dry THF at 0 °C. After 24 h, the product was purified by flash column chromatography to afford **(2.34)** as a crystalline white solid in good yield (76%; Scheme 2.29).

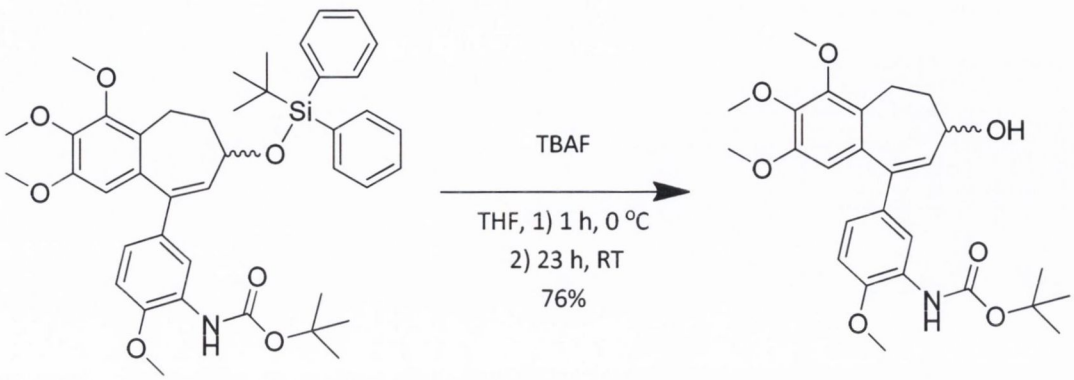

(2.32) **(2.34)**

Scheme 2.29 Removing the silyl protecting group from **(2.32)**

Following removal of the silyl group, the secondary alcohol at the C-7 position was oxidised to the ketone using PDC. After 2 h the carbonyl containing product **(2.35)** was purified by flash column chromatography to afford **(1.38)** as a yellow oil in moderate yield (65%; Scheme 2.30).

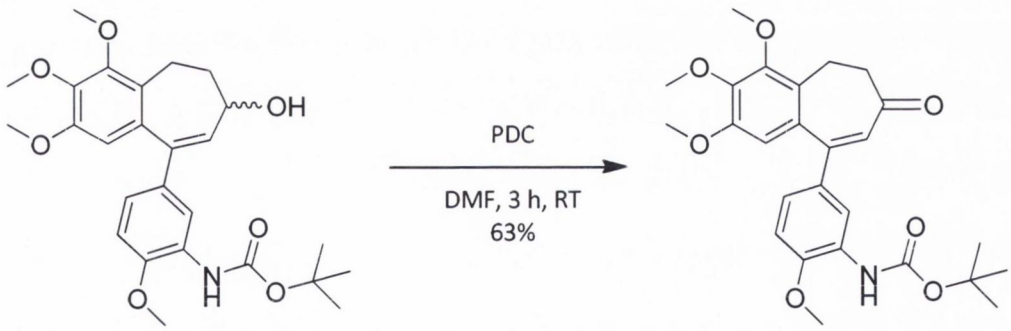

(2.34) **(2.35)**

Scheme 2.30 PDC oxidation of alcohol to form **(2.35)**

The oxidation of **(2.34)** to **(2.35)** was subsequently carried out using Dess-Martin periodinane in an attempt to further increase the yield of this reaction (Scheme 2.31). The alcohol **(2.34)** was dissolved in DCM and DMP was added. After 30 min, the reaction was deemed to have gone to completion and the product was isolated in excellent yield (99%).

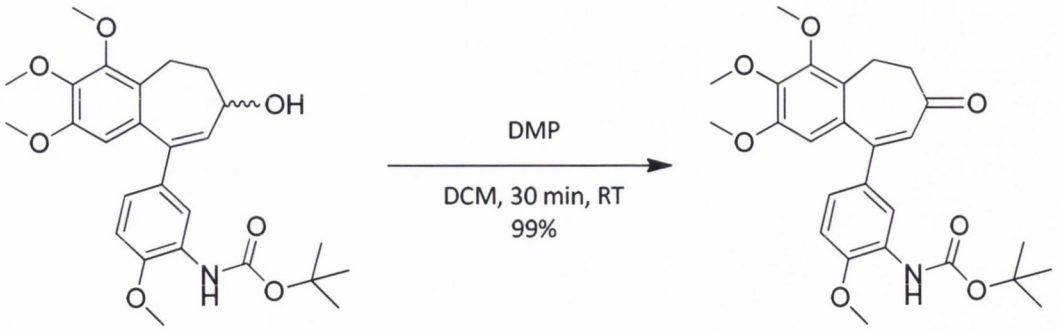

(2.34) **(2.35)**

Scheme 2.31 DMP oxidation of alcohol **(2.34)**

A significantly improved yield was obtained using DMP compared with PDC. (99% v 65%) Other advantages of using DMP over PDC were the relatively non-toxic nature of the DMP and the ease at which the product could be isolated due to the use of DCM, rather than DMF, as reaction solvent.

The BOC group of compound **(2.35)** was then removed. The compound was dissolved in dry DCM under an atmosphere of nitrogen and the temperature cooled to 0 °C. TFA was then added under anhydrous conditions. After 1 h, the solvent was removed and the residue washed with saturated sodium bicarbonate aqueous solution and extracted with diethyl ether. Following purification by flash column chromatography, compound **(2.25)** was obtained as a yellow oil in moderate yield (50%; Scheme 2.32).

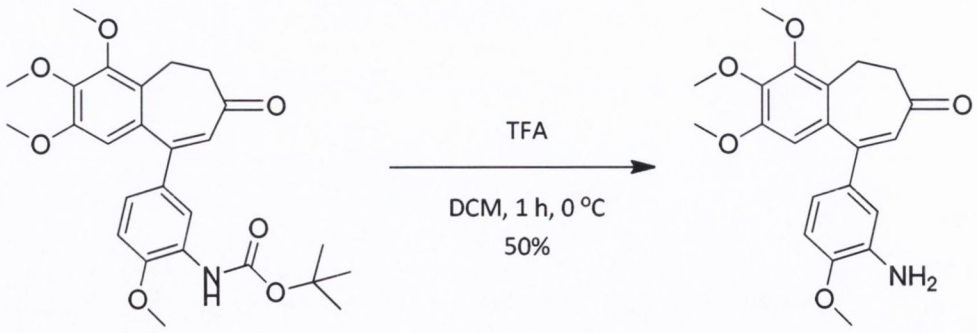

(2.35) **(2.25)**

Scheme 2.32 BOC deprotection of **(2.35)**

2.5.7 Characterisation of aniline (2.25)

A full structural elucidation was carried out in order to confirm the identity of **(2.25)**. Using one and two-dimensional NMR spectroscopy techniques, the proton and carbon signals were assigned (Figures 2.14-2.17). The four CH_2 protons were found to resonate as two distinct multiplets at 2.72 ppm and 3.15 ppm utilising the HSQC spectrum. The four methoxy CH_3 proton signals were found to resonate as four singlets at 3.65 ppm, 3.91 ppm, 3.92 ppm and 3.96 ppm. Using a combination of the HSQC and HMBC spectra, the vinylic proton was found to correspond to the singlet at 6.39 ppm and the A-ring aromatic proton was found to resonate as a singlet at 6.43 ppm. The three remaining aromatic protons were found to resonate at 6.74 ppm (2 x ArH) and 6.78 ppm.

The two CH_2 signals were readily apparent from the DEPT 135 spectrum, resonating at 20.28 ppm and 45.71 ppm (Figure 2.15). Similarly, the four methoxy carbon atoms were found to resonate at 55.57 ppm, 56.09 ppm, 60.95 ppm and 61.43 ppm. Using the HSQC spectrum, the double bond CH carbon was found to resonate at 127.82 ppm while the A-ring aromatic CH carbon was found to resonate at 112.01 ppm. The three remaining aromatic CH carbons were found to correspond to the signals at 109.76 ppm, 115.54 ppm and 119.78 ppm. The distinctive downfield signal at 204.32 ppm on the ^{13}C spectrum confirmed the presence of the carbonyl group. The 9 remaining quaternary carbon signals were identified as corresponding to signals at 129.06 ppm, 132.71 ppm, 135.45 ppm, 135.80 ppm, 143.14 ppm, 148.07 ppm, 149.87 ppm, 151.00 ppm and 152.30 ppm.

Mass spectrometry further confirmed the formation of the desired compound. The mass of the molecular ion [M+H] was found to be 370.1657, correlating closely with the calculated value of 370.1654.

IR spectroscopy revealed a characteristic carbonyl stretching absorption at 1651.25 cm^{-1}, indicating the presence of the C-7 ketone group within the structure of **(2.25)**.

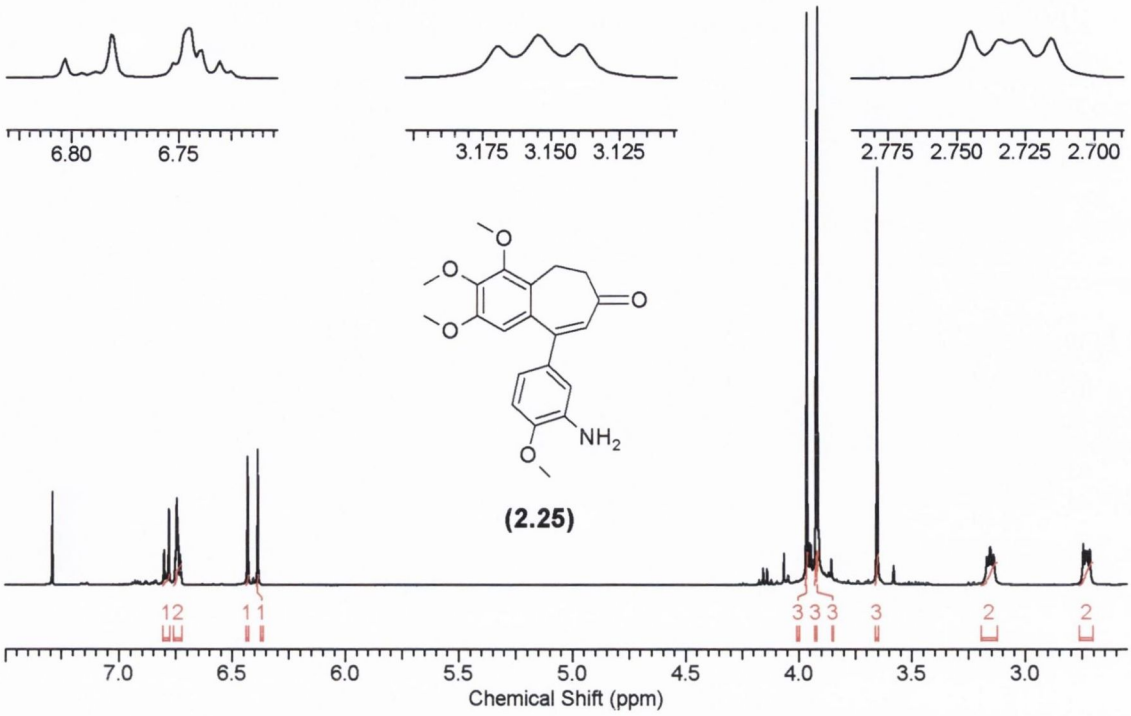

Figure 2.14 ^{1}H NMR spectrum of **(2.25)**

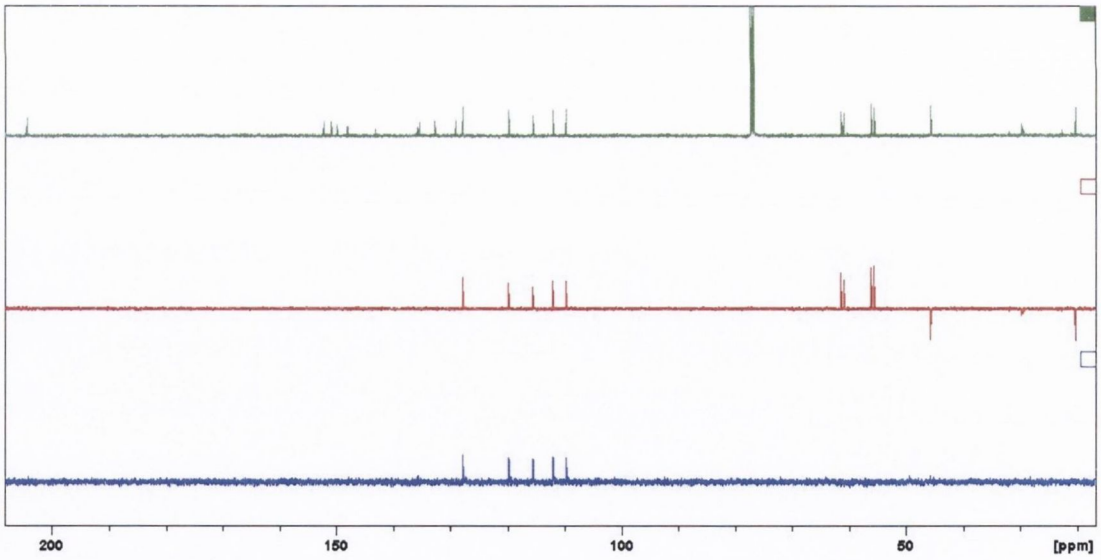

Figure 2.15 ^{13}C, DEPT 135 and DEPT 90 NMR spectra of **(2.25)**

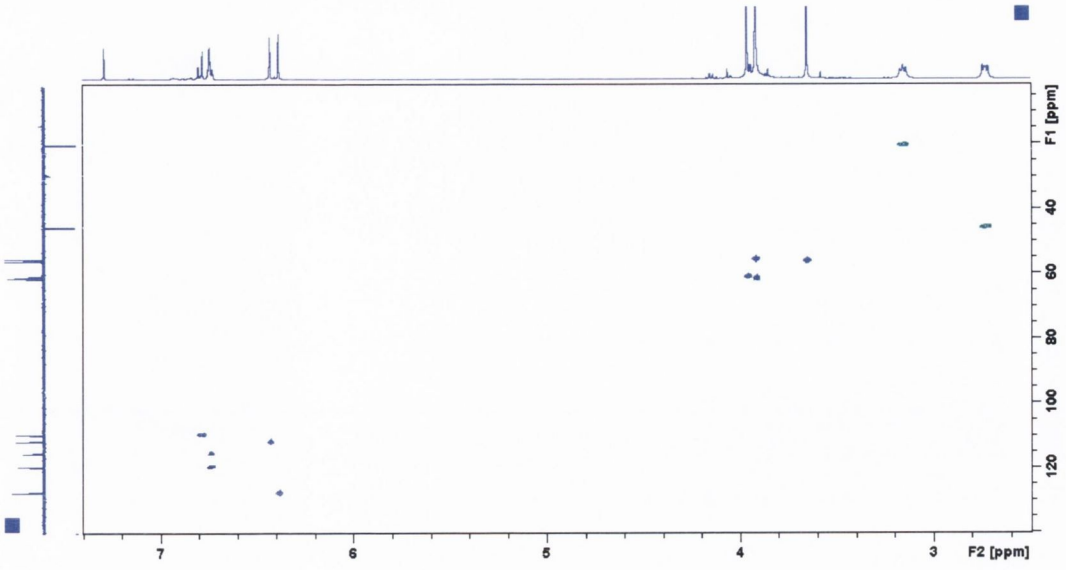

Figure 2.16 HSQC spectrum of **(2.25)**

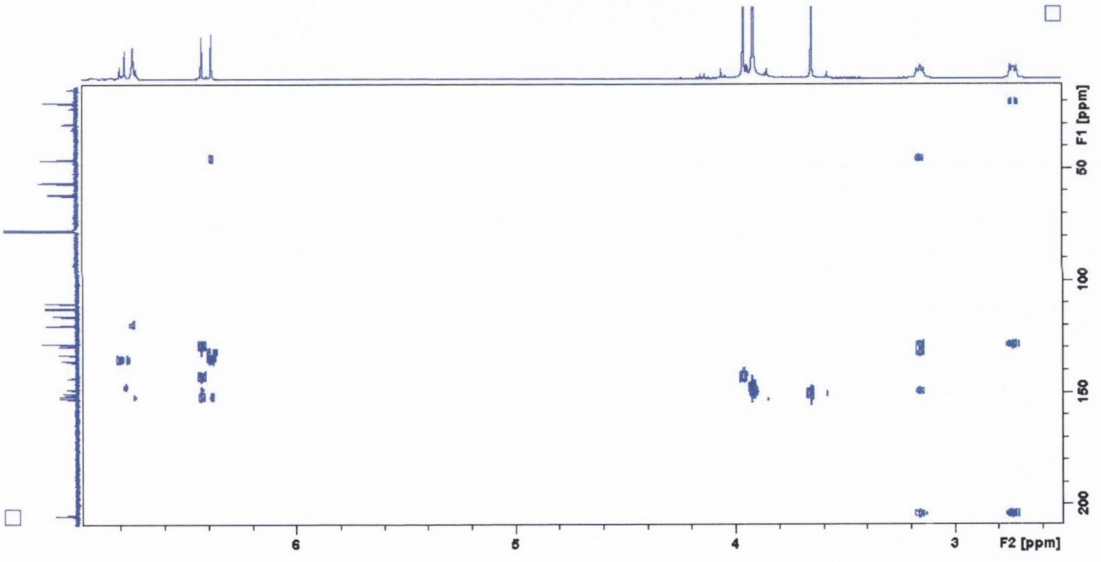

Figure 2.17 HMBC spectrum of **(2.25)**

2.5.8 Synthesis of aniline hydrochloride salt (2.36)

The hydrochloride salt of the aniline **(2.25)** was formed by bubbling HCl gas through a diethyl ether solution of the aniline. The resulting white solid **(2.36)** was washed with diethyl ether and dried under high vacuum before submission for biological testing.

2.6 Biological evaluation

The lead molecule **(2.03)**, the phosphate ester prodrug **(2.24)** and the hydrochloride salt of the aniline analogue **(2.36)** were all subject to biological evaluation by E. Prokopiou as part of the work submitted for her doctoral thesis [210]. The following is a brief overview of this work.

2.6.1 Cell proliferation inhibition assays

Compounds **(2.03)** and (**2.36)** were tested for cell proliferation inhibition activity in both human umbilical vein endothelial cells (HUVECs) and prostate carcinoma (PC-3) cells (Table 2.2).

	HUVECs (nM)	PC-3 cells (nM)
CA-4	4.03 ± 1.73	14.01 ± 0.58
(2.03)	65.05 ± 1.10	50.65 ± 1.19
(2.36)	8.58 ± 1.06	9.70 ± 0.88

Table 2.2 Best fit IC_{50} values ± SEM for CA-4 and compounds **(2.03)** and **(2.36)** following MTT assay in HUVECS and PC-3 cells (n = 3)

Both compound **(2.03)** and **(2.36)** were found to possess *in vitro* anti-proliferative activity comparable with CA-4. Interestingly, the aniline modification in the C-ring of **(2.36)** appeared to confer a greater degree of anti-proliferative activity to the pharmacophore compared with the lead compound **(2.03)**. In fact, the IC_{50} value obtained for **(2.36)** in PC-3 cells was found to be even lower than that of the reference compound CA-4.

2.6.2 Immunofluorescence staining of the microtubules

Compounds **(2.03)** and **(2.36)** were subsequently evaluated for their ability to disrupt the tubulin cytoskeleton of HUVECs. Following treatment with the compounds for 30 min, the cells were stained and observed under the microscope (Figure 2.18).

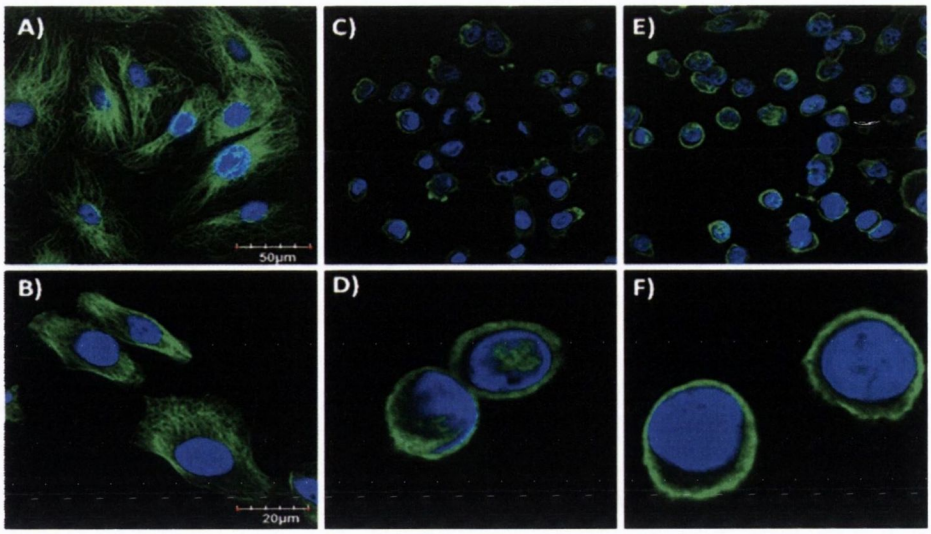

Figure 2.18 Microtubule disruption of endothelial cells. HUVECs were treated for 30 min and stained for α-tubulin (green) and nucleus (blue). Images were taken using an Olympus FV1000 point scanning confocal microscope (x60). A-B) Control (0.1% DMSO), C-D) 1 μM **(2.03)** and E-F) 1 μM **(2.36)**

The images clearly demonstrate the microtubule disrupting effects of both **(2.03)** and **(2.36)**. Severe microtubule disruption was apparent following treatment with **(2.03)** and **(2.36)**. Microtubule fibres were also found to be absent in the treated cells (Figure 2.18; C-F).

2.6.3 Cell cycle analysis

The anti-mitotic effect of the compounds was then established by analysing the cell cycle stages of treated cells using propidium iodide (PI) staining followed by flow cytometry (Figure 2.19).

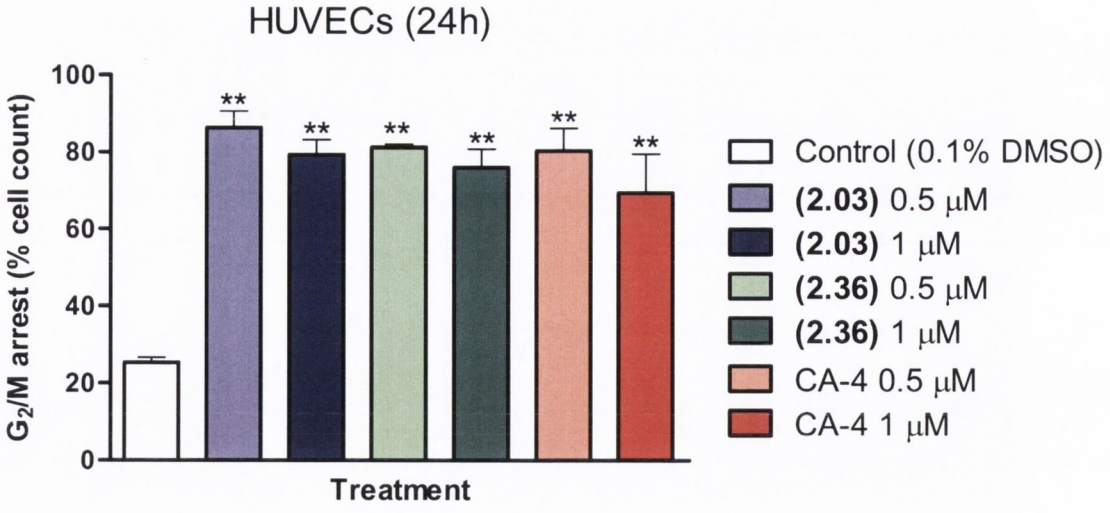

** $p < 0.01$, significantly higher mean % cell count in the G_2/M phase compared with the untreated controls as determined by Student's *t*-test.

Figure 2.19 Percentage of G2/M phase cell count of **(2.03)**, **(2.36)** and CA-4. Data represent mean ± SEM (n=3).

It is well established that treatment of cells with tubulin polymerisation inhibitors causes a G_2/M phase arrest [211]. Therefore, it is unsurprising that a dramatic increase in the proportion of cells having undergone arrest at the G_2/M phase is clearly apparent for both the **(2.03)** and **(2.36)** treated cells, as well as those treated with CA-4.

2.6.4 Endothelial cell morphology analysis

Tubulin inhibitors are widely reported to have an anti-vascular effect, as distinct from their anti-mitotic activity, particularly at low doses. Treatment with such agents has been shown to cause vascular shutdown within solid tumours independently of a direct cytotoxic effect [212]. Morphological changes to the endothelial cells of the tumour vasculature are thought to play a central role in mediating this effect. Accordingly, analysis of the morphological changes in endothelial cells following treatment with **(2.03)**, **(2.36)** and CA-4 was also undertaken.

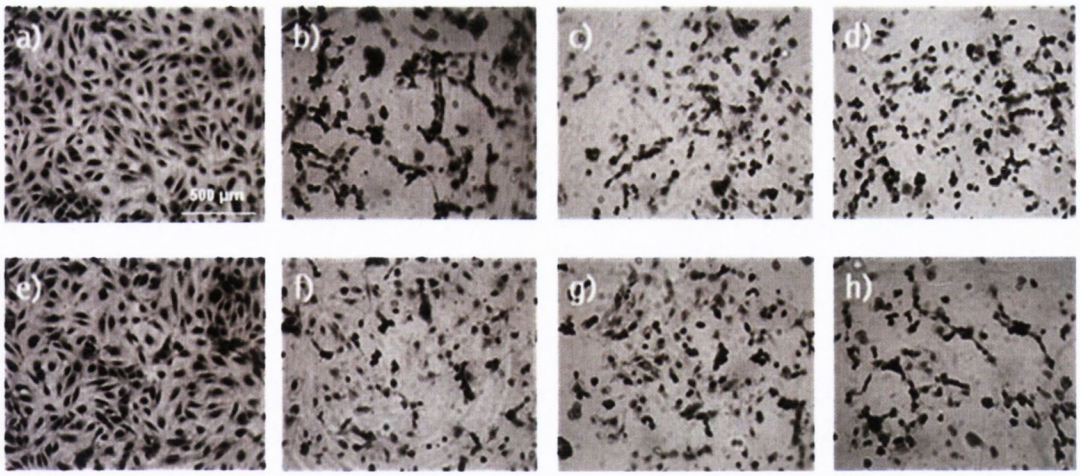

Figure 2.20 The effect of **(2.03)** and CA-4 on endothelial cells' morphology. HUVECs were exposed to the compounds for 40 min and photomicrographs (x 10) were taken 1 h after drug washout. a/e) Control (0.1% DMSO), b) 0.1 µM **(2.03)**, c) 0.5 µM **(2.03)**, d) 1 µM **(2.03)**, f) CA-4 0.1 µM, g) CA-4 0.5 µM and h) CA-4 1 µM

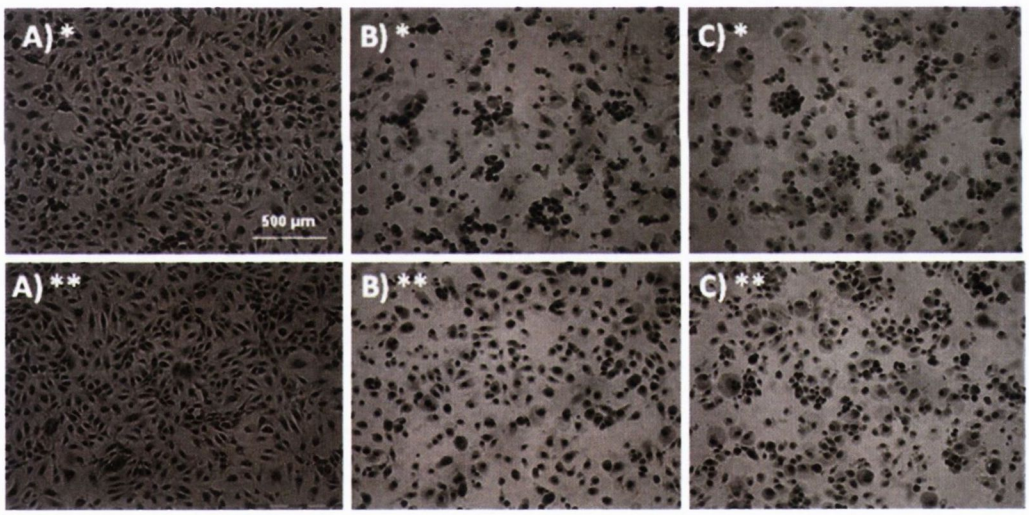

Figure 2.21 The effect of **(2.36)** on endothelial cells' morphology. HUVECs were exposed to the compounds for 40 min and photomicrographs (x10) were taken 1 h (*) and 3 h (**) after drug washout. A) Control (0.1% DMSO) B) 0.1 **(2.36)** µM and C) 0.5 µM **(2.36)**

All three compounds evaluated were found to induce rapid morphological changes to endothelial cells at concentrations as low as 0.1 µM. Cell contraction, membrane blebbing, intercellular gaps and darkening of the cell contents were all observed in the treated cells. These results suggested that both **(2.03)** and **(2.36)** may have the potential to act as anti-vascular agents *in vivo*.

2.6.5 Angiogenesis inhibition assay

An Angiokit assay (supplied by TCS Cellworks) consisting of a co-culture assay of HUVECs and fibroblasts was used to determine the anti-angiogenic activity of **(2.03)**. The effects of treatment with **(2.03)** on the growth of microvessel, and hence angiogenesis, was thus determined (Figures 2.22 and 2.23).

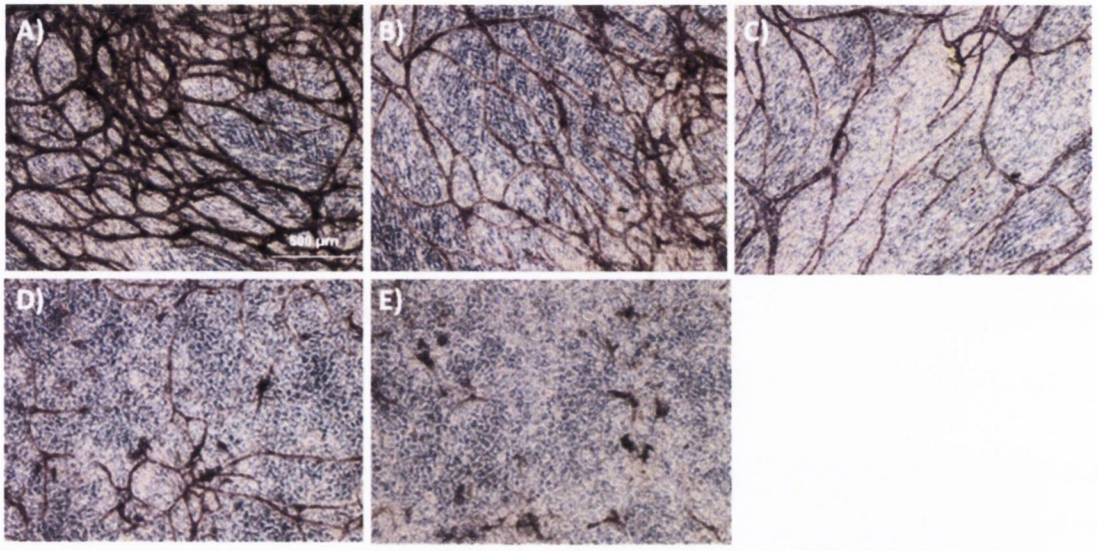

Figure 2.22 Angiokit angiogenesis assay. Cells were cultured for 12 days resulting in a confluent co-culture. A) 2 ng/mL VEGF, B) Control (0.1% DMSO), C) 20 μM suramin, D) 25 nM **(2.03)** and E) 50 nM **(2.03)**

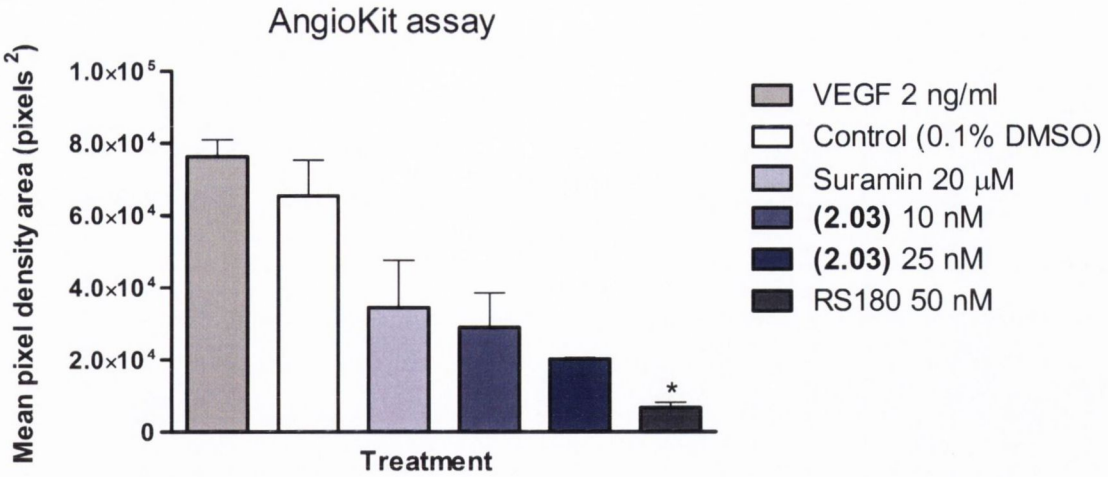

* $p < 0.01$, significantly lower mean pixel density area compared with the control (0.1% DMSO) as determined by Student's *t*-test.

Figure 2.23 The effect of **(2.03)** on microvessel formation. An estimation of the mean pixel density area of the vessels was calculated by Adobe Photoshop CS4. Data represents mean ± SEM (n = 3).

Treatment with **(2.03)** resulted in a visible decrease in microvessel formation at both 25 nM and 50 nM (Figure 2.22; D-E).The reduction achieved at a dose of 50 nM was subsequently shown to be of statistical significance, suggesting the anti-angiogenic efficacy of this agent (Figure 2.23).

2.6.6 Aortic ring: angiogenesis assay

The aortic ring assay was also used to determine the anti-angiogenic effects of **(2.03)** and **(2.36)**.

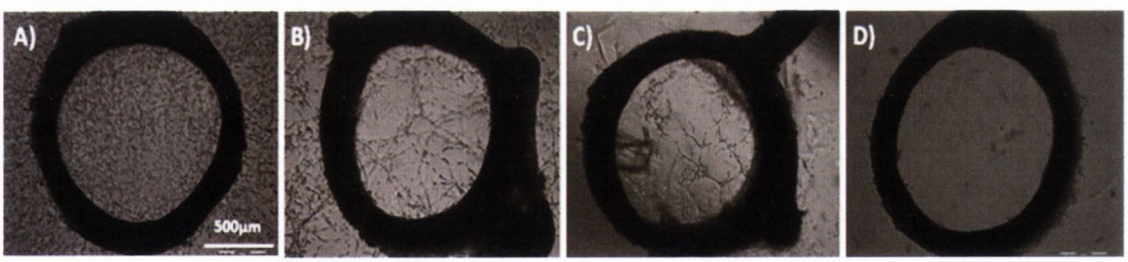

Figure 2.24 Effect of treatment with **(2.03)** on the growth of new blood vessel capillaries in an *ex vivo* aortic ring assay. The aortic rings were kept in a humidified CO_2 incubator at 37 °C and the medium was changed every other day, starting from day 3. Test compounds were added on day 8. Photomicrographs of the aortic cultures were taken under bright field microscopy using a digital camera (x4). A) Control (0.1% DMSO), B) 1 nM **(2.03)**, C) 10 nM **(2.03)** and D) 100 nM **(2.03)**

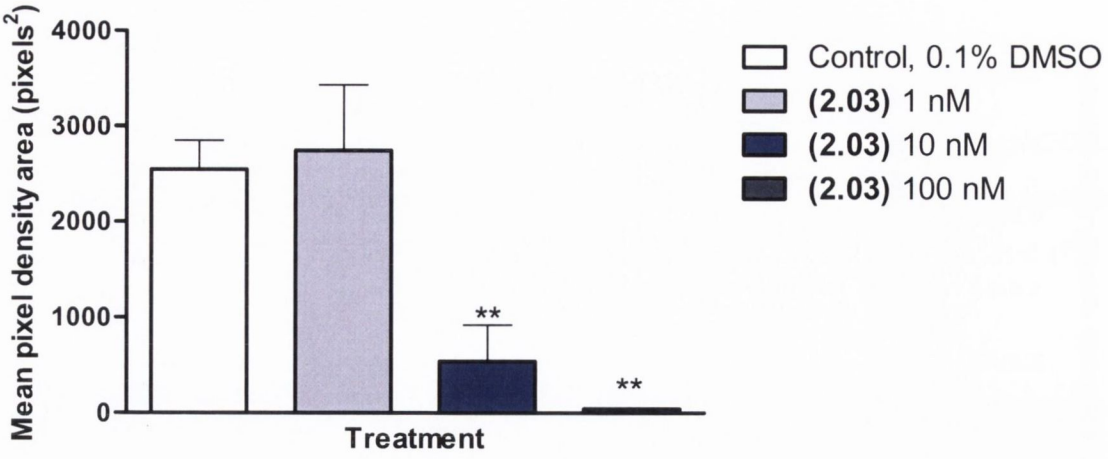

** $p < 0.01$, significantly lower mean pixel density area compared with the untreated controls as determined by Student's *t*-test.

Figure 2.25 The effect of **(2.03)** on new blood vessel capillary formation. An estimation of the mean pixel density area of the vessels was calculated by Adobe Photoshop CS4

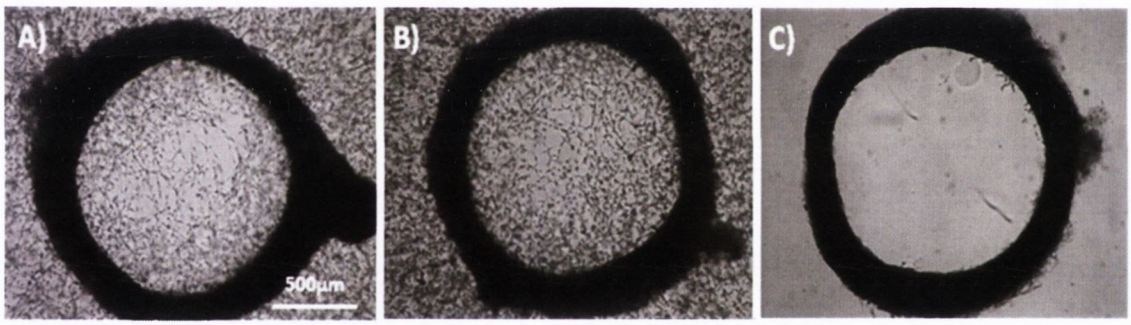

Figure 2.26 Effect of treatment with **(2.36)** on the growth of new blood vessel capillaries in an *ex vivo* aortic ring assay The aortic rings were kept in a humidified CO_2 incubator at 37 °C and the medium was changed every other day, starting from day 3. Test compounds were added on day 8. Photomicrographs of the aortic cultures were taken under bright field microscopy using a digital camera (x4). A) Control (0.1% DMSO), B) 10 nM **(2.36)**, C) 50 nM **(2.36)** and D) 100 nM **(2.36)**

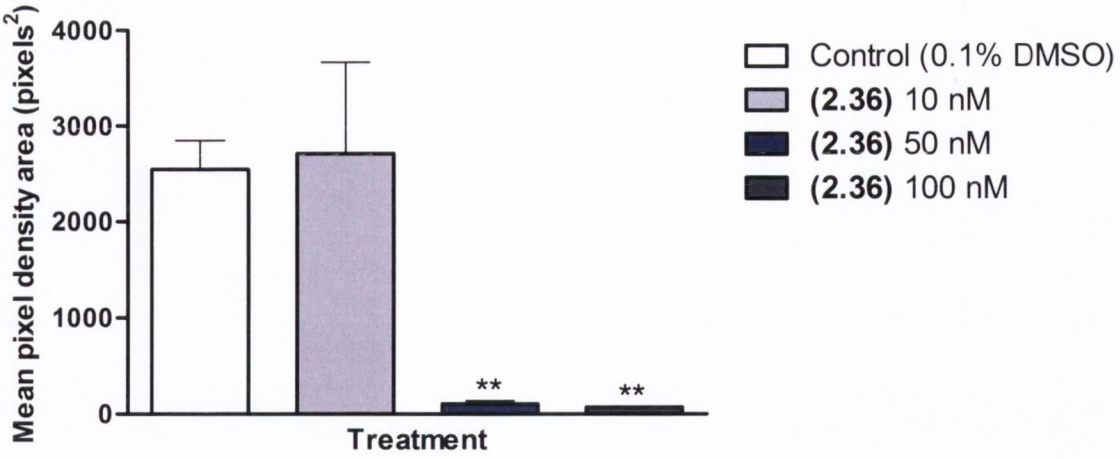

** $p < 0.01$, significantly lower mean pixel density area compared with the untreated controls as determined by Student's *t*-test.

Figure 2.27 The effect of **(2.36)** on new blood vessel capillary formation. An estimation of the mean pixel density area of the vessels was calculated by Adobe Photoshop CS4

A dose dependent reduction in new blood vessel formation following treatment with **(2.03)** was clearly apparent (Figure 2.24). A statistically significant reduction in new blood vessel formation was observed at both 10 nM and 100 nM indicating that compound **(2.03)** possessed potent anti-angiogenic activity (Figure 2.25).

In a comparable manner to **(2.03)**, compound **(2.36)** was also found to cause a significant reduction in the amount of new blood vessels formed, particularly at 50 nM and 100 nM (Figures 2.26 and 2.27). This suggested the potent anti-angiogenic efficacy of **(2.36)**.

2.6.7 Aortic ring: anti-vascular assay

The aortic ring assay was also used to determine the effect of **(2.03)** and **(2.36)** on established vasculature.

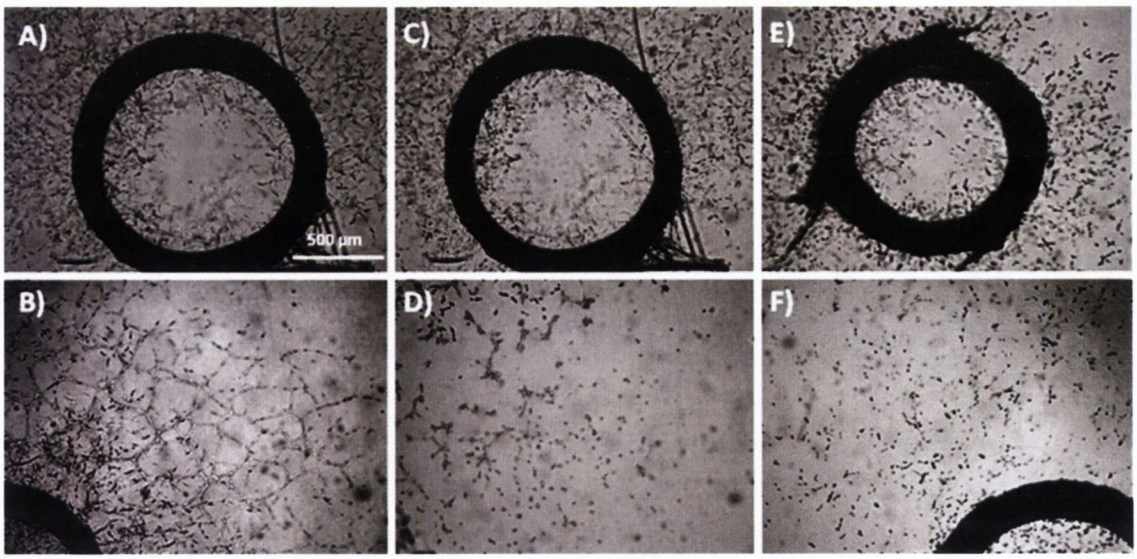

Figure 2.28 Anti-vascular effect of **(2.03)**. The aortic rings were kept in a humidified CO_2 incubator at 37 °C and the medium was changed every other day, starting from day 3. Test compounds were added on day 8. Photomicrographs of the aortic cultures were taken under bright field microscopy using a digital camera (x4). A-B) Before the addition of test compound, C-D) 100 nM **(2.03)** (4 h) and E-F) 100 nM **(2.03)** (24 h).

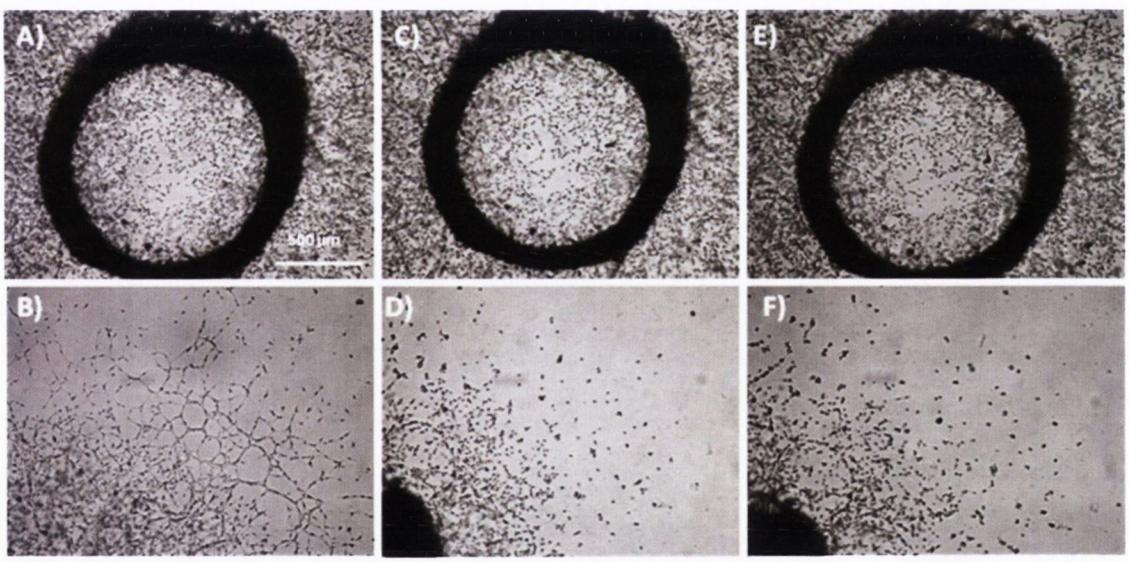

Figure 2.29 Anti-vascular effect of **(2.03)**.The aortic rings were kept in a humidified CO_2 incubator at 37 °C and the medium was changed every other day, starting from day 3. Test compounds were added on day 8. Photomicrographs of the aortic cultures were taken under bright field microscopy using a digital camera (x4). A-B) Before the addition of test compound, C-D) 100 nM **(2.36)** (4 h) and E-F) 100 nM **(2.36)** (24 h).

The ability of compounds **(2.03)** and **(2.36)** to disrupt existing vasculature is readily apparent (Figures 2.28 and 2.29). This further supports the hypothesis that these agents have the potential to act as vascular disrupting agents *in vivo.*

2.6.8 *In vivo* evaluation of phosphate ester prodrug (2.24)

Following the encouraging *in vitro* and *ex vivo* performance of the lead compound **(2.03)**, the phosphate ester prodrug **(2.24)** was evaluated *in vivo.*

The compound was evaluated in a PC-3 tumour xenograft model in mice. Combretastatin A-4 phosphate (CA-4P) was evaluated in tandem as a control.

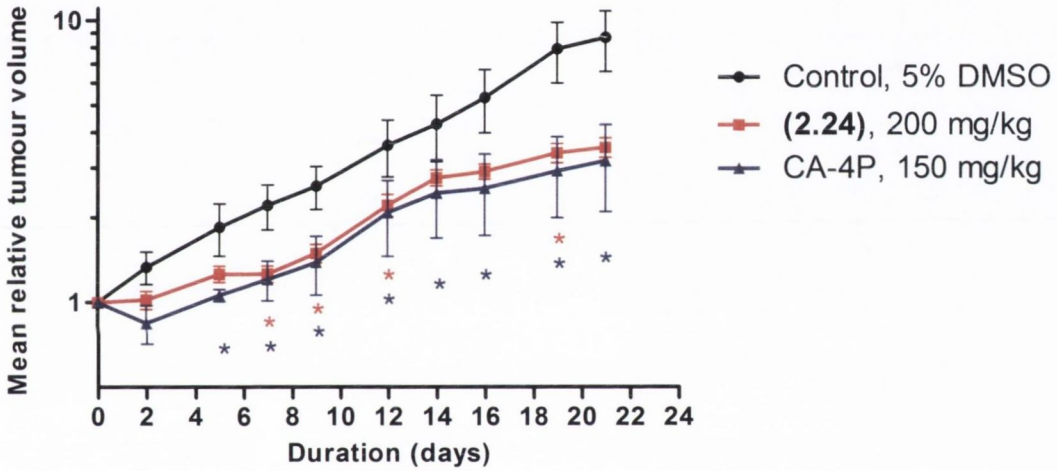

* $p < 0.05$, significantly higher mean relative tumour volume compared with the control group as determined by the Mann-Whitney *U*-test.

Figure 2.30 Evaluation of the efficacy of 200 mg/kg **(2.24)** and 150 mg/kg CA-4P administered once a week for three weeks in a PC-3 tumour xenograft model. Data points represent the mean relative tumour volume ± SEM (n=8).

A statistically significant reduction in mean relative tumour volume compared with the control was observed following treatment with **(2.24)** (Figure 2.30). The efficacy of the compound was found to be comparable with that of the control compound combretastatin A-4 phosphate. This extremely encouraging result demonstrated that the *in vitro* potential of the parent compound **(2.03)** was maintained *in vivo.*

In a separate study, the effect of a single dose of **(2.24)** on PC-3 tumour xenograft vasculature was evaluated.

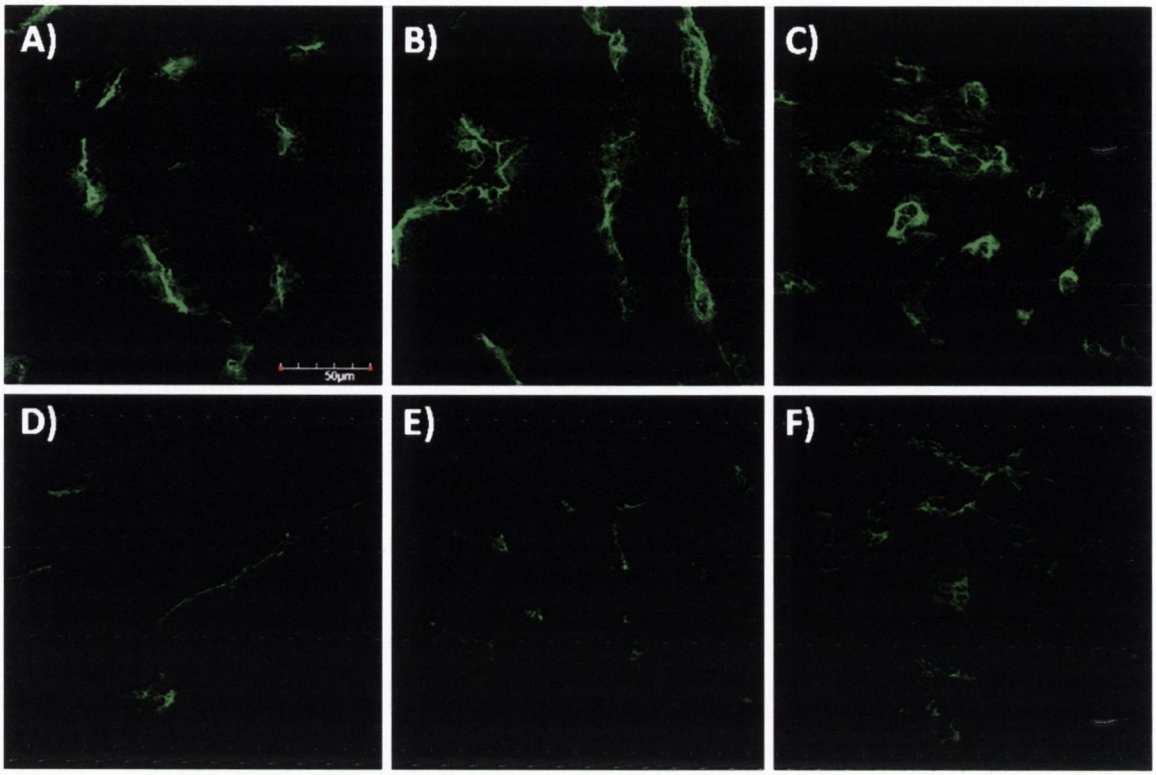

Figure 2.31 The effect of **(2.24)** treatment on tumour vasculature. Images of CD31-stained endothelial cells in cryosections of PC-3 tumours treated with A-C) vehicle (5% DMSO) and D-F) 200 mg/kg **(2.24)**, for 6 h (n = 3).

The anti-vascular effects observed for **(2.03)** *in vitro* were again preserved following evaluation of **(2.24)** *in vivo* (Figure 2.31). These results again suggest the potential utility of **(2.24)** as a clinical drug candidate.

2.7 Conclusions

The new synthetic route for the lead molecules **(2.02)** and **(2.03)**, outlined in this chapter, represented a progressive revision of the initial work conducted by Shah and Hudson [187-188]. An overall yield of 12% over 11 steps was obtained for the improved synthetic route compared with a yield of 1% over 12 steps obtained utilising the original synthesis. In addition, the new pathway avoided the need for two large scale reflux reactions and developed an alternative oxidation strategy for the C-7 position alcohol without the use of the toxic chromium based reagent PDC.

The synthesis of the water soluble, phosphate ester prodrug **(2.24)** was readily accomplished in satisfactory yield following a three step process from the lead compound **(2.03)**. The use of the phosphate ester prodrug strategy was a particularly important development, as it permitted the *in vivo* evaluation of the parent compound **(2.03)**.

Replacement of the hydroxyl of **(2.02)** with an amine group presented a significant synthetic challenge. The poor yield obtained for the synthesis of the enol triflate **(2.26)** and failure of initial attempts to furnish the boronic acid **(2.28)** were both judiciously overcome. The synthesis of the enol triflate **(2.28)** was revised and a substantially improved yield was obtained (72% v 45%). A change in strategy also enabled the synthesis of the boronic acid **(2.31)**, containing a BOC protected aniline group. Despite the successful coupling of the boronic acid **(2.31)** and enol triflate **(2.28)**, the boronic acid was found to be unstable. The boronate ester **(2.33)** was thus synthesised, offering more convenient preparation, increased stability and a comparable performance in the Suzuki coupling reaction.

Biological evaluation of compounds **(2.03)** and **(2.36)** demonstrated the potent anti-mitotic, anti-vascular and anti-angiogenic efficacy of these agents. Significantly, it was established that they possessed biological efficacy comparable with that of the model compound combretastatin A-4. As a consequence of the encouraging biological assessment of the aniline **(2.36)**, it was subsequently utilised by E. Breen in the synthesis of conjugate drugs [213]. The favourable *in vivo* results obtained for the phosphate ester prodrug **(2.24)**, offered further encouragement for the development of this agent as a preclinical drug candidate.

3 Chapter 3

3.0 Introduction

The C-7 position substituent of the tubulin inhibitors synthesised by Shah and Hudson was shown to be a major determinant of the potency of these molecules (Figure 3.1) [187-188]. Therefore, the effect of modification of this position was deemed to be of particular interest in the synthesis of novel tubulin inhibitors suitable for molecular conjugation.

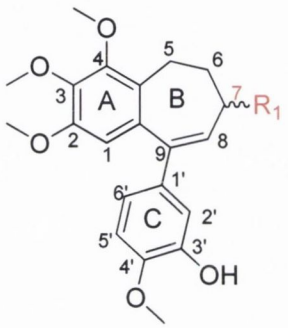

Figure 3.1 Schematic of tubulin inhibitory pharmacophore (The C-7 substituent is highlighted in red)

The potent alcohol **(2.02)** was initially synthesised and evaluated as a racemic mixture. It was thus proposed to stereoselectively synthesise and evaluate both the (*S*) and (*R*)-enantiomers of this compound in order to investigate the effect of stereochemistry at the C-7 position (Figure 3.2).

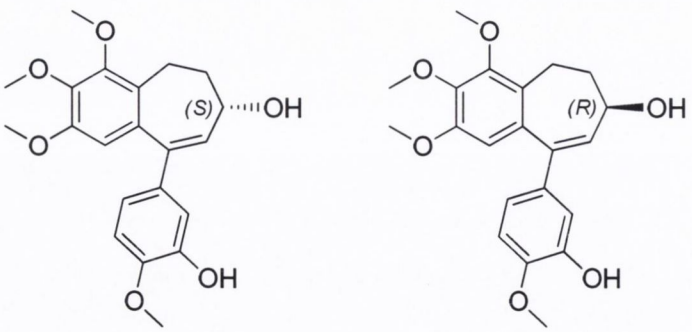

(3.01) **(3.02)**

Figure 3.2 (*S*) and (*R*)-enantiomers of racemic lead compound **(2.02)**

3.1 Aims and Objectives

The primary objective of the work laid out in this chapter was to develop a methodology to introduce stereoselectivity into the synthesis of the lead compound **(2.02)**. Once this had been accomplished an appropriate technique to determine the stereochemical purity of the resultant molecules would be required. Determination of the absolute configuration of any enantiomerically pure compound synthesised would also be of integral importance. Finally, it would be necessary to develop a synthetic scheme to achieve the efficient synthesis of both enantiomers of compound **(2.02)** in acceptable yield.

3.2 Homochiral drug substances

Enantiomers are stereoisomers that are composed of the same atoms connected in the same order, which differ only in the arrangement in space of substituents at the chiral centre [190]. (*R*) and (*S*)-enantiomers of a substance have identical NMR and IR spectra and identical physical properties and differ only in the direction in which they rotate plane polarised light [190].

Pharmacologically, (*R*) and (*S*)-enantiomer of bioactive molecules have the potential to interact in different ways with the asymmetric environment of drug targets [214]. The chirality of active pharmaceutical ingredients has become a major theme in the design and synthesis of new drug products in recent years [215]. The top three selling drugs of 2008, Lipitor, Plavix and Nexium, with combined sales of over $30 billion, are single enantiomer drugs [216]. The worldwide market share of chiral drugs in single enantiomer form has grown from 27% in 1996, to 39% in 2002 and is still growing [215].

Traditionally, enantiomers of biologically active molecules were divided by Ariëns into the eutomer, which possessed the desirable pharmacologically activity and the distomer, which was either inactive or in some cases largely responsible for the side effects of the racemate [217]. The more complex reality of the situation has since been revealed. It has since been established that if one enantiomer is responsible for the desired pharmacologically activity the other enantiomer can:

- Possess some desired pharmacological activity (warfarin [218] and verapamil [219])
- Be inactive
- Be an antagonist of the desired pharmacological activity

- Possess a different, but desirable activity (ketamine and labetalol [220]
- Possess a different, but undesirable activity [221]

Depending on the situation the potential advantages of the synthesis of stereochemically pure drug molecules include:

- Reduction of total drug dose administered
- Enhancement of the therapeutic window
- Reduction of patient response variability
- More precise estimation of dose-response relationship [215]

Esomeprazole **(3.03)** is one example of a compound which has been presented clinically in single enantiomer form (Figure 3.3). Esomeprazole is a proton-pump inhibitor and is the active pharmaceutical ingredient in Nexium, a product licensed for the treatment of various gastro-oesophageal reflux disorders and peptic ulceration. The substituted benzimidazole esomeprazole is the (*S*)-isomer of omeprazole **(3.04)**, which is also marketed as a racemic mixture for largely identical indications as Losec [222]. In head to head clinical trials, the (*S*)-enantiomer (esomeprazole) was found to be more efficacious than racemic omeprazole, when administered at the same dose [223].

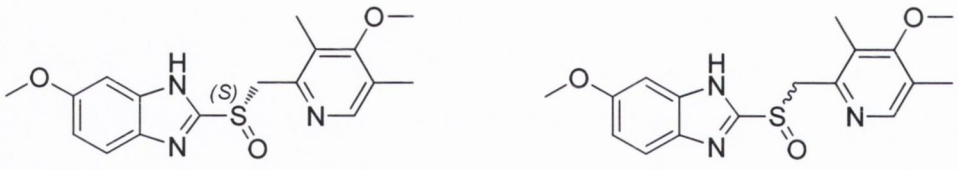

(3.03) **(3.04)**

Figure 3.3 Structure of (*S*)-omeprazole **(3.03)** and racemic omeprazole **(3.04)**

Similarly, the fluoroquinolone antibiotic, levofloxacin **(3.05)** (marketed as Tavanic), consists of the (*S*)-enantiomer of the racemic drug substance ofloxacin **(3.06)**. The (*S*)-enantiomer is reported to have an antibacterial activity up to two orders of magnitude higher than the (*R*)-enantiomer [224].

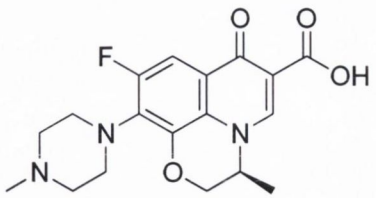

(3.05)

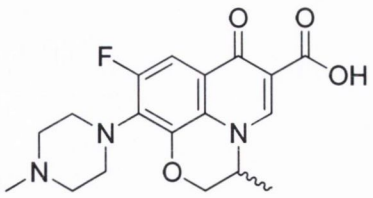

(3.06)

Figure 3.4 (*S*)-ofloxacin (Levofloxacin) **(3.05)** and racemic ofloxacin **(3.06)**

Other chiral drugs remain marketed as racemates despite convincing arguments for stereochemically pure presentations. Examples include the anticoagulant warfarin, where (*S*)-warfarin has been shown to possess a anticoagulant potency 3–5 times greater than (*R*)-warfarin [225]. Similarly, (*S*)-ketoprofen is 2-4 times more potent than the racemate [221] Methadone is also still presented as a racemate despite the fact that (*R*)-methadone accounts for the majority, if not the entirety, of its opioid effect [226]. The anaesthetic ketamine is also marketed as a racemic mixture. Comparison of the potencies of the individual enantiomers suggest an vastly superior potency for the (*S*)-(+)-ketamine as compared with that of the (*R*)-(-)-enantiomer [41,42]. Conversely, (*R*)-(-)-ketamine but not (*S*)-(+)-ketamine was found to be responsible for side effects such as hallucinations, restlessness and agitation in surgical patients [227-228].

Taking into consideration the potential for dramatic differences between enantiomers in terms of pharmacological activity, attention turned to the technical aspects of how best to achieve the desired synthesis of **(3.01)** and **(3.02)**. In the synthesis of **(2.02)** described previously, chirality was introduced by reduction of the achiral ketone **(2.07)** using sodium borohydride (Scheme 2.3). Both sides of the ketone were equally amenable to hydride attack and since both the reducing agent and the starting material were achiral, a racemic mixture of both the (*S*) and (*R*)-alcohols was obtained [190]. In order to synthesise both the (*R*) and (*S*)-enantiomers of **(2.02)** in stereochemically pure form, the possibility of the stereoselective reduction of the prochiral ketone **(2.07)** was explored.

3.3 Asymmetric reduction of ketones

The asymmetric reduction of ketones has become a key approach in the synthesis of stereochemically pure organic molecules [190]. The transformation can be achieved in a number of different ways. Resolution of the racemic mixture [190], use of a chiral auxiliary [229], use of chiral reducing agents [230] and chiral catalysts [231] and use of an oxido-reductase enzyme

system [232] have all been employed in asymmetric syntheses. Each of these methods has their inherent advantages and disadvantages.

The synthesis of a pair of diastereomers by the esterification of the racemic alcohol **(2.08)** with a stereochemically pure acid was initially considered. Subsequent chromatographic separation of the resulting pair of diastereomers and hydrolysis of the esters would afford both the (*R*) and the (*S*) enantiomers in homochiral form. Alternatively, the use of a chiral column would allow the separation of the enantiomers without derivatisation [190]. This solution would provide convenient access to both enantiomers of the alcohol in high enantiomeric excess. The principal disadvantage of this approach was that complete duplication of the synthetic route at this early stage would be required, resulting in a halving of the ultimate yield of each enantiomerically pure final compound. The use of a chiral auxiliary also receives considerable attention in the literature but in the absence of a suitable procedure for the desired reaction, this avenue was not further explored [190].

There are many examples of chiral reducing agents in the literature. The chiral reducing system developed by Yatagai utilised a sodium borohydride/(L)-tartaric acid system. This method was reported to reduce a variety of β-keto ester containing compounds in variable yields (16-100%) and with varying degrees of stereoselectivity (0-86% enantiomeric excess) [229]. Similarly the alpine-borane chiral reducing agent championed by Midland achieved modest yields and poor stereoselectivity in the reduction of β-keto esters, despite the use of high pressures and long reaction times [230].

Chiral catalysis has similarly been extensively exploited in the asymmetric reduction of ketones. Enantioselective hydrogenation catalysts, in particular those derived from 2,2'-bis(diphenylphosphino)-1,1'-binaphthyl (BINAP) ligands, are reported to be capable of reducing β-keto esters in extremely high enantiomeric excesses [231, 233-235]. These reactions typically employ expensive catalysts and extreme conditions of pressure under hydrogen and thus were not deemed feasible for the large scale reaction sequence being attempted. However, another class of chiral catalyst, examined in more detail, were the CBS reagents.

Since 1987, the chiral oxazaborolidines known as CBS reagents (after the work of Corey, Bakshi and Shibata) have been employed for the enantioselective reduction of prochiral ketones [236]. These reagents have been utilised in a variety of complex syntheses, accomplishing the enantioselective reduction of various functionalised ketones in excellent yield and enantiomeric

purity [237-239]. It was hypothesised that these reagents could be exploited to introduce the desired chirality into the synthesis of stereochemically pure **(2.02)**. Thus, this approach was further explored (Section 3.8.2).

The enantiomerically selective reduction of β-keto esters utilising the oxido-reductase enzyme system in baker's yeast is another methodology reported extensively in the literature. Satisfactory yields and high degrees of enantiomeric selectivity have been reported for such transformations. Due to the convenient and inexpensive nature of this approach, this method was chosen for the initial attempt to introduce the desired stereochemistry into the synthesis of **(3.01)** and **(3.02)**.

3.4 Yeast reduction of β-keto ester (2.07)

Typically, a bioreduction reaction involves adding the substrate to incubating fermenting yeast in an aqueous medium [232]. However, this method involves considerable difficulty in the isolation of the product from the large volume of aqueous solvent. Emulsions can also form, further hindering the work-up [240-241]. The use of petroleum ether as solvent greatly simplified the work-up as the yeast could simply be decanted off [240-241]. According to the procedure outlined by North *et al.*, the β-keto ester was combined with yeast from *Saccharomyces cerevisiae* type II (obtained from Sigma-Aldrich) together with distilled water and petroleum ether as solvent [240-241]. The water was found to be essential for the normal functioning of the yeast and hence the oxidative enzyme system [242]. The reaction was shaken overnight. The solvent was then decanted and together with the washings, was concentrated and purified by flash column chromatography to afford the desired β-hydroxy ester in reasonable yield (43%; Scheme 3.1).

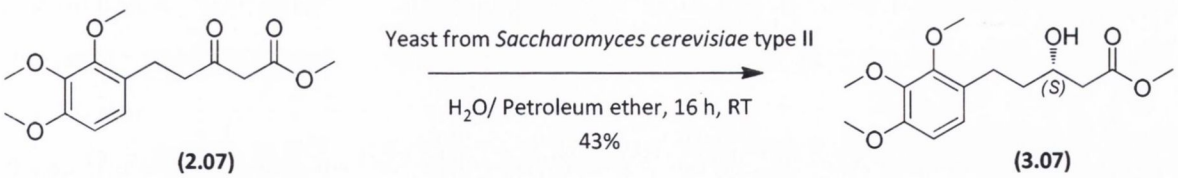

(2.07) **(3.07)**

Scheme 3.1 Bioreduction of **(2.07)**

It has been reported that the amount of reduced cofactor present in the yeast cells and thus, the amount of yeast used in the reaction was the rate limiting factor for this reaction [241]. Cognisant of this fact, the procedure employed for subsequent reactions was modified to use a higher

proportion of yeast according to the procedure established by Athanasiou *et al.* [243]. After 18 h, complete conversion was achieved with a significant improvement in isolated yield (60%).

In order to establish the broader applicability of this reaction, it was decided to examine the results of the yeast bioreduction of the ethyl ester **(2.17)**

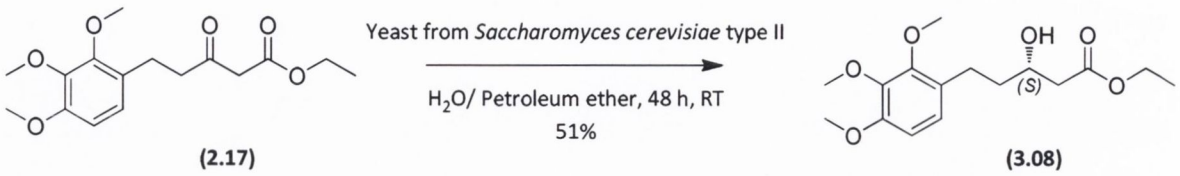

(2.17) **(3.08)**

Scheme 3.2 Bioreduction of **(2.17)**

The yeast reduced the β-keto ester **(2.17)** effectively and in a comparable yield to that attained for the corresponding methyl ester **(2.07)** (51% v 60%) thus, demonstrating the versatility of the reaction.

According to the literature, an enantiomeric excess of the order of 45-98% would be expected for the β-keto ester reduction reaction, with stereoselectivity for the (S)-enantiomer [241, 244]. However, the enantioselectivity of the reduction still had to be established.

3.5 Determination of enantiomeric purity of (3.07) by NMR

Enantiomers cannot be distinguished by NMR in an achiral medium, since the resonances of enantiotopic nuclei are isochronous [245]. However, diastereomers may be distinguished because the resonances (of certain diastereotopic nuclei) are anisochronous [245]. Thus, the determination of stereochemical purity of a chiral compound can be achieved by the use of a chiral auxiliary, which converts the mixture of enantiomers into diastereomers which can be distinguished by NMR.

The use of chiral derivatising agents remains one of the most reliable NMR techniques for assaying enantiomeric purity [245]. One of the most widely used reagents is α-methoxy-α-(trifluoromethyl)phenylacetic-acid (MTPA or Mosher's acid; Figure 3.5).



(3.09)

Figure 3.5 (*R*)-3,3,3-trifluoro-2-methoxy-2-phenylpropanoic acid ((*R*)-MTPA or (*R*)-Mosher's acid)

This reagent found favour following introduction by Mosher in 1969 for a number of reasons [246]. Firstly, because there is no hydrogen α to the carboxylic acid, racemisation during the derivatisation process is impossible [245]. Secondly, the constituent trifluoromethyl group of Mosher's acid allows the relatively uncluttered ^{19}F NMR spectrum to be utilised for unambiguous and accurate determination of enantiomeric purity. This is usually possible, since in the case of a pair of diastereomers only two peaks would be apparent in the ^{19}F spectrum (provided the molecule whose stereochemistry is being assessed does not contain any additional fluorine atoms). Therefore, owing to the relative ease of derivatisation and the reported reliability of this methodology, the (*R*)-Mosher's esters of the bioreduced alcohol and the sodium borohydride reduced alcohols were synthesised [245].

The (*R*)-Mosher's ester of the racemic alcohol **(2.08)** was prepared by coupling with (*R*)-Mosher's acid. 2,6-Dichlorobenzoyl chloride was used as coupling reagent. DIPEA was employed as base. DMAP was added as acylation catalyst. The product **(3.10)** was then purified by flash column chromatography ensuring that no discrimination between diastereomers occurred in the process (Scheme 2.3).

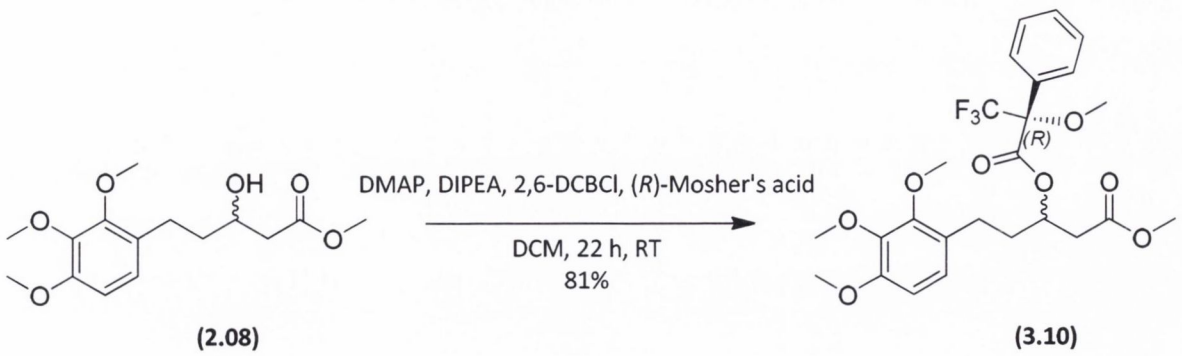

(2.08) **(3.10)**

Scheme 3.3 Synthesis of (*R*)-Mosher's ester **(3.10)**

The (*R*)-Mosher's ester of the bioreduced alcohol **(3.07)** was synthesised similarly to afford **(3.11)** (Scheme 3.4).

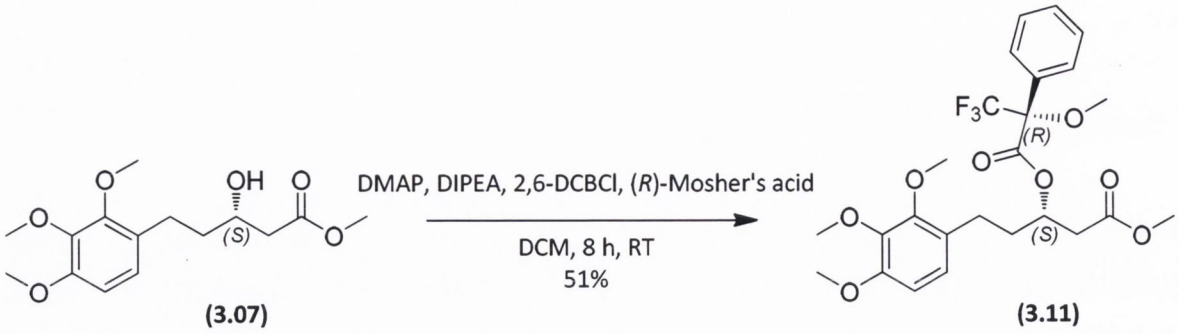

Scheme 3.4 Synthesis of (*R*)-Mosher's ester **(3.11)**

The ^{19}F NMR spectra of both compounds were then obtained (Figure 3.6 and 3.7). The spectrum of the racemic alcohol ester **(3.10)** was, as expected, observed to have two peaks at -72.01 ppm and -71.84 ppm with essentially equivalent integration (100:86). The (*R*)-Mosher's ester of the bioreduced alcohol, compound **(3.11)** however, was observed to have one majorly predominant peak at -72.01 ppm with a much less significant peak at -71.84 ppm (100:1). The two signals in the racemic ester **(3.10)** arose as a result of the two diastereomers formed, namely (*S,R*) and (*R,R*)-diastereomers of the alcohol and chiral (*R*)-Mosher's acid. Since the trifluoromethyl groups were in different chemical environments in both diastereomers, they resonated at different frequencies. In the ester of the enantiomerically pure alcohol **(3.11)**, only one enantiomer, (*S,R*), is formed to an appreciable extent and hence only one peak is observed. The enantiomeric purity of the bioreduced alcohol **(3.07)** was thus estimated to be in excess of 99%. Thus, the enantiomeric excess of the (*S*)-enantiomer was estimated to be of the order of 98%.

The specific optical rotation $[\alpha]_D^{25}$ of the alcohol **(3.07)** was determined using a polarimeter and was found to be - 10.70 (*c* = 1.68, DCM). As a control measurement, the specific optical rotation of the racemic alcohol **(2.08)** was also determined. It was not found to be optically active, with a rotation of 0 (*c* = 0.8, DCM) observed.

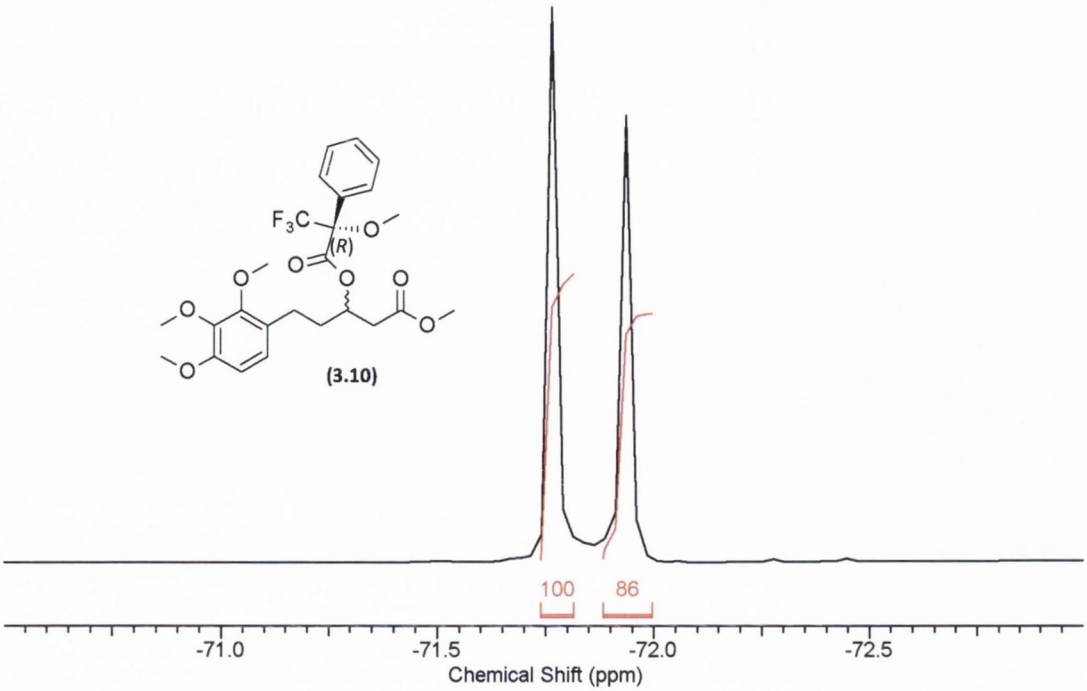

Figure 3.6 ^{19}F NMR spectrum of racemic alcohol (R)-Mosher's ester **(3.10)**

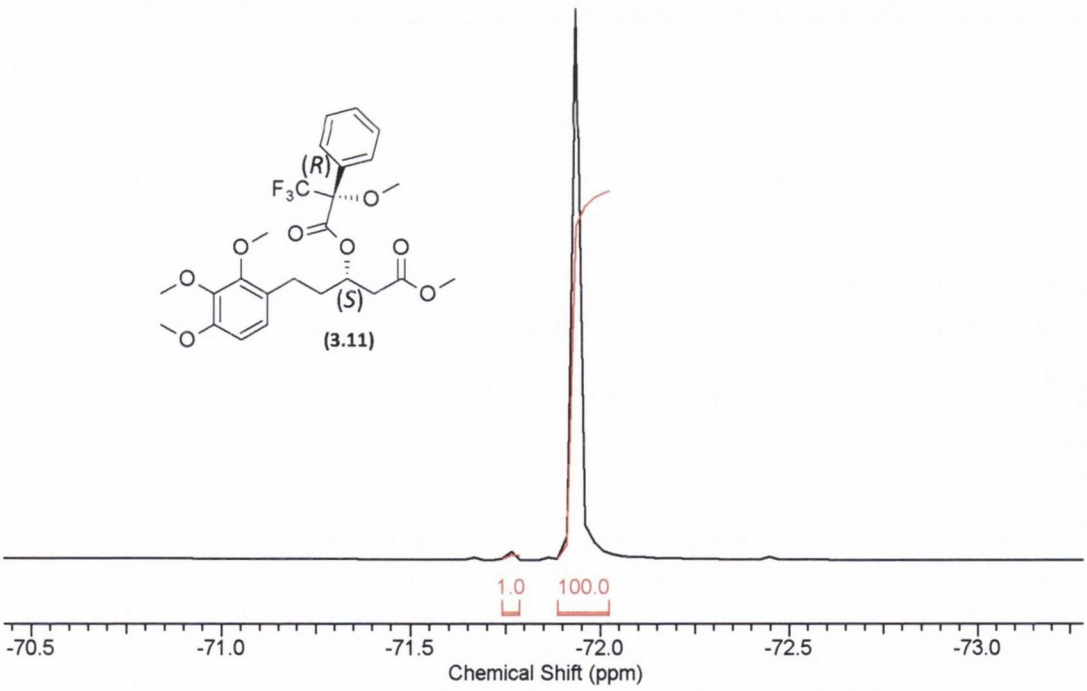

Figure 3.7 ^{19}F NMR spectrum of bio reduced alcohol R-Mosher's ester **(3.11)**

3.6 Confirmation of absolute configuration of bioreduced alcohol by NMR

Examination of the published literature for baker's yeast reductions of β-keto esters suggested that the bioreduced alcohol **(3.07)** would be of (*S*)-configuration [241]. However, in order to confirm that it was in fact the (*S*)-enantiomer that was isolated, an NMR-based procedure taken from Ohtani *et al.* was employed [247]. The procedure undertaken was as follows:

1. Assign as many protons as possible with respect to each of the (*R*) and (*S*) Mosher's acid esters of the alcohol under investigation
2. Calculate the difference in the resonance frequency for each proton between the (*S*) and (*R*) esters, $\Delta\delta$ (where $\Delta\delta = \delta_S - \delta_R$)
3. Put the protons with positive $\Delta\delta$ values on the right side and those with negative $\Delta\delta$ values on the left side of model A (Figure 3.8)
4. Construct a molecular model of the compound in question and confirm that all the assigned protons with positive and negative $\Delta\delta$ values are actually found on the right and left sides of the Mosher's ester plane, respectively. When all these conditions are satisfied, model A will indicate the absolute conformation of the compound.

The method is based on the premise that due to the diamagnetic shielding effect of the aromatic ring, the H_A, H_B and H_C signals of the (*R*)-Mosher's ester should resonate upfield relative to those of the (S)-Mosher's ester. Conversely, the reverse should hold true for the H_X H_Y, H_Z signals.

In accordance with the method prescribed by Ohtani, the (*S*)-Mosher's ester of the bioreduced alcohol was synthesised. The procedure outlined for the synthesis of the (*R*)-Mosher's ester **(3.11)** was employed (Scheme 3.4). The (S)-Mosher's ester **(3.12)** was subsequently isolated in acceptable yield (77%) and along with the (*R*)-Mosher's ester **(3.11)** was analysed by NMR (Figure 3.9 and 3.10).

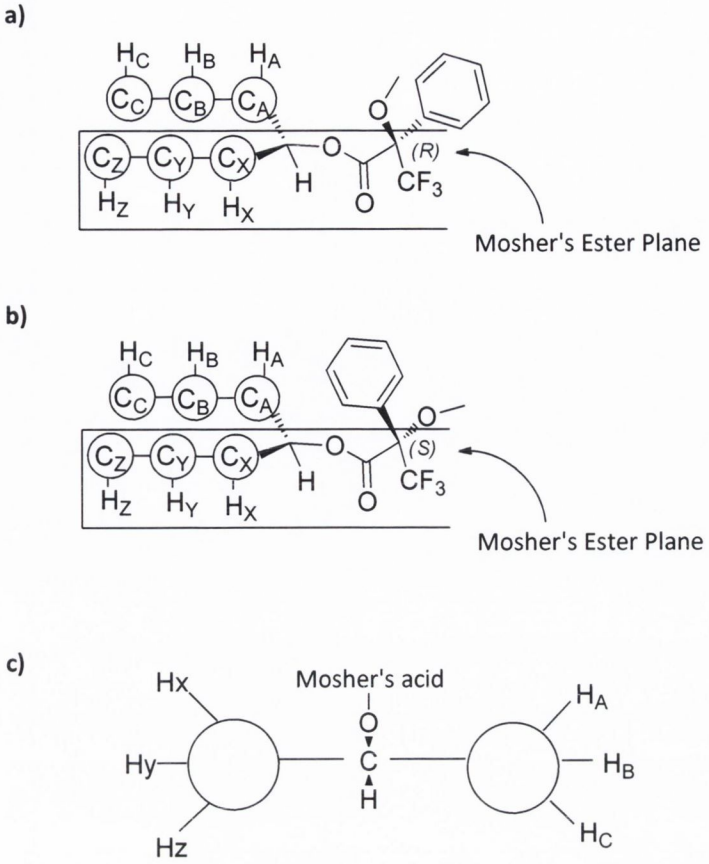

Figure 3.8 Ohtani's Model for determination of absolute configuration by NMR

a) and b) illustrate the configurational correlation model for the (*R*) and (*S*)-Mosher's esters used by Ohtani. The arrow indicates the ester plane. It is from the direction of this arrow that the model in part c) is derived, with the H_A, H_B and H_C protons on the right of the ester plane and the H_X, H_Y and H_Z protons on the left hand side

c) Model A proposed by Ohtani to determine the configuration of secondary alcohols.

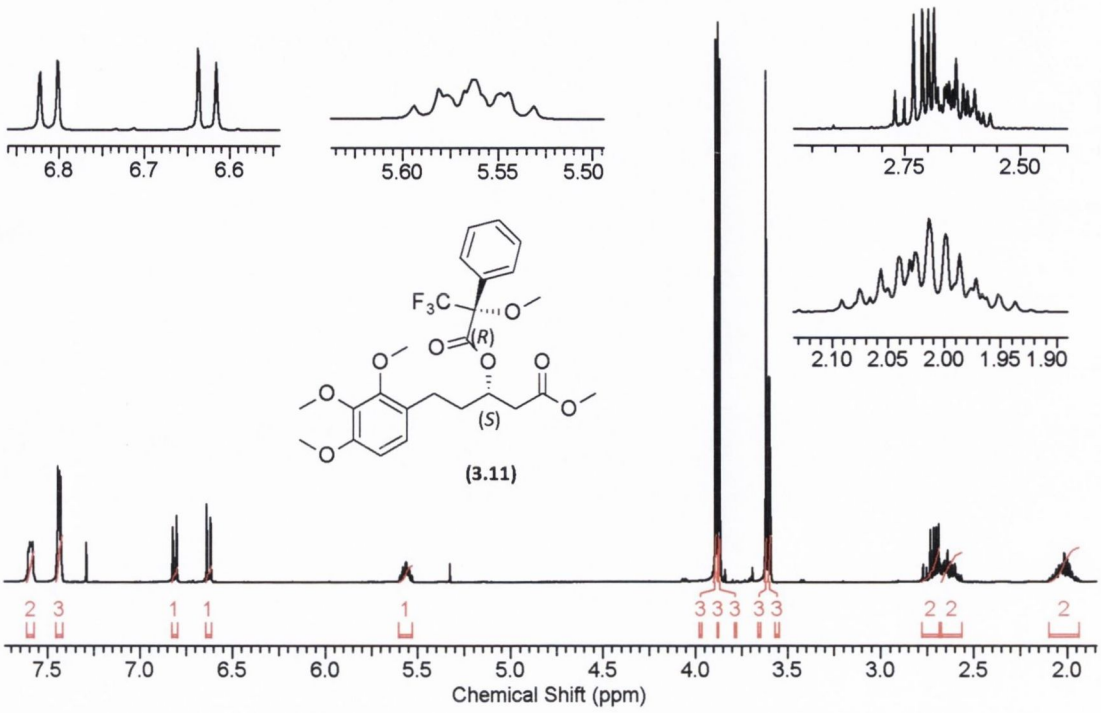

Figure 3.9 ^{1}H NMR of (*R*)-Mosher's ester **(3.11)**

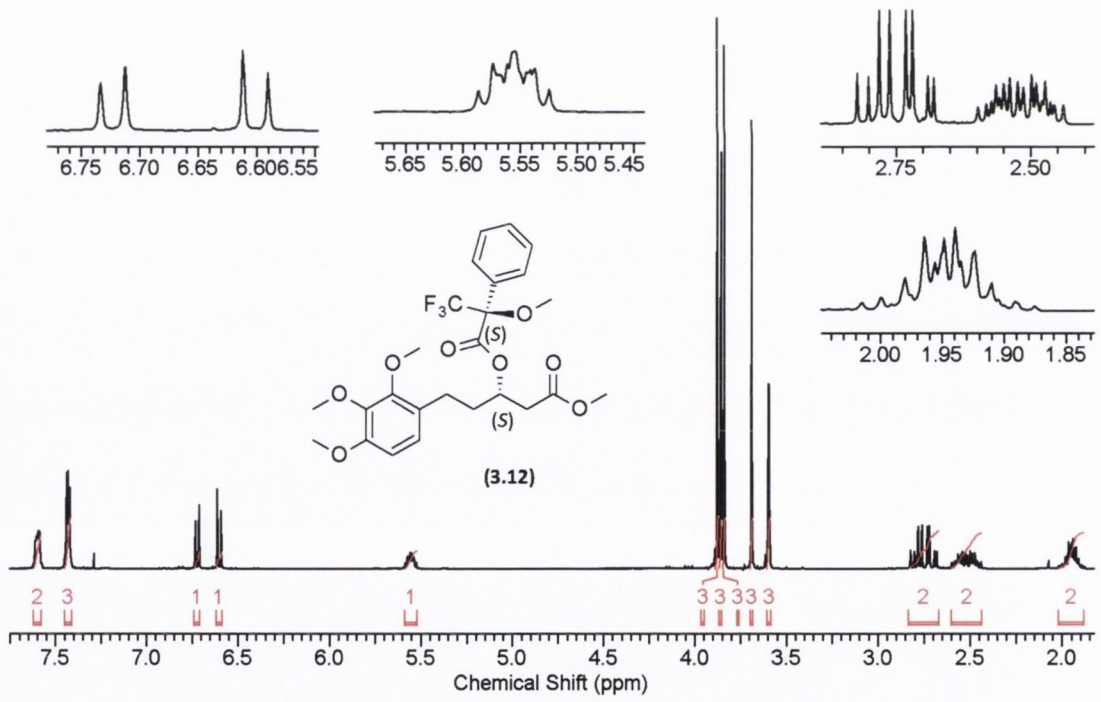

Figure 3.10 ^{1}H NMR of (*S*)-Mosher's ester **(3.12)**

The ^{1}H NMR spectra of **(3.11)** and **(3.12)** were assigned using a combination of one and two dimensional NMR experiments. The difference in chemical shift between the esters for each proton (Δδ) was calculated (where $\Delta\delta = \delta_S - \delta_R$; Table 3.1).

Proton*	(*S*)-Mosher's ester **(3.12)** ^{1}H NMR resonance (ppm)	(*R*)-Mosher's ester **(3.11)** ^{1}H NMR resonance (ppm)	Δδ (ppm)
1	1.95	2.00	-0.05
2	2.51	2.61	-1.0
3	2.74	2.70	+0.04
4	3.68	3.61	+0.07
5	3.83	3.86	-0.03
6	3.86	3.87	-0.08
7	3.88	3.88	0
8	6.60	6.63	-0.02
9	6.72	6.80	0

Table 3.1 Calculation of Δδ for (*R*) and (*S*)-esters, **(3.11)** and **(3.12).** *The proton designations are as shown in Figure 3.11).

Once the Δδ values were obtained, the model devised by Ohtani was constructed by placing the protons with positive values on the right side of model A and the protons with negative values on the left hand side (Figure 3.11; a)). The structure was then re-drawn in the more conventional format taking into consideration the configuration determined by Model A (Figure 3.11; b)).

Hence, the configuration of the bioreduced alcohol **(3.07)** was confirmed as the (*S*)-enantiomer, corroborating the evidence available from review of the literature. The stereochemistry of the ethyl ester **(3.08)** was confirmed similarly, by the synthesis and subsequent NMR analysis of the equivalent (*S*) and (*R*) Mosher's esters **(3.13)** and **(3.14)** (Figure 3.12).

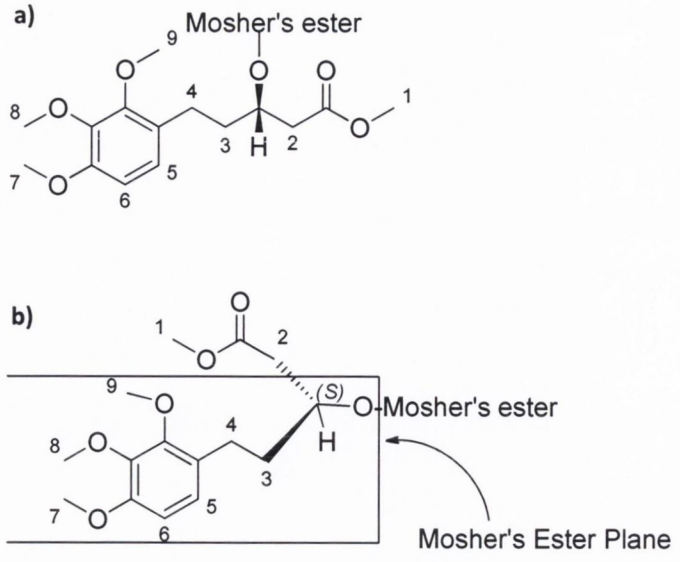

Figure 3.11 a) Model A re-drawn with the positive value Δδ protons on the right side and the negative Δδ values on the left side b) Configurational correlation model illustrating the (*S*)-stereochemistry of the alcohol **(3.07)**

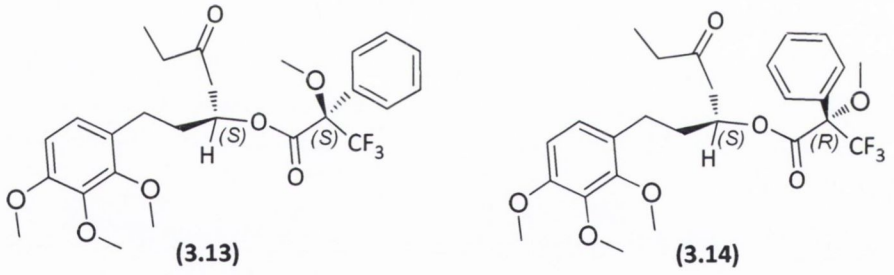

Figure 3.12 (*S*) and (*R*)-Mosher's esters of ethyl ester **(3.08)**

It was thus shown that the yeast had selectively reduced the β-keto ester **(2.17)** to the (*S*)-enantiomer alcohol **(3.08)** and that the transformation had resulted in a product with an enantiomeric purity greater than 99%.

3.7 Synthesis of enantiomerically pure (3.01)

Once the methodology to successfully introduce the desired stereoselectivity had been established, this knowledge was employed in the synthesis of the (*S*)-enantiomer of the lead

compound **(2.02)** to afford **(3.01)**. The synthesis was accomplished in an analogous manner to that employed for the racemate.

3.7.1 Silyl protection of (3.07) and hydrolysis of ester (3.15)

The enantiomerically pure alcohol **(3.07)** was protected as a *tert*-butyldiphenylsilyl ether by reacting with TBDPSCl using imidazole as base. After 16 h, the reaction was deemed to have gone to completion and after purification the desired protected compound **(3.15)** was isolated as a clear oil in excellent yield (98%). The protected alcohol **(3.15)** was then dissolved in a mixture of methanol and THF and subject to base catalysed hydrolysis using sodium hydroxide aqueous solution. Following purification, the carboxylic acid **(3.16)** was obtained in modest yield (46%; Scheme 3.5).

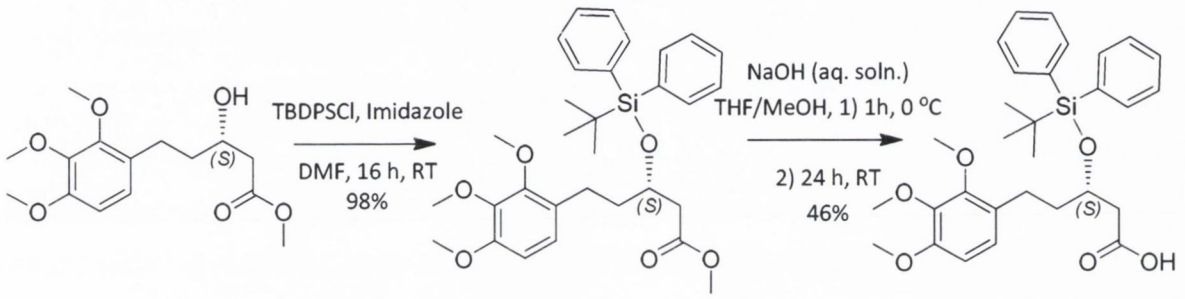

(3.07) **(3.15)** **(3.16)**

Scheme 3.5 Protection of alcohol **(3.07)** and hydrolysis of methyl ester **(3.15)**

3.7.2 Cyclisation of (3.16) and removal of silyl protecting group of (3.17)

Intramolecular cyclisation of the carboxylic acid **(3.16)** was then carried out. The carboxylic acid **(3.16)** was dissolved in dry DCM under an atmosphere of nitrogen and oxalyl chloride, together with a catalytic quantity of DMF, was added at 0 °C. After 2 h, the volatile organic phase of the reaction mixture was removed under vacuum and the resulting acid chloride intermediate was reconstituted with fresh, dry DCM. Tin (IV) chloride was then added to the reaction mixture at -15 °C to catalyse the intramolecular cyclisation. Following purification, the desired ketone **(3.17)** was obtained in moderate yield (54% over two steps) as a yellow oil. Compound **(3.17)** was subsequently dissolved in dry THF and TBAF solution was added at 0 °C under nitrogen. The temperature was the allowed to reach ambient after 30 min. After a further 3 h, the reaction

mixture was added directly to a silica gel flash column. Following purification, the free alcohol **(3.18)** was obtained in moderate yield (56%) as a yellow oil (Scheme 3.6).

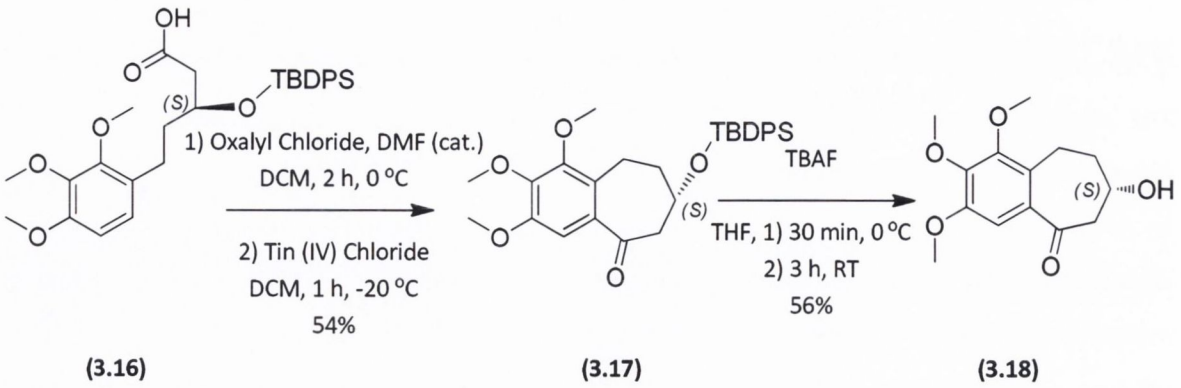

(3.16) **(3.17)** **(3.18)**

Scheme 3.6 Cyclisation of carboxylic acid **(3.16)** and deprotection of alcohol **(3.17)**

3.7.3 Coupling of (2.14) and (3.18) and removal of silyl groups

The C-ring bromide **(2.14)** was then dissolved in dry THF under an atmosphere of nitrogen and subject to lithiation at -78 °C by treatment with *n*-butyllithium. After 40 min, a solution of the AB-ring compound **(3.18)** in dry THF was added dropwise under anhydrous conditions. After 1 h, the temperature of the reaction was allowed to increase to ambient and after a further 4 h, the reaction was quenched by the addition of HCl aqueous solution. Following purification, compound **(3.19)** was obtained in satisfactory yield (59%) as a yellow resin. The phenol protecting group on **(3.19)** was then readily removed by treatment with TBAF solution at 0 °C. After 1 h, the reaction mixture was purified by flash column chromatography to afford the desired product **(3.01)** as a white solid in excellent yield (96%; Scheme 3.7).

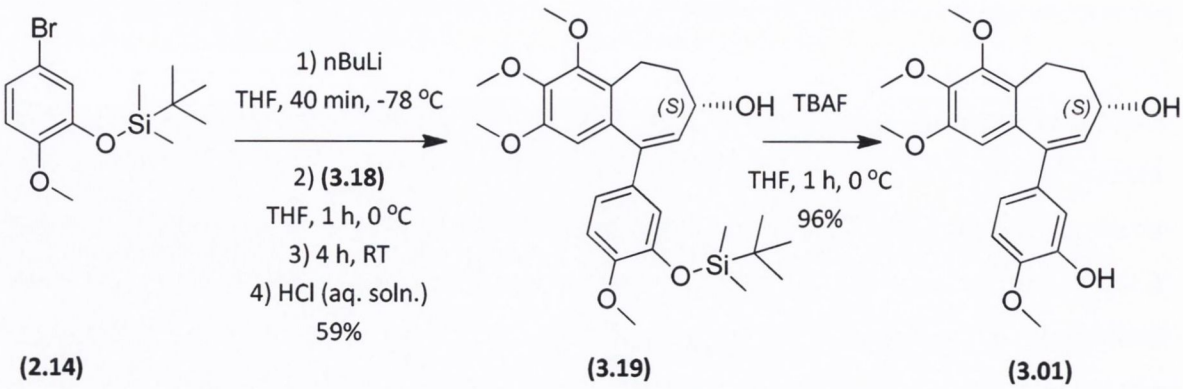

(2.14) **(3.19)** **(3.01)**

Scheme 3.7 Organolithium coupling of **(2.14)** and **(3.18)** and silyl deprotection of **(3.19)**

3.8 Introducing (*R*)-configuration at the C-7 position

Once the successful synthesis of **(3.01)** had been accomplished, attention turned to the synthesis of the opposite enantiomer, **(3.02)**. The main obstacle to this objective was devising a suitable method of obtaining (*R*)-configuration at the C-7 position.

3.8.1 Synthetic strategy

In order to introduce the required (*R*)-configuration into the synthesis, a variety of different approaches were explored. Initial attempts focused on the stereoselective reduction of the β-keto ester **(2.07)**, to afford the (*R*)-enantiomer alcohol, utilising the CBS reagents. The Mitsunobu reaction was then carried out to try to effect clean inversion of configuration of the (*S*)-enantiomer alcohol **(3.07)**

Following the failure of these approaches, inversion of configuration at the C-7 position alcohol of the cyclised compound **(3.18)** was proposed. Due to previous experience with the chemistry of this molecule, suitable protection of the C-9 carbonyl group was deemed necessary in order to remove the potential for elimination. Therefore, the C-9 position carbonyl was reduced and protected. Inversion of configuration of the suitably protected compound using the Mitsunobu reaction was then attempted. Once again, unsatisfactory stereochemistry was obtained with this approach.

The S_N2 displacement of a mesylate at the C-7 position by an acetate anion was thus proposed as an alternative method of achieving inversion of configuration. It is ultimately this method which provided the desired access to the (*R*)-configuration C-7 alcohol. Therefore, this approach was employed in the synthesis of **(3.02)**

3.8.2 Use of CBS reagents to reduce (2.07)

The chiral catalyst CBS reagents were investigated as a method of introducing the desired (*R*)-chirality to the C-7 position. These oxazaborolidine based reagents have been reported to mediate the reduction of functionalised ketones with a high degree of enantioselectivity and in excellent yields [236-238]. Therefore, the stereoselective reduction of the prochiral ketone **(2.07)** using the chiral catalyst (*S*)-(−)-2-methyl-CBS-oxazaborolidine was attempted.

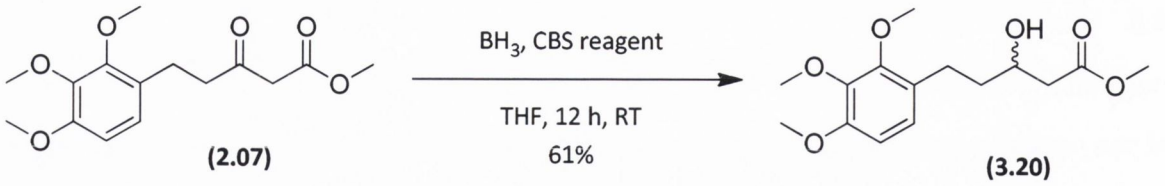

Scheme 3.8 Attempted stereoselective reduction of **(2.07)** using CBS catalyst

Various procedures, obtained from the literature, utilising (S)-(−)-2-Methyl-CBS-oxazaborolidine as chiral catalyst and borane solution in THF as reducing agent were undertaken [236, 248-250]. The alcohol **(3.20)** was obtained in variable yield (0-61%; Scheme 3.8). Initially, the quantity of borane used was kept to the recommended 0.6 equivalents and the temperature was maintained at ambient as increasing either of these variables was reported to reduce the enantioselectivity of the reaction [250]. Particular attention was paid to the exclusion of all moisture from the reaction, as the catalysts were reported to give erratic results in the presence of water [239].

In order to establish the stereoselectivity of the transformation, the (*R*)-Mosher's ester of **(3.20)** was synthesised following the procedure used for previous Mosher's acid esterification reactions (Scheme 3.9). Following purification, the Mosher's ester **(3.21)** was obtained in good yield (90%) as a yellow oil.

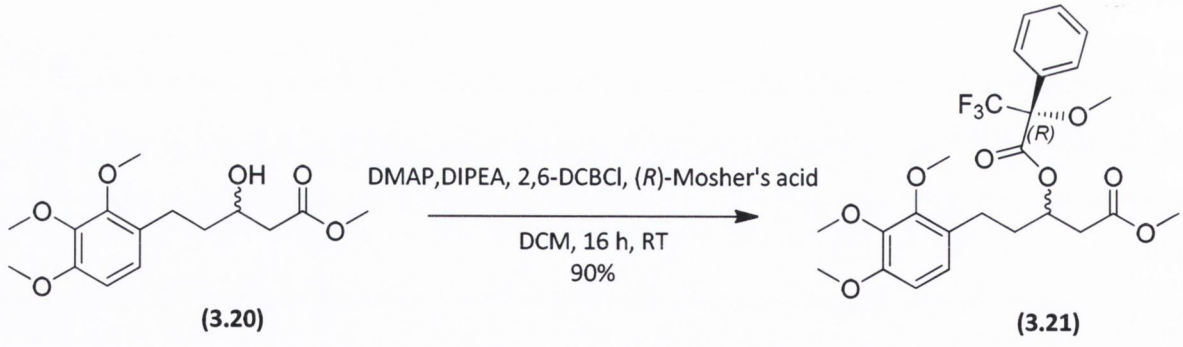

Scheme 3.9 Synthesis of Mosher's ester **(3.21)**

The (*R*)-Mosher's ester **(3.21)** was then subject to ^{19}F NMR in order to establish the stereochemistry of the CBS reduced alcohol **(3.20)** (Figure 3.13).

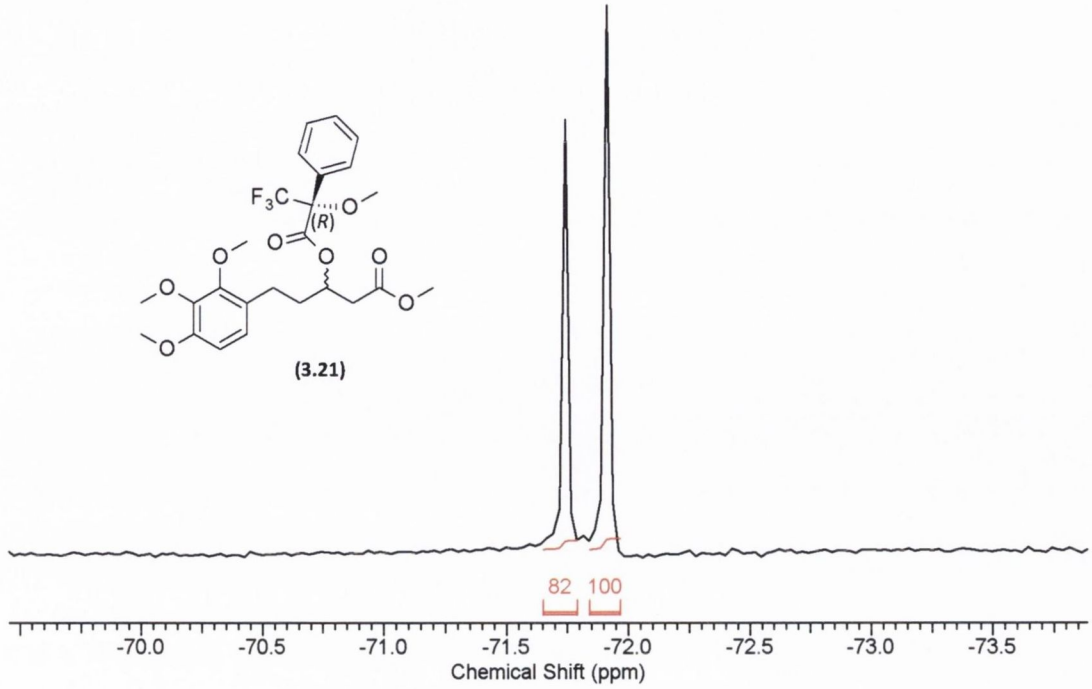

Figure 3.13 ^{19}F NMR spectrum of (*R*)-Mosher's ester **(3.21)**

As can be seen from the ^{19}F NMR spectrum of compound **(3.21)** (Figure 3.13), negligible stereoselectivity was obtained using the CBS mediated reduction (82:100). It is interesting to note that slight selectivity was obtained for the (*S*)-enantiomer. This interesting finding is the opposite result obtained following sodium borohydride reduction of the β-keto ester (Figure 3.6) and the opposite result expected for this reaction according to the literature [236, 248-250]. This approach was not pursued further.

3.8.3 Attempted inversion of configuration using the Mitsunobu reaction

Due to the high yield and excellent enantioselectivity afforded by the yeast reduction, it was hypothesised that a simple inversion of configuration using the well known Mitsunobu reaction would provide ready access to the desired molecule **(3.02)**.

According to the literature, the Mitsunobu reaction allows the conversion of primary and secondary alcohols into esters, phenyl esters, thioesters and other compounds with clean inversion of configuration [190]. The reaction requires diethylazodicarboxylate (DIAD) and triphenylphosphine together with formic acid as a nucleophile. The reaction proceeds by the formation of a triphenylphosphine-DIAD complex which is then attacked by the alcohol which activates the alcohol as a good leaving group. The formic acid then acts as a nucleophile and

carries out a substitution reaction resulting in the formation of a formate ester. The driving force for the reaction is the formation of a stable phosphorous oxygen bond. Triphenylphosphine oxide is thus formed as a side product of the reaction. It was postulated that the (*S*)-β-hydroxy ester **(3.07)** could be converted to the formate ester **(3.22)** (Scheme 3.10). This formate ester could then be readily hydrolysed under mildly basic conditions to liberate the (*R*)-β-hydroxy ester.

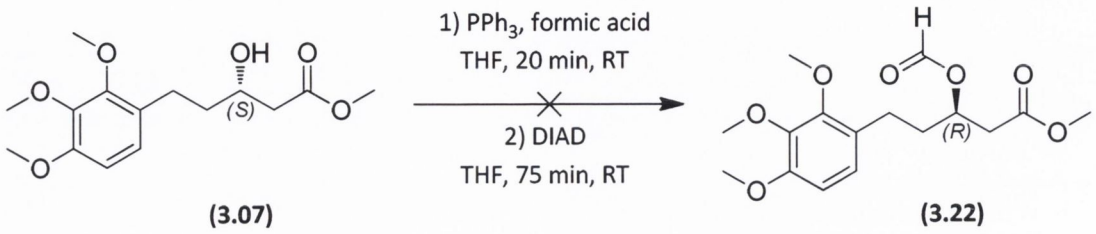

(3.07) **(3.22)**

Scheme 3.10 Attempted Mitsunobu reaction

Despite attempting the reaction using a variety of different reaction conditions, the desired product was not isolated. It was proposed that due to the strong drive for conjugation in the system, rather than undergoing a substitution reaction with the formic acid, an elimination reaction was favoured, yielding a more conjugated side product.

3.8.4 Removing the source of conjugation: Reduction of the C-7 position carbonyl and protection of the resultant alcohol

Due to the preference for elimination rather than substitution, as outlined for the Mitsunobu reaction on compound **(3.07)** above, it was decided to attempt the inversion of configuration at a later stage in the synthesis. The cyclised compound **(3.17)** was adjudged to be the most appropriate point in the synthesis to carry out the Mitsunobu reaction. However, it had been observed from previous chemistry with this compound, that the alcohol at the C-7 position was also prone to elimination. The drive for elimination occurs due to the highly conjugated structure of the enone-containing elimination product **(3.23)** [188].

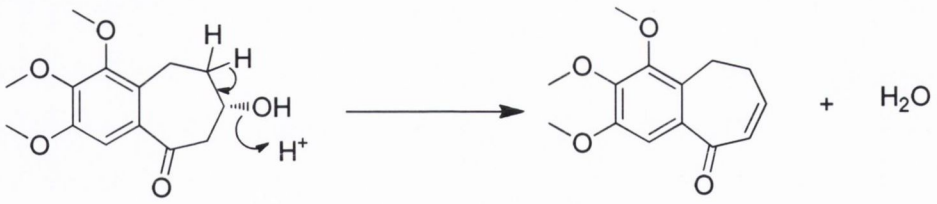

(3.18) (3.23)

Scheme 3.11 Conjugation as a driving force for elimination at the C-7 position alcohol

Therefore, in order to successfully carry out the Mitsunobu reaction, it would first be necessary to modify the carbonyl group at the C-9 position, thus negating the potential for the formation of the highly conjugated AB ring system **(3.23).** It was decided to pursue a strategy, first employed by Hudson, of reducing the C-9 ketone and protecting it appropriately [188]. This would allow the necessary chemistry to be carried out at the C-7 position. Removal of the protecting group and oxidation of the alcohol would then be undertaken to re-introduce the C-9 carbonyl.

3.8.5 The acetate protecting group

The first protection strategy employed was the use of an acetate ester. This technique had previously been employed by Hudson in a related synthesis [188].

3.8.5.1 Reduction of ketone (3.17) and synthesis of acetate ester

The ketone **(3.17)** was dissolved in a mixture of methanol and THF and the reaction cooled to 0 °C. Sodium borohydride was then added. After 5 min, the reaction was deemed to have gone to completion. Following purification, the desired alcohol **(3.24)** was obtained in good yield (75%), as a white solid (Scheme 3.12).

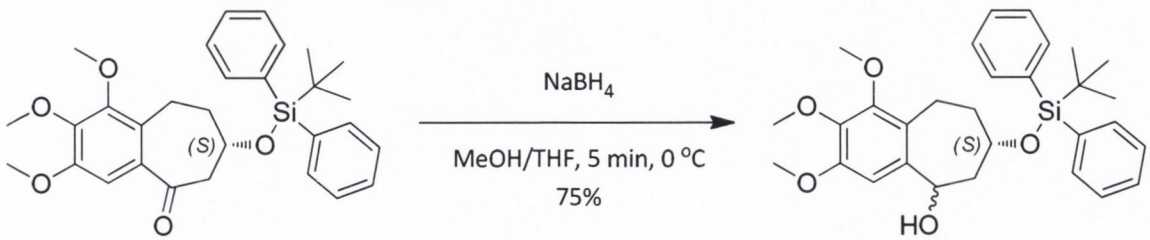

(3.17) (3.24)

Scheme 3.12 Reduction of ketone **(3.17)**

The alcohol **(3.24)** was dissolved in dry DCM under an atmosphere of nitrogen. DIPEA was added as base, DMAP was utilised as an acylation catalyst and acetic anhydride was added at 0 °C. After 1 h, the reaction was deemed to have gone to completion. Following purification, the acetate **(3.25)** was obtained in excellent yield (100%) as a yellow oil.

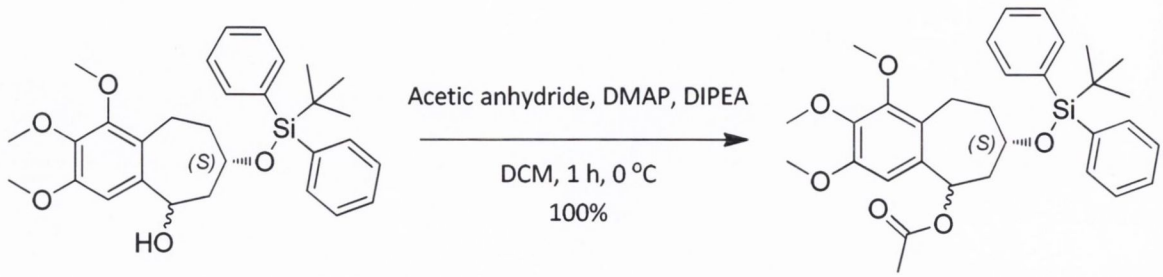

(3.24) **(3.25)**

Scheme 3.13 Acetate protection of C-9 alcohol

3.8.5.2 Mitsunobu reaction on acetate protected alcohol (3.26)

The C-7 alcohol *tert*-butyldiphenylsilyl ether protecting group of compound **(3.25)** was first removed, in preparation for the attempted Mitsunobu reaction. TBAF solution was added to a solution of **(3.25)** in dry THF, at 0 °C under anhydrous conditions. After 24 h, the reaction was deemed to have gone to completion. Following purification, the alcohol **(3.26)** was obtained as an off-white solid in excellent yield (100%; Scheme 3.14).

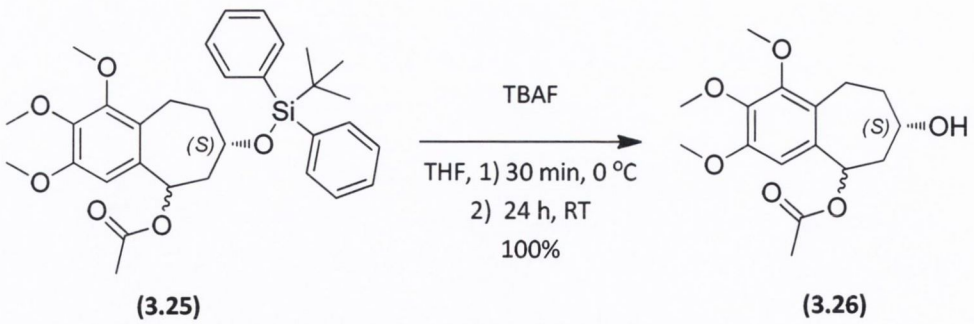

(3.25) **(3.26)**

Scheme 3.14 Removal of silyl protecting group from compound **(3.25)**

The Mitsunobu reaction was then attempted. Triphenylphosphine, formic acid and compound **(3.26)** were dissolved in dry THF under an atmosphere of nitrogen. After 20 min, DIAD was added dropwise (Scheme 3.15).

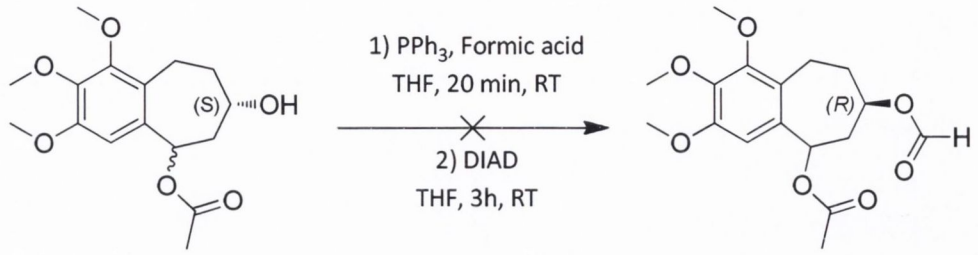

(3.26) **(3.27)**

Scheme 3.15 Attempted Mitsunobu reaction on compound **(3.26)**

After a further 3 h, a complex mixture of products was observed to have formed by TLC analysis. Following purification and rudimentary analysis of the principal products formed, it was established that the desired transformation had not taken place. It was hypothesised that the acetate group was extremely labile under the conditions employed. In order to carry out the chemistry required at the C-7 position alcohol, it became apparent that a more robust protection strategy would have to be found for the C-9 alcohol. Therefore, a number of alternative protecting groups were explored.

3.8.6 The 2-methoxyethoxymethyl ether protecting group

The 2-methoxyethoxymethyl ether (MEM) protecting group was explored as an alternative protection strategy for the C-9 hydroxyl functionality. The MEM group was first introduced by Corey *et al.* in 1976. Due to ease of introduction and removal of the MEM ether and its high stability to a range of acidic and basic conditions, it has been frequently employed for the protection of hydroxyl groups [204, 251].

3.8.6.1 Synthesis of MEM ether containing compound (3.28)

Following a procedure outlined by Corey *et al.*, the benzylic alcohol **(3.24)** was combined with 2-methoxyethoxymethyl chloride (MEMCl) in dry DCM, utilising DIPEA as base [251]. However, after 24 h, the starting material remained unchanged.

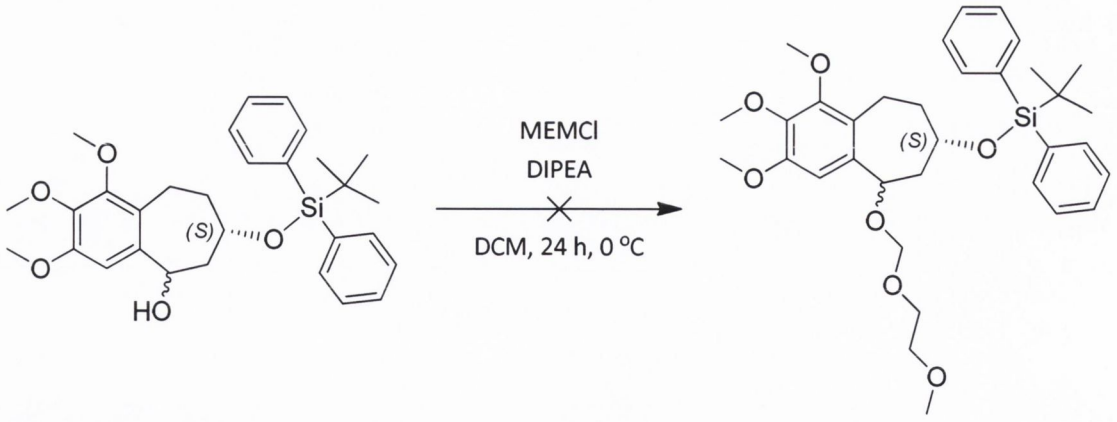

(3.24) **(3.28)**

Scheme 3.16 Attempted MEM protection of **(3.24)**

An alternative procedure for the MEM protection of alcohols outlined by Corey *et al.* was then explored [251]. Using sodium hydride as base, the MEM ether was obtained in good yield (77%; Scheme 3.17).

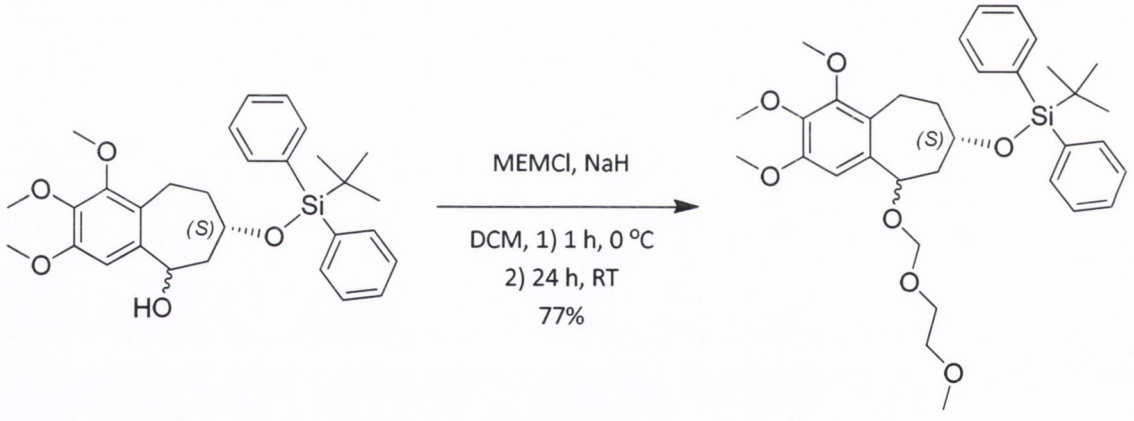

(3.24) **(3.28)**

Scheme 3.17 MEM protection of **(3.24)**

In order to establish the ultimate usefulness of the MEM ether as a protection strategy, it was first necessary to determine the relative ease with which it could eventually be removed. Accordingly, a trial deprotection reaction using the Lewis acid zinc bromide in dry DCM was undertaken.

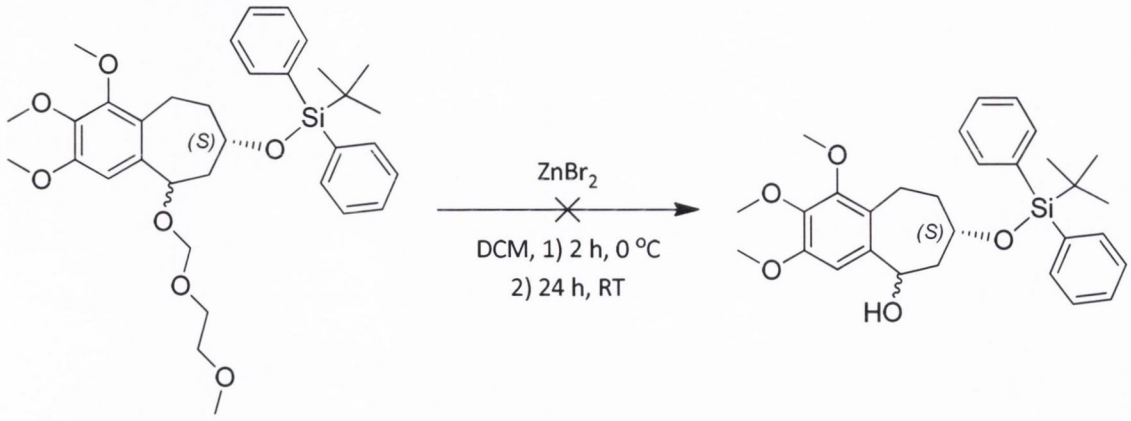

(3.28) **(3.24)**

Scheme 3.18 Attempted removal of MEM protecting group

Despite repeated assurances in the literature of the relative ease with which this group could be removed, no change in the MEM protected compound was observed after 24 h [204, 251]. A variety of alternate reaction conditions were explored. However, the MEM group proved particularly resilient to removal and thus other protection strategies were examined.

3.8.7 The tetrahydropyranyl ether protecting group

The tetrahydropyranyl ether (THP) protecting group is another protection strategy introduced by Corey *et al.* [252]. The THP protecting group has been used extensively as a protection strategy in complex organic synthesis due to its low cost, ease of introduction and general stability to most non-acidic conditions [204]. The THP protecting group was readily introduced to compound **(3.24)**. The compound was dissolved in DCM and 3,4-dihydro-*2H*-pyran and *p*-toluenesulfonic acid were added. After 25 min, the reaction was deemed to have gone to completion. Following purification, the desired THP ether **(3.29)**, was obtained in excellent yield (94%) as a yellow oil (Scheme 3.19).

While the introduction of the THP protecting group proceeded cleanly and in high yield, the introduction of a third chiral centre posed a number of difficulties in the chromatography and analysis of the resulting compound. The THP ether **(3.29)** potentially consisted of 8 stereoisomers which manifested themselves on TLC as three distinct entities. Furthermore, the extreme complexity of the ^{1}H NMR spectrum strongly discouraged the use of this protecting group. Thus, an alternative protection strategy was sought.

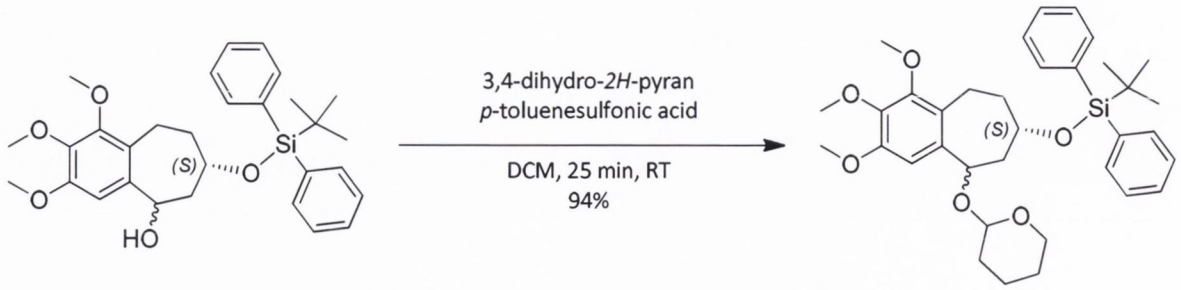

(3.24) **(3.29)**

Scheme 3.19 THP protection of **(3.24)**

3.8.8 The methoxymethyl ether protecting group

The methoxymethyl ether (MOM) protecting group is a substituted ether closely related to the MEM protecting group (Section 3.8.6). The MOM ether was reported to be robust in the presence of a wide range of reaction conditions and, according to the literature, was readily and conveniently introduced and removed [204].

3.8.8.1 MOM ether synthesis

The MOM ether was introduced using a procedure described by Walsh [253-254]. The alcohol **(3.24)** was dissolved in dimethoxymethane and lithium bromide and *para*-toluenesulfonic acid were added to catalyse the reaction. This afforded the MOM ether **(3.30)** readily and in satisfactory yield (74%).

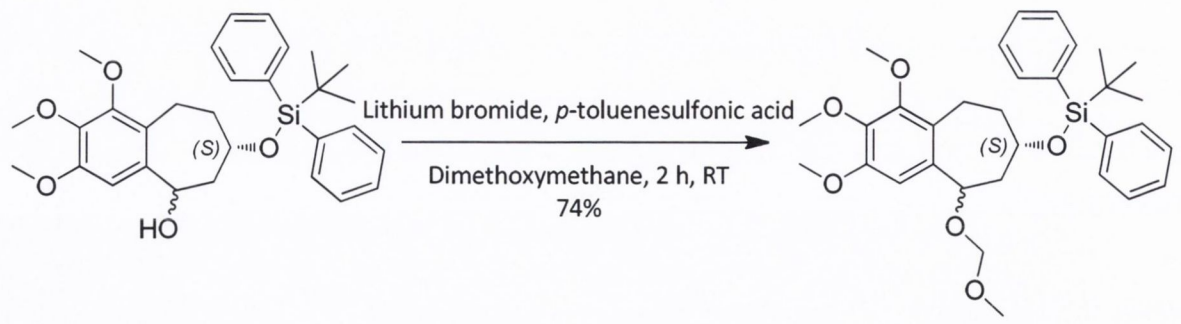

(3.24) **(3.30)**

Scheme 3.20 MOM protection of **(3.24)**

3.8.8.2 Characterisation of MOM ether (3.30)

The MOM ether **(3.30)** was characterised by NMR spectroscopy. Compound **(3.30)** was possessed of two chiral centres which complicated the assignment of both the proton and carbon spectra. While configuration at the C-7 carbon was exclusively (*S*) due to the stereoselectivity of the yeast bioreduction, the stereochemistry at the C-9 carbon was found to be either (*R*) or (*S*). Therefore, one major and one minor diastereomer were found to be present within **(3.30)**.

The distinctive *tert*-butyl group protons of the C-7 protecting group were found to resonate furthest upfield as a singlet at 1.08 ppm for the major diastereomer and 1.17 ppm for the minor diastereomer. The aromatic protons of the *tert*-butyldiphenylsilyl protecting group of both the major and minor diastereomers were found to resonate as two distinct multiplets at 7.38-7.50 ppm and at 7.70-7.80 ppm. The four methoxy methyl group protons of the major diastereomer were found to resonate at 3.25 ppm, 3.82 ppm, 3.87 ppm and 3.90 ppm while the equivalent minor diastereomer protons were found to resonate at 3.35 ppm, 3.80 ppm, 3.87 ppm and 3.90 ppm. The C-7 proton (C<u>H</u>OSi) of the major and minor diastereomers was found to resonate together as a multiplet at 3.94-4.05 ppm by reference to the HSQC spectrum (Figure 3.17). Similarly, the C-9 proton (C<u>H</u>OCH_2) of the major diastereomer was found to resonate as a doublet (J = 10.85 Hz) at 4.44 ppm while the minor diastereomer C-9 proton resonated as a broad singlet at 4.32 ppm. The MOM protecting group protons (OCH_2O) of the major diastereomer resonated as two distinct doublets (J = 6.6 Hz) at 4.51 ppm and 4.55 ppm, while the equivalent minor diastereomer protons resonated as broad singlet at 4.61 ppm. The A-ring aromatic proton of the major diastereomer was found to correspond to a singlet at 6.87 ppm. The equivalent A-ring proton of the minor diastereomer meanwhile, resonated as a singlet at 6.79 ppm. The assignment of the B-ring CH_2 protons for **(3.30)** relied heavily on the HSQC spectrum. An expansion of the HSQC, focusing on the most pertinent region for these assignments is shown in Figure 3.18. The six B-ring CH_2 protons of the major diastereomer were found to resonate at 1.28-1.39 ppm, 1.65-1.78 ppm, 1.89-2.05, 2.15-2.24 ppm (2 x CH_2) and 3.13-3.22 ppm. The minor diastereomer CH_2 protons were found to resonate at 1.28-1.39 ppm, 1.65-1.78 ppm, 1.89-2.05 ppm (2 x CH_2), 2.83 ppm and 2.98-3.04 ppm.

Examination of the DEPT 135 spectrum revealed that the six B-ring CH_2 carbons resonated as five distinct peaks at 18.14 ppm, 19.29 ppm, 34.41 ppm, 42.55 ppm, and 44.73 ppm while the MOM group CH_2 carbons were found to resonate at 94.44 ppm (Figure 3.15). The *tert*-butyl methyl carbons ($C(\underline{C}H_3)_3$) were found to resonate at 26.95 ppm and 27.09 ppm. The methoxy carbons

were identified as resonating as six signals at 55.46 ppm, 55.56 ppm, 56.00 ppm, 60.87 ppm, 61.34 ppm and 61.39 ppm. The C-7 carbons (CHOSi) were found to resonate at 73.49 ppm and the C-9 carbons ($CHOCH_2$) were assigned as resonating at 69.89 ppm and 70.89 ppm. The aromatic CH carbons were found to resonate at 103.14 ppm, 127.62 ppm, 129.65 ppm, 135.83 ppm, 135.87 ppm, and 135.89 ppm with the aid of the DEPT 90 spectrum (Figure 3.15). The quaternary *tert*-butyl carbons were found to resonate at 19.17 ppm and 19.35 ppm, while the remainder of the quaternary carbons were assigned to peaks appearing at 134.36 ppm, 134.38 ppm, 134.41ppm, 134.51 ppm, 138.07 ppm, 140.71 ppm, 150.86 ppm, 150.89 ppm, 151.10 ppm, and 151.42 ppm.

The identity of **(3.30)** was further analysed by mass spectrometry. The molecular ion peak [M+Na] was found to have a mass of 573.2669. This value was in close approximation to the calculated value of 573.2648, further confirming the identity of **(3.30)**

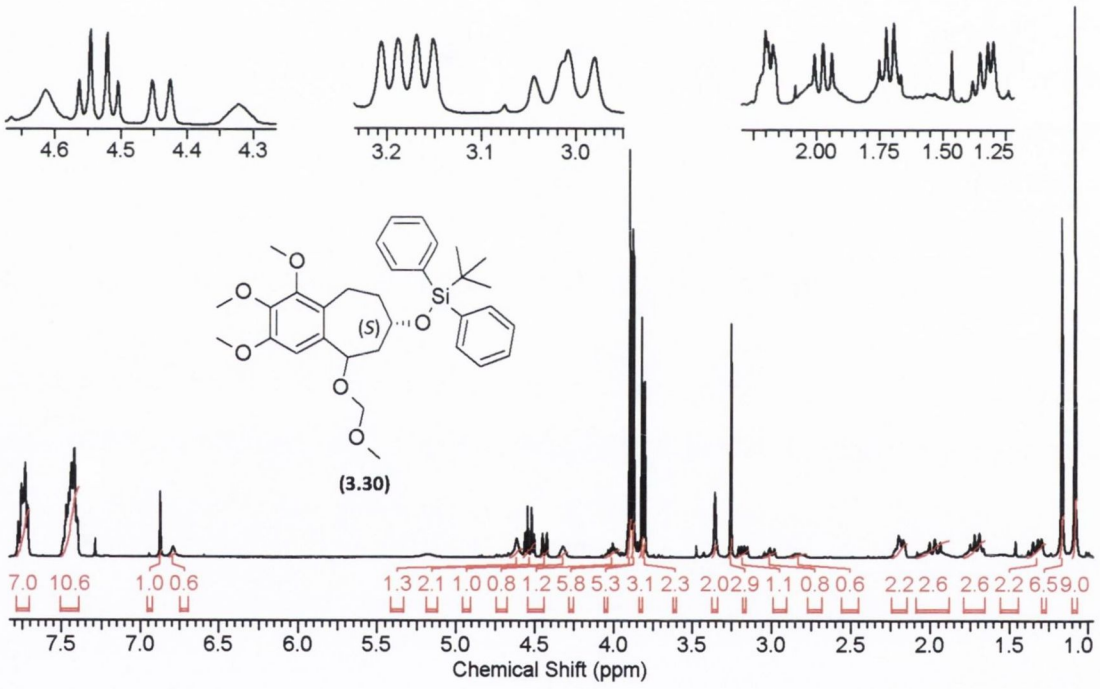

Figure 3.14 ^{1}H NMR spectrum of **(3.30)**

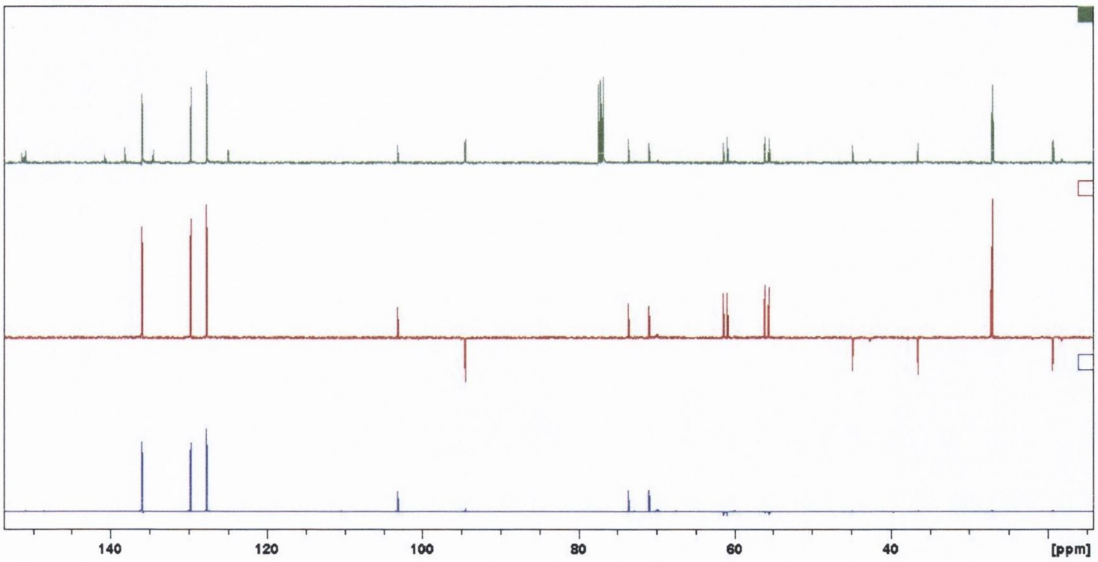

Figure 3.15 ^{13}C, DEPT 135 and DEPT 90 spectra of **(3.30)**

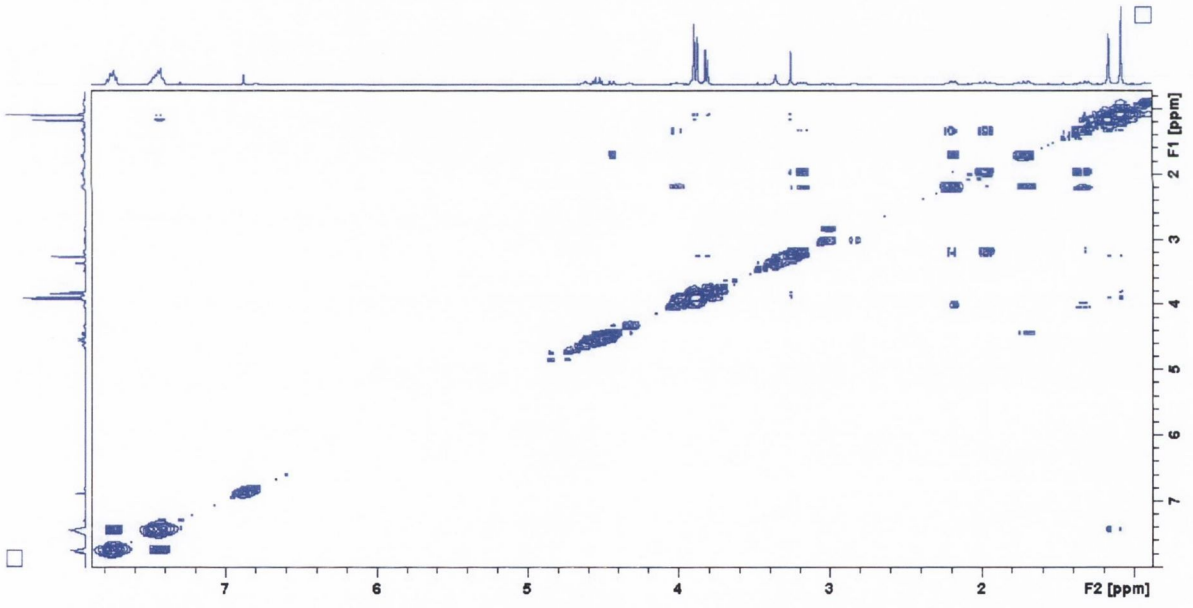

Figure 3.16 HH COSY spectrum of **(3.30)**

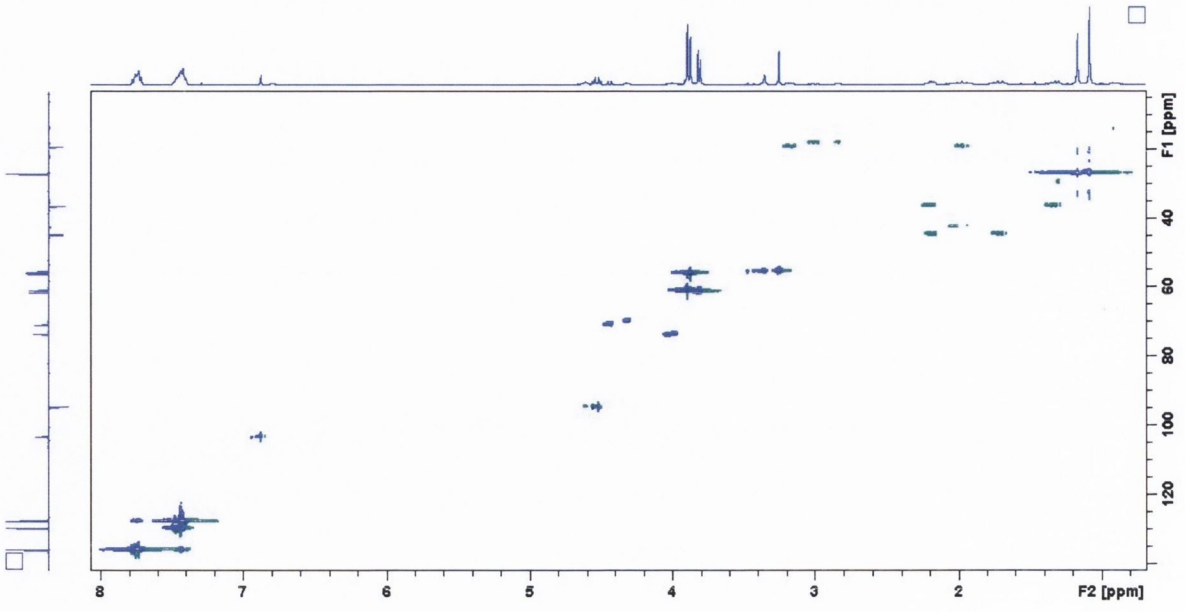

Figure 3.17 HSQC spectrum of **(3.30)**

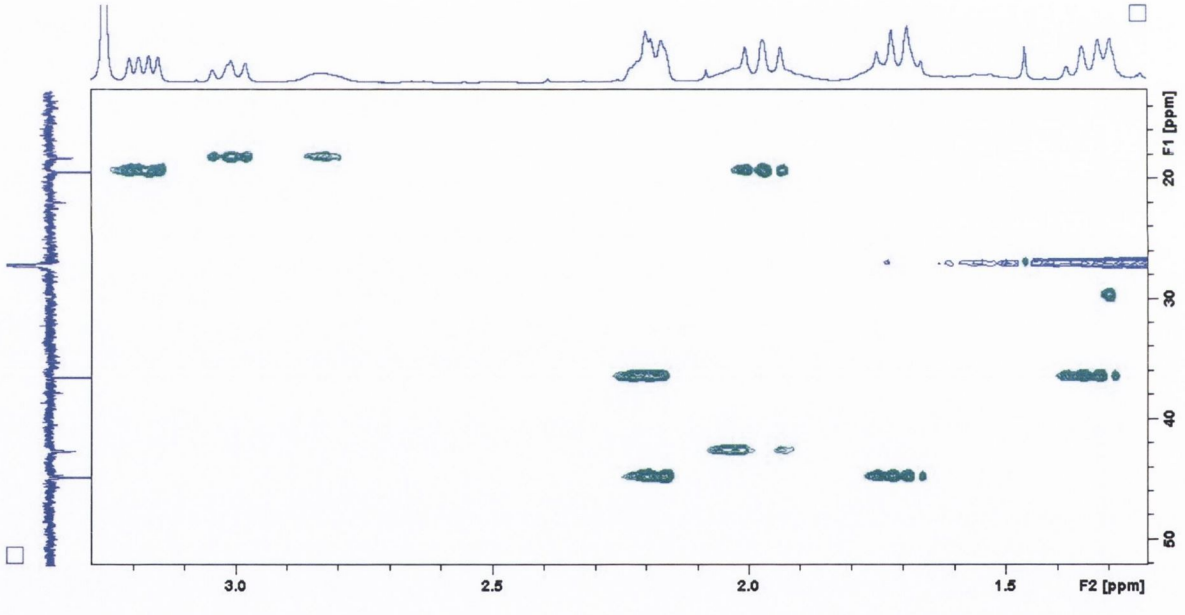

Figure 3.18 Selected expansion of HSQC of **(3.30)**

3.8.8.3 Removal of MOM protecting group

Once inversion of configuration at the C-7 position had been ultimately achieved (Section 3.8.10), it was necessary to remove the MOM ether selectively and in satisfactory yield. However, removal of the MOM ether posed a considerable challenge and a number of methods of MOM ether removal were explored before an acceptable procedure was found.

Of the multitude of procedures described in the literature for the removal of MOM ethers, the method presented by Sharma *et al.* appeared to be among the most convenient [204, 255]. According to the protocol outlined by Sharma *et al.*, the Lewis acid zirconium (IV) chloride ($ZrCl_4$), can be used to achieve the facile deprotection of the MOM ether in a diverse range of functionalised compounds [255]. Accordingly, **(3.30)** was dissolved in IPA and $ZrCl_4$ added.

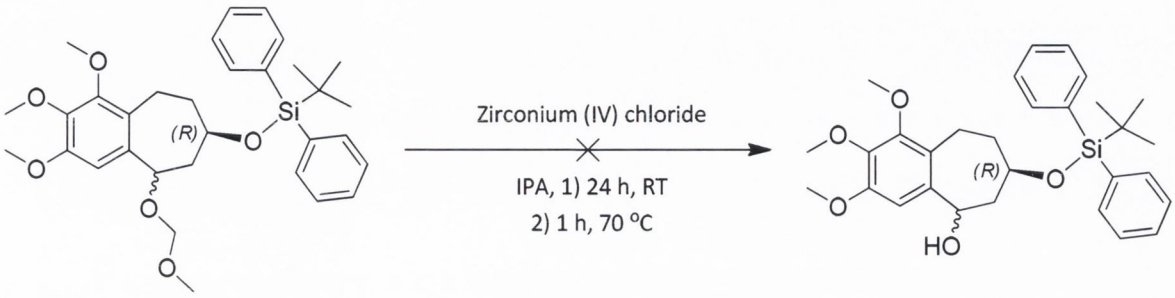

(3.31) **(3.32)**

Scheme 3.21 Attempted deprotection of **(3.31)** using zirconium (IV) chloride

After 24 h at room temperature, **(3.31)** remained unchanged. The reaction was subsequently refluxed at 70 °C for 1 h. This resulted in the complete consumption of the starting material and the formation of an undesired side product. The non-polar side product was hypothesised to be the alkene containing compound **(3.33)**. It was hypothesised that elimination of the MOM ether as a result of coordination with the zirconium complex allowed the formation of a benzylic carbocation. The subsequent loss of a proton resulted in the formation of the highly conjugated compound **(3.33)** (Scheme 3.22).

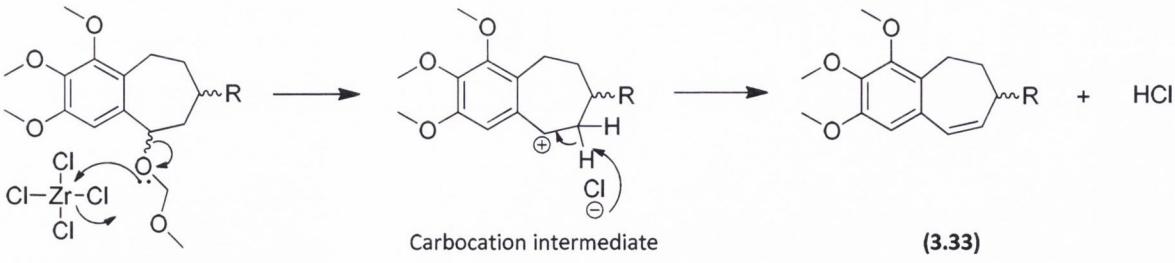

Carbocation intermediate **(3.33)**

Scheme 3.22 Purported mechanism for benzylic elimination reaction during MOM deprotection

It was hypothesised that the strong drive for conjugation and hence the formation of **(3.33)** would make the competing hydroxyl deprotection difficult to achieve by the use of a Lewis acid. Nevertheless, an alternative procedure to effect the MOM deprotection was explored.

Another procedure detailed in the literature for the removal of MOM ether protecting groups describes the use of the halosilane Lewis acid trimethylsilyl bromide [204]. Following a protocol described by Hanessian *et al.*, the MOM ether protected compound **(3.31)** was dissolved in DCM at -30 °C and trimethylsilyl bromide was added (Scheme 3.23) [256].

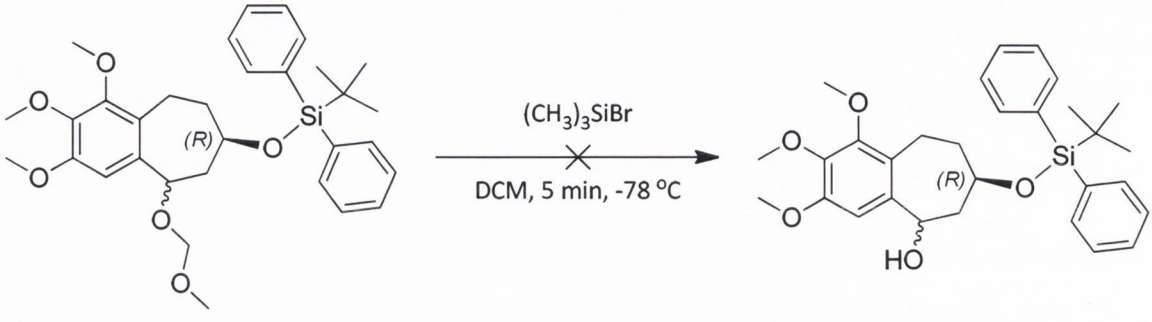

(3.31) **(3.32)**

Scheme 3.23 Attempted trimethylsilyl bromide deprotection of **(3.31)**

Immediate consumption of the starting material **(3.31)** was apparent by TLC analysis. Unfortunately, there was no evidence for the formation of the product of interest. It was hypothesised that elimination, resulting in the formation of the unsaturated side product **(3.33)**, had again occurred. The reaction was repeated at -78 °C with more encouraging results. The formation of the alcohol **(3.32)** was suggested by comparison with a TLC reference sample. The crude product was concentrated at room temperature and added directly to a silica gel column but was found to be unstable to chromatography. Therefore, the product of interest was not isolated.

A final attempt to remove the MOM ether protecting group was embarked upon following a procedure described by Moher *et al.* [257]. **(3.31)** was dissolved in a mixture of acetonitrile and DCM at 0 °C and aluminium chloride and sodium iodide were added. The formation of the free hydroxyl **(3.32)** was monitored by TLC. After 30 min, the starting material was consumed and the reaction was quenched by the addition of saturated sodium bicarbonate aqueous solution. The reaction was extracted with DCM. This DCM extract was not concentrated. Dess-Martin

periodinane was then added. After 1 h, the desired ketone **(3.34)** was obtained in moderate yield (42%) following purification (Scheme 3.24).

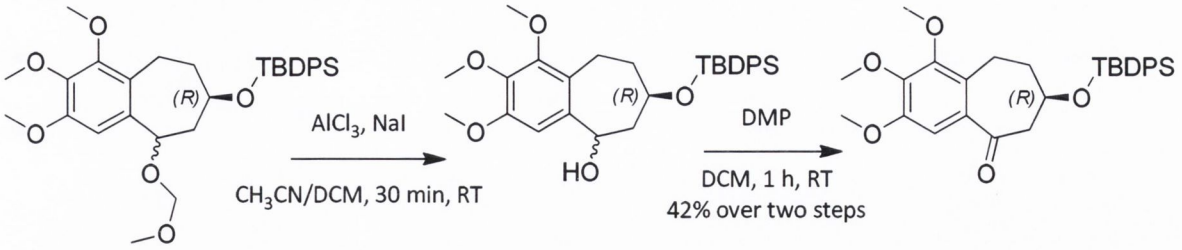

(3.31) **(3.32)** **(3.34)**

Scheme 3.24 MOM deprotection and oxidation of alcohol **(3.32)**

The aluminium chloride/sodium iodide/acetonitrile system that eventually proved successful for removal of the MOM ether protecting group was initially described for the dealkylation of a variety of different ether groups by Node *et al.* [258]. The acetonitrile was chosen as it was found to solvate the aluminium chloride and sodium iodide particularly well. According to Node, the aluminium chloride acts as a Lewis acid, coordinating with the oxygen lone pair of electrons and weakening the carbon-oxygen bond of the ether linkage, while the sodium iodide acts as nucleophile ultimately causing breakage of the ether linkage and resulting in deprotection of the hydroxyl group [258]. The prompt oxidation of the benzylic alcohol group without purification or concentration of the DCM extract was found to be essential to the ultimate success of the synthetic approach. It was felt that the benzylic hydroxyl was particularly prone to elimination and that even the heat utilised to remove the solvent under reduced pressure could be enough to encourage this. Armed with the knowledge that the MOM ether could be successfully introduced and subsequently removed, attention once again turned to the Mitsunobu reaction.

3.8.9 Attempted inversion of configuration using the Mitsunobu reaction on MOM protected alcohol (3.30)

Once the MOM group was successfully introduced to afford **(3.30)**, the C-7 position silyl protecting group was removed. Compound **(3.30)** was dissolved in dry THF under an atmosphere of nitrogen. TBAF solution was then added at 0 °C under anhydrous conditions. After 24 h, the reaction was deemed to have gone to completion. Following purification, the desired alcohol **(3.35)** was obtained in excellent yield (87%) as a yellow oil (Scheme 3.25)

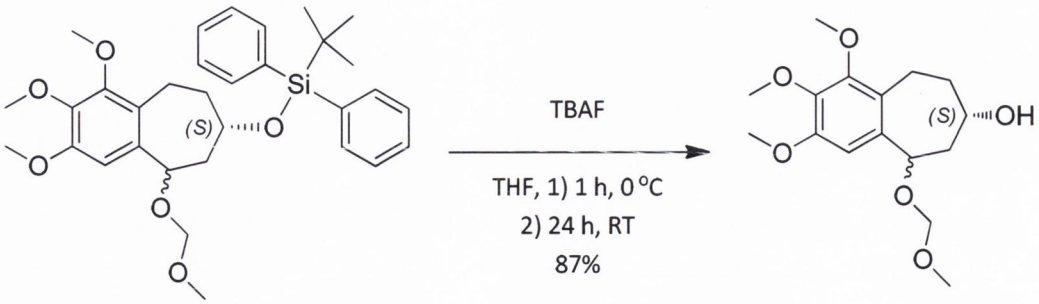

(3.30) **(3.35)**

Scheme 3.25 Removal of silyl group using TBAF to afford **(3.35)**

The Mitsunobu reaction was then re-attempted. The MOM protected alcohol **(3.35)** was dissolved in dry THF at 0 °C and triphenylphosphine (1 eq) and formic acid (2 eq) were added. DIAD (1 eq) was then added dropwise. However, the starting materials were found to remain unchanged after 16 h. An alternative procedure modified from Maruyama *et al.,* involving greater equivalents of the reagents was subsequently carried out (Scheme 3.26) [259].

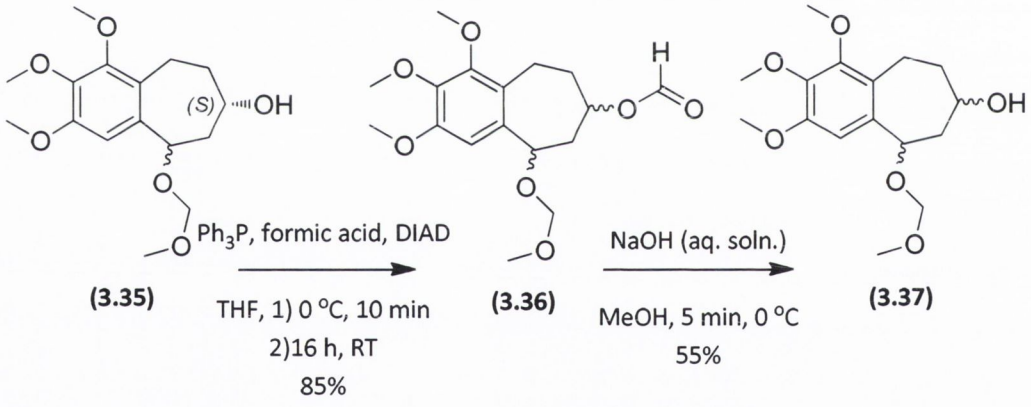

(3.35) **(3.36)** **(3.37)**

Scheme 3.26 Mitsunobu reaction on (3.35) and hydrolysis of formate ester (3.36)

The alcohol **(3.35)** was dissolved in dry THF and the solution cooled to 0 °C. Triphenylphosphine (3 eq) and formic acid (3 eq) were then added to the reaction. The DIAD (3 eq) was then slowly added dropwise. After 16 h, the formation of the product was observed by TLC analysis using vanillin as visualisation reagent. The product was isolated by flash column chromatography to afford the formate ester **(3.36)** in satisfactory yield (85%). The labile formate ester **(3.36)** was readily hydrolysed by the addition of NaOH aqueous solution to a methanolic solution of the ester

at 0 °C. Following purification, the alcohol **(3.37)** was obtained in moderate yield (55%) as a yellow oil (Scheme 3.26).

3.8.9.1 Synthesis of a derivative of (3.37) suitable for esterification with Mosher's acid

In order to establish if the attempted inversion of configuration at the C-7 position had been successful, derivatisation with (*R*)-Mosher's acid was required. However, before this could be attempted, the synthesis of a more robust intermediate with more straightforward stereochemistry at the C-9 position was required.

The C-7 position hydroxyl of **(3.37)** was protected as a *tert*-butyldiphenylsilyl ether using an excess of *tert*-butyldiphenylsilyl chloride, together with imidazole as base, to afford **(3.38)** in excellent yield (97%; Scheme 3.27)

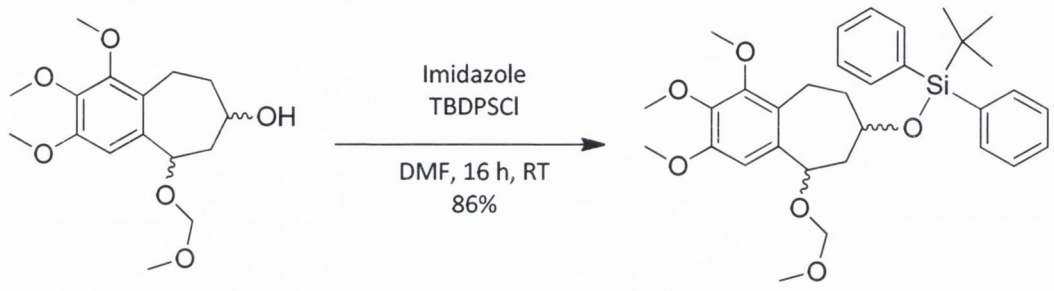

(3.37) **(3.38)**

Scheme 3.27 Silyl protection of **(3.37)**

The MOM ether protecting group of compound **(3.38)** was then removed using the aluminium chloride/sodium iodide/acetonitrile system (Scheme 3.24). Subsequent oxidation of the resultant benzylic alcohol **(3.39)** using DMP afforded **(3.40)** in good yield (89%) after purification (Scheme 3.28).

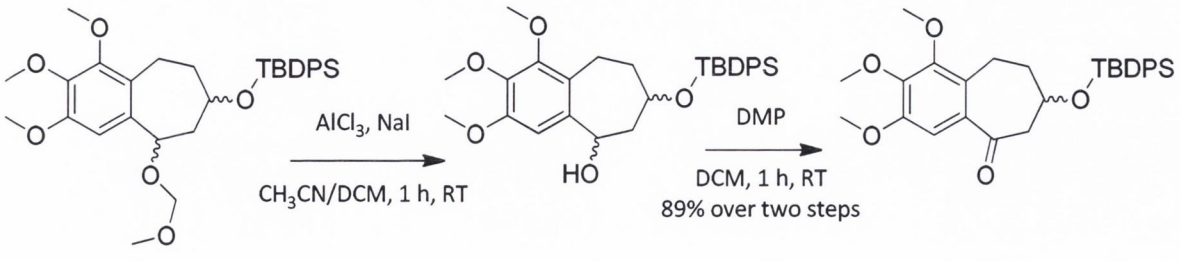

(3.38) **(3.39)** **(3.40)**

Scheme 3.28 MOM deprotection of **(3.38)** and oxidation of resultant alcohol **(3.39)**

The silyl protecting group of **(3.40)** was then removed utilising TBAF in THF at 0 °C. After 16.5 h, the reaction was deemed to have gone to completion. Following purification, the alcohol **(3.41)** was isolated in good yield (83%) as a yellow oil (Scheme 3.29).

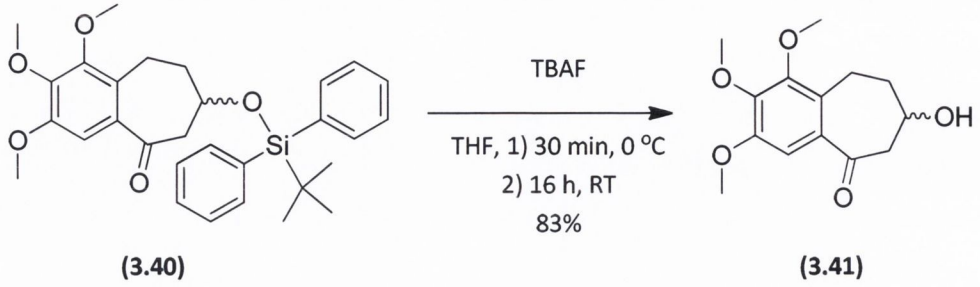

(3.40) **(3.41)**

Scheme 3.29 Silyl deprotection of **(3.40)**

Organolithium coupling methodology was then used to attach the C-ring **(2.14)** to the AB-ring compound **(3.41)**. The C-ring **(2.14)** was dissolved in dry THF under an atmosphere of nitrogen. The reaction was then cooled to -78 °C and *n*-butyllithium was added dropwise under anhydrous conditions. After 40 min, a solution of **(3.41)** in THF was added dropwise. After a further 4 h stirring at ambient temperature, the reaction was quenched by the addition of HCl aqueous solution. Following purification the desired tricyclic compound **(3.42)** was obtained in poor yield (16%; Scheme 3.30).

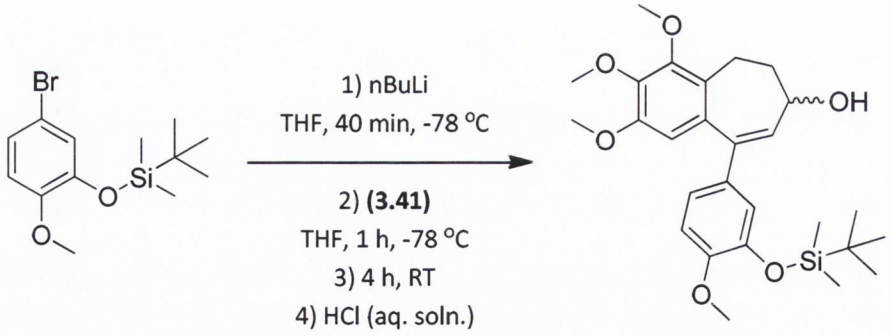

(2.14) **(3.42)**

Scheme 3.30 Organolithium coupling of **(2.14)** and **(3.41)**

3.8.9.2 Determination of stereoselectivity of Mitsunobu reaction

The hydroxyl containing compound **(3.42)** was derivatised with *(R)*-Mosher's acid according to the standard procedure. The compound was dissolved in dry DCM under an atmosphere of nitrogen. 2,6-dichlorobenzoyl chloride was utilised as coupling reagent. DMAP was added as acylation catalyst. DIPEA was added as base. After 16 h, the reaction was deemed to have gone to completion. Following purification, the desired ester **(3.43)** was obtained in good yield (71%) as a yellow oil (Scheme 3.31). Compound **(3.43)** was then subject to ^{19}F NMR analysis (Figure 3.19).

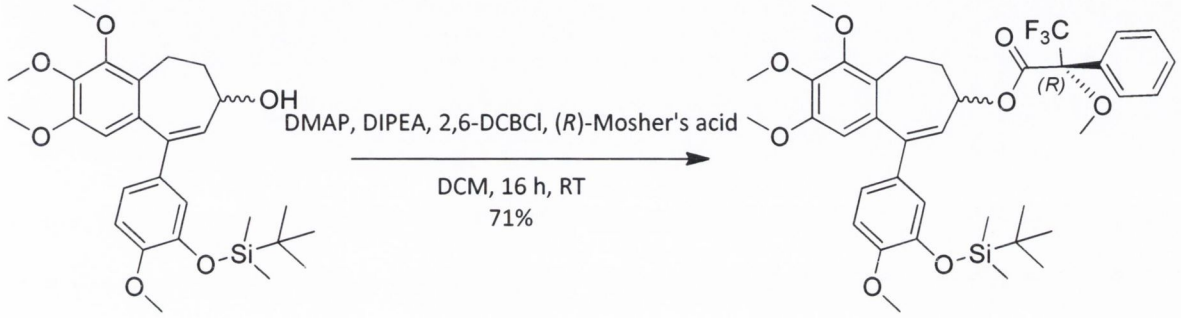

(3.42) **(3.43)**

Scheme 3.31 Synthesis of *(R)*-Mosher's ester **(3.43)**

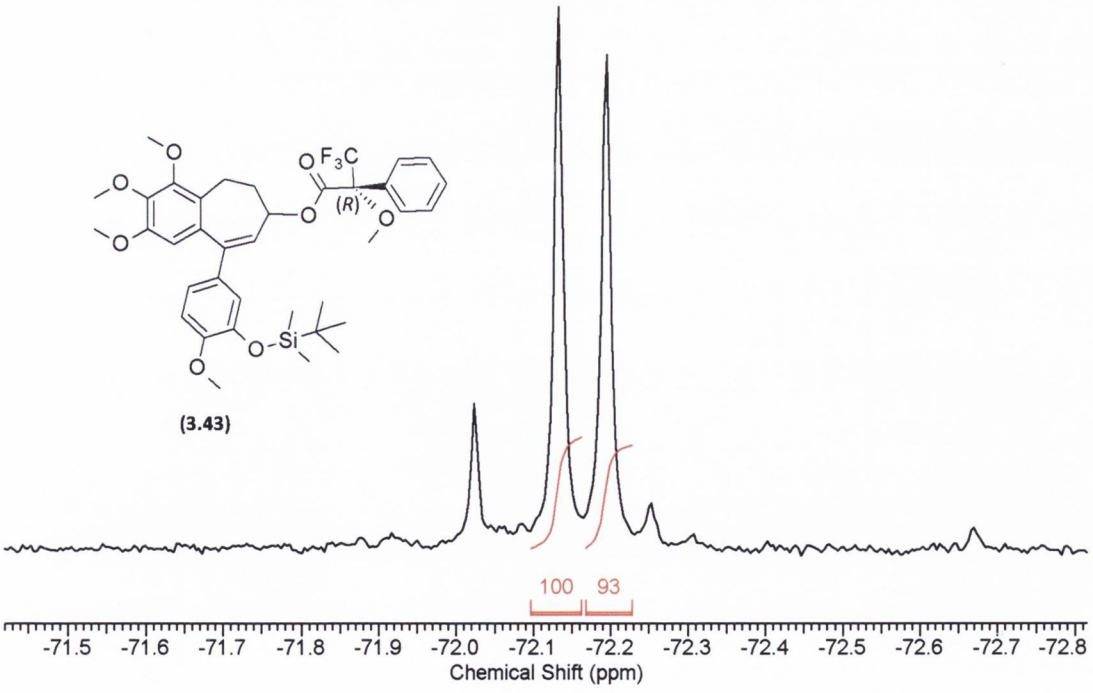

Figure 3.19 ^{19}F NMR of **(3.43)**

Perplexingly, two almost equivalent peaks were observed in the ^{19}F NMR spectrum of compound **(3.43)** (Figure 3.19). This suggested that clean inversion of configuration had not been achieved with the Mitsunobu reaction (Scheme 3.26). In order to confirm that this second major peak apparent in the spectrum was not an artefact of the derivatisation process, the (*R*)-Mosher's ester of the enantiomerically pure (*S*)-configuration alcohol **(3.19)** was synthesised. Utilising the same procedure as used for the synthesis of **(3.43),** compound **(3.44)** was obtained in good yield (71%) as a yellow oil (Scheme 3.32). This compound was then subject to ^{19}F NMR (Figure 3.20).

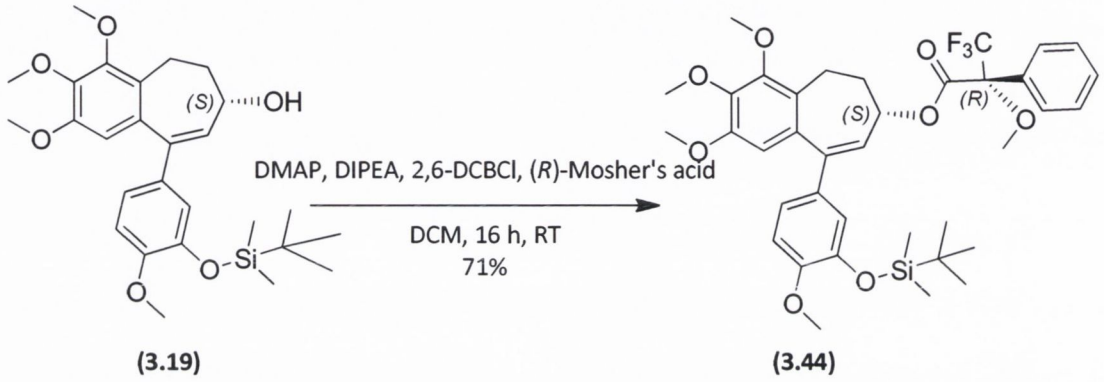

(3.19) **(3.44)**

Scheme 3.32 Synthesis of (*R*)-Mosher's ester **(3.44)**

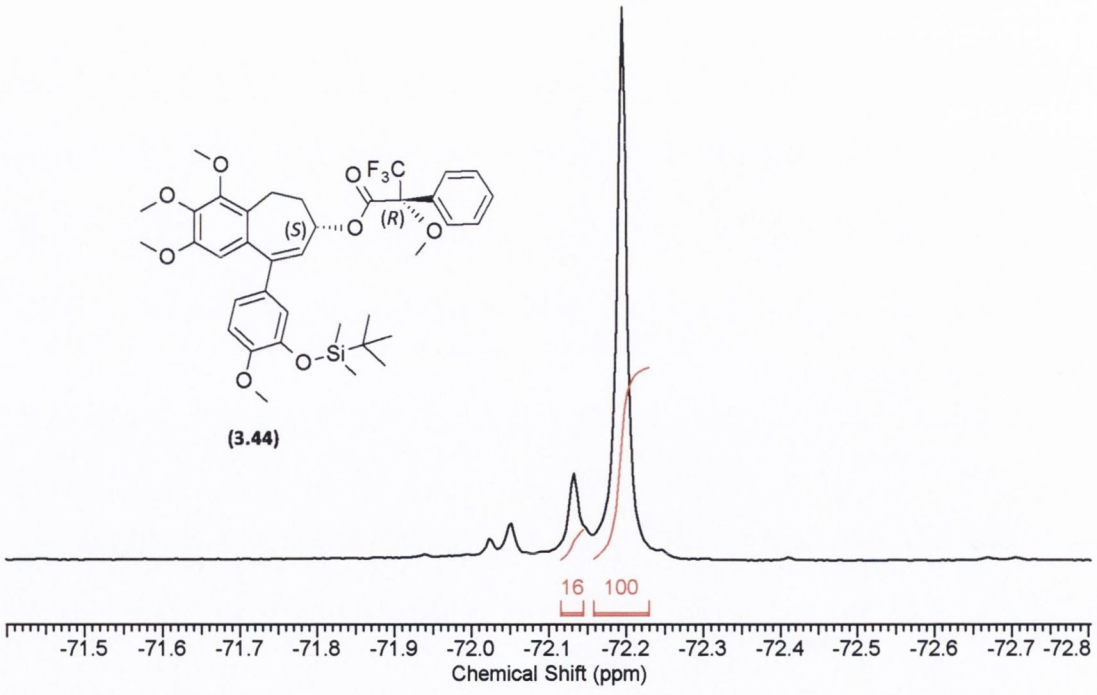

Figure 3.20 ^{19}F NMR of **(3.44)**

The alcohol **(3.19)** was thus shown to be of high enantiomeric purity by derivatisation and subsequent analysis by ^{19}F NMR. A small quantity of the (*R*)-enantiomer did appear to be present as indicated by the secondary peak (Figure 3.20). However, the dominant major peak was that of the (*S*)-enantiomer. This slight stereochemical contamination was deemed to be batch specific, as no such reduction in stereochemical purity was observed at the bioreduction phase, despite extensive quality control measures at that point.

The disappointing result obtained using the Mitsunobu reaction was particularly difficult to explain. This reaction was widely reported to proceed by clean inversion of configuration [190]. One possible explanation for the result is that the formate ester formed was itself displaced by the excess formate in solution. It is possible that this was encouraged by the use of excess reagents and the elevated temperatures required to concentrate the organic fraction following work-up. Thus, an alternative procedure for the clean inversion of configuration was investigated.

3.8.10 Mesylate formation and acetate substitution

It is generally accepted that S_N2 reactions typically proceed with inversion of configuration [190]. This principal was thus exploited to obtain inversion of configuration in the synthesis of **(3.02)**. The starting point for this potential synthetic scheme was the MOM protected alcohol **(3.35)**.

The alcohol **(3.35)** was reacted with methanesulfonyl chloride in a solution of dry DCM under nitrogen at 0 °C using DIPEA as base. After 1 h, the reaction was subjected to an ether/water work-up. Cesium acetate was prepared in parallel by slow addition of a stoichiometric quantity of acetic acid to a dry methanolic suspension of cesium carbonate. The methanol was removed under reduced pressure and the resulting white solid dried under high vacuum. The crude mesylate was mixed with the cesium acetate using DMF as solvent and the reaction was heated to 70 °C under reflux for 40 h. The product was then isolated by flash column chromatography to afford the acetate in an acceptable yield (56%) as a colourless oil. The reaction was repeated substituting DMSO for DMF as solvent resulting in a much shorter reaction time (24 h v 40 h) with an equivalent chemical yield (56%; Scheme 3.33).

Cesium acetate was utilised as the source of the acetate nucleophile for this reaction due to a particular collection of characteristics known as "the cesium effect" [260]. In the context of the chemistry undertaken, this effect primarily referred to the readiness with which cesium carboxylates cause S_N2 displacement of mesylates, allowing clean inversion to occur even for

racemisation prone compounds [260]. DMF and DMSO were chosen as solvents as they are both polar, aprotic solvents said to favour an S_N2 nucleophilic substitution reaction [190]. Cesium carboxylates are also found to be an order of magnitude more soluble in DMSO than DMF possibly explaining the shortened reaction time observed with this solvent [260]. Some evidence also suggests that DMSO resulted in shortened reaction times and higher yields compared to DMF for a number of S_N2 nucleophilic substitution reactions involving the azide ion [5]. Furthermore, cesium carboxylates were reported to be two orders of magnitude more soluble in DMSO than their sodium counterparts [260]. It was felt that optimisation of the reaction conditions to ensure the shortest possible reaction time maximised the possibility of clean inversion of configuration occurring at the chiral centre.

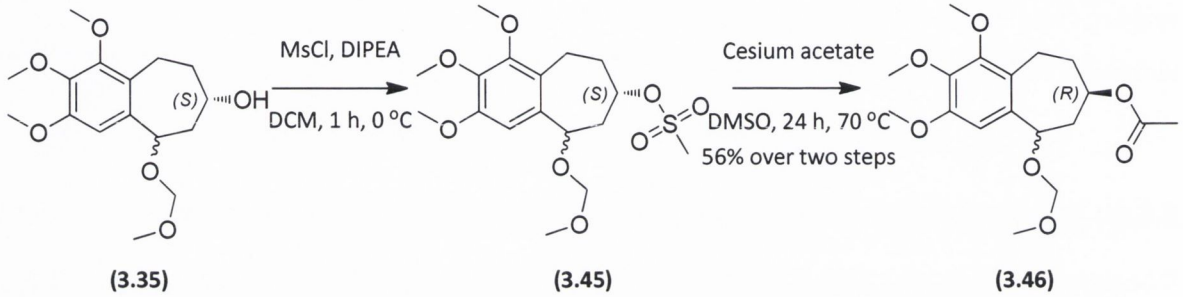

(3.35) **(3.45)** **(3.46)**

Scheme 3.33 Formation of mesylate **(3.45)** followed by acetate substitution

The acetate ester **(3.46)** was then dissolved in methanol and the acetate removed by base-catalysed hydrolysis using NaOH aqueous solution to afford the alcohol **(3.47)** in excellent yield (100%) as a yellow oil.

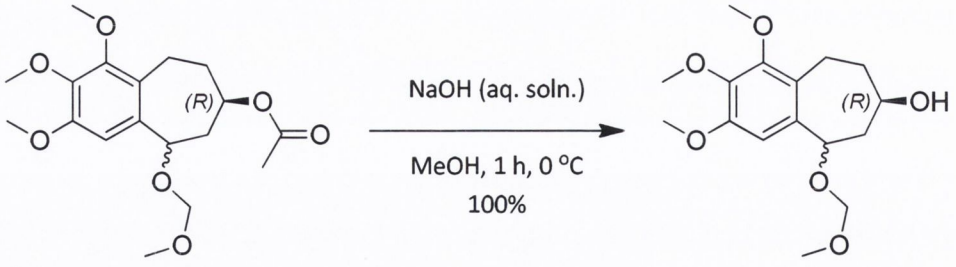

(3.46) **(3.47)**

Scheme 3.34 Hydrolysis of acetate **(3.46)**

In order to confirm that the mesylate displacement reaction had resulted in inversion of configuration at the C-7 position, esterification of a suitable derivative with Mosher's acid was required.

3.8.10.1 Synthesis of derivative of (3.47) suitable for esterification with Mosher's acid

The C-7 position alcohol of **(3.47)** was suitably protected with a silyl protecting group. Compound **(3.47)** was dissolved in dry DMF under nitrogen and *tert*-butyldiphenylsilyl chloride and imidazole were added under anhydrous conditions. After 4 h, the reaction was deemed to have gone to completion. Following purification **(3.31)** was obtained as a colourless oil in excellent yield (97%; Scheme 3.35).

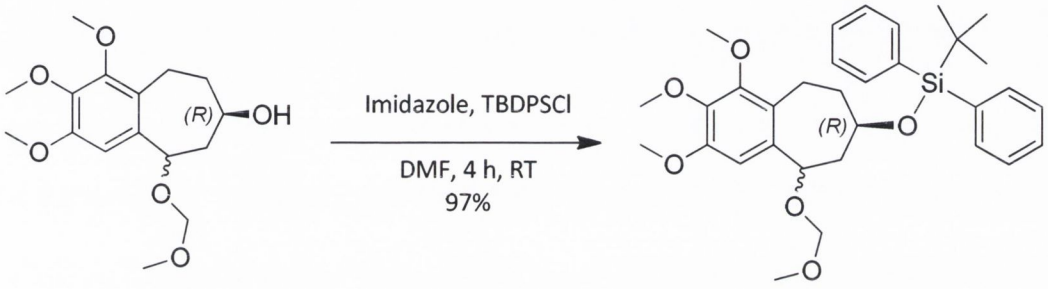

(3.47) **(3.31)**

Scheme 3.35 Silyl protection of **(3.47)**

The C-9 MOM ether of **(3.31)** was removed and the resulting benzylic alcohol **(3.32)** oxidised to afford compound **(3.34)** (Scheme 3.24). The C-7 position silyl protecting group was then removed. **(3.34)** was dissolved in dry THF under nitrogen. TBAF solution was then added at 0 °C. After 30 min, the temperature of the reaction was allowed to increase to ambient. After a further 16 h, the reaction was deemed to have gone to completion. Following purification, compound **(3.48)** was obtained in moderate yield (54%) as a yellow oil (Scheme 3.36).

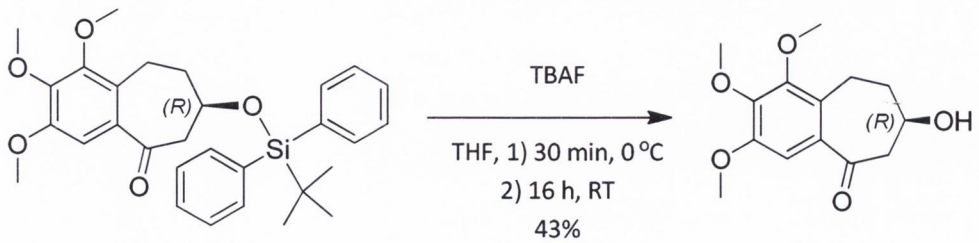

(3.34) **(3.48)**

Scheme 3.36 Silyl deprotection of **(3.34)**

Organolithium coupling of **(3.48)** and **(2.14)** was then undertaken. **(2.14)** was dissolved in dry THF under an atmosphere of nitrogen and *n*-butyllithium was added at -78 °C. After 40 min, a solution of **(3.48)** was added. After 1 h, the temperature of the reaction was allowed to increase to ambient. After a further 4 h, the reaction was quenched by the addition of HCl aqueous solution and following purification, **(3.49)** was obtained as a yellow oil in poor yield (34%; Scheme 3.37).

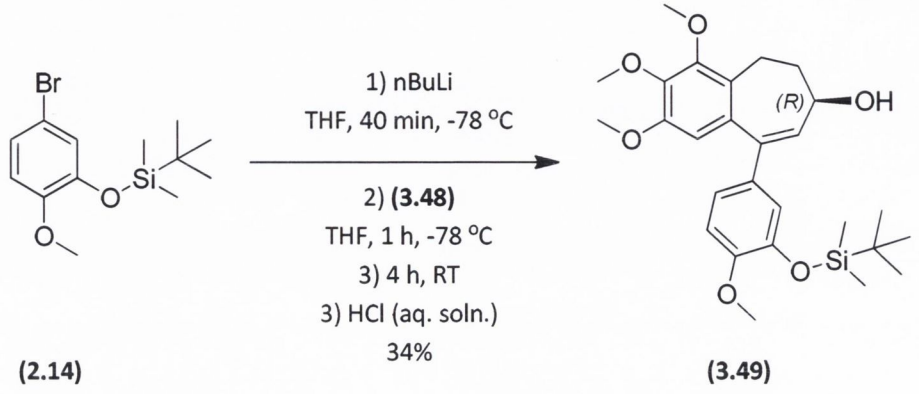

Scheme 3.37 Organolithium coupling of **(2.14)** and **(3.48)**

3.8.10.2 Determination of stereoselectivity of mesylate displacement reaction

The (*R*)-Mosher's ester of **(3.49)** was subsequently synthesised according to the standard procedure. Following purification, **(3.50)** was obtained in good yield (71%) as a yellow oil (Scheme 3.38). Compound **(3.50)** was then subject to ^{19}F NMR analysis (Figure 3.21).

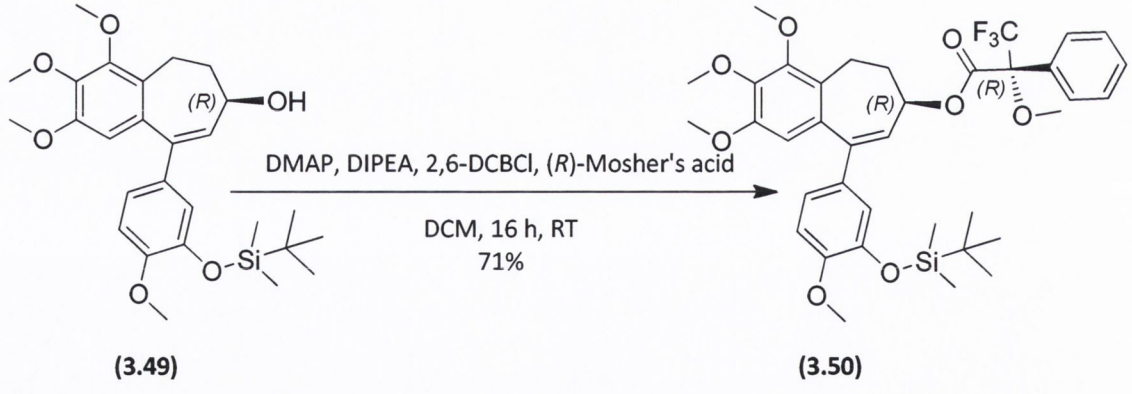

Scheme 3.38 Synthesis of (*R*)-Mosher's ester **(3.50)**

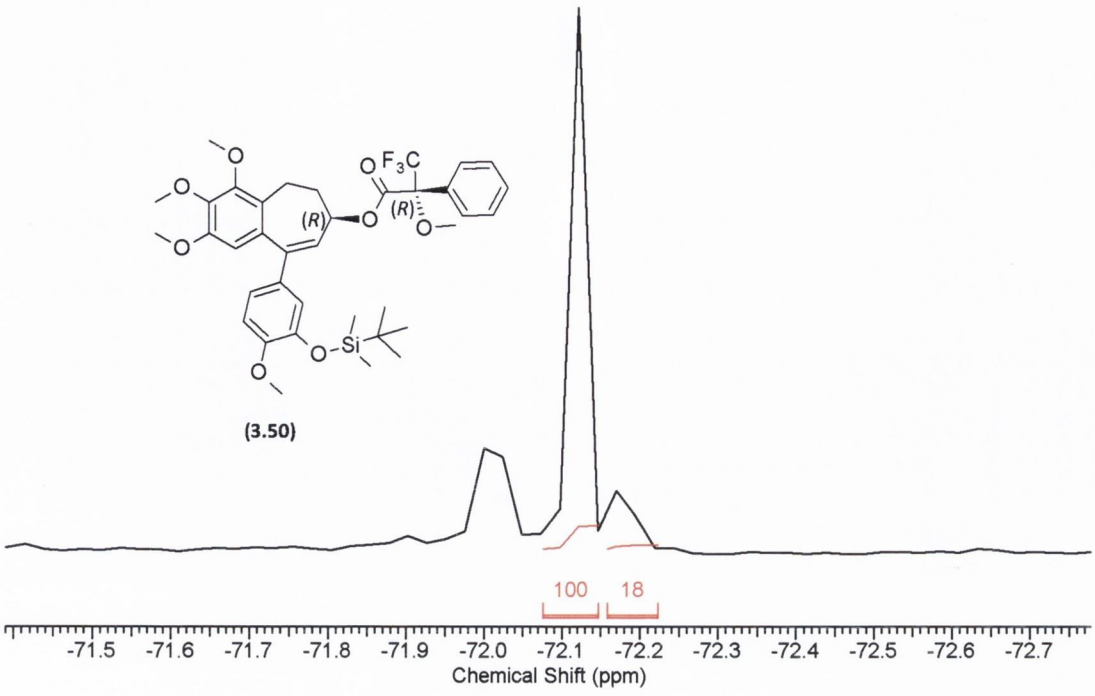

Figure 3.21 ^{19}F NMR spectrum of **(3.50)**

The ^{19}F NMR spectrum illustrated the formation of one major stereoisomer following derivatisation with Mosher's acid, indicating the enantiomeric purity of **(3.49)**. By comparison with the ^{19}F NMR spectrum of compound **(3.44)**, it was apparent that the alcohol **(3.49)** was of opposite configuration to that of the (*S*)-enantiomer **(3.19)** (Figure 3.20). Therefore, it had been demonstrated that successful inversion of configuration had been achieved by the mesylate displacement methodology and that introduction of (*R*)-configuration into the synthesis was accessible through this procedure.

3.9 Synthesis of (*R*)-enantiomer alcohol (3.02)

Once it had been established that clean inversion of configuration had been obtained via a mesylation and subsequent acetate substitution at the C-7 position alcohol, this methodology was employed to synthesise the (*R*)-enantiomer of the initial lead compound **(2.02)**.

TBAF was used to remove the silyl protecting group of **(3.49)** in excellent yield (98%) to afford **(3.02)** as a white solid (Scheme 3.39).

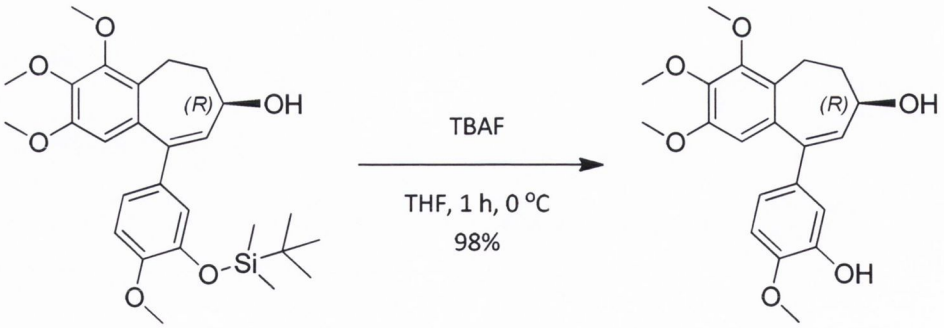

(3.49) **(3.02)**

Scheme 3.39 Silyl deprotection of **(3.49)**

Compound **(3.02)** was then dried under high vacuum for several days to remove any traces of residual solvents before being subjected to biological evaluation (Section 3.10).

3.10 Biological evaluation

The (*S*)-configuration alcohol **(3.01)** and its optical antipode **(3.02)** were tested for their antiproliferative activity in PC-3 cells using the MTT assay (Section 6.2).

Compound	IC_{50} value (nM)
(3.01)	21.04 ± 1.18
(3.02)	273.7 ± 1.09

Table 3.2 Best fit IC_{50} values ± SEM for compounds **(3.01)** and **(3.02)** following MTT assay in PC-3 cells (n = 3)

The results of the MTT assay raised some very interesting issues regarding the effect of configuration of the C-7 position substituent on biological activity. The (*S*)-enantiomer alcohol **(3.01)** was found to have an IC_{50} value greater than one order of magnitude lower than that of the (*R*)-enantiomer alcohol **(3.02)**.

3.11 Conclusions

The desired stereoselectivity was introduced into the synthesis of **(3.01)** using a bioreduction reaction utilising the yeast of *Sacchoromyces cervesiae* type II. This reaction was found to be convenient, high yielding and highly stereoselective for the (*S*)-enantiomer. Determination of the stereoselectivity and the absolute configuration of the resultant alcohol products was successfully accomplished utilising the chiral derivatisation reagent Mosher's acid, together with the use of NMR spectroscopy. The synthesis of the enantiomerically pure tubulin inhibitor **(3.01)** in satisfactory yield was thus achieved.

A significant technical challenge was presented by the synthesis of the (*R*)-enantiomer alcohol **(3.02)**. Following the unsuccessful stereoselective reduction of **(2.07)** using the CBS reagents and the failure of the Mitsunobu reaction to invert the configuration of the alcohol **(3.07)** an alternative methodology was explored. However, before further attempts at inverting the C-7 position stereochemistry were possible, a novel protection strategy for the C-9 position was needed.

Various protecting groups were scrutinised before the MOM protecting group was ultimately chosen for use in the synthesis of **(3.02)**. The MOM ether protection proved pivotal to the synthesis of **(3.02)** and also became a fundamental strategy in the synthesis of a number of other key compounds (Chapters 4 and 5). However, despite its undoubted utility, significant difficulties were encountered in its removal. These difficulties were adroitly surmounted utilising a combination of aluminium chloride, sodium iodide and acetonitrile together with rapid oxidation of the resultant alcohol before elimination could occur.

The MOM protection allowed the Mitsunobu reaction to be undertaken on the more robust intermediate **(3.35).** Despite the high yield obtained, the transformation was ultimately shown to be of negligible stereoselectivity, with an almost racemic configuration at the C-7 position the final result.

The ultimately successful inversion of configuration was accomplished by the formation of a mesylate at the C-7 position and its subsequent displacement. This simple and high yielding procedure provided ready access to the (*R*)-configuration at the C-7 position. The (*R*)-enantiomer alcohol **(3.02)** was thus synthesised in high enantiomeric purity.

Biological evaluation of both the (*R*) and (*S*) alcohols revealed the integral importance of configuration at the C-7 position of the pharmacophore on activity. A greater that 10-fold difference in IC_{50} values was observed between **(3.01)** and **(3.02)** in the MTT cell proliferation assay (21.04 ± 1.18 nM and 273.7 ± 1.09 nM respectively). Therefore, a eudismic ratio of 13 was apparent between the eutomer, **(3.01)**, and the distomer, **(3.02)**. This result was deemed of tremendous significance given the importance of the racemic compound **(2.02)** in the synthesis of conjugate drugs. This result was also particularly relevant to the design of future analogues, with diverse functionalities at the C-7 position, which was subsequently undertaken (Chapter 4).

4 Chapter 4

4.0 Introduction

The dramatic effect of C-7 stereochemistry on the antiproliferative activity of compounds **(3.01)** and **(3.02)** served to emphasise the importance of this position on the activity of the tubulin inhibitory pharmacophore. It was thus envisaged, that modification of the substituents at this position could lead to further improvements in biological activity. Furthermore, it was hypothesised that when such modifications were combined with the enantioselective synthetic methodology developed previously, novel compounds with alternate C-7 substituents and defined stereochemistry could be synthesised. The synthesis of compounds with diverse functionality at the C-7 position was also deemed of particular importance for the design of molecular conjugates with other bioactive principals. By developing tubulin inhibitors with different functional groups at the C-7 position, it would enable various linker methodologies to be utilised in the synthesis of such conjugates.

4.1 Aims and objectives

The principal aim of the work outlined in this chapter was the synthesis of a series of enantiomerically pure analogues of **(2.02)** with diverse functionalities at the C-7 position. In order to accomplish this feat, it was first necessary to develop a convenient method of C-7 position manipulation. The synthesis of analogues with amine and carboxylic acid groups were designated a priority due to their potential for further conjugation. The synthesis of analogues with an extended methylene side chain was also deemed desirable due to the potential for increased stability in these molecules. Finally, the biological evaluation of the novel tubulin inhibitors synthesised was of paramount importance, in order to further the understanding of the structure activity relationship of these compounds.

4.2 Synthesis of the enantiomerically pure acetamide (4.01)

Hudson synthesised a racemic analogue of **(2.02)** with an amine group at the C-7 position as part of the work submitted for her doctoral thesis [188]. Structure activity relationship studies subsequently revealed that the acetamide derivative of this compound was significantly more biologically active [188]. It was thus decided to synthesis the enantiomerically pure version of this

compound, **(4.01)**, in order to establish what effect stereochemistry at the C-7 position might have on its biological activity.

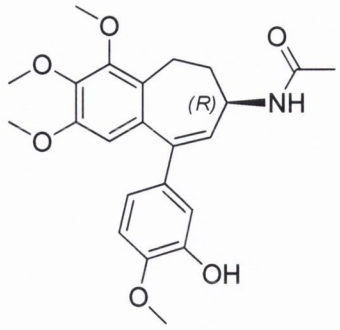

(4.01)

Figure 4.1 (*R*)-enantiomer acetamide **(4.01)**

4.2.1 Synthetic strategy

The basic strategy for the synthesis of this compound was the separate synthesis of an enol triflate, containing the amine functionality, and a boronic acid of the C-ring component. Both elements were then to be combined using standard Suzuki coupling methods.

4.2.2 Synthesis of enol triflate (4.07)

4.2.2.1 Mesylation of (3.26) and subsequent azide displacement

The acetate **(3.26)** was reacted with methanesulfonyl chloride utilising DIPEA as base. Following ether/water work-up, the mesylate **(4.02)** was obtained as a crude mixture. The mesylate was then dissolved in DMSO and sodium azide was added. The reaction was heated under reflux. After 2 h, the reaction was deemed to have gone to completion. Following purification, the azide **(4.03)** was obtained in moderate yield (63%; Scheme 4.1).

The S_N2 displacement of the mesylate proceeded with clean inversion of configuration resulting in a change in stereochemistry at the C-7 position from (*S*) to (*R*). The reaction was initially attempted with DMF, which resulted in a longer reaction time and an equivalent yield. Therefore, DMSO became the solvent of choice for the reaction. It was found that pulverising the sodium

azide powder, before addition to the reaction, avoided clumping and ensured rapid dissolution in the DMSO.

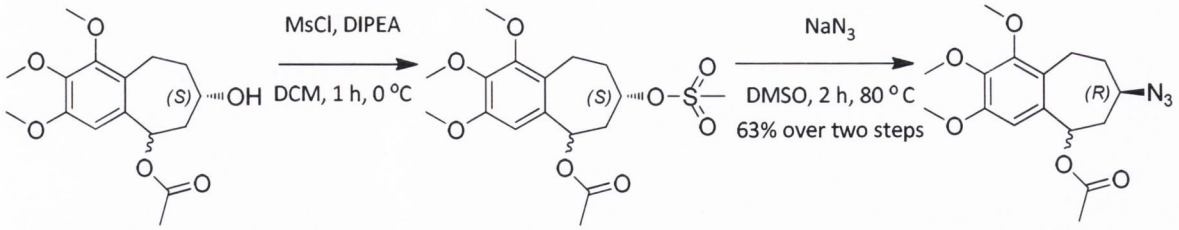

(3.26) **(4.02)** **(4.03)**

Scheme 4.1 Synthesis of mesylate **(4.02)** and subsequent displacement with azide

The identity of **(4.03)** was confirmed by reference to the data described by Hudson [188]. The formation of the azide was also confirmed by mass spectrometry. The mass obtained for the molecular ion peak $[M+Na]^+$ was in close correlation with the calculated value (calculated 358.1379, found 358.1394). The presence of the azide functional group was further confirmed by IR. The azide absorption peak was particularly prominent at 2094.29 cm^{-1}, while the acetate carbonyl was also apparent at 1739.46 cm^{-1}.

4.2.2.2 Acetate deprotection

The acetate protecting group was then removed by addition of NaOH aqueous solution to a methanolic solution of **(4.03)**. Due to the inherent instability of the benzylic hydroxyl group observed in previous reactions, **(4.04)** was neither purified nor characterised. The alcohol of **(4.04)** was instead oxidised using Dess-Martin periodinane to afford the ketone **(4.05)** in moderate yield (58%; Scheme 4.2).

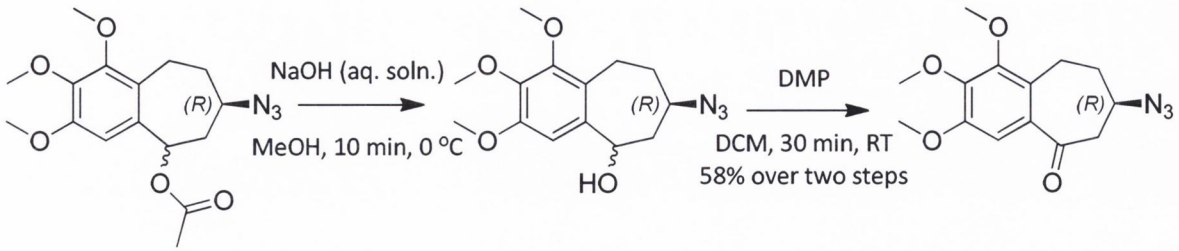

(4.03) **(4.04)** **(4.05)**

Scheme 4.2 Hydrolysis of acetate ester **(4.03)** and oxidation of alcohol **(4.04)**

4.2.2.3 Azide reduction and BOC protection of amine

The azide group of **(4.05)** was reduced and the resultant amine simultaneously protected as an *N*-*tert*-butoxycarbonyl group by reaction with di-*tert*-butyl-dicarbonate and palladium on activated carbon under an atmosphere of hydrogen gas. The desired compound **(4.06)** was thus obtained as a clear oil in satisfactory yield (77%; Scheme 4.3).

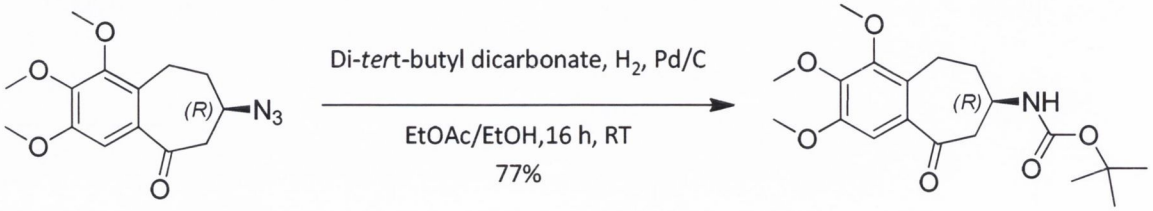

(4.05) **(4.06)**

Scheme 4.3 Reduction of azide **(4.05)** and simultaneous BOC protection of resultant amine

4.2.2.4 Formation of enol triflate (4.07)

The synthesis of the enol triflate **(4.07)** was effected using a procedure first exploited by Hudson [188, 261]. The enolate of the BOC protected amine **(4.06)** was generated using potassium bis(trimethylsilyl)amide (KHMDS) as base at 0 °C. The triflating reagent 2-[*N,N*-bis(fluoromethylsulfonyl)amino]-5-chloropyridine was then added to furnish the enol triflate **(4.08)** in modest yield (50%) as a yellow oil (Scheme 4.4).

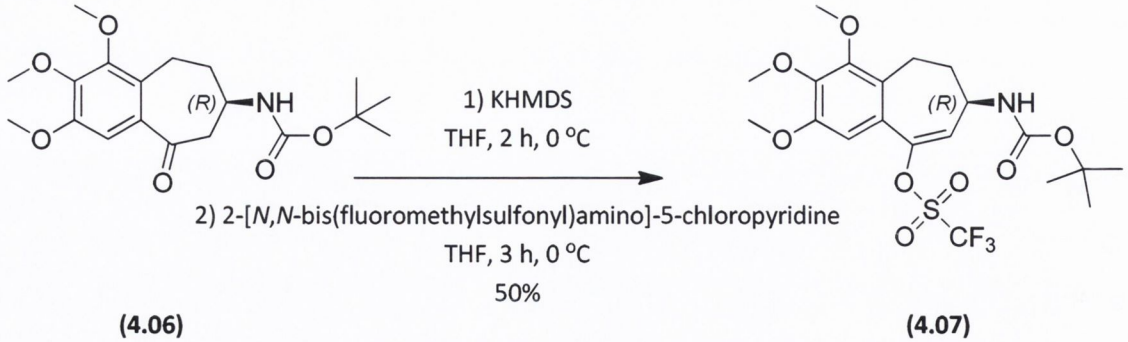

(4.06) **(4.07)**

Scheme 4.4 Synthesis of enol triflate **(4.07)**

While LDA was typically used to furnish the enolate of the analogous protected alcohol **(2.26)**, it has been reported to cause deprotection of the BOC group and elimination of the resulting free amine [188]. KHMDS is a weaker base than LDA and is reportedly used for more sensitive compounds. However, it was still capable of deprotonating the hydrogen α to the ketone, resulting in the formation of the enolate [261].

4.2.3 Synthesis of boronic acid (4.08)

Compound **(2.14)** was dissolved in dry THF at -78°C under an atmosphere of nitrogen. *N*-butyllithium was then added under anhydrous conditions to create the lithiated derivative of **(2.14)**. Excess triisopropyl borate was then added and following acidic work-up and purification, the desired boronic acid **(4.08)** was obtained in moderate yield (66%) as a white solid (Scheme 4.5).

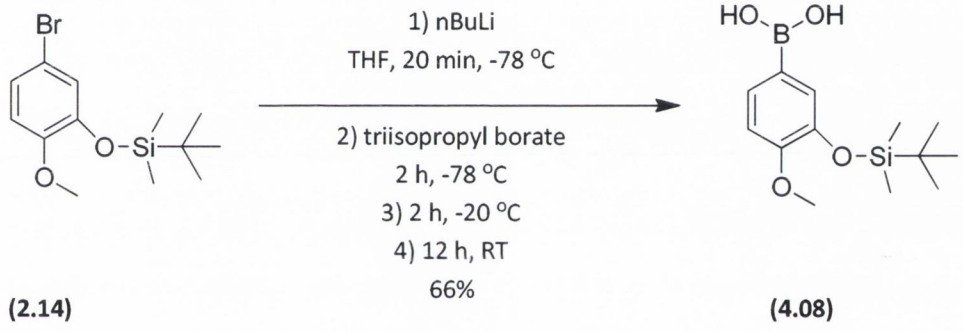

(2.14) **(4.08)**

Scheme 4.5 Synthesis of boronic acid **(4.08)**

4.2.4 Suzuki coupling and synthesis of (4.01)

4.2.4.1 Suzuki coupling of enol triflate (4.07) and boronic acid (4.08)

The enol triflate **(4.07)** and boronic acid **(4.08)** were dissolved in a mixture of toluene, ethanol and water. Potassium carbonate was added as base and (tetrakis(triphenyl)phosphine) palladium was utilised as coupling catalyst. The reaction was heated under reflux at 60 °C for 1 h to afford the coupled compound **(4.09)** in satisfactory yield (80%; Scheme 4.6).

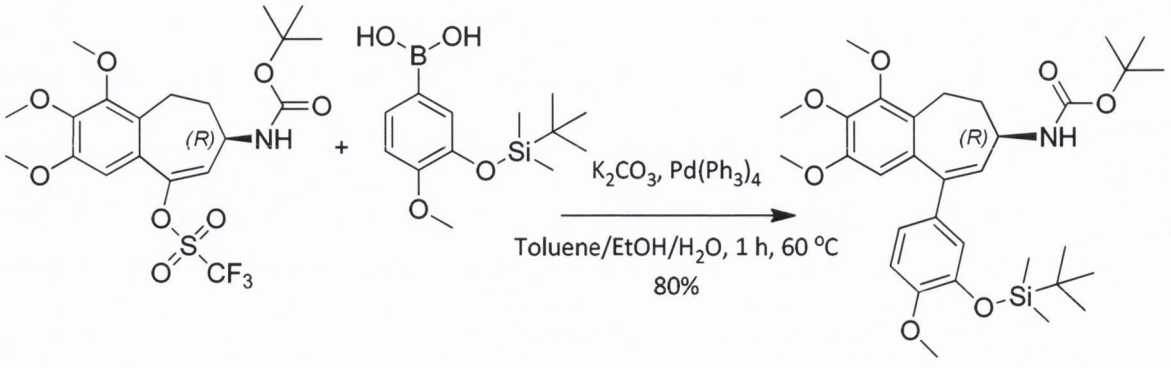

(4.07) **(4.08)** **(4.09)**

Scheme 4.6 Suzuki coupling of **(4.07)** and **(4.08)**

The coupled compound **(4.09)** was found to have an identical R_f value to the enol triflate starting material **(4.07)**, complicating the monitoring of the reaction by TLC. Therefore, the reaction was repeated on a number of occasions and the optimal reaction conditions were determined by trial and error.

4.2.4.2 Removal of BOC and silyl protecting groups

Compound **(4.09)** was dissolved in a mixture of methanol and THF. HCl aqueous solution was then added. This mixture was then heated at 40 °C to simultaneously remove both the BOC and TBDMS protecting groups. The progress of the reaction was monitored by TLC using ninhydrin as visualisation reagent. After 30 min, both acid sensitive protecting groups were deemed to have been removed. Following purification, **(4.10)** was obtained in modest yield (38%) as a white solid (Scheme 4.7).

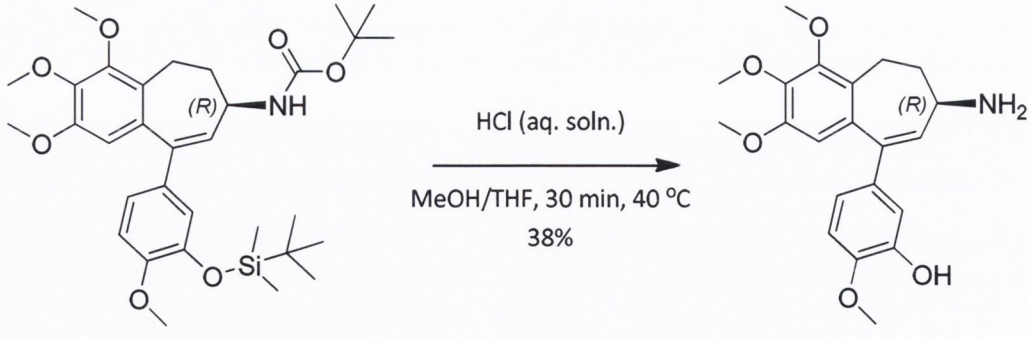

(4.09) **(4.10)**

Scheme 4.7 Simultaneous removal of BOC and silyl protecting groups from **(4.09)**

4.2.4.3 Acetylation and hydrolysis of phenolic ester

The amino and hydroxyl groups of **(4.10)** were acetylated using acetic anhydride, together with triethylamine as base to afford **(4.11)** in moderate yield (41%) as a yellow oil (Scheme 4.8).

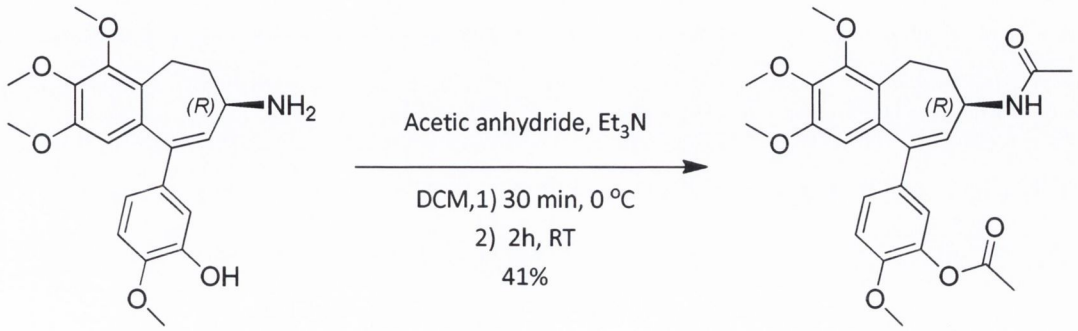

(4.10) **(4.11)**

Scheme 4.8 Acetylation of **(4.10)**

The phenolic ester of **(4.11)** was then readily hydrolysed, by reacting with a mixture of methanol and saturated sodium bicarbonate aqueous solution, to afford the desired acetamide **(4.01)** in good yield (74%) as a white solid (Scheme 4.9).

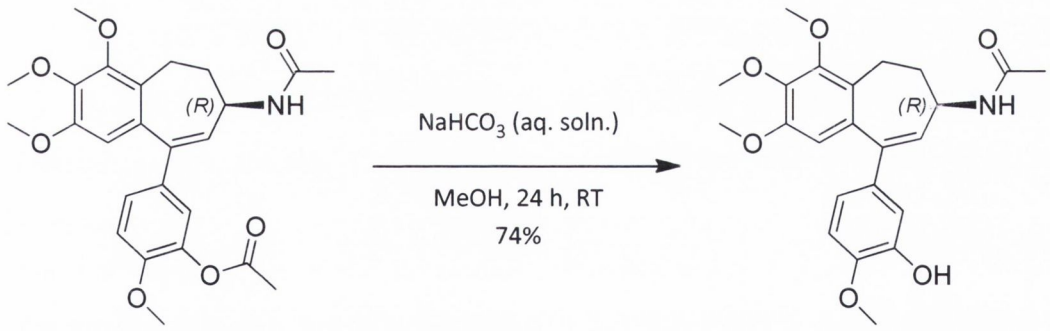

(4.11) **(4.01)**

Scheme 4.9 Hydrolysis of phenolic ester of **(4.11)**

The identity of compound **(4.01)** was confirmed by comparison with the data provided by Hudson [188]. The compound was also found to have a specific optical activity $[\alpha]_D^{25}$ of + 35.2 (*c* = 2,

DCM), indicating the chiral stereochemistry of the molecule. The acetamide **(4.01)** was subsequently dried under vacuum and subject to biological evaluation (Section 4.6.1).

4.3 Synthesis of C-7 methylene acetamide analogue (4.12)

The synthesis of an analogue of **(4.01)** containing an additional C-7 methylene linker substituent was proposed (Figure 4.2). It was anticipated that this compound would offer additional insight into the structure activity relationship surrounding C-7 substituent modification. Furthermore, it was hypothesised that the additional methylene unit could potentially confer additional stability to the structure.

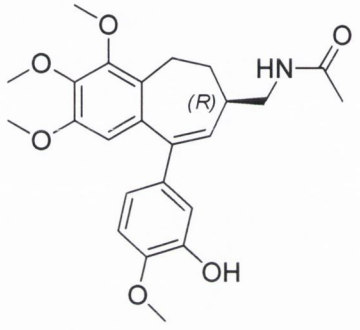

(4.12)

Figure 4.2 Methylene containing acetamide analogue **(4.12)**

4.3.1 Synthetic strategy

The synthetic route followed was analogous to that for **(4.01).** An enol triflate containing the amine functionality was synthesised and subsequently coupled with the boronic acid **(4.09)**. The major challenge encountered was how to confer the structure with the additional methylene unit. It was hypothesised that the introduction of a nitrile at the C-7 position, followed by its reduction, would facilitate the insertion of the desired functionality into the molecule. However, in order to carry out the desired transformation, a more robust protection strategy was required for the C-9 position. It was proposed that the MOM group would be suitable for this purpose.

4.3.2 Synthesis of enol triflate containing additional methylene unit

In trial reactions, the acetate protected compound **(3.26)** was mesylated and underwent nucleophilic substitution with cyanide. However, the formation of significant quantities of an

unwanted elimination side product was observed. Furthermore, the acetate ester was not deemed a suitable protection strategy due to the use of diisobutylaluminium hydride (DIBAL-H) later in the synthesis, which would cause hydrolysis of the ester group [190].

4.3.2.1 Mesylation and cyanide displacement

Therefore, the more robust MOM protected compound **(3.35)** was chosen as the starting point for the synthesis of **(4.12)**. The MOM protection was known from previous experience, to be stable to a wide range of reaction conditions. Furthermore, the stability of the MOM group was evident from a review of the literature [204].

The alcohol of **(3.35)** was readily transformed into the mesylate **(4.13)** by reacting with methanesulfonyl chloride together with DIPEA as base. The crude mesylate was then dissolved in DMSO and excess sodium cyanide was added. After heating to 70 °C for 24 h, the desired nitrile was obtained in moderate yield (41%) as a yellow oil (Scheme 4.10).

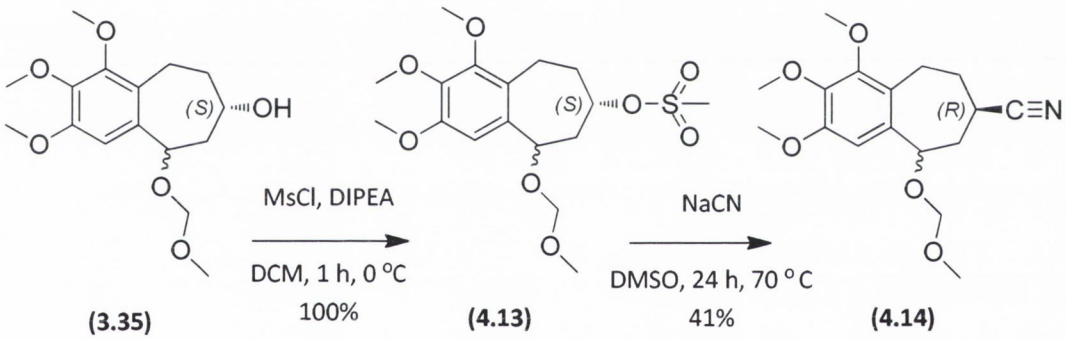

Scheme 4.10 Mesylation of **(3.35)** and subsequent cyanide displacement

The sodium cyanide was pulverised, using a pestle and mortar, before addition to the reaction to aid dissolution and avoid the formation of insoluble lumps. The reaction proceeded with inversion of configuration at the C-7 position from (*S*) to (*R*). The resulting compound was characterised by NMR as a pair of diastereomers (major and minor). The identity was further confirmed by the use of mass spectrometry. The observed mass of the molecular ion peak $[M+Na]^+$ was found to be in close correlation with the theoretical mass (calculated 349.1627, found 349.1633). The identity of **(4.14)** was also confirmed by IR. The nitrile (CN stretch) absorption at 2237.47 cm^{-1} clearly indicated the presence of a nitrile functionality in the molecule.

4.3.2.2 Reduction of nitrile (4.14)

The nitrile **(4.14)** was readily reduced by the addition of lithium aluminium hydride ($LiAlH_4$) at 0 °C to exclusively afford the primary amine **(4.15)** in moderate yield (77%) as a colourless oil (Scheme 4.11).

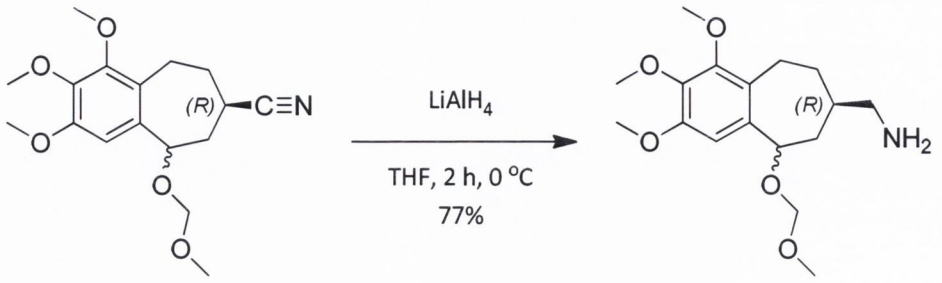

(4.14) **(4.15)**

Scheme 4.11 Reduction of nitrile **(4.14)** to primary amine **(4.15)**

The formation of the amine was monitored by TLC using ninhydrin as visualisation reagent. Mass spectrometry confirmed the identity of the product. The observed mass of the molecular ion peak $[M+H]^+$ was found to be in close correlation with the theoretical calculated mass (calculated 326.1967, found 326.1970). The IR spectrum confirmed the transformation of the nitrile functionality, with the absence of a discernable nitrile peak in the 2210-2260 cm^{-1} region. Characteristic amine absorption bands were apparent however, at 3376.36 cm^{-1} (NH stretch) and 1599.56 cm^{-1} (NH bending).

4.3.2.3 BOC protection of primary amine (4.15)

The primary amine **(4.15)** was reacted with di-*tert*-butyl dicarbonate solution under anhydrous conditions in THF at room temperature. The formation of the BOC protected amine **(4.16)** was monitored by TLC. After 2 h, the reaction was deemed to have gone to completion and the product was isolated in good yield (79%) as a clear oil (Scheme 4.12).

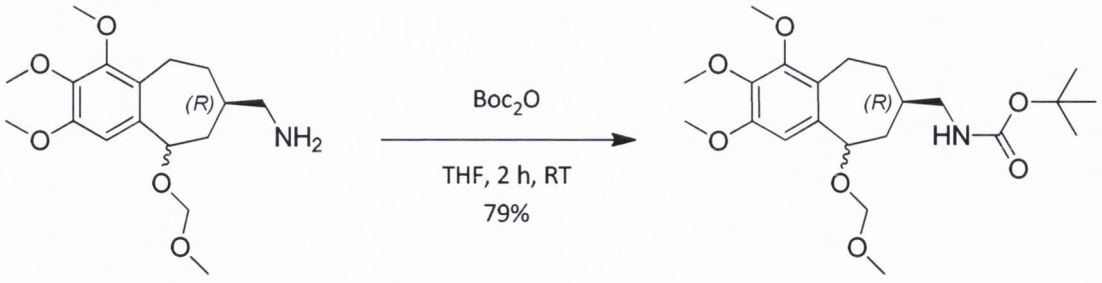

(4.15) **(4.16)**

Scheme 4.12 BOC protection of **(4.15)**

4.3.2.4 MOM deprotection and oxidation of benzylic alcohol

The MOM ether protecting group of **(4.16)** was removed utilising the aluminium chloride/sodium iodide/acetonitrile system. Compound **(4.16)** was dissolved in a mixture of DCM and acetonitrile. Aluminium chloride and sodium iodide were then added. After 30 min, complete consumption of the starting material was observed and the reaction was quenched by the addition of saturated sodium bicarbonate aqueous solution. A combination of the desired benzylic alcohol **(4.17)** and undesired, purported elimination product were detected on TLC. Due to the unstable nature of the benzylic alcohol, no further purification was attempted. The alcohol **(4.17)** was promptly oxidised by the addition of DMP to the DCM extract of the deprotection reaction. After 1 h, the oxidation was adjudged to have gone to completion. The ketone product **(4.18)** was isolated, after purification, in moderate yield (31% over two steps) as a yellow oil (Scheme 4.13).

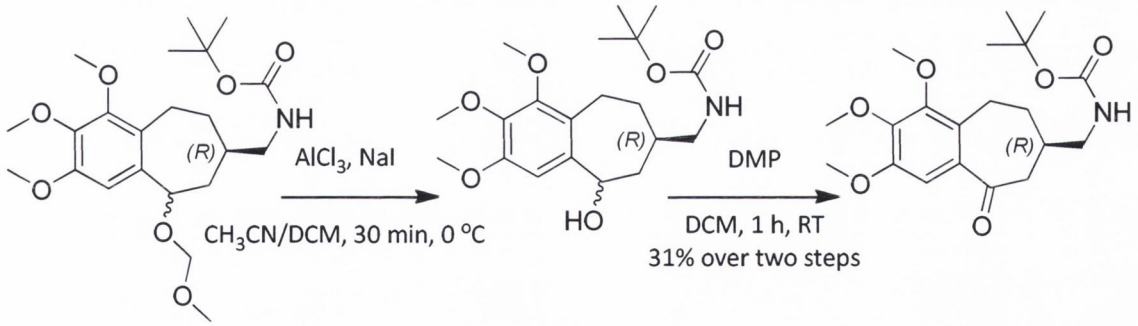

(4.16) **(4.17)** **(4.18)**

Scheme 4.13 MOM deprotection of **(4.16)** and oxidation of alcohol **(4.17)**

Significant difficulty was encountered in the removal of the MOM ether protecting group as outlined previously (Section 3.8.8.3). Numerous attempts were made to isolate the benzylic alcohol, but none were successful as the compound proved extremely unstable to heat and silica gel column chromatography. The alcohol was thus oxidised as a crude mixture. A significant amount of a competing side product, purported to be the elimination product **(3.33)**, was again observed during the deprotection. The ketone **(4.18)** proved much more stable and was readily isolated.

The identity of **(4.18)** was confirmed by mass spectrometry. The molecular ion peak $[M+Na]^+$ was found to have a mass in close correlation with the calculated value (calculated 402.1893, found 402.1862). The IR spectrum suggested the presence of two carbonyl groups with two overlapping peaks at 1711.95 cm^{-1} providing further confirmation of the identity of **(4.18)**.

4.3.2.5 Synthesis of enol triflate (4.19)

The enolate of **(4.18)** was generated using KHMDS and the triflating reagent 2-[*N*,*N*-bis(fluoromethylsulfonyl)amino]-5-chloropyridine was then added. After 3 h, the reaction was still not adjudged to have gone to completion. However, due to the increasing formation of undesirable side-products, the reaction was worked up and the product isolated in poor yield (24%) as a yellow oil (Scheme 4.14).

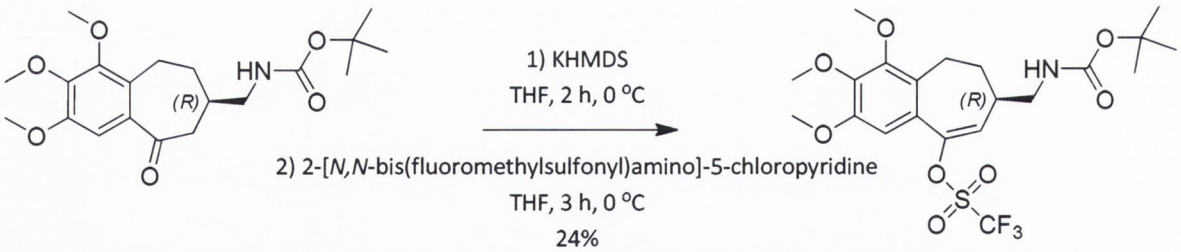

(4.18) **(4.19)**

Scheme 4.15 Synthesis of enol triflate **(4.19)**

4.3.3 Suzuki coupling and synthesis of (4.12)

4.3.3.1 Suzuki coupling of enol triflate (4.19) and boronic acid (4.08)

A palladium catalysed cross-coupling reaction between the enol triflate **(4.19)** and the boronic acid **(4.08)** was carried out using standard Suzuki coupling conditions. Potassium carbonate was added as base The catalyst used was $Pd(Ph_3)_4$. The reaction was heated at 60 °C for 1 h and following purification, **(4.20)** was isolated in modest yield (56%) as a yellow oil (Scheme 4.16).

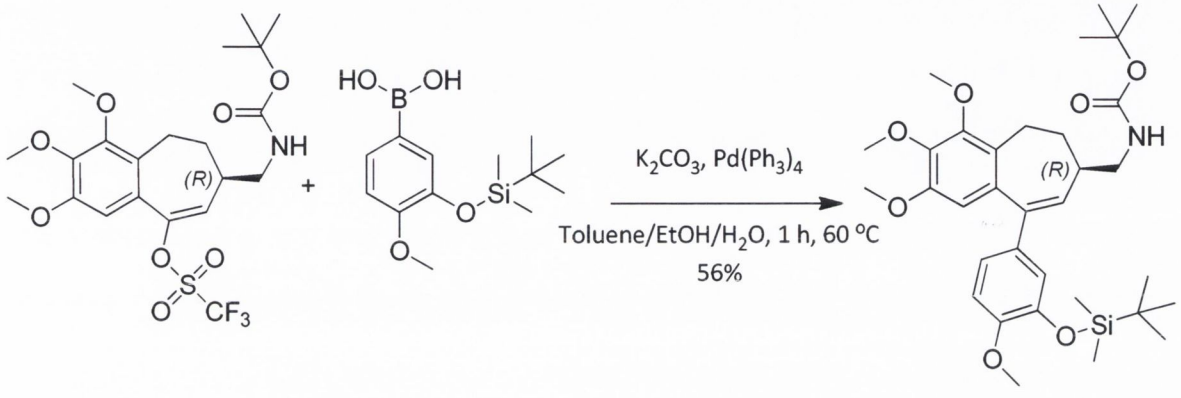

Scheme 4.16 Suzuki coupling of **(4.19)** and **(4.08)**

The difference in R_f value between the enol triflate starting material **(4.19)** and the product **(4.20)** allowed convenient monitoring of the progress of the reaction by TLC, unlike the equivalent reaction in the synthesis of the related compound **(4.01)**. The product **(4.20)** was isolated in disappointing yield considering the apparent clean and complete conversion indicated by TLC analysis.

The identity of **(4.20)** was confirmed by mass spectrometry. The mass of the molecular ion peak $[M+Na]^+$ was found to be in close agreement with the calculated value (calculated 622.3176, found 622.3192). The IR spectrum indicated the presence of a carbonyl group in the compound, with a distinctive absorption peak at 1945.92 cm^{-1}, further confirming the identity of **(4.20)**.

4.3.3.2 Removal of BOC protecting group of (4.20)

Following the disappointing yield obtained from the dual deprotection of the analogous compound **(4.01)**, an alternative strategy was employed. The BOC group of **(4.20)** was selectively

removed by treatment with trifluoroacetic acid in DCM under anhydrous conditions. The deprotection was monitored by TLC using ninhydrin as visualisation reagent. The deprotection was complete in 5 min. Removal of the volatile organic phase and washing with saturated sodium bicarbonate aqueous solution allowed ready isolation of pure **(4.21)** in excellent yield (86%) as a yellow oil without the need for further purification (Scheme 4.17).

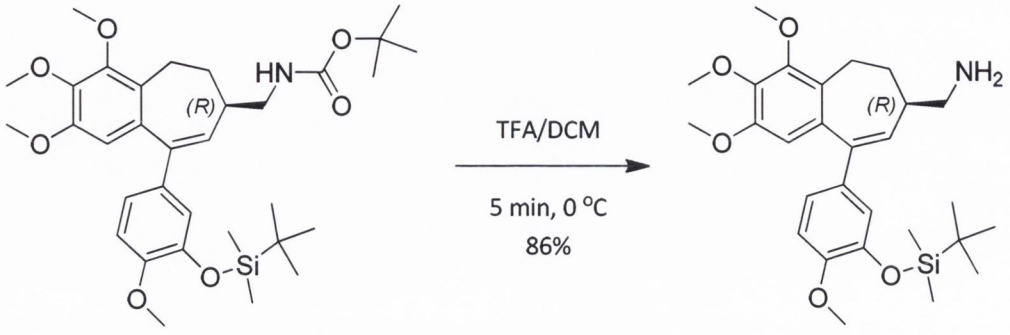

(4.20) **(4.21)**

Scheme 4.17 BOC deprotection of **(4.20)**

4.3.3.3 Acetylation of (4.21)

The primary amine of **(4.21)** was readily acetyled using acetic anhydride together with triethylamine as base under anhydrous conditions in DCM. After 2.5 h, the reaction was adjudged to have gone to completion and the product **(4.22)** was isolated in satisfactory yield (62%) as a yellow resin (Scheme 4.18).

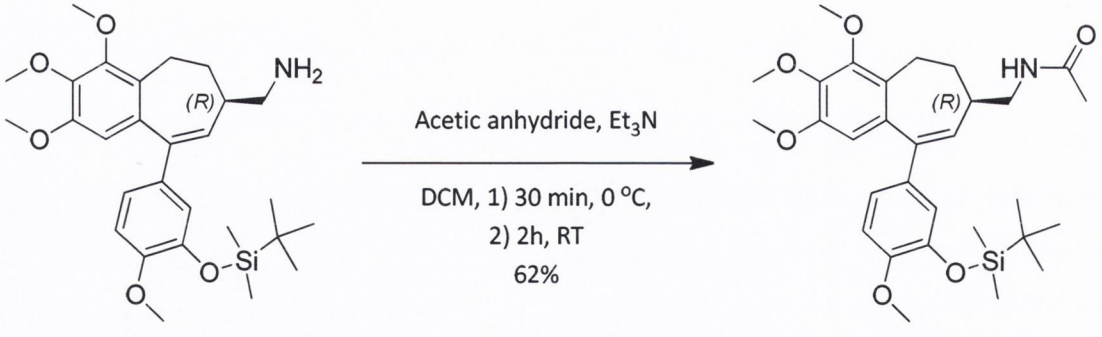

(4.21) **(4.22)**

Scheme 4.18 Acetylation of **(4.21)**

4.3.3.4 Removal of phenolic silyl protecting group of (4.22)

The phenolic *tert*-butyldimethylsilyl ether protection of **(4.22)** was readily removed using TBAF in dry THF under nitrogen. Complete and exclusive conversion was apparent by TLC after 30 min. The product **(4.12)** was isolated in quantitative yield as a white solid (Scheme 4.19).

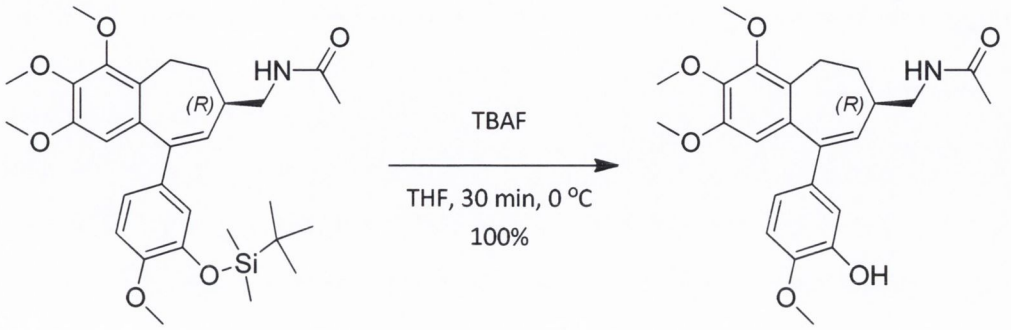

(4.22) **(4.12)**

Scheme 4.19 Removal of phenolic silyl protecting group on **(4.12)**

The approach outlined above, involving selective removal of the BOC group, was deemed superior to that used for the analogue **(4.01)** involving simultaneous removal of both the BOC and silyl groups. Compound **(4.12)** was obtained from the coupled product **(4.20)** in moderate yield of 53% over 3 steps. The equivalent overall transformation from **(4.09)** to **(4.01)** was realised with a yield of only 12% over 3 steps.

4.3.3.5 Characterisation of compound (4.12)

Compound **(4.12)** was characterised by NMR. The acetamide methyl group protons were found to resonate as a singlet at 2.02 ppm. The four methoxy group proton signals were found to resonate as four singlets at 3.72 ppm, 3.92 ppm, 3.93 ppm and 3.95 ppm. The alkene proton was found to resonate as a doublet (J = 6.01 Hz) at 6.07 ppm with the aid of the HSQC spectrum (Figure 4.5). The four aromatic protons were similarly identified as corresponding to the singlet at 6.39 ppm, the double doublet (J_1 = 8.44 Hz, J_2 = 1.86 Hz) at 6.78 ppm, the doublet (J = 8.44 Hz) at 6.82 ppm and the doublet (J = 1.86 Hz) at 6.90 ppm. The HSQC spectrum allowed ready identification of the aliphatic protons (Figure 4.5). The six aliphatic CH_2 protons were found to correspond to five distinct multiplets at 1.84-1.92 ppm, 2.17-2.32 ppm (2 x CH_2), 3.05-3.08 ppm, 3.29-3.35 ppm and 3.40-3.45 ppm. The C-7 CH proton was found to resonate as part of the multiplet at 2.17-2.32 ppm. Meanwhile, the phenolic proton was found to correspond to the broad singlet at 5.54 ppm.

In the carbon spectrum, the four methoxy carbons were readily assigned to the peaks at 56.02 ppm, 56.04 ppm, 60.89 ppm and 61.58 ppm. The acetate methyl group was identified as the peak at 23.42 ppm. The alkene CH carbon was found to resonate at 128.67 ppm using the DEPT 90 and HSQC spectra (Figure 4.4 and 4.5). The four aromatic CH carbons resonated at 108.93 ppm, 110.33 ppm, 114.14 ppm and 119.76 ppm. The three CH_2 carbons were assigned, using the DEPT 135 spectrum, as resonating at 23.14 ppm, 39.34 ppm and 43.82 ppm. The C-7 position CH carbon resonated at 37.40 ppm. The acetamide carbonyl carbon was identified as corresponding to the furthest downfield signal at 170.26 ppm. The nine remaining quaternary carbon signals were found to resonate at 127.99 ppm, 135.04 ppm, 135.72 ppm, 141.36 ppm, 142.48 ppm, 145.29 ppm, 146.18 ppm, 150.83 ppm, and 151.15 ppm.

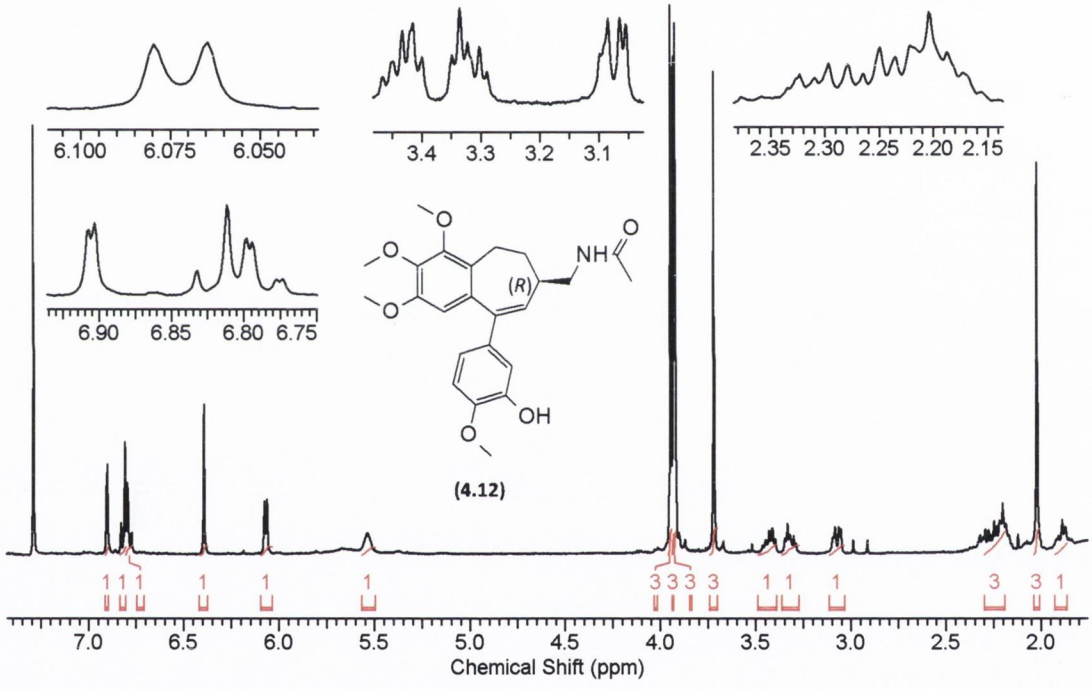

Figure 4.3 ^{1}H NMR spectrum of **(4.12)**

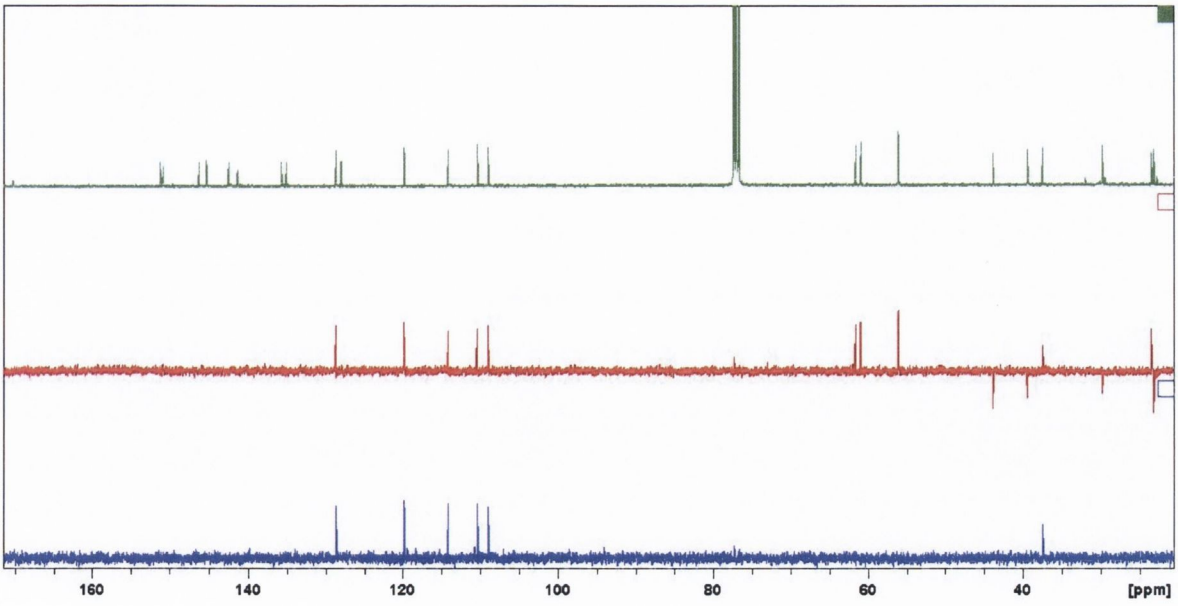

Figure 4.4 ^{13}C, DEPT 135 and DEPT 90 spectra of **(4.12)**

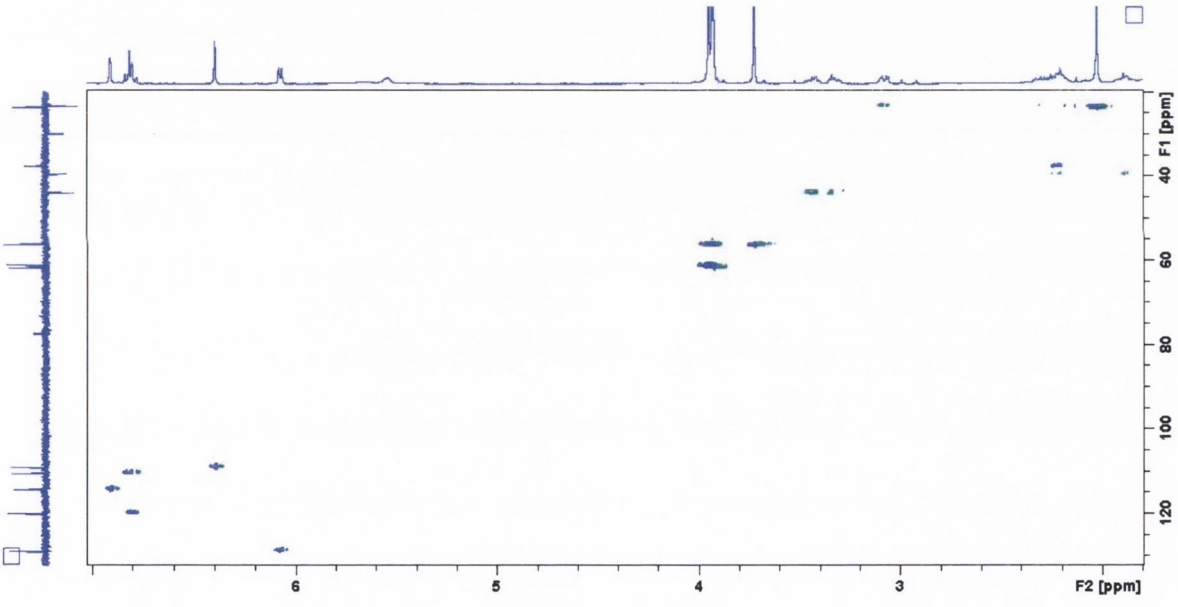

Figure 4.5 HSQC spectrum of **(4.12)**

The identity of **(4.12)** was further confirmed by mass spectrometry. The mass of the molecular ion peak $[M+H]^+$ was found to be in close agreement with the calculated value (calculated 428.2073, found 428.2066). Furthermore, the IR spectrum of **(4.12)** clearly showed an absorption peak at 1650.34 cm^{-1} indicating the presence of the amide carbonyl.

The compound **(4.12)** was also found to have a specific optical activity $[\alpha]_D^{25}$ of + 162 (*c* = 1.11, DCM), indicating the chiral stereochemistry of the molecule. Compound **(4.12)** was subsequently subject to biological evaluation (Section 4.6.1).

4.4 Synthesis of C-7 methylene alcohol analogues

Following the successful synthesis of **(4.12)** and the enantiomerically pure (*R*) and (*S*) alcohols **(3.01)** and **(3.02)**, it was decided to combine methodology from both syntheses to produce analogues of **(2.02)** with an additional methylene unit linking the alcohol to the C-7 position (Figure 4.6). It was anticipated that the additional methylene spacer unit in compounds **(4.23)** and **(4.24)** would confer them with additional chemical stability. The effect of stereochemistry at the C-7 position on biological activity could also be further explored. Furthermore, once the pharmacological activity of these compounds had been evaluated, their potential suitability for the synthesis of molecular conjugates could be established.

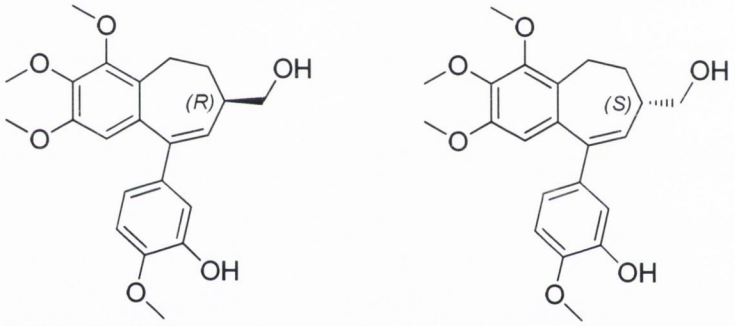

(4.23) **(4.24)**

Figure 4.6 (*R*) and (*S*)-enantiomers of methylene containing **(2.02)** analogues

4.4.1 Synthetic strategy

In order to introduce the required stereochemistry into the synthesis of compounds **(4.23)** and **(4.24)**, the same methodology as used for the synthesis of the (*R*) and (*S*) alcohols **(3.01)** and **(3.02)** was employed. Once the C-9 MOM protected alcohols were obtained, introduction of the nitrile group in an analogous manner to that employed for compound **(4.12)** was proposed. Following reduction of the nitrile groups to primary alcohols and their suitable production, the synthesis of enol triflates was envisioned. These enol triflates could then be coupled with the C-ring boronic acid to provide ready access to the desired compounds.

4.4.2 Synthesis of (*R*)-enantiomer methylene alcohol

4.4.2.1 Nitrile reduction

The first step in the synthesis of compound **(4.23)** utilised the common nitrile intermediate **(4.14)**. DIBAL-H was added to a solution of the nitrile **(4.14)** at -78 °C. After acidic work-up, the aldehyde **(4.25)** was afforded as a crude mixture. The aldehyde **(4.25)** was then readily reduced using sodium borohydride to afford the alcohol **(4.26)**. The product was isolated in good yield (61% over two steps) as a yellow oil (Scheme 4.20).

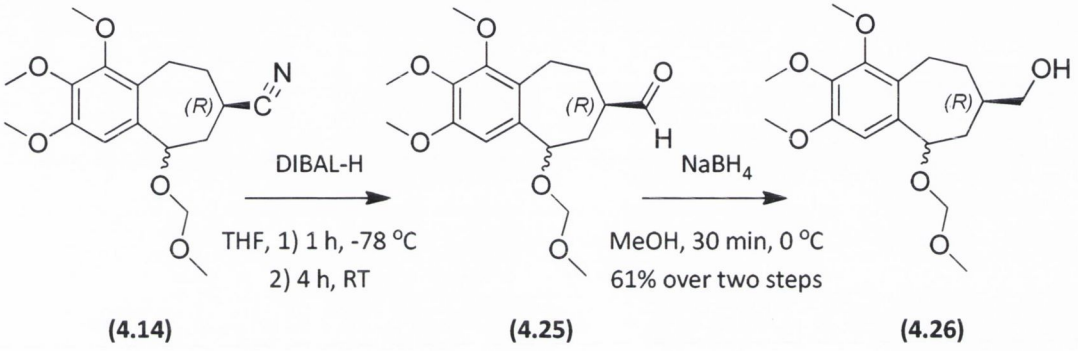

Scheme 4.20 Two step reduction of nitrile **(4.14)** to alcohol **(4.26)**

The aluminium based reducing reagent DIBAL-H was reported to have found particular utility in the selective reduction of nitriles to aldehydes [190]. DIBAL-H causes the formation of a stable imine intermediate (especially at low temperature) which is hydrolysed upon acid work-up [190]. The DIBAL-H reduction was accomplished utilising a procedure modified from Enders *et al.* [262]. The reduction was monitored by TLC, utilising vanillin as visualisation reagent. Monitoring of the reaction was complicated by the fact that both the nitrile **(4.14)** and aldehyde **(4.25)** had identical R_f values on TLC. Fortuitously, the vanillin selectively stained for the aldehyde, allowing its formation to be monitored. Initial attempts to isolate and characterise the aldehyde proved fruitless, as it appeared to be very unstable. It was therefore decided to reduce the aldehyde **(4.25)** using sodium borohydride, without purification, to afford the much more stable alcohol **(4.26)**.

4.4.2.2 Silyl protection of alcohol (4.26)

In order to achieve selective oxidation of the C-9 position alcohol following MOM ether removal, the C-7 methylene alcohol of **(4.26)** was protected as a TBDPS ether. This was accomplished using *tert*-butyldiphenylsilyl chloride together with imidazole as base in DMF under anhydrous conditions. The product **(4.27)** was isolated after 4 h in excellent yield (88%) as a colourless oil (Scheme 4.21).

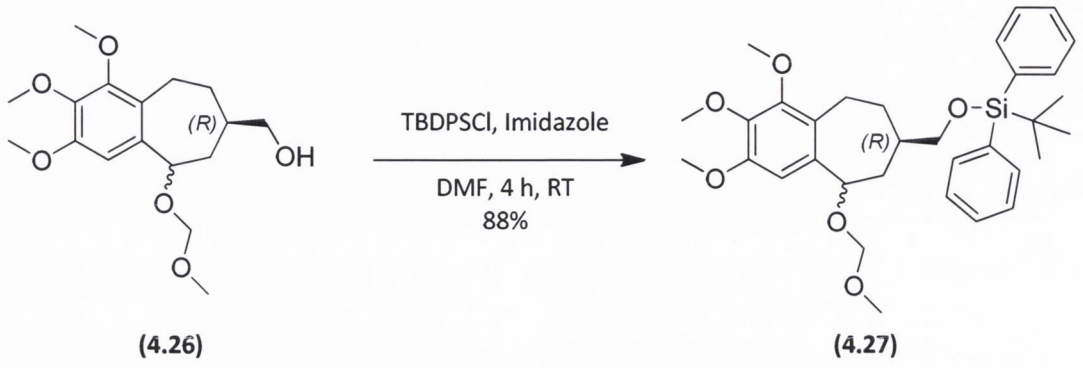

(4.26) **(4.27)**

Scheme 4.21 Silyl protection of **(4.26)**

4.4.2.3 MOM deprotection and alcohol oxidation

The MOM ether of compound **(4.27)** was then removed using the aluminium chloride/sodium iodide/acetonitrile system developed by Node *et al.* [258]. Compound **(4.27)** was dissolved in a mixture of DCM and acetonitrile. Aluminium chloride and sodium iodide were then added. After 20 min, consumption of the starting material was apparent by TLC analysis. The formation of two products was observed. As expected, the desired benzylic alcohol **(4.28)** was observed. However, an unknown substance, purported to be the elimination side product **(4.30)**, was also observed (Scheme 4.23). The reaction was quenched by the addition of saturated sodium bicarbonate aqueous solution and extracted with DCM. Dess-Marin periodinane was added to this DCM extract. The reaction was quenched after 30 min by the addition of saturated sodium bicarbonate aqueous solution and the ketone **(4.29)** was isolated as a yellow oil in reasonable yield (74% over two steps; Scheme 4.22).

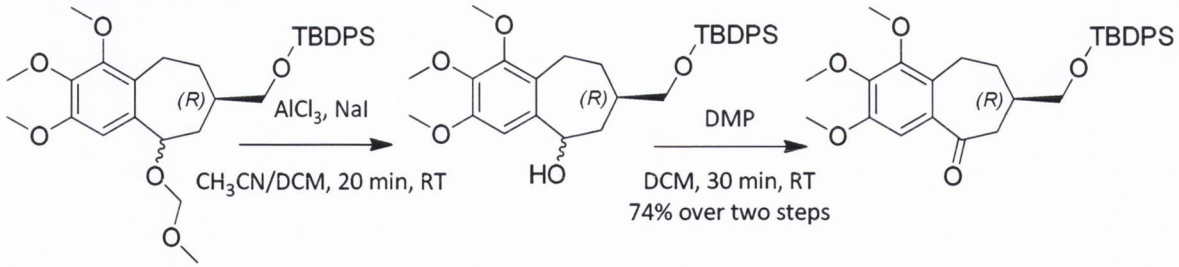

(4.27) **(4.28)** **(4.29)**

Scheme 4.22 Removal of MOM group of **(4.27)** and oxidation of alcohol **(4.28)**

In order to investigate the hypothesised elimination reaction proposed previously (Section 3.8.8.3), the purported elimination side product **(4.30)** was also isolated and characterised. The identity of compound **(4.30)** was confirmed, providing evidence for the proposed elimination mechanism outlined previously (Section 3.8.8.3; Scheme 3.22).

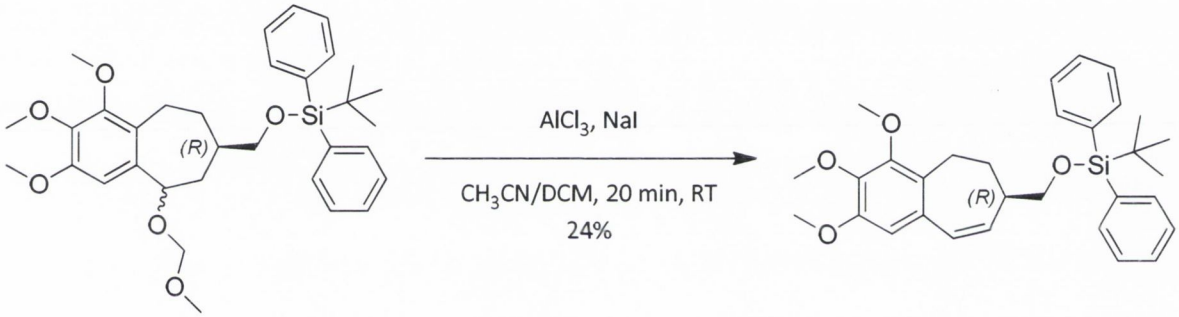

(4.27) **(4.30)**

Scheme 4.23 Formation of elimination side product **(4.30)**

4.4.2.4 Formation of enol triflate (4.31)

The lithium enolate was first generated by the *in situ* formation of lithium diisopropylamide (LDA) at -78 °C, followed by addition of a solution of the ketone **(4.29)** in THF under anhydrous conditions. After 2 h, the triflating reagent 2-[*N*,*N*-bis(fluoromethylsulfonyl)amino]-5-chloropyridine was added as a solution in THF and the reaction stirred for a further 3 h. The enol triflate **(4.31)** was then isolated in moderate yield (58%) as a yellow oil (Scheme 4.24).

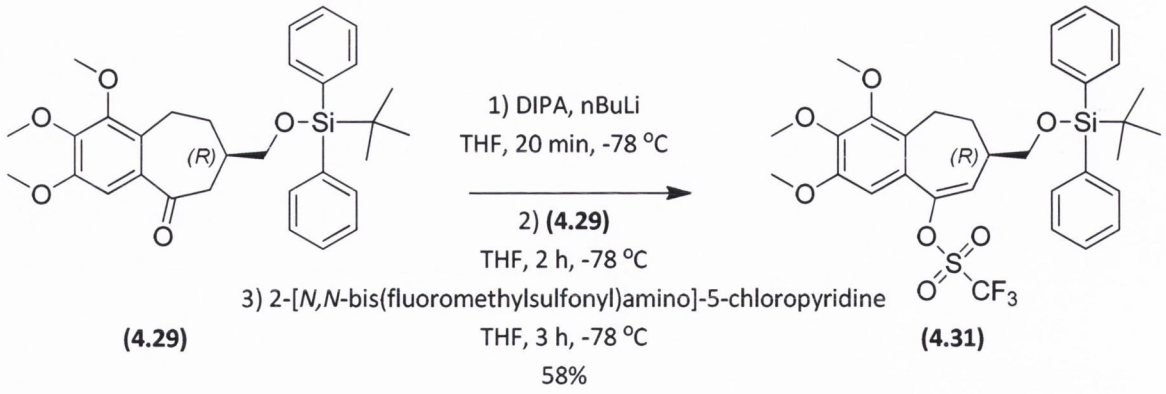

Scheme 4.24 Synthesis of enol triflate **(4.31)**

4.4.2.5 Suzuki coupling of enol triflate (4.31) and boronic acid (4.08)

Standard Suzuki coupling reaction conditions were used for the palladium catalysed cross coupling reaction. The enol triflate **(4.31)** and boronic acid **(4.08)** were dissolved in a mixture of toluene, ethanol and water. Potassium carbonate was added as base. The palladium based catalyst (tetrakis(triphenyl)phosphine) palladium was added and the reaction was heated under reflux for 1 h. The tricyclic product **(4.32)** was then isolated as a yellow oil in quantitative yield (Scheme 4.25).

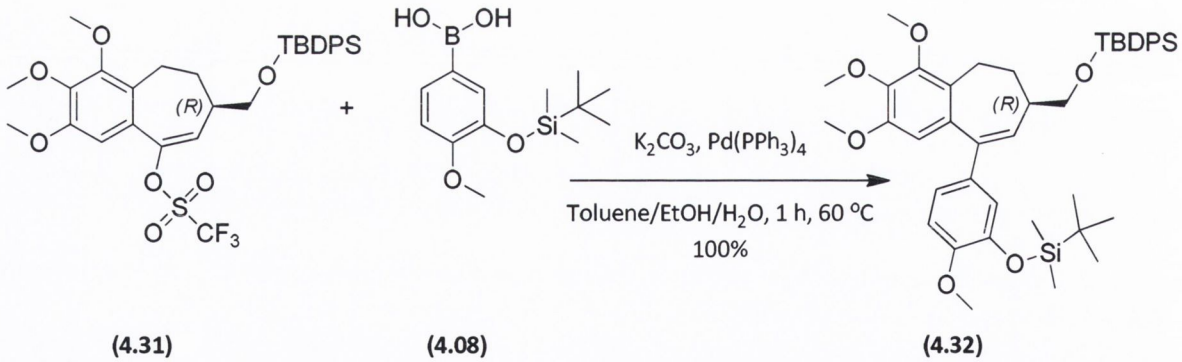

Scheme 4.25 Suzuki coupling of enol triflate **(4.31)** and boronic acid **(4.08)**

The progress of the reaction was monitored by TLC. The enol triflate **(4.31)** was observed to have an almost identical R_f value to the coupled product **(4.32)**. The two compounds could only be resolved using a very non-polar mobile phase (10:1; hexane: ethyl acetate) and a long

development distance (15 cm). Once the enol triflate **(4.31)** had been consumed, the product **(4.32)** was conveniently isolated by flash column chromatography.

4.4.2.6 Simultaneous removal of both silyl protecting groups of (4.32)

The simultaneous removal of both silyl protecting groups of compound **(4.32)** was achieved by the addition of TBAF in dry THF under anhydrous conditions. After 16 h, the product **(4.23)** was isolated in moderate yield (65%) as a white solid (Scheme 4.26).

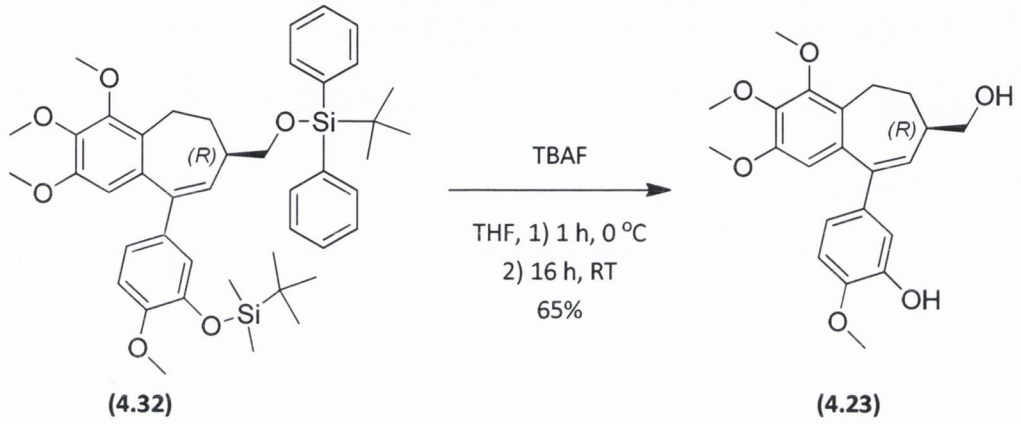

(4.32) **(4.23)**

Scheme 4.26 Simultaneous removal of both silyl protecting groups to afford compound **(4.23)**

4.4.2.7 Increased stability of (4.23)

The silyl deprotection reaction was observed to occur cleanly, affording exclusively the desired diol **(4.23)** in satisfactory yield. This compares favourably with the equivalent deprotection of **(2.02)** which resulted in the formation of a number of undesirable side products and afforded the desired product in a substantially lower yield (65% v 37%).

It was hypothesised that the driving force for the elimination of the C-7 hydroxyl in compound **(2.02)** was the potential for significantly increased conjugation throughout the eliminated compound **(4.33)** (Figure 4.27). The allylic character of the C-7 hydroxyl was hypothesised to contribute significantly to this effect.

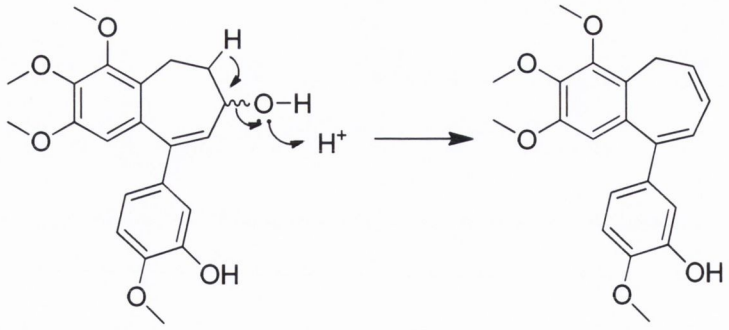

(2.02) **(4.33)**

Scheme 4.27 Proposed elimination product of **(2.02)**

The alcohol group in compound **(4.23)**, however, was not allylic and thus experienced a significantly reduced tendency towards elimination. The increased stability hypothesised to arise from insertion of the additional methylene group was manifested in the increased yield and cleaner conversion obtained in the silyl deprotection reaction (Figure 4.26).

4.4.2.8 Characterisation of (4.23)

The diol **(4.23)** was fully characterised by NMR spectroscopy. The four distinct methoxy proton signals were found to resonate as four distinct signals at 3.70 ppm, 3.91 ppm, 3.92 ppm and 3.93 ppm. The double bond proton was found to correspond to a doublet (J = 6.18 Hz) at 6.09 Hz with the aid of the HSQC spectrum (Figure 4.9). The four aromatic CH protons were found to resonate as three distinct signals at 6.40 ppm, 6.77-6.81 ppm (2 x CH) and 6.93 ppm. The six aliphatic CH_2 protons were assigned as corresponding to four distinct multiplets at 1.88-1.92 ppm, 2.16-2.29 ppm (2 x CH_2), 3.05-3.10 ppm and 3.63-3.70 ppm (2 x CH_2) by reference to the HSQC spectrum (Figure 4.9). The C-7 CH proton was found to resonate as part of a multiplet at 2.16-2.29 ppm.

Utilising the DEPT 135 spectrum, the three CH_2 carbons were readily assigned as the peaks at 22.67 ppm, 37.38 ppm and 65.91 ppm (Figure 4.8). Similarly, the four methoxy carbons were found to resonate as three distinct signals at 55.55 ppm (2 x OCH_3), 60.44 ppm and 61.14 ppm. The C-7 CH carbon was assigned to the signal at 39.45 ppm with the aid of the HSQC spectrum (Figure 4.9). The double bond CH carbon was determined to resonate at 128.37 ppm by reference to the HSQC spectrum. The four aromatic CH signals were identified at 108.44 ppm, 109.84 ppm, 113.80 ppm and 119.27 ppm by reference to the DEPT 90 spectrum (Figure 4.8). The nine quaternary carbons were found to resonate at 127.66 ppm, 134.87 ppm, 135.58 ppm, 140.72 ppm, 141.49 ppm, 144.79 ppm, 145.62 ppm, 150.31 ppm and 150.57 ppm.

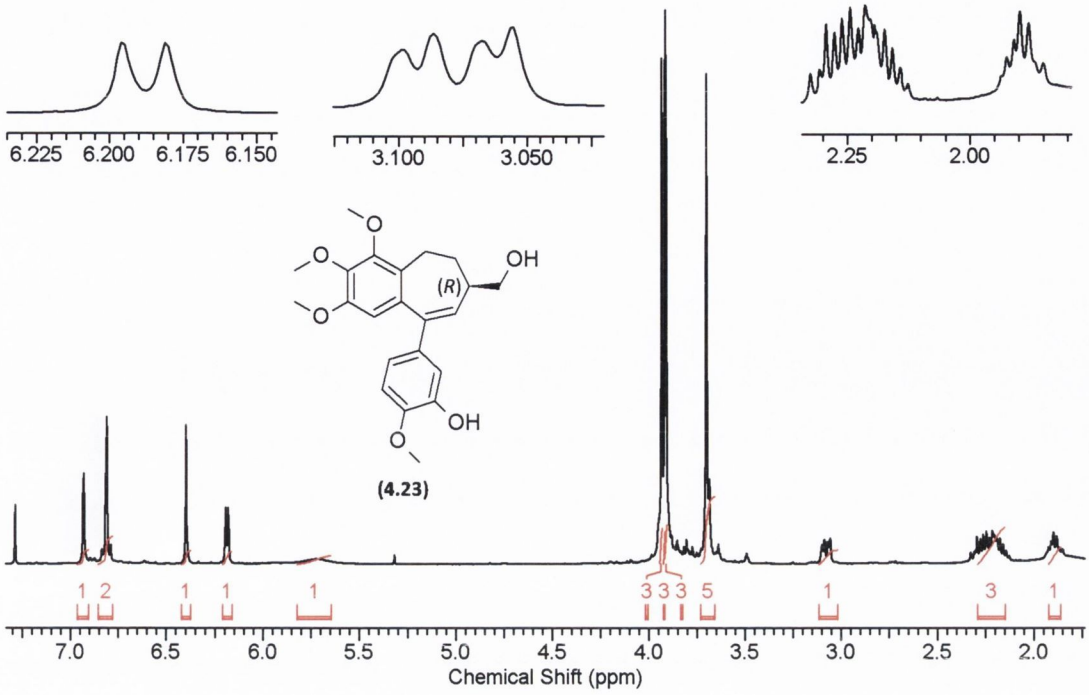

Figure 4.7 ^{1}H NMR spectrum of **(4.23)**

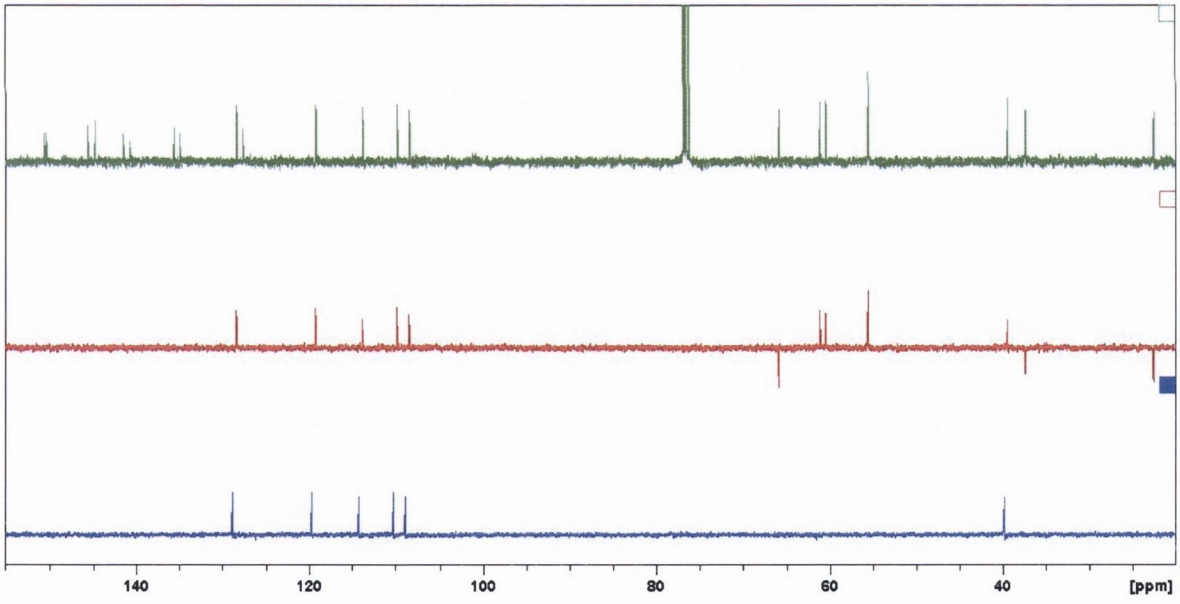

Figure 4.8 ^{13}C, DEPT 135 and DEPT 90 spectra of **(4.23)**

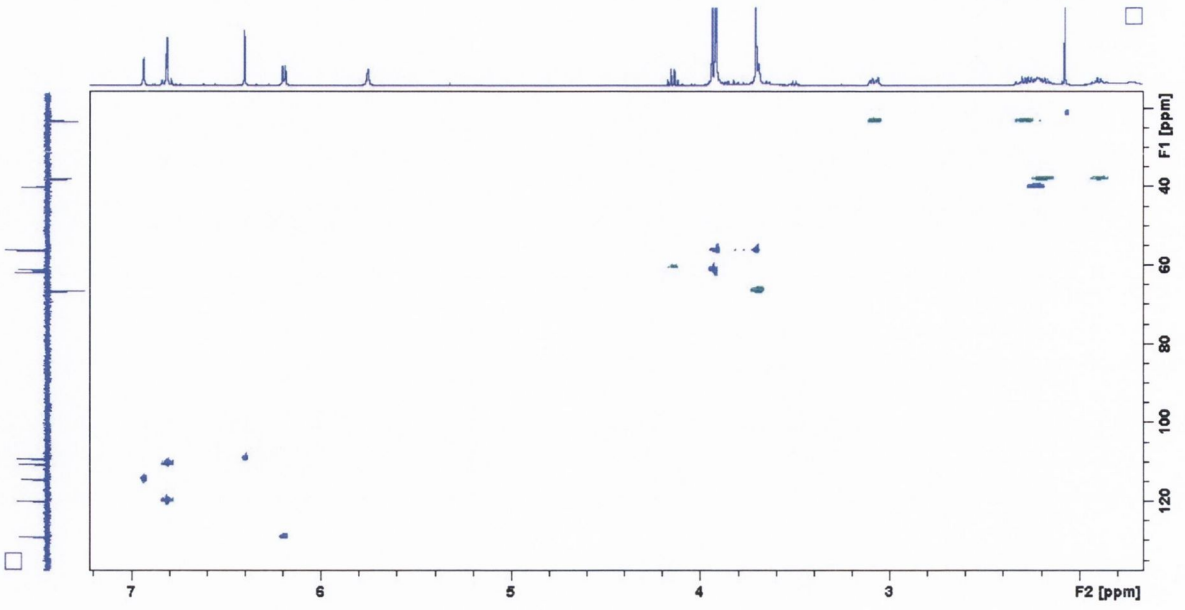

Figure 4.9 HSQC NMR spectrum of **(4.23)**

Mass spectrometry further confirmed the identity of **(4.23)**. The mass of the molecular ion peak $[M+H]^+$ was found to be in close agreement with the calculated value (calculated 387.1808, found 387.1834). The specific optical rotation $[\alpha]_D^{25}$ of 102.4 (*c* = 3.13, DCM) also suggested that although inversion of configuration had occurred, the stereochemical purity of the C-7 position had been maintained. The compound was then subject to biological evaluation (Section 4.6.2).

4.4.3 Synthesis of (*S*)-enantiomer methylene alcohol (4.24)

The (*S*)-enantiomer of the methylene containing alcohol, compound **(4.24)** was then synthesised using similar methodology. The intermediate **(3.47)** served as the starting point for this synthesis.

4.4.3.1 Synthesis of mesylate (4.35) and displacement with cyanide

The mesylate of **(3.47)** was synthesised by the addition of methanesulfonyl chloride and DIPEA to a solution of the alcohol in DCM under anhydrous conditions at 0 °C. After 1 h, the mesylate **(4.34)** was isolated as a crude mixture. The mesylate was dissolved in DMSO. A large excess of sodium cyanide was pulverised using a mortar and pestle and added to the reaction. The reaction was heated to 70 °C for 24 h. Following consumption of the starting material, the nitrile **(4.35)** was isolated as a yellow oil in modest yield (46% over two steps; Scheme 4.28).

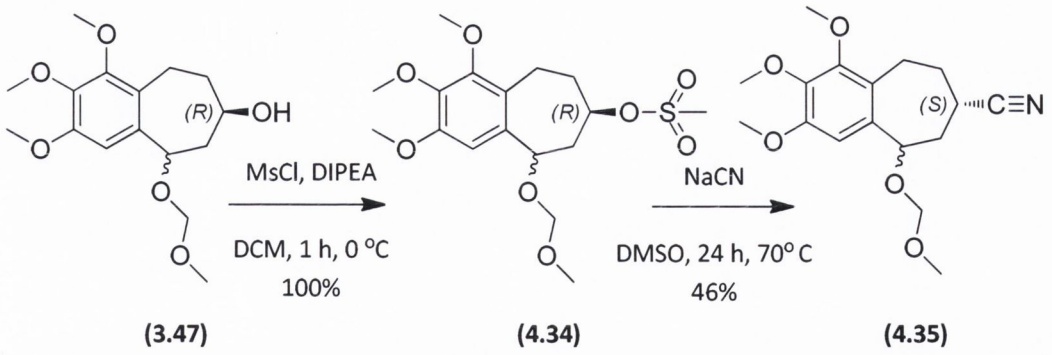

Scheme 4.28 Synthesis of mesylate **(4.34)** followed by cyanide displacement

4.4.3.2 Two-step reduction of nitrile (4.35) to alcohol (4.37)

The nitrile **(4.35)** was treated with DIBAL-H in THF under anhydrous conditions. Following work-up with tartaric acid aqueous solution, the aldehyde **(4.36)** was obtained as a crude mixture. The aldehyde was not purified, due to the inherent instability of the compound observed during the synthesis of the (*R*)-enantiomer equivalent **(4.25)**. The aldehyde **(4.36)** was then readily reduced to the alcohol **(4.37)** using sodium borohydride in methanol. Following purification, the alcohol **(4.37)** was isolated as a white oil in good yield (75%; Scheme 4.29).

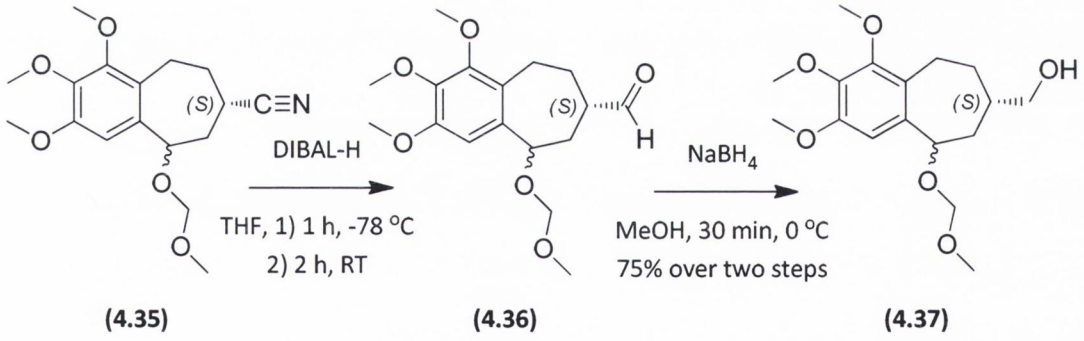

Scheme 4.29 Two-step reduction of nitrile **(4.35)** to alcohol **(4.37)**

4.4.3.3 Silyl protection of the alcohol (4.37)

The alcohol **(4.37)** was then protected as *tert*-butyldiphenylsilyl ether by combining with *tert*-butyldiphenylsilyl chloride and imidazole in DMF under anhydrous conditions. After 16 h, the protected compound **(4.38)** was isolated in excellent yield (94%) as a colourless oil (Scheme 4.30).

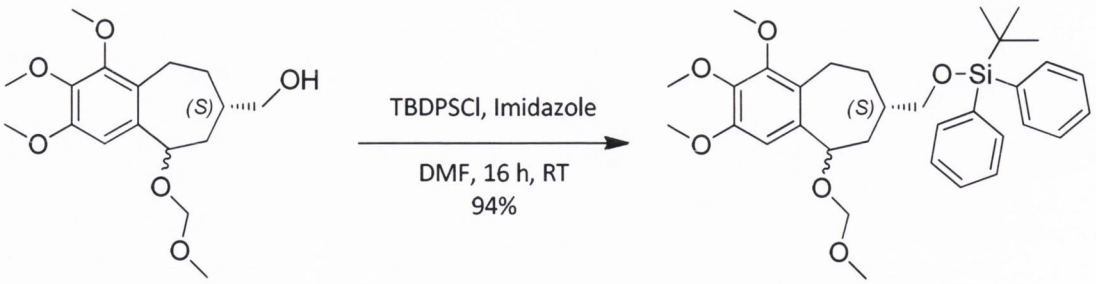

(4.37) **(4.38)**

Scheme 4.30 Silyl protection of the alcohol **(4.37)**

4.4.3.4 Removal of the MOM group of (4.38) and oxidation of alcohol (4.39)

The aluminium chloride/sodium iodide/acetonitrile system was again utilised for the removal of the MOM ether protection [258]. Compound **(4.38)** was dissolved in a mixture of acetonitrile and DCM. Aluminium chloride and sodium iodide were then added at 0 °C. After 1 h, the reaction was quenched by the addition of saturated sodium bicarbonate aqueous solution and the reaction was extracted with DCM. Dess-Martin periodinane was added to this DCM extract. After 30 min, the ketone **(4.40)** was isolated as a yellow oil in excellent yield (83% over two steps; Scheme 4.31).

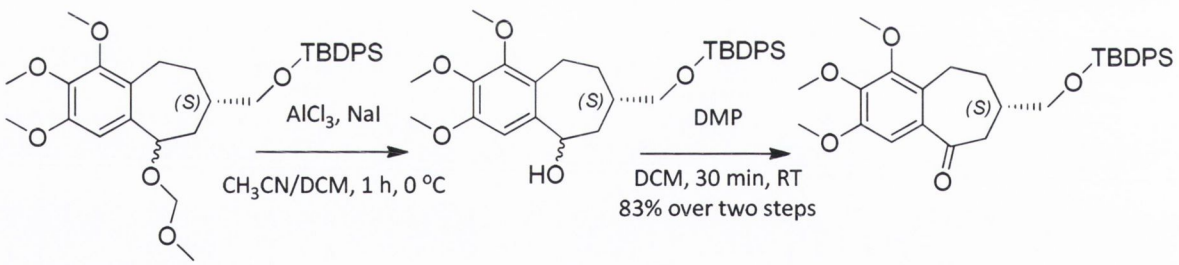

(4.38) **(4.39)** **(4.40)**

Scheme 4.31 Removal of MOM protecting group of **(4.38)** and oxidation of alcohol **(4.39)**

4.4.3.5 Removal of silyl protecting group of (4.40)

The silyl protecting group of compound **(4.40)** was then removed using TBAF under anhydrous conditions. After 3 h, the alcohol **(4.41)** was isolated as a yellow oil in excellent yield (91%; Scheme 4.32). The high yield and clean conversion observed for this transformation compared very favourably with the analogous reaction involving the C-7 alcohol without the additional

methylene unit (91% v 51%; Section 2.3.4; Scheme 2.14). This provided further evidence for the enhanced stability in the molecule afforded by the presence of the C-7 methylene group.

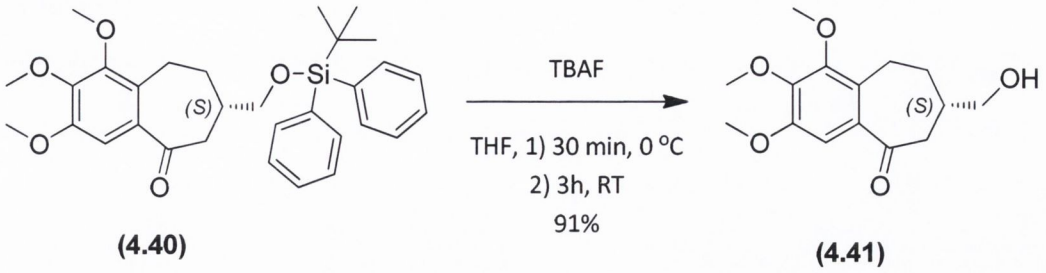

(4.40) **(4.41)**

Scheme 4.32 Removal of silyl protecting group of **(4.40)**

The removal of the silyl protecting group at this juncture represented a deviation in the synthetic route followed for the (*R*)-enantiomer **(4.23)**. It was proposed to couple the C-ring to the AB-ring ketone **(4.41)** using the organolithium coupling methodology employed in the improved synthesis of **(2.02)**. This would facilitate chemoselective modification of the C-7 functionality, in the synthesis of additional analogues, while maintaining protection of the C-ring phenol.

4.4.3.6 Coupling of the ketone (4.41) with the C-ring bromide (2.14)

The C-ring **(2.14)** was dissolved in THF and *n*-butyllithium was added at -78 °C under anhydrous conditions. After 40 min, following formation of the lithiated derivative, a solution of the ketone **(4.41)** in THF was added under anhydrous conditions. After a further 4 h, the reaction was quenched by the addition of HCl aqueous solution. Following purification, the desired coupled compound **(4.42)** was isolated as a yellow oil in moderate yield (54%; Scheme 4.33).

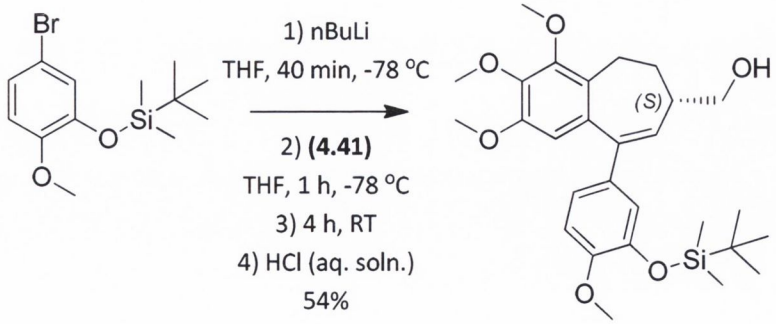

(2.14) **(4.42)**

Scheme 4.33 Organolithium coupling of ketone **(4.41)** and C-ring bromide **(2.14)**

4.4.3.7 Removal of the phenolic silyl group of compound (4.42)

The phenolic silyl protecting group of compound **(4.42)** was removed by the addition of TBAF in THF at 0 °C under anhydrous conditions. After 3.5 h, the desired product **(4.24)** was isolated as a white solid in excellent yield (98%; Scheme 4.34).

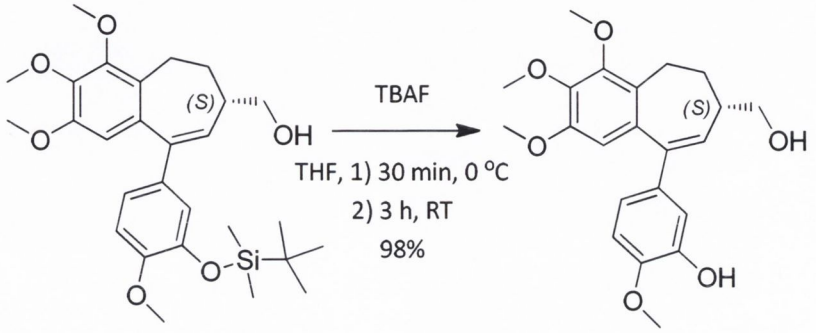

Scheme 4.34 Removal of phenolic silyl group of **(4.42)**

As expected, the diol **(4.24)** was found to have identical physical and chemical properties to its stereochemical antipode **(4.23)** apart from its specific optical rotation. The specific optical rotation, $[\alpha]_D^{25}$ of the (*R*)-enantiomer **(4.23)** was found to be - 71.4 (*c* = 3.13, DCM) while the $[\alpha]_D^{25}$ of the (S)-enantiomer **(4.24)** was found to be + 102.4 (*c* = 0.48, DCM). The close approximation of the values for both enantiomers together with their opposite sign indicated that the stereochemical integrity of the molecules had been maintained through the synthesis. Both compounds were subsequently evaluated *in vitro* (Section 4.6.2).

4.5 Synthesis of C-7 carboxylic acid tubulin inhibitors

In order to further probe the structure activity relationship of the tubulin inhibitory pharmacophore, a pair of enantiomerically pure C-7 carboxylic acid containing analogues was designed (Figure 4.10). It was proposed that these compounds would also significantly increase the options available for molecular conjugation.

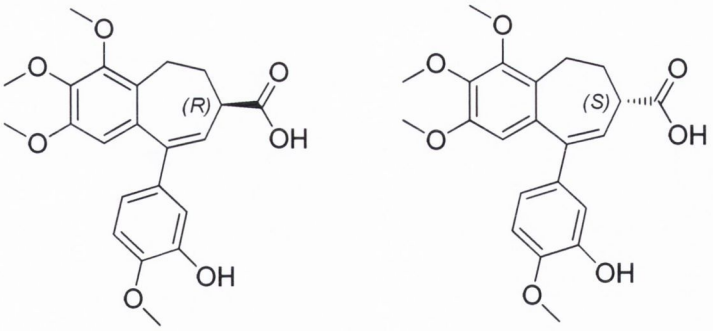

(4.43) **(4.44)**

Figure 4.10 (*R*) and (*S*) carboxylic acid containing tubulin inhibitors **(4.43)** and **(4.44)**

4.5.1 Synthetic strategy

It was proposed to utilise the intermediate **(4.42)** and its (*R*)-enantiomer equivalent in the synthesis of these molecules. It was envisioned that facile oxidation of these primary alcohol intermediates would be possible to afford the desired carboxylic acid products. These intermediates would provide suitable protection to the C-ring phenol while oxidation at the C-7 position alcohol was undertaken. This strategy was deemed of fundamental importance, given previous negative experiences of oxidation in the presence of a free phenolic group (Section 2.2; Scheme 2.7 and Section 2.3.3; Scheme 2.13). Cognisant of the propensity of the B-ring double bond for oxidation under suitable conditions, selection of an appropriate oxidising reagent was given particular attention. Ultimately a two step oxidation, utilising DMP and oxone in sequence was employed for the central oxidative transformation of this synthetic strategy.

4.5.2 Synthesis of (*R*)-enantiomer carboxylic acid (4.43)

The first step in the synthesis of **(4.43)** was removal of the silyl group of **(4.29)**. This would allow the addition of the C-ring bromide **(2.14)** using organolithium coupling methodology and would furnish an intermediate possessing a silyl protected phenol with a free C-7 alcohol.

4.5.2.1 Silyl deprotection of (4.29)

The silyl ether of **(4.29)** was removed using TBAF under anhydrous conditions. After 3 h, the desired alcohol **(4.45)** was isolated in excellent yield (86%) as a yellow oil (Scheme 4.35).

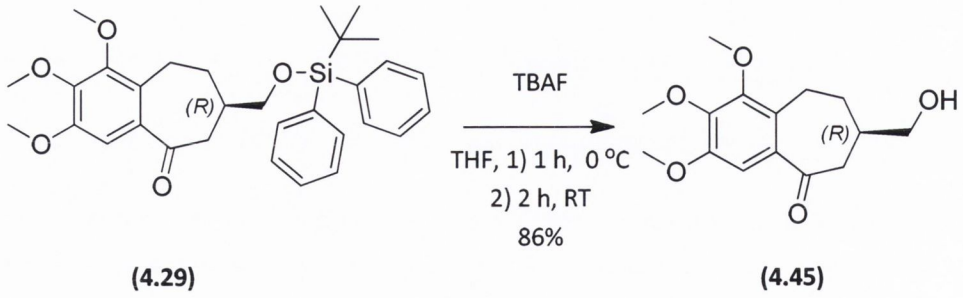

(4.29) **(4.45)**

Scheme 4.35 Removal of silyl group on **(4.29)**

4.5.2.2 Organolithium coupling of ketone (4.45) and C-ring bromide (2.14)

The ketone **(4.45)** was then coupled to the C-ring bromide **(2.14)** using the familiar organolithium coupling procedure. The C-ring bromide **(2.14)** was lithiated at -78 °C by the addition of *n*-butyllithium. After 40 min, a THF solution of the ketone **(4.45)** was added under anhydrous conditions. After 5 h, the reaction underwent acidic workup. Following purification, the desired coupled compound **(4.46)** was isolated in moderate yield (53%) as a yellow oil (Scheme 4.36).

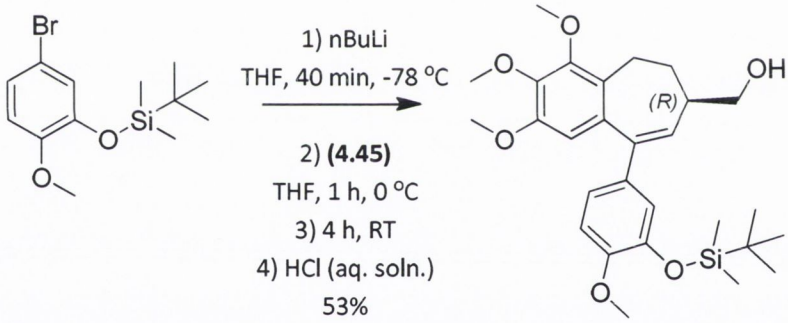

(2.14) **(4.46)**

Scheme 4.36 Organolithium coupling of ketone **(4.45)** and C-ring bromide **(2.14)**

4.5.2.3 Direct oxidation of alcohol (4.46) to carboxylic acid (4.47)

The crucial transformation in the synthesis of the carboxylic acid containing compound **(4.43)** was the oxidation of the alcohol functional group of **(4.46)** to a carboxylic acid. The situation was complicated by the presence of a double bond at C-8 and C-9, as a number of the most commonly used oxidising agents are known to react with such a system [190]. For example, it was hypothesised that aqueous solutions of chromic acid (Jones' reagent) or potassium permanganate

would result in unwanted side reactions taking place. Therefore, it was necessary to utilise a methodology which would chemoselectively oxidise the alcohol while leaving the double-bond unchanged.

4.5.2.4 Attempted PDC oxidation of (4.46)

The chromium based oxidation reagent PDC had been previously used to selectively oxidise the alcohol of **(2.02)** to the ketone **(2.03)** in DCM, albeit in poor yield (Section 2.2; Scheme 2.7). This suggested that this reagent might be chemoselective for the alcohol even in the presence of the double bond. In the oxidation of primary alcohols with PDC, it has been shown that solvent plays a significant role in the product formed [263]. PDC was reported to conveniently oxidise primary alcohols to aldehydes in DCM, whereas, in DMF, oxidation to carboxylic acids has been achieved [263]. Therefore, the direct oxidation of the alcohol **(4.46)** to the carboxylic acid **(4.47)** was attempted using PDC in DMF. After 6 h, TLC analysis suggested the formation of a complex mixture of substances. Accordingly, this approach was not pursued.

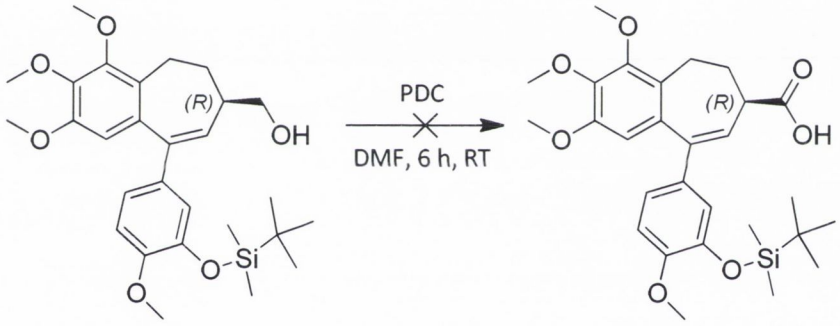

(4.46) **(4.47)**

Scheme 4.37 Attempted PDC oxidation of alcohol **(4.46)** to carboxylic acid **(4.47)**

4.5.2.5 Attempted DMP/NHS oxidation of (4.46)

A procedure detailed by Mazitschek *et al.* outlined the use of the pentavalent iodine based oxidising reagent 1-hydroxy-1,2-benziodoxole-3(1H)-one-1-oxide (IBX) together with *N*-hydroxysuccinimide (NHS) to oxidise primary alcohols to carboxylic acids [264]. A modification of this procedure, substituting the related oxidising agent DMP for IBX, was subsequently attempted. DMP was added to a solution of the alcohol **(4.47)** in DCM. After 10 min, the consumption of the alcohol and the formation of an aldehyde intermediate was suggested by TLC. NHS was then

added. After consumption of the purported aldehyde was observed by TLC, the reaction was subjected to basic work-up with sodium hydroxide aqueous solution and extraction with diethyl ether. TLC analysis of the concentrated organic fraction revealed no indication of the formation of the desired product **(4.47)**. Therefore, this approach was not subsequently pursued.

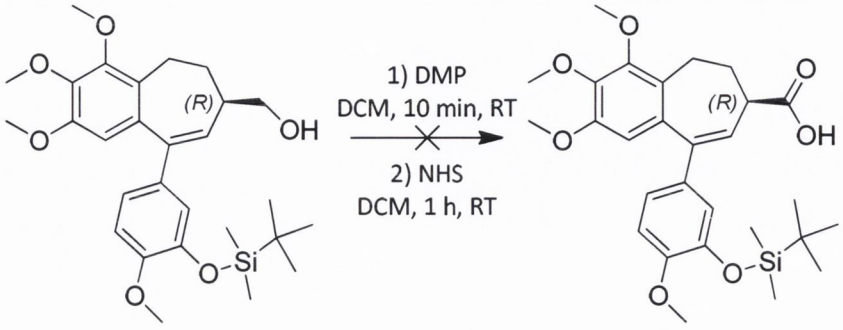

(4.46) **(4.47)**

Scheme 4.38 Attempted DMP/NHS oxidation or alcohol **(4.46)** to carboxylic acid **(4.47)**

4.5.2.6 Oxidation of alcohol (4.46) to aldehyde (4.48)

It was decided that a two-step oxidation of the alcohol **(4.46)** *via* an aldehyde intermediate **(4.48)** might be the most efficient route to obtaining the desired carboxylic acid. Accordingly, oxidation of the alcohol **(4.46)** to the aldehyde **(4.48)** was undertaken. Dess-Martin periodinane was added to a solution of the alcohol **(4.46)** in DCM. After 1 h, the desired aldehyde **(4.48)** was obtained in excellent yield (82%) following purification (Scheme 4.39).

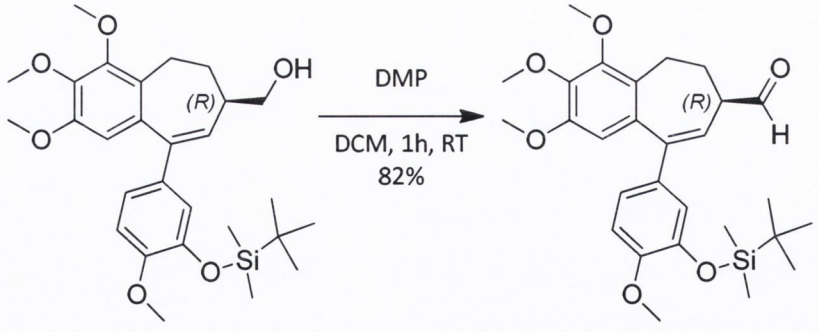

(4.46) **(4.48)**

Scheme 4.39 Dess-Martin periodinane oxidation of **(4.46)**

It was hoped that oxidation of the aldehyde **(4.48)** to the carboxylic acid would occur much more readily than was observed for direct oxidation of the alcohol to the carboxylic acid. The aldehyde **(4.48)** was found to be unstable. The formation of several significant degradants was observed by TLC analysis after only 3 days. It was thus decided to react the aldehyde promptly following purification. However, before the reaction could be repeated on a larger scale, an efficient procedure for synthesising the carboxylic acid was desired.

4.5.2.7 Characterisation of aldehyde (4.48)

The aldehyde compound **(4.48)** was characterised in full by NMR. The distinctive dimethyl silyl protons were found to resonate furthest upfield as a doublet (J =4.56 Hz) at 0.17 ppm. The *tert*-butyl group protons were found to resonate as a singlet at 1.00 ppm. The four methoxy group protons were assigned to four distinct signals at 3.70 ppm, 3.85 ppm, 3.94 ppm and 3.95 ppm. The double bond proton was found to correlate with a doublet (J = 7.32 Hz) at 6.46 ppm with the aid of the DEPT 90 and HSQC spectra (Figure 4.12 and 4.13). The four aromatic protons resonated as a singlet at 6.39 ppm, a multiplet at 6.81-6.85 ppm and a double doublet (J_1 =8.03 Hz, J_2 = 2.01 Hz) at 6.92 ppm. The four aliphatic B-ring CH_2 protons were found to resonate as two multiplets at 2.40-2.56 ppm (3 x CH_2) and 2.88-2.98 ppm by reference to the HSQC spectrum. The C-7 CH proton was assigned similarly and identified to resonate as part of the multiplet at 2.88-2.98 ppm. The aldehyde proton was found to resonate furthest downfield, as a singlet at 9.61 ppm.

The signal resonating furthest upfield in the ^{13}C spectrum at -4.53 ppm was assigned to the dimethyl silyl group carbons. The *tert*-butyl group methyl carbons were found to resonate at 25.73 ppm. The four methoxy carbons were readily identified as those signals at 55.50 ppm, 55.91 ppm, 60.89 ppm and 61.55 ppm. The two CH_2 carbons were readily identified from the DEPT 135 spectrum as corresponding to the two signals at 22.69 ppm and 36.77 ppm. The C-7 CH carbon was found to resonate at 49.81 ppm using the DEPT 90 and HSQC spectra (Figure 4.12 and 4.13). The double bond CH carbon was found to resonate at 121.26 ppm. The four aromatic CH carbons were assigned to the signals at 109.00 ppm, 111.61 ppm, 120.76 ppm and 121.59 ppm. The *tert*-butyl quaternary carbon was found to resonate at 18.47 ppm. The distinct aldehyde carbonyl carbon signal was identified as the furthest downfield signal 202.16 ppm. The nine remaining quaternary carbons were assigned as corresponding to those signals at 127.92 ppm, 134.12 ppm, 135.12 ppm, 141.66 ppm, 143.79 ppm, 144.67 ppm, 150.84 ppm, 150.99 ppm and 151.42 ppm.

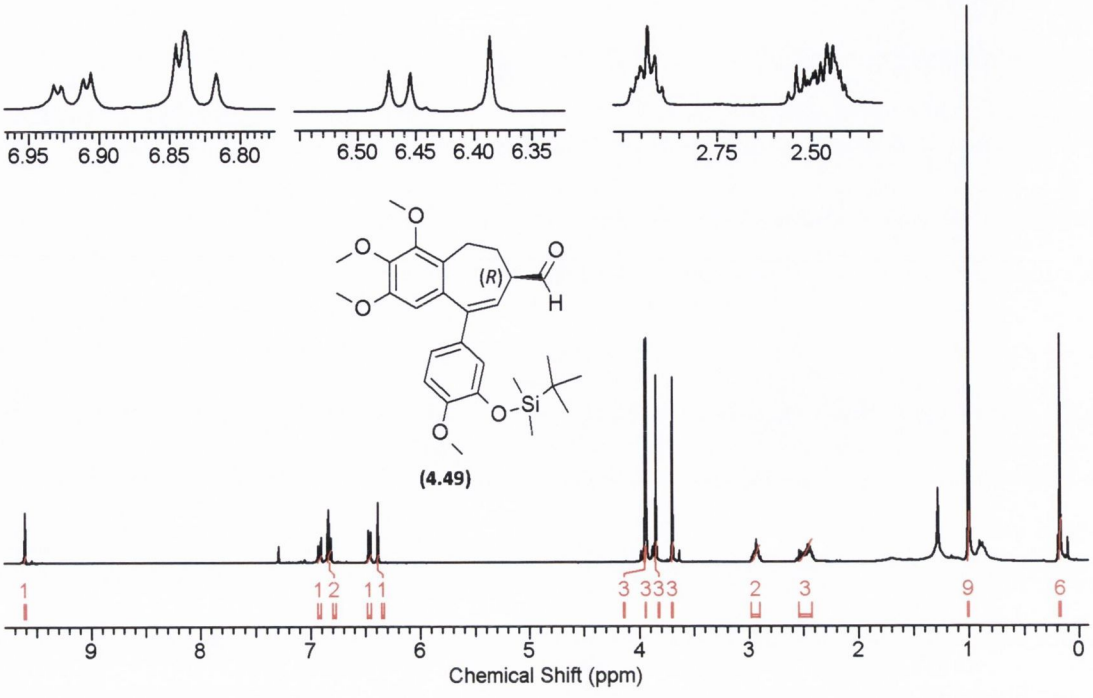

Figure 4.11 ^{1}H NMR spectrum of **(4.48)**

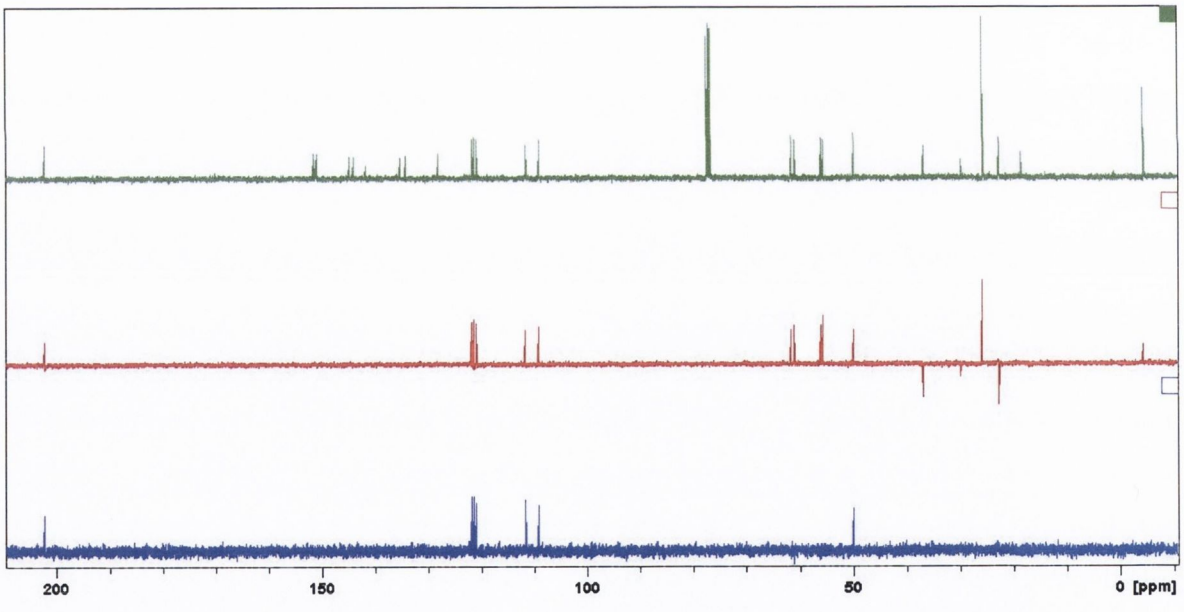

Figure 4.12 ^{13}C, DEPT 135 and DEPT 90 NMR spectra of **(4.48)**

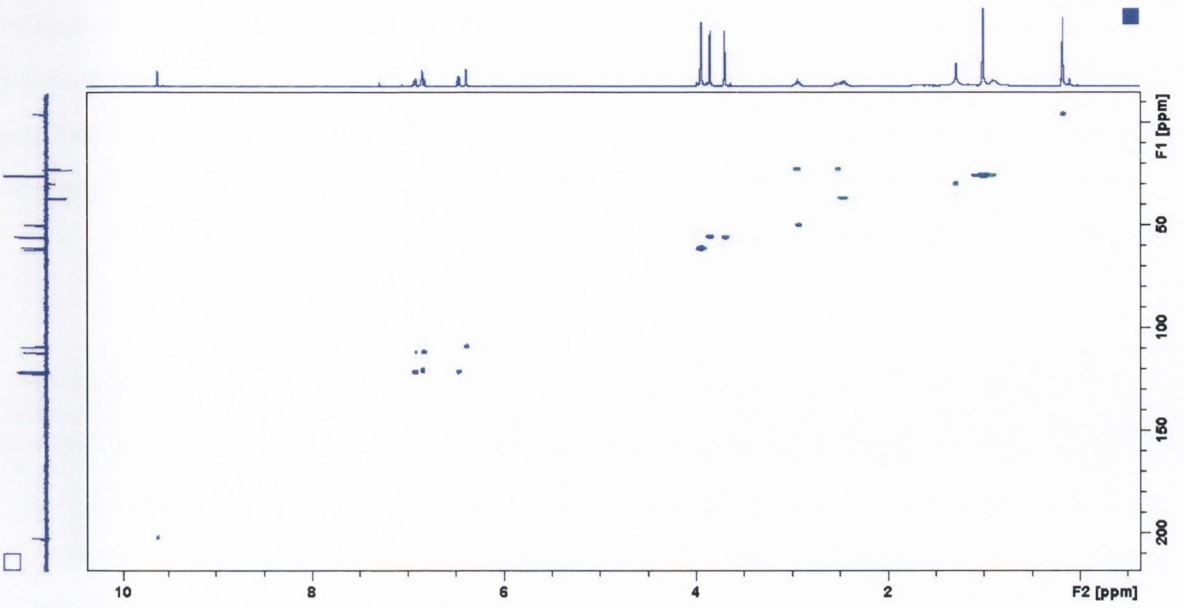

Figure 4.13 HSQC NMR spectrum of **(4.48)**

The identity of **(4.48)** was further confirmed by IR spectroscopy. A distinctive carbonyl stretching absorption at 1726.29 cm^{-1} was observed clearly indicating the presence of an aldehyde carbonyl group in the molecule. The mass spectrometry data provided further confirmation of the identity of **(4.48)**. The observed mass of the molecular ion peak $[M+H]^+$ was found to be in close agreement with the calculated value (calculated 499.2516, found 499.2520).

4.5.2.8 Attempted PDC oxidation of aldehyde (4.48)

Once a facile procedure for the synthesis of the aldehyde **(4.48)** had been established, an attempt was made to oxidise the aldehyde **(4.48)** to the carboxylic acid **(4.47)** using PDC (Scheme 4.40).

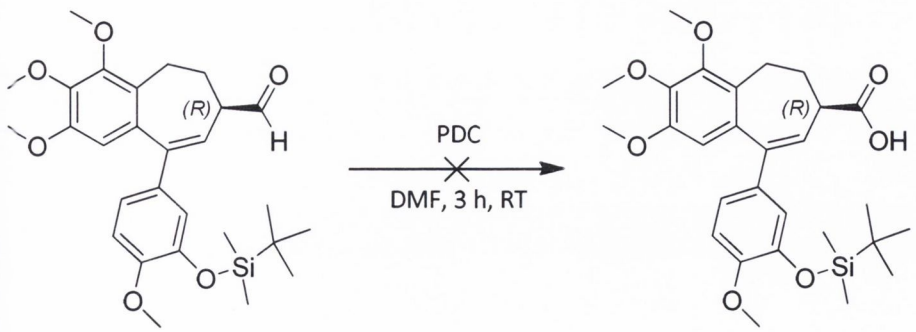

(4.48) **(4.47)**

Scheme 4.40 Attempted PDC oxidation of **(4.48)**

As mentioned previously, there was substantial evidence in the literature, that when the reaction was carried out in DMF, PDC was capable of oxidising primary alcohols to aldehydes and subsequently to carboxylic acids [190]. Therefore, the aldehyde **(4.48)** was dissolved in DMF and PDC was added. After 3 h, TLC analysis revealed the formation of a complex mixture of products. Therefore, this method was not pursued.

4.5.2.9 Attempted oxidation of aldehyde (4.48) using sodium chlorite and hydrogen peroxide

The facile oxidation of aldehydes to carboxylic acids under mild conditions using sodium chlorite and hydrogen peroxide has been described by Dalcanale *et al.* and Raach *et al.* [265-266]. A wide range of functional groups were reported to be tolerant of this oxidative system. However, as stated by Raach, there appeared to be a delicate balance of success and failure for the oxidation of olfenic aldehyde starting materials [266]. α,β-unsaturated aldehydes and double bonds said to be in conjugation with electron demanding substituents or another double bond, were reported to be readily and exclusively oxidised to their respective carboxylic acids [266]. Conversely, isolated double bonds were reported to be particularly sensitive to this reagent system, yielding chlorinated side products [265-266].

Sodium chlorite is reported to oxidise aldehydes under mild conditions according to Equation 4.1.



Equation 4.1 Oxidation of aldehyde with chlorite [265]

A significant limitation of this approach was the formation of the hypochlorite species and subsequent formation of chlorine dioxide (Equation 4.2).



Equation 4.2 Formation of chlorine dioxide [265]

Both the hypochlorite and chlorine dioxide species were implicated in undesirable side reactions involving addition and chlorination across the double bond [265-266]. Consequently, hydrogen

peroxide was added as a hypochlorite scavenger, to reduce the hypochlorite to largely inert by-products (Equation 4.3).

$$HOCl + H_2O_2 \longrightarrow HCl + O_2 + H_2O$$

Equation 4.3 Reaction of hydrogen peroxide with hypochlorite species [266]

Following the procedure outlined by Dalcanle *et al.*, the aldehyde **(4.48)** was dissolved in a mixture of acetonitrile and water (1:1). Hydrogen peroxide (30% aqueous solution) and sodium dihydgrogen phosphate were then added. The pH was adjusted to 4.3 [265]. A solution of sodium chlorite in water was then added dropwise to the reaction. After 1 h, the formation of a major product, together with a significant minor product of very similar R_f value, was observed by TLC. Following purification, the desired product was obtained as a mixture in poor yield (25%; Scheme 4.41).

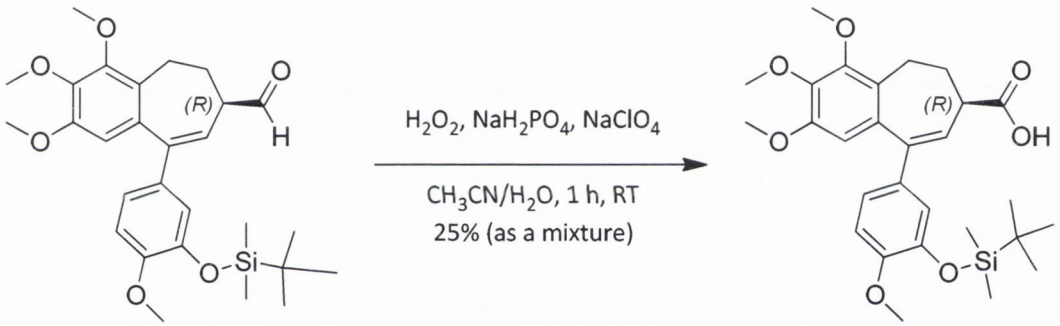

(4.48) **(4.47)**

Scheme 4.41 Sodium chlorite/hydrogen peroxide oxidation of aldehyde **(4.48)**

Mass spectrometry confirmed the presence of the desired carboxylic acid **(4.47)** in the mixture isolated from the reaction. The mass of the molecular ion peak $[M+H]^+$ obtained by mass spectrometry was in close agreement to the calculated mass (calculated 515.2465, found 515.2490). However, a secondary product was apparent on TLC with an almost equivalent R_f value. NMR analysis revealed that the secondary compound accounted for approximately one third of the total product isolated. Separation of this impurity was attempted by flash column chromatography. This ultimately proved futile, with only minute quantities of the desired material obtained in pure form following extensive purification. It was hypothesised that the impurity was a chlorination product formed following reaction of the hypochlorite or chlorine dioxide species

with the double bond. Therefore, an alternative hypochlorite scavenger was employed in an attempt to suppress this unwanted side-reaction.

4.5.2.10 Attempted oxidation of (4.48) using sodium chlorite and DMSO

DMSO has been employed as scavenger in cases where the reaction of the hypochlorite and related species with the substrate is deemed faster than the reaction with the hydrogen peroxide [265]. Therefore, the oxidation of the aldehyde **(4.48)** was attempted replacing the hydrogen peroxide with DMSO. The aldehyde was dissolved in a mixture of water and DMSO (1:1) and sodium dihydrogen phosphate was added. An aqueous solution of sodium chlorite was then added dropwise. After 3 h, TLC analysis indicated the formation of the desired product, together with a significant amount of purported chlorination product. Due to the difficulty in separating the impurity from the desired product, as outlined previously, no attempt was made to isolate the product.

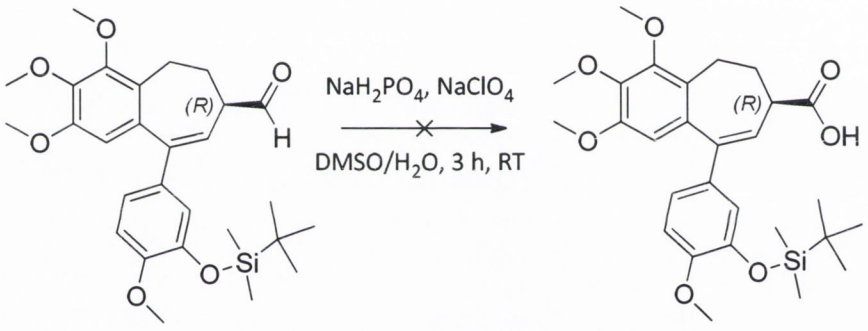

(4.48) **(4.47)**

Scheme 4.42 Attempted sodium chlorite-DMSO oxidation of aldehyde **(4.48)**

It was concluded that chlorination of the double bond could not be circumvented utilising either of the scavengers examined. The absence of exclusivity in the transformation, together with the disappointing yield, discouraged further exploration of this procedure. Therefore, an alternative methodology for the oxidation of the aldehyde was investigated.

4.5.2.11 Oxone oxidation of aldehyde (4.48)

Oxone® is a triple salt with molecular formula $KHSO_5 \cdot 0.5KHSO_4 \cdot 0.5K_2SO_4$. This reagent has achieved widespread use as an oxidising reagent for a wide variety of chemical transformations

due to its stability, ease of use and low cost [267]. The active constituent of oxone is potassium peroxymonosulfate (Scheme 4.43).

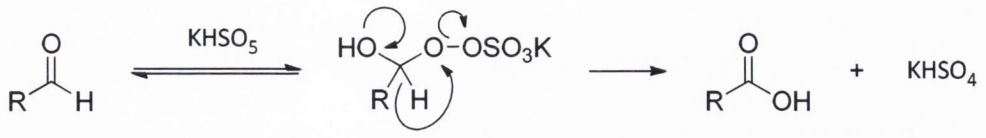

Scheme 4.43 Proposed mechanism for oxone oxidation of aldehyde to carboxylic acid [267]

Travis *et al.* have reported a procedure utilising oxone for the oxidation of aldehydes to carboxylic acids [267]. This procedure was reported to be tolerant of isolated double bonds (unlike the sodium chlorite based procedures outlined above) and was described as simple, effective and high yielding (Scheme 4.43). Following the procedure outlined by Travis *et al.*, the aldehyde **(4.48)** was dissolved in DMF and oxone was added [267]. After 2 h, the reaction was deemed to have gone to completion by TLC analysis. After purification, the desired product **(4.47)** was obtained as yellow resin in acceptable yield (54%; Scheme 4.44).

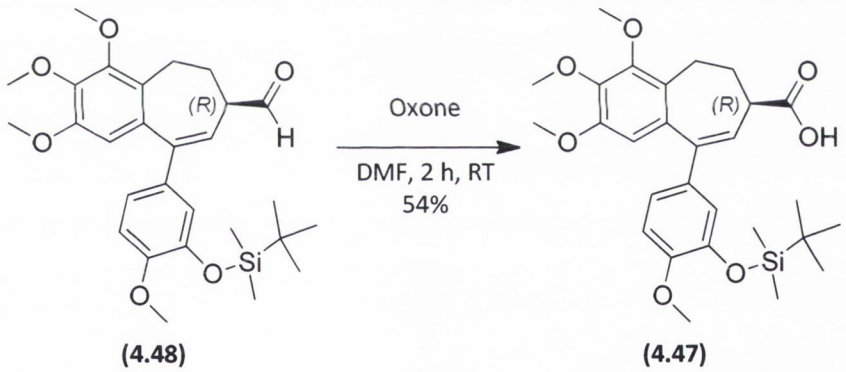

(4.48) **(4.47)**

Scheme 4.44 Oxone oxidation of aldehyde **(4.48)**

The facile and convenient nature of the reaction was particularly amenable to the scaling up required for such a long synthetic route. Efficient conversion of the aldehyde **(4.48)** to the carboxylic acid **(4.47)**, without the formation of undesirable side products, greatly simplified the isolation of the carboxylic acid.

4.5.2.12 Removal of the silyl protecting group of (4.47)

The *tert*-butyldimethylsilyl ether on the phenolic C-ring of **(4.47)** was readily removed by the addition of TBAF under anhydrous conditions. Following purification, the desired carboxylic acid **(4.43)** was obtained as a white solid in satisfactory yield (75%; Scheme 4.45).

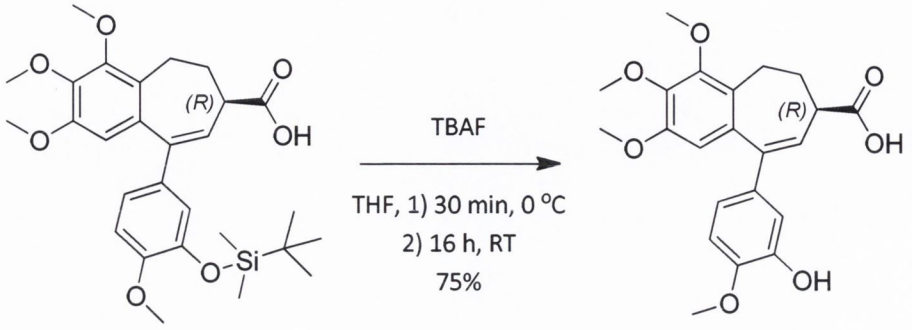

(4.47) **(4.43)**

Scheme 4.45 Removal of silyl protecting group on **(4.47)**

4.5.2.13 Characterisation of compound (4.43)

The carboxylic acid **(4.43)** was initially characterised by NMR spectroscopy. The four methoxy proton signals were immediately apparent at 3.72 ppm, 3.93 ppm, 3.94 ppm and 3.96 ppm. The double bond proton was found to resonate as a doublet (J = 6.66 Hz) at 6.51 ppm by reference to the HSQC spectrum (Figure 4.16). The four aromatic protons were found to correspond to the singlet at 6.40 ppm, the doublet (J = 8.46 Hz) at 6.82 ppm, the double doublet (J_1 = 8.46 Hz, J_2 = 2.05 Hz) at 6.86 ppm and the doublet (J = 2.05 Hz) at 6.93 ppm. Utilising the HSQC spectrum, the C-7 CH proton was found to resonate as a multiplet at 2.99-3.05 ppm. Similarly, the four aliphatic CH_2 proton signals were identified as three distinct multiplets at 2.27-2.39 ppm (2 x CH_2), 2.49-2.60 ppm and 3.11-3.16 ppm.

The two CH_2 carbons were readily identified from the DEPT 135 spectrum as corresponding to the signals at 22.81 ppm and 39.34 ppm (Figure 4.15). The DEPT 90 and HSQC spectra allowed ready assignment of the double bond CH carbon at 119.90 and the four aromatic CH carbons at 108.91 ppm, 110.32 ppm, 114.37 ppm and 119.90 ppm (Figure 4.15 and 4.16). The DEPT 135 spectrum then allowed ready identification of the four methoxy carbon signals at 56.02 ppm, 56.06 ppm, 60.90 ppm and 61.61 ppm. The C-7 CH carbon was identified utilising both the HSQC and DEPT 90 spectra as the signal at 42.72 ppm (Figure 4.15 and 4.16). The distinct signal at 180.43 ppm was

assigned to the carboxylic acid carbonyl carbon. The nine remaining quaternary carbons were then found to resonate at 127.28 ppm, 134.70 ppm, 135.22 ppm, 141.54 ppm, 141.99 ppm, 145.29 ppm, 146.31 ppm, 150.92 ppm and 151.41 ppm.

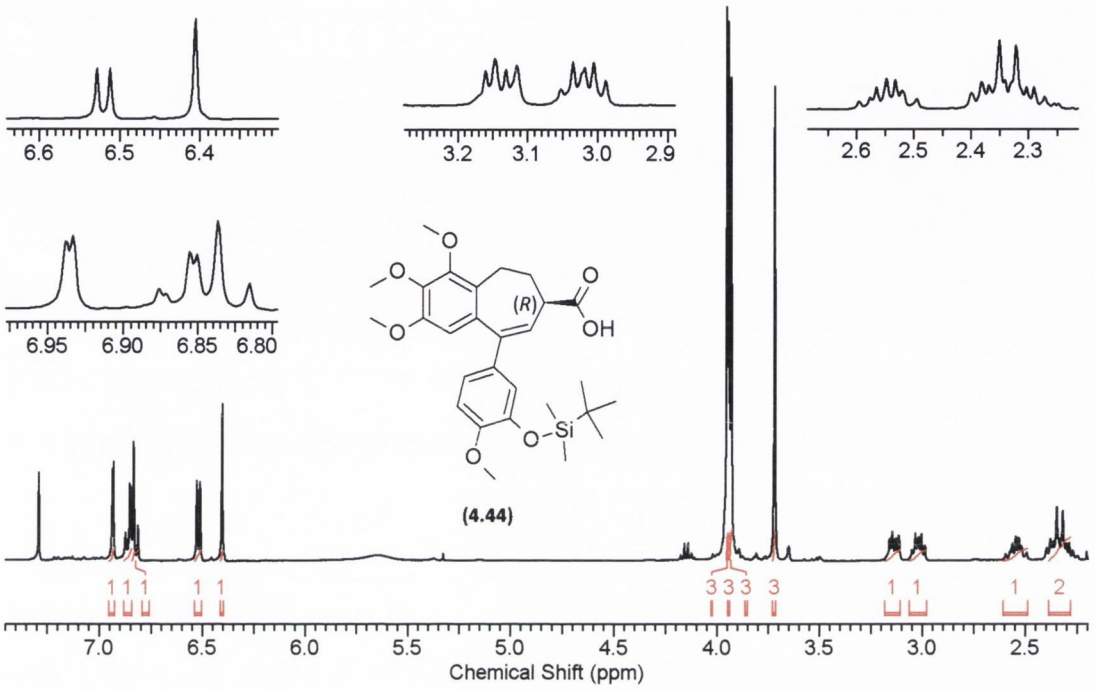

Figure 4.14 ^{1}H NMR spectrum of **(4.43)**

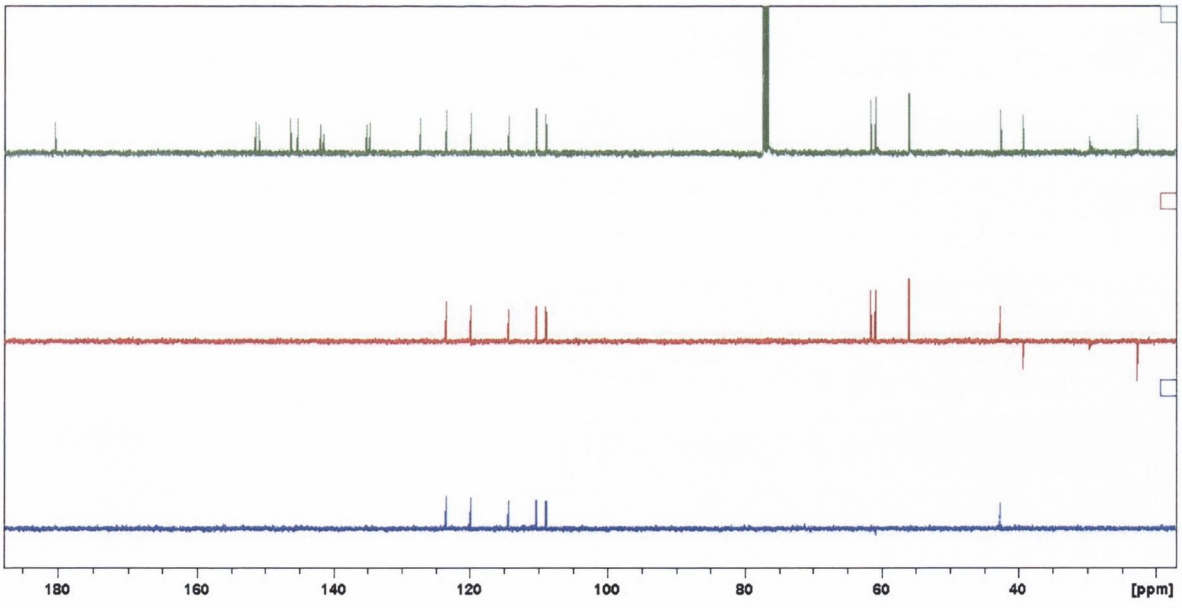

Figure 4.15 ^{13}C, DEPT 135 and DEPT 90 spectra of **(4.43)**

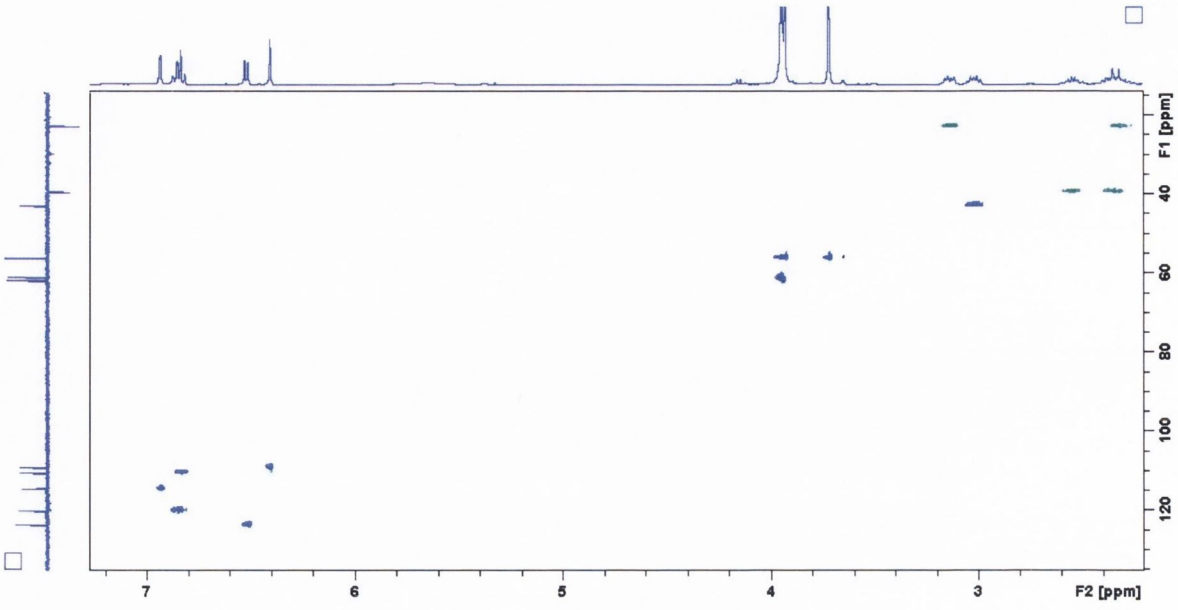

Figure 4.16 HSQC NMR spectrum of **(4.43)**

The identity of the product **(4.43)** was further confirmed by mass spectrometry. The molecular ion peak $[M+Na]^+$ was found to have a mass in close correlation with the calculated mass (found 515.2443, calculated 515.2465). Furthermore, the IR spectrum clearly indicated a carbonyl absorption peak at 1706.92 cm^{-1}, corresponding to the distinct carbonyl stretching absorption peak of a carboxylic acid. Once the identity of **(4.43)** had been confirmed, it was subject to biological evaluation (Section 4.6.3).

4.5.3 Synthesis of (*S*)-enantiomer carboxylic acid (4.44)

Once the synthetic methodology had been established for compound **(4.43)**, the (*S*)-enantiomer **(4.44)** was synthesised in an analogous fashion from related C-7 (*S*)-configuration intermediates.

4.5.3.1 Two-step oxidation of alcohol (4.42) to carboxylic acid (4.50)

In order to further optimise the methodology employed for the synthesis of the (*R*)-enantiomer, the Dess-Martin periodinane oxidation of the alcohol **(4.42)** and the subsequent oxidation of the aldehyde **(4.49)** by oxone, were carried out contiguously without purification of the intermediate aldehyde **(4.49)**. Following purification, the carboxylic acid **(4.50)** was isolated in excellent yield (85% over two steps; Scheme 4.46).

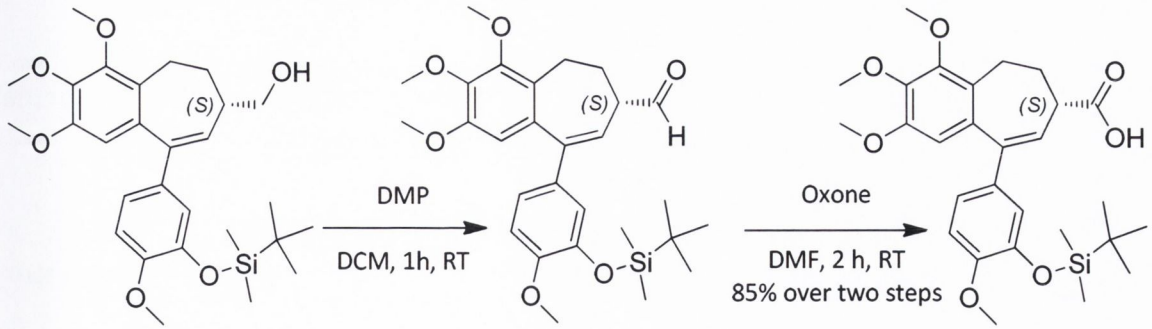

(4.42) **(4.49)** **(4.50)**

Scheme 4.46 Two-step oxidation of alcohol **(4.42)** to carboxylic acid **(4.50)**

A significant improvement in yield for the two step transformation from alcohol to carboxylic acid was obtained compared to that observed in the oxidation of **(4.46)** (85% v 44%). It was hypothesised that this was as a result of the rapid reaction of the aldehyde, before appreciable degradation of this unstable intermediate had occurred.

4.5.3.2 Silyl deprotection of compound (4.50)

The silyl protecting group of compound **(4.50)** was readily removed by the addition of TBAF in THF under anhydrous conditions. Following purification the desired carboxylic acid was isolated in excellent yield (87%) as an off-white solid **(4.44)** (Scheme 4.47).

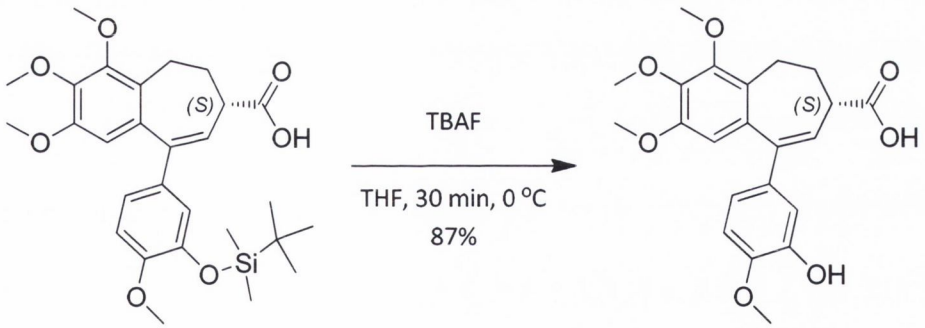

(4.50) **(4.44)**

Scheme 4.47 Silyl deprotection of compound **(4.44)**

Compound **(4.44)** was subsequently subject to biological evaluation (Section 4.6.3).

4.6 Biological Evaluation

The novel, stereochemically pure, tubulin inhibitors described in this chapter were tested for their antiproliferative activity in PC-3 cells using the MTT assay (Section 6.2).

4.6.1 MTT assay results for (4.01) and (4.12)

The (*R*)-configuration acetamide **(4.01)** and the methylene containing (*R*)-configuration acetamide analogue **(4.12)** were tested for antiproliferative activity (Table 4.1)

Compound	IC_{50} value (nM)
(4.01)	2130 ± 1.07
(4.12)	595.7 ± 1.06

Table 4.1 Best fit IC_{50} values ± SEM for compounds **(4.01)** and **(4.12)** following MTT assay in PC-3 cells (n = 3)

As expected from preliminary tubulin polymerisation inhibition data obtained by Hudson for the racemate of compound **(4.01)**, the acetamide was shown to be of moderate activity, with an IC_{50} value in the low μM range [188]. The methylene containing analogue **(4.12)** however, was found to have an IC_{50} value considerably lower, in the mid-nM range. This interesting result suggested that extension of the C-7 substituent could, in some cases, result in an improvement in pharmacological efficacy. It should be noted however, that both compound **(4.01)** and **(4.12)** were of (*R*)-configuration. It would appear from evaluation of both enantiomers of other C-7 position analogues, that the eutomer in each case tends to be of (*S*)-configuration. Therefore, it has been proposed that further improvements in the potency of both of these agents may be acchievable by the synthesis of their stereochemical antipodes.

4.6.2 MTT assay results for (4.23) and (4.24)

The (*R*) and (*S*) methylene containing C-7 alcohols **(4.23)** and **(4.24)** were tested for antiproliferative activity *in vitro* using PC-3 cells (Table 4.2).

Compound	IC_{50} value (nM)
(4.23)	516.2 ± 1.06
(4.24)	29.88 ± 1.18

Table 4.2 Best fit IC_{50} values ± SEM for compounds **(4.23)** and **(4.24)** following MTT assay in PC-3 cells (n = 3)

The (*S*)-enantiomer C-7 methylene alcohol **(4.24)** was shown to be substantially more active in the cell proliferation assay than its (*R*)-configuration counterpart **(4.23)**. The eudismic ratio of 17.28 obtained for these compounds further emphasised the importance of stereochemistry at the C-7 position for tubulin binding activity. Compound **(4.24)** exhibited an IC_{50} value comparable with that obtained for the C-7 alcohol **(3.01)** (29.88 ± 1.18 nM v 21.04 ± 1.18). This result provided further confirmation that the insertion of a methylene group at the C-7 position could result in tubulin inhibitors with comparable pharmacological activity. The potency of compound **(4.24)** was deemed of particular relevance to the future synthesis of molecular conjugates, given the proposed increased stability conferred by the additional methylene group.

4.6.3 MTT assay results for (4.43) and (4.44)

The biological activity of both the (*R*) and (*S*) configuration C-7 carboxylic acids **(4.43)** and **(4.44)** was also determined by assaying their antiproliferative activity in PC-3 cells (Table 4.3)

Compound	IC_{50} value (nM)
(4.43)	144.8 ± 1.11
(4.44)	144.4 ± 1.12

Table 4.3 Best fit IC_{50} values ± SEM for compounds **(4.43)** and **(4.44)** following MTT assay in PC-3 cells (n = 3)

The (*R*) and (*S*) configuration carboxylic acids **(4.43)** and **(4.44)** were both found to possess similar activity *in vitro*. Both compounds were found to possess IC_{50} values greater than the eutomers of the C-7 alcohol **(3.01)** and the methylene containing C-7 alcohol **(4.24)**. However, the compounds were still found to possess significant antiproliferative activity, with IC_{50} values an order of

magnitude less than the acetamides **(4.01)** and **(4.12)**. Therefore, it was suggested that either **(4.43)** or **(4.44)**, or perhaps even a racemic mixture of these agents, could be readily utilised in the synthesis of molecular conjugates by the attachment of additional bioactive compounds onto the C-7 carboxylic acid substituent.

4.7 Conclusions

The synthesis of the acetamide **(4.01)** in enantiomerically pure form was readily accomplished by combining the methodology for stereoselective synthesis, with a scheme devised by Hudson [188]. Compound **(4.01)** was found to possess significant antiproliferative activity in PC-3 cells. However, it was proposed that a further improvement in activity might be achievable if the (*S*)-enantiomer of this compound was synthesised.

The introduction of a nitrile group at the C-7 position, together with the use of the MOM protection strategy, devised previously, allowed convenient introduction of a methylene acetamide, a methylene alcohol and ultimately a carboxylic acid functional group into the tubulin inhibitory pharmacophore.

The methylene acetamide **(4.12)** was shown to possess an IC_{50} value considerably lower than that of the acetamide **(4.01)**. This result suggested that modification of the C-7 position still had the potential to increase the activity of the tubulin inhibitory pharmacophore. It was again suggested that the (*S*)-enantiomer of this compound might possess greater pharmacological activity.

The synthesis and evaluation of both the (*R*) and (*S*) enantiomers of the methylene containing C-7 alcohol, compounds **(4.23)** and **(4.24)**, served to further emphasise the importance of stereochemistry at the C-7 position for biological activity in these compounds. A eudismic ratio of 17.28 was found between the eutomer and distomer of this molecule. The potent antiproliferative activity of the (*S*)-enantiomer **(4.24)** was found to be comparable to that of the alcohol **(3.01)**. It was proposed that the increased stability offered by the additional methylene unit would be particularly important in the synthesis of robust molecular conjugates.

The synthesis of the C-7 carboxylic acid compounds **(4.43)** and **(4.44)** presented a particularly formidable synthetic challenge. While it was initially envisaged that simple oxidation of the primary alcohol precursors would allow facile synthesis of the desired carboxylic acid functional groups, a number of different strategies proved unsuccessful. Ultimately, a two step oxidation, utilising DMP and oxone, was required to carryout the desired transformation with acceptable chemoselectivity. The resultant carboxylic acid containing compounds **(4.43)** and **(4.44)** were found to possess significant antiproliferative activity. Interestingly, both enantiomers were possessed of roughly equivalent activity suggesting that the stereochemistry of these compounds was perhaps not as important as it appeared to be for other compounds in the series.

Overall, a synthetic methodology had been established for the stereoselective introduction of a variety of amine, alcohol and carboxylic acid functional groups at the C-7 position. In addition to contributing to the optimisation of the tubulin inhibitory pharmacophore, it was proposed that these functionally diverse compounds offered multiple opportunities for the synthesis of molecular conjugate drugs.

5 Chapter 5

5.0 Introduction

The work outlined in the preceding chapters described the various attempts made to maximise the potential of the novel tubulin inhibitory pharmacophore both as a drug entity and also as component of a molecular conjugate. The analogues containing diverse functionalities on the C-ring or C-7 position were designed to facilitate the synthesis of conjugate drugs. It was envisaged that the analogues would retain the core tubulin inhibitory activity of the lead compounds but would offer additional opportunities for molecular conjugation. Two types of conjugate drugs utilising these tuneable molecular conjugation sites were contemplated. Firstly, conjugates containing a homing moiety to increase the selectivity of the active principal and secondly, conjugates containing a complimentary pharmacophore, to offer dual biological activity.

5.0.1 Conjugates containing a homing moiety

An exhaustive assessment of the arguments for and against molecular conjugation to a homing moiety to improve the *in vivo* performance of a tubulin inhibitor was presented in the literature review in chapter one. Furthermore, the synthesis of conjugates containing the tubulin inhibitors described in this thesis is being actively explored within the Walsh group.

5.0.2 Conjugates containing a complimentary pharmacophore

A comprehensive review of tubulin targeting hybrid drugs has previously been conducted by Breen and Walsh [268]. This review outlined the various advantages and disadvantages of various multi-target conjugates containing a tubulin inhibitor component. G. Hudson synthesised a number of such conjugates as part of the work conducted for her doctoral thesis [188]. These conjugates consisted of a tubulin inhibitor attached to the aminopeptidase N (APN) inhibitor bestatin. Furthermore, as part of the work conducted for her doctoral thesis, E. Breen synthesised a number of conjugates of **(2.03)**, **(2.25)** and **(3.01)** with the aminopeptidase N (APN) inhibitor bestatin, in order to obtain molecules with dual biological activity (Figure 5.1) [213].

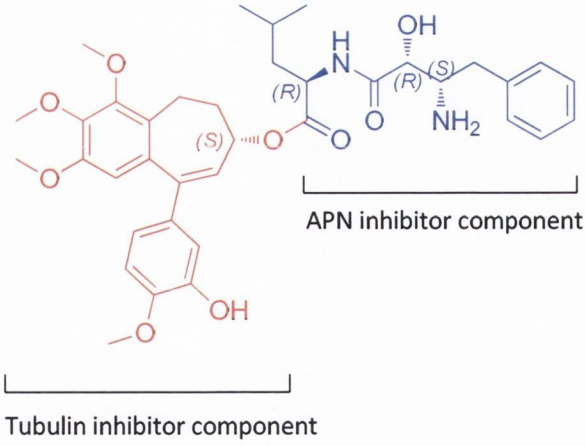

Figure 5.1 Compound **(5.01)**: Conjugate of tubulin inhibitor **(3.01)** and bestatin **(5.02)**

Thus, the design and synthesis of dual inhibitors of tubulin polymerisation and APN activity had received considerable attention by previous members of the Walsh group. Therefore, it was proposed to utilise this experience and focus on the optimisation of this dual target approach. However, it was suggested that the synthesis of a compound with dual tubulin polymerisation/APN inhibition activity could be realised without the need for molecular conjugation.

5.0.3 Aminopeptidase N inhibition as a complimentary target for dual acting compounds

Aminopeptidase N (APN; EC 3.4.11.2 also known as CD13, microsomal aminopeptidase, aminopeptidase M and alanine aminopeptidase) is a zinc-dependent, membrane-bound ectopeptidase with ubiquitous expression throughout a whole host of human organs, tissues and cell types [269]. APN is said to be a multi-functional protein, with enzymatic activity being but one of many aspects of its biological significance. Physiologically, APN is reported to be implicated in antigen presentation, cholesterol uptake, cell signalling and modulation of immune system processes [270]. APN is expressed in the renal and intestinal epithelia, in certain neurons and in monocytes and macrophages [270]. It is also reported to be expressed in endothelial cells, with its expression reportedly significantly upregulated in activated or angiogenic endothelial cells [270]. APN is also found to be essential for the development and progression of malignancy.

APN activity is associated with tumour cell proliferation, differentiation, apoptosis, invasion, motility and angiogenesis [269-270]. Crucially, expression of APN has been reported to be far

higher in angiogenic vasculature than resting vasculature [271]. Furthermore, APN has been shown to be of functional importance in immature vasculature and inhibition of its activity has been reported to suppress both angiogenesis and tumour growth [271]. *In vivo* studies in animals have demonstrated that treatment with APN inhibitors significantly impaired retinal and chorioallantoic angiogenesis as well as xenograft tumour growth [269]. *Ex vivo* studies carried out on vascular endothelial cells also demonstrated that APN inhibitors interfered with tube formation but had no effect on endothelial cell proliferation [272]. Increased APN expression has also been observed in a number of cancer cell types including breast, ovarian, colon and thyroid cancer cells [273-276].

N-[(2*S*,3*R*)-3-Amino-2-hydroxy-4-phenylbutyryl]-L-leucine or bestatin **(5.01)** is a dipeptide originally isolated from a culture filtrate of *Streptomyces olivoreticuli* [277]. Bestatin has been shown to exhibit potent APN inhibition and has been extensively evaluated as an anticancer agent in a wide variety of haematological malignancies and solid tumour types [269]. The efficacy of this agent either alone or in combination with established chemotherapeutic regimens has been demonstrated in acute myeloid leukaemia, lymphoma, carcinoma of the head and neck, bladder, stomach, lung, oesophageal and skin cancers [269].

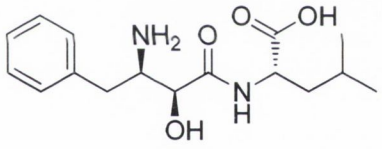

Figure 5.2 Structure of bestatin **(5.02)**

Tosedostat is another novel zinc metalloprotease inhibitor. Upon intracellular activation, Tosedostat inhibits a whole host of intracellular proteases including aminopeptidase N [278]. It has demonstrated antiproliferative activity against a number of tumour cell types both *in vitro* [278-279] and *in vivo* and is currently undergoing clinical evaluation in the adjunctive treatment of various haematological and solid tumour malignancies [278].

The natural product curcumin has also displayed potent APN inhibition. Originally isolated from the rhizome of *Curcuma longa* (turmeric), this phenolic compound has been shown to inhibit angiogenesis by virtue of its role as an irreversible APN inhibitor [280].

A number of other APN inhibitors are also reported to be at various stages of preclinical and clinical evaluation [281]. Thus, APN inhibition as a desirable target for cancer chemotherapy appears to be in the midst of a renaissance.

5.0.4 Disadvantages of the molecular conjugation drug design paradigm

As outlined previously, Breen synthesised a number of bestatin conjugates containing the tubulin inhibitors described in the preceding chapters [213]. These compounds showed considerable activity, both *in vitro* and *in vivo,* against the human prostate cancer cell line PC-3. PC-3 cells are known to express high levels of APN and form highly vascularised tumours in xenograft tumour models [282]. Therefore, the positive results obtained from the evaluation of these conjugates provided significant encouragement to the dual target approach. However, dual targeting compounds are also possessed of a number of significant disadvantages.

Lipinski's rule of 5 has often been quoted as a reliable predictor of drug candidates potential solubility or permeability difficulties, two factors which can significantly impede a drug candidates progression to the next stage of pre-clinical evaluation [283].

Lipinski's rule of 5 predicts that poor absorption or permeation of a drug in a biological setting is likely if a compound has:

- More than 5-H bond donors
- More than 10 H-bond acceptors
- A molecular weight greater than 500
- A calculated Log P greater than 5

While compounds of the type shown in Figure 5.1 have exhibited significant pharmacological activity as antitumour agents, a number of the parameters of the conjugate are in violation of Lipinski's rule of 5 [283].

For example, compound **(5.01)** was found to have 11 H-bond acceptors and a molecular weight of 661.7844 thus violating Lipinski's rule of 5 on two accounts and suggesting that the compound may experience absorption and distribution issues *in vivo*.

Cognisant of the inherent disadvantages of the high molecular weight conjugates outlined above, an alternative approach to increasing the pharmacological range of the novel tubulin inhibitors synthesised was explored.

5.0.5 Hydroxamic acid containing APN inhibitors

Many metallo-enzyme inhibitors currently under evaluation contain a hydroxamic acid functionality. This functional group is known to have a high chelating power to bind to the zinc ion present in the active site of the enzymes [284-285]. Conversely, a number of metallo-enzyme inhibitors containing a hydroxamic acid functionality are at an advanced stage of clinical evaluation.

Prinomastat is a potent mixed inhibitor of a number of matrix-metalloproteases (MMP's) and is currently being evaluated for its effects in inhibiting tumour growth and angiogenesis [286]. Trocade is another hydroxamic acid containing drug at an advanced stage of evaluation. It is a potent and selective inhibitor of MMP 1, 8 and 13 and is currently under investigation as a therapeutic agent for the prevention of joint damage in patients with rheumatoid arthritis [287]. The histone deacetylase inhibitor suberoylanilide hydroxamic acid (SAHA, Vorinostat) is currently in clinical use for the treatment of cutaneous T-cell lymphoma [288]. The progress of these agents to clinical evaluation provides evidence for the potential of hydroxamic acid containing compounds as clinically useful agents.

A number of APN inhibitors containing a hydroxamic acid functional groups within their structures are also currently in various stages of development. The hydroxamic acid compounds investigated by Wang *et al.* displayed potent and selective inhibition of APN and APN expressing cell lines *in vitro*. The most active compound in the series is shown in Figure 5.3 [289].

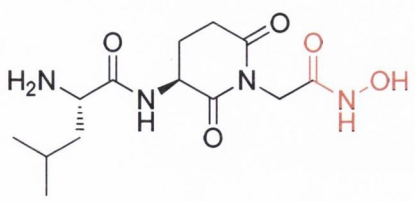

Figure 5.3 APN inhibitor **(5.03)** synthesised by Wang *et al.* [289] (hydroxamic acid functionality highlighted in red)

Furthermore, the related novel antiangiogenic and antiproliferative APN inhibitor **(5.04)** evaluated by Inagaki *et al.* was also found to contain a hydroxamic acid functionality [290].

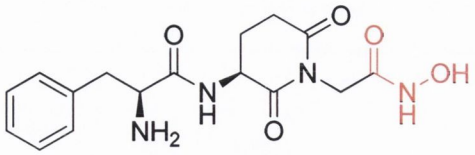

Figure 5.4 APN inhibitor **(5.04)** evaluated by Inagaki *et al.* [290]

A library of 217 hydroxamic acid containing compounds was synthesised by Flipo *et al.* and screened for APN inhibitory activity [284]. A number of these compounds were shown to potently inhibit APN *in vitro* with IC_{50} values as low as 82 nM.

The encouraging clinical development of these hydroxamic acid compounds, together with the development of hydroxamic acid containing APN inhibitors, suggested that this functional group could provide the desired pharmacological diversity to the existing tubulin inhibitor compounds.

5.0.6 Designed multiple ligands

In an attempt to overcome the perceived limitations of molecular conjugation as a drug design approach, a designed multiple ligand (DML) was envisaged. This dual inhibitor was designed to utilise the scaffold of the tubulin inhibitor pharmacophore, to which an aminopeptidase N inhibitor component would be anchored. The tubulin inhibitor scaffold was proposed to consist of the novel pharmacophore first devised by Shah [187]. It was then hypothesised that functionalisation of the C-7 position on the B-ring would permit the attachment of a hydroxamic acid functional group to afford the compound with APN inhibitory activity. It was proposed that the design of the DML would afford a compound with dual biological activity at least equivalent to the conjugate drugs synthesised previously, but with superior physicochemical characteristics. The structure of the proposed DML **(5.05)** is shown in Figure 5.5.

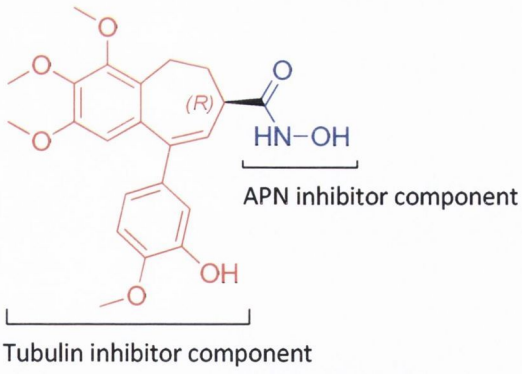

Figure 5.5 Structure of proposed DML compound **(5.05)** (tubulin inhibitor scaffold shown in red; hydroxamic acid shown in blue)

5.1 Aims and objectives

The principal objective of the work described in this chapter was the synthesis of a small molecule DML which would possess both tubulin polymerisation and APN inhibition activity. Initially, it was envisaged that compound **(5.05)** would fulfil that objective. However, following the difficulties encountered in its production, the design and synthesis of an alternative DML became the main priority. Once this objective had been achieved, it was then necessary to determine the biological activity of the DML. Evaluation of the compound in an assay suitable to determine APN inhibitory activity was deemed essential. Similarly, it was deemed of integral importance to demonstrate that the DML retained the antiproliferative activity of the parent compounds by determining its activity *in vitro*. In the course of the synthesis of the DML, a number of novel intermediates with diverse functionality on the C-7 side chain were synthesised. The biological evaluation of these compounds became a welcome ancillary objective to the work to be undertaken.

5.2 Attempted synthesis of (5.05)

Initial attempts to synthesise a DML possessing the desired dual inhibitor structure focused on the synthesis of compound **(5.05)**.

5.2.1 Synthetic strategy

The approach utilised in the attempted synthesis of **(5.05)** relied upon the derivatisation of existing intermediates. It was envisaged that the phenol protected carboxylic acid containing

intermediate **(4.47)** could be activated as a PFP ester. This activated ester could then be reacted with hydroxylamine to yield the desired hydroxamic acid group.

5.2.2 Synthesis of pentafluorophenyl ester of (4.47)

The synthesis of the proposed hydroxamic acid containing DML compound **(5.05)** began with the common intermediate carboxylic acid **(4.47)**. The acid was activated by the formation of a PFP ester. The acid was dissolved in dry DCM and pentafluorophenol and the coupling reagent DCC were added under anhydrous conditions at 0 °C. After 4 h, the reaction was deemed to have gone to completion by TLC. Following purification, the PFP ester compound **(5.06)** was isolated in good yield (83%) as a yellow oil.

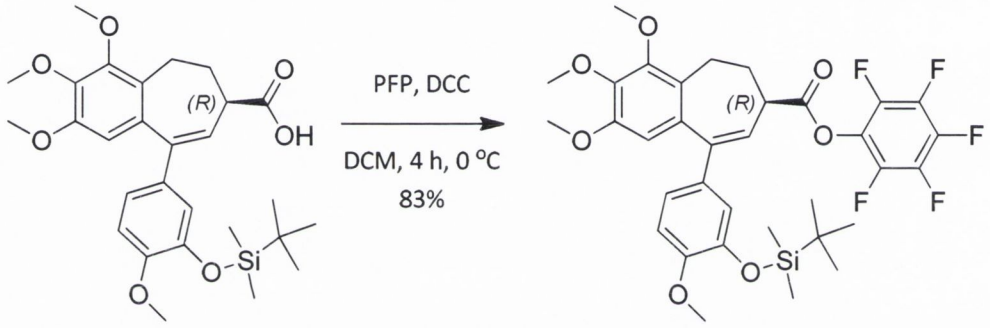

(4.47) **(5.06)**

Scheme 5.1 Synthesis of pentafluorophenyl ester of **(4.47)**

5.2.3 Displacement of PFP ester of (5.06) with hydroxylamine

The activated PFP ester **(5.06)** was dissolved in DMF and DIPEA was added. Hydroxylamine hydrochloride was then added to the reaction. After 20 min, consumption of the starting material was observed by TLC. A single spot was apparent by TLC analysis suggesting that exclusive conversion to the desired product had been achieved. Following purification by silica gel flash column chromatography, compound **(5.07)** was obtained in moderate yield (65%; Scheme 5.2).

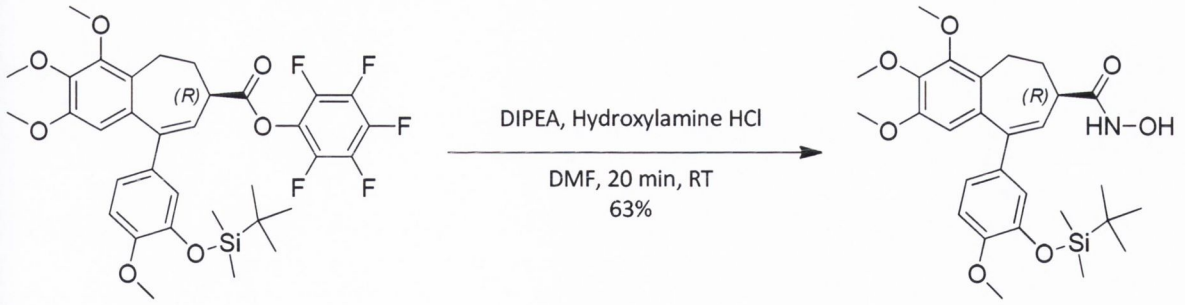

(5.06) (5.07)

Scheme 5.2 Displacement of PFP ester **(5.06)** with hydroxylamine

The compound was placed under high vacuum to remove residual solvent traces in preparation for NMR analysis. Mass spectrometry of the compound was also undertaken.

The mass spectrometry analysis was conducted promptly and confirmed the formation of the desired compound **(5.07)**. The molecular ion peak $[M+Na]^+$ was found to have a mass which agreed closely with the calculated mass (calculated mass 552.2393, found 552.2377). After 24 h, the dry sample was re-examined in preparation for NMR analysis. TLC analysis revealed that compound **(5.07)** had completely degraded into several unknown substances. The reaction was repeated, this time taking particular care to protect the pure product isolated from light and heat. However, disappointingly, after 24 h, none of the product of interest was found to remain intact.

The relatively poor stability of the hydroxamic acid functional group has previously been reported in the literature. This group has been shown to undergo hydrolysis and reduction reactions under certain conditions [285].

In the case of compound **(5.07)**, it was hypothesised that the push towards greater conjugation throughout the system acted as the driving force for the instability of the molecule. The formation of a double bond at the C-7 position would result in conjugation throughout the system. The elimination of the hydroxamic acid and formation of this double bond was thus proposed as the root cause of instability within the molecule. A number of the potential mechanisms for the formation of this double bond and elimination of the hydroxamic acid group are outlined in Figure 5.6.

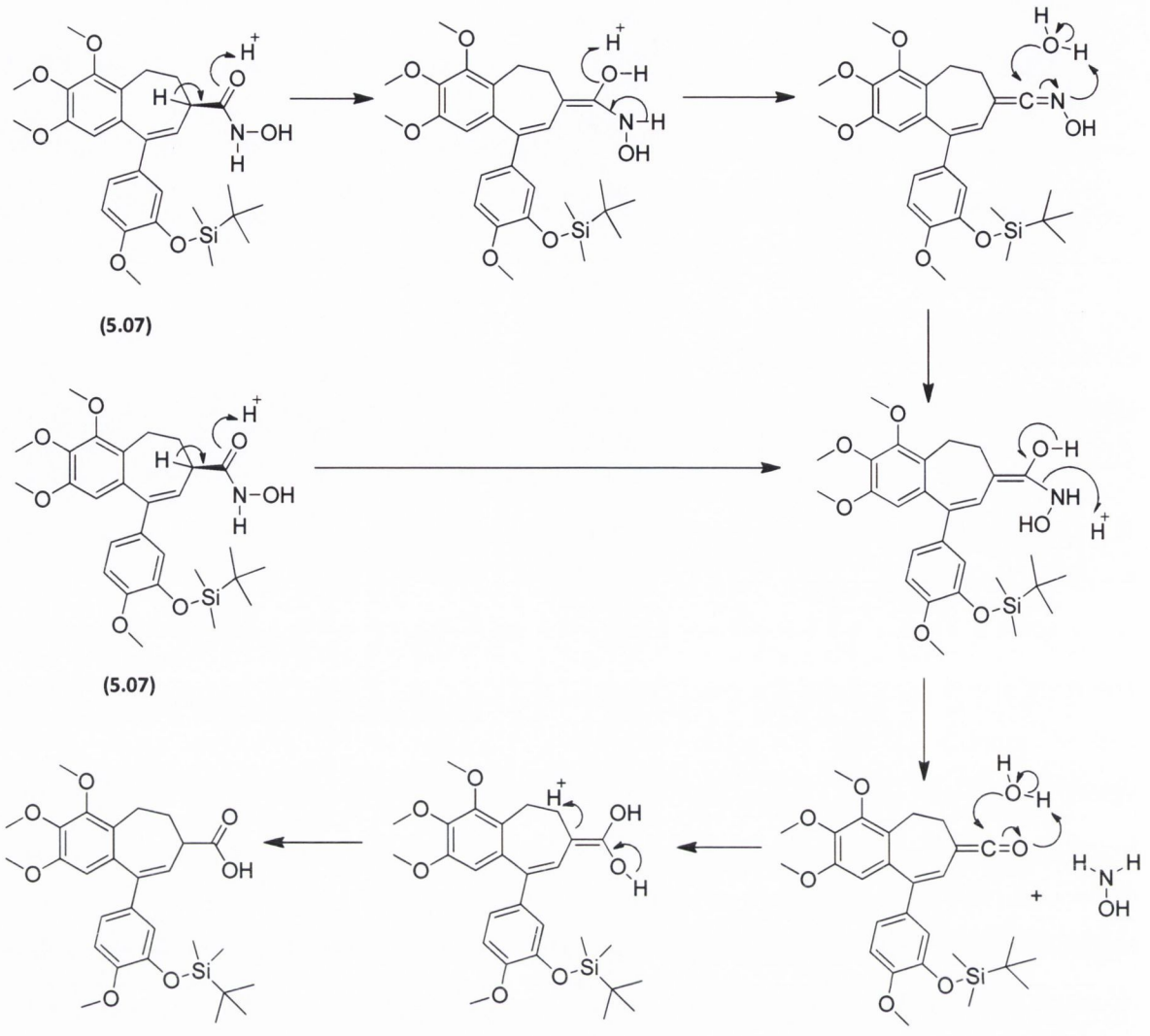

Figure 5.6 Proposed mechanisms for the instability of **(5.07)**

It was hypothesised that the synthesis of an analogue of **(5.05)**, containing an additional inert linker group between the hydroxamic acid and the double bond at the C-8 position, would result in a molecule with improved stability.

5.3 Attempted synthesis of ether containing hydroxamic acid compound

It was hypothesised that a compound containing an ether group in the C-7 position side chain would permit the introduction of a terminal hydroxamic acid group. It was hypothesised that the presence of the ether linkage would abrogate the drive for further conjugation deemed to be responsible for the instability of **(5.07)**. The proposed ether containing compound **(5.08)** is shown in Figure 5.7.

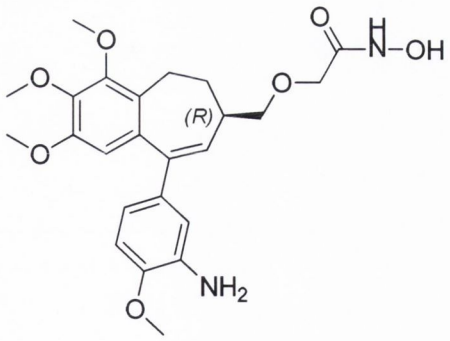

Figure 5.7 Proposed ether containing hydroxamic acid compound **(5.08)**

5.3.1 Synthetic strategy

A number of derivatives of the tubulin inhibitors described in chapter 4, containing an aniline functional group, were synthesised in order to demonstrate the tuneable nature of the synthetic approach. The synthetic strategy employed was to react the methylene alcohol of one such analogue with a suitable ester-containing alkylating reagent. It was hypothesised that once the ether linkage had been formed, convenient hydrolysis of the ester and activation of the resulting acid would allow the desired hydroxamic acid group to be introduced by a displacement reaction with hydroxylamine.

5.3.2 Suzuki coupling of enol triflate (4.31) and boronic ester (2.33)

The intermediates **(4.31)** and **(2.33)** were coupled using standard Suzuki coupling conditions. Both compounds were dissolved in a mixture of toluene, ethanol and water (3:1:1). Potassium carbonate was added as base. The palladium based catalyst $Pd(Ph_3)_4$ was also added. The reaction was then heated for 1.5 h at 70 °C. TLC monitoring of the reaction proved particularly difficult as the boronic ester **(2.33)** was found to have an identical R_f value to the desired product **(5.09)**. As a result, a certain degree of trial and error was involved in optimising the reaction time necessary to achieve optimal conversion. The reaction did not go to completion under any of the reaction conditions employed. Following flash column chromatography, compound **(5.09)** was isolated as a mixture with the boronic ester **(2.33)** in modest yield (53%). Compound **(5.09)** was then carried forward to the next reaction without further purification (Scheme 5.3).

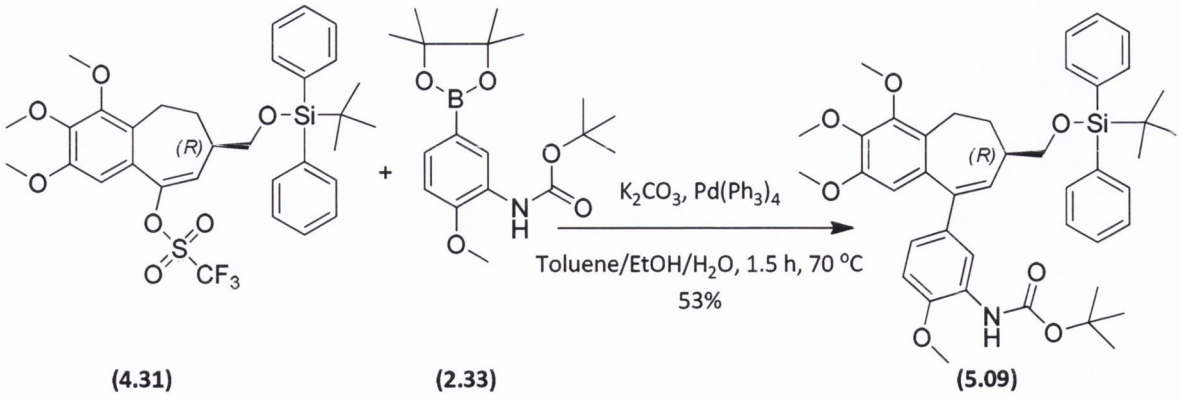

(4.31) **(2.33)** **(5.09)**

Scheme 5.3 Suzuki coupling of enol triflate **(4.31)** and boronic ester **(2.33)**

5.3.3 Removal of silyl protecting group on (5.09)

The crude mixture containing **(5.09)** was dissolved in THF and TBAF was added under anhydrous conditions. After 5.5 h, the reaction was deemed to have gone to completion and following purification the desired product **(5.10)** was isolated in poor yield (29%) as a yellow oil (Scheme 5.4).

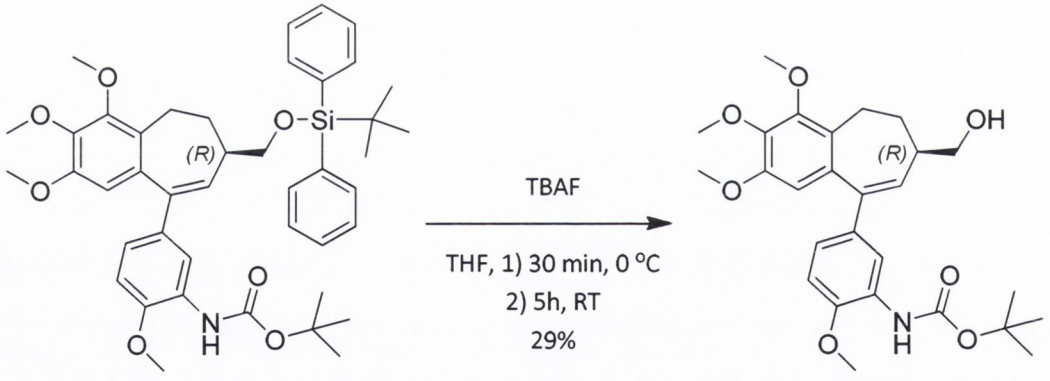

(5.09) **(5.10)**

Scheme 5.4 Removal of silyl group on compound **(5.09)**

5.3.4 Attempted O-alkylation of compound (5.10)

The key reaction in the synthesis of **(5.08)** was deemed to be the formation of an ether linkage by the O-alkylation of the free alcohol group on compound **(5.10)**. As outlined previously, it was hypothesised that this ether group would negate the possibility of increased conjugation, through

chemical rearrangement, thought to be responsible for the instability of compound **(5.07)**. Compound **(5.10)** was dissolved in THF and sodium hydride was slowly added under anhydrous conditions at 0 °C as a suspension in THF. Ethyl bromoacetate was then added and the reaction was left stirring for 16 h. TLC analysis suggested the formation of one principal product together with negligible amounts of a further three compounds. Mass spectrometry of a sample of the crude reaction mixture suggested the formation of the product of interest **(5.11)**. Therefore, the principal product was isolated by flash column chromatography in good yield (82%). Further analysis subsequently revealed that this compound was in fact **(5.12)** (Scheme 5.5).

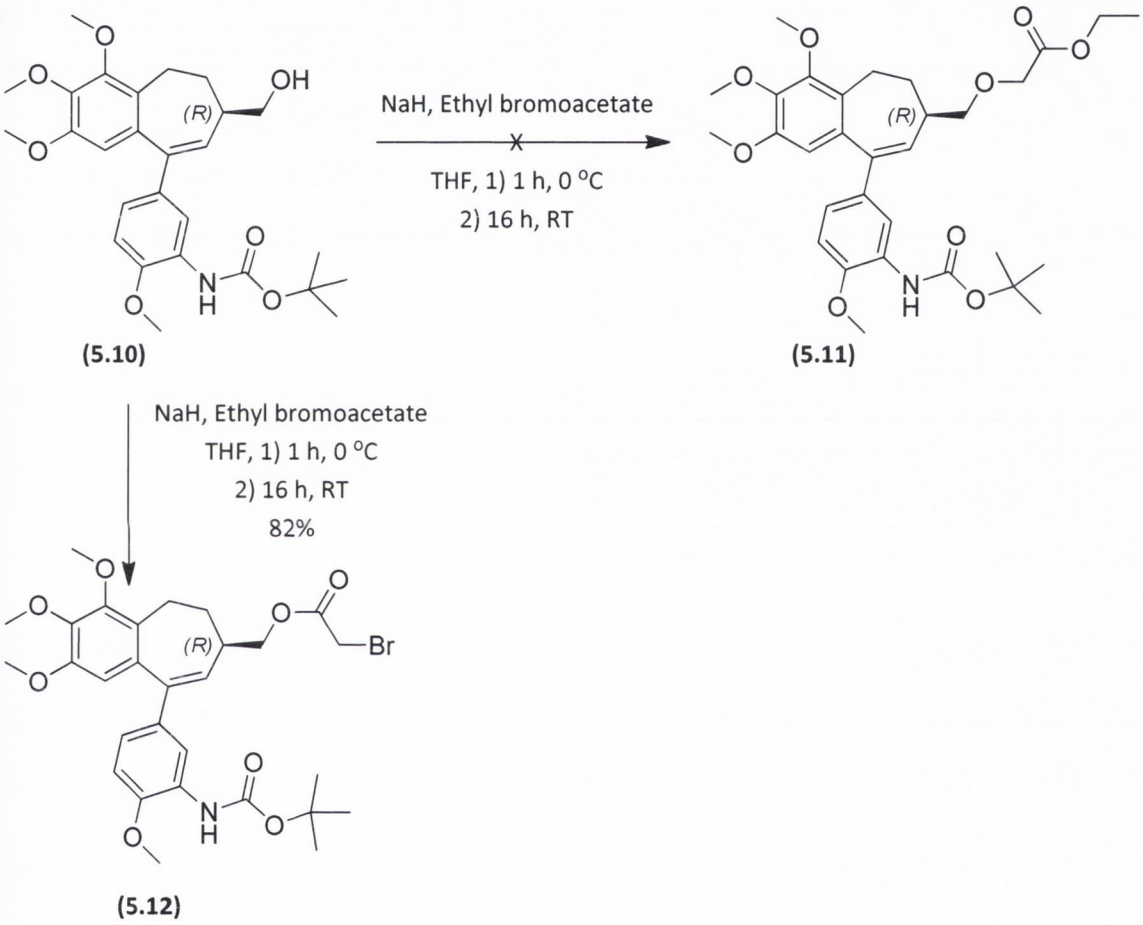

Scheme 5.5 Attempted O-alkylation of compound **(5.10)**

5.3.4.1 Characterisation of compound (5.12)

NMR analysis was used to confirm the identity of the principal product as compound **(5.12)**. The distinctive singlet resonating furthest upfield at 1.53 ppm was readily identified as corresponding to the methyl protons of the BOC group. The methoxy group protons were found to resonate as

four singlets at 3.72 ppm, 3.90 ppm, 3.93 ppm and 3.95 ppm. The double bond proton was found to correspond to a multiplet at 2.39-2.45 ppm by reference to the HSQC spectrum (Figure 5.11). The eight distinct CH_2 protons expected to be found within the molecule were identified as seven distinct multiplets at 1.92-2.00 ppm, 2.18-2.26 ppm, 2.29-2.36 ppm, 3.08-3.12 ppm, 3.91-3.92 ppm (2 x CH_2), 4.19-4.24 ppm and 4.25-4.32 ppm using the HSQC spectrum. The four expected aromatic protons were found to resonate at 6.41 ppm, 6.79 ppm (2 x ArH) and 7.08 ppm.

Analysis of the DEPT 135 spectrum readily revealed the presence of the four expected CH_2 signals at 23.13 ppm, 25.94 ppm, 38.14 ppm and 69.08 ppm (Figure 5.9). Similarly, the four methoxy carbon signals were identified at 55.77 ppm, 56.07 ppm, 60.87 ppm and 61.56 ppm. The C-7 CH carbon was found to correspond to a signal at 36.50 ppm by reference to the DEPT 90 spectrum (Figure 5.9). The BOC group methyl carbons were found to resonate at 28.38 ppm. The double bond CH carbon was identified, using the HSQC data, as corresponding to the signal at 127.32 ppm (Figure 5.11). The four aromatic CH carbons were clearly observed on the DEPT 90 spectrum and identified as resonating at 109.08 ppm, 109.46 ppm, 117.72 ppm and 122.41 ppm (Figure 5.9). The *tert*-butyl group quaternary carbon signal proved elusive due to its resonance position overlapping with the residual chloroform signals at approximately 77 ppm. The carbon was eventually found to resonate at 77.24 ppm (Figure 5.10). The remaining eleven quaternary carbon signals were found to resonate at 126.32 ppm, 127.87 ppm, 127.92 ppm, 135.93 ppm, 137.90 ppm, 141.40 ppm, 142.47 ppm, 147.20 ppm, 150.81 ppm, 167.49 ppm and 170.7 ppm.

The identity of **(5.12)** was further confirmed by mass spectrometry. The molecular ion peak $[M+H]^+$ was found to have a mass of 628.1577, which was in close agreement with the calculated mass of 628.1522.

It became apparent that the use of the strong base, sodium hydride had formed the alkoxide ion of the alcohol **(5.10)**. This anion nucleophile then preferentially attacked the electron deficient carbonyl of ethyl bromoacetate rather than the bromide carbon. This resulted in a transesterification reaction product rather than the desired O-alkylation product **(5.11)**. Following the failure of this approach, an alternative strategy was investigated.

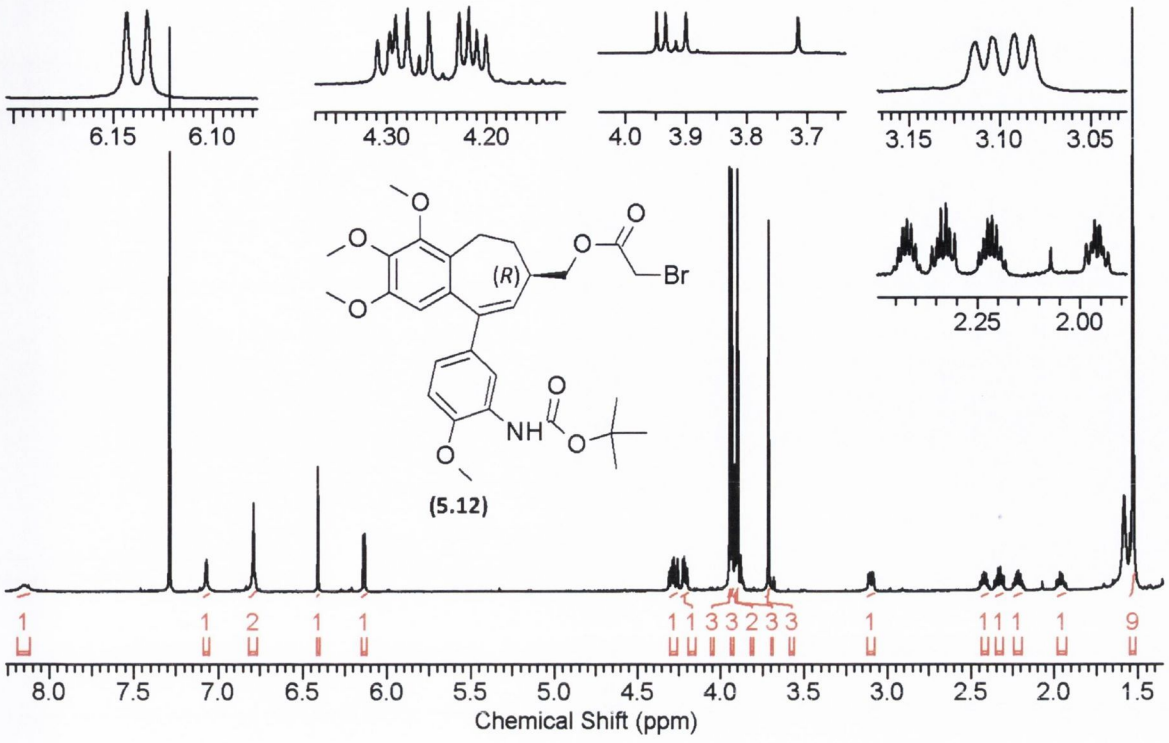

Figure 5.8 ^{1}H NMR spectrum of **(5.12)**

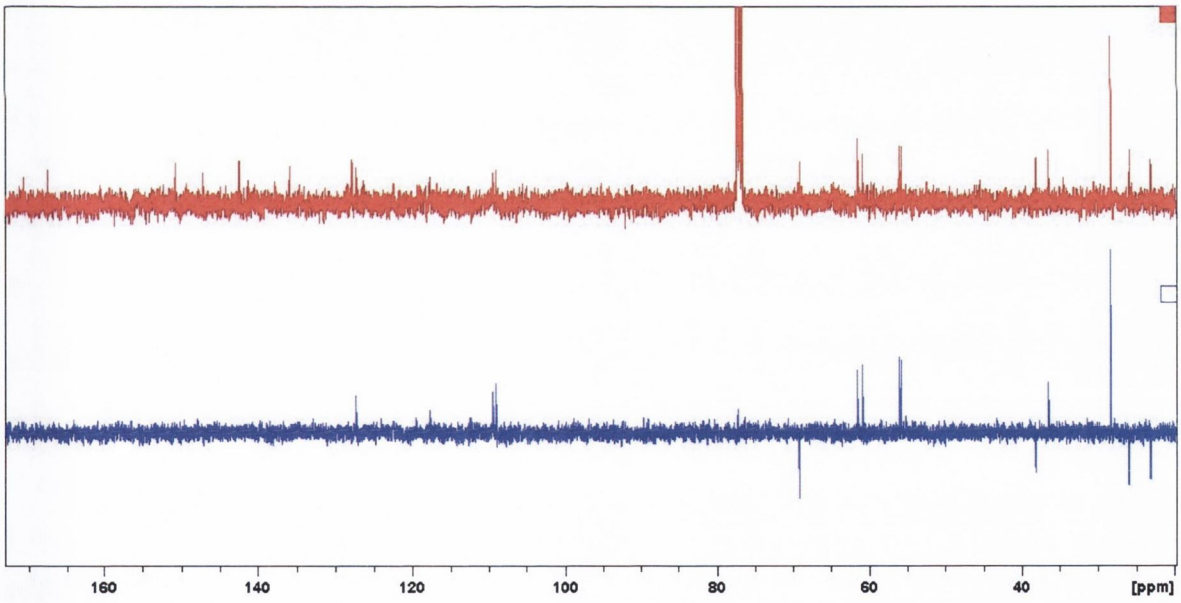

Figure 5.9 ^{13}C and DEPT 135 NMR spectrum of **(5.12)**

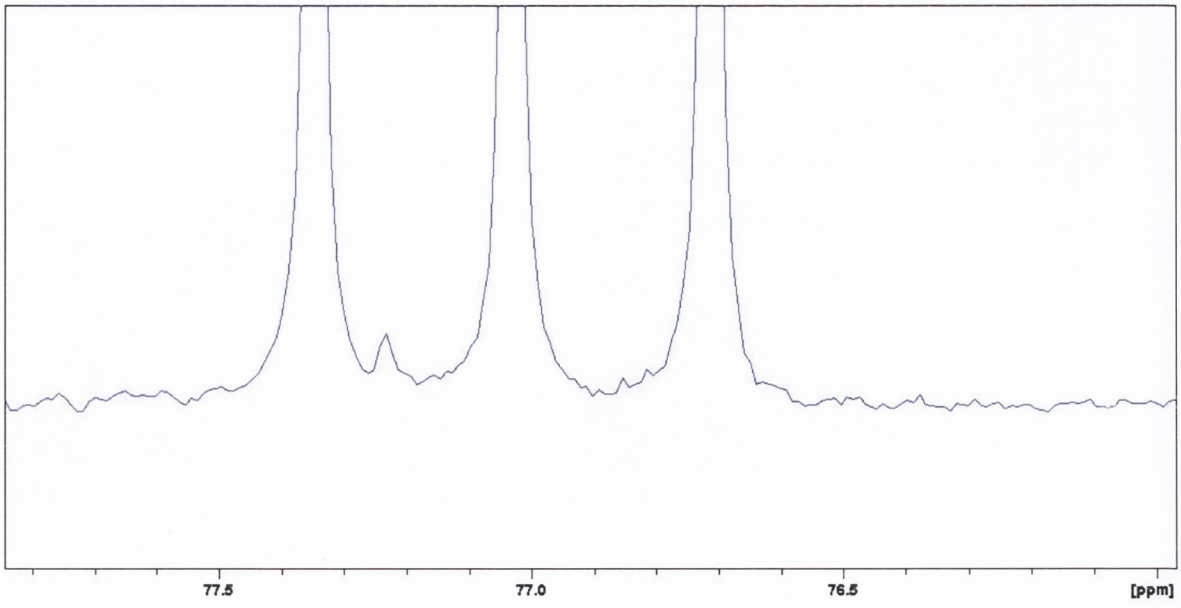

Figure 5.10 Expansion of ^{13}C spectrum of **(5.12)** from 76-78 ppm

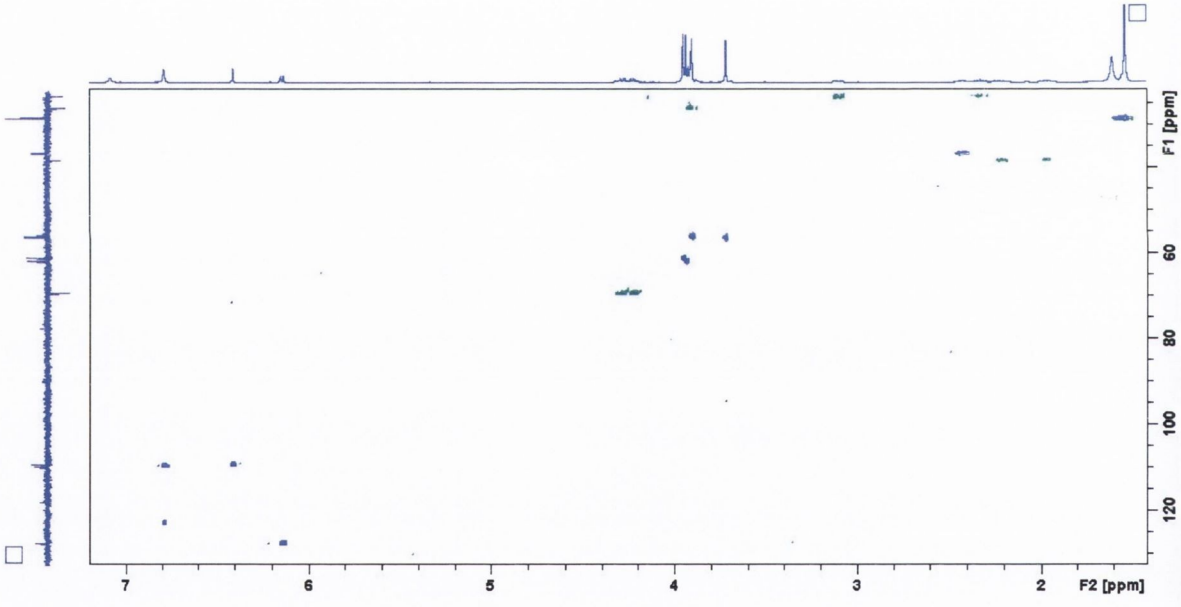

Figure 5.11 HSQC NMR spectrum of **(5.12)**

5.4 Synthesis of methylene containing hydroxamic acid compound (5.13)

It was proposed to synthesise a molecule containing an inert methylene linker unit between the C-7 position and the hydroxamic acid side chain (Figure 5.12). It was posited that the additional

methylene group would ensure that rearrangements, of the kind hypothesised to have taken place in the case of compound **(5.08)** (Figure 5.6), would not be possible and that the molecule **(5.13)** would be chemically stable.

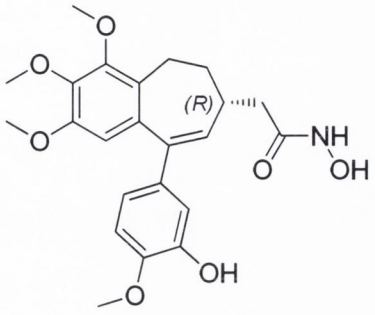

Figure 5.12 Methylene-containing hydroxamic acid compound **(5.13)**

5.4.1 Synthetic strategy

It was suggested that the introduction of the additional methylene unit would have to take place at a relatively early stage of the synthetic route. The common intermediate **(4.37)** was thus chosen as the starting point for the divergent synthesis. It was envisaged that the required C-7 carbon chain extension could be achieved by the formation of a nitrile group and its subsequent reduction to a primary alcohol. Once this key transformation had been accomplished, the synthetic scheme was deemed to be theoretically straight forward, mirroring that employed for the failed synthesis of **(5.08)**.

5.4.2 Synthesis of mesylate (5.14) and displacement with cyanide

The synthesis of **(5.13)** commenced with the mesylation of the alcohol intermediate **(4.37)**. The alcohol was dissolved in DCM and methanesulfonyl chloride and DIPEA were added at 0 °C. After 1 h, the reaction was quenched and the desired product **(5.14)** isolated as a crude mixture. Without further purification, the mesylate **(5.14)** was dissolved in DMSO and sodium cyanide was added. After 3 h, TLC analysis revealed that consumption of the mesylate had occurred. Exclusive formation of the desired nitrile **(5.15)** was observed. Following purification, the nitrile **(5.15)** was isolated as a colourless oil in excellent yield (85% over two steps).

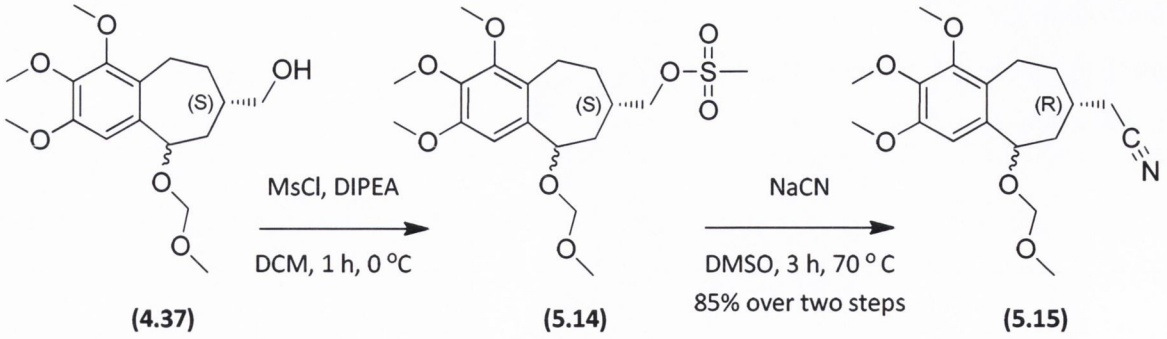

Scheme 5.6 Synthesis of mesylate **(5.14)** and displacement with cyanide

The sodium cyanide was pulverised using a mortar and pestle in order to aid dissolution in the DMSO. The facile and exclusive nature of the cyanide displacement reaction was in stark contrast to the long reaction time, poor yield and formation of substantial quantities of eliminated side product observed for the analogous reaction of the mesylate **(4.34)** (reaction time 3 h v 24 h; yield 85% v 46%). It was hypothesised that compound **(4.34)** would experience greater steric hindrance during the displacement reaction due to the proximity of the mesylate group to the B-ring. Conversely, it was proposed that the presence of the additional methylene unit in compound **(5.14)** allowed the cyanide nucleophile less sterically hindered access to the mesylate group. Thus a shorter reaction time and higher yield was obtained.

It was interesting to observe that although compound **(4.37)** was of (S)-configuration, the configuration of the resultant nitrile **(5.15)** was in fact (*R*). It should be noted that inversion of configuration at the C-7 position did not occur in this case. This phenomenon arose as a consequence of the IUPAC rules for nomenclature of chiral centres. The carbon chain extension resulted in the C-7 side chain having a lower priority. Thus, the chiral centre at C-7 of compound **(5.15)** was designated as having an (*R*)-configuration.

5.4.3 Two step reduction of nitrile (5.15)

The nitrile group of compound **(5.15)** was reduced to the corresponding alcohol **(5.17)** *via* two consecutive reactions. DIBAL-H was added to a solution of **(5.15)** in dry THF at - 78 °C under anhydrous conditions. After 3 h, the reaction was deemed to have gone to completion by TLC analysis and tartaric acid aqueous solution was added. The reaction was extracted and the resulting ethereal solution concentrated to afford the aldehyde **(5.16)** in crude form. The mixture containing the aldehyde **(5.16)** was then reconstituted in methanol and the aldehyde was further

reduced with sodium borohydride. Following purification, the desired alcohol **(5.17)** was obtained in good yield (75%) as a colourless oil (Scheme 5.7).

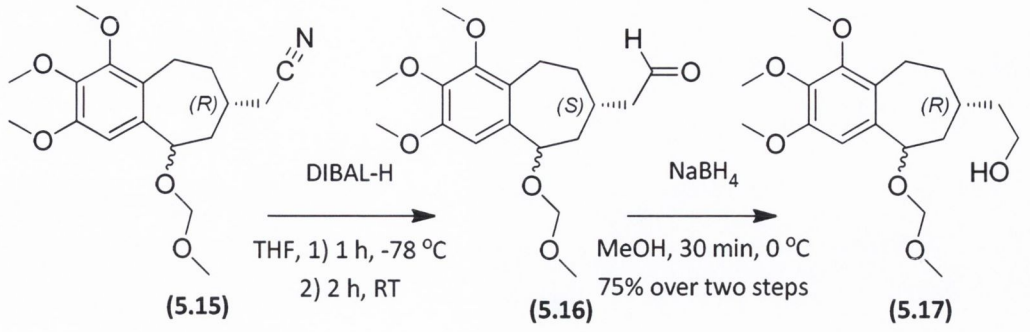

Scheme 5.7 Two step reduction of nitrile **(5.15)** to alcohol **(5.17)**

Monitoring of the reaction by TLC was greatly simplified by the fact that the nitrile **(5.15)** and aldehyde **(5.16)** had distinguishably different R_f values. This compared favourably with the analogous reduction of the nitrile of **(4.35)**, where both the starting material and aldehyde intermediate **(4.36)** had identical R_f values on TLC.

5.4.4 Silyl protection of alcohol (5.17)

The free alcohol group of compound **(5.17)** was protected as the *tert*-butyldiphenylsilyl ether. The alcohol **(5.17)** was combined with *tert*-butyldiphenylsilyl chloride and imidazole and dissolved in DMF under anhydrous conditions. After 16, the reaction was deemed to have gone to completion by TLC. Following purification, the desired product **(5.18)** was isolated in excellent yield (98%) as a colourless oil (Scheme 5.8).

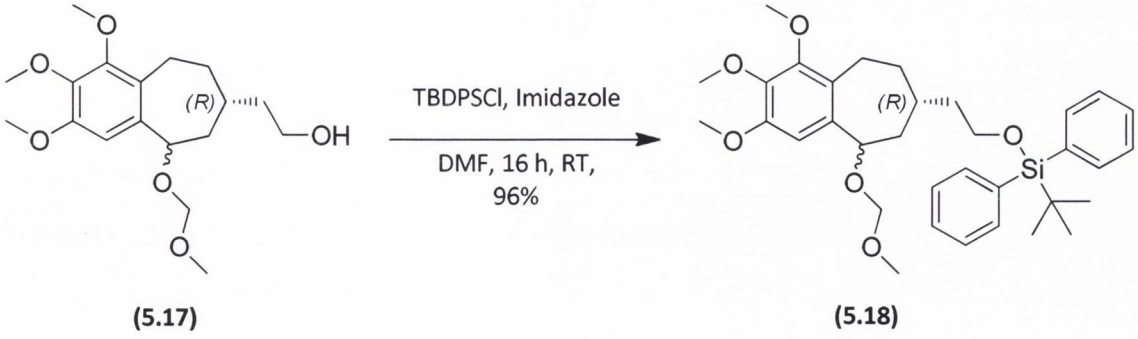

Scheme 5.8 Silyl protection of alcohol **(5.17)**

5.4.5 Removal of MOM protecting group of (5.18) and oxidation of alcohol (5.19)

The MOM ether of compound **(5.18)** was removed using the aluminium chloride/sodium iodide/acetonitrile system outlined previously (section 3.8.8.3). Compound **(5.18)** was dissolved in a mixture of DCM and acetonitrile (1:2). Aluminium chloride and sodium iodide were then added at 0 °C. After 15 min, the starting material was adjudged to have been consumed by TLC. The reaction was quenched by the addition of sodium bicarbonate aqueous solution. The benzylic alcohol intermediate **(5.19)** was extracted with DCM. Dess-Martin periodinane was then added to this crude DCM extract containing the alcohol **(5.19)**. After a further 30 min, TLC analysis revealed that the alcohol had been consumed. Following purification, the desired ketone product **(5.20)** was isolated as a colourless oil in excellent yield (90% over two steps; Scheme 5.9).

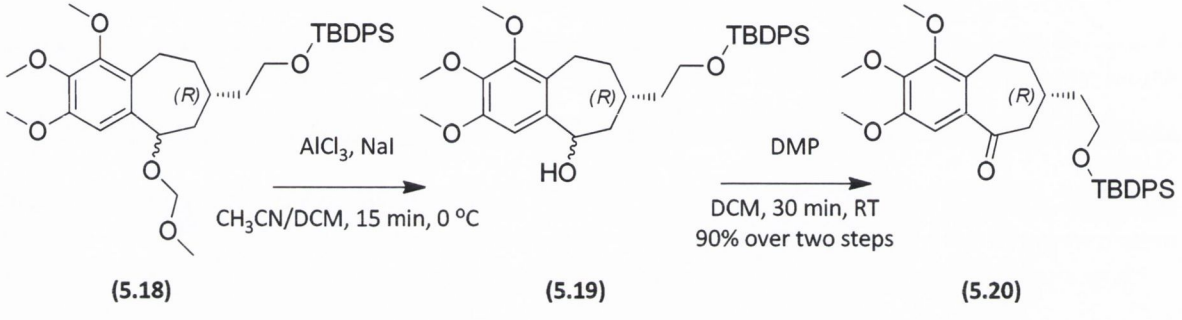

Scheme 5.9 Removal of MOM group of **(5.18)** and oxidation of alcohol **(5.19)**

The excellent yield obtained for the MOM deprotection and alcohol oxidation compared favourably with the equivalent deprotection of the methylene containing alcohol **(4.41)** and very favourably with deprotection of the C-7 position alcohol containing compound **(3.31)** (90%; 83% and 42% respectively). This reaffirmed the suggestion that additional stability to elimination at the C-9 position was potentially conferred by the extended carbon chain at the C-7 position.

5.4.6 Removal of the silyl protecting group of (5.20)

The *tert*-butyldiphenylsilyl ether of compound **(5.20)** was removed by the addition of TBAF to a solution of the compound in THF under anhydrous conditions. Following purification, the desired alcohol **(5.21)** was obtained in satisfactory yield (74%) as a yellow oil (Scheme 5.10).

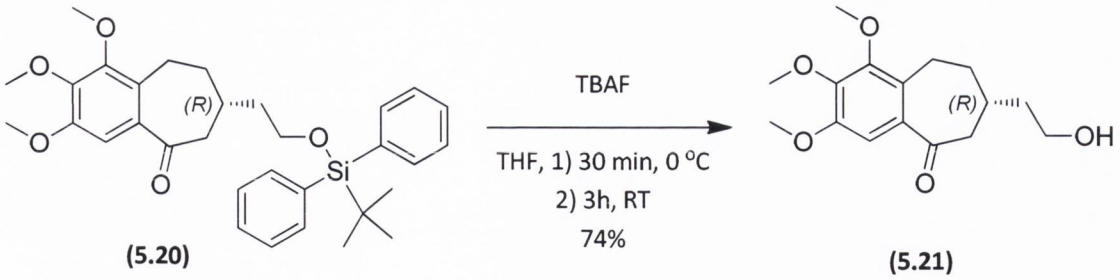

(5.20) (5.21)

Scheme 5.10 Removal of silyl group of **(5.20)**

5.4.7 Organolithium coupling of AB-ring ketone (5.20) and C-ring bromide (2.14)

An organolithium coupling reaction was utilised to attach the C-ring component **(2.14)** to the AB-ring component **(5.20)**. The C-ring **(2.14)** was dissolved in THF and *n*-butyllithium solution was added at - 78 °C under anhydrous conditions. After 40 min, a solution of compound **(5.20)** in THF was added. TLC analysis revealed that the reaction had gone to completion after 4 h. HCl aqueous solution was added to quench the reaction. Following purification, the desired tricyclic coupled compound **(5.21)** was obtained as a yellow oil in moderate yield (57%; Scheme 5.11).

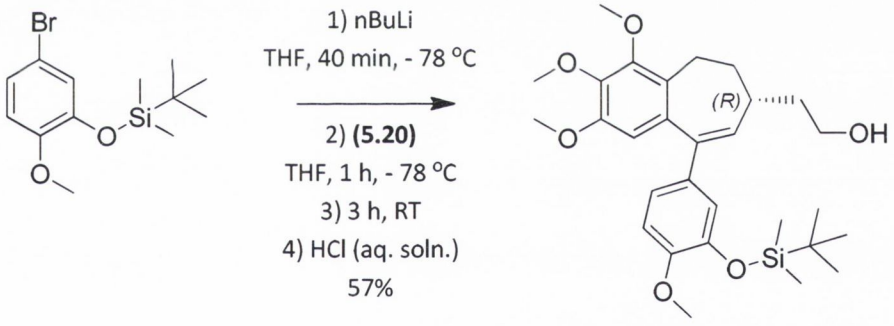

(2.14) (5.21)

Scheme 5.11 Organolithium coupling of ketone **(5.20)** and bromide **(2.14)**

5.4.8 Removal of phenolic silyl protecting group of (5.21)

In order to further probe the effect of C-7 position modification on the activity of the tubulin inhibitor pharmacophore, it was decided to synthesise the C-7 ethylene analogue of **(2.02)**. Hence, the silyl group of **(5.21)** was removed using TBAF in THF under anhydrous conditions. Following purification, the desired diol compound **(5.22)** was obtained in moderate yield (52%) as a white solid (Scheme 5.12).

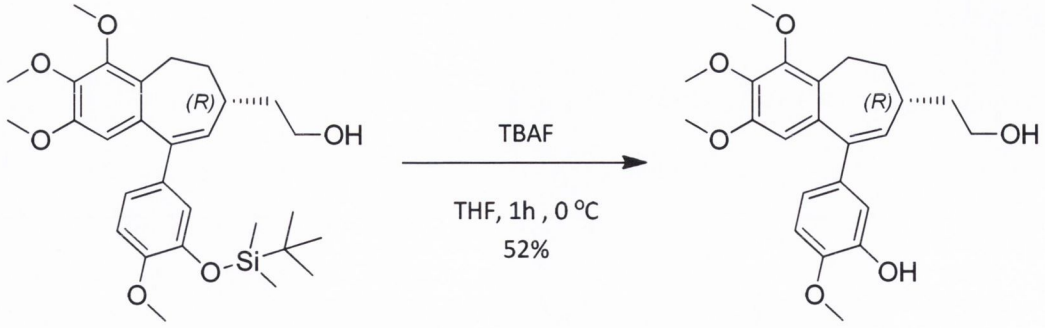

(5.21) **(5.22)**

Scheme 5.12 Removal of phenol silyl group of **(5.21)**

5.4.8.1 Characterisation of compound (5.22)

The identity of compound **(5.22)** was confirmed by the use of NMR spectroscopy. The four methoxy group proton signals were identified as resonating as three distinct peaks at 3.71 ppm, 3.91 ppm (2 X OCH_3) and 3.94 ppm. The double bond proton was found to resonate as a doublet (J = 5.82 Hz) at 6.06 ppm by reference to the HSQC spectrum (Figure 5.15). The four aromatic CH protons were found to resonate at 6.39 ppm, 6.76-6.81 (2 x ArH) and 6.91 ppm. The aliphatic C-7 CH proton was assigned to the multiplet at 2.07-2.13 ppm again using the HSQC proton-carbon correlation data (Figure 5.14 and 5.15). The HSQC spectrum also proved invaluable in assigning the eight aliphatic CH_2 protons (Figure 5.16). They were found to resonate as six distinct signals at 1.62-1.71 ppm, 1.77-1.80 ppm, 1.82-1.90 ppm, 2.16-2.31 ppm (2 x CH_2), 3.03-3.05 ppm and 3.71 ppm (2 x CH_2).

The DEPT 135 spectrum permitted identification of the CH_2 carbon signals at 23.04 ppm, 37.92 ppm, 41.58 ppm and 61.24 ppm (Figure 5.14). The methoxy group carbons were identified as corresponding to the peaks at 55.53 ppm (2 x OCH_3), 60.43 ppm and 61.13 ppm, again by reference to the DEPT 135 spectrum. The DEPT 90 spectrum allowed convenient identification of the aromatic CH proton signals at 108.42 ppm, 109.81 ppm, 113.71 ppm and 119.25 ppm (Figure 5.14). The double bond CH carbon signal was found to correspond to the peak at 131.67 ppm, utilising the data available from the HSQC spectrum (Figure 5.15). Similarly, the aliphatic C-7 CH carbon was found to resonate at 33.15 ppm. The nine quaternary carbon signals were assigned to the peaks at 125.44 ppm, 127.79 ppm, 134.99 ppm, 135.62 ppm, 140.70 ppm, 144.78 ppm, 145.54 ppm, 150.30 ppm and 150.52 ppm.

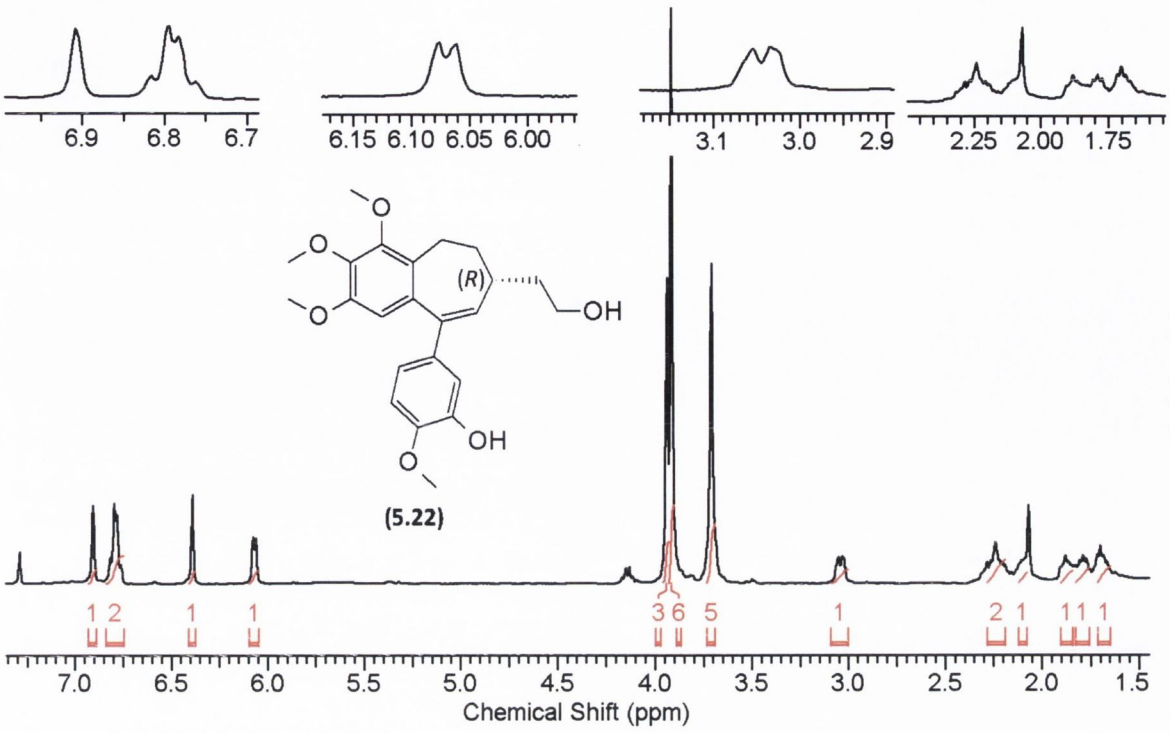

Figure 5.13 ^{1}H NMR spectrum of **(5.22)**

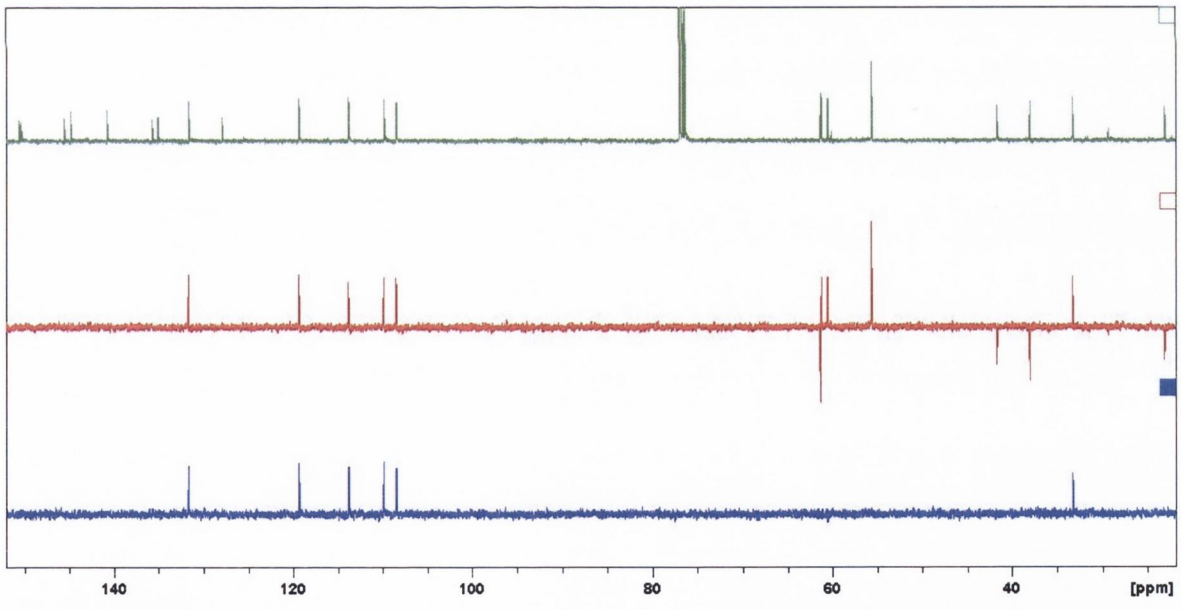

Figure 5.14 ^{13}C, DEPT 135 and DEPT 90 NMR spectra of **(5.22)**

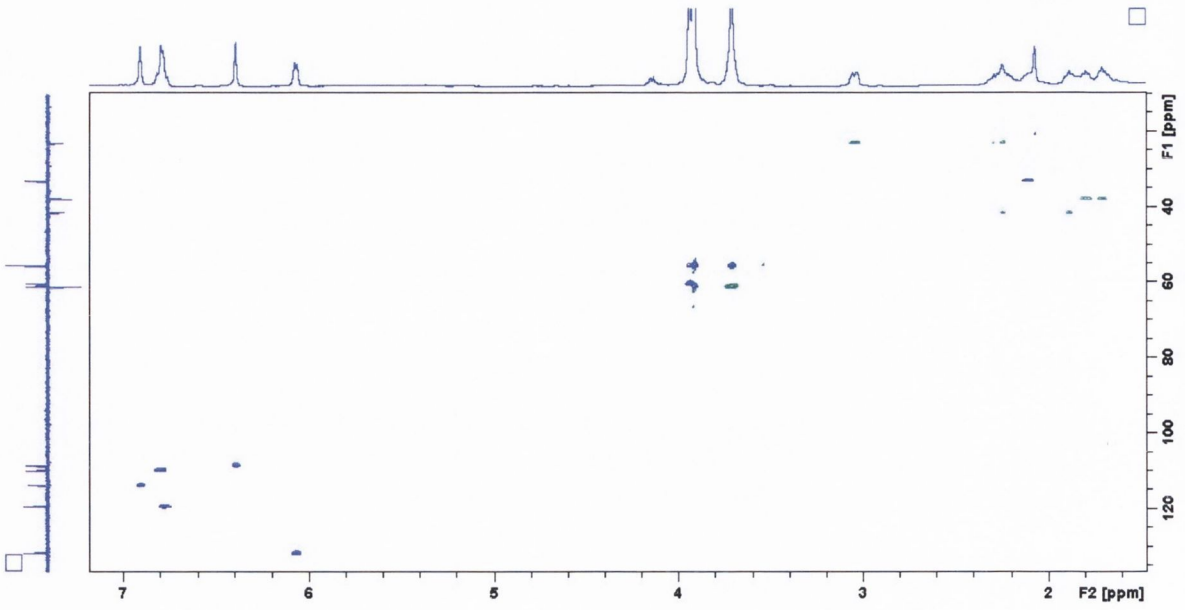

Figure 5.15 HSQC NMR spectrum of **(5.22)**

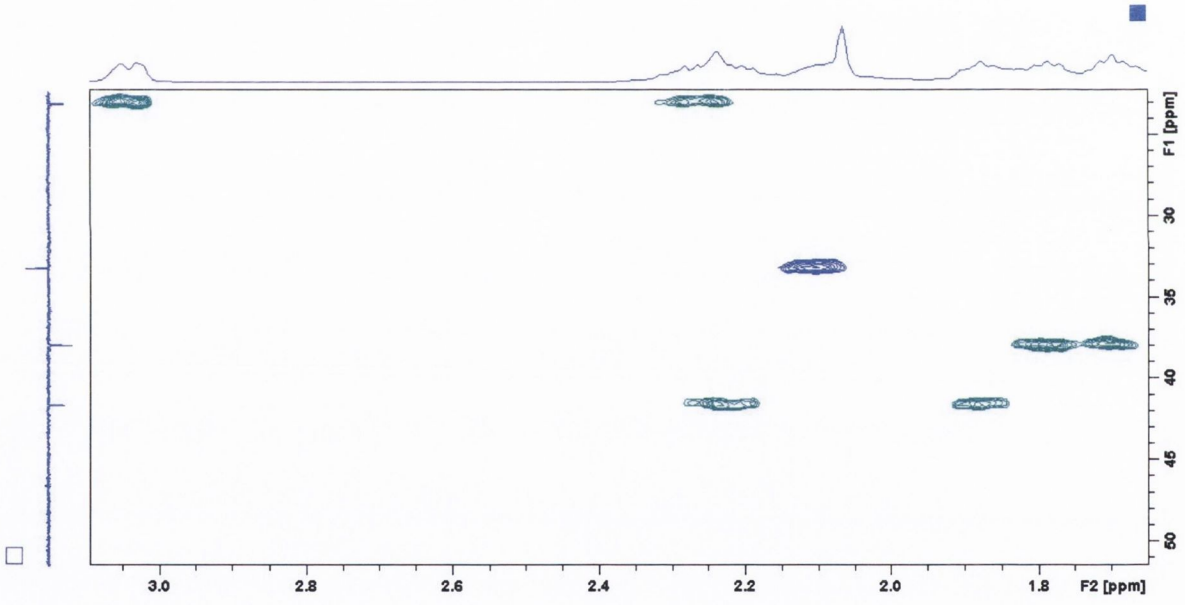

Figure 5.16 HSQC NMR spectrum expansion of **(5.22)**

The identity of **(5.22)** was further confirmed by mass spectrometry. The molecular ion peak $[M+Na]^+$ was found to have a mass in close correlation with the calculated value (found 423.1818, calculated 423.1784).

The specific optical rotation of the molecule $[\alpha]_D^{25}$ was found to be - 95.7 (*c* = 0.61, DCM). This suggested that the stereochemistry at the C-7 position had been maintained throughout the synthesis. Compound **(5.22)** was then subject to biological evaluation (Section 5.5.1).

5.4.9 Two step oxidation of alcohol (5.21) to carboxylic acid (5.24)

Compound **(5.21)** was dissolved in DCM and Dess-Martin periodinane was added to effect oxidation of the primary alcohol group to an aldehyde. TLC analysis revealed that complete and exclusive transformation had been achieved within 30 min. The reaction was quenched with sodium bicarbonate and the product **(5.23)** extracted with diethyl ether. Following removal of the diethyl ether, the crude mixture was reconstituted in DMF. Oxone was added and the reaction was left stirring for a further 2 h. Complete and exclusive conversion from the aldehyde to the carboxylic acid was observed on TLC. Following purification, the desired carboxylic acid **(5.24)** was isolated in excellent yield (85% over two steps) as a yellow resin (Scheme 5.13).

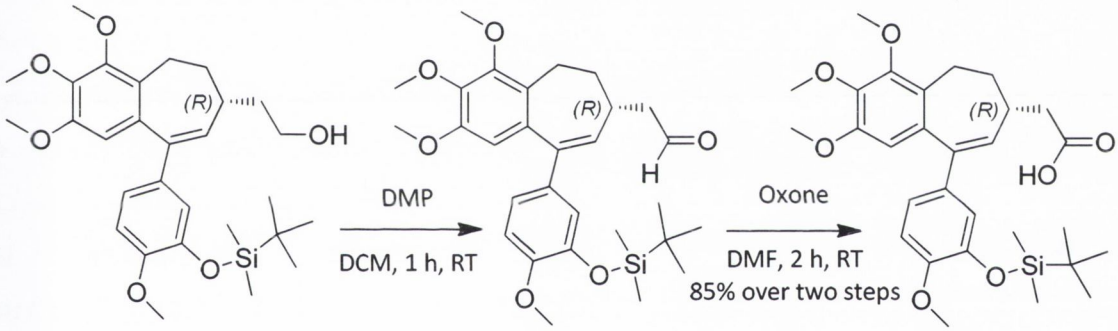

Scheme 5.13 Two step oxidation of alcohol **(5.21)** to carboxylic acid **(5.24)**

5.4.10 Removal of silyl protecting group of (5.24)

The silyl protected compound **(5.24)** was dissolved in THF and TBAF was added under anhydrous conditions at 0 °C. After 1 h, the reaction was deemed to have gone to completion and following purification the desired carboxylic acid containing tubulin inhibitor **(5.25)** was isolated in good yield (80%) as an off-white solid (Scheme 5.14).

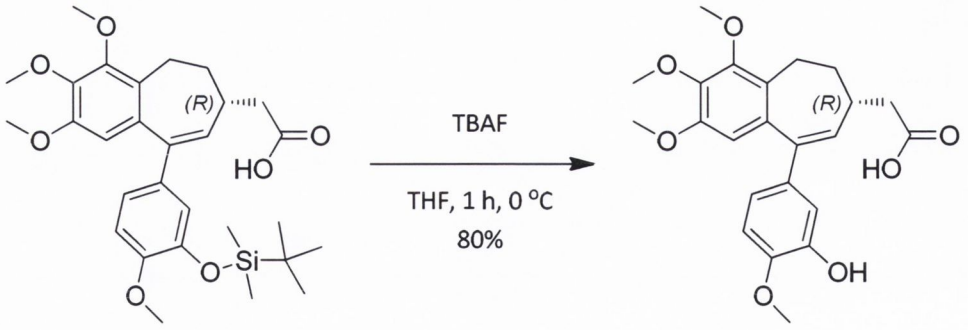

(5.24) **(5.25)**

Scheme 5.14 Removal of silyl group of compound **(5.24)** to afford compound **(5.25)**

5.4.10.1 Characterisation of (5.25)

Compound **(5.25)** was characterised by NMR spectroscopy. The four methoxy group proton signals were identified at 3.71 ppm, 3.92 (2 x OCH_3) and 3.94 ppm. The double bond proton was found to resonate as a doublet (J =4.36 Hz) at 6.09 ppm by reference to the HSQC spectrum (Figure 5.21). Similarly, the four aromatic protons were identified as corresponding to the three singlets at 6.40 ppm, 6.80 ppm (2 x ArH) and 6.90 ppm. The HSQC correlation data proved essential in the assignment of the aliphatic protons in the molecule (Figure 5.19). The C-7 CH proton was found to resonate as part of a multiplet at 2.45-2.47 ppm along with one of the CH_2 protons. The five remaining aliphatic CH_2 protons were identified as corresponding to the multiplets at 1.92-1.96 ppm, 2.20-2.35 (2 x CH_2), 2.54-2.58 ppm and 3.06-3.06 ppm. The phenol proton was identified as corresponding to the broad singlet at 5.60 ppm.

The four methoxy carbons were identified as resonating at 55.55 ppm (2 x OCH_3), 60.44 ppm and 61.15 ppm. The three CH_2 carbons were readily identified from the DEPT 135 spectrum as corresponding to the peaks at 22.88 ppm, 38.92 ppm and 41.10 ppm (Figure 5.18). The aliphatic C-7 carbon was found to resonate at 33.31 ppm while the double bond CH carbon was found to resonate at 129.41 ppm by reference to the HSQC spectrum (Figure 5.21). The four aromatic CH carbons were found to correspond to the four signals at 108.54 ppm, 109.80 ppm, 113.80 ppm and 119.40 ppm. The distinctive carboxylic acid carbon was identified as corresponding to the furthest downfield peak at 177.34 ppm. The nine remaining quaternary carbons were found to resonate at 127.35 ppm, 134.76 ppm, 135.31 ppm, 140.82 ppm, 140.95 ppm, 144.74 ppm, 145.61 ppm, 150.32 ppm and 150.67 ppm.

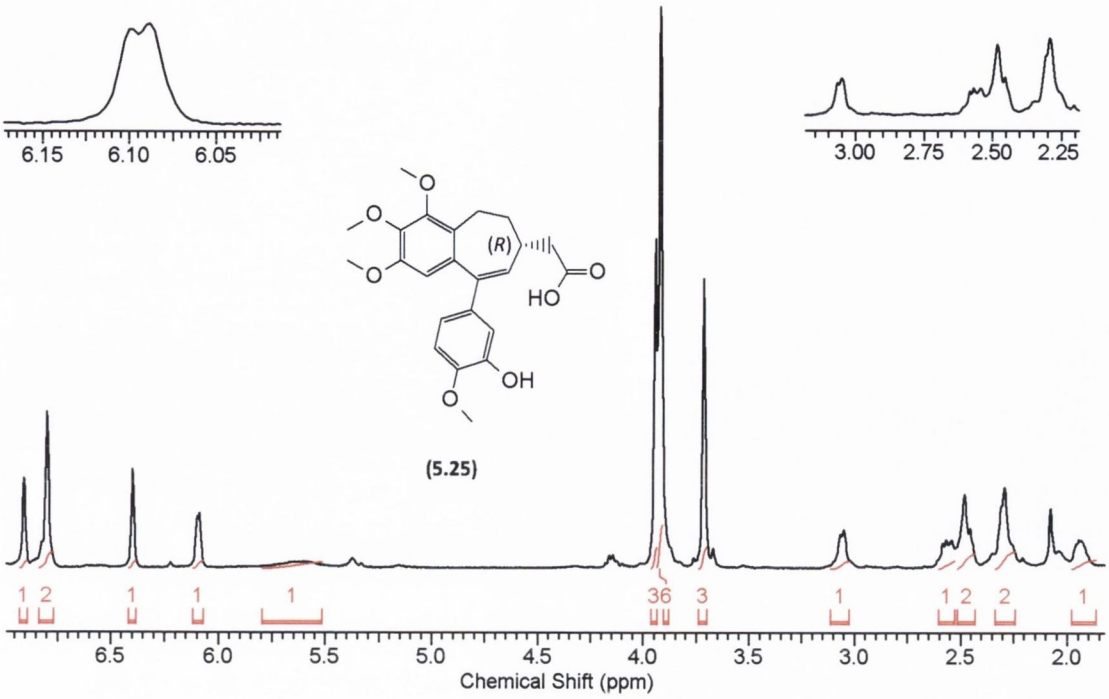

Figure 5.17 ^{1}H NMR spectrum of **(5.25)**

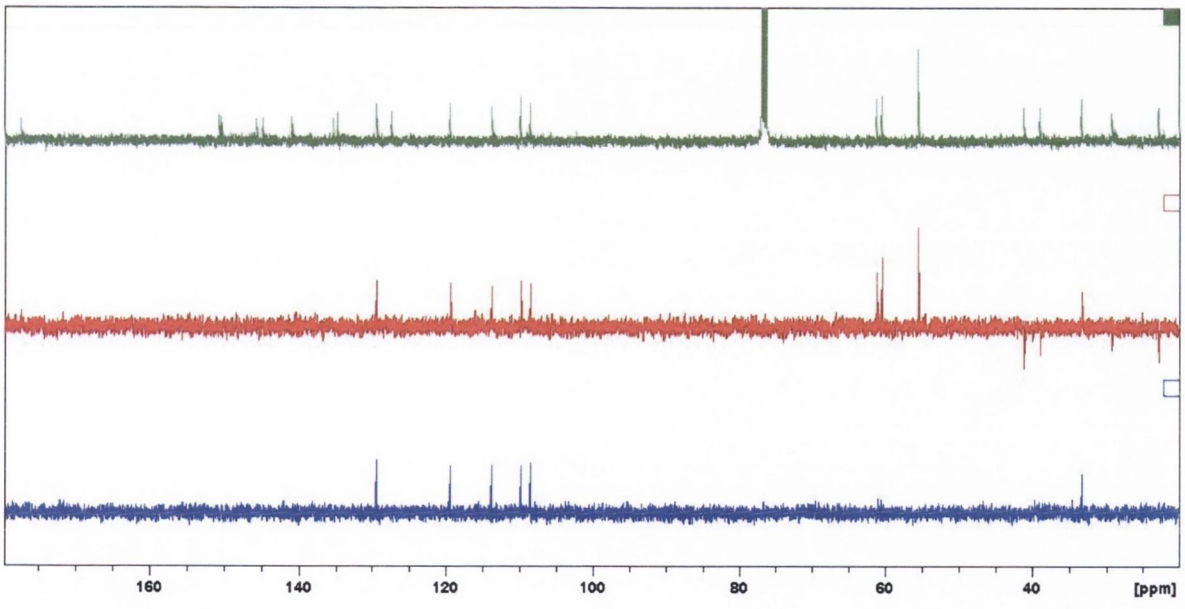

Figure 5.18 ^{13}C, DEPT 135 and DEPT 90 NMR spectra of **(5.25)**

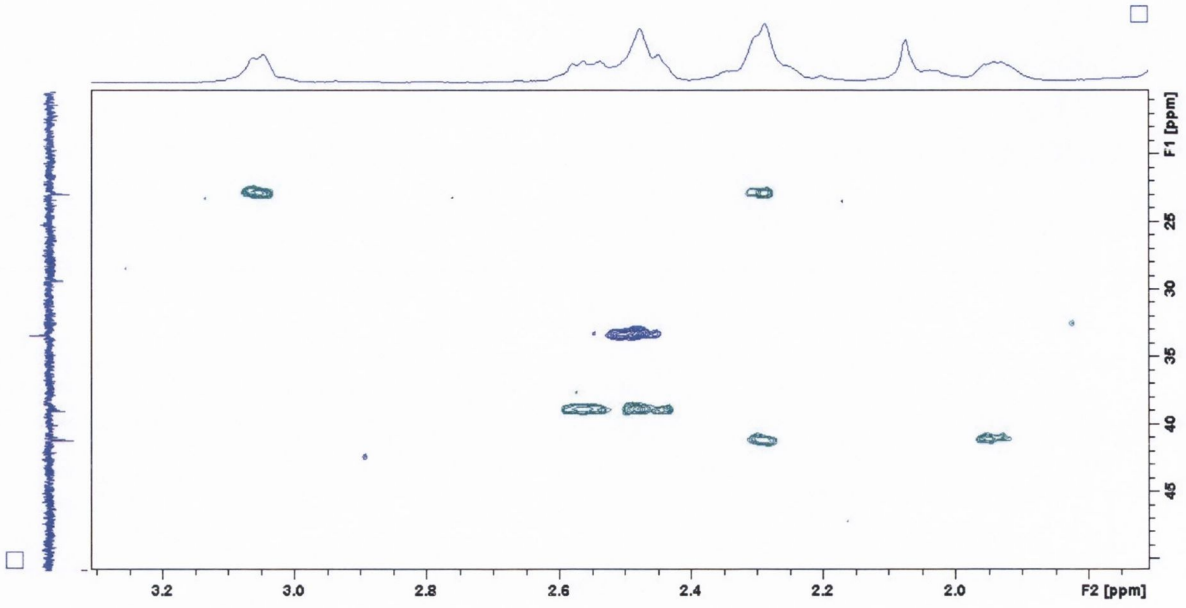

Figure 5.19 Expansion of aliphatic region of HSQC NMR spectrum of **(5.25)**

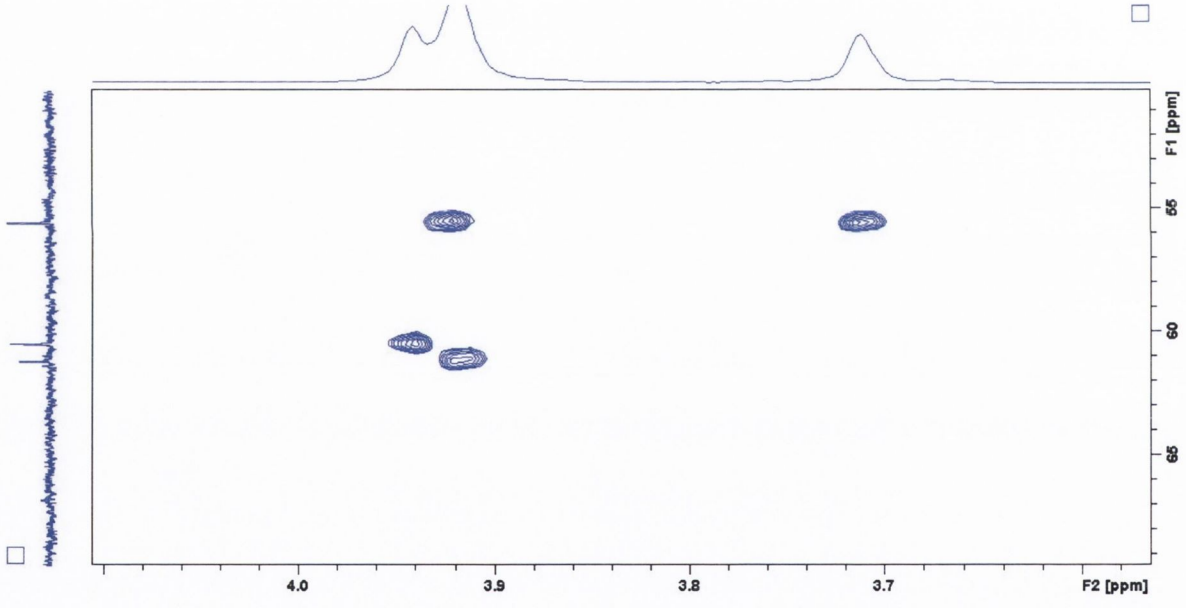

Figure 5.20 Expansion of HSQC NMR spectrum of **(5.25)** illustrating methoxy carbon and proton signals

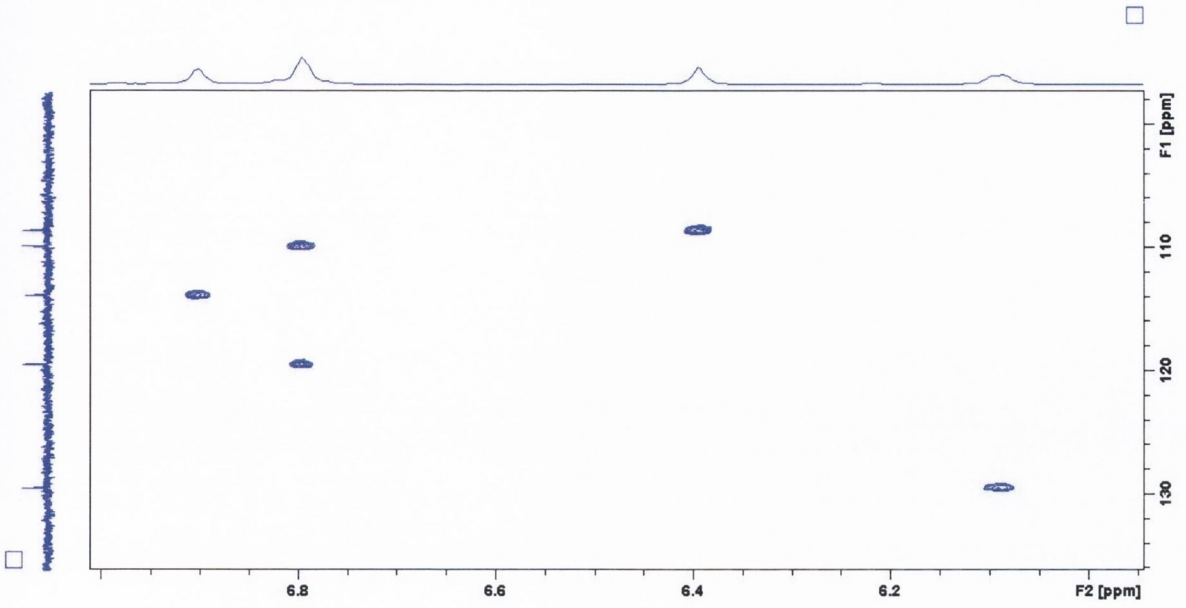

Figure 5.21 Expansion of aromatic region of HSQC NMR spectrum of **(5.25)**

Mass spectrometry further confirmed the identity of **(5.25)**. The mass of the molecular ion peak $[M+Na]^+$ was found to be in close approximation to that of the calculated value (found 437.1613, calculated 437.1576).

The presence of the carboxylic acid group was further suggested by the distinct carbonyl stretch absorption apparent in the IR spectrum of **(5.25)** at 1707.44 cm^{-1}.

Compound **(5.25)** was also found to have a specific optical rotation $[\alpha]_D^{25}$ of - 40 (*c* = 1, DCM), suggesting that the stereochemistry at the C-7 position had been preserved throughout the synthesis. Compound **(5.25)** was subsequently evaluated for biological activity (Section 5.5.1).

5.4.11 Formation of PFP ester of compound (5.24)

In order to introduce the hydroxamic acid group into the molecule, the carboxylic acid first had to be activated by the formation of a PFP ester. Compound **(5.24)** was dissolved in DCM and pentafluorophenol and DCC were added to the solution at 0 °C. After 1 h, the reaction was deemed to have gone to completion by TLC and the volatile organic solvent was removed under reduced pressure. The crude reaction mixture was then purified to afford compound **(5.26)** as a yellow oil in moderate yield (58%; Scheme 5.15).

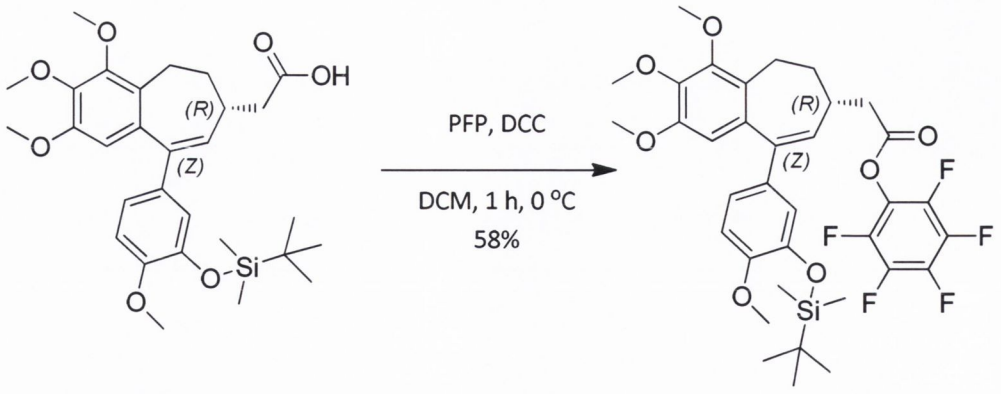

(5.24) **(5.26)**

Scheme 5.15 Formation of PFP ester of compound **(5.24)**

Particular care was taken in the purification of the PFP ester **(5.26)** by flash column chromatography due to its inherent instability on silica. Therefore, the product was eluted rapidly from the column using a relatively polar mobile phase. Notwithstanding the haste with which the purification was carried out, a relatively poor yield was obtained. However, it was decided that the removal of the coupling reagent side product, (*N*,*N*′-dicyclohexylurea) prior to the next step, was essential.

5.4.12 Displacement of PFP ester (5.26) with hydroxylamine

The hydroxamic acid functionality was introduced by the displacement of the PFP ester group on compound **(5.26)** with hydroxylamine. The PFP ester **(5.26)** was dissolved in DMF and DIPEA was added. Hydroxylamine hydrochloride was then added to the reaction mixture. After 10 min, no trace of the starting material was apparent on TLC and the reaction was quenched by the addition of dilute HCl aqueous solution. Following extraction and purification, the desired product **(5.27)** was isolated as a yellow resin in good yield (79%; Scheme 5.16).

Chromatography of the hydroxamic acid containing compound **(5.27)** was complicated by the extreme polarity of the acidic hydroxamic acid residue. In order to more easily elute the product from the column, a mobile phase employing formic acid (1%) was used.

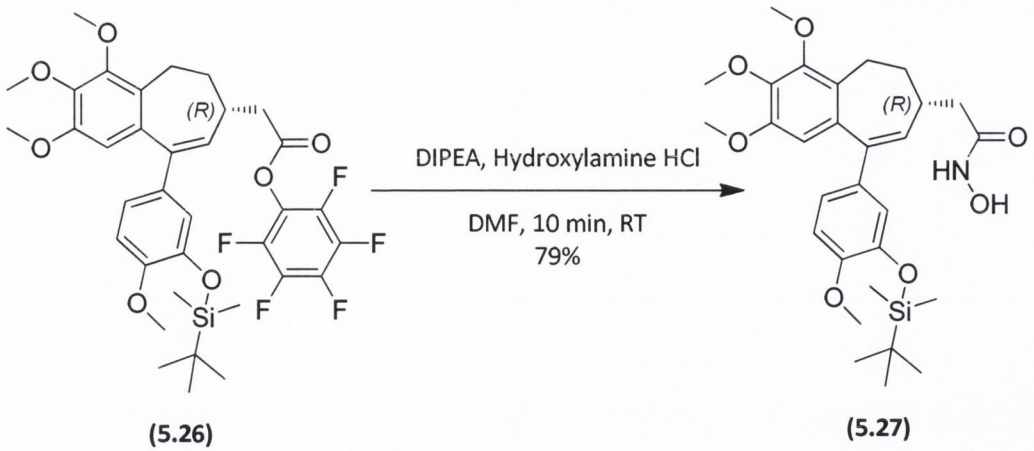

(5.26) **(5.27)**

Scheme 5.16 Displacement of PFP ester of **(5.26)** with hydroxylamine

5.4.13 Removal of silyl group on compound (5.27)

The silyl ether of compound **(5.27)** was readily removed by the addition of TBAF in THF at 0 °C. After 1 h, the reaction was deemed to have gone to completion by TLC analysis. Following purification the desired hydroxamic acid compound **(5.13)** was isolated in good yield (89%) as an off-white solid (Scheme 5.17).

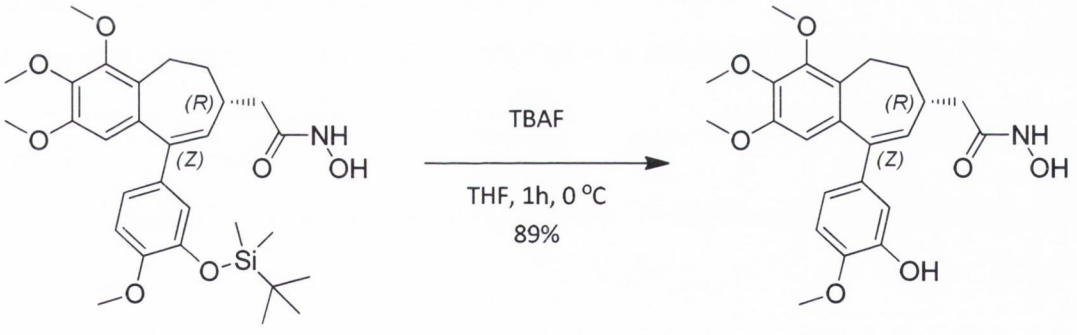

(5.26) **(5.13)**

Scheme 5.17 Removal of silyl group of compound **(5.27)**

A mobile phase containing formic acid (1%) was again required to purify compound **(5.13)** by silica gel flash column chromatography. Once isolated, compound **(5.13)** was characterised in full.

5.4.13.1 Characterisation of (5.13)

Compound **(5.13)** was characterised by NMR spectroscopy. The four methoxy group proton signals were found to resonate as three singlets at 3.63 ppm, 3.83 ppm (2 x OCH_3) and 3.85 ppm. Using the HQSC spectrum, the double bond CH proton was found to resonate as a doublet (J = 6.10 Hz) at 6.04 ppm (Figure 5.25). Similarly, the four aromatic protons were identified as corresponding to the signals at 6.35 ppm, 6.66-6.72 ppm (2 x ArH) and 6.84 ppm. The aliphatic C-7 CH proton was found to resonate as a multiplet at 2.31-2.37 ppm by reference to the HSQC correlation data (Figure 5.26). The six aliphatic CH_2 signals were also assigned to the multiplets at 1.81-1.88 ppm, 2.11-2.16 ppm, 2.19-2.27 ppm (3 x CH_2) and 2.99-3.05 ppm using the HSQC spectrum correlation information (Figure 5.26).

The three CH_2 carbon signals were readily identified from the DEPT 135 NMR spectrum at 22.98 ppm, 37.79 ppm and 41.27 ppm (Figure 5.23). The aliphatic CH proton at the C-7 position was identified as resonating at 34.43 ppm by reference to the DEPT 90 and HSQC spectra (Figure 5.23 and 5.26). The four methoxy group carbon signals were readily identified at 54.96 ppm, 55.00 ppm, 59.81 ppm and 60.63 ppm by comparison of the DEPT 135 and DEPT 90 spectra. The double bond carbon was found to resonate at 129.01 ppm utilising the HQSC and DEPT 90 spectra. The four aromatic CH carbon signals were similarly identified as those peaks at 108.89 ppm, 110.96 ppm, 114.62 ppm and 119.17 ppm. The carbonyl carbon of the hydroxamic acid proved particularly elusive. However, 600 MHz NMR spectroscopy and an extended data acquisition period allowed the identification of this signal at 162.90 ppm (Figure 5.24). The nine remaining quaternary carbons were then found to resonate at 127.78 ppm, 134.70 ppm, 136.29 ppm, 141.17 ppm, 141.62 ppm, 145.80 ppm, 147.25 ppm, 150.66 ppm and 151.15 ppm.

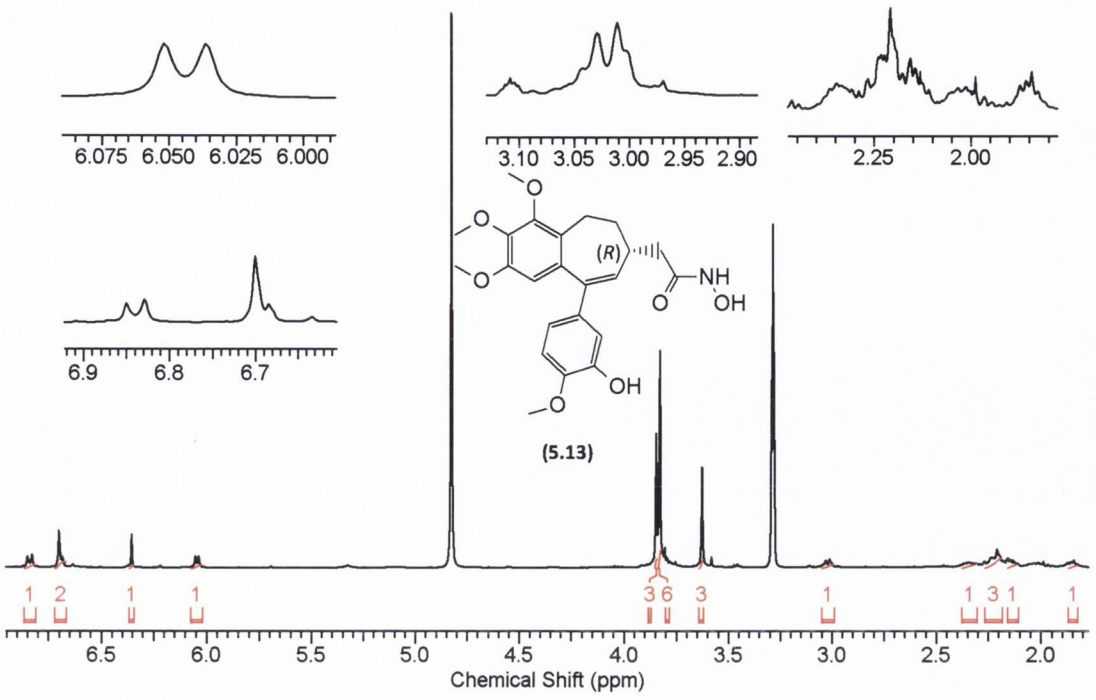

Figure 5.22 ^{1}H NMR spectrum of **(5.13)**

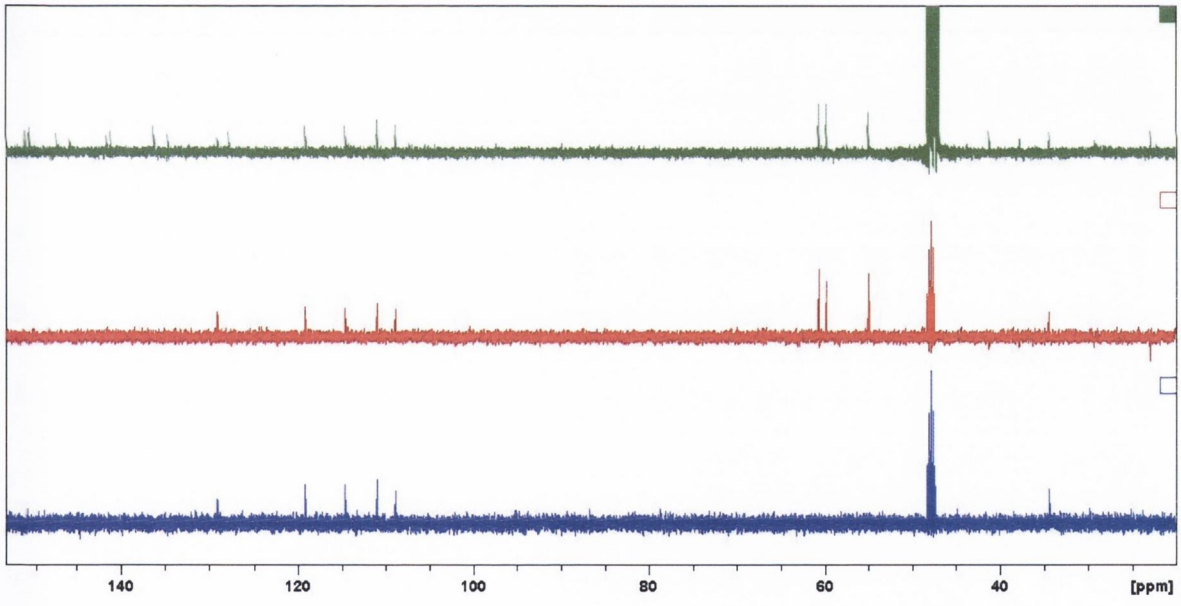

Figure 5.23 ^{13}C, DEPT 135 and DEPT 90 NMR spectra of **(5.13)**

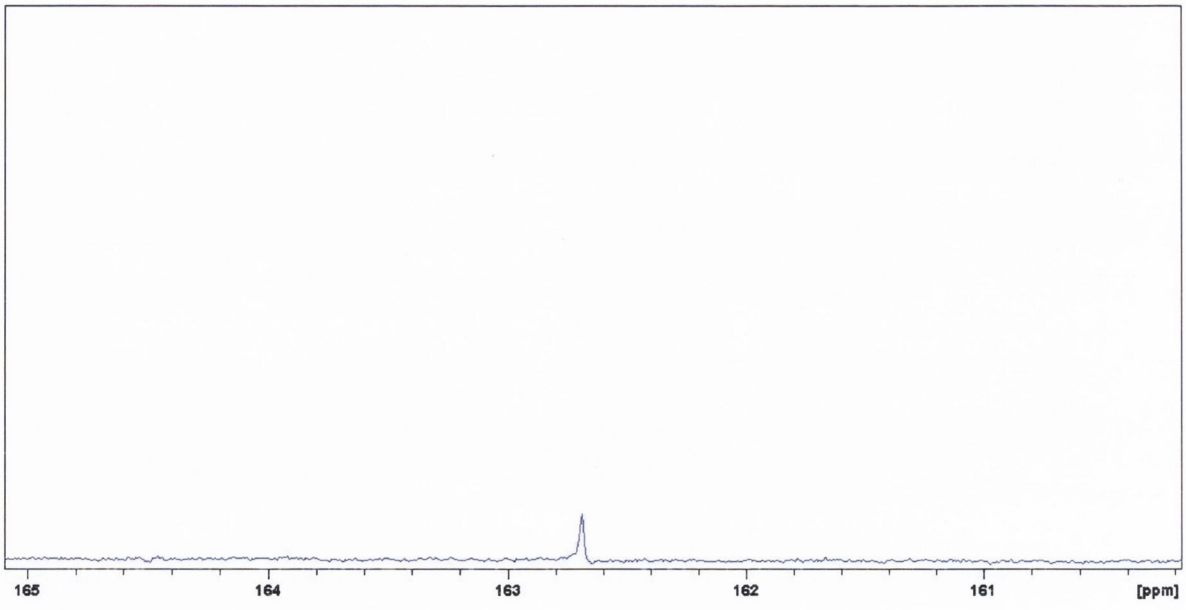

Figure 5.24 Expansion of ^{13}C NMR spectrum of **(5.13)** from 160-165 ppm

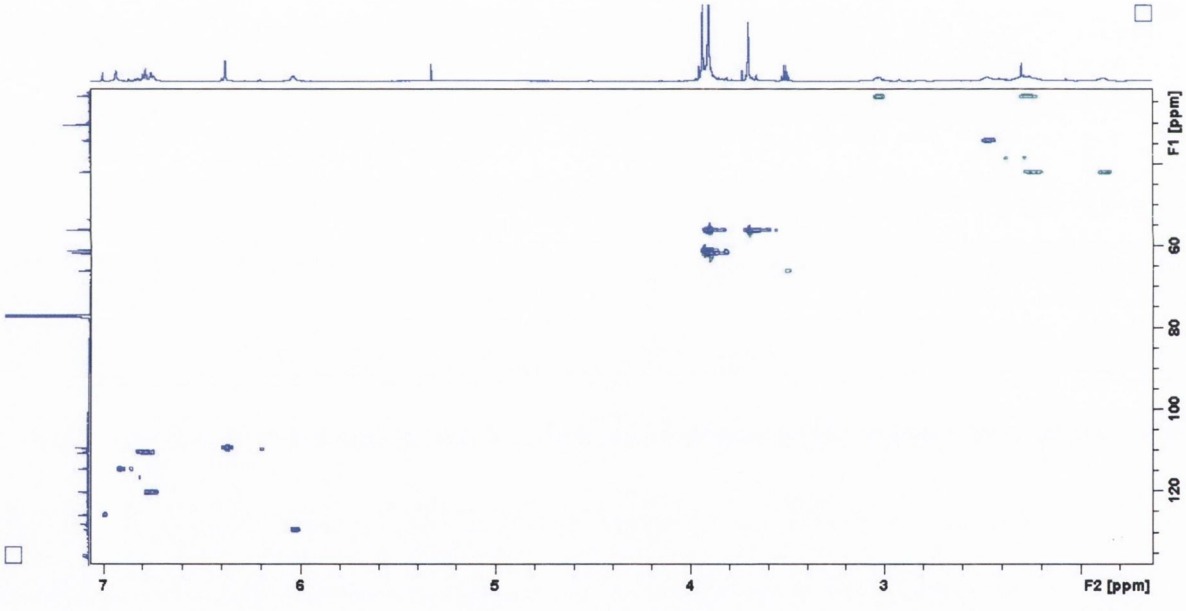

Figure 5.25 HSQC NMR spectrum of **(5.13)**

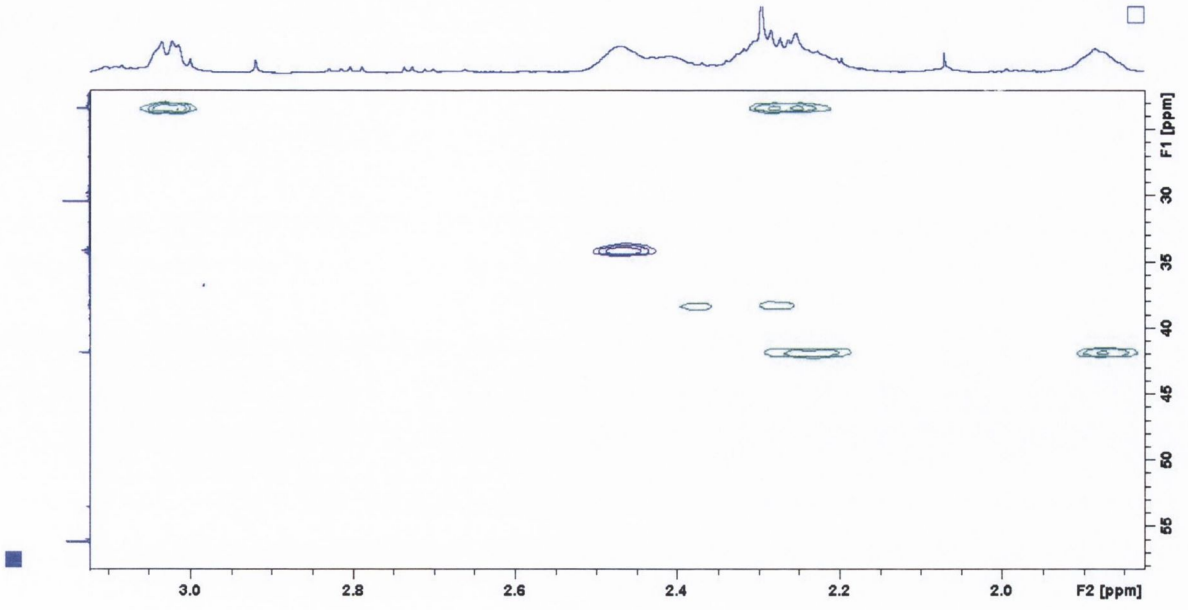

Figure 5.26 Expansion of aliphatic region of HSQC NMR spectrum of **(5.13)**

The identity of compound **(5.13)** was confirmed by mass spectrometry. The mass of the molecular ion $[M+Na]^+$ was found to be in close agreement with the calculated value (found 452.1684, calculated 452.1685).

Compound **(5.13)** was found to have a relatively narrow melting point range (104-106 °C) suggesting that it was isolated in relatively pure form. Furthermore, it was found to be optically active, with a specific optical rotation $[\alpha]_D^{25}$ of - 61.2 (*c* = 0.56, DCM). This suggested that the enantiomeric purity of the compound had not been compromised during the synthesis.

The IR spectrum of the compound was found to have an absorption peak at 1660.04 cm^{-1}. This provided further evidence for the presence of a carbonyl functional group within the molecule.

The hydroxamic acid **(5.13)** was then subject to biological evaluation in both the MTT cell proliferation assay and the APN inhibition assay (Section 5.5).

5.5 Biological evaluation

The novel tubulin inhibitors **(5.22)** and **(5.25)**, together with the DML **(5.13)** were evaluated for their antiproliferative activity using the MTT assay. This allowed a crude determination of their tubulin polymerisation inhibition activity to be estimated. The APN inhibitory activity of the DML

(5.13) was determined using an aminopeptidase N UV spectrophotometric assay as described by Melzig *et al.* (Section 6.3) [291]. The IC_{50} value of the control compound bestatin **(5.02)** was also calculated.

5.5.1 MTT assay results for (5.22), (5.25) and (5.13)

Compounds **(5.22)**, **(5.25)** and the DML **(5.13)** were all evaluated for their antiproliferative activity using the MTT cell proliferation assay (Table 5.1).

Compound	IC_{50} value (nM)
(5.22)	147.6 ± 1.26
(5.25)	727.7 ± 1.07
(5.13)	245 ± 1.15

Table 5.1 Best fit IC_{50} values ± SEM for compounds **(5.22)**, **(5.25)** and **(5.13)** following MTT assay in PC-3 cells (n = 3)

Compound **(5.22)** exhibited an antiproliferative potency comparable with that of the carboxylic acids **(4.43)** and **(4.44)**. However, the activity of this molecule was significantly less than that observed for the methylene eutomer **(4.24)** and dramatically less than that observed for the C-7 alcohol eutomer **(3.01)**. While the configuration of compound **(5.22)** was designated (*R*), it should be noted that it had the same orientation of substituents at the C-7 position as compound **(4.24)** and **(3.01)**, both of which are designated (*S*). Therefore, this result suggested that the activity of the compounds in this series of alcohols decreased with increasing carbon chain length.

Compound **(5.25)** was found to possess moderate activity, in the upper nM range. Its activity was substantially less than that of compounds **(4.43)** and **(4.44)** suggesting that the added methylene unit had a detrimental effect on biological activity of the compound.

The DML **(5.13)** was found to possess significant antiproliferative activity with an IC_{50} of 245 ± 1.15 nM. This represented an antiproliferative activity comparable with that of the carboxylic acids **(4.43)** and **(4.44)**. It is interesting to observe that the activity of this molecule in the MTT assay was substantially higher than that observed for the related methylene containing carboxylic acid **(5.25)**. In fact, the DML **(5.13)** was found to possess an IC_{50} almost three-fold lower than the

related carboxylic acid **(5.25)**. It was suggested that this additional activity may be related to its purported APN inhibition activity. However, more comprehensive biological evaluation would be required to confirm the veracity of this assertion.

5.5.2 Aminopeptidase N UV spectrophotometric assay results

Bestatin **(5.02)** and the DML compound **(5.13)** were evaluated for their APN inhibition activity in the aminopeptidase N UV spectrophotometric assay (Table 5.2).

Compound	IC_{50} value (μM)
(5.02)	26.59 ± 1.13
(5.13)	6.39 ± 1.06

Table 5.2 Best fit IC_{50} values ± SEM for Bestatin **(5.02)** and compound **(5.13)** following APN UV assay (n = 3)

Compound **(5.13)** was found to possess an IC_{50} value approximately four-fold lower than that of the model compound bestatin **(5.02)**. Given the current status of bestatin in clinical evaluation, this impressive result was deemed extremely encouraging. Furthermore, when taken together with the favourable antiproliferative activity demonstrated *in vitro*, the dual acting DML **(5.13)** could be considered to represent a suitable candidate for further biological evaluation as a pre-clinical drug candidate.

5.6 Conclusions

Initial attempts to furnish a DML possessing both APN and tubulin polymerisation inhibition activity were fraught with difficulty. The synthesis of **(5.05)** ultimately ended prematurely as a result of the instability of the hydroxamic acid containing intermediate **(5.07)**. It became apparent that the chemical instability in the molecule arose as a result of a series of rearrangement and elimination reactions encouraged by the drive for greater conjugation within the molecule. It was proposed that the insertion of a chemically inert linker group at the C-7 position would remove this drive for greater conjugation and allow the introduction of the desired hydroxamic acid functionality.

The synthesis of the ether containing compound **(5.08)** was thus proposed. Significant difficulty surrounded the essential O-alkylation reaction of the proposed synthetic pathway and this strategy also ended fruitlessly. An analogue of compound **(5.05)** containing an additional C-7 linkage was ultimately envisaged. It was hypothesised that the extra methylene group of compound **(5.13)** would prevent the rearrangements and elimination reactions purported to be responsible for the instability of the related compound **(5.05)**.

The strategy employed to afford **(5.13)** involved a lengthy synthetic scheme mirroring that employed for the synthesis of compounds **(4.43)** and **(4.44)**. As a fortuitous consequence of the synthesis of **(5.13)**, the novel tubulin inhibitors **(5.22)** and **(5.25)** were also produced.

The evaluation of the ethylene containing compound **(5.22)** suggested that lengthening of the C-7 carbon chain beyond one methylene group resulted in a significant reduction in antiproliferative activity. Furthermore, the evaluation of **(5.25)** suggested that the carboxylic acid series of compounds also exhibited a significant reduction in activity upon introduction of an additional C-7 methylene group.

The desired compound **(5.13)** was eventually obtained following a challenging thirty-one step synthetic scheme. Biological evaluation of this compound revealed that it was possessed of favourable antiproliferative activity and also potent APN inhibitor efficacy. The small molecule, dual acting DML **(5.13)** was thus deemed to have realised the aspiration of a multi-targeted approach without resorting to the synthesis of a molecular conjugate.

6 Biological Experimental

6.0 Introduction

The compounds synthesised were subject to biological evaluation using the MTT cell proliferation assay and the APN inhibition assay as appropriate. The compounds were dried *in vacuo* for several days prior to testing to remove any remaining solvent residue. Stock solutions of compounds were obtained by weighing quantities using a microbalance and reconstituting in DMSO. Sequential dilution of these stock solutions afforded solutions of appropriate concentration for assay.

6.1 MTT Cell proliferation assay

The MTT assay was used to assess the antiproliferative activity of the novel tubulin inhibitors synthesised. This assay, initially described by Mosmann *et al*, is quantitative colorimetric assay which detects viable, but not dead cells by generating a signal proportional to the degree of cellular function [292]. In the presence of viable cells, the yellow tetrazole MTT is reduced by an active reductase enzyme system, to afford purple formazan crystals. These crystals are then dissolved in DMSO to give a coloured solution. The absorbance of this solution can then be quantified using a spectrophotometer.

6.1.1 Materials

Dimethyl sulfoxide (DMSO), thiazolyl blue tetrazolium bromide (MTT), foetal bovine serum (FBS), streptomycin/penicillin solution and 0.25% trypsin/EDTA solution were all purchased from Sigma-Aldrich®, Ireland. Phosphate buffered saline (PBS) tablets were purchased from Invitrogen, Ireland. Greiner CELLSTAR® 75 cm^2 cell culture flasks and Greiner 96-well cell culture microplates with solid U-bottom were purchased from Cruinn, Ireland.

6.1.2 Equipment

Fluostar Optima 96 well plate reader equipped with a thermostat function

NuAire class II biological safety cabinet

Olympus CKX41 inverted microscope (Mason Technology, Ireland)

6.1.3 Test compounds

All dilutions of DMSO stock solutions were carried out using cell culture medium to a afford a final DMSO concentration of ≤ 0.1%. Control solutions consisted of 0.1 % DMSO in cell culture medium. Fresh solutions were prepared prior to each experiment.

6.1.4 Cell line

The PC-3 human prostate adenocarcinoma cell line was purchased from LGC Standards, UK. The cells were cultured in F12K medium supplemented with 0.02 mg/mL sodium pyruvate, 10% FBS and 10 mL/L penicillin/streptomycin solution. Cells were incubated at 37 °C in a humidified atmosphere, containing 5% CO_2 at all times.

6.1.5 Cell maintenance and sub-culture

Cell culture experiments were performed in a NuAire class II biological safety cabinet. Aseptic techniques were followed at all times to prevent contamination. The cells were cultured in 75 cm^2 cell culture flasks using 15 mL of complete medium. The cell culture medium was typically replaced every 2 days. Cells were monitored using an Olympus CKX41 inverted microscope (Mason Technology, Ireland). Cells were sub-cultured into fresh flasks once they had reached 70-80% confluence. The protocol followed for sub-culture was as follows:

1. The old medium was removed from the cell culture flask.
2. The cell monolayer was gently rinsed with PBS solution (10 mL).
3. Trypsin/EDTA solution (3 mL) was added and the cells were incubated at 37 °C until 90% of the cells took on a rounded morphology.
4. The flask was tapped to encourage detachment of the cells and complete medium (5 mL) was added. The contents of the flask was then transferred to a sterile centrifuge tube.
5. The flask was rinsed with a further aliquot of medium (5 mL) and this was also added to the centrifuge tube.
6. The cell suspension was centrifuged at 1000 rpm at 25 °C for 5 min.
7. The supernatant was removed and fresh medium (2-3 mL) was added to the tube to re-suspend the cell pellet.

8. New flasks containing fresh medium (15 mL) at 37 °C were prepared in parallel. The cell suspension was then sub-cultured into these new flasks at 1:4 or 1:6 seeding densities and returned to the incubator.
9. After 24 h, the cells were examined under the microscope and the medium was replaced with fresh, pre-equilibrated medium.

6.1.6 Cell count

A haemocytometer was used to determine the concentration of cells in a given cell suspension for use in the MTT cell proliferation assay. Once cells reached 70-80% confluence, the cells were trypsinised and centrifuged as outlined above (Section 6.1.5). Following removal of the supernatant, the cell pellet was re-suspended in 10 mL of cell medium. The haemocytometer was cleaned thoroughly with 70% ethanol solution and the cover slip was affixed using gentle pressure and circular motions. The haemocytometer was filled by carefully pipetting the appropriate volume of suspension (10 µL) onto the haemocytometer, adjacent to the cover slip. The haemocytometer was thus filled by capillary action. The haemocytometer was then viewed under the microscope using the x4 objective lens to focus on the grid lines. The number of cells in the 16 corner squares was counted using a hand tally counter. Cells were only included in the count if they were within the square or positioned on the left or top boundary lines. This process was repeated for the 5 sets of corner squares (including the middle set of 16 squares) on the haemocytometer. The average count was then obtained by dividing the total cell count for the 5 sets of squares by 5. Due to the design of the haemocytometer, the concentration of cells in the original cell suspension was equal to the average cell count x 10^4 cells/mL.

6.1.7 Assay protocol

PC-3 cells were seeded into a 96-well plate at a density of 2000 cells per well using an appropriate volume of cell suspension. The volume of liquid in each well was then adjusted to 180 µL. The plate was incubated for 24 h at 37 °C. Compound test solutions or control solutions (20 µL) were then added to each well and the plate was incubated for 72 h at 37 °C. CA-4 was used as a positive control. After incubation, the cell medium was removed and 0.5 mg/mL MTT solution in complete medium (200 µL) was added. The plate was then incubated for a further 4 h. The supernatant was then removed from the plate and the purple formazan crystals dissolved in DMSO (180 µL). Absorbance values for the resulting solutions were obtained using the Fluostar Optima 96 well

plate reader. Each compound concentration was tested in quadruplicate and each experiment was performed three independent times.

6.1.8 Plate reader settings

Measurement type	Kinetic, 1 cycle of 20 readings
Absorbance wavelength	485 nm
Temperature	Ambient
Shaking	Once before first measurement, 10 seconds, double orbital

6.1.9 Interpretation of data

The percentage growth inhibition was calculated according to the following formula:

Percentage growth Inhibition (%) = [(control absorbance-test absorbance)/control absorbance] x 100

Statistical analysis of the data was carried out using GraphPad Prism, version 5. The normalised percentage inhibition was plotted against the log(compound concentration) and analysed by non-linear regression. The best fit IC_{50} values ± SEM were then calculated by Prism.

6.2 Aminopeptidase N UV Spectrophotometric Assay

The APN inhibition activity of the test compounds was determined using a UV spectrophotometric assay as described by Melzig et al [291]. The amount of the chromigenic substrate L-Leucine-*p*-nitroanilide enzymatically hydrolysed by APN in the presence of the test compounds in a given time was determined by spectrophotometry. By comparing the blank absorbance with the test absorbance the percentage inhibition caused by the test compound was determined.

6.2.1 Materials

Bestatin, aminopeptidase N, L-Leucine-*p*-nitroanilide, Leucine aminopeptidase (microsomal from porcine kidney, Type VI-S, lyophilized powder, 15-25 units/mg protein), and 4-(2-

Hydroxyethyl)piperazine-1-ethanesulfonic acid (HEPES) were purchased from Sigma-Aldrich®. Greiner 96-well cell culture microplates with solid U-bottom were purchased from Cruinn, Ireland.

6.2.2 Equipment

Fluostar Optima 96 well plate reader equipped with a thermostat function

6.2.3 Buffers and Solutions

HEPES buffer consisting of 50 mM HEPES dry powder and 154 mM NaCl was prepared with deionised water. The pH of the resultant solution was adjusted to 7.4 by the dropwise addition of 2.5 M NaOH aqueous solution. The buffer was then stored at 4 °C.

The substrate solution containing 2 mM L-Leucine-*p*-nitroanilide was prepared using HEPES buffer.

The enzyme solution containing 95 mU leucine aminopeptidase was prepared using HEPES buffer.

6.2.4 Assay protocol

The 2 mM enzyme substrate (L-Leucine-*p*-nitroanilide) solution (50 µL) and HEPES buffer solution (40 µL) were pipetted into the wells of a 96 well plate. The test compound solution (50 µL), control containing DMSO (0.1%) in HEPES buffer (50 µL) or 200 µM bestatin solution in HEPES (50 µL) were then added. The reaction was commenced by the addition of 95 mU enzyme solution (10 µL) to each well. Each test well of the 96 well plate contained a final volume of 200 µL. The plate was incubated at 37 °C for 2 h. The absorbance at 405 nm was then determined using the microplate reader. The 200 µM bestatin solution in HEPES acted as negative control while the solutions containing DMSO (0.1%) in HEPES were used as positive controls. A blank containing HEPES buffer (150 µL) and substrate (50 µL) only also acted as a negative control. Each concentration of compound was assayed in triplicate. Furthermore, all assays were carried out on three separate occasions. APN inhibitory activity was determined by comparison to blank controls.

6.2.5 Plate reader settings

Measurement type	Kinetic, 1 cycle of 20 readings
Absorbance wavelength	405 nm
Temperature	37 °C
Shaking	Once before first measurement, 15 seconds, double orbital

6.2.6 Interpretation of data

Percentage inhibition was calculated according to the following formula:

Percentage Inhibition (%) = [(blank absorbance-test absorbance)/Blank absorbance] x 100

The results were analysed using GraphPad Prism software. Dose-response curves were obtained by plotting the percentage APN inhibition (%) against log (compound concentration). Non-linear regression was used to analyse the data. The best fit IC_{50} values ± SEM were then calculated by Prism.

7 Chemistry Experimental

Starting materials and reagents were obtained from Sigma-Aldrich® and Apollo Scientific® and were not characterised.

Melting points were determined using an Electrothermal® melting point apparatus and were uncorrected.

Optical rotations were obtained using an Optical Activity Ltd AA-55 polarimeter together with a 0.5 dm path length cell.

Spectral data were obtained using the following instruments:

Infra-red (IR) spectra: A Perkin Elmer FT-IR spectrophotometer Paragon 100 was used to obtain IR spectra. Solid samples were analysed by potassium bromide (KBr) discs. Oils were analysed as films on NaCl discs (DCM).

Nuclear Magnetic Resonance (NMR): All ^{1}H and ^{13}C NMR spectra were obtained using a Bruker MSL 400 MHz and 600 MHz (as indicated). All spectra were analysed using Bruker Topspin 2.0 software. Samples were prepared in deuterated chloroform ($CDCl_3$) unless otherwise stated. Resonance positions in ppm were assigned relative to the $CHCl_3$ resonance at 7.27 ppm for ^{1}H spectra and 76.5 ppm, 76.8 ppm and 77.2 ppm for ^{13}C spectra. Signal descriptions are abbreviated as follows:
S = singlet; d = doublet; t = triplet; dd = double doublet; dt = double triplet; ddd = double double doublet; q = quartet; m = multiplet; br = broad; ArC<u>H</u> = proton attached directly to an aromatic ring; Ar<u>C</u> = carbon of an aromatic ring; Q<u>C</u> = quaternary carbon)

High Resolution Mass Spectrometry (HRMS): All high resolution mass spectral data was obtained using a Thermo LTQ-Oribtrap Discovery mass spectrometer. Data analysis was performed using Xcalibre software.

Column chromatography was carried out using silica gel 60 (230-400 mesh) (Merck Millipore). Thin layer chromatography was carried out with silica gel 60 F_{254} pre-coated aluminium sheets

(Merck Millipore). Compounds were visualised using UV at both 254 nm and 365 nm and a variety of spray reagents.

Anhydrous THF was prepared by refluxing over powder lithium aluminium hydride for 2 h and then collecting the distillate and allowing it to fall back down over sodium lumps and benzophenone. The resulting mixture was refluxed until a purple colour was obtained. The colourless distillate was used immediately.

Anhydrous DCM was prepared by distillation over powdered calcium hydride.

7.1 Original Synthesis of 9-(3-hydroxy-4-methoxyphenyl)-2,3,4-trimethoxy-5H-benzo[7]annulen-7(6H)-one (2.03)

7.1.1 Malonic Acid Coupling: Synthesis of intermediate (*E*)-3-(2,3,4-trimethoxyphenyl)acrylic acid (2.04)

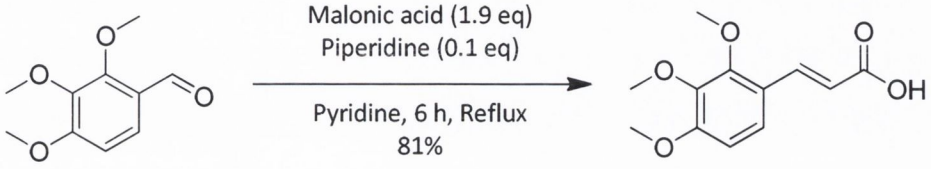

(2.04)

To a stirred solution of 2,3,4-trimethoxybenzaldehyde (15.92 g, 81.14 mmol) in pyridine (45 mL) and piperidine (0.9 mL) was added malonic acid (15.93 g, 153.03 mmol). The solution was refluxed for 6 h and then quenched by the addition of 2 M HCl (100 mL). The product was extracted with DCM (3 x 100 mL), dried over $MgSO_4$, filtered and the solvent removed *in vacuo* to afford **(2.04)** as a yellow solid (15.92 g, 81%). The product was not further purified.

R_f: 0.17 (2:1, hexane/ethyl acetate)

^{1}H NMR ($CDCl_3$, 400 MHz) δ_H ppm: 3.90 (3H, s, OC<u>H</u>$_3$), 3.93 (3H, s, OC<u>H</u>$_3$), 3.96 (3H, s, OC<u>H</u>$_3$), 6.45 (1H, d, J = 16.0 Hz, C<u>H</u>=CH), 6.73 (1H, d, J = 8.5 Hz, Ar<u>H</u>), 7.32 (1H, d, J = 8.5 Hz, Ar<u>H</u>), 8.01 (1H, d, J = 16.0 Hz, C<u>H</u>=CH)

^{13}C NMR ($CDCl_3$, 400 MHz) δ_c ppm: 55.63 (O<u>C</u>H$_3$), 60.47 (O<u>C</u>H$_3$), 61.04 (O<u>C</u>H$_3$), 107.15 (Ar<u>C</u>H), 115.60 (<u>C</u>H=CH), 120.68 (Q<u>C</u>), 123.13 (Ar<u>C</u>H), 141.56 (<u>C</u>H=CH), 141.88 (Q<u>C</u>), 153.08 (Q<u>C</u>), 155.48 (Q<u>C</u>), 172.49 (<u>C</u>=O)

ν_{MAX} (DCM)/cm^{-1} 3452.6, 2944.1, 1694.2, 1619.4, 1590.0

HRMS [M-H]$^-$: calculated 237.08, found 237.1691, molecular formula ($C_{12}H_{13}O_5$)

Melting point: 160-162 °C

7.1.2 Reduction of double bond: Synthesis of 3-(2,3,4-trimethoxyphenyl)propanoic acid (2.05)

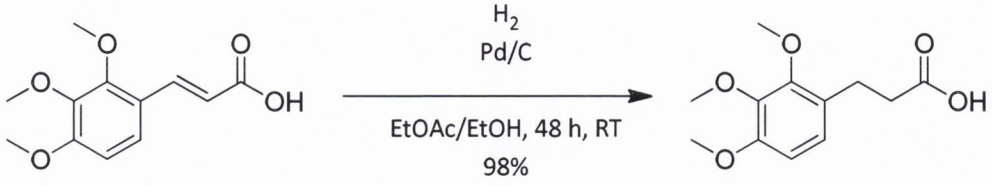

(2.04) **(2.05)**

To a stirred solution of **(2.04)** (15.65 g, 65.69 mmol) in a mixture of ethanol and ethyl acetate (1:1; 200 mL) was added palladium 5% w/w on activated carbon (0.5g). The solution was stirred under an atmosphere of hydrogen for a period of 48 h. The solution was then filtered and concentrated under reduced pressure. The resulting residue was then purified by flash column chromatography (stationary phase; silica gel 230-400 mesh, mobile phase; ethyl acetate). The homogenous fractions were collected and the solvent was removed *in vacuo* to afford **(2.05)** as a yellow solid (15.50 g, 98%).

R_f: 0.17 (2:1, hexane/ethyl acetate)

^{1}H NMR ($CDCl_3$, 400 MHz) δ_H ppm: 2.64 (2H, t, J = 8 Hz, CH=C<u>H</u>), 2.90 (2H, t, J = 8 Hz, CH=C<u>H</u>), 3.84 (3H, s, OC<u>H</u>$_3$), 3.87 (3H, s, OC<u>H</u>$_3$), 3.90 (3H, s, OC<u>H</u>$_3$), 6.60 (1H, d, J = 8.4 Hz, Ar<u>H</u>), 6.86 (1H, d, J = 8.4 Hz, Ar<u>H</u>)

^{13}C NMR ($CDCl_3$, 400 MHz) δ_c ppm: 24.69 (<u>C</u>H$_2$), 34.45 (<u>C</u>H$_2$), 55.48 (O<u>C</u>H$_3$), 60.23 (O<u>C</u>H$_3$), 60.38 (O<u>C</u>H$_3$), 106.64 (Ar<u>C</u>H), 123.33 (Ar<u>C</u>H), 125.61 (Q<u>C</u>), 141.71 (Q<u>C</u>), 151.41 (Q<u>C</u>), 152.02 (Q<u>C</u>), 190.00 (<u>C</u>=O)

ν_{MAX} (DCM)/cm^{-1} 3004.2, 2834.9, 1212.9, 1599.5

HRMS $[M+Na]^+$: calculated 263.0895, found 263.0845, molecular formula ($C_{12}H_{16}O_5Na$)

Melting point: 65-67 °C

7.1.3 Meldrum's Acid coupling and methanolysis: Synthesis of methyl 3-oxo-5-(2,3,4-trimethoxyphenyl)pentanoate (2.07)

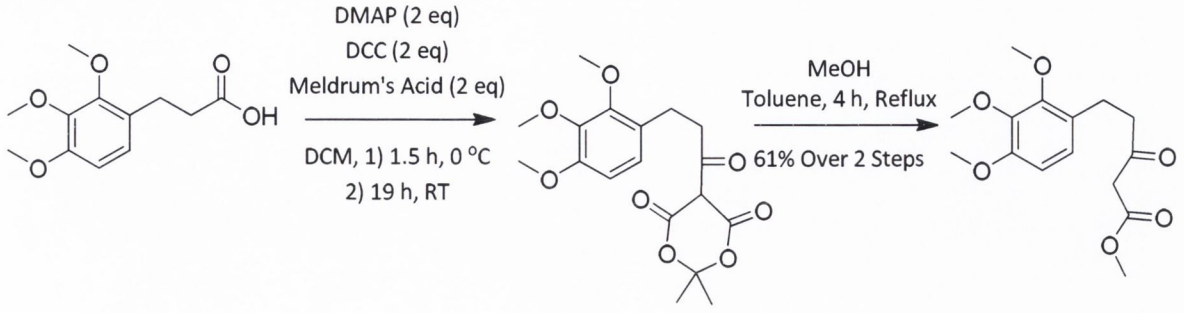

(2.05) **(2.06)** **(2.07)**

To a stirred solution of **(2.05)** (15.65 g, 59.49 mmol) in dry DCM (45 mL) under an atmosphere of nitrogen was added DMAP (14.53 g, 118.98 mmol) and Meldrum's acid (17.12 g, 118.98 mmol). The temperature of the reaction mixture was reduced to 0 °C using an ice bath. Using a pressure equalising dropping funnel, DCC (24.55 g, 118.98 mmol) dissolved in dry DCM (20 mL) was added dropwise to the reaction mixture, while maintaining the temperature at 0 °C. The reaction was left stirring under nitrogen for 90 min at 0 °C and then stirred at room temperature for 19 h. The reaction was monitored by TLC and once the coupling reaction had been deemed to have gone to completion the reaction mixture was filtered to remove the DCU. The reaction mixture was then washed with 2.5 M HCl aqueous solution (2 x 200 mL) and then with water (2 x 200 mL). The DCM solution was then dried over $MgSO_4$, filtered and concentrated under reduced pressure to afford a yellow residue. This residue was dissolved in a mixture of toluene and methanol (4:1; 300 mL) and refluxed at 110 °C for 4 h. The solvent was then removed *in vacuo* and the resulting mixture purified by flash column chromatography (stationary phase; silica gel 230-400 mesh, mobile phase; 8:1, hexane/ethyl acetate). All homogenous fractions were collected and the solvent was evaporated to afford **(2.07)** as a yellow oil (10.76 g, 61%).

R_f: 0.69 (1:1, hexane/ethyl acetate)

^{1}H NMR ($CDCl_3$, 400 MHz) δ_H ppm: 2.84 (4H, s, 2 x $C\underline{H}_2$), 3.46 (2H, s, $C\underline{H}_2$), 3.74 (3H, s, $COOC\underline{H}_3$), 3.84 (3H, s, $OC\underline{H}_3$), 3.87 (3H, s, $OC\underline{H}_3$), 3.89 (3H, s, $OC\underline{H}_3$), 6.60 (1H, d, J = 8.8 Hz, Ar$\underline{H}$), 6.83 (1H, d, J = 8.3 Hz, Ar$\underline{H}$)

^{13}C NMR ($CDCl_3$, 400 MHz) δ_c ppm: 23.72 ($\underline{C}H_2$), 43.43 ($\underline{C}H_2$), 48.64 ($\underline{C}H_2$), 51.90 ($O\underline{C}H_3$), 55.27 ($O\underline{C}H_3$), 60.29 ($O\underline{C}H_3$), 60.40 ($O\underline{C}H_3$), 107.06 (Ar$\underline{C}$H), 123.88 (Ar$\underline{C}$H), 125.83 ($\underline{Q}C$), 141.78 ($\underline{Q}C$), 151.37 ($\underline{Q}C$), 151.99 ($\underline{Q}C$), 167.16 ($\underline{C}$=O), 201.78 ($\underline{C}$=O)

ν_{MAX} (DCM)/cm^{-1} 2928.6, 1747.19, 1716.35, 1658.35, 1602.86

HRMS $[M+Na]^+$: calculated 319.1158, found 319.1156, molecular formula ($C_{15}H_{20}NaO_6$)

7.1.4 Reduction of β-keto ester: Synthesis of methyl 3-hydroxy-5-(2,3,4-trimethoxyphenyl)pentanoate (2.08)

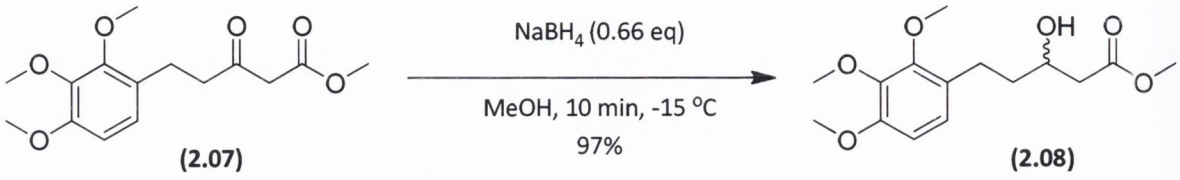

(2.07) **(2.08)**

To a stirred solution of **(2.07)** (3.97 g, 13.4 mmol) in methanol (65 mL) at -15 °C was added sodium borohydride (0.34 g, 8.93 mmol). After 10 min, the reaction was quenched by the addition of water (100 mL). The resulting solution was the acidified by the addition of 2 M HCl aqueous solution (10 mL). The methanol was removed under reduced pressure and the resulting aqueous solution was extracted with diethyl ether (3 x 100 mL). The ethyl ether extracts were dried over $MgSO_4$, filtered and concentrated *in vacuo*. The resulting residue was then purified by flash column chromatography (stationary phase; silica gel 230-400 mesh, mobile phase; 4:1, hexane/ethyl acetate). All homogenous fractions were collected and the solvent was removed to afford **(2.08)** as a clear oil (3.89 g, 97%).

R_f: 0.36 (1:1, hexane/ethyl acetate)

^{1}H NMR ($CDCl_3$, 400 MHz) δ_H ppm: 1.69-1.80 (2H, m, C$\underline{H_2}$), 2.48-2.51 (2H, m, C$\underline{H_2}$), 2.68-2.73 (2H, m, C$\underline{H_2}$), 2.18 (H, s, br, O$\underline{H}$), 3.71 (3H, s, COOC$\underline{H_3}$), 3.85 (3H, s, OC$\underline{H_3}$), 3.88 (3H, s, OC$\underline{H_3}$), 3.90 (3H, s, OC$\underline{H_3}$), 3.97-4.00 (1H, m, C$\underline{H}$OH), 6.63 (1H, d, J = 8.5 Hz, Ar$\underline{H}$), 6.86 (1H, d, J = 8.5 Hz, Ar$\underline{H}$)

^{13}C NMR ($CDCl_3$, 400 MHz) δ_c ppm: 25.13 (C$\underline{H_2}$), 37.19 (C$\underline{H_2}$), 40.73 (C$\underline{H_2}$), 51.29 (COOC$\underline{H_3}$), 55.54 (OC$\underline{H_3}$), 60.31 (OC$\underline{H_3}$), 60.55 (OC$\underline{H_3}$), 66.73 (C$\underline{H}$OH) 106.92 (ArC$\underline{H}$), 123.53 (ArC$\underline{H}$), 126.91 (Q$\underline{C}$), 141.72 (Q$\underline{C}$), 151.30 (Q$\underline{C}$), 151.64 (Q$\underline{C}$), 172.82 ($\underline{C}$=O)

ν_{MAX} (DCM)/cm^{-1} 3448.07, 2934.16, 1736.64, 1602.64

HRMS $[M+Na]^+$: calculated 321.1314, found 321.1301 , molecular formula ($C_{15}H_{22}NaO_6$)

7.1.5 Protection of secondary alcohol: Synthesis of methyl 3-((*tert*-butyldiphenylsilyl)oxy)-5-(2,3,4-trimethoxyphenyl)pentanoate (2.09)

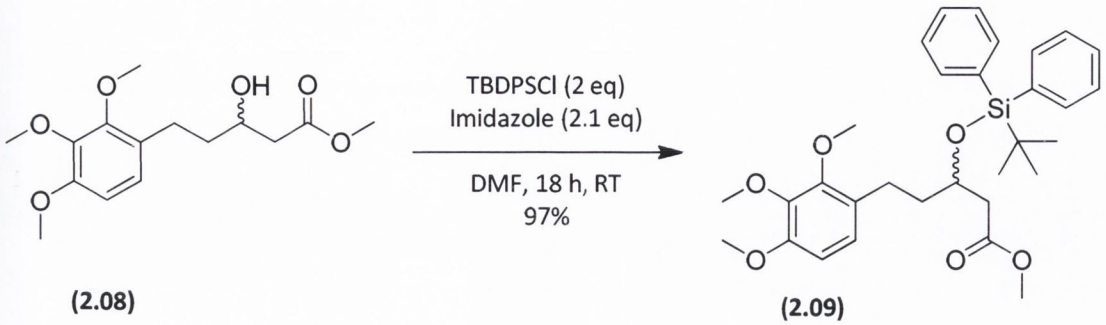

(2.08) **(2.09)**

To a stirred solution of **(2.08)** (4.09 g, 13.8 mmol) in dry DMF (30 mL) under anhydrous conditions was added *tert*-butyldiphenylsilyl chloride (5.39 mL, 13.8 mmol) and imidazole (1.5 g, 22.09 mmol). After 18 h, the reaction was quenched by the addition of water (3 x 100 mL). The reaction mixture was then extracted with diethyl ether (3 x 100 mL). The diethyl ether extracts were dried over $MgSO_4$, filtered and concentrated under vacuum. The resulting residue was purified by flash column chromatography (stationary phase; silica gel 230-400 mesh, mobile phase; 10:1, hexane/ethyl acetate) to yield **(2.09)** as a clear oil (7.2 g, 97%).

R_f: 0.15 (7:1, hexane/ethyl acetate)

^{1}H NMR ($CDCl_3$, 400 MHz) δ_H ppm: 1.08 (9H, s, C(CH_3)$_3$), 1.73-1.78 (2H, m, CH_2), 2.4-2.59 (4H, m, 2 x CH_2), 3.56 (3H, s, COOCH_3), 3.77 (3H, s, OCH_3), 3.84 (3H, s, OCH_3), 3.85 (3H, s, OCH_3), 4.27-4.30 (1H, m, CHOSi), 6.54 (1H, d, J = 8.5 Hz, ArH), 6.60 (1H, d, J = 8.5 Hz, ArH), 7.28-7.38 (6H, m, ArH), 7.68-7.78 (4H, m, ArH)

^{13}C NMR ($CDCl_3$, 400 MHz) δ_c ppm: 18.90 (C(CH_3)$_3$), 24.59 (CH_2), 26.47 (C(CH_3)$_3$, 37.8 (CH_2), 41.35 (CH_2), 50.98 (COOCH_3), 55.54 (OCH_3), 60.24 (OCH_3), 60.33 (OCH_3), 69.87 (CHOSi) 106.64 (ArCH), 123.04 (ArCH), 127.05 (2 x ArCH), 127.09 (2 x ArCH), 129.12 (ArCH), 129.15 (ArCH), 135.44 (2 x ArCH), 135.5 (2 x ArCH), 127.40 (2 x QC), 133.54 (QC), 141.70 (QC), 151.28 (QC), 151.43 (QC), 171.46 (C=O)

ν_{MAX} (DCM)/cm^{-1} 3399.49, 1740, 750

HRMS $[M+Na]^+$: calculated 559.2492, found 559.2488, molecular formula ($C_{31}H_{40}NaO_6Si$)

7.1.6 Hydrolysis of methyl ester: Synthesis of 3-((*tert*-butyldiphenylsilyl)oxy)-5-(2,3,4-trimethoxyphenyl)pentanoic acid (2.10)

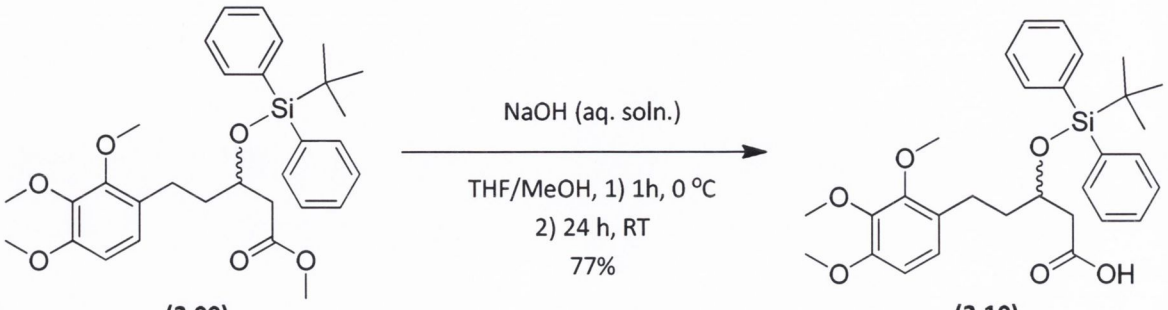

(2.09) **(2.10)**

To a stirred solution of **(2.09)** (1.75 g, 3.26 mmol) in a mixture of methanol (17 mL) and THF (13 mL) at 0 °C was added 2.5 M NaOH aqueous solution (4 mL). After 1 h, the temperature was increased to room temperature and the reaction was left stirring for 24 h. The solution was then acidified with 2 M HCl aqueous solution and the volatile solvents removed under reduced pressure. The aqueous reaction mixture was then extracted with diethyl ether (3 x 100 mL). The diethyl ether extracts were dried over $MgSO_4$, filtered and concentrated *in vacuo.* The resulting residue was then purified by flash column chromatography (stationary phase; silica gel 230-400 mesh, mobile phase; 3:1, hexane/ethyl acetate) to yield **(2.10)** as a white solid (1.32 g, 77%).

R_f: 0.32 (1:1, hexane/ethyl acetate)

^{1}H NMR ($CDCl_3$, 400 MHz) δ_H ppm: 1.09 (9H, s, C(C$\underline{H}_3$)$_3$), 1.8 (2H, m, C$\underline{H}_2$), 2.42-2.51 (2H, m, C$\underline{H}_2$), 2.62 (2H, m, C$\underline{H}_2$), 3.77 (3H, s, OC$\underline{H}_3$), 3.84 (3H, s, OC$\underline{H}_3$), 3.85 (3H, s, OC$\underline{H}_3$), 4.21 (1H, m, C$\underline{H}$OSi), 6.53 (1H, d, J = 8.5 Hz, Ar$\underline{H}$), 6.58 (1H, d, J = 8.5 Hz, Ar$\underline{H}$), 7.39-7.44 (6H, m, Ar$\underline{H}$), 7.67-7.71 (4H, m, Ar$\underline{H}$)

^{13}C NMR ($CDCl_3$, 400 MHz) δ_c ppm: 19.29 (C(CH$_3$)$_3$), 25.25 (C$\underline{H}_2$), 26.94 (C(C$\underline{H}_3$)$_3$, 37.84 (C$\underline{H}_2$), 40.87 (C$\underline{H}_2$), 56.00 (OC$\underline{H}_3$), 60.69 (OC$\underline{H}_3$), 60.77 (OC$\underline{H}_3$), 70.25 (C$\underline{H}$OSi) 107.14 (ArC$\underline{H}$), 123.49 (ArC$\underline{H}$), 127.38 (Q$\underline{C}$), 127.67 (2 x ArC$\underline{H}$), 127.69 (2 x ArC$\underline{H}$), 129.84 (ArC$\underline{H}$), 129.87 (ArC$\underline{H}$), 133.27 (2 x Q$\underline{C}$), 135.87 (2 x ArC$\underline{H}$), 135.92 (2 x ArC$\underline{H}$), 141.72 (Q$\underline{C}$), 151.30 (Q$\underline{C}$), 151.50 (Q$\underline{C}$), 177.26 ($\underline{C}$=O)

ν_{MAX} (DCM)/cm^{-1} 2933.36, 1720, 1709.58, 1602.65, 1494.82

HRMS $[M+Na]^+$: calculated 545.2335, found 545.2374 , molecular formula ($C_{30}H_{38}O_6SiNa$)

Melting point: 109-112 °C

7.1.7 Cyclisation: Synthesis of 7-((*tert*-butyldiphenylsilyl)oxy)-1,2,3-trimethoxy-6,7,8,9-tetrahydro-5*H*-benzo[7]annulen-5-one (2.11)

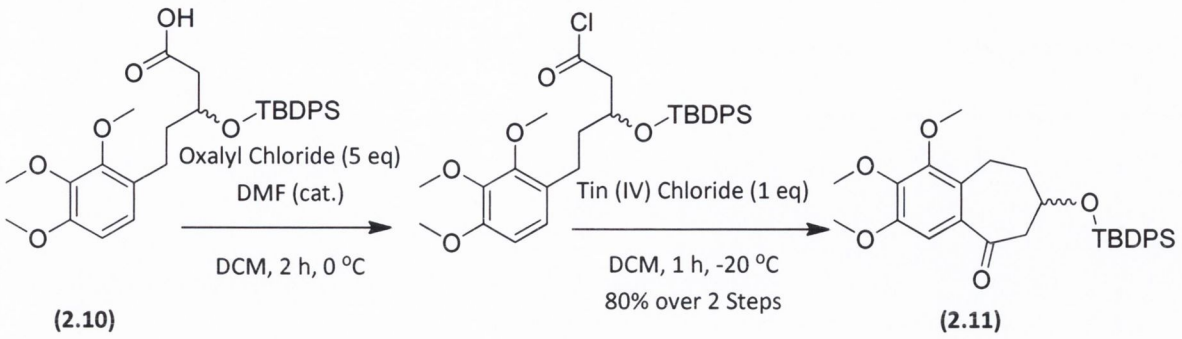

(2.10) **(2.11)**

To a stirred solution of **(2.10)** (0.99 g, 1.89 mmol) in dry DCM (8 mL) and DMF (0.2 mL) at 0 °C under an atmosphere of nitrogen was added 2 M oxalyl chloride solution (4.74 mL, 9.46 mmol) dropwise. The solution was left stirring for 2 h at 0 °C after which time the solvent was removed under high vacuum at room temperature. The residue was left to dry under high vacuum for 2 h after which time the residue was reconstituted with dry DCM (20 mL) under an atmosphere of nitrogen. The temperature of the solution was reduced to -20 °C using a sodium chloride ice bath and 1 M Tin (IV) Chloride solution in DCM (1.89 mL, 1.89 mmol) was added dropwise. After 1 h, the reaction was quenched by the addition of saturated sodium chloride aqueous solution (50 mL) and the mixture was extracted with diethyl ether (3 x 50 mL). The organic fractions were dried over $MgSO_4$, filtered and concentrated *in vacuo.* The resulting residue was then purified by flash column chromatography (stationary phase; silica gel 230-400 mesh, mobile phase; 10:1, hexane/ethyl acetate) to yield **(2.11)** as a yellow oil (0.76 g, 80%).

R_f: 0.63 (1:1, hexane/ethyl acetate)

^{1}H NMR ($CDCl_3$, 400 MHz) δ_H ppm: 1.06 (9H, s, C(CH_3)$_3$), 1.88-1.90 (1H, m, CH_2), 2.00-2.10 (1H, m, CH_2), 2.92-2.98 (2H, m, CH_2), 3.04-3.10 (1H, m, CH_2), 3.10-3.19 (1H, m, CH_2), 3.86 (3H, s, OCH_3), 3.89 (3H, s, OCH_3), 3.95 (3H, s, OCH_3), 4.34 (1H, m, CHOSi), 7.19 (1H, s, ArH), 7.38-7.45 (6H, m, ArH), 7.46-7.67 (4H, m, ArH)

^{13}C NMR ($CDCl_3$, 400 MHz) δ_c ppm: 19.18 (C(CH_3)$_3$), 21.02 (CH_2), 26.92 (C(CH_3)$_3$, 38.38 (CH_2), 50.27 (CH_2), 55.95 (OCH_3), 60.85 (OCH_3), 61.13 (OCH_3), 68.30 (CHOSi) 107.59 (ArCH), 127.71 (2 x ArCH), 127.74 (2 x ArCH), 129.80 (ArCH), 129.85 (ArCH), 130.84 (QC), 133.75 (QC), 133.93 (QC), 134.69 (QC), 135.78 (2 x (ArCH), 135.84 (2 x ArCH), 145.61 (QC), 151.12 (QC), 151.46 (QC), 199.58 (C=O)

ν_{MAX} (DCM)/cm^{-1} 3054.40, 2987.13, 2305.64, 1551.22, 1421.66

HRMS $[M+Na]^+$: calculated 527.2230 found 527.2264, molecular formula ($C_{30}H_{36}NaO_5Si$)

7.1.8 Synthesis of 5-bromo-2-methoxyphenol (2.13)

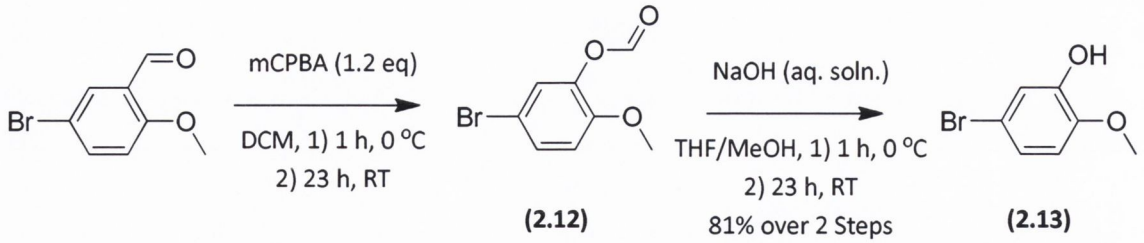

(2.12) **(2.13)**

To a stirred solution of 5-bromo-2-methoxybenzaldehyde (10.07 g, 46.83 mmol) in DCM (50 mL) at 0 °C was added mCPBA (9.75 g, 56.52 mmol) dissolved in DCM (100 mL) dropwise. After 1 h, the temperature was allowed to increase to room temperature and the reaction was left stirring for 23 h. The reaction mixture was then filtered to remove the precipitated 3-chlorobenzoic acid and the DCM solution was washed with saturated sodium hydrogen carbonate aqueous solution (2 x 100 mL), water (100 mL) and then saturated sodium chloride solution (100 mL). The DCM was then removed *in vacuo* and the resulting residue dissolved in methanol (97 mL) and THF (75 mL). 2.5 M NaOH aqueous solution (2.5 mL) was then added to the stirred solution at 0°C. After 1 h, the temperature was allowed to increase to room temperature and the reaction was left stirring for a further 23 h. The reaction was then quenched by the addition of 2 M HCl aqueous solution (50 mL) and the organic solvents were removed under reduced pressure. The resulting aqueous mixture was extracted with diethyl ether (3 x 50 mL). The organic fractions were dried over $MgSO_4$, filtered and concentrated *in vacuo.* The resulting residue was then purified by flash column chromatography (stationary phase; silica gel 230-400 mesh, mobile phase; 4:1, hexane/ethyl acetate) to yield **(2.13)** as an off white solid (7.65 g, 81%).

R_f: 0.19 (5:1, hexane/ethyl acetate)

^{1}H NMR ($CDCl_3$, 400 MHz) δ_H ppm: 3.85 (3H, s, OC<u>H</u>$_3$), 6.00 (1H, s, br, ArO<u>H</u>), 6.70 (1H, d, J = 8.5 Hz, Ar<u>H</u>), 6.98 (1H, dd, J_1 = 8.5 Hz, J_2 = 2.4 Hz, Ar<u>H</u>), 7.10 (1H, d, J = 2.4 Hz, Ar<u>H</u>)

^{13}C NMR ($CDCl_3$, 400 MHz) δ_c ppm: 56.12 (O<u>C</u>H$_3$), 112.03 (Ar<u>C</u>H), 113.20 (Q<u>C</u>), 117.91 (Ar<u>C</u>H), 122.89 (Ar<u>C</u>H), 145.99 (Q<u>C</u>), 146.48 (Q<u>C</u>)

ν_{MAX} (DCM)/cm^{-1} 3519.06, 5053.97, 2843.41, 1593.21, 1499.56

HRMS $[M+H]^+$: calculated 201.9629, found 201.9860, molecular formula ($C_7H_7BrO_2$)

Melting point: 59 °C

7.1.9 Protection of Phenol: Synthesis of (5-bromo-2-methoxyphenoxy)(*tert*-butyl)dimethylsilane (2.14)

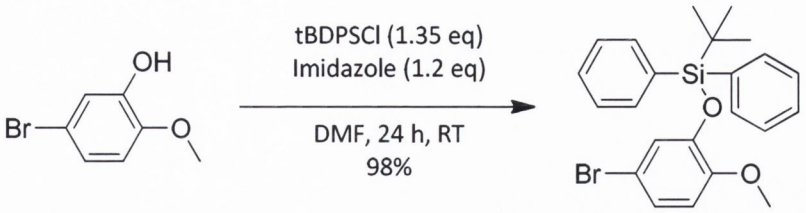

(2.13) **(2.14)**

To a stirred solution of **(2.13)** (7.65 g, 37.68 mmol) in dry DMF (60 mL) under an atmosphere of nitrogen was added imidazole (6.41 g, 94.21 mmol) and *tert*-butyldimethylsilyl chloride (7.67 g, 50.87 mmol). The reaction was left stirring for 24 h. The reaction was then quenched by the addition of water (100 mL). The aqueous mixture was extracted with diethyl ether (3 x 100 mL). The organic fractions were dried over $MgSO_4$, filtered and concentrated *in vacuo.* The resulting residue was then purified by flash column chromatography (stationary phase; silica gel 230-400 mesh, mobile phase; 20:1, hexane/ethyl acetate) to afford **(2.14)** as a clear, colourless oil (11.72 g, 98%).

R_f: 0.71 (3:1, hexane/ethyl acetate)

^{1}H NMR ($CDCl_3$, 400 MHz) δ_H ppm: 0.18 (6H, s, Si($C\underline{H}_3$)$_2$), 1.02 (9H, s, C($C\underline{H}_3$)$_3$), 3.80 (3H, s, O$C\underline{H}_3$), 6.73 (1H, d, J = 8.6 Hz, Ar$\underline{H}$), 7.02 (1H, m, Ar$\underline{H}$), 7.04 (1H, d, J = 6 Hz, Ar$\underline{H}$)

^{13}C NMR ($CDCl_3$, 400 MHz) δ_c ppm: -4.60 (Si($\underline{C}H_3$)$_2$), 18.46 ($\underline{C}$(CH_3)$_3$), 25.66 (C($\underline{C}H_3$)$_3$, 55.55 (O$\underline{C}H_3$), 112.39 ($\underline{Q}C$), 113.22 (Ar$\underline{C}$H), 124.08 (Ar$\underline{C}$H), 146.00 (Ar$\underline{C}$H), 150.45 (Ar$\underline{C}$H)

ν_{MAX} (DCM)/cm^{-1} 3546.14, 2955.31, 2930.67, 1585.93

HRMS $[M+H]^+$: calculated 339.0392, found 339.0374, molecular formula ($C_{13}H_{21}BrO_2SiNa$)

7.1.10 Organolithium coupling: Synthesis of *tert*-butyl((9-(3-((*tert*-butyldimethylsilyl)oxy)-4-methoxyphenyl)-2,3,4-trimethoxy-6,7-dihydro-5*H*-benzo[7]annulen-7-yl)oxy)diphenylsilane (2.15)

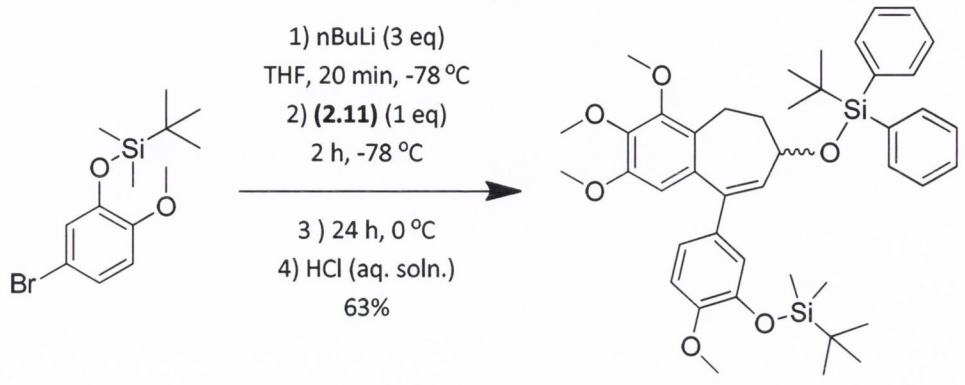

(2.14) **(2.15)**

To a stirred solution of **(2.14)** (1.40 g, 4.4 mmol) dissolved in dry THF (4 mL) under anhydrous conditions at -78 °C was added 2.5 M *n*-butyllithium in hexane (1.1 mL, 4.4 mmol) dropwise. After 20 min, a solution of **(2.11)** (0.74 g, 1.46 mmol) in dry THF (20 mL) was added dropwise. After 2 h, the temperature was allowed to increase to 0°C and the reaction was stirred at this temperature for 24 h. The reaction was quenched by the addition of 2 M HCl aqueous solution (50 mL) and the aqueous layer was extracted with diethyl ether (3 x 50 mL). The organic fractions were dried over $MgSO_4$, filtered and concentrated *in vacuo.* The resulting residue was then purified by flash column chromatography (stationary phase; silica gel 230-400 mesh, mobile phase; 10:1, hexane/ethyl acetate) to afford **(2.15)** as a viscous, yellow oil (0.67 g, 63%).

R_f: 0.75 (4:1, hexane/ethyl acetate)

^{1}H NMR ($CDCl_3$, 400 MHz) δ_H ppm: 0.20 (3H, s, Si($C\underline{H}_3$)$_2$), 0.22 (3H, s, Si($C\underline{H}_3$)$_2$), 1.06 (9H, s, C($C\underline{H}_3$)$_3$), 1.13 (9H, s, C($C\underline{H}_3$)$_3$), 2.33 (3H, m, 2 x $C\underline{H}_2$), 2.96 (1H, m, $C\underline{H}_2$), 3.68 (3H, s, $OC\underline{H}_3$), 3.79 (3H, s, $OC\underline{H}_3$), 3.88 (3H, s, $OC\underline{H}_3$), 3.92 (3H, s, $OC\underline{H}_3$), 4.20 (1H, m, C<u>H</u>OH), 6.25 (1H, s, Ar<u>H</u>), 6.31 (1H, d, J = 5.0 Hz, C=C<u>H</u>), 6.70 (3H, m, Ar<u>H</u>), 6.75 (6H, m, Ar<u>H</u>), 7.36 (4H, m, Ar<u>H</u>)

^{13}C NMR ($CDCl_3$, 400 MHz) δ_c ppm: -4.99 (Si($\underline{C}H_3$)$_2$), 18.06 ($\underline{C}$(CH_3)$_3$), 18.72 ($\underline{C}$(CH_3)$_3$), 21.40 ($\underline{C}H_2$), 25.34 (C($\underline{C}H_3$)$_3$), 26.53 (C($\underline{C}H_3$)$_3$), 43.42 ($\underline{C}H_2$), 55.11 ($O\underline{C}H_3$), 55.45 ($O\underline{C}H_3$), 60.42 ($O\underline{C}H_3$), 61.13 ($O\underline{C}H_3$), 70.88 (<u>C</u>H), 108.19 (Ar<u>C</u>H), 111.19 (Ar<u>C</u>H), 120.29 (Ar<u>C</u>H), 121.06 (Ar<u>C</u>H), 127.02 (2 x Ar<u>C</u>H), 127.28 (2 x Ar<u>C</u>H), 127.52 (Q<u>C</u>), 129.09 (Ar<u>C</u>H), 129.19 (Ar<u>C</u>H), 132.14 (Q<u>C</u>), 133.83 (Q<u>C</u>), 133.97 (Ar<u>C</u>H), 134.40 (Q<u>C</u>), 135.36 (2 x Ar<u>C</u>H), 135.61 (2 x Ar<u>C</u>H), 137.25 (Q<u>C</u>), 140.75 (Q<u>C</u>), 144.14 (Q<u>C</u>), 150.03 (Q<u>C</u>), 150.19 (Q<u>C</u>), 150.40 (Q<u>C</u>)

ν_{MAX} (DCM)/cm^{-1} 1509.19, 1113.77, 838.33

HRMS $[M+Na]^+$: calculated 747.3513, found 747.3469, molecular formula ($C_{43}H_{56}O_6Si_2Na$)

7.1.11 Deprotection: Synthesis of 9-(3-hydroxy-4-methoxyphenyl)-2,3,4-trimethoxy-6,7-dihydro-5*H*-benzo[7]annulen-7-ol (2.02)

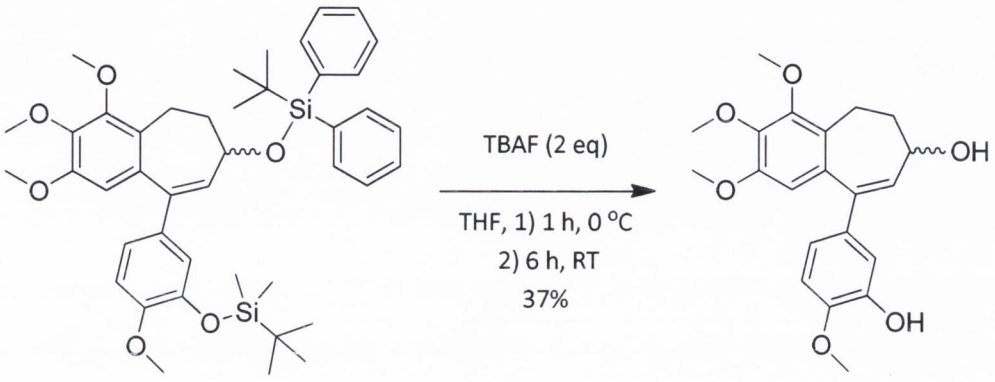

(2.15) **(2.02)**

To a stirred solution of **(2.15)** (0.61 g, 1.21 mmol) in THF (6.1 mL) at 0 °C was added 1 M tetrabutylammonium fluoride solution (2.42 mL, 2.42 mmol). After 1 h, the temperature was allowed to increase to room temperature and the reaction was left stirring for 6 h. The solvent was removed by blowing with nitrogen and the resulting residue was purified by flash column chromatography (stationary phase; silica gel 230-400 mesh, mobile phase; 4:1, hexane/ethyl acetate) to yield **(2.02)** as a white solid (0.17 g, 37% yield).

R_f: 0.31 (1:1, hexane/ethyl acetate)

^{1}H NMR ($CDCl_3$, 400 MHz) δ_H ppm: 2.06-2.14 (1H, m, C$\underline{H}_2$), 2.29-2.37 (1H, m, C$\underline{H}_2$), 2.26-2.55 (1H, m, C$\underline{H}_2$), 2.63 (1H, br s, O$\underline{H}$), 2.99-3.04 (1H, m, C$\underline{H}_2$), 3.66 (3H, s, OC$\underline{H}_3$), 3.88 (3H, s, OC$\underline{H}_3$), 3.89 (3H, s, OC$\underline{H}_3$), 3.91 (3H, s, OC$\underline{H}_3$), 4.10-4.18 (1H, m, C$\underline{H}$OH), 6.02 (1H, s br, O$\underline{H}$), 6.28 (1H, d, J = 5 Hz, C=C$\underline{H}$), 6.36 (1H, s , Ar$\underline{H}$), 6.78 (2H, s, 2 x Ar$\underline{H}$), 6.89 (1H, s, Ar$\underline{H}$)

^{13}C NMR ($CDCl_3$, 400 MHz) δ_c ppm: 21.08 (C$\underline{H}_2$), 43.3 (C$\underline{H}_2$), 55.99 (2 x OC$\underline{H}_3$), 60.91 (OC$\underline{H}_3$), 61.59 (OC$\underline{H}_3$), 69.74 (C$\underline{H}$OH), 108.83 (Ar$\underline{C}$H), 110.48 (Ar$\underline{C}$H), 114.42 (Ar$\underline{C}$H) 119.81 (Ar$\underline{C}$H), 128.01 (Q$\underline{C}$), 131.8 (C=$\underline{C}$H)), 134.6 (Q$\underline{C}$), 135.28 (Q$\underline{C}$), 138.51 (Q$\underline{C}$), 141.39 (Q$\underline{C}$), 145.35 (Q$\underline{C}$), 146.36 (Q$\underline{C}$), 150.7 (Q$\underline{C}$), 151.1 (Q$\underline{C}$)

ν_{MAX} (DCM)/cm^{-1}: 3411.41, 2935.49, 2838.98, 1717.00, 1580.70

HRMS $[M-H]^-$: calculated 371.15, found 371.1484, molecular formula ($C_{21}H_{23}O_6$)

Melting point: 54-56 °C

7.1.12 Oxidation: Synthesis of 9-(3-hydroxy-4-methoxyphenyl)-2,3,4-trimethoxy-5*H*-benzo[7]annulen-7(6*H*)-one (2.03)

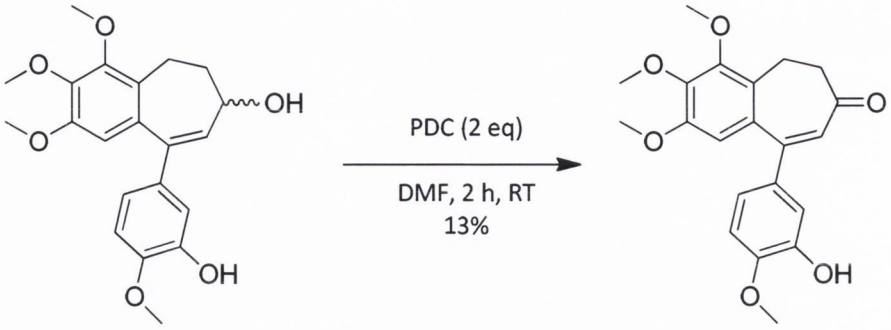

(2.02) **(2.03)**

To a stirred solution of **(2.02)** (2.3 g, 6.20 mmol) in DMF (20 mL) was added pyridinium dichromate (4.66 g, 12.39 mmol). After 1 h, the reaction was quenched by the addition of 2 M HCl aqueous solution (20 mL) and extracted with diethyl ether (3 x 25 mL). The organic fractions were dried over $MgSO_4$, filtered and concentrated *in vacuo.* The resulting residue was then purified by flash column chromatography (stationary phase; silica gel 230-400 mesh, mobile phase; 4:1, hexane/ethyl acetate) to yield **(2.03)** as an off white solid (0.3 g, 13%).

R_f: 0.53 (1:1, hexane/ethyl acetate)

^{1}H NMR ($CDCl_3$, 400 MHz) δ_H ppm: 2.72 (2H, t, J = 7 Hz, C$\underline{H}_2$), 3.16 (2H, t, J = 6 Hz C$\underline{H}_2$), 3.65 (3H, s, OC$\underline{H}_3$), 3.90 (3H, s, OC$\underline{H}_3$), 3.91 (3H, s, OC$\underline{H}_3$), 3.93 (3H, s, OC$\underline{H}_3$), 5.63 (1H, s, br, ArO$\underline{H}$), 6.39 (1H, s, C=C$\underline{H}$), 6.39 (1H, s, Ar$\underline{H}$), 6.87 (1H, d, J = 8.3 Hz Ar$\underline{H}$), 6.92 (2H,m,2 x Ar$\underline{H}$)

^{13}C NMR ($CDCl_3$, 400 MHz) δ_c ppm: 20.10 (C$\underline{H}_2$), 45.54 (C$\underline{H}_2$), 55.91 (OC$\underline{H}_3$), 55.85 (OC$\underline{H}_3$), 60.78 (OC$\underline{H}_3$), 61.26 (OC$\underline{H}_3$), 110.04 (ArC$\underline{H}$), 111.80 (C=C$\underline{H}$), 115.27 (ArC$\underline{H}$), 121.02 (ArC$\underline{H}$), 128.02 (ArC$\underline{H}$), 128.96 (Q$\underline{C}$), 132.33 (Q$\underline{C}$), 135.87 (Q$\underline{C}$), 143.13 (Q$\underline{C}$), 145.10 (Q$\underline{C}$), 147.15 (Q$\underline{C}$), 149.83 (Q$\underline{C}$), 150.95 (Q$\underline{C}$), 151.52 (Q$\underline{C}$), 203.97 ($\underline{C}$=O)

ν_{MAX} (DCM)/cm^{-1}: 2098.99, 1643.16, 1509.08, 1493.06

HRMS [M-H]$^-$: calculated 369.13, found 369.1561, molecular formula ($C_{21}H_{21}O_6$)

Melting Point: 132 °C

7.2 Alternative Synthesis of 9-(3-hydroxy-4-methoxyphenyl)-2,3,4-trimethoxy-5H-benzo[7]annulen-7(6H)-one (2.03)

7.2.1 Wittig Reaction: Synthesis of (*E*)-ethyl 3-oxo-5-(2,3,4-trimethoxyphenyl)pent-4-enoate (2.16)

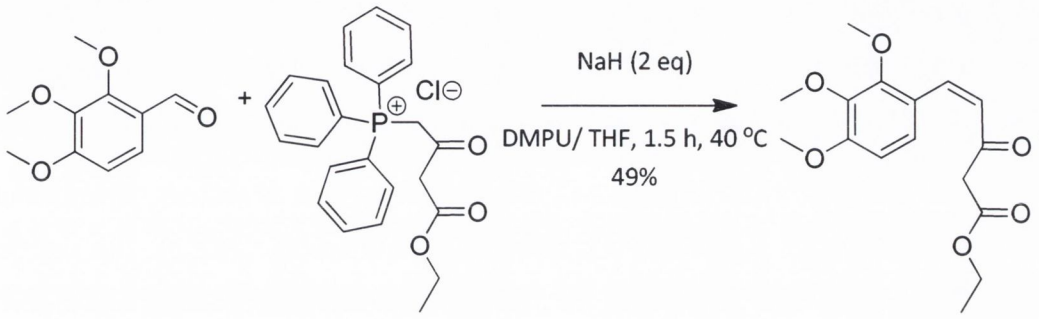

(2.16)

To a stirred solution of [3-(ethoxycarbonyl)-2-oxypropyl] triphenylphosphonium chloride (4.35 g, 10.19 mmol) in dry THF (10 mL) and *N*,*N*-dimethylpropyleneurea (5 mL) under an atmosphere of nitrogen was added sodium hydride 60% dispersion in mineral oil (0.82 g, 20.39 mmol). After 20 min, a solution of 2,3,4-trimethoxybenzaldehyde (1.00 g, 5.1 mmol) in dry THF (5 mL) was added to the reaction. The reaction was then heated to 40 °C and left stirring for 90 min. The reaction was quenched by the addition of saturated ammonium chloride aqueous solution (50 mL) and extracted with diethyl ether (3 x 50 mL). The organic fractions were dried over $MgSO_4$, filtered and concentrated *in vacuo.* The resulting oily residue was then subjected to flash column chromatography (stationary phase; silica gel 230-400 mesh, mobile phase; 4:1, hexane/ethyl acetate) to yield a crude, bright yellow oil. The mixture containing **(2.16)** (0.76 g, 49%) was not purified further.

7.2.2 Reduction: Synthesis of ethyl 3-oxo-5-(2,3,4-trimethoxyphenyl)pentanoate (2.17) and ethyl 3-hydroxy-5-(2,3,4-trimethoxyphenyl)pentanoate (2.18)

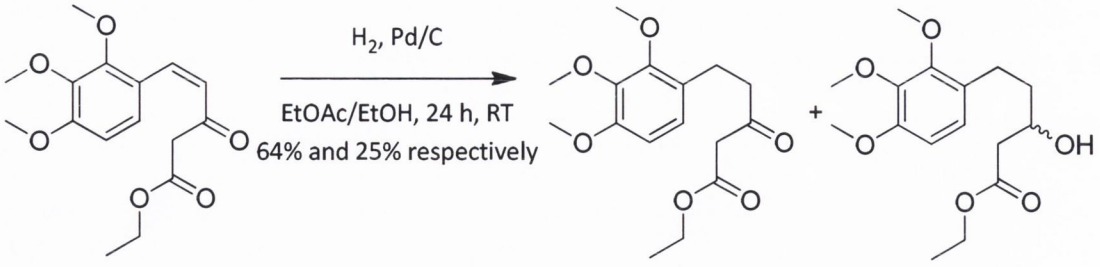

(2.16) **(2.17)** **(2.18)**

To a stirred solution of **(2.16)** (0.76 g, 2.46 mmol) in a mixture of ethanol (25 mL) and ethyl acetate (25 mL) was added palladium 5% w/w on activated carbon (0.1 g). The reaction was stirred under an atmosphere of hydrogen for 24 h. The palladium on activated carbon was filtered off and the solvent removed *in vacuo*. The resulting residue was purified by flash column chromatography (stationary phase; silica gel 230-400 mesh, mobile phase; 10:1, hexane/ethyl acetate) to yield **(2.17)** as a yellow oil (0.49 g, 64%) and **(2.18)** as a clear oil (0.19 g, 25%).

(2.17)

R_f: 0.52 (1:1, hexane/ethyl acetate)

^{1}H NMR ($CDCl_3$, 400 MHz) δ_H ppm: 1.17 (3H, t, J = 7.27 Hz, C$\underline{H}_3$), 2.74 (4H, s, 2 x C$\underline{H}_2$), 3.36 (2H, s, C$\underline{H}_2$), 3.73 (3H, s, OC$\underline{H}_3$), 3.76 (3H, s, OC$\underline{H}_3$), 3.79 (3H, s, OC$\underline{H}_3$), 4.08 (2H, q, J = 7.02 Hz, C$\underline{H}_2$), 6.50 (1H, d, J = 8.7 Hz, Ar$\underline{H}$), 6.73 (1H, d, J = 8.7 Hz, Ar$\underline{H}$)

^{13}C NMR ($CDCl_3$, 400 MHz) δ_c ppm: 13.52 (C$\underline{H}_3$), 23.54 (C$\underline{H}_2$), 43.22 (C$\underline{H}_2$), 48.71 (C$\underline{H}_2$), 55.34 (OC$\underline{H}_3$), 60.06 (OC$\underline{H}_3$), 60.21 (OC$\underline{H}_3$), 60.66 (C$\underline{H}_2$), 106.61 (C$\underline{H}$), 123.37 (C$\underline{H}$), 125.80 (Q$\underline{C}$), 141.64 (Q$\underline{C}$), 151.25 (Q$\underline{C}$), 151.85 (Q$\underline{C}$), 166.64 ($\underline{C}$=O), 201.80 ($\underline{C}$=O)

ν_{MAX} (DCM)/cm^{-1}: 2979.52, 2938.41, 2836.11, 1743.98 (C=O), 1716.23 (C=O), 1602.86

HRMS $[M+Na]^+$: calculated 333.1314, found 333.1320, molecular formula ($C_{16}H_{22}NaO_6$)

(2.18)

R_f: 0.37 (1:1, hexane/ethyl acetate)

^{1}H NMR ($CDCl_3$, 400 MHz) δ_H ppm: 1.25 (3H, t, J = 7.42 Hz, C$\underline{H}_3$), 1.72 (2H, m, C$\underline{H}_2$), 2.47 (2H, m, C$\underline{H}_2$) 2.69 (2H, m, C$\underline{H}_2$), 3.28 (1H, s, CHO$\underline{H}$), 3.83 (3H, s, OC$\underline{H}_3$), 3.86 (3H, s, OC$\underline{H}_3$), 3.88 (3H, s, OC$\underline{H}_3$), 3.98 (1H, m, C$\underline{H}$OH), 4.15 (2H, m, C$\underline{H}_2$), 6.60 (1H, d, J = 8.5 Hz, Ar$\underline{H}$), 6.84 (1H, d, J = 8.5 Hz, Ar$\underline{H}$)

^{13}C NMR ($CDCl_3$, 400 MHz) δ_c ppm: 13.70 (<u>CH_3</u>), 25.14 (<u>CH_2</u>), 37.20 (<u>CH_2</u>), 40.95 (<u>CH_2</u>), 55.51 (<u>CH_3</u>), 60.15 (<u>CH_2</u>), 60.27 (<u>CH_3</u>), 60.51 (<u>CH_3</u>), 66.78 (<u>CH</u>OH), 106.88 (<u>CH</u>), 123.51 (<u>CH</u>), 127.00 (Q<u>C</u>), 141.70 (Q<u>C</u>), 151.31 (Q<u>C</u>), 151.60 (Q<u>C</u>), 172.39 (<u>C</u>=O)

ν_{MAX} (DCM)/cm^{-1}: 3501.04, 2935.26, 1726.08 (C=O), 1602.29, 1493.66, 1467.89

HRMS $[M+Na]^+$: calculated 335.1471 , found 335.1474, molecular formula ($C_{16}H_{24}NaO_6$)

7.2.3 Reduction of β-keto ester: Synthesis of ethyl 3-hydroxy-5-(2,3,4-trimethoxyphenyl)pentanoate (2.18)

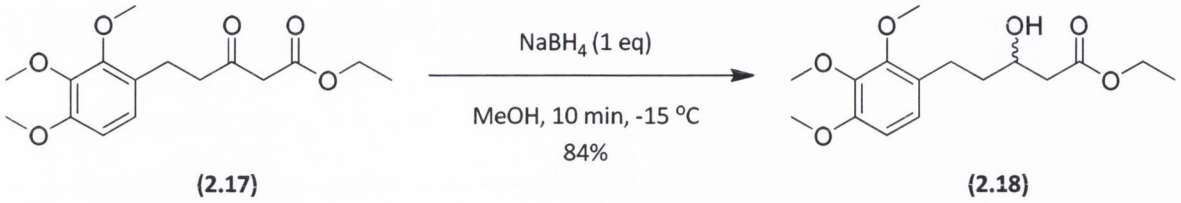

(2.17) **(2.18)**

To a stirred solution of **(2.17)** (4.75 g, 15.31 mmol) in methanol (50 mL) at -15 °C was added sodium borohydride (0.58 g, 15.31 mmol). After 10 min, the methanol was removed under reduced pressure and water (50 mL) added to the resulting residue. The aqueous phase was then extracted with diethyl ether (3x 100 mL). The ethyl ether extracts were dried over $MgSO_4$, filtered and concentrated *in vacuo*. The resulting residue was then purified by flash column chromatography (stationary phase; silica gel 230-400 mesh, mobile phase; 4:1, hexane/ethyl acetate). All homogenous fractions were collected and the solvent was removed to afford **(2.18)** as a clear oil (3.95 g, 84%).

Data already described.

7.2.4 Wittig reaction using commercial ylide: Synthesis of (*E*)-ethyl 3-oxo-5-(2,3,4-trimethoxyphenyl)pent-4-enoate (2.16)

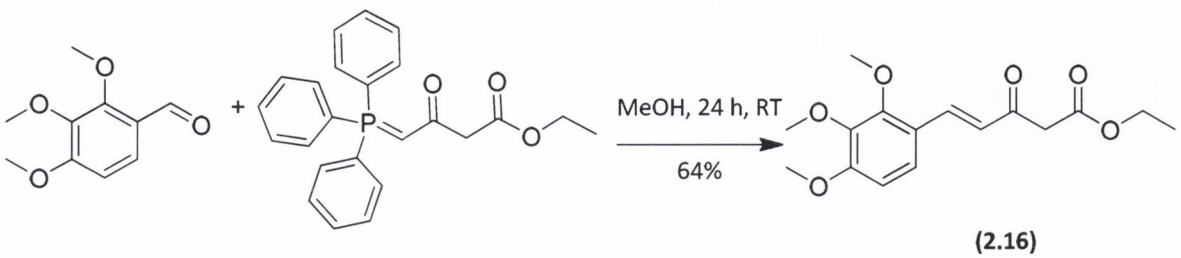

(2.16)

To a stirred solution of 2,3,4-trimethoxybenzaldehyde (0.5 g, 2.55 mmol) in methanol (5 mL) was added ethyl 3-oxo-4-(triphenylphosphoranylidene) butyrate (1.19 g, 3.06 mmol). After 24 h, the solvent was removed under reduced pressure and the resulting residue was subjected to flash column chromatography (stationary phase; silica gel 230-400 mesh, mobile phase; 4:1, hexane/ethyl acetate) to yield **(2.16)** as constituent of a bright yellow oil (0.5 g, 64%). The product was not purified further.

7.2.5 Silyl protection of alcohol: Synthesis of ethyl 3-(2,2-dimethyl-1,1-diphenylpropoxy)-5--trimethoxyphenyl)pentanoate (2.19)

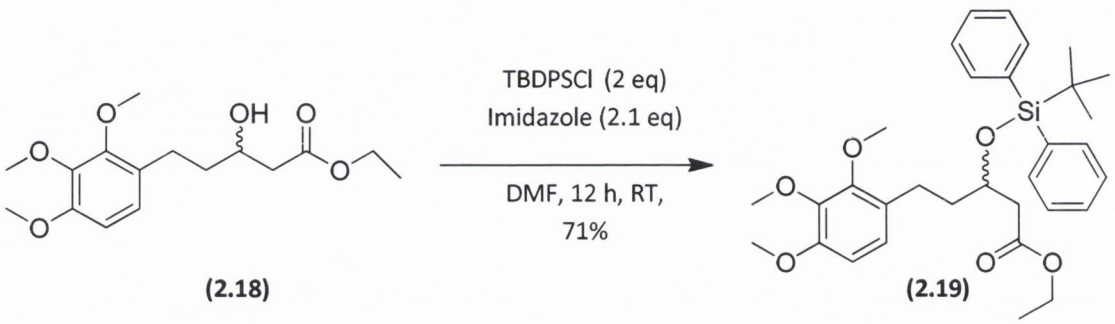

(2.18) **(2.19)**

To a stirred solution of **(2.18)** (3.11 g, 10.50 mmol) in dry DMF (25 mL) under an atmosphere of nitrogen was added imidazole (1.5 g, 22.04 mmol) and *tert*-butyldiphenylsilyl chloride (5.46 mL, 20.99 mmol). The reaction was left stirring for 12 h and then quenched by the addition of water (100 mL). The reaction mixture was then extracted with diethyl ether (3 x 100 mL). The organic fractions were dried over $MgSO_4$, filtered and concentrated *in vacuo.* The resulting oily residue was then purified by flash column chromatography (stationary phase; silica gel 230-400 mesh, mobile phase; 10:1, hexane/ethyl acetate) to afford **(2.19)** as bright yellow oil (4 g, 71%).

R_f: 0.56 (3:1, hexane/ethyl acetate)

^{1}H NMR ($CDCl_3$, 400 MHz) δ_H ppm: 1.09 (9H, s, C($C\underline{H}_3$)$_3$, 1.21 (3H, t, J = 7 Hz, $C\underline{H}_3$), 1.77 (2H, m, $C\underline{H}_2$), 2.49 (2H, m, $C\underline{H}_2$), 2.58 (2H, m, $C\underline{H}_2$), 3.78 (3H, s, $OC\underline{H}_3$), 3.85 (3H, s, $OC\underline{H}_3$), 3.86 (3H, s, $OC\underline{H}_3$), 4.04 (2H, m, $C\underline{H}_2$), 4.31 (1H, m, C$\underline{H}$OSi), 6.54 (1H, d, J = 9 Hz, Ar$\underline{H}$), 6.61 (1H, d, J = 9 Hz, Ar$\underline{H}$), 7.41 (6H, m, Ar$\underline{H}$), 7.73 (4H, m, Ar$\underline{H}$)

^{13}C NMR ($CDCl_3$, 400 MHz) δ_c ppm: 13.66 ($\underline{C}H_3$), 18.92 ($\underline{C}(CH_3)_3$), 24.61 ($\underline{C}H_2$), 26.51 (C($\underline{C}H_3$)$_3$), 37.77 ($\underline{C}H_2$), 41.58 ($\underline{C}H_2$), 55.53 ($O\underline{C}H_3$), 59.84 ($O\underline{C}H_3$), 60.25 ($\underline{C}H_2$), 60.34 ($O\underline{C}H_3$), 69.91 ($\underline{C}$HOSi), 106.63 (Ar$\underline{C}$H), 123.06 (Ar$\underline{C}$H), 127.06 (2 x Ar$\underline{C}$H), 127.09 (2 x Ar$\underline{C}$H), 127.47 (2 x Q$\underline{C}$), 129.16 (2 x Ar$\underline{C}$H),

133.58 (QC), 135.47 (2 x ArCH), 135.52 (2 x ArCH), 141.70 (QC), 151.30 (QC), 151.42 (QC), 171.06 (C=O)

ν_{MAX} (DCM)/cm^{-1}: 2960.35, 2934.16, 2091.36, 1734.62, 1644.78, 1494.76, 1466.34

HRMS $[M+K]^+$: calculated 573.2618, found 573.2623, molecular formula ($C_{33}H_{42}O_6K$)

7.2.6 Hydrolysis of ethyl ester: Synthesis of 3-(2,2-dimethyl-1,1-diphenylpropoxy)-5-(2,3,4-trimethoxyphenyl)pentanoic acid (2.10)

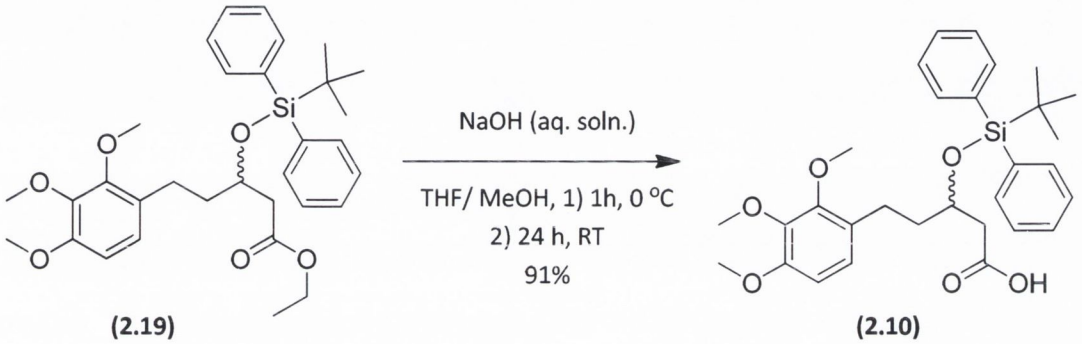

(2.19) **(2.10)**

To a stirred solution of **(2.19)** (0.09 g, 0.17 mmol) in a mixture of methanol (0.85 mL) and THF (0.66 mL) at 0 °C was added 2.5 M NaOH solution (0.25 mL) dropwise. After 24 h, the pH of the solution was adjusted to pH 7 by the addition of 2 M HCl aqueous solution. The organic solvent was removed under reduced pressure and the aqueous phase was extracted with diethyl ether (3 x 10 mL). The organic fractions were dried over $MgSO_4$, filtered and concentrated *in vacuo.* The resulting residue was then purified by flash column chromatography (stationary phase; silica gel 230-400 mesh, mobile phase; 2:1, hexane/ethyl acetate) to yield **(2.10)** as a white solid (0.08 g, 91%).

Data described previously.

7.27 Dess-Martin oxidation of alcohol: Synthesis of 9-(3-hydroxy-4-methoxyphenyl)-2,3,4-trimethoxy-5*H*-benzo[7]annulen-7(6*H*)-one (2.03)

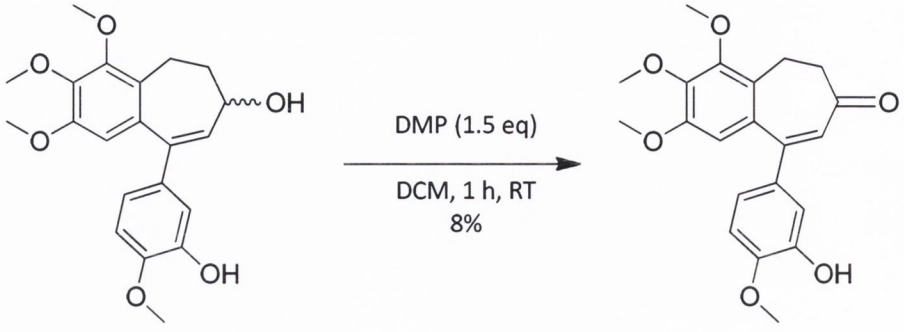

(2.02) **(2.03)**

To a stirred solution of **(2.02)** (0.31 g, 0.64 mmol) in DCM (2 mL) was added Dess-Martin periodinane (0.41 g, 0.96 mmol). After 1 h, saturated sodium hydrogen carbonate aqueous solution (10 mL) was added and the reaction was left stirring for 30 min. The reaction was extracted with diethyl ether (3 x 25 mL). The organic fractions were dried over $MgSO_4$, filtered and concentrated *in vacuo.* The resulting oily residue was then subjected to flash column chromatography (stationary phase; silica gel 230-400 mesh, mobile phase; 1:1, hexane/ethyl acetate) to afford **(2.03)** as a white solid (0.02 g, 8%).

Data already described.

7.2.8 Deprotection: Synthesis of 7-hydroxy-1,2,3-trimethoxy-6,7,8,9-tetrahydro-5*H*-benzo[7]annulen-5-one (2.20)

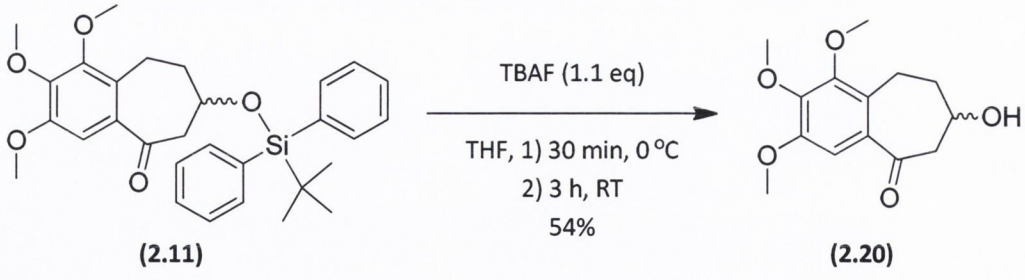

(2.11) **(2.20)**

To a stirred solution of **(2.11)** (0.63 g, 1.25 mmol) in THF (5 mL) at 0 °C was added 1 M tetrabutylammonium fluoride solution (1.37 mL, 1.37 mmol) dropwise. After 30 min, the temperature was allowed to increase to room temperature and left stirring for 3 h. The reaction

mixture was then added directly to a silica gel column and purified by flash column chromatography (stationary phase; silica gel 230-400 mesh, mobile phase; 4:1, hexane/ethyl acetate) to yield **(2.20)** as a yellow oil (0.18 g, 54%).

R_f: 0.20 (1:1, hexane/ethyl acetate)

^{1}H NMR ($CDCl_3$, 400 MHz) δ_H ppm: 1.87 (1H, m, C$\underline{H}_2$), 2.12 (1H, m, C$\underline{H}_2$), 3.02 (4H, m, C$\underline{H}_2$), 3.82 (3H, s, OC$\underline{H}_3$), 3.86 (3H, s, OC$\underline{H}_3$), 3.91 (3H, s, OC$\underline{H}_3$), 4.32 (1H, m, C$\underline{H}$OH), 7.14 (1H, s, Ar$\underline{H}$)

^{13}C NMR ($CDCl_3$, 400 MHz) δ_c ppm: 21.04 (C$\underline{H}_2$), 35.79 (C$\underline{H}_2$), 50.35 (C$\underline{H}_2$), 55.96 (OC$\underline{H}_3$), 60.88 (OC$\underline{H}_3$), 61.13 (OC$\underline{H}_3$), 67.07 (C$\underline{H}$OH), 107.45 (Ar$\underline{C}$H), 131.01 ($\underline{Q}$C), 134.02 ($\underline{Q}$C), 145.71 ($\underline{Q}$C), 151.13 ($\underline{Q}$C), 151.47 ($\underline{Q}$C), 199.87 ($\underline{C}$=O)

ν_{MAX} (DCM)/cm^{-1}: 2939.17, 1668.19, 1589.43, 1487.68, 1455.77, 1431.71

HRMS $[M+Na]^+$: calculated 267.1232, found 267.1256, molecular formula ($C_{14}H_{19}O_5$)

7.2.9 Organolithium Coupling: Synthesis of (*S*)-9-(3-((*tert*-butyldimethylsilyl)oxy)-4-methoxyphenyl)-2,3,4-trimethoxy-6,7-dihydro-5*H*-benzo[7]annulen-7-ol (2.21)

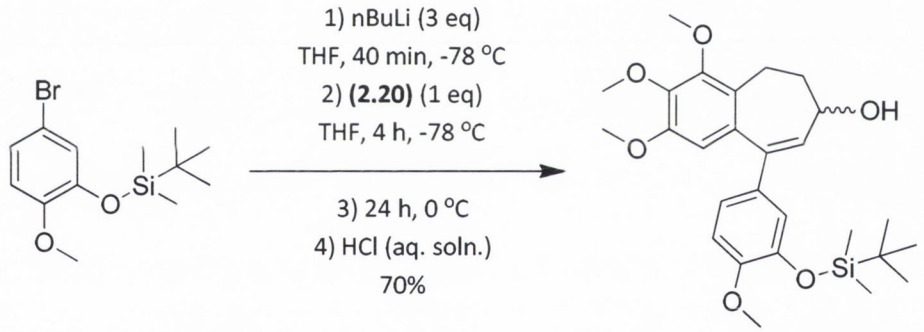

(2.14) **(2.21)**

To a stirred solution of **(2.14)** (0.64 g, 2.03 mmol) in dry THF (4 mL) under an atmosphere of nitrogen at -78 °C was added 2.5 M *n*-butyllithium solution in hexane (0.81 mL, 2.3 mmol) dropwise. After 40 min, a solution of **(2.20)** (0.18 g, 0.68 mmol) in dry THF (5 mL) was added to the reaction. After 4 h, the temperature was increased to 0 °C and left stirring for a further 24 h. The reaction was quenched by the addition of 2 M HCl aqueous solution (50 mL) and then extracted with diethyl ether (3 x 50 mL). The organic fractions were combined, dried over $MgSO_4$ and concentrated *in vacuo*. The resulting residue was then purified by flash column chromatography (stationary phase; silica gel 230-400 mesh, mobile phase; 4:1, hexane/ethyl acetate) to yield **(2.21)** as a yellow oil (0.23 g, 70%).

R_f: 0.52 (1:1, hexane/ethyl acetate)

^{1}H NMR ($CDCl_3$, 400 MHz) δ_H ppm: 0.16 (6H, d, J = 5.6 Hz, Si(C<u>H</u>$_3$)$_2$), 0.99 (9H, s, C(C<u>H</u>$_3$)$_3$), 1.28 (1H, s, br, CHO<u>H</u>), 2.13 (1H, m, C<u>H</u>$_2$), 2.36 (1H, m, C<u>H</u>$_2$), 2.51 (1H, m, C<u>H</u>$_2$), 3.03 (1H, m, C<u>H</u>$_2$), 3.68 (3H, s, OC<u>H</u>$_3$), 3.83 (3H, s, OC<u>H</u>$_3$), 3.92 (3H, s, OC<u>H</u>$_3$), 4.16 (1H, m, C<u>H</u>OH), 6.27 (1H, d, J = 4.12 Hz, C<u>H</u>=C), 6.36 (1H, s, Ar<u>H</u>), 6.80 (3H, m, 3 x Ar<u>H</u>)

^{13}C NMR ($CDCl_3$, 400 MHz) δ_c ppm: -5.00 (Si(<u>C</u>H$_3$)$_2$), -4.98 (Si(<u>C</u>H$_3$)$_2$), 18.00 (<u>C</u>(CH$_3$)$_2$), 21.34 (<u>C</u>H$_2$), 25.28 (C(<u>C</u>H$_3$)$_3$), 43.00 (<u>C</u>H$_2$), 55.04 (O<u>C</u>H$_3$), 55.44 (O<u>C</u>H$_3$), 60.43 (O<u>C</u>H$_3$), 61.12 (O<u>C</u>H$_3$), 69.32 (<u>C</u>H=C), 108.23 (Ar<u>C</u>H), 111.16 (Ar<u>C</u>H), 120.20 (Ar<u>C</u>H), 121.06 (Ar<u>C</u>H), 127.51 (Q<u>C</u>), 130.86 (Ar<u>C</u>H), 133.59 (Q<u>C</u>), 134.92 (Q<u>C</u>), 138.14 (Q<u>C</u>), 140.89 (Q<u>C</u>), 144.16 (Q<u>C</u>), 150.12 (Q<u>C</u>), 150.24 (Q<u>C</u>), 150.60 (Q<u>C</u>)

ν_{MAX} (DCM)/cm^{-1}: 3054.45, 2987.23, 2685.74, 2410.86, 2305.64, 1509.06, 1488.89

HRMS $[M+Na]^+$: calculated 509.2335, found 509.2339, molecular formula ($C_{27}H_{38}NaO_6Si$)

7.2.10 Dess-Martin oxidation of alcohol: Synthesis of 9-{3-[(*tert*-butyldimethylsilyl)oxy]-4-methoxyphenyl}-2,3,4-trimethoxy-6,7-dihydro-5*H*-benzo[7]annulen-7-ol (2.22)

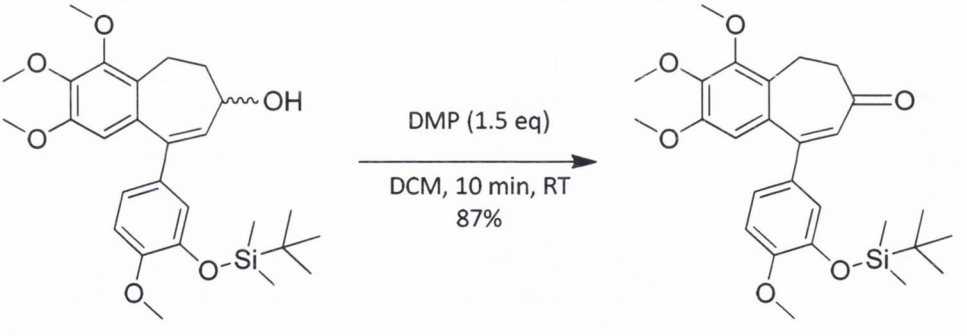

(2.21) **(2.22)**

To a stirred solution of **(2.21)** (0.1 g, 2.06 mmol) in DCM (30 mL) was added Dess-Martin periodinane (1.31 g, 3.08 mmol). After 10 min, saturated sodium hydrogen carbonate aqueous solution (50 mL) was added and the reaction was left stirring for 30 min. The reaction was extracted with diethyl ether (3 x 100 mL). The organic fractions were dried over $MgSO_4$, filtered and concentrated *in vacuo.* The resulting oily residue was then subjected to flash column chromatography (stationary phase; silica gel 230-400 mesh, mobile phase; 4:1, hexane/ethyl acetate) to afford **(2.22)** as a yellow oil (0.87 g, 87%).

R_f: 0.75 (1:1, hexane/ethyl acetate)

^{1}H NMR ($CDCl_3$, 400 MHz) δ_H ppm: 0.16 (6H, s, Si(C<u>H</u>$_3$)$_2$), 0.99 (9H, s, C(C<u>H</u>$_3$)$_3$), 2.67-2.70 (2H, m, C<u>H</u>$_2$), 3.10-3.13 (2H, t, J = 5.5 Hz, C<u>H</u>$_2$), 3.62 (3H, s, OC<u>H</u>$_3$), 3.86 (3H, s, OC<u>H</u>$_3$), 3.91 (3H, s, OC<u>H</u>$_3$),

3.94 (3H, s, $OC\underline{H}_3$), 6.36 (2H, s, 1 x Ar$\underline{H}$, 1 x C$\underline{H}$=C), 6.84 (2H, m, 2 x Ar$\underline{H}$), 6.92 (1H, dd, J_1 = 8 Hz, J_2 = 2 Hz, Ar$\underline{H}$)

^{13}C NMR ($CDCl_3$, 400 MHz) δ_c ppm: - 5.03 Si($\underline{C}H_3)_2$, 17.99 $\underline{C}(CH_3)_3$), 19.80 ($\underline{C}H_2$), 25.22 C($\underline{C}H_3)_3$), 45.21 ($\underline{C}H_2$), 54.96 ($O\underline{C}H_3$), 55.46 ($O\underline{C}H_3$), 60.47 ($O\underline{C}H_3$), 60.96 ($O\underline{C}H_3$), 110.88 (Ar$\underline{C}$H), 111.34 (Ar$\underline{C}$H), 121.25 (Ar$\underline{C}$H), 122.47 (Ar$\underline{C}$H), 127.47 (Ar$\underline{C}$H), 128.60 ($\underline{Q}C$), 132.16 ($\underline{Q}C$). 134.89 ($\underline{Q}C$), 142.73 ($\underline{Q}C$), 144.13 ($\underline{Q}C$), 149.46 ($\underline{Q}C$), 150.56 ($\underline{Q}C$), 151.31 ($\underline{Q}C$), 151.34 ($\underline{Q}C$), 203.70 (C=O)

ν_{MAX} (DCM)/cm^{-1}: 2933.36, 2856.52, 2095.35, 1653.05 (C=O), 1509.71

HRMS $[M+Na]^+$: calculated 507.2179, found 507.2179, molecular formula ($C_{27}H_{36}NaO_6Si$)

7.2.11 Deprotection of C ring phenol: Synthesis of (*Z*)-8,9-dihydro-5-(3-hydroxy-4-ethoxyphenyl)-1,2,3-trimethoxybenzo[7]annulen-7-one (2.03)

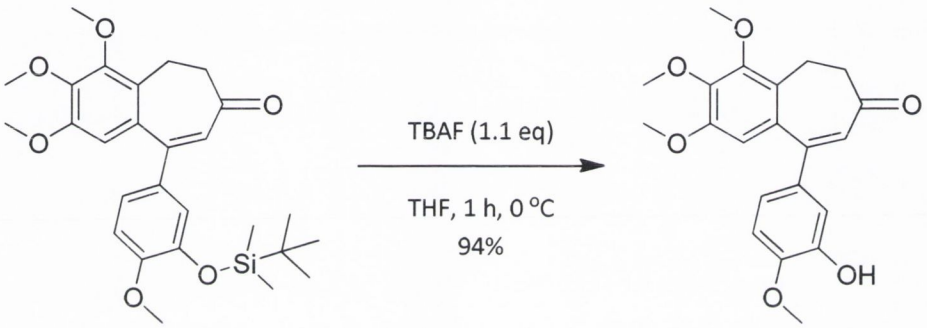

(2.22) **(2.03)**

To a stirred solution of **(2.22)** (0.21 g, 0.43 mmol) in dry THF (5 mL) under an atmosphere of nitrogen at 0 °C was added 1 M TBAF solution in THF (0.48 mL, 0.48 mmol). After 1 h, the THF was blown off in a stream of nitrogen gas and the reaction mixture added directly to a silica gel column and purified by flash column chromatography (stationary phase; silica gel 230-400 mesh, mobile phase; ethyl acetate) to yield **(2.03)** as a white solid (0.15 g, 94%).

Data already described.

7.3 Synthesis of sodium (5-((Z)-6,7-dihydro-2,3,4-trimethoxy-7-oxo-5H-benzo[7]annulen-9-yl)-2-methoxyphenyl)methylphosphonate (2.24)

7.3.1 Phosphate dibenzyl ester synthesis: Synthesis of dibenzyl (5-((*Z*)-6,7-dihydro-2,3,4-trimethoxy-7-oxo-5*H*-benzo[7]annulen-9-yl)-2-methoxyphenyl)methylphosphonate (2.23)

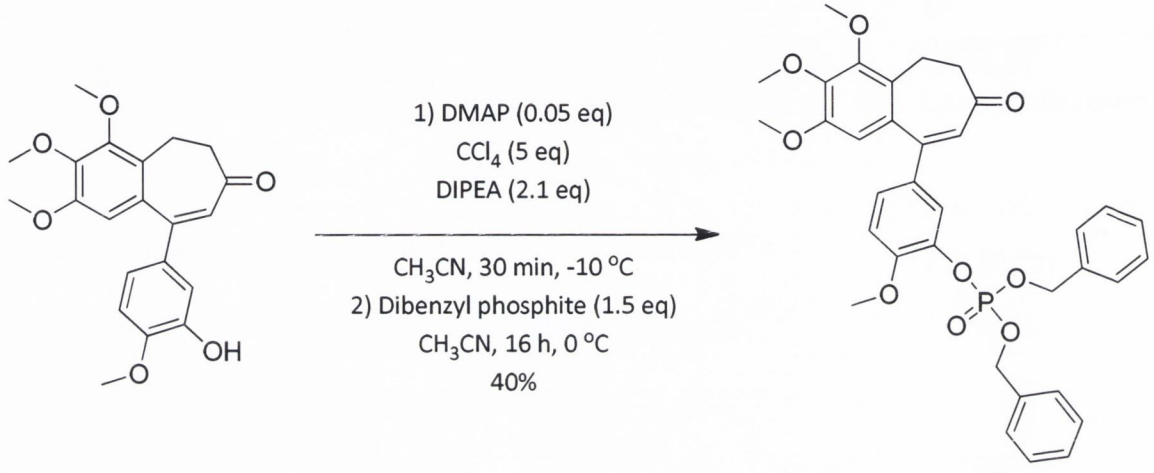

(2.03) **(2.23)**

To a stirred solution of **(2.03)** (0.23 g, 0.62 mmol) and DMAP (0.004 g, 0.033 mmol) in anhydrous acetonitrile (10 mL) under an atmosphere of nitrogen at -10 °C was added carbon tetrachloride (0.3 mL, 3.10 mmol) and *N,N*-diisopropylethylamine (0.23 mL, 1.30 mmol) dropwise. After 30 min, a solution of dibenzyl phosphite (0.24 g, 0.93 mmol) in anhydrous acetonitrile (1 mL) was added dropwise. The temperature of the reaction was allowed to increase to 0 °C and was left stirring at this temperature for 16 h. The reaction was then quenched by the addition of 0.5 M monobasic potassium phosphate aqueous solution (50 mL). The reaction mixture was then extracted with diethyl ether (3 x 50 mL). The organic fractions were dried over $MgSO_4$, filtered and concentrated *in vacuo.* The resulting residue was then purified by flash column chromatography (stationary phase; silica gel 230-400 mesh, mobile phase; 10:1, hexane/ethyl acetate) to yield **(2.23)** as a green oil (0.16 g, 40%).

R_f: 0.25 (1:2, hexane/ethyl acetate)

^{1}H NMR ($CDCl_3$, 400 MHz) δ_H ppm: 2.73 (2H, m, C$\underline{H}_2$), 3.15 (2H, m, C$\underline{H}_2$), 3.62 (3H, s, OC$\underline{H}_3$), 3.85 (3H, s, OC$\underline{H}_3$), 3.91 (3H, s, OC$\underline{H}_3$), 3.94 (3H, s, OC$\underline{H}_3$), 5.16 (4H, d, J = 8.16 Hz, 2 x OC$\underline{H}_2$) 6.34 (2H, s, 1 x C=C$\underline{H}$ and 1 x Ar$\underline{H}$), 6.94 (1H, d, J = 8.67 Hz, Ar$\underline{H}$), 7.08 (1H, s, Ar$\underline{H}$), 6.22 (1H, d, J = 9 Hz, Ar$\underline{H}$)

^{13}C NMR ($CDCl_3$, 400 MHz) δ_c ppm: 20.28 ($\underline{C}H_2$), 45.62 ($\underline{C}H_2$), 55.97 (O$\underline{C}H_3$), 56.01 (O$\underline{C}H_3$), 60.91 (O$\underline{C}H_3$), 61.41 (O$\underline{C}H_3$), 69.69 (CH_2), 69.94 (CH_2), 111.69 (C=$\underline{C}$H), 112.24 (Ar$\underline{C}$H), 122.55 (Ar$\underline{C}$H), 122.58 (Ar$\underline{C}$H), 126.78 (Ar$\underline{C}$H), 127.89 (5 x Ar$\underline{C}$H), 128.47 (Ar$\underline{C}$H), 128.58 (4 x Ar$\underline{C}$H), 129.19 (Q$\underline{C}$), 132 (Q$\underline{C}$), 135.17 (Q$\underline{C}$), 135.50 (Q$\underline{C}$), 135.57 (Q$\underline{C}$), 139.23 (Q$\underline{C}$), 139.31 (Q$\underline{C}$), 143.38 (Q$\underline{C}$), 150.08 (Q$\underline{C}$), 150.51 (Q$\underline{C}$), 151.20 (Q$\underline{C}$), 151.49 (Q$\underline{C}$), 203.81 ($\underline{C}$=O)

ν_{MAX} (DCM)/cm^{-1}: 2091.99, 1650.96, 1512.87, 1493.77, 1454.10

HRMS $[M+Na]^+$: calculated 653.1916, found 653.1913, molecular formula ($C_{36}H_{37}NaO_9P$)

7.3.2 Removal of benzyl groups and formation of disodium salt: Synthesis of sodium (5-((*Z*)-6,7-dihydro-2,3,4-trimethoxy-7-oxo-5*H*-benzo[7]annulen-9-yl)-2-methoxyphenyl)methylphosphonate (2.24)

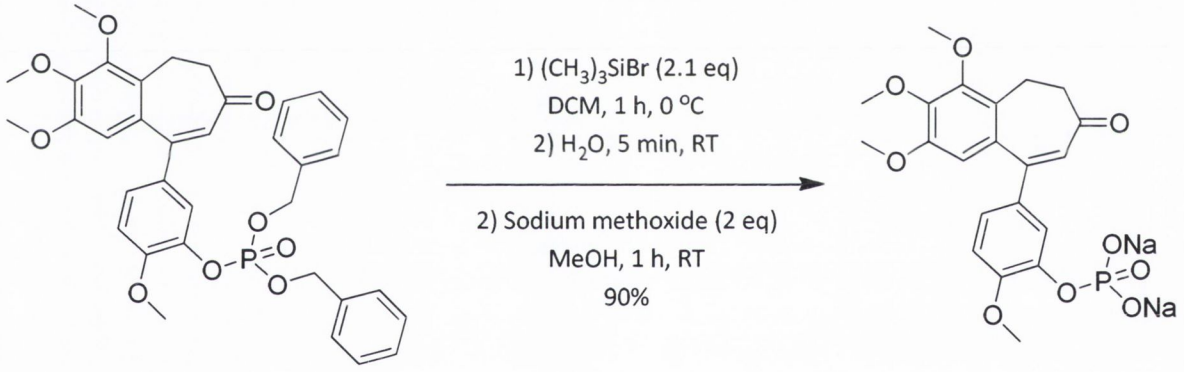

(2.23) **(2.24)**

To a stirred solution of **(2.23)** (0.16 g, 0.25 mmol) in dry DCM under an atmosphere of nitrogen at 0 °C was added bromotrimethylsilane (0.07 mL, 0.52 mmol). After 1 h, the DCM was removed using a stream of nitrogen at room temperature and the resulting residue dissolved in distilled water (50 mL). The aqueous solution was then washed with diethyl ether (5 x 25 mL) and removed under reduced pressure. This residue was then re-dissolved in methanol (2 mL) and sodium methoxide (0.2 g, 0.37 mmol) was added to the stirred solution. After 1 h, the methanol was removed under reduced pressure to afford the disodium salt **(2.24)** as an off-white solid (0.8 g, 90%).

R_f: n/a

^{1}H NMR (CD_3OD, 400 MHz) δ_H ppm: 2.67 (2H, m, C<u>H</u>$_2$), 3.14 (2H, m, C<u>H</u>$_2$), 3.64 (3H, s, OC<u>H</u>$_3$), 3.90 (6H, s, OC<u>H</u>$_3$), 3.91 (3H, s, OC<u>H</u>$_3$), 6.43 (1H, s, C=C<u>H</u>), 6.51 (1H,s, Ar<u>H</u>), 7.00 (1H, dd, J_1 = 8.28 Hz, J_2 = 2.03 Hz, Ar<u>H</u>), 7.03 (1H, d, J = 8.48 Hz, Ar<u>H</u>), 7.54 (1H, s, Ar<u>H</u>),

^{13}C NMR (CD_3OD, 400 MHz) δ_c ppm: 19.72 (<u>C</u>H$_2$), 45.17 (<u>C</u>H$_2$), 55.03 (O<u>C</u>H$_3$), 55.10 (O<u>C</u>H$_3$), 59.86 (O<u>C</u>H$_3$), 60.50 (O<u>C</u>H$_3$), 111.68 (Ar<u>C</u>H), 112.07 (Ar<u>C</u>H), 121.51 (Ar<u>C</u>H), 123.88 (Ar<u>C</u>H), 127.12 (C=<u>C</u>H), 128.92 (Q<u>C</u>), 132.38 (Q<u>C</u>), 134.68 (Q<u>C</u>), 142.63 (Q<u>C</u>), 143.32 (Q<u>C</u>), 149.83 (Q<u>C</u>), 151.24 (Q<u>C</u>), 152.06 (Q<u>C</u>), 152.81 (Q<u>C</u>), 205.01 (<u>C</u>=O)

^{31}P NMR (CD_3OD, 400 MHz) δ_P ppm: -3.00

ν_{MAX} (KBr)/cm^{-1}: 3540.22, 2935.47, 1660.91, 1599.01, 1566.73

HRMS $[M+H]^+$: calculated 449.1007, found 449.1022, molecular formula ($C_{21}H_{22}O_9P$)

Melting point: 166-167 °C

7.4 Synthesis of 9-(3-amino-4-methoxyphenyl)-2,3,4-trimethoxy-5H-benzo[7]annulen-7(6H)-one (2.25)

7.4.1 Preparation of Triflate: Synthesis of 7-((*tert*-butyldiphenylsilyl)oxy)-2,3,4-trimethoxy-6,7-dihydro-5*H*-benzo[7]annulen-9-yl trifluoromethanesulfonate (2.26)

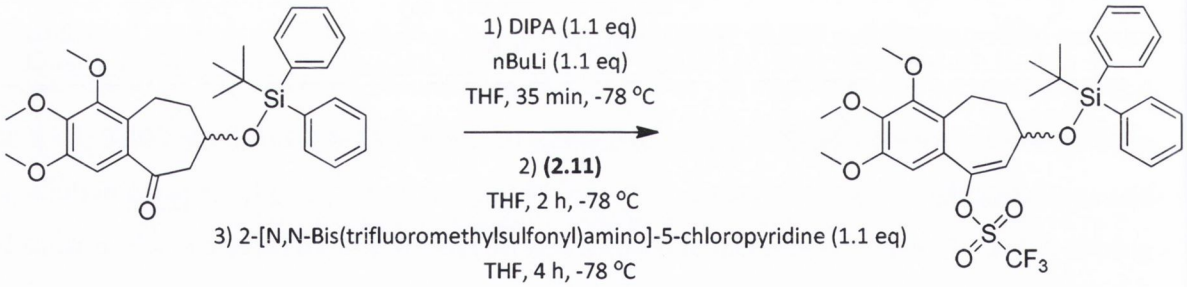

(2.11) **(2.26)**

To a stirred solution of diisopropylamine (0.19 mL, 1.35 mmol) in dry THF at -78 °C under an atmosphere of nitrogen was added 2.5 M *n*-butyllithium solution in hexane (0.54 mL, 1.35 mmol). After 35 min, a solution of **(2.11)** (0.62 g, 1.23 mmol) in dry THF (8 mL) was added dropwise. The solution was stirred at -78 °C for 2 h and then a solution of 2-[*N,N*-Bis(trifluoromethylsulfonyl)amino]-5-chloropyridine (0.53 g, 1.35 mmol) in dry THF (8 mL) was added. The solution was stirred at -78 °C for a further 4 h after which time the reaction was quenched with saturated sodium chloride aqueous solution (50 mL). The reaction mixture was

then extracted with diethyl ether (3 x 25 mL). The organic fractions were dried over $MgSO_4$, filtered and concentrated *in vacuo.* The resulting residue was then purified by flash column chromatography (stationary phase; silica gel 230-400 mesh, mobile phase; 10:1, hexane/ethyl acetate) to yield **(2.26)** as an off white oil (0.35 g, 45%).

R_f: 0.66 (3:1, hexane/ethyl acetate)

^{1}H NMR ($CDCl_3$, 400 MHz) δ_H ppm: 1.23 (9H, s, C(CH_3)$_3$), 1.92 (1H, m, CH_2), 2.27 (1H, m, CH_2), 2.59 (1H, m, CH_2), 3.00 (1H, m, CH_2), 3.76 (3H, s, OCH_3), 3.87 (3H, s, OCH_3), 3.93 (3H, s, OCH_3), 4.30 (1H, m, CHOSi), 6.13 (1H, d, J = 4.7 Hz, C=CH), 6.82 (1H, s, ArH), 7.38-7.48 (6H, m, ArH) 7.67-7.78 (4H, m, ArH)

^{13}C NMR ($CDCl_3$, 400 MHz) δ_c ppm: 19.13 (C(CH_3)$_3$), 20.44 (CH_2), 26.59 (C(CH_3)$_3$, 39.75 (CH_2), 55.97 (OCH_3), 60.94 (OCH_3), 61.53 (OCH_3), 68.60 (CHOSi) 105.95 (ArCH), 126.55 (CH=C) 127.02 (QC) 127.74 (2 x ArCH), 127.77 (2 x ArCH), 128.98 (QC), 129.67 (ArCH), 133.41 (QC), 133.58 (QC), 134.84 (2 x ArCH), 135.26 (QC), 135.78 (2 x ArCH), 143.54 (QC), 143.88 (QC), 150.89 (QC), 151.52 (QC)

ν_{MAX} (DCM)/cm^{-1}: 1645.38, 1491.19, 1211.82

HRMS $[M+Na]^+$: calculated 659.1723, found 659.1707 , molecular formula ($C_{31}H_{35}F_3O_7SSiNa$)

7.4.2 Alternative preparation of triflate: Synthesis of 7-((*tert*-butyldiphenylsilyl)oxy)-2,3,4-trimethoxy-6,7-dihydro-5*H*-benzo[7]annulen-9-yl trifluoromethanesulfonate (2.26)

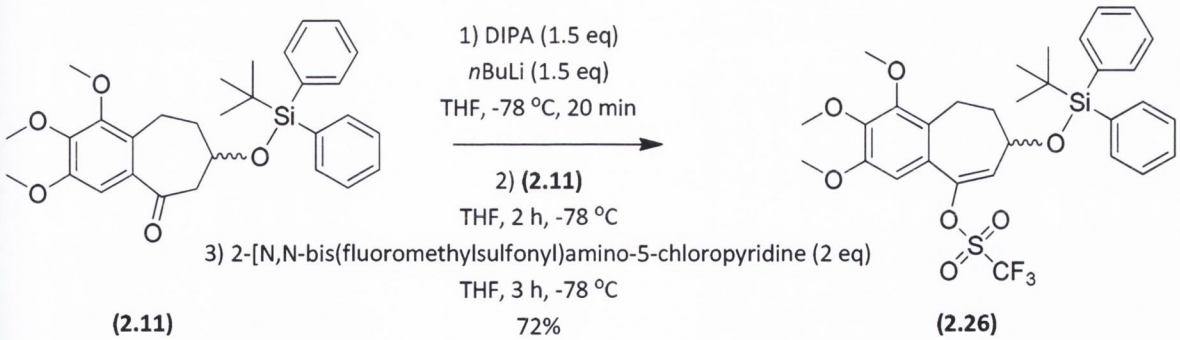

To a stirred solution of diisopropylamine (1.39 mL, 9.91 mmol) in dry THF (5 mL) at -78 °C under an atmosphere of nitrogen was added 2.5 M *n*-butyllithium solution in hexane (3.96 mL, 9.91 mmol). After 20 min, a solution of **(2.11)** (3.33 g, 6.6 mmol) in dry THF (20 mL) was added dropwise. The solution was stirred at -78 °C for 2 h and then a solution of 2-[*N,N*-bis(fluoromethylsulfonyl)amino]-5-chloropyridine (5.19 g, 13.21 mmol) in dry THF (20 mL) was

added. The solution was stirred at -78 °C for a further 3 h after which time the reaction wa quenched with saturated sodium chloride aqueous solution (100 mL). The reaction mixture wa then extracted with diethyl ether (3 x 100 mL). The organic fractions were dried over MgSO filtered and concentrated *in vacuo.* The resulting residue was then purified by flash colum chromatography (stationary phase; silica gel 230-400 mesh, mobile phase; 10:1, hexane/eth acetate) to yield **(2.26)** as an off-white oil (3.03 g, 72%).

Data already described.

7.4.3 Methylation of Phenol: Synthesis of 4-bromo-1-methoxy-2-nitrobenzene (2.27)

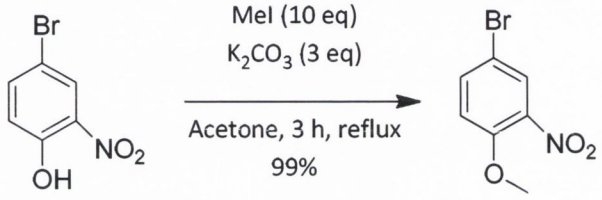

(2.27)

To a stirred solution of 4-bromo-2-nitrophenol (5.46 g, 25.04 mmol) in acetone (60 mL) was adde potassium carbonate (10.38 g, 75.13 mmol) and iodomethane (15.59 mL, 250.45 mmol). Th reaction was heated under reflux for 3 h. The reaction was quenched by the addition of 2 M H aqueous solution (200 mL) and extracted with diethyl ether (3 x 100 mL). The organic fractio were dried over $MgSO_4$, filtered and concentrated *in vacuo.* The product was not purified furth and afforded **(2.27)** as an off-white solid (5.78 g, 99%).

R_f: 0.39 (3:1, hexane/ethyl acetate)

^{1}H NMR ($CDCl_3$, 400 MHz) δ_H ppm: 3.98 (3H, s, OC<u>H</u>$_3$), 7.01 (1H, d, J = 8.92 Hz, Ar<u>H</u>), 7.65 (1H, dd, = 9 Hz, J_2 = 2.48 Hz, Ar<u>H</u>), 7.98 (1H, d, J = 2.5 Hz, Ar<u>H</u>)

^{13}C NMR ($CDCl_3$, 400 MHz) δ_c ppm: 56.29 (O<u>C</u>H$_3$), 111.35 (Q<u>C</u>), 114.74 (Ar<u>C</u>H), 127.89 (Ar<u>C</u>H 136.50 (Ar<u>C</u>H), 139.51 (Q<u>C</u>), 151.69 (Q<u>C</u>)

ν_{MAX} (DCM)/cm^{-1}: 3105.13, 2980.33, 2948.81, 2845.25, 1906.06, 1605.52, 1516.15

HRMS $[M+H]^+$: calculated 231.9609, found 231.9254, molecular formula ($C_7H_7BrNO_3$)

Melting Point: 86 °C

7.4.4 Attempted Boronic Acid Synthesis: Attempted Synthesis of (4-methoxy-3-nitrophenyl)boronic acid (2.28)

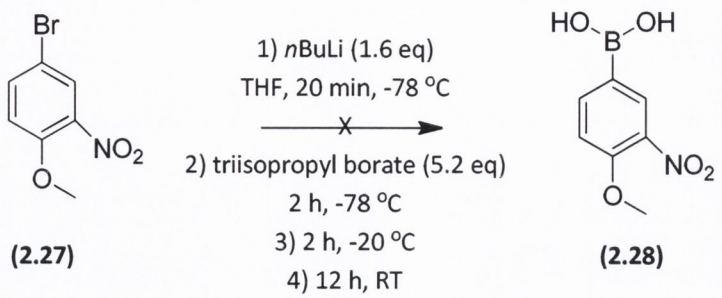

(2.27) **(2.28)**

To a stirred solution of **(2.27)** (2.12 g, 9.14 mmol) in dry THF (4 mL) under an atmosphere of nitrogen at -78 °C was added 2.5 M *n*-butyllithium hexane solution (5.85 mL, 14.62 mmol) dropwise. After 20 min, triisopropyl borate (7.28 mL, 47.51 mmol) was added and the solution was left stirring at -78 °C for 2 h. The temperature was then increase to -20 °C and left to stir for a further 2 h. The temperature of the reaction was then allowed to increase to ambient and left stirring for 12 h. The reaction was then quenched by the addition of 2 M HCl aqueous solution (100 mL) and extracted with diethyl ether (3 x 75 mL). The organic fractions were combined, dried over $MgSO_4$ and concentrated under reduced pressure to afford a crude black residue. The reaction mixture was deemed to contain a complex mixture of compounds and thus the reaction was not pursued further.

7.4.5 Reduction of nitro group: Synthesis of 5-bromo-2-methoxyaniline (2.29)

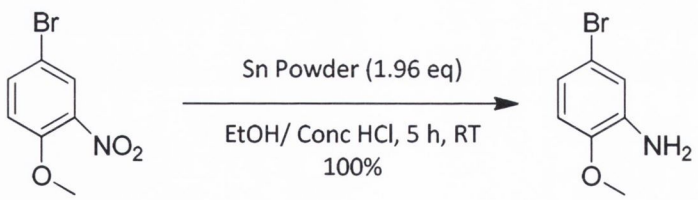

(2.27) **(2.29)**

To a stirred solution of **(2.27)** (0.95 g, 4.09 mmol) in ethanol (30 mL) was added concentrated HCl (15 mL) and tin powder (0.95 g, 8 mmol). The reaction was stirred for 5 h. The solvent was then removed *in vacuo* and the acid was neutralised by the slow addition of 2.5 M NaOH aqueous solution (13 mL) at 0 °C. The aqueous mixture was then extracted with diethyl ether (3 x 50 mL).

The organic fractions were dried over $MgSO_4$, filtered and concentrated *in vacuo* to afford **(2.2** as a brown solid (0.86 g, 100 %). The product was not purified further.

R_f: 0.43 (2:1, hexane/ethyl acetate)

^{1}H NMR ($CDCl_3$, 400 MHz) δ_H ppm: 3.85 (3H, s, OC<u>H</u>$_3$), 6.65 (1H, dd, J_1 = 10.12, J_2 = 2 Hz, Ar<u>H</u>), 6. (1H, dd, J_1 = 8.2 Hz, J_2 = 2.44 Hz, Ar<u>H</u>), 6.85 (1H, s, Ar<u>H</u>)

^{13}C NMR ($CDCl_3$, 400 MHz) δ_c ppm: 55.18 (O<u>C</u>H$_3$), 111.14 (Ar<u>C</u>H), 116.87 (Ar<u>C</u>H), 117.72 (Q 120.23 (Ar<u>C</u>H), 137.15 (Q<u>C</u>), 145.90 (Q<u>C</u>)

ν_{MAX} (DCM)/cm^{-1}: 3460.96, 3370.98, 1611.91, 1573.81

HRMS $[M+H]^+$: calculated 201.9862, found 201.9855, molecular formula (C_7H_9BrNO)

Melting Point: 110 °C

7.4.6 Boc protection: Synthesis of *tert*-butyl (5-bromo-2-methoxyphenyl)carbama (2.30)

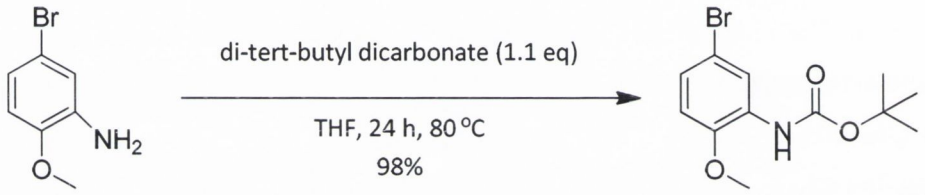

(2.29) **(2.30)**

To a stirred solution of **(2.30)** (0.63 g, 3.12 mmol) in dry THF (5 mL) under an atmosphere nitrogen was added 1 M di-*tert*-butyl dicarbonate solution in THF (3.43 mL, 3.43 mmol). T reaction was heated under reflux at 80 °C for 24 h. The solvent was removed *in vacuo* and t resulting residue was purified by purified by flash column chromatography (stationary phas silica gel 230-400 mesh, mobile phase; 20:1, hexane/ethyl acetate) to yield **(2.30)** as clear oil (0. g, 98%).

R_f: 0.56 (3:1, hexane/ethyl acetate)

^{1}H NMR ($CDCl_3$, 400 MHz) δ_H ppm: 1.55 (9H, s, C(C<u>H</u>$_3$)$_3$), 3.87 (3H, s, OC<u>H</u>$_3$), 6.71 (1H, d, J = 8.6 H Ar<u>H</u>), 7.08 (2H, dd, J_1 = 8.6 Hz, J_2 = 2.4 Hz, 2 x Ar<u>H</u>), 8.30 (1H, s, br, ArN<u>H</u>)

^{13}C NMR ($CDCl_3$, 400 MHz) δ_c ppm: 27.85 (C(<u>C</u>H$_3$)$_3$, 55.39 (O<u>C</u>H$_3$), 80.33 (<u>C</u>(CH$_3$)$_3$), 110.67 (Ar<u>C</u>I 113.09 (Q<u>C</u>), 120.17(Ar<u>C</u>H), 124.22 (Ar<u>C</u>H), 128.89(Q<u>C</u>), 145.99 (Q<u>C</u>), 151.95 (<u>C</u>=O)

ν_{MAX} (DCM)/cm^{-1}: 3434.78, 2977.96, 2934.83, 1729.29, 1595.81

HRMS $[M+Na]^+$: calculated 324.0211, found 324.0197, molecular formula ($C_{12}H_{16}BrNO_3Na$)

7.4.7 Synthesis of carbamate protected boronic acid: Synthesis of (3-((*tert*-butoxycarbonyl)amino)-4-methoxyphenyl)boronic acid (2.31)

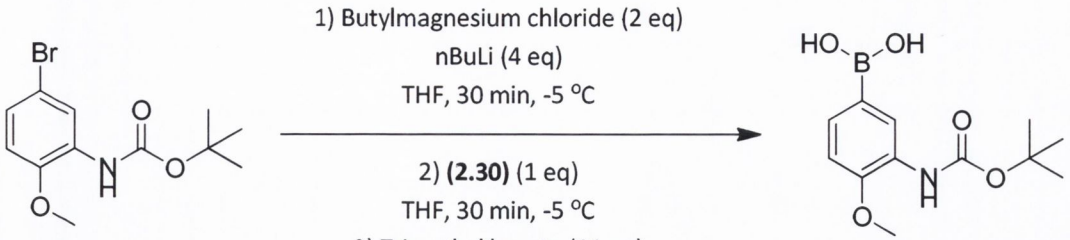

(2.30) **(2.31)**

To a stirred 3-necked round bottomed flask containing THF (7 mL) at -5 °C under an atmosphere of nitrogen was added 2 M butylmagnesium chloride solution in THF (1.69 mL, 3.38 mmol). After 10 min, 2.5 M *n*-butyllithium solution in hexane (2.7 mL, 6.75 mmol) was added dropwise. The solution was stirred at -5 °C for 30 min. A solution of **(2.30)** (0.51 g, 1.69 mmol) in dry THF (5 mL) was added dropwise and the solution was stirred for 30 min. Whilst maintaining the temperature at -5 °C, trimethyl borate (2.07 mL, 18.57 mmol) was added to the reaction mixture in a dropwise manner. The temperature of the reaction was allowed to gradually increase to 0 °C and was left stirring at this temperature for 3 h. The reaction was quenched with ammonium chloride aqueous solution (50 mL) and extracted with diethyl ether (3 x 50 mL). The organic fractions were dried over $MgSO_4$, filtered and concentrated *in vacuo.* The resulting residue was purified by flash column chromatography (stationary phase; silica gel 230-400 mesh, mobile phase; 3:1, hexane/ethyl acetate) to yield **(2.31)** as part of a crude mixture. The crude product was not purified further but was carried forward to the next step.

R_f: 0.22 (2:1, hexane/ethyl acetate)

7.4.8 Suzuki Coupling: Synthesis of *tert*-butyl (5-(7-((*tert*-butyldiphenylsilyl)oxy)-2,3 trimethoxy-6,7-dihydro-5*H*-benzo[7]annulen-9-yl)-2-methoxyphenyl)carbamate (2.32

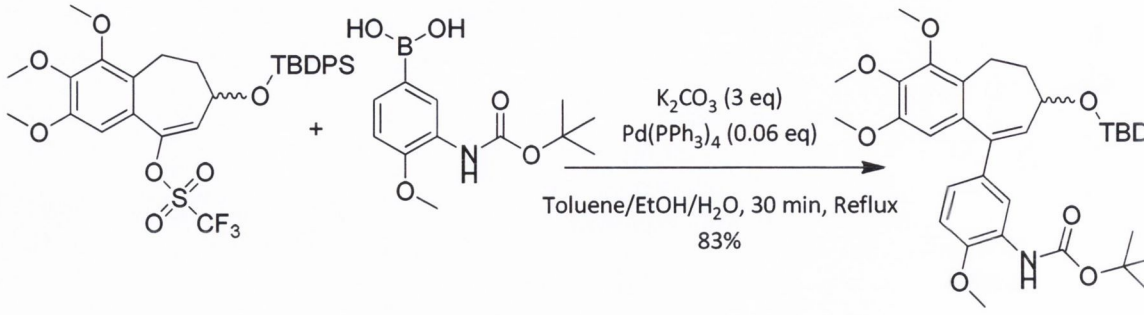

(2.26) **(2.31)** **(2.32)**

To a stirred solution of **(2.26)** (0.11 g, 0.17 mmol) in a mixture of toluene, ethanol and wate mL; 3: 1: 1) was added potassium carbonate (0.07 g, 0.52 mmol), (tetrakis(triphenyl)phosph palladium (0.01 g, 0.01 mmol) and **(2.31)** (0.06 g, 0.20 mmol). The reaction was heated un reflux for 30 min after which time it was quenched by the addition of water (50 mL). The reac mixture was then extracted with diethyl ether (3 x 50 mL). The organic fractions were dried o $MgSO_4$, filtered and concentrated *in vacuo.* The resulting residue was then purified by fl column chromatography (stationary phase; silica gel 230-400 mesh, mobile phase; 1 hexane/ethyl acetate) to yield **(2.32)** as a yellow oil (0.1 g, 83%).

R_f: 0.29 (3:1, hexane/ethyl acetate)

^{1}H NMR ($CDCl_3$, 400 MHz) δ_H ppm: 1.09 (9H, s, SiC(CH_3)$_3$), 1.52 (9H, s, COOC(CH_3)$_3$), 2.18-2.34 (m, 2 x CH_2), 3.67 (3H, s, OCH_3), 3.71 (3H, s, OCH_3), 3.88 (3H, s, OCH_3), 3.90 (3H, s, OCH_3), 4.10-4 (1H, m, CHOSi), 6.23 (1H, s, ArH), 6.36 (1H, d, J = 4.8 Hz, CH=C), 6.69 (1H, dd, J_1 = 8.5 Hz, J_2 = 2.1 ArH), 7.03 (1H,s , br, ArNH), 7.30 (1H, s, ArH), 7.32-7.40 (6H, m, ArH), 7.62-7.70 (4H, m, ArH)

^{13}C NMR ($CDCl_3$, 400 MHz) δ_c ppm: 19.15 (SiC(CH_3)$_3$), 21.86 (CH_2), 26.98 (C(CH_3)$_3$), 28.35 (C(CH 43.83 (CH_2), 55.75 (CH_3), 56.03 (CH_3), 60.83 (CH_3), 61.53 (CH_3), 71.33 (CH), 80.36 (COOC(CH 108.79 (CH), 109.45 (CH), 118.13 (CH), 122.24 (CH), 127.43 (2 x CH), 127.52 (2 x CH), 127.76 (128.01 (QC), 129.41 (CH), 129.44 (CH), 133.02 (CH), 134.24 (QC), 134.36 (QC), 134.41 (QC), 134 (QC), 135.74 (2 x CH), 135.84 (2 x CH), 137.88 (QC), 141.13 (QC), 147.15 (QC), 150.63 (QC), 150 (QC), 152.68 (C=O)

ν_{MAX} (DCM)/cm^{-1}: 2931.45, 2856.77, 1730.76, 1589.65, 1527.16

HRMS $[M+Na]^+$: calculated 732.3332, found 732.2711, molecular formula ($C_{42}H_{51}NO_7SiNa$)

4.9 Boronic acid ester synthesis: Synthesis of *tert*-butyl (2-methoxy-5-(4,4,5,5-tetramethyl-1,3,2-dioxaborolan-2-yl)phenyl)carbamate (2.33)

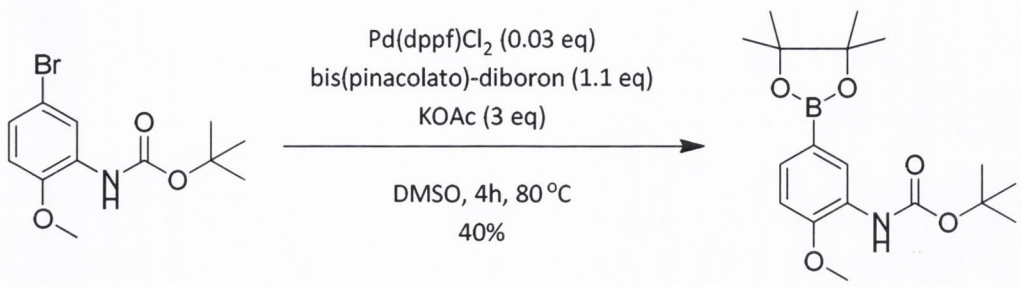

(2.30) **(2.33)**

a dry round bottomed flask containing [1,1′-s(diphenylphosphino)ferrocene]dichloropalladium(II) (0.01, 0.01 mmol), potassium acetate .11 g, 1.09 mmol) and bis(pinacolato)-diboron (0.1 g, 0.4 mmol) under an atmosphere of trogen was added a solution of **(2.30)** (0.11 g, 0.36 mmol) in dry DMSO (6 mL). The reaction was en heated under reflux at 80 °C under anhydrous conditions for 4 h. The reaction was quenched ith water (25 mL). The reaction mixture was then extracted with diethyl ether (3 x 50 mL). The rganic fractions were dried over $MgSO_4$, filtered and concentrated *in vacuo.* The resulting residue as then purified by flash column chromatography (stationary phase; silica gel 230-400 mesh, obile phase; 10:1, hexane/ethyl acetate) to yield **(2.33)** as a white solid (0.05 g, 40%).

: 0.44 (3:1, hexane/ethyl acetate)

I NMR ($CDCl_3$, 400 MHz) δ_H ppm: 1.33 (12H, s, 2 x C($C\underline{H}_3$)$_2$, 1.54 (9H, s, C($C\underline{H}_3$)$_3$), 3.88 (3H, s, $C\underline{H}_3$), 6.87 (1H, d, J = 8.08 Hz, Ar$\underline{H}$), 7.06 (1H, s, br Ar$\underline{H}$), 7.48 (1H, dd, J_1 = 8.08 Hz, J_2 = 1.03 Hz, r$\underline{H}$), 8.47 (1H, s, br, N$\underline{H}$)

C NMR ($CDCl_3$, 400 MHz) δ_c ppm: 25.04 (2 x C($\underline{C}H_3$)$_2$), 28.39 (C($\underline{C}H_3$)$_3$), 55.59 (O$\underline{C}H_3$), 80.05 ($\underline{C}$(CH$_3$)$_3$), 83.58 (2 x $\underline{C}$(CH$_3$)$_2$), 109.23 (Ar$\underline{C}$H), 124.11 (Q$\underline{C}$), 127.52 (Q$\underline{C}$), 129.80 (2 x Ar$\underline{C}$H), 150.09 Q$\underline{C}$), 152.50 ($\underline{C}$=O)

$_{MAX}$ (DCM)/cm^{-1}: 3443.03, 2979.23, 1732.52, 1604.30, 1536.44

RMS $[M+Na]^+$: calculated 372.1958, found 372.1958, molecular formula ($C_{18}H_{28}BNNaO_5$)

elting Point: 104 °C

7.4.10 Suzuki coupling of boronic ester with triflate: Alternative synthesis of *tert*-bu (5-(7-((*tert*-butyldiphenylsilyl)oxy)-2,3,4-trimethoxy-6,7-dihydro-5*H*-benzo[7]annulen- yl)-2-methoxyphenyl)carbamate (2.32)

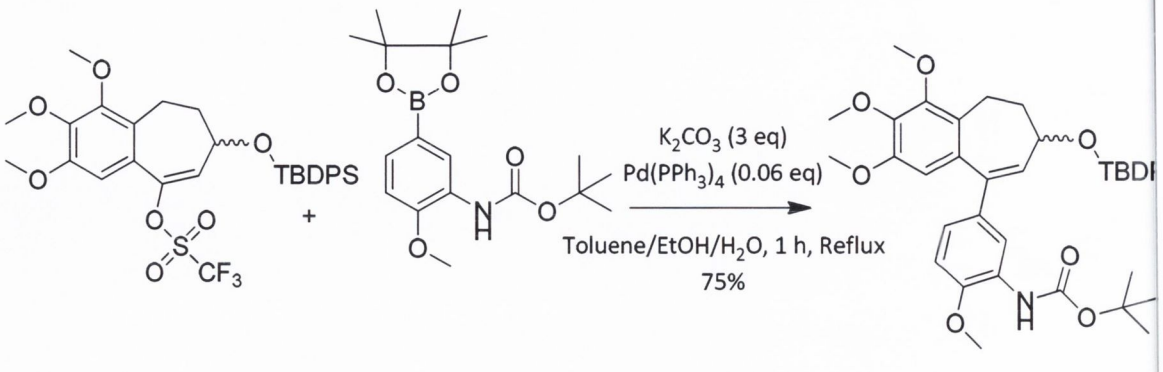

(2.26) **(2.33)** **(2.32)**

To a stirred solution of **(2.26)** (0.05 g, 0.07 mmol) in a mixture of toluene, ethanol and water mL; 3: 1: 1) was added potassium carbonate (0.03 g, 0.22 mmol), (tetrakis(triphenyl)phosphin palladium (0.005 g, 0.004 mmol) and **(2.33)** (0.03 g, 0.09 mmol). The reaction was heated unc reflux for 1 h after which time it was quenched by the addition of water (50 mL). The reacti mixture was then extracted with diethyl ether (3 x 50 mL). The organic fractions were dried ov $MgSO_4$, filtered and concentrated *in vacuo*. The resulting residue was then purified by fla column chromatography (stationary phase; silica gel 230-400 mesh, mobile phase; 10 hexane/ethyl acetate) to yield **(2.32)** as a yellow oil (0.04 g, 75%).

Data already described.

7.4.11 One pot biaryl synthesis via in situ boronate formation: Alternative synthesis of *tert*-butyl (5-(7-((*tert*-butyldiphenylsilyl)oxy)-2,3,4-trimethoxy-6,7-dihydro-5*H*-benzo[7]annulen-9-yl)-2-methoxyphenyl)carbamate (2.32)

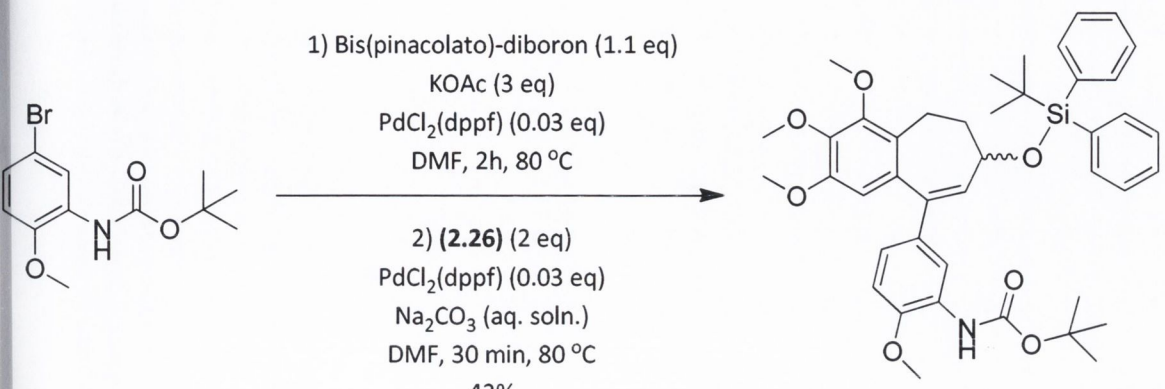

(2.31) **(2.32)**

To a clean, dry, round bottomed flask containing **(2.31)** (0.2 g, 0.66 mmol) was added bis(pinacolato)-diboron (0.18 g, 0.73 mmol), potassium acetate (0.2 g, 1.99 mmol) and [1,1′-Bis(diphenylphosphino)ferrocene]dichloropalladium(II) (0.015 g, 0.02 mmol). The reaction vessel was flushed with nitrogen and maintained under an atmosphere of nitrogen. Dry DMF (4 mL) was added to the mixture and the reaction was heated under reflux at 80°C for 2 h. A solution of **2.26)** (0.84 g, 1.32 mmol) in dry DMF (2 mL) and 2 M sodium carbonate aqueous solution (2 mL) were added to the reaction mixture. A fresh quantity of $PdCl_2$(dppf) (0.015 g, 0.02 mmol) was also added to the reaction which was then heated for a further 30 min at 80 °C. The reaction was quenched by the addition of water (50 mL) and extracted with diethyl ether (3 x 50 mL). The organic fractions were dried over $MgSO_4$, filtered and concentrated *in vacuo.* The resulting black residue was then purified by flash column chromatography (stationary phase; silica gel 230-400 mesh, mobile phase; 4:1, hexane/ethyl acetate) to yield **(2.32)** as a yellow oil (0.2 g, 43%).

Data already described.

7.4.12 Silyl Deprotection: Synthesis of *tert*-butyl (5-(7-hydroxy-2,3,4-trimethoxy-6 dihydro-5*H*-benzo[7]annulen-9-yl)-2-methoxyphenyl)carbamate (2.34)

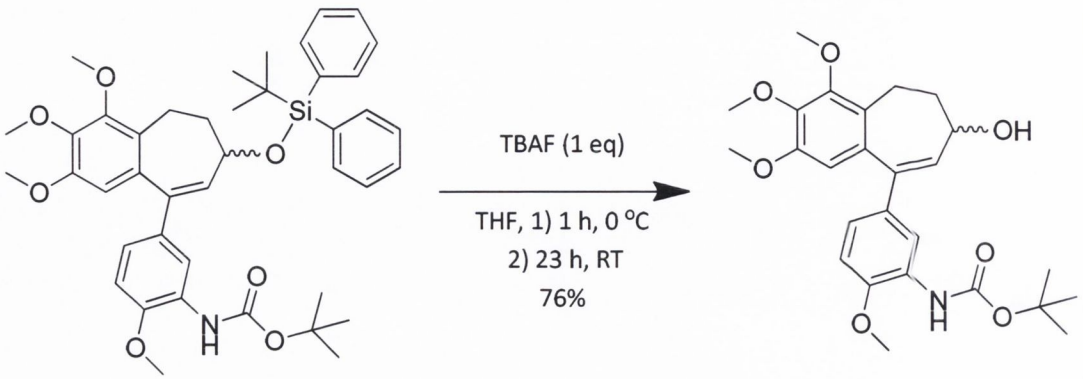

(2.32) **(2.34)**

To a stirred solution of **(2.32)** (0.04 g, 0.06 mmol) in THF (1 mL) at 0 °C was added 1 tetrabutylammonium fluoride solution (0.06 mL, 0.06 mmol) dropwise. The reaction was stirre 0 °C for 1 h and then allowed to increase to room temperature and stirred for 23 h. The react mixture was then diluted with DCM (1 mL) and added directly to a silica column and purifie flash column chromatography (stationary phase; silica gel 230-400 mesh, mobile phase; hexane/ethyl acetate) to yield **(2.34)** as an off-white solid (0.02 g, 76%).

R_f: 0.45 (1:1, hexane/ethyl acetate)

^{1}H NMR ($CDCl_3$, 400 MHz) δ_H ppm: 1.53 (9H, s, C(C$\underline{H}_3$)$_3$, 2.11 (1H, m, C$\underline{H}_2$), 2.37 (1H, m, C$\underline{H}_2$), 2 (1H, m, C$\underline{H}_2$), 3.02 (1H, m, C$\underline{H}_2$), 3.70 (3H, s, OC$\underline{H}_3$), 3.90 (3H, s, OC$\underline{H}_3$), 3.93 (3H, s, OC$\underline{H}_3$), 3.94 s, OC$\underline{H}_3$), 4.18 (1H, m, C$\underline{H}$OH), 6.36 (1H, d, J = 4.84 Hz, C=C$\underline{H}$), 6.39 (1H, s, Ar$\underline{H}$), 6.79 (2H, s, Ar$\underline{H}$), 7.09 (1H, s, Ar$\underline{H}$), 8.20 (1H, s, br, N$\underline{H}$)

^{13}C NMR ($CDCl_3$, 400 MHz) δ_c ppm: 21.39 (C$\underline{H}_2$), 27.90 (C(C$\underline{H}_3$)$_3$), 42.86 (C$\underline{H}_2$), 55.31 (OC$\underline{H}_3$), 5 (OC$\underline{H}_3$), 60.42 (OC$\underline{H}_3$), 61.09 (OC$\underline{H}_3$), 69.42 (C$\underline{H}$OH), 79.94 (C(CH$_3$)$_3$), 108.43 (Ar$\underline{C}$H), 109.00 (Ar 117.11 (Ar$\underline{C}$H), 122.00 (Ar$\underline{C}$H), 127.48 (Q$\underline{C}$), 127.65 (Q$\underline{C}$), 131.52 (C$\underline{H}$=C), 133.70 (Q$\underline{C}$), 134.91 (138.39 (Q$\underline{C}$), 140.92 (Q$\underline{C}$), 147.73 (Q$\underline{C}$), 150.28 (Q$\underline{C}$), 150.63 (Q$\underline{C}$), 152.28 (Q$\underline{C}$)

ν_{MAX} (DCM)/cm^{-1}: 2066.14, 1643.67, 1528.58, 1488.47, 1406.30

HRMS [M+Na]$^+$: calculated 494.2155, found 494.2211 , molecular formula ($C_{26}H_{33}NNaO_7$)

Melting Point: 180 °C

.13 Oxidation: Synthesis of *tert*-butyl (2-methoxy-5-(2,3,4-trimethoxy-7-oxo-6,7-ydro-5*H*-benzo[7]annulen-9-yl)phenyl)carbamate (2.35)

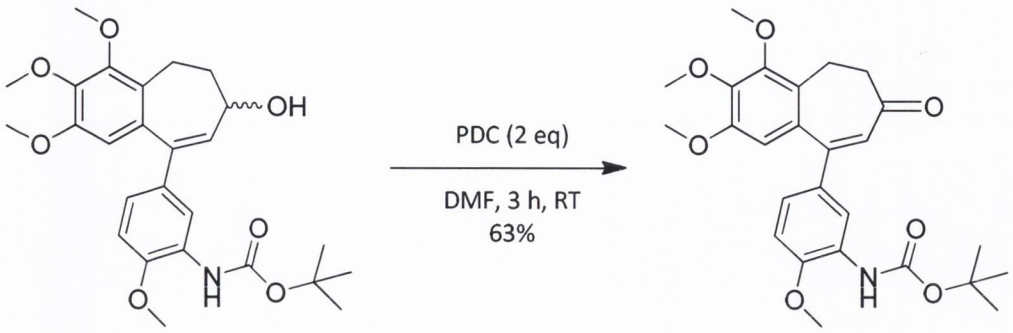

(2.34) **(2.35)**

a stirred solution of **(2.34)** (0.08 g, 0.17 mmol) in DMF (2 mL) was added pyridinium hromate (0.13 g, 0.34 mmol). After 3 h, the reaction was quenched by the slow addition of 2 M aqueous solution (15 mL) and the mixture was extracted with diethyl ether (3 x 25 mL). The anic fractions were dried over $MgSO_4$, filtered and concentrated *in vacuo.* The resulting residue s then purified by flash column chromatography (stationary phase; silica gel 230-400 mesh, bile phase; 4:1, hexane/ethyl acetate) to yield **(2.35)** as a yellow oil (0.05 g, 63%).

0.43 (1:1, hexane/ethyl acetate)

NMR ($CDCl_3$, 400 MHz) δ_H ppm: (1.51 (9H, s, C($C\underline{H}_3$)$_3$, 2.72 (2H, m, $C\underline{H}_2$), 3.15 (2H, m, $C\underline{H}_2$), 3.64 , s, $OC\underline{H}_3$), 3.91 (3H, s, $OC\underline{H}_3$), 3.93 (3H, s, $OC\underline{H}_3$), 3.96 (3H, s, $OC\underline{H}_3$), 6.40 (1H, s, C=C$\underline{H}$), 6.41 , s, Ar$\underline{H}$), 6.85 (1H, d, J = 8.5 Hz, Ar$\underline{H}$), 6.96 (1H, dd, J_1 = 8.5 Hz, J_2 = 2 Hz, Ar$\underline{H}$), 7.10 (1H, s, Ar$\underline{H}$), 1 (1H, s, br, N$\underline{H}$)

NMR ($CDCl_3$, 400 MHz) δ_c ppm: 20.24 ($\underline{C}H_2$), 28.33 (C($\underline{C}H_3$)$_3$), 45.50 ($\underline{C}H_2$), 55.79 ($O\underline{C}H_3$), 56.11 $\underline{C}H_3$), 60.92 ($O\underline{C}H_3$), 61.39 ($O\underline{C}H_3$), 80.60($\underline{C}(CH_3)_3$), 109.39 (Ar$\underline{C}$H), 112.18 ($\underline{C}$H=C), 118.74 (Ar$\underline{C}$H), 3.56 (Ar$\underline{C}$H), 127.89 (Q$\underline{C}$), 128.42 (Ar$\underline{C}$H), 129.22 (Q$\underline{C}$), 132.55 (Q$\underline{C}$), 135.57 (Q$\underline{C}$), 143.25 (Q$\underline{C}$), 3.15 (Q$\underline{C}$), 149.93 (Q$\underline{C}$), 151.02 (Q$\underline{C}$), 152.12 (Q$\underline{C}$), 152.57 (Q$\underline{C}$), 204.01 ($\underline{C}$=O)

$_{IX}$ (DCM)/cm^{-1}: 3435.99, 2930.00, 2854.43, 1728.64, 1652.10, 1590.88

MS $[M+H]^+$: calculated 470.2179, found 470.2173, molecular formula ($C_{26}H_{32}NO_7$)

7.4.14 Alternative oxidation of alcohol: Synthesis of Synthesis of *tert*-butyl (2-meth 5-(2,3,4-trimethoxy-7-oxo-6,7-dihydro-5*H*-benzo[7]annulen-9-yl)phenyl)carbamate (2.35)



(2.34) **(2.35)**

To a stirred solution of **(2.34)** (0.07 g, 0.15 mmol) in DCM at room temperature was added Martin periodinane (0.09 g, 0.22 mmol). After 30 min, the reaction was quenched by the ad of saturated sodium bicarbonate aqueous solution (10 mL) and the reaction was extracted diethyl ether (3 x 25 mL). The organic fractions were combined, dried over $MgSO_4$, concentrated *in vacuo*. The resulting residue was then purified by flash column chromatog (stationary phase; silica gel 230-400 mesh, mobile phase; 10:1, hexane/ethyl acetate) to **(2.35)** as a yellow oil (0.07 g, 99%).

Data already described.

7.4.15 Removal of BOC group: Synthesis of 9-(3-amino-4-methoxyphenyl)-2 trimethoxy-5*H*-benzo[7]annulen-7(6*H*)-one (2.25)

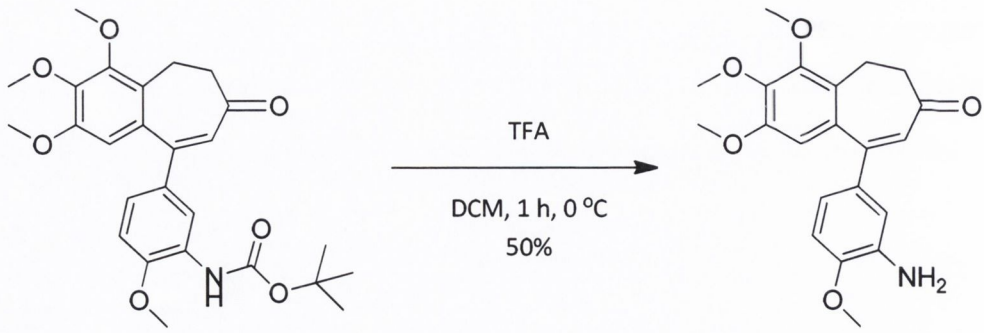

(2.35) **(2.25)**

a round bottom flask containing **(2.25)** (0.04 g, 0.11 mmol) under an atmosphere of nitrogen as added a mixture of TFA and dry DCM (2 mL, 1:1) at 0 °C. After 1 h, the solvent was removed *in cuo*. The resulting residue was then washed with sodium bicarbonate saturated aqueous lution (5 mL) and extracted with diethyl ether (3 x 5 mL). The organic fractions were dried over gSO_4, filtered and concentrated *in vacuo.* The resulting residue was then purified by flash lumn chromatography (stationary phase; silica gel 230-400 mesh, mobile phase; 4:1, xane/ethyl acetate) to yield **(2.25)** as a yellow oil (0.02 g, 50%).

: 0.75 (1:2, hexane/ethyl acetate)

NMR ($CDCl_3$, 400 MHz) δ_H ppm: 2.72 (2H, m, C<u>H</u>$_2$), 3.15 (2H, m, C<u>H</u>$_2$), 3.65 (3H, s, OC<u>H</u>$_3$), 3.91 H, s, OC<u>H</u>$_3$), 3.92 (3H, s, OC<u>H</u>$_3$), 3.96 (3H, s, OC<u>H</u>$_3$), 6.39 (1H, s, C=C<u>H</u>), 6.43 (1H, s, Ar<u>H</u>), 6.74 (2H, 2 x Ar<u>H</u>), 6.78 (1H, d, J = 8.7 Hz, Ar<u>H</u>)

NMR ($CDCl_3$, 400 MHz) δ_c ppm: 20.28 (<u>C</u>H$_2$), 45.71 (<u>C</u>H$_2$), 55.57 (O<u>C</u>H$_3$), 56.09 (O<u>C</u>H$_3$), 60.95 <u>C</u>H$_3$), 61.43 (O<u>C</u>H$_3$), 109.76 (Ar<u>C</u>H), 112.01 (Ar<u>C</u>H), 115.54 (Ar<u>C</u>H), 119.78 (Ar<u>C</u>H), 127.82 (<u>C</u>H=C), 9.06 (<u>Q</u>C), 132.71 (<u>Q</u>C), 135.45 (<u>Q</u>C), 135.80 (<u>Q</u>C), 143.14 (<u>Q</u>C), 148.07 (<u>Q</u>C), 149.87 (<u>Q</u>C), 151.00 <u>C</u>), 152.30 (<u>Q</u>C), 204.32 (<u>C</u>=O)

$_{AX}$ (DCM)/cm^{-1}: 2933.52, 1651.25 (C=O), 1513.03, 1492.79, 1464.70

RMS $[M+H]^+$: calculated 370.1654, found 370.1657, molecular formula ($C_{27}H_{38}O_6Si$)

4.16 Salt Formation: Synthesis of 2-methoxy-5-(2,3,4-trimethoxy-7-oxo-6,7-dihydro-5*H*-benzo[7]annulen-9-yl)benzenaminium chloride (2.36)

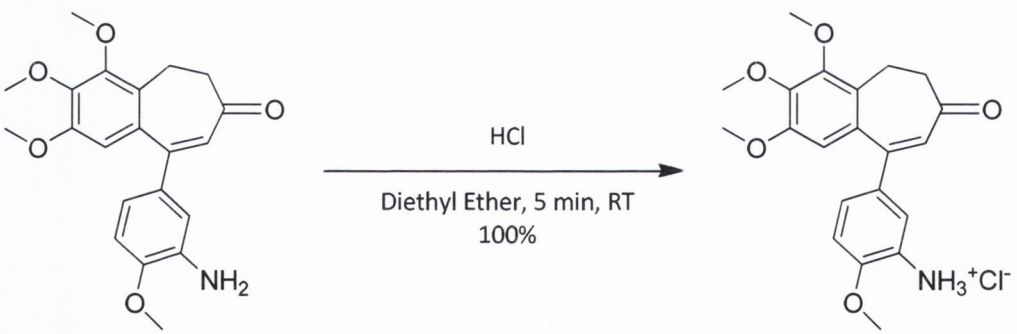

(2.25) **(2.36)**

seous HCl was bubbled through a solution of **(2.25)** (0.02 g, 0.05 mmol) in diethyl ether (2 mL). e resulting white precipitate was allowed to settle and the diethyl ether supernatant was moved. The precipitate was then washed with diethyl ether (3 x 2 mL) and then dried under cuum to yield **(2.36)** as a white solid (0.02 g, 100%)

7.5 Synthesis of enantiomerically pure (S)-methyl 3-hydroxy-5-(2,3, trimethoxyphenyl)pentanoate (3.01)

7.5.1 Bioreduction: Synthesis of (*S*)-methyl 3-hydroxy-5-(2,3, trimethoxyphenyl)pentanoate (3.07)

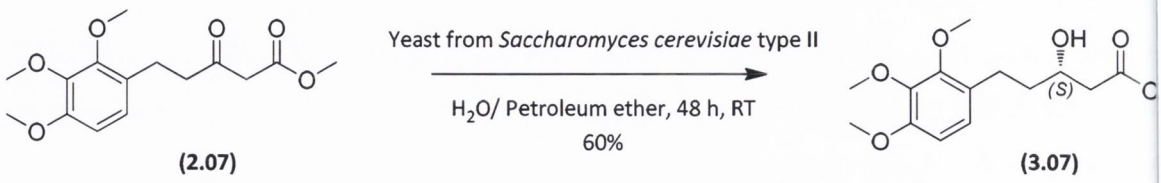

(2.07) **(3.07)**

To a clean, round bottomed flask was added **(2.07)** (1 g, 3.37 mmol), yeast from *Saccharomyc cerevisiae* type II (10g), water (10 mL) and petroleum ether (150 mL). The flask was stoppered a shaken for 48 h. The supernatant was decanted through filter paper and the yeast extracted wi ethyl acetate (3 x 100 mL). The organic fractions were combined, dried over $MgSO_4$, a concentrated *in vacuo*. The resulting oily residue was then purified by flash colun chromatography (stationary phase; silica gel 230-400 mesh, mobile phase; 4:1, hexane/eth acetate) to yield **(3.07)** as clear, colourless oil (0.6 g, 60%).

$[\alpha]_D^{25}$ = - 10.70 (*c* = 1.68, DCM)

All other data already described.

7.5.2 Bioreduction: Synthesis of (*S*)-ethyl 3-hydroxy-5-(2,3, trimethoxyphenyl)pentanoate (3.08)

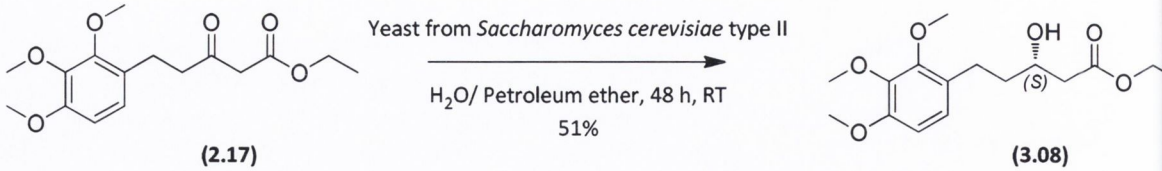

(2.17) **(3.08)**

To a clean, round bottomed flask was added **(2.17)** (0.45 g, 1.45 mmol), yeast fro *Saccharomyces cerevisiae*, type II (4g), water (6 mL) and petroleum ether (100 mL). The flask w stoppered and shaken for 48 h. The supernatant was decanted through filter paper and the yea extracted with ethyl acetate (3 x 100 mL). The organic fractions were combined, dried ov

$MgSO_4$, and concentrated *in vacuo*. The resulting oily residue was then purified by flash column chromatography (stationary phase; silica gel 230-400 mesh, mobile phase; 4:1, hexane/ethyl acetate) to yield **(3.08)** as a clear colourless oil (0.23 g, 51%).

Data already described.

7.6 Determination of stereochemistry and absolute configuration of bioreduced alcohols (3.07) and (3.08)

7.6.1. Synthesis of (*R*)-Mosher's ester of (2.08): Synthesis of methyl 3-(((*R*)-3,3,3-trifluoro-2-methoxy-2-phenylpropanoyl)oxy)-5-(2,3,4-trimethoxyphenyl)pentanoate (3.10)

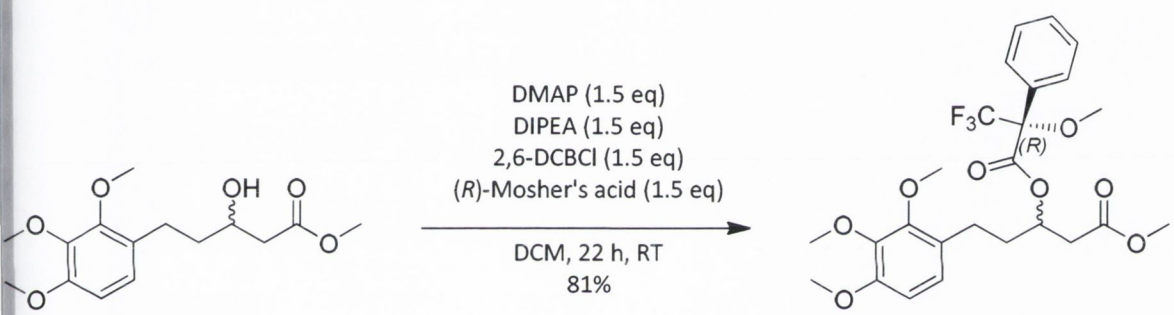

(2.08) **(3.10)**

To a stirred solution of **(2.08)** (0.05 g, 0.17 mmol) in dry DCM (2 mL) was added DMAP (0.03 g, 0.25 mmol), diisopropylethylamine (0.04 mL, 0.25 mmol), 2,6-dichlorobenzoyl chloride (0.04 mL, 0.25 mmol) and (*R*)-(+)-α-Methoxy-α-(trifluoromethyl)phenylacetic acid (0.06 g, 0.25 mmol) under an atmosphere of nitrogen. After 22 h, the reaction was quenched by the addition of saturated sodium bicarbonate aqueous solution (5 mL) and the product was extracted with diethyl ether (3 x 10 mL). The diethyl ether was dried over $MgSO_4$ and concentrated *in vacuo.* The resulting oily residue was then purified by flash column chromatography (stationary phase; silica gel 230-400 mesh, mobile phase; 4:1, hexane/ethyl acetate) to yield **(3.10)** as a yellow oil (0.7 g, 81%).

R_f: 0.53 (2:1, hexane/ethyl acetate)

^{19}F NMR ($CDCl_3$, 400 MHz) δ_F ppm: - 71.81 (1F, s, $C\underline{F}_3$), - 71.99 (1F, s, $C\underline{F}_3$)

7.6.2 Synthesis of (*R*)-Mosher's acid ester of (3.07): (*S*)-methyl 3-(((*R*)-3,3,3-trifluor methoxy-2-phenylpropanoyl)oxy)-5-(2,3,4-trimethoxyphenyl)pentanoate (3.11)

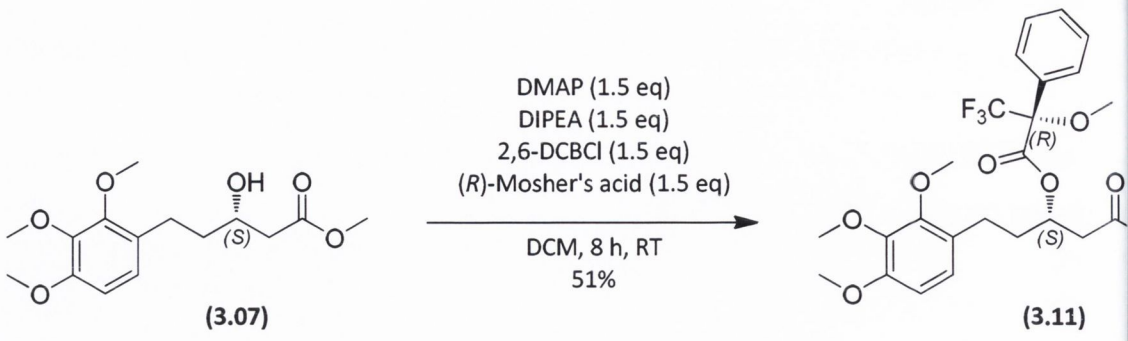

(3.07) **(3.11)**

To a stirred solution of **(3.07)** (0.06 g, 0.2 mmol) in dry DCM (2 mL) was added DMAP (0.04 g mmol), diisopropylethylamine (0.05 mL, 0.3 mmol), 2,6-dichlorobenzoyl chloride (0.04 mL mmol) and (*R*)-(+)-α-Methoxy-α-(trifluoromethyl)phenylacetic acid (0.07 g, 0.3 mmol) unde atmosphere of nitrogen. After 8 h, the reaction was quenched by the addition of satu sodium bicarbonate aqueous solution (5 mL) and the product was extracted with diethyl eth x 10 mL). The diethyl ether was dried over $MgSO_4$ and concentrated *in vacuo.* The resultin residue was then purified by flash column chromatography (stationary phase; silica gel 230 mesh, mobile phase; 4:1, hexane/ethyl acetate) to yield **(3.11)** as a yellow oil (0.50 g, 51%).

R_f: 0.53 (2:1, hexane/ethyl acetate)

^{1}H NMR ($CDCl_3$, 400 MHz) δ_H ppm: 2.00 (2H, m, C$\underline{H}_2$), 2.61 (2H, m, C$\underline{H}_2$), 2.70 (2H, m, C$\underline{H}_2$), (3H, s, OC$\underline{H}_3$), 3.61 (3H, s, OC$\underline{H}_3$), 3.86 (3H, s, OC$\underline{H}_3$), 3.87 (3H, s, OC$\underline{H}_3$), 3.88 (3H, s, OC$\underline{H}_3$), (1H, m, C$\underline{H}$OCO), 6.63 (1H, d, J = 8.5 Hz, Ar$\underline{H}$), 6.80 (1H, d, J = 8.5 Hz, Ar$\underline{H}$), 7.44 (3H, m, Ar$\underline{H}$), (2H, m, Ar$\underline{H}$)

^{13}C NMR ($CDCl_3$, 400 MHz) δ_c ppm: 25.67 ($\underline{C}H_2$), 29.72 (Q$\underline{C}$), 34.96 ($\underline{C}H_2$), 38.39 ($\underline{C}H_2$), 51.84 (C 55.44 (O$\underline{C}H_3$), 56 (O$\underline{C}H_3$), 60.75 (O$\underline{C}H_3$), 60.86 (O$\underline{C}H_3$), 73.31 ($\underline{C}$HOCO), 107.17 (Ar$\underline{C}$H), 1 (Ar$\underline{C}$H), 124.74 (Q$\underline{C}$), 126.48 (Q$\underline{C}$), 127.49 (2 x Ar$\underline{C}$H), 128.41 (2 x Ar$\underline{C}$H), 129.60 (Ar$\underline{C}$H), 1 (Q$\underline{C}$), 142.26 (Q$\underline{C}$), 151.80 (Q$\underline{C}$), 152.41 (Q$\underline{C}$), 165.91 ($\underline{C}$=O), 170.25 ($\underline{C}$=O)

^{19}F NMR ($CDCl_3$, 400 MHz) δ_F ppm: - 71.81 (1F, s, C$\underline{F}_3$), - 71.99 (1F, s, C$\underline{F}_3$)

HRMS $[M+Na]^+$: calculated 537.1712, found 537.1679, molecular formula ($C_{25}H_{29}F_3O_8Na$)

6.3 Synthesis of (*S*)-Mosher's ester of (3.07): Synthesis of (*S*)-methyl 3-(((*S*)-3,3,3-ifluoro-2-methoxy-2-phenylpropanoyl)oxy)-5-(2,3,4-trimethoxyphenyl)pentanoate .12)

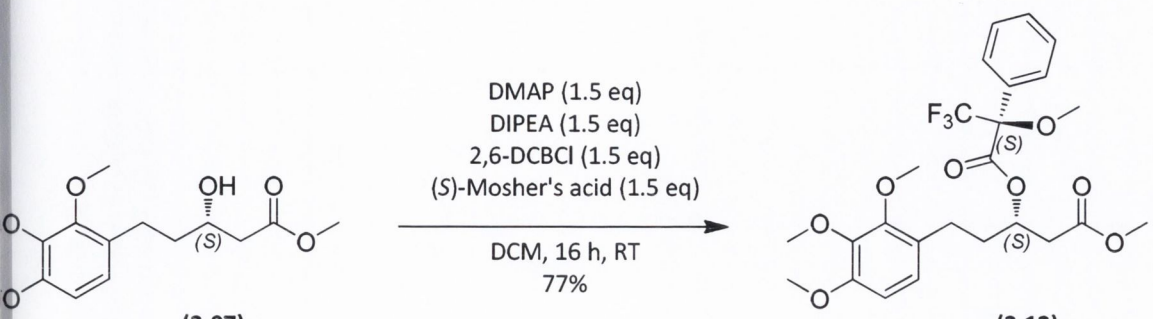

(3.07) **(3.12)**

a stirred solution of **(3.07)** (0.06 g, 0.2 mmol) in dry DCM (2 mL) was added DMAP (0.04 g, 0.3 mol), diisopropylethylamine (0.05 mL, 0.3 mmol), 2,6-dichlorobenzoyl chloride (0.04 mL, 0.3 mol) and (*S*)-(+)-α-Methoxy-α-(trifluoromethyl)phenylacetic acid (0.07 g, 0.3 mmol) under an mosphere of nitrogen. After 16 h, the reaction was quenched by the addition of saturated dium bicarbonate aqueous solution (5 mL) and the product was extracted with diethyl ether (3 10 mL). The diethyl ether was dried over $MgSO_4$ and concentrated *in vacuo.* The resulting oily sidue was then purified by flash column chromatography (stationary phase; silica gel 230-400 esh, mobile phase; 4:1, hexane/ethyl acetate) to yield **(3.12)** as a yellow oil (0.50 g, 77%).

0.82 (3:1, hexane/ethyl acetate)

NMR ($CDCl_3$, 400 MHz) δ_H ppm: 1.95 (2H, m, C<u>H</u>$_2$), 2.51 (2H, m, C<u>H</u>$_2$), 2.74 (2H, m, C<u>H</u>$_2$), 3.59 H, s, OC<u>H</u>$_3$), 3.68 (3H, s, OC<u>H</u>$_3$), 3.83 (3H, s, OC<u>H</u>$_3$), 3.86 (3H, s, OC<u>H</u>$_3$), 3.88 (3H, s, OC<u>H</u>$_3$), 5.55 H, m, C<u>H</u>OCO), 6.60 (1H, d, J = 8.5 Hz, Ar<u>H</u>), 6.72 (1H, d, J = 8.5 Hz, Ar<u>H</u>), 7.42 (3H, m, Ar<u>H</u>), 7.60 H, m, Ar<u>H</u>)

NMR ($CDCl_3$, 400 MHz) δ_c ppm: 25.43 (<u>C</u>H$_2$), 34.87 (<u>C</u>H$_2$), 38.53 (<u>C</u>H$_2$), 51.92 (O<u>C</u>H$_3$), 55.44 <u>C</u>H$_3$), 55.98 (O<u>C</u>H$_3$), 60.72 (O<u>C</u>H$_3$), 60.82 (O<u>C</u>H$_3$), 73.21 (<u>C</u>HOCO), 107.14 (Ar<u>C</u>H), 123.71 (Ar<u>C</u>H), 6.55 (<u>Q</u>C), 127.43 (2 x Ar<u>C</u>H), 128.41 (2 x Ar<u>C</u>H), 129.62 (Ar<u>C</u>H), 132.23 (<u>Q</u>C), 142.25 (<u>Q</u>C), 1.80 (<u>Q</u>C), 152.36 (<u>Q</u>C), 165.99 (<u>C</u>=O), 170.45 (<u>C</u>=O)

NMR ($CDCl_3$, 400 MHz) δ_F ppm: - 71.31 (1F, s, C<u>F</u>$_3$), - 71.49 (1F, s, C<u>F</u>$_3$)

7.6.4 Synthesis of (*S*)-Mosher's ester of (3.08): Synthesis of (*S*)-ethyl 3-(((*S*)-3 trifluoro-2-methoxy-2-phenylpropanoyl)oxy)-5-(2,3,4-trimethoxyphenyl)pentanoat (3.13)

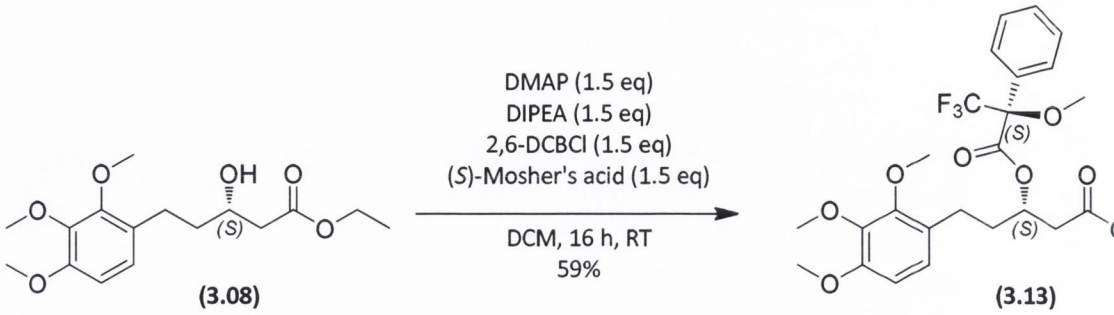

(3.08) (3.13)

To a stirred solution of **(3.08)** (0.05 g, 0.16 mmol) in dry DCM (2 mL) was added DMAP (0 0.24 mmol), diisopropylethylamine (0.04 mL, 0.24 mmol), 2,6-dichlorobenzoyl chloride (0.0 0..24 mmol) and (*S*)-(+)-α-Methoxy-α-(trifluoromethyl)phenylacetic acid (0.06 g, 0.24 under an atmosphere of nitrogen. After 16 h, the reaction was quenched by the addit saturated sodium bicarbonate aqueous solution (5 mL) and the product was extracted diethyl ether (3 x 10 mL). The diethyl ether was dried over $MgSO_4$ and concentrated *in vacu* resulting oily residue was then purified by flash column chromatography (stationary phase gel 230-400 mesh, mobile phase; 4:1, hexane/ethyl acetate) to yield **(3.13)** as a yellow oil (0 59%).

R_f: 0.44 (3:1, hexane/ethyl acetate)

^{1}H NMR ($CDCl_3$, 400 MHz) δ_H ppm: 1.26 (3H, m, C<u>H</u>$_3$), 1.93 (2H, m, C<u>H</u>$_2$), 2.49 (2H, m, C<u>H</u>$_2$ (2H, m, C<u>H</u>$_2$), 3.59 (3H, s, OC<u>H</u>$_3$), 3.83 (3H, s, OC<u>H</u>$_3$), 3.85 (3H, s, OC<u>H</u>$_3$), 3.87 (3H, s, OC<u>H</u>$_3$), 4.1 m, C<u>H</u>$_2$), 5.57 (1H, m, C<u>H</u>OCO), 6.59 (1H, d, J = 8.5 Hz, Ar<u>H</u>), 6.71 (1H, d, J = 8.5 Hz, Ar<u>H</u>), 7.4 m, Ar<u>H</u>), 7.59 (2H, m, Ar<u>H</u>)

^{13}C NMR ($CDCl_3$, 400 MHz) δ_c ppm: 13.62 (<u>C</u>H$_3$), 24.96 (<u>C</u>H$_2$), 34.72 (<u>C</u>H$_2$), 38.31 (<u>C</u>H$_2$), (O<u>C</u>H$_3$), 55.52 (O<u>C</u>H$_3$), 60.27 (O<u>C</u>H$_3$), 60.36 (O<u>C</u>H$_3$), 60.48 (<u>C</u>H$_2$), 72.76 (<u>C</u>HOCO), 83.93 (<u>Q</u>C), (Ar<u>C</u>H), 123.24 (Ar<u>C</u>H), 126.15 (<u>Q</u>C), 126,95 (2 x Ar<u>C</u>H), 127.93 (2 x Ar<u>C</u>H), 129.14 (Ar<u>C</u>H), (<u>Q</u>C), 141.76 (<u>Q</u>C), 151.33 (<u>Q</u>C), 151.87 (<u>Q</u>C), 165.49 (<u>C</u>=O), 169.54 (<u>C</u>=O)

^{19}F NMR ($CDCl_3$, 400 MHz) δ_F ppm: - 71.57 (1F, s, C<u>F</u>$_3$), - 71.81 (1F, s, C<u>F</u>$_3$)

.5 Synthesis of (*R*)-Mosher's ester of (3.08): Synthesis of (*S*)-ethyl 3-(((*R*)-3,3,3-luoro-2-methoxy-2-phenylpropanoyl)oxy)-5-(2,3,4-trimethoxyphenyl)pentanoate 14)

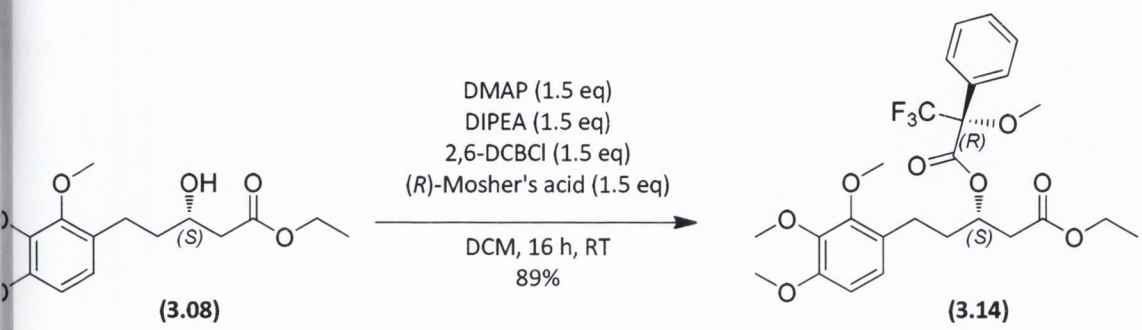

(3.08) **(3.14)**

a stirred solution of **(3.08)** (0.06 g, 0.19 mmol) in dry DCM (2 mL) was added DMAP (0.04 g, 9 mmol), diisopropylethylamine (0.05 mL, 0.29 mmol), 2,6-dichlorobenzoyl chloride (0.04 mL, 9 mmol) and (*R*)-(+)-α-Methoxy-α-(trifluoromethyl)phenylacetic acid (0.07 g, 0.29 mmol) under atmosphere of nitrogen. After 16 h, the reaction was quenched by the addition of saturated lium bicarbonate aqueous solution (5 mL) and the product was extracted with diethyl ether (3 0 mL). The diethyl ether was dried over $MgSO_4$ and concentrated *in vacuo.* The resulting oily idue was then purified by flash column chromatography (stationary phase; silica gel 230-400 sh, mobile phase; 4:1, hexane/ethyl acetate) to yield **(3.14)** as a yellow oil (0.09 g, 89%).

0.44 (3:1, hexane/ethyl acetate)

NMR ($CDCl_3$, 400 MHz) δ_H ppm: 1.21 (3H, m, C<u>H</u>$_3$), 2.00 (2H, m, C<u>H</u>$_2$), 2.62 (2H, m, C<u>H</u>$_2$), 2.73 , m, C<u>H</u>$_2$), 3.59 (3H, s, OC<u>H</u>$_3$), 3.86 (3H, s, OC<u>H</u>$_3$), 3.87 (3H, s, OC<u>H</u>$_3$), 3.88 (3H, s, OC<u>H</u>$_3$), 4.07 (2H, C<u>H</u>$_2$), 5.57 (1H, m, C<u>H</u>OCO), 6.61 (1H, d, J = 8.5 Hz, Ar<u>H</u>), 6.80 (1H, d, J = 8.5 Hz, Ar<u>H</u>), 7.42 (3H, Ar<u>H</u>), 7.58 (2H, m, Ar<u>H</u>)

NMR ($CDCl_3$, 400 MHz) δ_c ppm: 13.58 (<u>C</u>H$_3$), 25.19 (<u>C</u>H$_2$), 29.25 (Q<u>C</u>), 35.50 (<u>C</u>H$_2$), 38.14 (<u>C</u>H$_2$), 97 (O<u>C</u>H$_3$), 55.52 (O<u>C</u>H$_3$), 60.26 (O<u>C</u>H$_3$), 60.36 (O<u>C</u>H$_3$), 60.38 (<u>C</u>H$_2$), 72.89 (<u>C</u>HOCO), 84.00 (Q<u>C</u>), .70 (Ar<u>C</u>H), 121.42 (Q<u>C</u>), 123.25 (Ar<u>C</u>H), 124.29 (Q<u>C</u>), 126.08 (Q<u>C</u>), 127.04 (2 x Ar<u>C</u>H), 127.93 (2 r<u>C</u>H), 129.13 (Ar<u>C</u>H), 131.67 (Q<u>C</u>), 141.78 (Q<u>C</u>), 151.34 (Q<u>C</u>), 151.93 (Q<u>C</u>), 165.43 (<u>C</u>=O), 169.35 O)

NMR ($CDCl_3$, 400 MHz) δ_F ppm: - 72.01 (1F, s, C<u>F</u>$_3$), - 72.11 (1F, s, C<u>F</u>$_3$)

7.7 Synthesis of enantiomerically pure (S)-9-(3-hydroxy-4-methoxyphe 2,3,4-trimethoxy-6,7-dihydro-5H-benzo[7]annulen-7-ol (3.01)

7.7.1 Silyl protection of β-hydroxy group: Synthesis of (3*S*)-3-[butyldiphenylsilyl)oxy]-5-(2,3,4-trimethoxyphenyl)pentanoate (3.15)

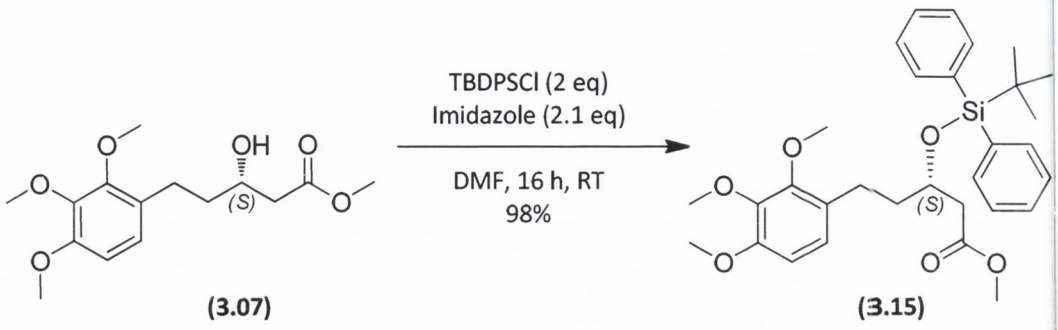

(3.07) **(3.15)**

To a stirred solution of **(3.07)** (7.48 g, 25.24 mmol) in dry DMF (30 mL) under anhy conditions was added *tert*-butyldiphenylsilyl chloride (13.13 mL, 50.49 mmol) and imidazole g, 53.01 mmol). After 16 h, the reaction was quenched by the addition of water (100 mL reaction mixture was then extracted with diethyl ether (3 x 100 mL). The diethyl ether ex were dried over $MgSO_4$, filtered and concentrated under vacuum. The resulting residue purified by flash column chromatography (stationary phase; silica gel 230-400 mesh, m phase; 10:1, hexane/ethyl acetate) to yield **(3.15)** as a clear oil (13.28 g, 98%).

$[\alpha]_D^{25}$ = + 28.86 (*c* = 18.5, DCM)

All other data already described.

.2 Hydrolysis of methyl ester: Synthesis of (3*S*)-3-[(*tert*-butyldiphenylsilyl)oxy]-5-,4-trimethoxyphenyl)pentanoic acid (3.16)

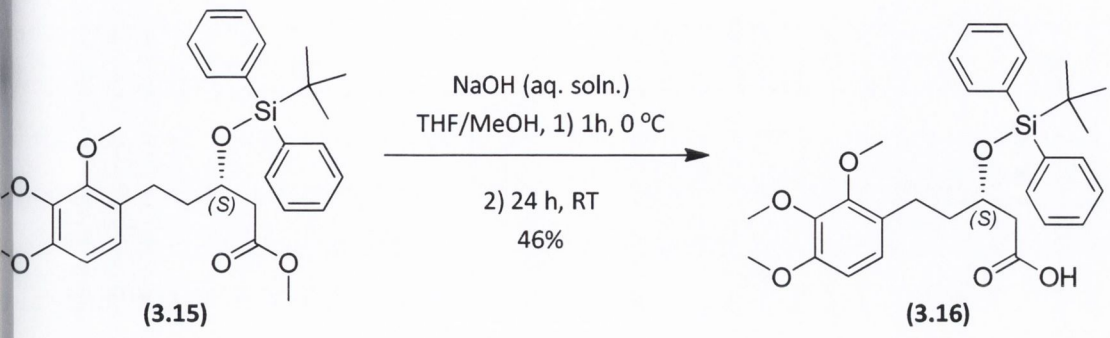

(3.15) **(3.16)**

a stirred solution of **(3.15)** (13.28 g, 24.74 mmol) in a mixture of methanol (100 mL) and THF mL) at 0 °C was added 2.5 M NaOH aqueous solution (30 mL). After 1 h, the temperature was eased to room temperature and the reaction was left stirring for a further 24 h. The solution then acidified with 2 M HCl aqueous solution (50 mL) and the volatile organic phase removed er reduced pressure. The aqueous reaction mixture was then extracted with diethyl ether (3 x mL). The diethyl ether extracts were dried over $MgSO_4$, filtered and concentrated *in vacuo.* resulting residue was then purified by flash column chromatography (stationary phase; silica 230-400 mesh, mobile phase; ethyl acetate) to yield **(3.16)** as a white solid (5.94 g, 46%).

$^{25}_{D}$ = + 33.14 (*c* = 7, DCM)

other data as previously described.

.3 Cyclisation: Synthesis of (7*S*)-7-[(*tert*-butyldiphenylsilyl)oxy]-1,2,3-trimethoxy-,8,9-tetrahydro-5*H*-benzo[7]annulen-5-one (3.17)

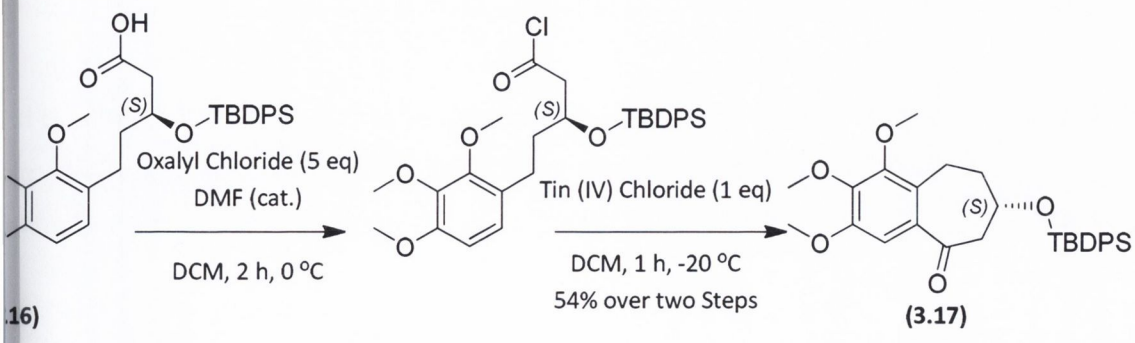

.16) **(3.17)**

To a stirred solution of **(3.16)** (5.94 g, 11.36 mmol) in dry DCM (30 mL) and DMF (0.5 mL) at 0 °C under an atmosphere of nitrogen was added 2 M oxalyl chloride solution (28.41 mL, 56.82 mmol) dropwise. The solution was left stirring for 2 h at 0 °C after which time the solvent was removed under high vacuum at room temperature. The residue was left to dry under high vacuum for 2 h after which time the residue was reconstituted with dry DCM (50 mL) under an atmosphere of nitrogen. The temperature of the solution was reduced to -20 °C using a sodium chloride ice bath and 1 M tin (IV) chloride solution in DCM (11.36 mL, 11.36 mmol) was added dropwise. After 1 h, the reaction was quenched by the addition of saturated sodium chloride aqueous solution (100 mL) and the mixture was extracted with diethyl ether (3 x 150 mL). The organic fractions were combined, dried over $MgSO_4$, filtered and concentrated *in vacuo.* The resulting residue was then purified by flash column chromatography (stationary phase; silica gel 230-400 mesh, mobile phase; 10:1, hexane/ethyl acetate) to yield **(3.17)** as a yellow oil (3.08 g, 54%).

$[\alpha]_D^{25}$ = + 7.14 (*c* = 7, DCM)

All other data as previously described.

7.7.3 Deprotection: Synthesis of (*S*)-6,7,8,9-tetrahydro-7-hydroxy-1,2,3-trimethoxybenzo[7]annulen-5-one (3.18)

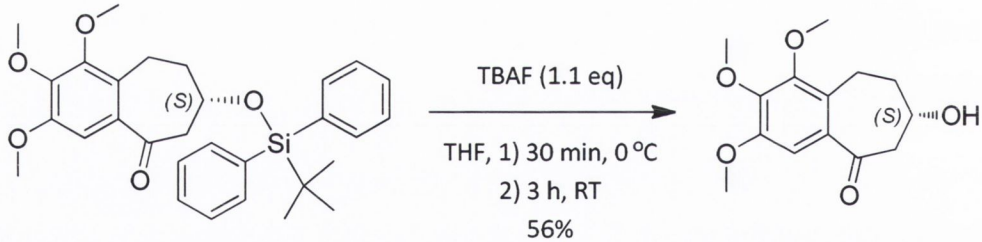

(3.17) **(3.18)**

To a stirred solution of **(3.17)** (3.34 g, 6.62 mmol) in THF (15 mL) at 0 °C was added 1 M tetrabutylammonium fluoride solution (7.29 mL, 7.29 mmol) dropwise. After 30 min, the temperature was allowed to increase to room temperature and left stirring for a further 3 h. The reaction mixture was then added directly to a silica gel column and purified by flash column chromatography (stationary phase; silica gel 230-400 mesh, mobile phase; 4:1, hexane/ethyl acetate) to yield **(3.18)** as a yellow oil (0.93 g, 56%).

$[\alpha]_D^{25}$ = - 8.24 (*c* =8.5, DCM)

All other data as previously described.

7.7.4 Organolithium Coupling: Synthesis of (7*S*)-9-{3-[(*tert*-butyldimethylsilyl)oxy]-4-methoxyphenyl}-2,3,4-trimethoxy-6,7-dihydro-5*H*-benzo[7]annulen-7-ol (3.19)

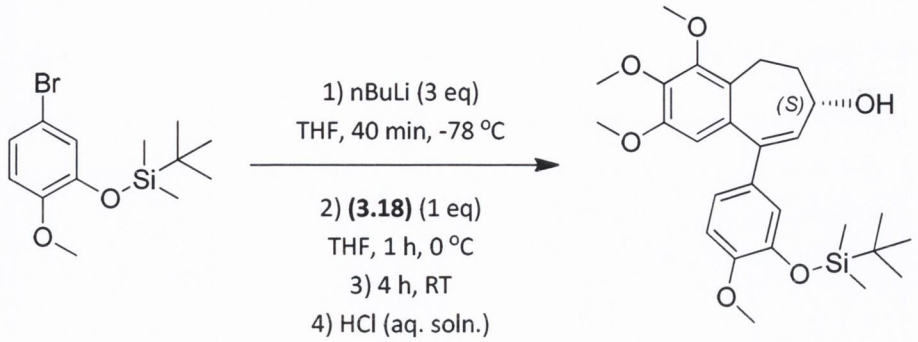

(2.14) **(3.19)**

To a stirred solution of **(2.14)** (3.33 g, 10.48 mmol) in dry THF (10 mL) under an atmosphere of nitrogen at -78 °C was added 2.5 M *n*-butyllithium solution in hexane (4.19 mL, 10.48 mmol) dropwise. After 40 min, a solution of **(3.18)** (0.93 g, 3.49 mmol) in dry THF (5 mL) was added to the reaction. After 1 h, the temperature was increased to ambient and left stirring for a further 4 h. The reaction was quenched by the addition of 2 M HCl aqueous solution (50 mL) and then extracted with diethyl ether (3 x 50 mL). The organic fractions were combined, dried over $MgSO_4$, filtered and concentrated *in vacuo*. The resulting residue was then purified by flash column chromatography (stationary phase; silica gel 230-400 mesh, mobile phase; 4:1, hexane/ethyl acetate) to yield **(3.19)** as a yellow resin (1 g, 59 %).

$[\alpha]_D^{25}$ = - 47.25 (*c* = 8, DCM)

All other data as previously described.

7.7.5 Deprotection of C-ring phenol: Synthesis of (*S*)-9-(3-hydroxy-4-methoxyphenyl)-2,3,4-trimethoxy-6,7-dihydro-5*H*-benzo[7]annulen-7-ol (3.01)

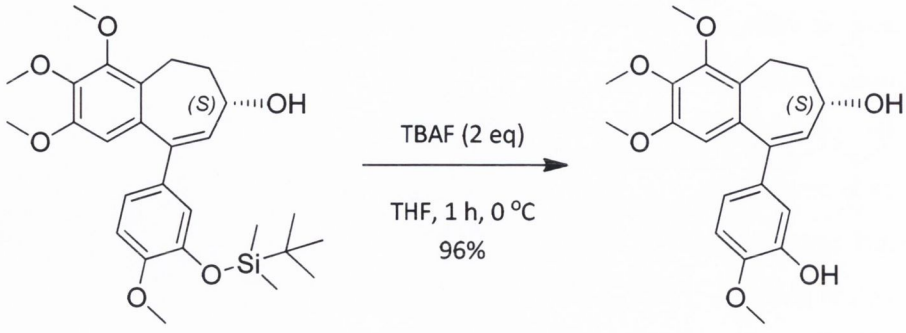

(3.19) **(3.01)**

To a stirred solution of **(3.19)** (0.04 g, 0.12 mmol) in dry THF (1 mL) under an atmosphere of nitrogen at 0 °C was added 1 M TBAF solution in THF (0.23 mL, 0.23 mmol). After 1 h, the THF was blown off in a stream of nitrogen gas and the reaction mixture added directly to a silica gel column and purified by flash column chromatography (stationary phase; silica gel 230-400 mesh, mobile phase; ethyl acetate) to yield **(3.01)** as a white solid (0.04 g, 96%).

$[\alpha]_D^{25}$ = - 63 (*c* = 2, DCM)

All other data as previously described.

7.8 CBS reduction: Attempted synthesis of (R)-methyl 3-hydroxy-5-(2,3,4-trimethoxyphenyl)pentanoate

7.8.1 CBS reduction of β-ketoester: Attempted synthesis of (*R*)-methyl 3-hydroxy-5-(2,3,4-trimethoxyphenyl)pentanoate (3.20)

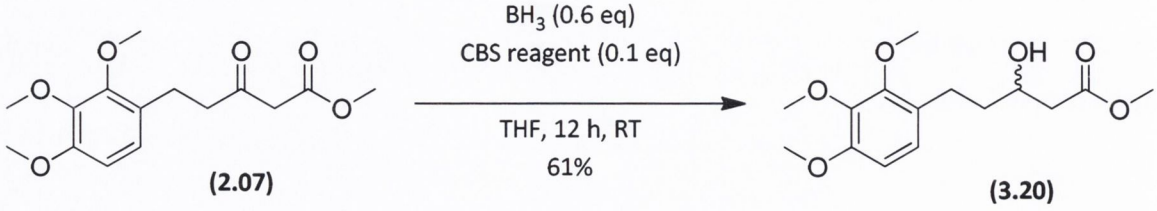

(2.07) **(3.20)**

Procedure A:

To a stirred solution of (*S*)-(−)-2-Methyl-CBS-oxazaborolidine (0.05 g, 0.17 mmol) in dry THF (5 mL) was added **(2.07)** (0.5 g, 1.69 mmol) in dry THF (2 mL) followed by 1 M BH_3 solution in THF (1.01 mL, 1.01 mmol) under an atmosphere of nitrogen. After 12 h, the reaction was quenched by the addition of water (20 mL). The reaction mixture was then extracted with diethyl ether (3 x 25 mL). The organic fractions were dried over $MgSO_4$, filtered and concentrated *in vacuo.* The resulting oily residue was then purified by flash column chromatography (stationary phase; silica gel 230-400 mesh, mobile phase; 4:1, hexane/ethyl acetate) to yield **(3.20)** as a clear oil (0.31 g, 61%).
Data already described.

Procedure B:

To a stirred solution of 1 M BH_3 in dry THF (0.28 mL, 0.28 mmol) and (*S*)-(−)-2-Methyl-CBS-oxazaborolidine (0.01 g, 0.05 mmol) in dry THF (3 mL) was added a solution of **(2.07)** (0.14 g, 0.46 mmol) in dry THF (1 mL) dropwise under an atmosphere of nitrogen. After 24 h, the reaction was quenched by the addition of water (5 mL). The reaction mixture was then extracted with diethyl ether (3 x 10 mL). The organic fractions were dried over $MgSO_4$, filtered and concentrated *in vacuo.* The resulting oily residue was then purified by flash column chromatography (stationary phase; silica gel 230-400 mesh, mobile phase; 4:1, hexane/ethyl acetate) to yield **(3.20)** as a clear oil (0.01 g, 7%).
Data already described.

Procedure C:

To a stirred solution of 1 M BH_3 in THF (0.20 mL, 0.20 mmol) and (S)-(−)-2-Methyl-CBS-oxazaborolidine (0.09 g, 0.34 mmol) in dry THF (3 mL) was added a solution of **(2.07)** (0.1 g, 0.34 mmol) in dry THF (1 mL) dropwise under an atmosphere of nitrogen. After 24 h, the reaction was quenched by the addition of water (5 mL). The reaction mixture was then extracted with diethyl ether (3 x 10 mL). The organic fractions were dried over $MgSO_4$, filtered and concentrated *in vacuo* to afford the starting materials unchanged.

7.8.2 Synthesis of (*R*)-Mosher's acid ester of CBS reduced alcohol (3.20): Synthesis of methyl 3-((*R*)-3,3,3-trifluoro-2-methoxy-2-phenylpropanoyloxy)-5-(2,3,4-trimethoxyphenyl)pentanoate (3.21)

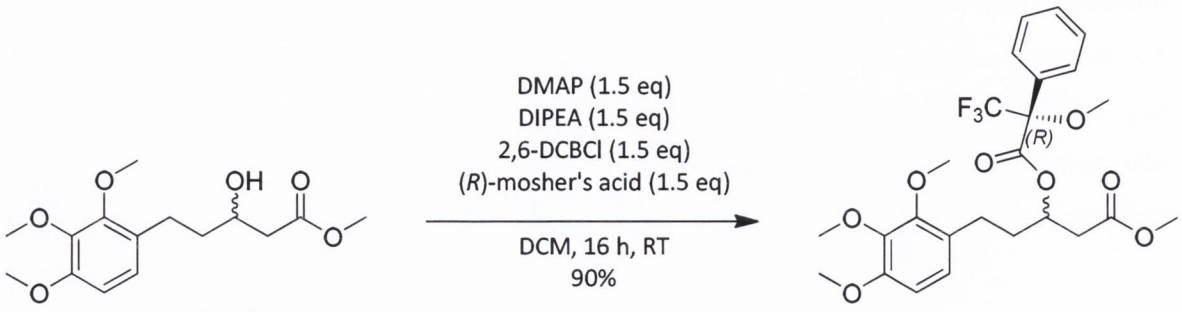

(3.20) **(3.21)**

To a stirred solution of **(3.20)** (0.06 g, 0.2 mmol) in dry DCM (2 mL) was added DMAP (0.04 g, 0.3 mmol), diisopropylethylamine (0.05 mL, 0.3 mmol), 2, 6-dichlorobenzoyl chloride (0.04 mL, 0.3 mmol) and (*R*)-(+)-α-Methoxy-α-(trifluoromethyl)phenylacetic acid (0.07 g, 0.3 mmol) under an atmosphere of nitrogen. After 16 h, the reaction was quenched by the addition of saturated sodium bicarbonate aqueous solution (5 mL) and the product was extracted with diethyl ether (3 x 10 mL). The diethyl ether was dried over $MgSO_4$, filtered and concentrated *in vacuo.* The resulting oily residue was then purified by flash column chromatography (stationary phase; silica gel 230-400 mesh, mobile phase; 4:1, hexane/ethyl acetate) to yield **(3.21)** as a yellow oil (0.1 g, 90%).

^{19}F NMR ($CDCl_3$, 400 MHz) δ_F ppm: - 71.81 (1F, s, C$\underline{F}_3$), - 71.99 (1F, s, C$\underline{F}_3$)

7.9 Mitsunobu reaction: Attempted inversion of configuration to afford (7R)-6,7,8,9-tetrahydro-1,2,3-trimethoxy-5-(methoxymethoxy)-5H-benzo[7]annulen-7-yl formate

7.9.1 Attempted Mitsunobu reaction: Attempted synthesis of (*R*)-methyl 3-(formyloxy)-5-(2,3,4-trimethoxyphenyl)pentanoate (3.22)

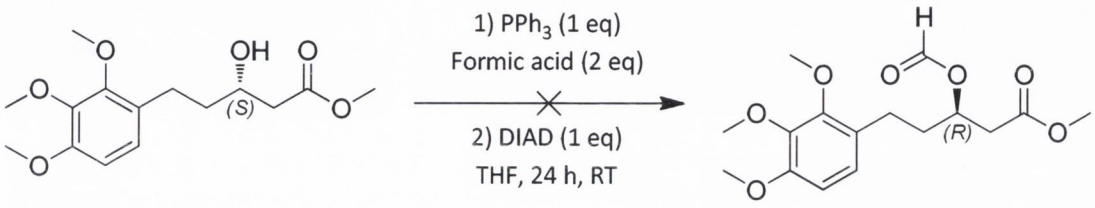

(3.07) **(3.22)**

To a stirred solution of **(3.07)** (0.08 g, 0.26 mmol), triphenylphosphine (0.07 g, 0.26 mmol) and formic acid (0.02 mL, 0.52 mmol) in dry THF under an atmosphere of nitrogen at 0 °C was added diisopropyl azodicarboxylate (0.05 mL, 0.26 mmol) dropwise. After 24 h, the starting material was recovered unchanged.

7.9.2 Attempted mitsunobu reaction: Alternate attempted Synthesis of (*R*)-methyl 3-(formyloxy)-5-(2,3,4-trimethoxyphenyl)pentanoate (3.22)

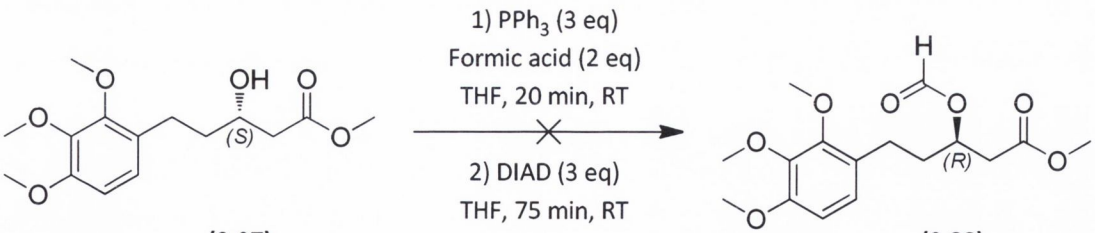

(3.07) **(3.22)**

To a stirred solution of **(3.07)** (0.12 g, 0.4 mmol) and triphenylphosphine (0.32 g, 1.2 mmol) in dry THF (15 mL) was added formic acid (0.03 mL, 0.8 mmol)) under an atmosphere of nitrogen. After 20 min DIAD (0.24 mL, 1.2 mmol) was added dropwise. After 75 min, the reaction was quenched by the addition of brine (50 mL) and the proposed product was extracted with diethyl ether (3 x

50 mL). The organic fractions were combined, dried over $MgSO_4$, filtered and concentrated under reduced pressure. The resulting residue was purified by flash column chromatography (stationary phase; silica gel 230-400 mesh, mobile phase; 4:1, hexane/ethyl acetate) and the major product isolated. However on subsequent analysis it was found not to be the product of interest.

7.10 Removing source of conjugation: Use of acetate, MEM, THP and MOM protecting groups

7.10.1 Reduction: Synthesis of (7*S*)-7-((*tert*-butyldiphenylsilyl)oxy)-1,2,3-trimethoxy-6,7,8,9-tetrahydro-5*H*-benzo[7]annulen-5-ol (3.24)

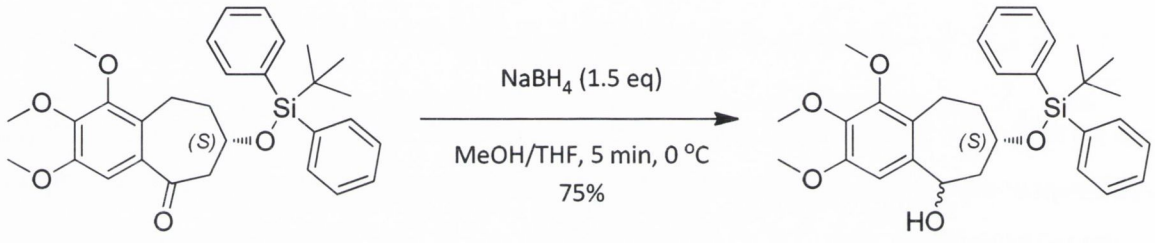

(3.17) **(3.24)**

To a stirred solution of **(3.17)** (0.32 g, 0.63 mmol) in methanol (3 mL) and THF (1.5 mL) at 0 °C was added $NaBH_4$ (0.04 g, 0.95 mmol). After 5 min, the reaction was quenched by the addition of water (25 mL). The organic solvent was then removed under reduced pressure and the resulting residue extracted with diethyl ether (3x 20 mL). The organic fractions were combined, dried over $MgSO_4$ and filtered. The solvent was then removed *in vacuo* to afford **(3.24)** as a white solid (0.24 g, 75%).

R_f: 0.06 (3:1, hexane/ethyl acetate)

^{1}H NMR ($CDCl_3$, 400 MHz) δ_H ppm: 1.12 (9H, s, major diastereomer, C(C$\underline{H}_3$)$_3$), 1.17 (9H, s, minor diastereomer C(C$\underline{H}_3$)$_3$), 1.33-1.43 (1H, m, minor diastereomer, C$\underline{H}_2$), 1.64 (2H, m, minor and major diastereomers, C$\underline{H}_2$), 1.69 (1H, s, minor diastereomer, C$\underline{H}_2$), 1.73-1.83 (2H, m, minor and major disastereomers, C$\underline{H}_2$), 1.86-1.96 (1H, major diastereomer, C$\underline{H}_2$), 1.96-2.05 (2H, m, minor and major diastereomers, C$\underline{H}_2$), 2.21 (1H, br s, major diastereomer, O$\underline{H}$), 2.45 (1H, br s, minor diastereomer, O$\underline{H}$), 2.98-3.02 (2H, m, minor and major diastereomers, C$\underline{H}_2$), 3.24-3.30 (1H, m, minor and major diastereomers, C$\underline{H}_2$), 3.80 (3H, s, major diastereomer, OC$\underline{H}_3$), 3.81 (3H, s, minor diastereomer, OC$\underline{H}_3$), 3.87 (3H, s, major diastereomer, OC$\underline{H}_3$), 3.88 (3H, s, minor diastereomer, OC$\underline{H}_3$), 3.88 (3H,

s, major diastereomer, OC$\underline{H}_3$), 3.89 (3H, s, minor diastereomer, OC$\underline{H}_3$) , 4.22 (1H, s br, major diastereomer, C$\underline{H}$), 4.30 (1H, m, minor diastereomer, C$\underline{H}$), 4.70 (1H, m, major diastereomer, C$\underline{H}$), 5.43 (1H, m, minor diastereomer, C$\underline{H}$), 6.78 (1H, s, major diastereomer, Ar$\underline{H}$), 6.95 (1H, s, minor diastereomer, Ar$\underline{H}$), 7.41-7.52 (6H, m, minor and major diastereomers, Ar$\underline{H}$), 7.72-7.80 4H, m, minor and major diastereomers, Ar$\underline{H}$).

^{13}C NMR ($CDCl_3$, 400 MHz) δ_c ppm: 17.70 ($\underline{C}H_2$), 18.29 ($\underline{C}H_2$), 19.16 ($\underline{C}(CH_3)_3$), 19.44 ($\underline{C}(CH_3)_3$), 26.98 (C($\underline{C}H_3$)$_3$), 27.13 (C($\underline{C}H_3$)$_3$), 34.99 ($\underline{C}H_2$), 35.47 ($\underline{C}H_2$), 44.80 ($\underline{C}H_2$), 55.99 (O$\underline{C}H_3$), 56.01 (O$\underline{C}H_3$), 60.87 (O$\underline{C}H_3$), 60.89 (O$\underline{C}H_3$), 61.37 (O$\underline{C}H_3$), 69.55 ($\underline{C}$HOSi), 73.86 ($\underline{C}$HOH), 103.71 (Ar$\underline{C}$H), 125.78 ($\underline{Q}C$), 127.68 (2 x Ar$\underline{C}$H), 127.72 (2 x Ar$\underline{C}$H), 129.74 (Ar$\underline{C}$H), 129.79 (Ar$\underline{C}$H), 129.87 (Ar$\underline{C}$H), 129.90 (Ar$\underline{C}$H), 133.64 ($\underline{Q}C$), 134.23 ($\underline{Q}C$), 134.55 ($\underline{Q}C$), 134.82 ($\underline{Q}C$), 135.85 (2 x Ar$\underline{C}$H), 135.90 (2 x Ar$\underline{C}$H), 139.49 ($\underline{Q}C$), 140.59 ($\underline{Q}C$), 141.00 ($\underline{Q}C$), 141.11 ($\underline{Q}C$), 150.94 ($\underline{Q}C$), 151.03 ($\underline{Q}C$), 151.07 ($\underline{Q}C$), 151.11 ($\underline{Q}C$)

ν_{MAX} (DCM)/cm^{-1}: 3468.99, 2933.46, 1603.34, 115.09

HRMS $[M+Na]^+$: calculated 529.2386, found 529.4425, molecular formula ($C_{30}H_{38}O_5SiNa$)

Melting point: 57-59 °C

7.10.2 Acetate Synthesis: Synthesis of (7*S*)-7-((*tert*-butyldiphenylsilyl)oxy)-1,2,3-trimethoxy-6,7,8,9-tetrahydro-5*H*-benzo[7]annulen-5-yl acetate (3.25)

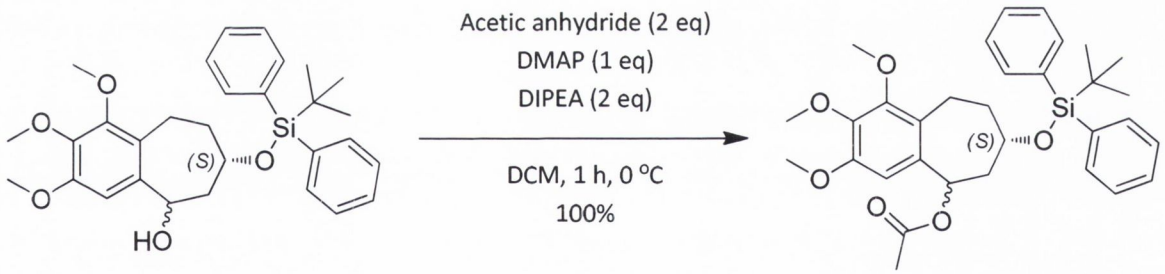

(3.24) **(3.25)**

To a stirred solution of **(3.24)** (0.24 g, 0.47 mmol) in dry DCM under an atmosphere of nitrogen at 0 °C was added acetic anhydride (0.09 mL, 0.95 mmol), DMAP (0.06 g, 0.47 mmol) and *N,N*-diisopropylethylamine (0.17 mL, 0.95 mmol). After 1 h, 2 M HCl aqueous solutions (25 mL) was added. The reaction mixture was then extracted with diethyl ether (3x 20 mL). The organic fractions were combined, dried over $MgSO_4$, filtered and concentrated *in vacuo* to yield **(3.25)** as a yellow oil (0.26 g, 100%)

R_f: 0.34 (3:1, hexane/ethyl acetate)

^{1}H NMR ($CDCl_3$, 400 MHz) δ_H ppm: 1.11 (9H, s, major diastereomer, C(C$\underline{H}_3$)$_3$), 1.16 (9H, s, minor diastereomer C(C$\underline{H}_3$)$_3$), 1.32 (1H, m, major diastereomer, C$\underline{H}_2$), 1.78 (2H, m, minor diastereomer, C$\underline{H}_2$), 1.90-1.93 (2H, m, minor and major diastereomers, C$\underline{H}_2$), 2.05 (3H, s, minor diastereomer, CHOCOC$\underline{H}_3$), 2.13 (5H, s, major and minor diastereomers, 1 x CHOCOC$\underline{H}_3$, 1 x C$\underline{H}_2$), 2.20 (1H, m, minor diastereomer, C$\underline{H}_2$), 2.74 (1H, m, minor diastereomer, C$\underline{H}_2$), 3.10-3.13 (3H, m, minor and major diastereomers, C$\underline{H}_2$), 3.82 (3H, s, major diastereomer, OC$\underline{H}_3$), 3.86 (3H, s, minor diastereomer, OC$\underline{H}_3$), 3.89 (3H, s, major diastereomer, OC$\underline{H}_3$), 3.90 (3H, s, major diastereomer, OC$\underline{H}_3$), 3.93 (3H, s, minor diastereomer, OC$\underline{H}_3$), 3.94 (3H, s, minor diastereomer, OC$\underline{H}_3$), 4.07-4.16 (1H, m, major diastereomer, C$\underline{H}$OSi), 4.22 (1H, m, major diastereomer, C$\underline{H}$OCOCH$_3$), 5.57 (1H, m, minor diastereomer, C$\underline{H}$OSi), 5.69 (1H, m, minor diastereomer, C$\underline{H}$OCOCH$_3$), 6.63 (1H, s, major diastereomer, Ar$\underline{H}$), 6.70 (1H, s, minor diastereomer, Ar$\underline{H}$), 7.39-7.49 (12H, m, major and minor diastereomers, Ar$\underline{H}$), 7.75-7.78 (8H, m, major and minor diastereomers, Ar$\underline{H}$)

^{13}C NMR ($CDCl_3$, 400 MHz) δ_c ppm: 18.66 (C$\underline{H}_2$), 19.05 (C(CH$_3$)$_3$), 19.19 (C(CH$_3$)$_3$), 20.78 (COCOC$\underline{H}_3$), 21.11 (COCOC$\underline{H}_3$), 25.39 (C$\underline{H}_2$), 26.60 (C(C$\underline{H}_3$)$_3$), 27.04 (C(C$\underline{H}_3$)$_3$), 36.01 (C$\underline{H}_2$), 36.30 (C$\underline{H}_2$), 41.38 (C$\underline{H}_2$), 43.71 (C$\underline{H}_2$), 56.02 (2 x OC$\underline{H}_3$), 60.85 (OC$\underline{H}_3$), 61.01 (OC$\underline{H}_3$), 61.36 (OC$\underline{H}_3$), 61.47 (OC$\underline{H}_3$), 69.78 (C$\underline{H}$OCOCH$_3$), 70.10 (C$\underline{H}$OCOCH$_3$), 72.48 (C$\underline{H}$OSi), 72.94 (C$\underline{H}$OSi), 103.20 (Ar$\underline{C}$H), 106.53 (Ar$\underline{C}$H), 122.99 (Q$\underline{C}$) , 126.33 (Ar$\underline{C}$H), 127.29 (Ar$\underline{C}$H), 127.51 (Ar$\underline{C}$H), 127.55 (Ar$\underline{C}$H), 127.62 (Ar$\underline{C}$H), 127.65 (Ar$\underline{C}$H), 127.71 (Ar$\underline{C}$H), 128.51 (Ar$\underline{C}$H), 129.62 (Ar$\underline{C}$H), 129.69 (Ar$\underline{C}$H), 132.41 (Q$\underline{C}$), 133.25 (Ar$\underline{C}$H), 134.25 (Q$\underline{C}$), 134.85 (Ar$\underline{C}$H), 135.31 (Q$\underline{C}$), 135.81 (Ar$\underline{C}$H) 135.88 (Ar$\underline{C}$H), 135.92 (Ar$\underline{C}$H), 136.07 (Q$\underline{C}$), 141.20 (Q$\underline{C}$), 141.63 (Q$\underline{C}$), 143.53 (Q$\underline{C}$), 149.44 (Q$\underline{C}$), 150.84 (Q$\underline{C}$), 150.92 (Q$\underline{C}$), 150.99 (Q$\underline{C}$), 151.26 (Q$\underline{C}$), 151.37 (Q$\underline{C}$), 169.71 ($\underline{C}$=O), 176.97 ($\underline{C}$=O)

ν_{MAX} (DCM)/cm^{-1}: 2932.91, 1740.77, 1604.43, 1240.40

HRMS [M+Na]$^+$: calculated 571.2492, found 571.2467, molecular formula ($C_{32}H_{40}O_6SiNa$)

7.10.3 Silyl deprotection: Synthesis of (7*S*)-6,7,8,9-tetrahydro-7-hydroxy-1,2,3-trimethoxy-5*H*-benzo[7]annulen-5-yl acetate (3.26)

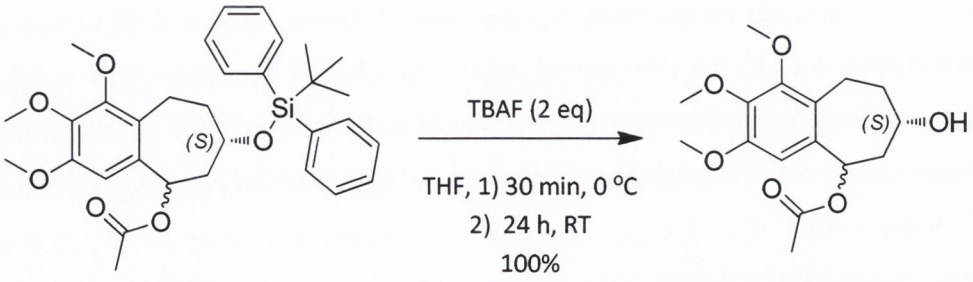

(3.25) **(3.26)**

To a stirred solution of **(3.25)** (0.24 g, 0.44 mmol) in dry THF (1 mL) at 0 °C under an atmosphere of nitrogen was added 1 M TBAF solution in THF (0.48 mL, 0.48 mmol). After 30 min, the temperature of the reaction was allowed to increase to ambient. After 24 h, the THF was removed under reduced pressure and the resulting residue added directly to a silica gel flash column and purified by flash column chromatography (stationary phase; silica gel 230-400 mesh, mobile phase; 1:1, hexane/ethyl acetate) to afford **(3.26)** as an off-white solid (0.14 g, 100%).

R_f: 0.17 (1:1, hexane/ethyl acetate)

^{1}H NMR ($CDCl_3$, 400 MHz) δ_H ppm: 1.24-1.37 (1H, m, major diastereomer, C$\underline{H}_2$), 1.64-1.68 (1H, m, minor diastereomer, C$\underline{H}_2$), 1.75-1.88 (2H, m, major and minor diastereomers, C$\underline{H}_2$), 1.94-1.95 (1H, m, minor diastereomer, C$\underline{H}_2$), 2.12 (4H, s, major and minor diastereomers, 1 x C$\underline{H}_2$ and 1 x CHOCOC$\underline{H}_3$), 2.21 (3H, s, major diastereomer, CHOCOC$\underline{H}_3$), 2.23-2.35 (3H, m, major and minor diastereomers, 3 x C$\underline{H}_2$), 2.74-2.80 (1H, m, minor diastereomer, C$\underline{H}_2$), 3.05-3.11 (1H, m, minor diastereomer, C$\underline{H}_2$), 3.24-3.30 (1H, m, major diastereomer, C$\underline{H}_2$), 3.80 (3H, s, minor diastereomer, OC$\underline{H}_3$), 3.81 (3H, s, major diastereomer, OC$\underline{H}_3$), 3.85 (3H, s, minor diastereomer, OC$\underline{H}_3$), 3.86 (3H, s, major diastereomer, OC$\underline{H}_3$), 3.87 (6H, s, major and minor diastereomers, 2 x OC$\underline{H}_3$), 4.04-4.15 (1H, m, major diastereomer, C$\underline{H}$OH), 4.18-4.24 (1H, m, minor diastereomer, C$\underline{H}$OSi), 5.83 (1H, d, J = 10.22 Hz, major diastereomer, C$\underline{H}$OCOCH$_3$), (1H, d, J = 8.63 Hz, minor diastereomer, C$\underline{H}$OCOCH$_3$), 6.68 (1H, s, minor diastereomer, Ar$\underline{H}$), 6.71 (1H, s, major diastereomer, Ar$\underline{H}$)

^{13}C NMR ($CDCl_3$, 400 MHz) δ_c ppm: 18.99 (C$\underline{H}_2$), 19.25 (C$\underline{H}_2$), 21.27 (COCOC$\underline{H}_3$), 21.29 (COCOC$\underline{H}_3$), 35.85 (C$\underline{H}_2$), 42.79 (C$\underline{H}_2$), 56.03 (2 x OC$\underline{H}_3$), 60.82 (OC$\underline{H}_3$), 60.85 (OC$\underline{H}_3$), 61.36 (2 x OC$\underline{H}_3$), 68.76 (C$\underline{H}$OH), 70.72 (C$\underline{C}$OCOCH$_3$), 71.41 (C$\underline{H}$OH), 72.33 (C$\underline{C}$OCOCH$_3$), 104.04 (Ar$\underline{C}$H), 107.70 (Ar$\underline{C}$H), 125.30 ($\underline{C}$), 127.20 ($\underline{C}$), 135.29 ($\underline{C}$), 135.65 ($\underline{C}$), 141.39 ($\underline{C}$), 141.85 ($\underline{C}$), 150.97 ($\underline{C}$), 151.10 ($\underline{C}$), 151.31 ($\underline{C}$), 151.38 ($\underline{C}$), 169.71 ($\underline{C}$=O), 170.09 ($\underline{C}$=O)

ν_{MAX} (DCM)/cm^{-1}: 3429.60 (OH), 2935.05, 2858.00, 1735.93 (C=O), 1601.83

HRMS $[M+Na]^+$: calculated 333.1314, found 333.1302, molecular formula ($C_{16}H_{22}NaO_6$)

Melting point: 28-30 °C

7.10.4 Mitsunobu attempt B: Attempted synthesis of (7*R*)-7-(formyloxy)-1,2,3-trimethoxy-6,7,8,9-tetrahydro-5*H*-benzo[7]annulen-5-yl acetate (3.27)

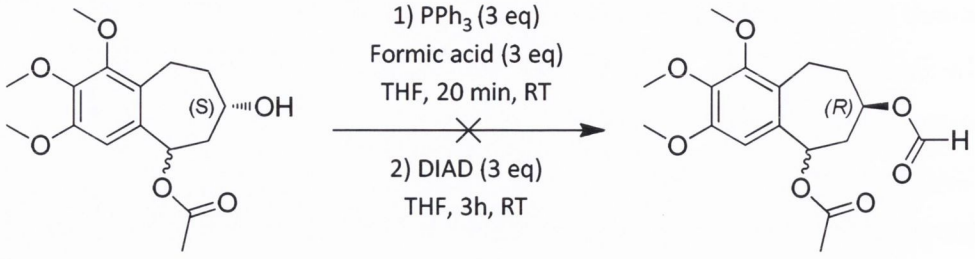

(3.26) **(3.27)**

To a stirred solution of triphenylphosphine (0.33 g, 1.26 mmol) and formic acid (0.05 mL, 1.26 mmol) in dry THF (5 mL) at room temperature under an atmosphere of nitrogen was added a solution of **(3.26)** (0.13 g, 0.42 mmol) in dry THF (1 mL). After 20 min, DIAD (0.25 mL, 1.26 mmol) was added and the reaction was left stirring for further 3 h. The reaction was then quenched by the addition of water (20 mL) and extracted with diethyl ether (3 x 20 mL). The organic fractions were combined, dried over $MgSO_4$ and concentrated *in vacuo*. The resulting oily residue was found to contain a complex mixture of compounds by TLC analysis and was not purified further.

7.10.5 Attempted MEM protection: Attempted synthesis of ((7*S*)-5-((2-methoxyethoxy)methoxy)-6,7,8,9-tetrahydro-1,2,3-trimethoxy-5H-benzo[7]annulen-7-yloxy)(*tert*-butyl)diphenylsilane (3.28)

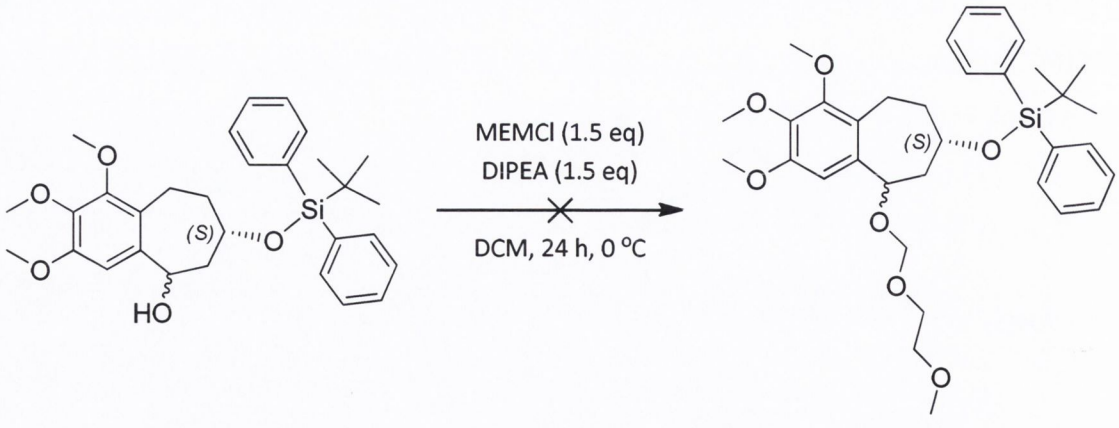

(3.24) **(3.28)**

To a stirred solution of **(3.24)** (0.84 g, 1.66 mmol) in dry DCM (10 mL) under an atmosphere of nitrogen at 0 °C was added methoxyethoxymethyl chloride (0.28 mL, 2.49 mmol) followed by DIPEA (0.43 mL, 2.49 mmol). After 24 h, the starting materials were found to remain unchanged and the reaction was not pursued.

7.10.6 MEM protection: Synthesis of ((7*S*)-5-((2-methoxyethoxy)methoxy)-6,7,8,9-tetrahydro-1,2,3-trimethoxy-5*H*-benzo[7]annulen-7-yloxy)(*tert*-butyl)diphenylsilane (3.28)

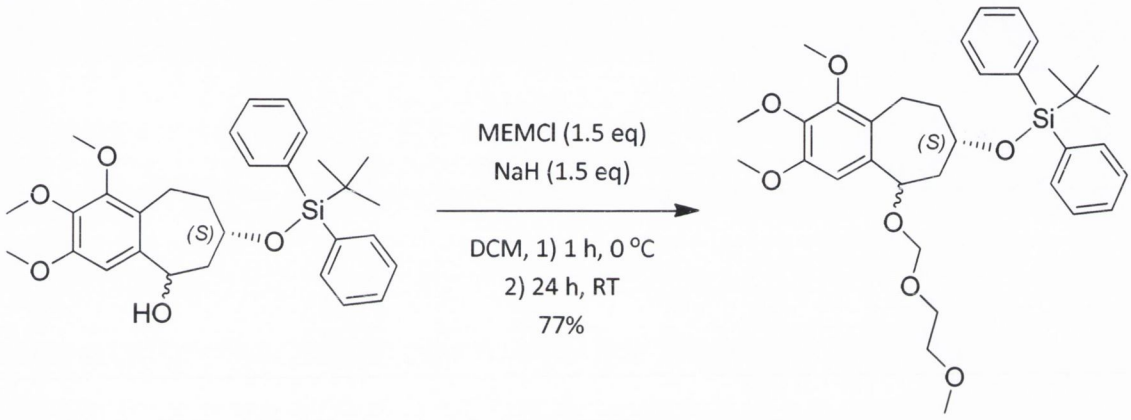

(3.24) **(3.28)**

To a stirred solution of **(3.24)** (0.77 g, 1.52 mmol) in dry DCM (10 mL) at 0 °C under an atmosphere of nitrogen was added MEMCl (0.26 mL, 2.28 mmol) and sodium hydride 60% dispersion in mineral oil (0.09 g, 2.28 mmol). After 1 h, the reaction was allowed to reach room temperature and the reaction was stirred for a further 24 h. The reaction was quenched by the addition of ice water (50 mL). The reaction mixture was then extracted with diethyl ether (3 x 100 mL). The diethyl ether extracts were dried over $MgSO_4$, filtered and concentrated under vacuum. The resulting residue was purified by flash column chromatography (stationary phase; silica gel 230-400 mesh, mobile phase; 4:1, hexane/ethyl acetate) to yield a mixture containing **(3.28)** as a yellow oil (0.7 g, 77%).

R_f: 0.34 (3:1, hexane/ethyl acetate)

HRMS $[M+Na]^+$: calculated 617.2911, found 617.2928, molecular formula ($C_{34}H_{46}NaO_7Si$)

7.10.7 Attempted MEM removal: Attempted synthesis of (7*S*)-7-((*tert*-butyldiphenylsilyl)oxy)-1,2,3-trimethoxy-6,7,8,9-tetrahydro-5*H*-benzo[7]annulen-5-ol (3.24)

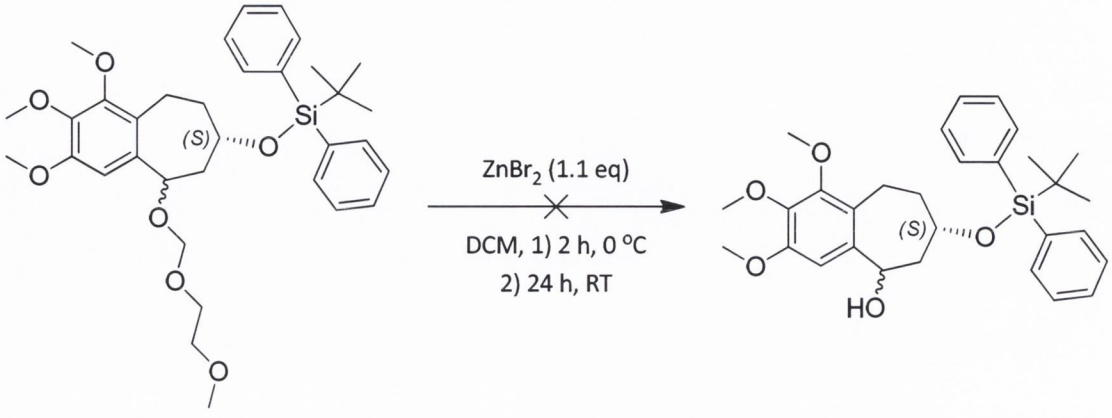

(3.28) **(3.24)**

To a stirred solution of **(3.28)** (0.07 g, 0.12 mmol) in DCM (2 mL) at 0 °C was added zinc bromide (0.03 g, 0.13 mmol). After 2 h, the temperature was allowed to reach ambient. The reaction was left stirring for a further 24 h after which time the starting materials remained unchanged. The reaction was thus not pursued.

7.10.8 THP protection: Synthesis of ((7*S*)-6,7,8,9-tetrahydro-1,2,3-trimethoxy-5-(tetrahydro-2*H*-pyran-2-yloxy)-5*H*-benzo[7]annulen-7-yloxy)(*tert*-butyl)diphenylsilane (3.29)

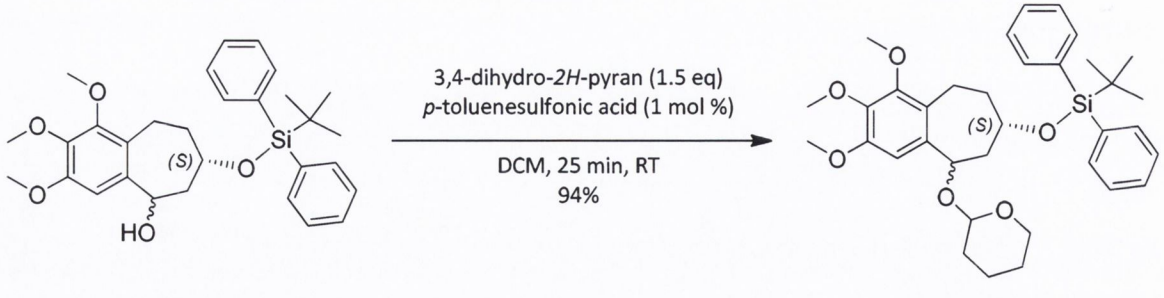

(3.24) **(3.29)**

To a stirred solution of **(3.24)** (0.17 g, 0.36 mmol) in DCM (5 mL) was added 3,4-dihydro-*2H*-pyran (0.05 mL, 0.5 mmol) and *p*-toluenesulfonic acid (0.6 mg, 3.34 µmol). After 25 min, the reaction

was quenched by the addition of saturated sodium bicarbonate aqueous solution (20 mL). The reaction was then extracted with diethyl ether (3 x 30 mL). The organic fractions were combined, dried over $MgSO_4$, filtered and concentrated *in vacuo*. The resulting residue was then purified by flash column chromatography (stationary phase; silica gel 230-400 mesh, mobile phase; 10:1, hexane/ethyl acetate) to yield **(3.29)** as a clear oil (0.20 g, 94%). Due to the complex stereochemistry of compound **(3.29)**, this approach was not pursued.

7.10.9 MOM protection: Synthesis of ((7*S*)-6,7,8,9-tetrahydro-1,2,3-trimethoxy-5-(methoxymethoxy)-5*H*-benzo[7]annulen-7-yloxy)(*tert*-butyl)diphenylsilane (3.30)

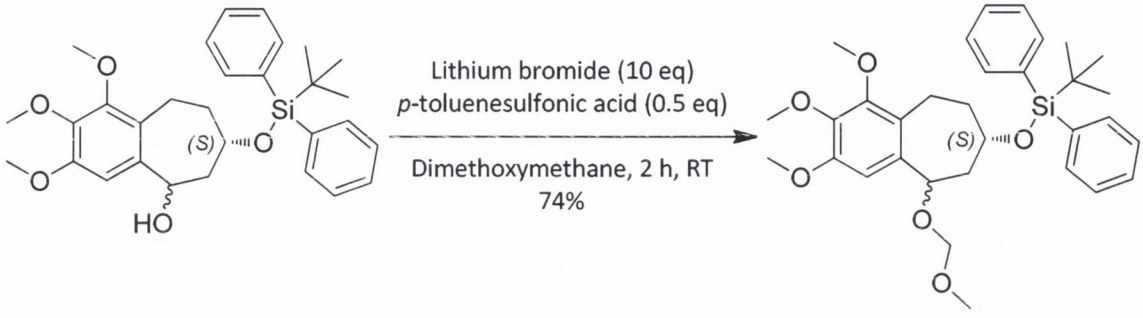

(3.24) **(3.30)**

To stirred solution of **(3.24)** (0.1 g, 0.2 mmol) in dimethoxymethane (2 mL) was added lithium bromide (0.17 g, 1.97 mmol) and *p*-toluenesulfonic acid (0.02 g, 0.1 mmol). After 2 h, the reaction was quenched by the addition of water (10 mL). The reaction mixture was then extracted with diethyl ether (3 x 20 mL). The organic fractions were combined, dried over $MgSO_4$, filtered and concentrated *in vacuo*. The resulting residue was then purified by flash column chromatography (stationary phase; silica gel 230-400 mesh, mobile phase; 10:1, hexane/ethyl acetate) to yield **(3.30)** as a clear oil (80 m g, 74%).

R_f: 0.40 (3:1, hexane/ethyl acetate)

^{1}H NMR ($CDCl_3$, 400 MHz) δ_H ppm: 1.08 (9H, s, major diastereomer, C($C\underline{H}_3$)$_3$), 1.17 (9H, s, minor diastereomer C($C\underline{H}_3$)$_3$), 1.28-1.39 (2H, m, minor and major diastereomers, $C\underline{H}_2$), 1.65-1.78 (2H, m, minor and major diastereomers, $C\underline{H}_2$), 1.89-2.05 (3H, m, minor and major diastereomers, $C\underline{H}_2$), 2.15-2.24 (2H, m, major diastereomer, $C\underline{H}_2$), 2.83 (1H, s, minor diastereomer, $C\underline{H}_2$), 2.98-3.04 (1H, m, minor diastereomer, $C\underline{H}_2$), 3.13-3.22 (1H, q, J = 7.16 Hz, major diastereomer, $C\underline{H}_2$), 3.25 (3H, s, major diastereomer, $OC\underline{H}_3$), 3.35 (3H, s, minor diastereomer, $OC\underline{H}_3$), 3.80 (3H, s, minor diastereomer, $OC\underline{H}_3$), 3.82 (3H, s, major diastereomer, $OC\underline{H}_3$), 3.87 (6H, s, major and minor diastereomers, $OC\underline{H}_3$), 3.90 (6H, s, minor and major diastereomers, $OC\underline{H}_3$), 3.94-4.05 (2H, m,

major and minor diastereomers, CHOSi), 4.32 (1H, s, br, minor diastereomer, $CHOCH_2$), 4.44 (1H, d, J = 10.85 Hz, major diastereomer, $CHOCH_2$) 4.51 (1H, d, J = 6.6 Hz, major diastereomer, $CHOCH_2OCH_3$), 4.55 (1H, d, J = 6.6 Hz, major diastereomer, $CHOCH_2OCH_3$), 4.61 (2H, br s, minor diastereomer, $CHOCH_2OCH_3$), 6.79 (1H, s, minor diastereomer, ArH), 6.87 (1H, s, major diastereomer, ArH), 7.38-7.50 (6H, m, minor and major diastereomers, ArH), 7.70-7.80 (4H, m, minor and major diastereomers, ArH).

^{13}C NMR ($CDCl_3$, 400 MHz) δ_c ppm: 18.14 (CH_2), 19.17 ($C(CH_3)_3$), 19.29 (CH_2), 19.35 ($C(CH_3)_3$), 26.95 ($C(CH_3)_3$), 27.09 ($C(CH_3)_3$), 34.41 (CH_2), 42.55 (CH_2), 44.73 (CH_2), 55.46 (OCH_3), 55.56 (OCH_3), 56.00 (OCH_3), 60.87 (OCH_3), 61.34 (OCH_3), 61.39 (OCH_3), 69.89 ($CHOCH_2$), 70.89 ($CHOCH_2$), 73.49 (CHOSi), 94.44 (OCH_2OCH_3), 103.14 (ArCH), 124.89 (QC), 127.62 (2 x ArCH), 129.65 (2 x ArCH), 134.36 (QC), 134.38 (QC), 134.41 (QC), 134.51 (QC), 135.83 (2 x ArCH), 135.87 (2 x ArCH), 135.89 (2 x ArCH), 138.07 (QC), 140.71 (QC), 150.86 (QC), 150.89 (QC), 151.10 (QC), 151.42 (QC).

ν_{MAX} (DCM)/cm^{-1}: 2932.45, 2857.24, 1643.74, 1600.21

HRMS $[M+Na]^+$: calculated 573.2648, found 573.2669, molecular formula ($C_{32}H_{42}NaO_6Si$)

7.10.10 MOM removal attempt A: Attempted synthesis of *tert*-butyldiphenyl{[(7*R*)-1,2,3-trimethoxy-5-(methoxymethoxy)-6,7,8,9-tetrahydro-5*H*-benzo[7]annulen-7-yl]oxy}silane (3.32)

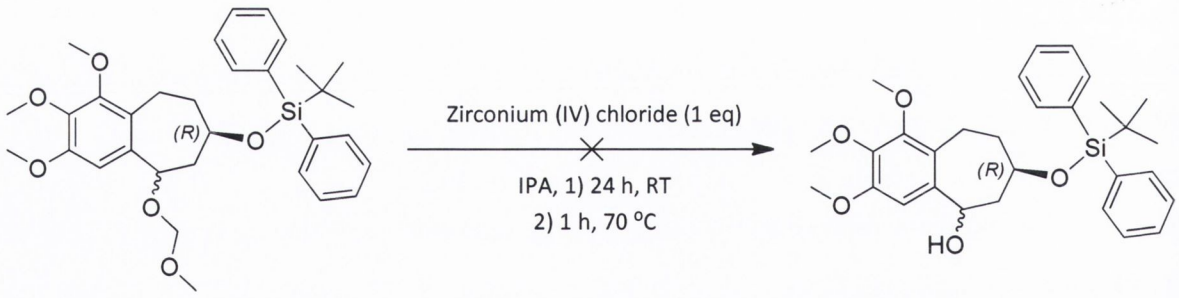

(3.31) **(3.32)**

To a stirred solution of **(3.31)** (0.2 g, 0.36 mmol) in IPA (6 mL) was added zirconium (IV) chloride (0.08 g, 0.36 mmol). The reaction was left stirring for 24 h after which time the starting materials remained unchanged. The reaction was then heated to 70 °C under reflux for 1 h after which time complete consumption of the starter material and the appearance of an elimination side product was detected. The reaction was thus not pursued.

7.10.11 MOM removal attempt B: Attempted synthesis of *tert*-butyldiphenyl{[(7*R*)-1,2,3-trimethoxy-5-(methoxymethoxy)-6,7,8,9-tetrahydro-5*H*-benzo[7]annulen-7-yl]oxy}silane (3.32)

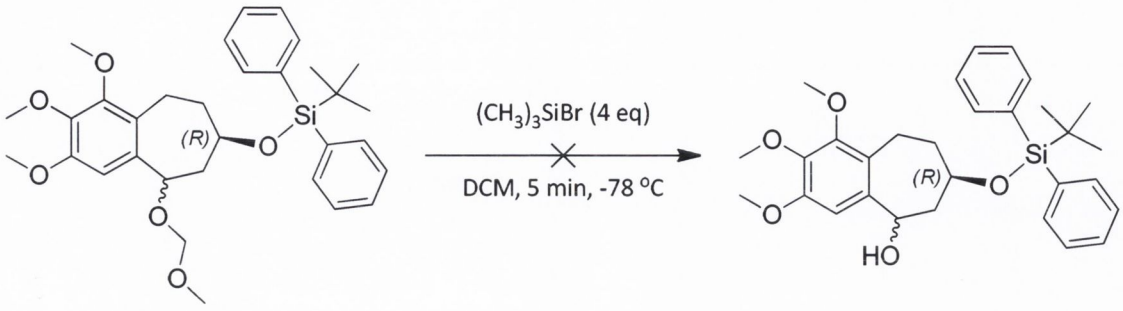

(3.31) **(3.32)**

To a stirred solution of **(3.31)** (0.02 g, 0.04 mmol) in dry DCM (1 mL) at -78 °C under an atmosphere of nitrogen was added bromotrimethylsilane (0.02 mL, 0.15 mmol). After 5 min, the reaction was quenched the addition of water (5 mL) and extracted with diethyl ether (3 x 5 mL). The organic fractions were combined, dried over $MgSO_4$, filtered and concentrated under reduced pressure to afford a crude mixture. A complex mixture of products was observed. Therefore, the reaction was not pursued.

7.10.12 MOM removal attempt C: Attempted synthesis of *tert*-butyldiphenyl{[(7*R*)-1,2,3-trimethoxy-5-(methoxymethoxy)-6,7,8,9-tetrahydro-5*H*-benzo[7]annulen-7-yl]oxy}silane (3.32)

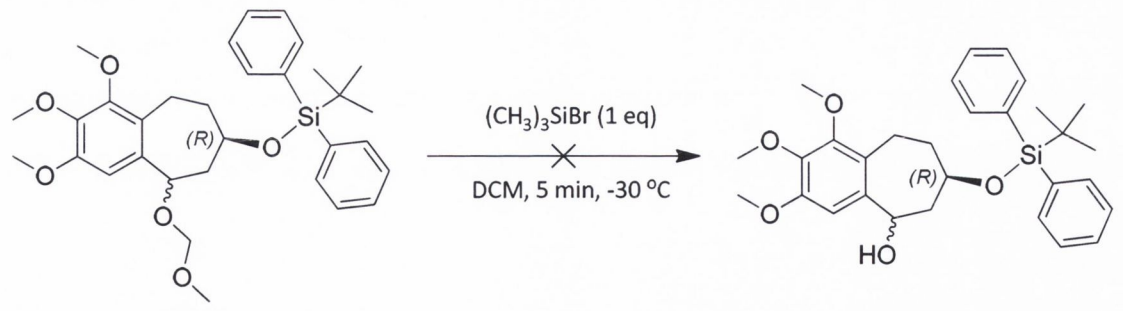

(3.31) **(3.32)**

To a stirred solution of **(3.31)** (0.02 g, 0.04 mmol) in dry DCM (1 mL) at -30 °C under an atmosphere of nitrogen was added bromotrimethylsilane (4.79 µL, 0.04 mmol). After 5 min, the DCM was removed by blowing with a stream of nitrogen gas. The resulting residue was added

directly to a silica gel column and purification by flash column chromatography was attempted (stationary phase; silica gel 230-400 mesh, mobile phase; 4:1, hexane/ethyl acetate). However, the proposed product was not stable to purification by a silica gel flash column. Therefore, the reaction was not pursued.

7.10.13 MOM removal attempt D and subsequent oxidation: Synthesis of *tert*-butyldiphenyl{[(7*R*)-1,2,3-trimethoxy-5-(methoxymethoxy)-6,7,8,9-tetrahydro-5*H*-benzo[7]annulen-7-yl]oxy}silane (3.34)

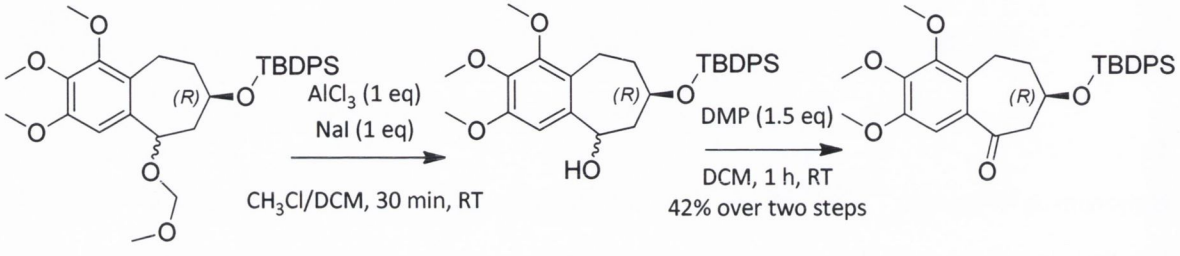

(3.31) **(3.32)** **(3.34)**

To a stirred solution of **(3.31)** (1.96 g, 3.47 mmol) in a mixture of acetonitrile and DCM (2:1, 24 mL) at room temperature was added aluminium chloride (0.46 g, 3.47 mmol) and sodium iodide (0.52 g, 3.47 mmol). After 30 min, the reaction was quenched by the addition of saturated sodium bicarbonate aqueous solution (50 mL) and the reaction extracted with DCM (3 x 10 mL). To a stirred solution of the combined organic fractions was added Dess-Martin periodinane (2.21 g, 5.21 mmol). After 1 h, the reaction was quenched by the addition of saturated sodium bicarbonate aqueous solution (50 mL) and the reaction was extracted with diethyl ether (3 x 50 mL). The organic fractions were combined, dried over $MgSO_4$, filtered and concentrated *in vacuo*. The resulting residue was then purified by flash column chromatography (stationary phase; silica gel 230-400 mesh, mobile phase; 10:1, hexane/ethyl acetate) to yield **(3.34)** as a yellow oil (0.73 g, 42%).

R_f: 0.32 (3:1, hexane/ethyl acetate)

$[\alpha]_D^{25}$ = - 55.56 (*c* = 9, DCM)

^{1}H NMR ($CDCl_3$, 400 MHz) δ_H ppm: 1.06 (9H, s, C(C$\underline{H}_3$)$_3$), 1.88-1.90 (1H, m, C$\underline{H}_2$), 2.00-2.10 (1H, m, C$\underline{H}_2$), 2.92-2.98 (2H, m, C$\underline{H}_2$), 3.04-3.10 (1H, m, C$\underline{H}_2$), 3.10-3.19 (1H, m, C$\underline{H}_2$), 3.86 (3H, s, OC$\underline{H}_3$), 3.89 (3H, s, OC$\underline{H}_3$), 3.95 (3H, s, OC$\underline{H}_3$), 4.30-4.35 (1H, m, C$\underline{H}$OSi), 7.17 (1H, s, Ar$\underline{H}$), 7.38-7.47 (6H, m, Ar$\underline{H}$), 7.64-7.77 (4H, m, Ar$\underline{H}$)

^{13}C NMR ($CDCl_3$, 400 MHz) δ_c ppm: 18.70 (C(CH_3)$_3$), 21.47 (CH_2), 26.40 (C(CH_3)$_3$, 35.88 (CH_2), 49.84 (CH_2), 55.52 (OCH_3), 60.44 (OCH_3), 60.71 (OCH_3), 67.76 (CHOSi) 107.00 (ArCH), 127.20 (2 x ArCH), 127.23 (2 x ArCH), 129.28 (ArCH), 129.34 (ArCH), 130.44 (QC), 133.27 (QC), 133.46 (QC), 134.17 (QC), 135.31 (2 x (ArCH), 135.36 (2 x ArCH), 145.05 (QC), 150.60 (QC), 150.29 (QC), 199.29 (C=O)

ν_{MAX} (DCM)/cm^{-1}: 2933.24, 2857.01, 1672.08 (C=O), 1589.68

HRMS $[M+Na]^+$: calculated 527.223, found 527.2244, molecular formula ($C_{30}H_{36}NaO_5Si$)

7.11 Attempted inversion of configuration: Mitsunobu reaction using MOM ether protected alcohol

7.11.1 Silyl deprotection: Synthesis of (7*S*)-6,7,8,9-tetrahydro-1,2,3-trimethoxy-5-(methoxymethoxy)-5*H*-benzo[7]annulen-7-ol (3.35)

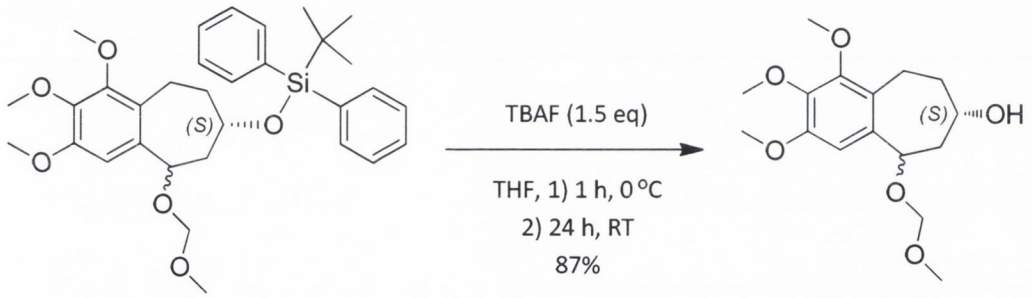

(3.30) **(3.35)**

To a stirred solution of **(3.30)** (2.65 g, 4.81 mmol) in dry THF under an atmosphere of nitrogen at 0 °C was added 1 M tetrabutylammonium fluoride solution (7.22 mL, 7.22 mmol) dropwise. After 1h, the temperature was allowed to increase to ambient. After a further 24 h, the reaction was quenched by the addition of water (50 mL). The reaction mixture was then extracted with diethyl ether (3 x 20 mL). The organic fractions were combined, dried over $MgSO_4$, filtered and concentrated *in vacuo.* The product was purified by flash column chromatography (stationary phase; silica gel 230-400 mesh, mobile phase; 1:1, hexane/ethyl acetate) to yield **(3.35)** as a yellow oil (1.31 g, 87%).

R_f: 0.17 (1:1, hexane/ethyl acetate)

^{1}H NMR ($CDCl_3$, 400 MHz) δ_H ppm: 1.52-2.31 (8H, m, minor and major diastereomers, CH_2), 2.56 (1H, s, br, major diastereomer, CH_2), 2.71-2.81 (1H, m, minor diastereomer, CH_2), 2.93-3.04 (1H,

m, minor diastereomer, C<u>H</u>$_2$), 3.11-3.21 (1H, m, major diastereomer, C<u>H</u>$_2$), 3.37 (3H, s, minor diastereomer, OC<u>H</u>$_3$), 3.39 (3H, s, major diastereomer, OC<u>H</u>$_3$), 3.78 (3H, s, minor diastereomer, OC<u>H</u>$_3$), 3.79 (3H, s, major diastereomer, OC<u>H</u>$_3$), 3.83 (6H, s, minor and major diastereomers, 2 x OC<u>H</u>$_3$), 3.86 (3H, s, minor diastereomer, OC<u>H</u>$_3$), 3.87 (3H, s, major diastereomer, OC<u>H</u>$_3$), 4.04-4.13 (1H, m, major diastereomer, C<u>H</u>OSi), 4.21-4.30 (1H, m, minor diastereomer, C<u>H</u>OSi), 4.55-4.68 (4H, m, minor and major diastereomers, 2 x OC<u>H</u>$_2$OCH$_3$), 4.71-4.77 (1H, m, major diastereomer, C<u>H</u>OCH$_2$O), 4.88-4.95 (1H, m, minor diastereomer, C<u>H</u>OCH$_2$O), 6.68 (1H, s, minor diastereomer, Ar<u>H</u>), 6.70 (1H, s, major diastereomer, Ar<u>H</u>)

^{13}C NMR ($CDCl_3$, 400 MHz) δ_c ppm: 18.41 (<u>C</u>H$_2$), 18.74 (<u>C</u>H$_2$), 35.73 (<u>C</u>H$_2$), 36.28 (<u>C</u>H$_2$), 41.79 (<u>C</u>H$_2$), 55.44 (O<u>C</u>H$_3$), 55.64 (O<u>C</u>H$_3$), 56.01 (O<u>C</u>H$_3$), 60.83 (O<u>C</u>H$_3$), 61.36 (O<u>C</u>H$_3$), 68.76 (<u>C</u>HOSi), 71.58 (<u>C</u>HOSi), 94.09 (O<u>C</u>H$_2$OCH$_3$), 94.21 (O<u>C</u>H$_2$OCH$_3$), 107.49 (Ar<u>C</u>H), 127.20 (<u>Q</u>C), 136.12 (<u>Q</u>C), 136.75 (<u>Q</u>C), 141.40 (<u>Q</u>C), 150.79 (<u>Q</u>C), 150.91 (<u>Q</u>C), 151.24 (<u>Q</u>C), 151.27 (<u>Q</u>C)

ν_{MAX} (DCM)/cm^{-1}: 3421.29 (OH), 2934.96, 1725.21, 1599.92

HRMS [M+Na]$^+$: calculated 335.1471, found 335.1463, molecular formula ($C_{16}H_{24}NaO_6$)

7.11.2 Mitsunobu attempt C: Attempted synthesis of (7*R*)-1,2,3-trimethoxy-5-(methoxymethoxy)-6,7,8,9-tetrahydro-5*H*-benzo[7]annulen-7-yl formate (3.36)

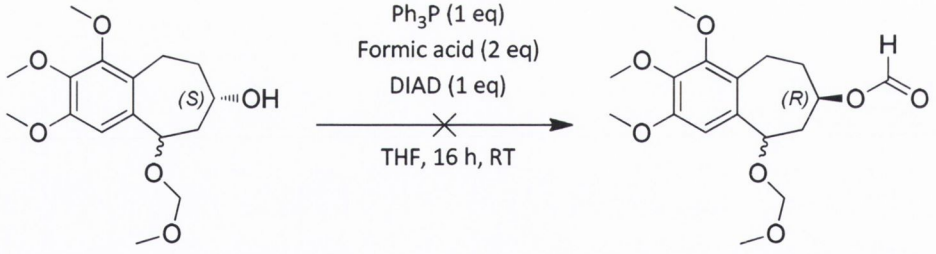

(3.35) **(3.36)**

To a stirred solution of **(3.35)** (0.08 g, 0.26 mmol), triphenylphosphine (0.07 g, 0.26 mmol), and formic acid (0.02 mL, 0.51 mmol) at 0 °C in dry THF (2 mL) under an atmosphere of nitrogen was added DIAD (0.05 mL, 0.26 mmol) dropwise. After 16 h, the starting materials were found to be unchanged therefore the reaction was not purified further.

7.11.3 Mitsunobu attempt D and hydrolysis of formate ester: Synthesis of 6,7,8,9-tetrahydro-1,2,3-trimethoxy-5-(methoxymethoxy)-5*H*-benzo[7]annulen-7-ol (3.37)

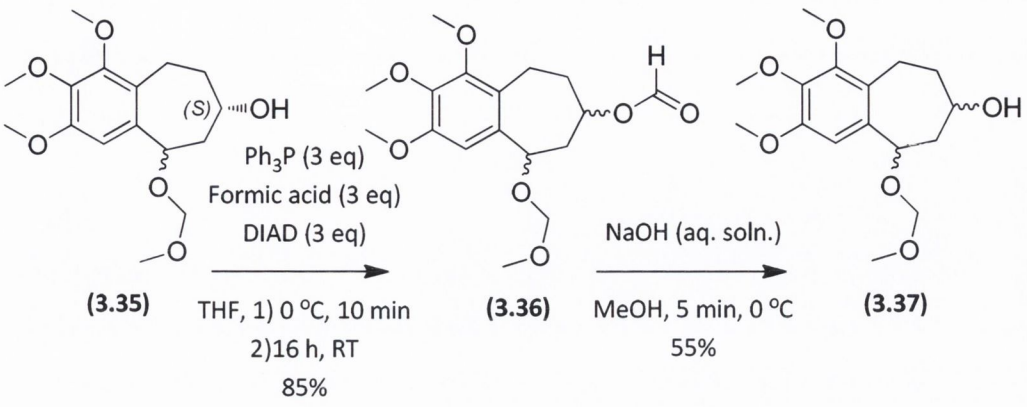

To a stirred solution of **(3.35)** (0.97 g, 3.11 mmol), triphenylphosphine (2.45 g, 9.32 mmol), and formic acid (0.35 mL, 9.32 mmol) in dry THF (10 mL) under an atmosphere of nitrogen at 0 °C was added DIAD (1.83 mL, 9.32 mmol) dropwise. After 10 min the reaction was allowed to increase to ambient and the reaction was left stirring for a further 16 h. The reaction was quenched by the addition of water (50 mL). The reaction mixture was then extracted with diethyl ether (3 x 25 mL). The organic fractions were combined, dried over $MgSO_4$, filtered and concentrated *in vacuo.* The resulting oily residue was then purified by flash column chromatography (stationary phase; silica gel 230-400 mesh, mobile phase; 10:1, hexane/ethyl acetate) to afford a mixture containing **(3.36)** as a yellow oil (0.9 g, 85%). The product was not purified further.

To a stirred solution of the mixture containing **(3.36)** (0.9 g, 2.64 mmol) in methanol (5 mL) at 0 °C was added 2.5 M NaOH aqueous solution (2 mL) dropwise. After 5 min, the methanol was removed under reduced pressure and the resulting aqueous phase was acidified with 2 M HCl aqueous solution (10 mL). The reaction mixture was then extracted with diethyl ether (3 x 25 mL). The organic fractions were combined, dried over $MgSO_4$, filtered and concentrated *in vacuo.* The resulting oily residue was then purified by flash column chromatography (stationary phase; silica gel 230-400 mesh, mobile phase; 4:1, hexane/ethyl acetate) to afford **(3.37)** as a yellow oil (0.45 g, 55%).

R_f: 0.17 (1:1, hexane/ethyl acetate)

^{1}H NMR ($CDCl_3$, 400 MHz) δ_H ppm: 1.52 (2H, m, major and minor diastereomers, C$\underline{H}_2$), 1.76-1.93 (4H, m, major and minor diastereomers, C$\underline{H}_2$), 2.14 (2H, m, major and minor diastereomers, C$\underline{H}_2$), 2.35 (1H, m, minor diastereomer, C$\underline{H}_2$), 2.64-2.70 (1H, m, major diastereomer, C$\underline{H}_2$), 2.88-2.93 (1H, m, major diastereomer, C$\underline{H}_2$), 3.07-3.13 (1H, m, minor diastereomer, C$\underline{H}_2$), 3.27 (3H, s, major

diastereomer, $OCH_2OC\underline{H}_3$), 3.32 (3H, s, minor diastereomer, $OCH_2OC\underline{H}_3$), 3.70 (3H, s, major diastereomer, $OC\underline{H}_3$), 3.71 (3H, s, minor diastereomer, $OC\underline{H}_3$), 3.75 (3H, s, major diastereomer, $OC\underline{H}_3$), 3.76 (3H, s, minor diastereomer, $OC\underline{H}_3$), 3.78 (3H, s, major diastereomer, $OC\underline{H}_3$), 3.93-3.99 (1H, m, major diastereomer, C<u>H</u>), 4.16 (1H, m, major diastereomer, C<u>H</u>), 4.48-4.54 (2H, m, major and minor diastereomers, $C\underline{H}_2$), 4.61-4.65 (2H, m, major and minor diastereomers, $C\underline{H}_2$), 4.82-4.84 2H, m, minor diastereomers, $C\underline{H}_2$), 6.61 (1H, s, major diastereomer, Ar<u>H</u>), 6.69 (1H, s, minor diastereomer, Ar<u>H</u>)

^{13}C NMR ($CDCl_3$, 400 MHz) δ_c ppm: 18.71 ($\underline{C}H_2$), 35.74 ($\underline{C}H_2$), 36.15 ($\underline{C}H_2$), 41.68 ($\underline{C}H_2$), 55.27 ($O\underline{C}H_3$), 55.49 ($O\underline{C}H_3$), 55.87 (2 x $O\underline{C}H_3$), 60.68 (2 x $O\underline{C}H_3$), 61.22 ($O\underline{C}H_3$), 61.23 ($O\underline{C}H_3$), 68.44 (<u>C</u>H), 69.60 (<u>C</u>H), 71.55 (<u>C</u>H), 74.15 (<u>C</u>H), 94.05 ($\underline{C}H_2$), 94.19 ($\underline{C}H_2$), 105.3 (Ar<u>C</u>H), 107.59 (Ar<u>C</u>H), 127.22 (<u>Q</u>C), 136.76 (<u>Q</u>C), 141.13 (<u>Q</u>C), 141.27 (<u>Q</u>C), 150.68 (<u>Q</u>C), 150.97 (<u>Q</u>C), 151.05 (<u>Q</u>C), 151.12 (<u>Q</u>C)

HRMS $[M+Na]^+$: calculated 335.1471, found 335.1496, molecular formula ($C_{16}H_{24}NaO_6$)

7.11.4 Silyl protection: Synthesis of *tert*-butyldiphenyl((1,2,3-trimethoxy-5-(methoxymethoxy)-6,7,8,9-tetrahydro-5*H*-benzo[7]annulen-7-yl)oxy)silane (3.38)

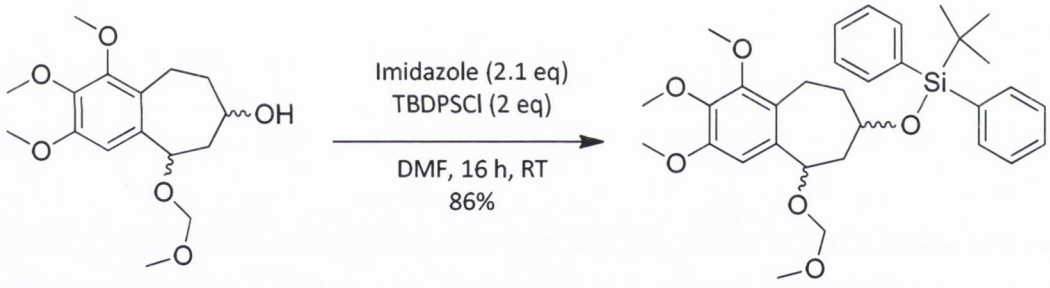

(3.37) **(3.38)**

To a stirred solution of **(3.37)** (0.42 g, 1.35 mmol) and imidazole (0.19 g, 2.84 mmol) in dry DMF (10 mL) under an atmosphere of nitrogen at room temperature was added *tert*-butyldiphenylsilyl chloride (0.7 mL, 2.69 mmol). After 16 h, the reaction was quenched by the addition of water (25 mL) and the reaction was extracted with diethyl ether (3 x 50 mL). The organic fractions were combined, dried over $MgSO_4$, filtered and concentrated *in vacuo*. The resulting residue was then purified by flash column chromatography (stationary phase; silica gel 230-400 mesh, mobile phase; 20:1, hexane/ethyl acetate) to yield **(3.38)** as a colourless oil (0.64 g, 86%).

R_f: 0.40 (3:1, hexane/ethyl acetate)

^1H NMR ($CDCl_3$, 400 MHz) δ_H ppm: 1.11 (9H, s, minor diastereomer, $C(C\underline{H}_3)_3$), 1.19 (9H, s, major diastereomer $C(C\underline{H}_3)_3$), 1.30-1.42 (2H, m, minor and major diastereomers, $C\underline{H}_2$), 1.70-1.78 (2H, m,

minor and major diastereomers, C$\underline{H}_2$), 1.97-2.09 (3H, m, minor and major diastereomers, C$\underline{H}_2$), 2.20-2.23 (2H, m, minor diastereomer, C$\underline{H}_2$), 2.86 (1H, s, major diastereomer, C$\underline{H}_2$), 3.01-3.08 (1H, m, major diastereomer, C$\underline{H}_2$), 3.18-3.23 (1H, q, J = 7.20 Hz, minor diastereomer, C$\underline{H}_2$), 3.28 (3H, s, minor diastereomer, OC$\underline{H}_3$), 3.38 (3H, s, major diastereomer, OC$\underline{H}_3$), 3.82 (3H, s, major diastereomer, OC$\underline{H}_3$), 3.84 (3H, s, minor diastereomer, OC$\underline{H}_3$), 3.88-3.91 (13H, m, minor and major diastereomers,1 x C$\underline{H}$OSi, 4 x OC$\underline{H}_3$), 4.03 (1H, m, minor diastereomer, C$\underline{H}$OSi), 4.35 (1H, s, br, major diastereomer, C$\underline{H}$OCH$_2$), 4.47 (1H, d, J = 10.62 Hz, minor diastereomer, C$\underline{H}$OCH$_2$) 4.53 (H, d, J = 6.77 Hz, minor diastereomer, CHOC$\underline{H}_2$OCH$_3$), 4.57 (H, d, J = 6.77 Hz, minor diastereomer, CHOC$\underline{H}_2$OCH$_3$), 4.63 (2H, br s, major diastereomer, CHOC$\underline{H}_2$OCH$_3$), 6.82 (1H, s, major diastereomer, Ar$\underline{H}$), 6.90 (1H, s, minor diastereomer, Ar$\underline{H}$), 7.42-7.48 (12H, m, minor and major diastereomers, Ar$\underline{H}$), 7.74-7.80 (8H, m, minor and major diastereomers, Ar$\underline{H}$)

^{13}C NMR ($CDCl_3$, 400 MHz) δ_c ppm: 18.73 (C$\underline{(CH_3)_3}$), 18.88 (2 x C$\underline{H}_2$), 18.91 (C$\underline{(CH_3)_3}$), 26.52 (C$\underline{(CH_3)_3}$), 26.66 (C$\underline{(CH_3)_3}$), 35.99 (C$\underline{H}_2$), 42.12 (C$\underline{H}_2$), 44.30 (C$\underline{H}_2$), 55.00 (OC$\underline{H}_3$), 55.11 (OC$\underline{H}_3$), 55.55 (OC$\underline{H}_3$), 60.41 (OC$\underline{H}_3$), 60.89 (OC$\underline{H}_3$), 60.93 (OC$\underline{H}_3$), 69.41 (C$\underline{H}$OCH$_2$), 70.42 (C$\underline{H}$OCH$_2$), 73.07 (C$\underline{H}$OSi), 93.99 (OC$\underline{H}_2$OCH$_3$), 102.67 (ArC$\underline{H}$), 124.44 (Q$\underline{C}$), 127.18 (2 x ArC$\underline{H}$), 129.23 (2 x ArC$\underline{H}$), 133.89 (Q$\underline{C}$), 133.93 (Q$\underline{C}$), 133.96 (Q$\underline{C}$), 134.05 (Q$\underline{C}$), 135.39 (2 x ArC$\underline{H}$), 135.42 (2 x ArC$\underline{H}$), 135.45 (2 x ArC$\underline{H}$), 137.65 (Q$\underline{C}$), 140.27 (Q$\underline{C}$), 150.43 (Q$\underline{C}$), 150.46 (Q$\underline{C}$), 150.68 (Q$\underline{C}$), 150.99 (Q$\underline{C}$)

ν_{MAX} (DCM)/cm^{-1}: 2932.45, 2857.24, 1643.74, 1600.21

HRMS $[M+Na]^+$: calculated 573.2648, found 573.2669, molecular formula ($C_{32}H_{42}NaO_6Si$)

7.11.5 MOM removal and subsequent oxidation: Synthesis of 7-((*tert*-butyldiphenylsilyl)oxy)-1,2,3-trimethoxy-6,7,8,9-tetrahydro-5*H*-benzo[7]annulen-5-one (3.40)

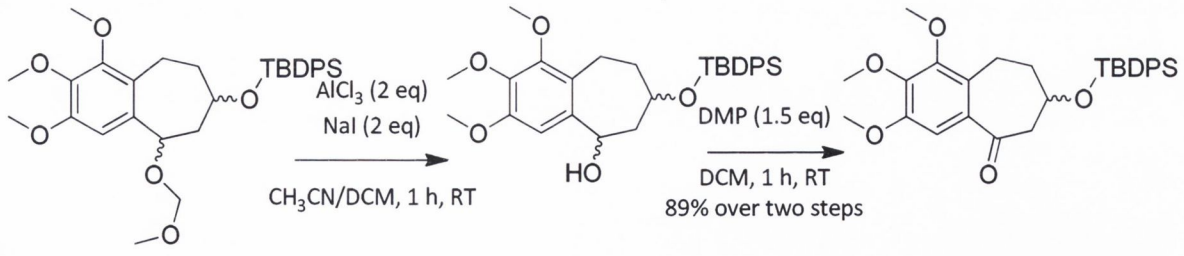

(3.38) **(3.39)** **(3.40)**

To a stirred solution of **(3.38)** (0.34 g, 0.62 mmol) in a mixture of acetonitrile and DCM (2:1, 24 mL) at room temperature was added aluminium chloride (0.16 g, 1.23 mmol) and sodium iodide (0.19 g, 1.23 mmol). After 1 h, the reaction was quenched by the addition of saturated sodium

bicarbonate aqueous solution (50 mL) and the reaction extracted with DCM (3 x 10 mL). To a stirred solution of the combined organic fractions was added Dess-Martin periodinane (2.21 g, 5.21 mmol). After 1 h, the reaction was quenched by the addition of saturated sodium bicarbonate aqueous solution (50 mL) and the reaction was extracted with diethyl ether (3 x 50 mL). The organic fractions were combined, dried over $MgSO_4$, filtered and concentrated *in vacuo*. The resulting residue was then purified by flash column chromatography (stationary phase; silica gel 230-400 mesh, mobile phase; 10:1, hexane/ethyl acetate) to yield **(3.40)** as a yellow oil (0.28 g, 89%).

$[\alpha]_D^{25}$ = - 4.6 (*c* = 10, DCM)

All other data previously described.

7.11.6 Deprotection: Synthesis of 7-hydroxy-1,2,3-trimethoxy-6,7,8,9-tetrahydro-5*H*-benzo[7]annulen-5-one (3.41)

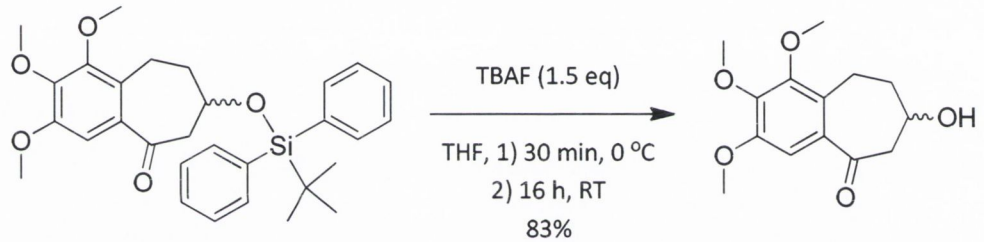

(3.40) **(3.41)**

To a stirred solution of **(3.40)** (0.27 g, 0.54 mmol) in dry THF (5 mL) at 0 °C was added 1 M tetrabutylammonium fluoride solution (0.59 mL, 0.59 mmol) dropwise. After 30, min the reaction was allowed to increase to room temperature and left stirring for a further 16 h. The reaction mixture was then added directly to a silica gel column and purified by flash column chromatography (stationary phase; silica gel 230-400 mesh, mobile phase; 4:1, hexane/ethyl acetate) to yield **(3.41)** as a yellow oil (0.12 g, 83%).

$[\alpha]_D^{25}$ = + 4.3 (*c* = 6, DCM)

All other data previously described.

7.11.7 Organolithium coupling: Synthesis of 9-(3-((*tert*-butyldimethylsilyl)oxy)-4-methoxyphenyl)-2,3,4-trimethoxy-6,7-dihydro-5*H*-benzo[7]annulen-7-ol (3.42)

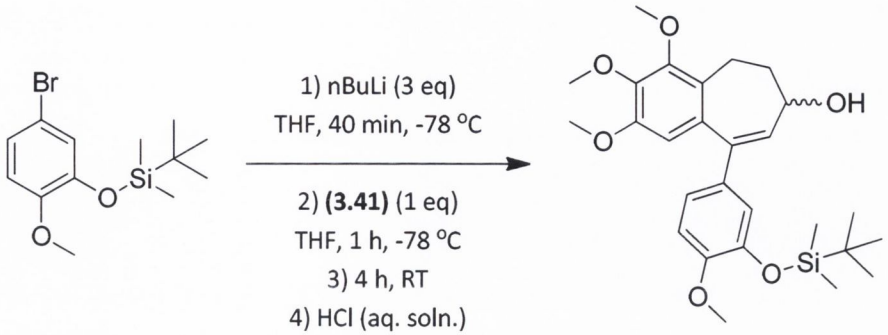

(2.14) **(3.42)**

To a stirred solution of **(2.14)** (0.25 g, 0.79 mmol) in dry THF (4 mL) under an atmosphere of nitrogen at -78 °C was added 2.5 M *n*-butyllithium solution in hexane (0.32 mL, 0.79 mmol) dropwise. After 40 min, a solution of **(3.41)** (0.07 g, 0.26 mmol) in dry THF (5 mL) was added to the reaction. After 1 h, the reaction was allowed to increase to ambient temperature and was left stirring for a further 4 h. The reaction was quenched by the addition of 2 M HCl aqueous solution (50 mL) and then extracted with diethyl ether (3 x 50 mL). The organic fractions were combined, dried over $MgSO_4$, filtered and concentrated *in vacuo*. The resulting residue was then purified by flash column chromatography (stationary phase; silica gel 230-400 mesh, mobile phase; 4:1, hexane/ethyl acetate) to yield **(3.42)** as a yellow oil (0.02 g, 16%).

$[\alpha]_D^{25}$ = + 0.7 (*c* = 1.43, DCM)

All other data as previously described.

7.11.8 Synthesis of (*R*)-Mosher's ester derivative of mitsunobu derived alcohol (3.42): Synthesis of (2*R*)-9-(3-((*tert*-butyldimethylsilyl)oxy)-4-methoxyphenyl)-2,3,4-trimethoxy-6,7-dihydro-5*H*-benzo[7]annulen-7-yl 3,3,3-trifluoro-2-methoxy-2-phenylpropanoate (3.43)

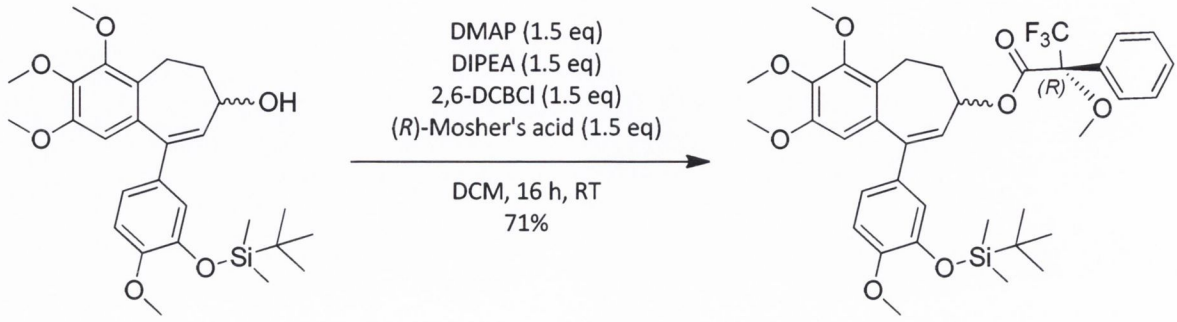

(3.42) **(3.43)**

To a stirred solution of **(3.42)** (0.02 g, 0.04 mmol) in dry DCM (1 mL) under an atmosphere of nitrogen was added DMAP (0.01 g, 0.06 mmol), diisopropylethylamine (0.01 mL, 0.06 mmol), 2,6-dichlorobenzoyl chloride (0.01 mL, 0.06 mmol) and (*R*)-(+)-α-Methoxy-α-(trifluoromethyl)phenylacetic acid (0.01 g, 0.06 mmol). After 16 h, the reaction was quenched by the addition of saturated sodium bicarbonate aqueous solution (5 mL) and the product was extracted with diethyl ether (3 x 10 mL). The diethyl ether was dried over $MgSO_4$, filtered and concentrated *in vacuo.* The resulting oily residue was then purified by flash column chromatography (stationary phase; silica gel 230-400 mesh, mobile phase; 4:1, hexane/ethyl acetate) to yield **(3.43)** as a yellow oil (0.02 g, 71%).

R_f: 0.47 (3:1, hexane/ethyl acetate)

^{19}F NMR ($CDCl_3$, 400 MHz) δ_F ppm: - 72.14 (1F, s, $C\underline{F}_3$), - 72.20 (1F, s, CF_3)

7.11.9 Synthesis of (*R*)-Mosher's ester derivative of enantiomerically pure alcohol (3.19): Synthesis of (*R*)-(S)-9-(3-((*tert*-butyldimethylsilyl)oxy)-4-methoxyphenyl)-2,3,4-trimethoxy-6,7-dihydro-5*H*-benzo[7]annulen-7-yl 3,3,3-trifluoro-2-methoxy-2-phenylpropanoate (3.44)

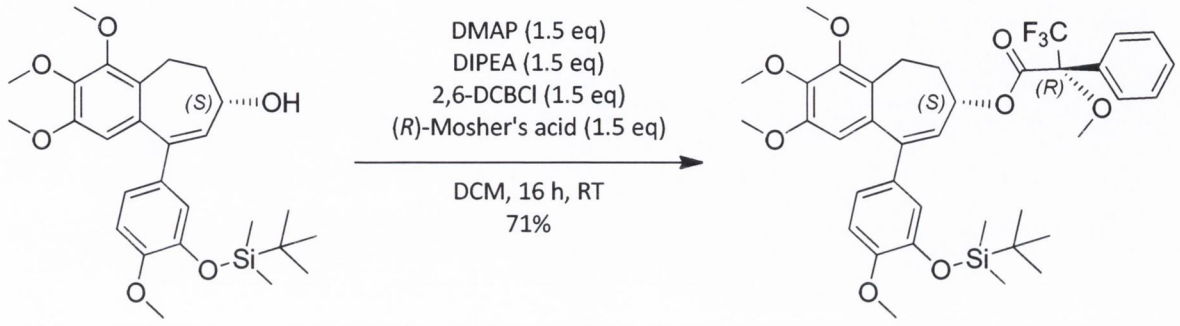

(3.19) **(3.44)**

To a stirred solution of **(3.19)** (0.02 g, 0.04 mmol) in dry DCM (1 mL) under an atmosphere of nitrogen was added DMAP (0.01 g, 0.06 mmol), diisopropylethylamine (0.01 mL, 0.06 mmol), 2,6-dichlorobenzoyl chloride (0.01 mL, 0.06 mmol) and (*R*)-(+)-α-Methoxy-α-(trifluoromethyl)phenylacetic acid (0.01 g, 0.06 mmol). After 16 h, the reaction was quenched by the addition of saturated sodium bicarbonate aqueous solution (5 mL) and the product was extracted with diethyl ether (3 x 10 mL). The diethyl ether was dried over $MgSO_4$, filtered and concentrated *in vacuo.* The resulting oily residue was then purified by flash column chromatography (stationary phase; silica gel 230-400 mesh, mobile phase; 4:1, hexane/ethyl acetate) to yield **(3.44)** as a yellow oil (0.02 g, 71%).

R_f: 0.47 (3:1, hexane/ethyl acetate)

^{19}F NMR ($CDCl_3$, 400 MHz) δ_F ppm: - 72.14 (1F, s, minor diastereomer $C\underline{F}_3$), - 72.20 (1F, s, major diastereomer, CF_3)

7.12 Synthesis of enantiomerically pure (7R)-9-(3-hydroxy-4-methoxyphenyl)-2,3,4-trimethoxy-6,7-dihydro-5H-benzo[7]annulen-7-ol (3.02)

7.12.1 Mesylate formation and displacement with cesium acetate: Synthesis of (7*R*)-6,7,8,9-tetrahydro-1,2,3-trimethoxy-5-(methoxymethoxy)-5*H*-benzo[7]annulen-7-yl acetate (3.46)

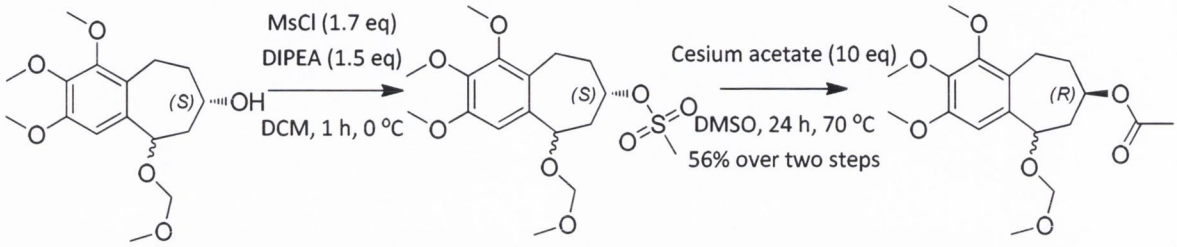

(3.35) **(3.45)** **(3.46)**

To stirred solution of **(3.46)** (0.11 g, 0.35 mmol) in dry DCM (1 mL) under an atmosphere of nitrogen at 0 °C was added methanesulfonyl chloride (0.05 mL, 0.60 mmol) followed by DIPEA (0.1 mL, 0.53 mmol). After 1 h, the reaction was quenched by the addition of water (5 mL) and the reaction extracted with diethyl ether (3 x 10 mL). The organic fractions were combined, dried over $MgSO_4$, filtered and concentrated *in vacuo*.

Cesium acetate was concurrently prepared as follows: To a stirred solution of cesium carbonate (0.57 g, 1.76 mmol) in dry methanol (10 mL) was added acetic acid (0.2 mL, 3.52 mmol). After 1 h, the methanol was removed under reduced pressure to yield cesium acetate as a white solid. The cesium acetate was added to a solution of the crude mesylate in DMSO (10 mL). The reaction was heated at 70 °C for 24 h. The reaction was then quenched by the addition of water (50 mL) and extracted with diethyl ether (3 x 50 mL). The organic fractions were combined, dried over $MgSO_4$, filtered and concentrated *in vacuo*. The resulting residue was then purified by flash column chromatography (stationary phase; silica gel 230-400 mesh, mobile phase; 4:1, hexane/ethyl acetate) to yield **(3.46)** as a colourless oil (0.07 g, 56%).

R_f: 0.46 (2:1, hexane/ethyl acetate)

^{1}H NMR ($CDCl_3$, 400 MHz) δ_H ppm: 1.27 (1H, m, major diastereomer, C$\underline{H}_2$), 1.67-1.76 (2H, m, minor diastereomer C$\underline{H}_2$), 1.89-2.00 (2H, m, major and minor diastereomers, C$\underline{H}_2$), 2.05 (3H, s, minor diastereomer, OC$\underline{H}_3$), 2.11 (3H, s, major diastereomer, OC$\underline{H}_3$), 2.19-2.25 (3H, m, minor and major diastereomers, C$\underline{H}_2$), 2.34-2.38 (1H, m, minor diastereomer, C$\underline{H}_2$), 2.89-2.97 (2H, m, major

diastereomer, $C\underline{H}_2$), 3.29-3.34 (1H, m, minor diastereomer, $C\underline{H}_2$), 3.40 (3H, s, major diastereomer, $OC\underline{H}_3$), 3.45 (3H, s, minor diastereomer, $OC\underline{H}_3$), 3.81 (3H, s, major diastereomer, $OC\underline{H}_3$), 3.82 (3H, s, minor diastereomer, $OC\underline{H}_3$), 3.87-3.89 (12H, m, major and minor diastereomers, 4 x $OC\underline{H}_3$), 4.61-4.66 (2H, m, major diastereomer, $OC\underline{H}_2OCH_3$), 4.70-4.74 (2H, m, minor diastereomer, 1 x $OC\underline{H}_2OCH_3$, 1 x C<u>H</u>OCO), 4.82 (1H, d, J = 6.82 Hz, minor diastereomer, $OC\underline{H}_2OCH_3$), 4.93 (1H, d, J = 8.71 Hz, major diastereomer, $C\underline{H}OCH_2$), 5.08-5.16 (1H, m, minor diastereomer, $C\underline{H}OCH_2$), 5.35-.5.40 (1H, m, major diastereomer, C<u>H</u>OCO), 6.71 (1H, s, major diastereomer, Ar<u>H</u>), 6.92 (1H, s, minor diastereomer, Ar<u>H</u>)

^{13}C NMR ($CDCl_3$, 400 MHz) δ_c ppm: 19.00 ($\underline{C}H_2$), 19.26 ($\underline{C}H_2$), 21.37 ($OCO\underline{C}H_3$), 21.46 ($OCO\underline{C}H_3$), 32.54 ($\underline{C}H_2$), 32.91 ($\underline{C}H_2$), 38.67 ($\underline{C}H_2$), 40.62 ($\underline{C}H_2$), 55.45 ($O\underline{C}H_3$), 55.77 ($O\underline{C}H_3$), 56.00 ($O\underline{C}H_3$), 56.04 ($O\underline{C}H_3$), 60.85 ($O\underline{C}H_3$), 61.37 ($O\underline{C}H_3$), 71.36 (<u>C</u>HOCO), 71.73 (<u>C</u>HOCO), 73.67 (2 x <u>C</u>HOCH_2), 94.16 ($O\underline{C}H_2O$), 94.87 ($O\underline{C}H_2O$), 103.64 (Ar<u>C</u>H), 107.25 (Ar<u>C</u>H), 124.54 (Q<u>C</u>), 126.68 (Q<u>C</u>), 136.79 (Q<u>C</u>), 137.66 (Q<u>C</u>), 140.89 (Q<u>C</u>), 141.45 (Q<u>C</u>), 150.98 (Q<u>C</u>), 150.99 (Q<u>C</u>), 151.36 (Q<u>C</u>), 151.56 (Q<u>C</u>), 170.20 (<u>C</u>=O), 170.25 (<u>C</u>=O)

ν_{MAX} (DCM)/cm^{-1}: 2931.11 2853.78, 1733.98 (C=O), 1644.29, 1600.43

HRMS $[M+Na]^+$: calculated 377.1576, found 377.1565, molecular formula ($C_{18}H_{26}NaO_7$)

7.12.2 Acetate hydrolysis: Synthesis of (7*R*)-6,7,8,9-tetrahydro-1,2,3-trimethoxy-5-(methoxymethoxy)-5*H*-benzo[7]annulen-7-ol (3.47)

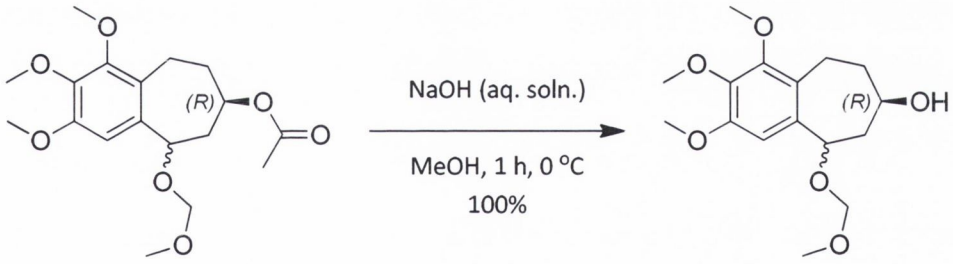

(3.46) **(3.47)**

To a stirred solution of **(3.46)** (0.62 g, 1.75 mmol) in methanol (10 mL) at 0 °C was added 2.5 M NaOH aqueous solution (5 mL) dropwise. After 1 h, the methanol was removed under reduced pressure. The reaction was quenched by the addition of 2 M HCl aqueous solution (20 mL) and the reaction was extracted with diethyl ether (3 x 50 mL). The organic fractions were combined, dried over $MgSO_4$, filtered and concentrated *in vacuo*. The resulting residue was then purified by flash

column chromatography (stationary phase; silica gel 230-400 mesh, mobile phase; 1:1, hexane/ethyl acetate) to yield **(3.47)** as a colourless resin (0.55 g, 100%).

R_f: 0.12 (2:1, hexane/ethyl acetate)

^{1}H NMR ($CDCl_3$, 400 MHz) δ_H ppm: 1.62-2.27 (8H, m, minor and major diastereomers, C$\underline{H}_2$), 2.62 (1H, s, br, minor diastereomer C$\underline{H}_2$), 2.75-2.81 (1H, major diastereomer C$\underline{H}_2$), 2.95-3.04 (1H, m, major diastereomer, C$\underline{H}_2$), 3.15-3.21 (1H, m, minor diastereomer, C$\underline{H}_2$), 3.40 (3H, s, major diastereomer, OC$\underline{H}_3$), 3.42 (3H, s, minor diastereomer, OC$\underline{H}_3$), 3.81 (3H, s, major diastereomer, OC$\underline{H}_3$), 3.82 (3H, s, minor diastereomer, OC$\underline{H}_3$), 3.86 (6H, s, minor and major diastereomers, 2 x OC$\underline{H}_3$), 3.88 (6H, s, major and minor diastereomers, 2 x OC$\underline{H}_3$), 4.10-4.16 (1H, m, minor diastereomer, C$\underline{H}$OSi), 4.26-4.31 (1H, m, major diastereomer, C$\underline{H}$OSi), 4.57-4.64 (4H, m, minor and major diastereomers, 2 x OC$\underline{H}_2$OCH$_3$), 4.74-4.78 (1H, m, minor diastereomer, C$\underline{H}$OCH$_2$O), 4.88-4.94 (1H, m, major diastereomer, C$\underline{H}$OCH$_2$O), 6.69(1H, s, major diastereomer, Ar$\underline{H}$), 6.73 (1H, s, minor diastereomer, Ar$\underline{H}$)

^{13}C NMR ($CDCl_3$, 400 MHz) δ_c ppm: 17.87 (C$\underline{H}_2$), 18.28 (C$\underline{H}_2$), 35.29 (C$\underline{H}_2$), 35.91 (C$\underline{H}_2$), 41.37 (C$\underline{H}_2$), 55.02 (OC$\underline{H}_3$), 55.21 (OC$\underline{H}_3$), 55.56 (2 x OC$\underline{H}_3$), 60.39 (OC$\underline{H}_3$), 60.92 (OC$\underline{H}_3$), 68.46 (C$\underline{H}$OSi), 71.36 (C$\underline{H}$OSi), 93.57 (OC$\underline{H}_2$OCH$_3$), 93.75 (OC$\underline{H}_2$OCH$_3$), 107.00 (Ar$\underline{C}$H), 126.74 (Q$\underline{C}$), 136.26 (Q$\underline{C}$), 13.45 (Q$\underline{C}$), 140.96 (Q$\underline{C}$), 150.35 (Q$\underline{C}$), 150.42 (Q$\underline{C}$), 150.82 (Q$\underline{C}$), 150.88 (Q$\underline{C}$)

ν_{MAX} (DCM)/cm^{-1}: 3421.29, 2934.96, 1725.21, 1599.92

HRMS $[M+Na]^+$: calculated 335.1471, found 335.1530, molecular formula ($C_{16}H_{24}NaO_6$)

7.12.3 Silyl protection: Synthesis of ((7*R*)-6,7,8,9-tetrahydro-1,2,3-trimethoxy-5-(methoxymethoxy)-5*H*-benzo[7]annulen-7-yloxy)(*tert*-butyl)diphenylsilane (3.31)

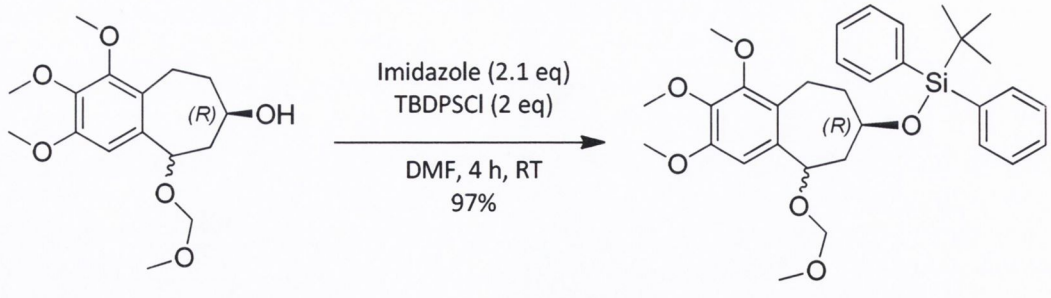

(3.47) **(3.31)**

To a stirred solution of **(3.47)** (0.55 g, 1.76 mmol) and imidazole (0.25 g, 3.52 mmol) in dry DMF (10 mL) under an atmosphere of nitrogen at room temperature was added *tert*-butyldiphenylsilyl chloride (0.92 mL, 3.52 mmol). After 4 h, the reaction was quenched by the addition of water (25

mL) and the reaction was extracted with diethyl ether (3 x 50 mL). The organic fractions were combined, dried over $MgSO_4$ and concentrated *in vacuo*. The resulting residue was then purified by flash column chromatography (stationary phase; silica gel 230-400 mesh, mobile phase; 20:1, hexane/ethyl acetate) to yield **(3.31)** as a colourless oil (0.94 g, 97%).

R_f: 0.40 (3:1, hexane/ethyl acetate)

^{1}H NMR ($CDCl_3$, 400 MHz) δ_H ppm: 1.07 (9H, s, minor diastereomer, C(C$\underline{H}_3$)$_3$), 1.15 (9H, s, major diastereomer C(C$\underline{H}_3$)$_3$), 1.22-1.37 (2H, m, minor and major diastereomers, C$\underline{H}_2$), 1.65-1.73 (2H, m, minor and major diastereomers, C$\underline{H}_2$), 1.93-2.00 (3H, m, minor and major diastereomers, C$\underline{H}_2$), 2.16-2.20 (2H, m, minor diastereomer, C$\underline{H}_2$), 2.82 (1H, s, major diastereomer, C$\underline{H}_2$), 2.97-3.03 (1H, m, major diastereomer, C$\underline{H}_2$), 3.14-3.19 (1H, q, J = 7.20 Hz, minor diastereomer, C$\underline{H}_2$), 3.24 (3H, s, minor diastereomer, OC$\underline{H}_3$), 3.35 (3H, s, major diastereomer, OC$\underline{H}_3$), 3.79 (3H, s, major diastereomer, OC$\underline{H}_3$), 3.81 (3H, s, minor diastereomer, OC$\underline{H}_3$), 3.86-3.90 (13H, m, minor and major diastereomers,1 x C$\underline{H}$OSi, 4 x OC$\underline{H}_3$), 3.96-4.06 (1H, m, minor diastereomer, C$\underline{H}$OSi), 4.31 (1H, s, br, major diastereomer, C$\underline{H}$OCH$_2$), 4.42 (1H, d, J = 10.62 Hz, minor diastereomer, C$\underline{H}$OCH$_2$) 4.50 (H, d, J = 6.77 Hz, minor diastereomer, CHOC$\underline{H}_2$OCH$_3$), 4.54 (H, d, J = 6.77 Hz, minor diastereomer, CHOC$\underline{H}_2$OCH$_3$), 4.60 (2H, br s, major diastereomer, CHOC$\underline{H}_2$OCH$_3$), 6.78 (1H, s, major diastereomer, Ar$\underline{H}$), 6.86 (1H, s, minor diastereomer, Ar$\underline{H}$), 7.39-7.48 (6H, m, minor and major diastereomers, Ar$\underline{H}$), 7.70-7.77 (4H, m, minor and major diastereomers, Ar$\underline{H}$).

^{13}C NMR ($CDCl_3$, 400 MHz) δ_c ppm: 18.71 (C(CH$_3$)$_3$), 18.81 (2 x $\underline{C}$H$_2$), 18.88 ($\underline{C}$(CH$_3$)$_3$), 26.48 (C($\underline{C}$H$_3$)$_3$), 26.61 (C($\underline{C}$H$_3$)$_3$), 35.93 ($\underline{C}$H$_2$), 42.08 ($\underline{C}$H$_2$), 44.25 ($\underline{C}$H$_2$), 55.00 (O$\underline{C}$H$_3$), 55.11 (O$\underline{C}$H$_3$), 55.54 (O$\underline{C}$H$_3$), 60.41 (O$\underline{C}$H$_3$), 60.89 (O$\underline{C}$H$_3$), 60.94 (O$\underline{C}$H$_3$), 69.35 ($\underline{C}$HOCH$_2$), 70.38 ($\underline{C}$HOCH$_2$), 73.01 ($\underline{C}$HOSi), 93.96 (O$\underline{C}$H$_2$OCH$_3$), 102.62 (Ar$\underline{C}$H), 124.42 (Q$\underline{C}$), 127.12 (2 x Ar$\underline{C}$H), 129.18 (2 x Ar$\underline{C}$H), 133.88 (Q$\underline{C}$), 133.90 (Q$\underline{C}$), 133.93 (Q$\underline{C}$), 134.03 (Q$\underline{C}$), 135.36 (2 x Ar$\underline{C}$H), 135.40 (2 x Ar$\underline{C}$H), 135.43 (2 x Ar$\underline{C}$H), 137.59 (Q$\underline{C}$), 140.21 (Q$\underline{C}$), 150.37 (Q$\underline{C}$), 150.41 (Q$\underline{C}$), 150.62 (Q$\underline{C}$), 150.93 (Q$\underline{C}$).

ν_{MAX} (DCM)/cm^{-1}: 2931.61, 2115.63, 1643.00, 1600.60

HRMS $[M+Na]^+$: calculated 573.2648, found 573.2645, molecular formula ($C_{32}H_{42}NaO_6Si$)

7.12.4 Deprotection: Synthesis of (*R*)-6,7,8,9-tetrahydro-7-hydroxy-1,2,3-trimethoxybenzo[7]annulen-5-one (3.48)

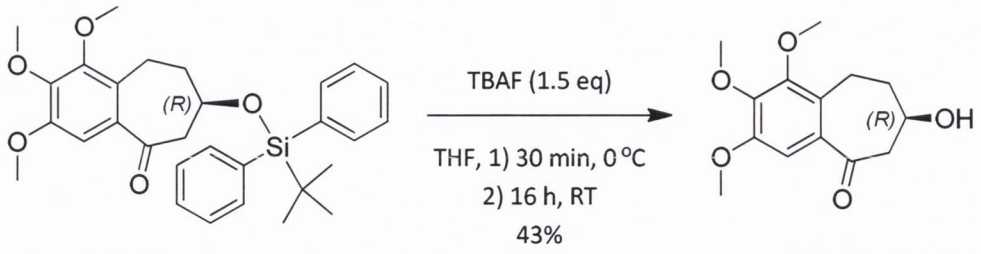

(3.34) **(3.48)**

To a stirred solution of **(3.34)** (0.48 g, 0.95 mmol) in dry THF (5 mL) at 0 °C was added 1 M tetrabutylammonium fluoride solution (1.43 mL, 1.43 mmol) dropwise. After 30 min, the reaction was allowed to increase to room temperature and left stirring for 16 h. The reaction mixture was then added directly to a silica gel column and purified by flash column chromatography (stationary phase; silica gel 230-400 mesh, mobile phase; 4:1, hexane/ethyl acetate) to yield **(3.48)** as a yellow oil (0.11 g, 54%).

$[\alpha]_D^{25}$ = + 6.33 (*c* = 6, DCM)

All other data as previously described.

7.12.5 Organolithium coupling: Synthesis of (7*R*)-9-{3-[(*tert*-butyldimethylsilyl)oxy]-4-methoxyphenyl}-2,3,4-trimethoxy-6,7-dihydro-5*H*-benzo[7]annulen-7-ol (3.49)

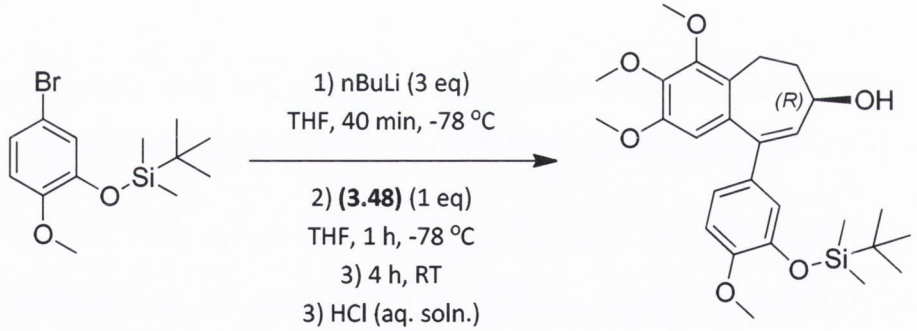

(2.14) **(3.49)**

To a stirred solution of **(2.14)** (0.39 g, 1.23 mmol) in dry THF (4 mL) under an atmosphere of nitrogen at -78 °C was added 2.5 M *n*-butyllithium solution in hexane (0.5 mL, 1.23 mmol) dropwise. After 40 min, a solution of **(3.48)** (0.11 g, 0.41 mmol) in dry THF (5 mL) was added to the reaction. After 1 h, the reaction was allowed to increase to ambient temperature and was left stirring for a further 4 h. The reaction was quenched by the addition of 2 M HCl aqueous solution (50 mL) and then extracted with diethyl ether (3 x 50 mL). The organic fractions were combined,

dried over $MgSO_4$, filtered and concentrated *in vacuo*. The resulting residue was then purified by flash column chromatography (stationary phase; silica gel 230-400 mesh, mobile phase; 4:1, hexane/ethyl acetate) to yield **(3.49)** as a yellow oil (0.07 g, 34%).

$[\alpha]_D^{25}$ = + 33 (*c* = 2.67, DCM)

All other data as previously described.

7.12.6 (*R*)-Mosher's ester of mesylate displacement derived alcohol (3.49): Synthesis of (*R*)-(*R*)-9-(3-((*tert*-butyldimethylsilyl)oxy)-4-methoxyphenyl)-2,3,4-trimethoxy-6,7-dihydro-5*H*-benzo[7]annulen-7-yl 3,3,3-trifluoro-2-methoxy-2-phenylpropanoate (3.50)

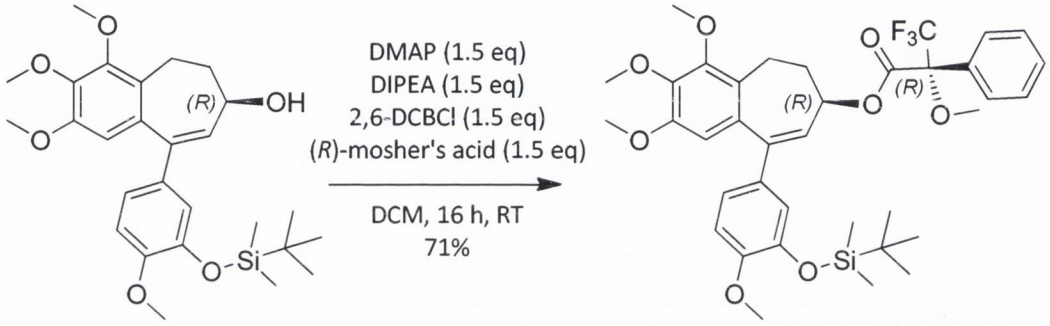

(3.49) **(3.50)**

To a stirred solution of **(3.49)** (0.02 g, 0.04 mmol) in dry DCM (1 mL) under an atmosphere of nitrogen was added DMAP (0.01 g, 0.06 mmol), diisopropylethylamine (0.01 mL, 0.06 mmol), 2,6-dichlorobenzoyl chloride (0.01 mL, 0.06 mmol) and (*R*)-(+)-α-Methoxy-α-(trifluoromethyl)phenylacetic acid (0.01 g, 0.06 mmol). After 16 h, the reaction was quenched by the addition of saturated sodium bicarbonate aqueous solution (5 mL) and the product was extracted with diethyl ether (3 x 10 mL). The diethyl ether was dried over $MgSO_4$, filtered and concentrated *in vacuo.* The resulting oily residue was then purified by flash column chromatography (stationary phase; silica gel 230-400 mesh, mobile phase; 4:1, hexane/ethyl acetate) to yield **(3.50)** as a yellow oil (0.02 g, 71%).

^{19}F NMR ($CDCl_3$, 400 MHz) δ_F ppm: - 72.13 (1F, s, major diastereomer, $C\underline{F}_3$), - 72.18 (1F, s, minor diastereomer CF_3)

7.12.7 Deprotection of C-ring phenol: Synthesis of (7*R*)-9-(3-hydroxy-4-methoxyphenyl)-2,3,4-trimethoxy-6,7-dihydro-5*H*-benzo[7]annulen-7-ol (3.02)

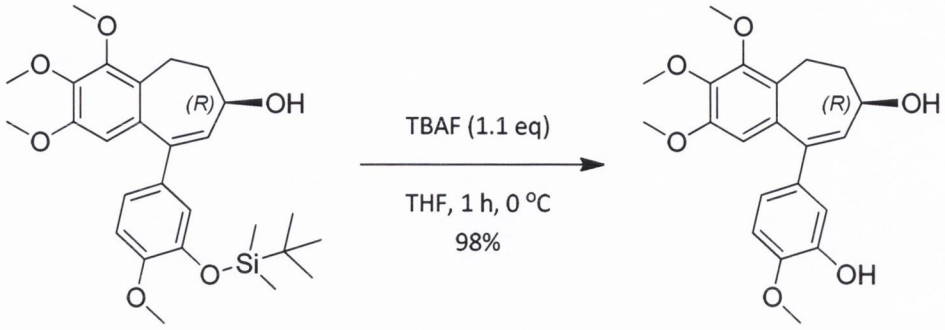

(3.49) **(3.02)**

To a stirred solution of **(3.49)** (0.0 4 g, 0.08 mmol) in dry THF (1 mL) under an atmosphere of nitrogen at 0 °C was added 1 M TBAF solution in THF (0.09 mL, 0.09 mmol). After 1 h, the THF was blown off in a stream of nitrogen gas and the reaction mixture added directly to a flash column of silica gel and purified by flash column chromatography (stationary phase; silica gel 230-400 mesh, mobile phase; ethyl acetate) to yield **(3.02)** as a white solid (0.08 g, 98%).

$[\alpha]_D^{25}$ = + 53.23 (*c* = 0.53, DCM)

All other data as previously described.

7.13 Synthesis of enantiomerically pure (R)-N-(9-(3-hydroxy-4-methoxyphenyl)-2,3,4-trimethoxy-6,7-dihydro-5H-benzo[7]annulen-7-yl)acetamide (4.01)

7.13.1 Mesylate formation and azide displacement: Synthesis of (7*R*)-7-azido-6,7,8,9-tetrahydro-1,2,3-trimethoxy-5*H*-benzo[7]annulen-5-yl acetate (4.03)

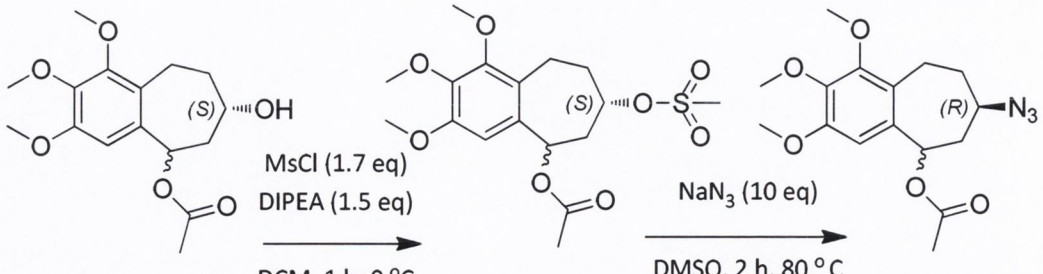

(3.26) **(4.02)** **(4.03)**

To a stirred solution of **(3.26)** (0.94 g, 3.03 mmol) in dry DCM (5 mL) under an atmosphere of nitrogen at 0 °C was added methanesulfonyl chloride (0.5 mL, 5.15 mmol) followed by *N,N*-diisopropylethylamine (0.53 mL, 4.54 mmol). After 1 h, the reaction was quenched by the addition of water (20 mL). The reaction mixture was extracted with diethyl ether (3 x 25 mL). The organic fractions were combined and dried over $MgSO_4$, filtered and concentrated *in vacuo* to yield the mesylate as a crude mixture. The mesylate was dissolved in DMSO (10 mL) at room temperature and sodium cyanide (1.97 g, 30.23 mmol) was added to the solution. The reaction was then refluxed at 80 °C for 2 h. The reaction was quenched by the addition of water (30 mL) and extracted with diethyl ether (3 x 30 mL). The organic fractions were combined, dried over $MgSO_4$, filtered and concentrated under reduced pressure. The product was purified by flash column chromatography (stationary phase; silica gel 230-400 mesh, mobile phase; 4:1, hexane/ethyl acetate) to yield **(4.03)** as a yellow oil (0.68 g, 63% over two steps).

R_f: 0.46 (2:1, hexane/ethyl acetate)

^{1}H NMR ($CDCl_3$, 400 MHz) δ_H ppm: 1.28-1.40 (1H, m, major diastereomer, C$\underline{H}_2$), 1.65-1.72 (1H, m, minor diastereomer, C$\underline{H}_2$), 1.78-1.90 (2H, m, major and minor diastereomers, C$\underline{H}_2$), 2.06-2.19 (4H, m, major and minor diastereomers, 1 x CHOCOC$\underline{H}_3$, 1 x C$\underline{H}_2$), 2.24 (3H, s, minor diastereomer, CHOCOC$\underline{H}_3$), 2.28-2.34 (2H, m, major and minor diastereomers, C$\underline{H}_2$), 2.37-2.42 (1H, m, major diastereomer, C$\underline{H}_2$), 2.75-2.82 (1H, m, major diastereomer, C$\underline{H}_2$), 3.14-3.20 (1H, m, major diastereomer, C$\underline{H}_2$), 3.37-3.41 (1H, m, minor diastereomer, C$\underline{H}_2$), 3.74-3.75 (1H, m, minor diastereomer, C$\underline{H}N_3$), 3.82 (3H, s, major diastereomer, OC$\underline{H}_3$), 3.83 (3H, s, minor diastereomer, OC$\underline{H}_3$), 3.86 (3H, s, major diastereomer, OC$\underline{H}_3$), 3.88 (9H, s, major and minor diastereomers, 3 x OC$\underline{H}_3$), 3.91-3.97 (1H, m, major diastereomer, C$\underline{H}N_3$), 5.86 (1H, d, J = 9.91 Hz, minor diastereomer, C$\underline{H}$OCOCH$_3$), 6.01 (1H, d, J = 7.83 Hz, major diastereomer, C$\underline{H}$OCOCH$_3$), 6.67 (1H, s, major diastereomer, Ar$\underline{H}$), 6.73 (1H, s, minor diastereomer, Ar$\underline{H}$)

^{13}C NMR ($CDCl_3$, 400 MHz) δ_c ppm: 20.09 (C$\underline{H}_2$), 20.39 (C$\underline{H}_2$), 21.19 (CO$\underline{C}$H$_3$), 21.21 (CO$\underline{C}$H$_3$), 32.35 (C$\underline{H}_2$), 32.92 (C$\underline{H}_2$), 37.41 (C$\underline{H}_2$), 39.56 (C$\underline{H}_2$), 56.04 (O$\underline{C}$H$_3$), 59.40 (C$\underline{H}$N$_3$), 60.81 (C$\underline{H}$N$_3$), 60.85 (O$\underline{C}$H$_3$), 61.38 (2 x O$\underline{C}$H$_3$), 61.41 (2 x O$\underline{C}$H$_3$), 70.31 (C$\underline{H}$OCOCH$_3$), 73.19 (C$\underline{H}$OCOCH$_3$), 103.57 (Ar$\underline{C}$H), 108.40 (Ar$\underline{C}$H), 124.45 (Q$\underline{C}$), 126.97 (Q$\underline{C}$), 134.38 (Q$\underline{C}$), 135.43 (Q$\underline{C}$), 141.46 (Q$\underline{C}$), 142.17 (Q$\underline{C}$), 151.11 (Q$\underline{C}$), 151.17 (Q$\underline{C}$), 151.40 (Q$\underline{C}$), 151.66 (Q$\underline{C}$), 169.68 ($\underline{C}$=O), 169.74 ($\underline{C}$=O)

ν_{MAX} (DCM)/cm^{-1}: 2936.17, 2094.20 (N_3), 1739.46 (C=O), 1600.97, 1584.17

HRMS $[M+Na]^+$: calculated 358.1379, found 358.1394, molecular formula ($C_{16}H_{21}N_3NaO_5$)

7.13.2 Acetate hydrolysis and alcohol oxidation: Synthesis of (*R*)-7-azido-6,7,8,9-tetrahydro-1,2,3-trimethoxybenzo[7]annulen-5-one (4.05)

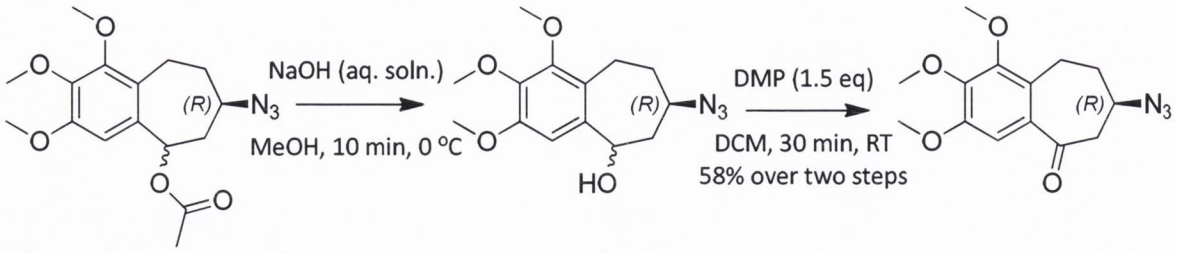

(4.03) **(4.04)** **(4.05)**

To a stirred solution of **(4.03)** (0.68 g, 2.13 mmol) in methanol (10 mL) at 0 °C was added 2.5 M NaOH aqueous solution (20 mL) dropwise. After 10 min, the metanol was removed under reduced pressure and the aqueous phase was acidified by the addition of 2 M HCl aqueous solution (40 mL). The aqueous phase was then extracted with diethyl ether (3 x 75 mL). The organic fractions were combined, dried over $MgSO_4$, filtered and concentrated under reduced pressure. To a stirred solution of this residue reconstituted in DCM (10 mL) was added Dess-Martin periodinane (1.35 g, 3.19 mmol). After 30 min, the reaction was quenched by the addition of saturated sodium bicarbonate solution (50 mL). After a further 30 min, the reaction mixture was extracted with diethyl ether (3 x 75 mL). The organic fractions were combined, dried over $MgSO_4$, filtered and concentrated under reduced pressure. The product was purified by flash column chromatography (stationary phase; silica gel 230-400 mesh, mobile phase; 10:1, hexane/ethyl acetate) to yield **(4.05)** as a yellow oil (0.36 g, 58% over two steps).

R_f: 0.88 (2:1, hexane/ethyl acetate)

$[\alpha]_D^{25}$ = + 14.8 (*c* = 10, DCM)

^{1}H NMR ($CDCl_3$, 400 MHz) δ_H ppm: 1.96-2.04 (1H, m, C<u>H</u>$_2$), 2.09-2.18 (1H, m, C<u>H</u>$_2$), 2.91-3.06 (3H, m, C<u>H</u>$_2$), 3.10-3.16 (1H, m, C<u>H</u>$_2$), 3.85 (3H, s, OC<u>H</u>$_3$), 3.88 (3H, s, OC<u>H</u>$_3$), 3.93 (3H, s, OC<u>H</u>$_3$), 3.97-4.04 (1H, m, C<u>H</u>N_3), 7.15 (1H, s, Ar<u>H</u>)

^{13}C NMR ($CDCl_3$, 400 MHz) δ_c ppm: 20.58 (<u>C</u>H_2), 31.73 (<u>C</u>H_2), 46.04 (<u>C</u>H_2), 55.53 (O<u>C</u>H_3), 56.14 (<u>C</u>HN_3), 60.43 (O<u>C</u>H_3), 60.78 (O<u>C</u>H_3), 107.05 (Ar<u>C</u>H), 129.04 (<u>Q</u>C), 133.19 (<u>Q</u>C), 145.54 (<u>Q</u>C), 150.64 (<u>Q</u>C), 151.33 (<u>Q</u>C), 198.09 (<u>C</u>=O)

ν_{MAX} (DCM)/cm^{-1}: 2939.03, 2102.28 (N_3), 1676.06 (C=O), 1589.10

HRMS $[M+Na]^+$: calculated 314.1117, found 314.1114, molecular formula ($C_{14}H_{17}N_3NaO_4$)

7.13.3 Reduction and BOC protection of azide group: Synthesis of *tert*-butyl (*R*)-6,7,8,9-tetrahydro-1,2,3-trimethoxy-5-oxo-5*H*-benzo[7]annulen-7-ylcarbamate (4.06)

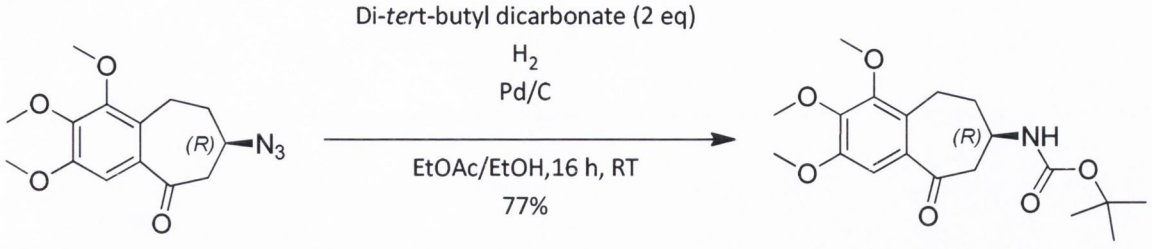

(4.05) **(4.06)**

To a stirred solution of **(4.05)** (0.36 g, 1.24 mmol) and palladium on activated carbon 10% w/w (0.5 g) in ethyl acetate and ethanol (1:1; 20 mL) was added di-*tert*-butyl dicarbonate (0.54 g, 2.47 mmol). The reaction was left stirring for 16 h. The reaction was then filtered to remove the palladium on activated carbon and the volatile organic solvents were removed under reduced pressure. The resulting residue was purified by flash column chromatography (stationary phase; silica gel 230-400 mesh, mobile phase; 4:1, hexane/ethyl acetate) to afford **(4.06)** as a clear oil (0.35 g, 77%).

R_f: 0.18 (3:1, hexane/ethyl acetate)

$[\alpha]_D^{25}$ = + 1.2 (*c* = 17.5, DCM)

^{1}H NMR ($CDCl_3$, 400 MHz) δ_H ppm: 1.38 (9H, s, C(C<u>H</u>$_3$)$_3$), 1.54 (1H, s, C<u>H</u>$_2$), 2.24 (1H, s, C<u>H</u>$_2$), 2.74-2.80 (1H, m, C<u>H</u>$_2$), 2.91-2.93 (2H, m, C<u>H</u>$_2$), 2.99-3.03(1H, m, C<u>H</u>$_2$), 3.78 (3H, s, OC<u>H</u>$_3$), 3.82 (3H, s, OC<u>H</u>$_3$), 3.87 (3H, s, OC<u>H</u>$_3$), 4.03-4.09 (1H, m, C<u>H</u>NH), 4.84 (1H, s, br, N<u>H</u>), 7.05 (1H, s, Ar<u>H</u>)

^{13}C NMR ($CDCl_3$, 400 MHz) δ_c ppm: 21.45 (<u>C</u>H$_2$), 27.85 (C(<u>C</u>H$_3$)$_3$), 32.65 (<u>C</u>H$_2$), 45.96 (<u>C</u>HNH), 47.14 (<u>C</u>H$_2$), 55.45 (O<u>C</u>H$_3$), 60.34 (O<u>C</u>H$_3$), 60.70 (O<u>C</u>H$_3$), 79.02 (<u>C</u>(CH$_3$)$_3$), 106.83 (Ar<u>C</u>H), 128.94 (Q<u>C</u>), 133.58 (Q<u>C</u>), 145.26 (Q<u>C</u>), 150.56 (Q<u>C</u>), 151.20 (Q<u>C</u>), 154.53 (Q<u>C</u>), 200.32 (<u>C</u>=O)

ν_{MAX} (DCM)/cm^{-1}: 3354.57 (NH), 2975.44, 2937.93, 1710.39 (C=O), 1680.72 (C=O), 1589.93

HRMS $[M+Na]^+$: calculated 388.1736, found 388.1748, molecular formula ($C_{19}H_{27}NNaO_6$)

7.13.4 Triflate synthesis: Synthesis of *tert*-butyl *N*-[(7*R*)-2,3,4-trimethoxy-9-(trifluoromethanesulfonyloxy)-6,7-dihydro-5*H*-benzo[7]annulen-7-yl]carbamate (4.07)

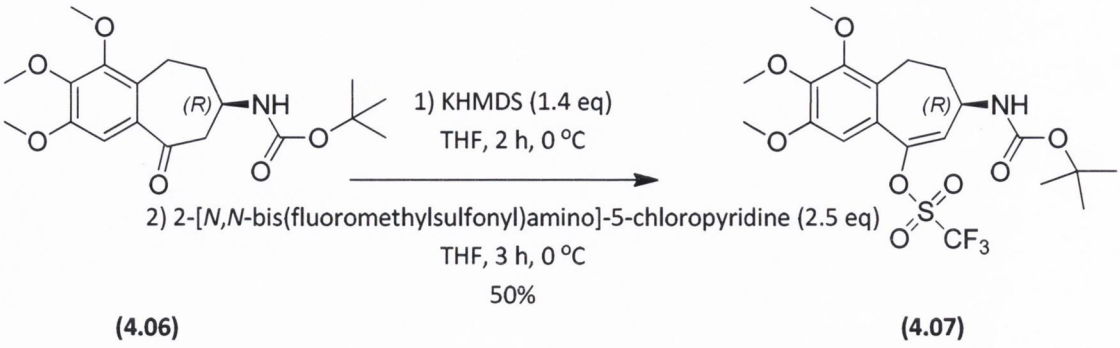

To a stirred solution of **(4.06)** (0.77 g, 2.11 mmol) in dry THF (10 mL) under an atmosphere of nitrogen at 0 °C was added 0.5 M KHMDS solution in toluene (5.9 mL, 2.95 mmol). After 2 h, a solution of 2-[*N,N*-bis(fluoromethylsulfonyl)amino]-5-chloropyridine (2.07 g, 5.27 mmol) in dry THF (5 mL) was added dropwise and the reaction was left stirring for a further 3 h. The reaction was then quenched by the addition of water (30 mL) and extracted with diethyl ether (3 x 50 mL). The organic fractions were combined, dried over $MgSO_4$, filtered and concentrated under reduced pressure. The product was purified by flash column chromatography (stationary phase; silica gel 230-400 mesh, mobile phase; 10:1, hexane/ethyl acetate) to yield **(4.07)** as a yellow oil (0.53 g, 50%).

R_f: 0.43 (3:1, hexane/ethyl acetate)

$[\alpha]_D^{25}$ = + 35.83 (*c* = 11.5, DCM)

^{1}H NMR ($CDCl_3$, 400 MHz) δ_H ppm: 1.44 (9H, s, C(C<u>H</u>$_3$)$_3$), 2.00-2.08 (1H, m, C<u>H</u>$_2$), 2.26-2.34 (1H, m, C<u>H</u>$_2$), 2.42-2.48 (1H, m, C<u>H</u>$_2$), 3.05-3.08 (1H, m, C<u>H</u>$_2$), 3.85 (3H, s, OC<u>H</u>$_3$), 3.86 (3H, s, OC<u>H</u>$_3$), 3.92 (3H, s, OC<u>H</u>$_3$), 4.01-4.17 (1H, m, C<u>H</u>NH), 6.05-6.06 (1H, d, J = 5.16 Hz, C=C<u>H</u>), 6.28 (1H, s, N<u>H</u>), 6.83 (1H, s, Ar<u>H</u>)

^{13}C NMR ($CDCl_3$, 400 MHz) δ_c ppm: 21.49 (<u>C</u>H$_2$), 28.27 (C(<u>C</u>H$_3$)$_3$), 38.51 (<u>C</u>H$_2$), 47.83 (<u>C</u>HNH), 55.99 (O<u>C</u>H$_3$), 60.87 (O<u>C</u>H$_3$), 61.50 (O<u>C</u>H$_3$), 80.15 (<u>C</u>(CH$_3$)$_3$), 106.07 (Ar<u>C</u>H), 116.89 (Q<u>C</u>), 120.07 (Q<u>C</u>), 125.04 (C=<u>C</u>H), 127.14 (Q<u>C</u>), 127.86 (Q<u>C</u>), 143.70 (Q<u>C</u>), 144.57 (Q<u>C</u>), 151.07 (Q<u>C</u>)), 151.91 (Q<u>C</u>), 155.07 (<u>C</u>=O)

ν_{MAX} (DCM)/cm^{-1}: 2939.84, 2371.85, 1687.49 (C=O), 1596.69

HRMS $[M+Na]^+$: calculated 520.1229, found 520.1237, molecular formula ($C_{20}H_{26}F_3NNaO_8S$)

7.13.5 Boronic acid synthesis: Synthesis of 3-*tert*-butyl-dimethylsilyloxy-4-methoxyphenylboronic acid (4.08)

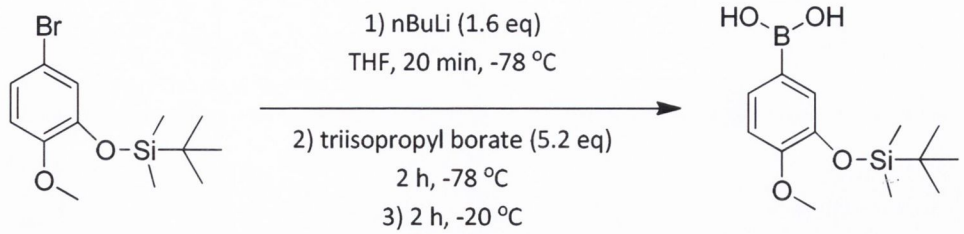

(2.14) **(4.08)**

To a stirred solution of **(2.14)** (2.22 g, 7.03 mmol) in dry THF (4 mL) under an atmosphere of nitrogen at -78 °C was added 2.5 M n-butyllithium in hexane (4.50 mL, 11.25 mmol) dropwise. After 20 min, triisopropyl borate (8.44 mL, 36.56 mmol) was added dropwise to the reaction. After a further 2 h, the temperature was allowed to increase to -20 °C and after an additional 2 h the temperature was allowed to increase to ambient. After a further 12 h, the reaction was quenched by the addition of 2 M HCl aqueous solution (1 x 100 mL). The product was extracted with diethyl ether (3 x 100 mL). The organic fractions were combined, dried over $MgSO_4$, filtered and concentrated *in vacuo*. The resulting residue was purified by flash column chromatography (stationary phase; silica gel 230-400 mesh, mobile phase; 9:1, ethyl acetate/methanol) to afford the 3-*tert*-butyl-dimethylsilyloxy-4-methoxyphenylboronic acid **(4.08)** as a white solid (1.3 g, 66%).

R_f: 0.14 (3:1, hexane/ethyl acetate)

^{1}H NMR ($CDCl_3$, 400 MHz) δ_H ppm: 0.25 (6H, s, Si($C\underline{H}_3$)$_2$), 1.09 (9H, s, C($C\underline{H}_3$)$_3$), 3.92 (3H, s, O$C\underline{H}_3$), 7.01 (1H, d, J = 8.0 Hz, Ar$\underline{H}$), 7.69 (1H, d, J = 1.5 Hz, Ar$\underline{H}$), 7.84 (1H, dd, J_1 = 8 Hz, J_2 = 1.5 Hz, Ar$\underline{H}$)

^{13}C NMR ($CDCl_3$, 400 MHz) δ_c ppm: - 4.96 (Si($\underline{C}H_3$)$_2$), 18.08 ($\underline{C}$(CH_3)$_3$), 25.38 (C($\underline{C}H_3$)$_3$), 54.86 (O$\underline{C}H_3$), 110.86 (Ar$\underline{C}$H), 126.95 (Ar$\underline{C}$H), 129.83 (Ar$\underline{C}$H), 144.07 (Q$\underline{C}$), 154.33 (Q$\underline{C}$)

ν_{MAX} (KBr)/cm^{-1} 2930.3, 1599.1, 1511.9, 1411.9

Melting point: 149 – 155 °C

7.13.6 Suzuki Coupling: Synthesis of *tert*-butyl *N*-[(7R)-9-{3-[(*tert*-butyldimethylsilyl)oxy]-4-methoxyphenyl}-2,3,4-trimethoxy-6,7-dihydro-5*H*-benzo[7]annulen-7-yl]carbamate (4.09)

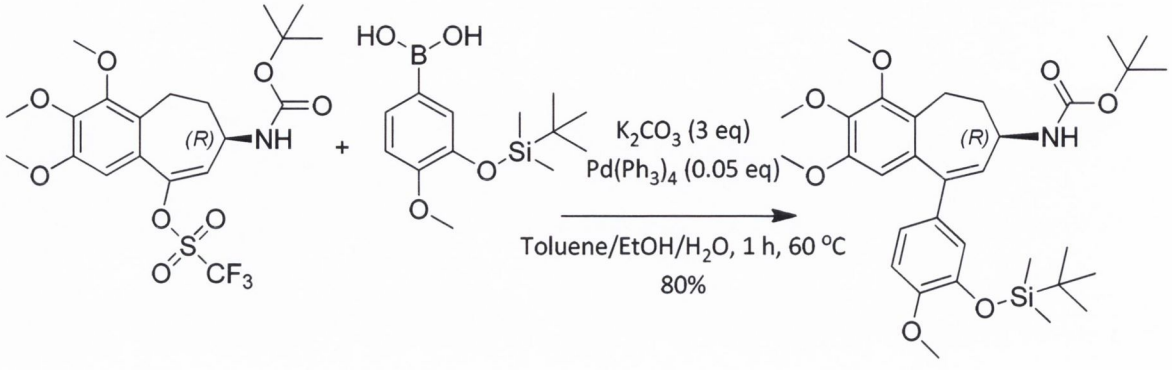

(4.07) **(4.08)** **(4.09)**

To a stirred solution of **(4.07)** (0.53 g, 1.07 mmol) in a mixture of toluene, ethanol and water (10 mL; 3: 1: 1) was added potassium carbonate (0.44 g, 3.20 mmol), (tetrakis(triphenyl)phosphine) palladium (0.06 g, 0.06 mmol) and **(4.08)** (0.36 g, 1.28 mmol). The reaction was heated under reflux to 60 °C for 1 h after which time it was quenched by the addition of water (50 mL). The reaction mixture was then extracted with diethyl ether (3 x 50 mL). The organic fractions were combined, dried over $MgSO_4$, filtered and concentrated *in vacuo.* The resulting residue was then purified by flash column chromatography (stationary phase; silica gel 230-400 mesh, mobile phase; 10:1, hexane/ethyl acetate) to afford **(4.09)** as a yellow oil (0.5 g, 80%).

R_f: 0.43 (3:1, hexane/ethyl acetate)

$[\alpha]_D^{25}$ = + 67.21 (*c* = 12.56, DCM)

^{1}H NMR ($CDCl_3$, 400 MHz) δ_H ppm: 0.16 (6H, d, J = 5.89, Si($C\underline{H}_2$)$_2$), 0.99 (9H, s, C($C\underline{H}_3$)$_3$), 1.46 (9H, s, C($C\underline{H}_3$)$_3$), 1.91-1.99 (1H, m, $C\underline{H}_2$), 2.28-2.37 (1H, m, $C\underline{H}_2$), 2.45-2.51 (1H, m, $C\underline{H}_2$), 3.04-3.08 (1H, m, $C\underline{H}_2$), 3.68 (3H, s, O$C\underline{H}_3$), 3.83 (3H, s, O$C\underline{H}_3$), 3.92 (6H, s, 2 x O$C\underline{H}_3$), 4.01-4.04 (1H, m, C$\underline{H}$NH), 4.73-4.74 (1H, d, J = 8.09 Hz, N$\underline{H}$), 6.02-6.03 (1H, d, J = 5.78 Hz, C=C$\underline{H}$), 6.37 (1H, s, Ar$\underline{H}$), 6.78-6.80 (2H, m, Ar$\underline{H}$), 6.84-6.88 (1H, m, Ar$\underline{H}$)

^{13}C NMR ($CDCl_3$, 400 MHz) δ_c ppm: -4.55 (Si($\underline{C}H_3$)$_2$), -4.53 (Si($\underline{C}H_3$)$_2$), 18.45 ($\underline{C}$(CH$_3$)$_3$), 22.26 ($\underline{C}H_2$), 25.73 (C($\underline{C}H_3$)$_3$), 28.41 (C($\underline{C}H_3$)$_3$), 41.95 ($\underline{C}H_2$), 49.13 ($\underline{C}$HNH), 55.50 (O$\underline{C}H_3$), 55.91 (O$\underline{C}H_3$), 60.87 (O$\underline{C}H_3$), 61.61 (O$\underline{C}H_3$), 79.39 ($\underline{C}$(CH$_3$)$_3$), 109.04 (Ar$\underline{C}$H), 111.58 (Ar$\underline{C}$H), 120.75 (Ar$\underline{C}$H), 121.52 (Ar$\underline{C}$H), 127.33 ($\underline{Q}$C), 129.38 (C=$\underline{C}$H), 134.19 ($\underline{Q}$C), 135.29 ($\underline{Q}$C), 140.00 ($\underline{Q}$C), 141.42 ($\underline{Q}$C), 144.58 ($\underline{Q}$C), 150.56 ($\underline{Q}$C), 150.76 ($\underline{Q}$C), 151.22 ($\underline{Q}$C), 155.26 (C=O)

ν_{MAX} (DCM)/cm^{-1}: 3418.71 (NH), 2956.97, 2933.15, 2857.59, 1690.14 (C=O), 1640.40 (NH)

HRMS: [M+Na]$^+$: calculated 608.3019, found 608.3038, molecular formula ($C_{32}H_{47}NNaO_7Si$)

7.13.7 Double deprotection: Synthesis of 5-((*R*,*Z*)-7-amino-6,7-dihydro-2,3,4-trimethoxy-5*H*-benzo[7]annulen-9-yl)-2-methoxyphenol (4.10)

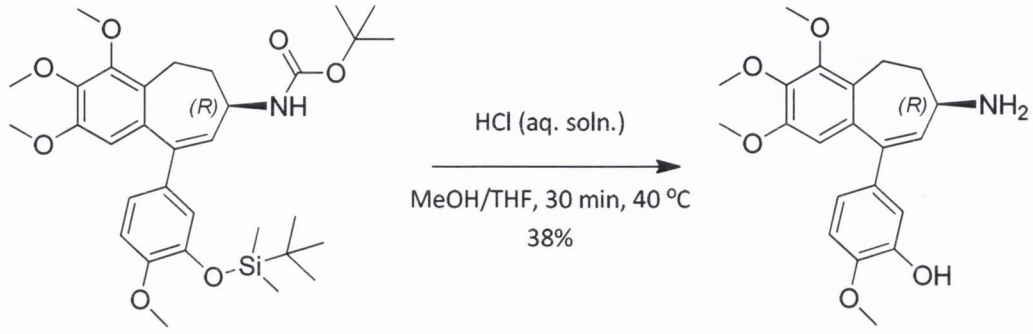

(4.09) **(4.10)**

To a stirred solution of **(4.09)** (0.5 g, 0.85 mmol) in a mixture of methanol and THF (1:1; 5 mL) was added 2 M HCl aqueous solution (2.5 mL). The reaction was heated under reflux at 40 °C for 30 min. The volatile organic solvents were then removed under reduced pressure. The aqueous phase was washed with diethyl ether (3 x 10 mL). The aqueous phase was then basified by the addition of saturated sodium bicarbonate aqueous solution (50 mL). The aqueous phase was then extracted with diethyl ether (3 x 50 mL). The organic fractions were combined, dried over $MgSO_4$, filtered and concentrated *in vacuo* to afford **(4.10)** as a white solid (0.12 g, 38%).

R_f: 0.5 (1:1, ethyl acetate/methanol)

$[\alpha]_D^{25}$ = + 107.52 (*c* = 3.13, DCM)

^{1}H NMR ($CDCl_3$, 400 MHz) δ_H ppm: 1.98-2.02 (1H, m, C<u>H</u>$_2$), 2.29-2.36 (1H, m, C<u>H</u>$_2$), 2.38-2.44 (1H, m, C<u>H</u>$_2$), 3.02-3.07 (1H, m, C<u>H</u>$_2$), 3.35 (1H, s, C<u>H</u>NH$_2$), 3.71 (3H, s, OC<u>H</u>$_3$), 3.91 (3H, s, OC<u>H</u>$_3$), 3.92 (3H, s, OC<u>H</u>$_3$), 3.94 (3H, s, OC<u>H</u>$_3$), 6.17-6.18 (1H, d, J = 5.53 Hz, C=C<u>H</u>), 6.38 (1H, s, Ar<u>H</u>), 6.76-6.82 (2H, m, Ar<u>H</u>), 6.93-6.94 (1H, d, J = 1.86 Hz, Ar<u>H</u>)

^{13}C NMR ($CDCl_3$, 400 MHz) δ_c ppm: 22.67 (<u>C</u>H$_2$), 44.38 (<u>C</u>H$_2$) 49.89 (<u>C</u>HNH$_2$), 55.97 (O<u>C</u>H$_3$), 56.03 (O<u>C</u>H$_3$), 60.89 (O<u>C</u>H$_3$), 61.57 (O<u>C</u>H$_3$), 108.79 (Ar<u>C</u>H), 110.44 (Ar<u>C</u>H), 114.36 (Ar<u>C</u>H), 119.73 (Ar<u>C</u>H), 128.15 (<u>Q</u>C), 132.97 (C=<u>C</u>H), 134.81 (<u>Q</u>C), 135.59 (<u>Q</u>C), 139.40 (<u>Q</u>C), 141.36 (<u>Q</u>C), 145.51 (<u>Q</u>C), 146.38 (<u>Q</u>C), 150.78 (<u>Q</u>C), 151.12 (<u>Q</u>C)

ν_{MAX} (DCM)/cm^{-1}: 3434.45, 2086.69, 1643.83

HRMS [M-H]$^-$: calculated 370.1654, found 370.1663, molecular formula ($C_{21}H_{24}NO_5$)

Melting point: 114-115 °C

7.13.8 Acetylation: Synthesis of 5-((*R*,*Z*)-7-acetamido-6,7-dihydro-2,3,4-trimethoxy-5*H*-benzo[7]annulen-9-yl)-2-methoxyphenyl acetate (4.11)

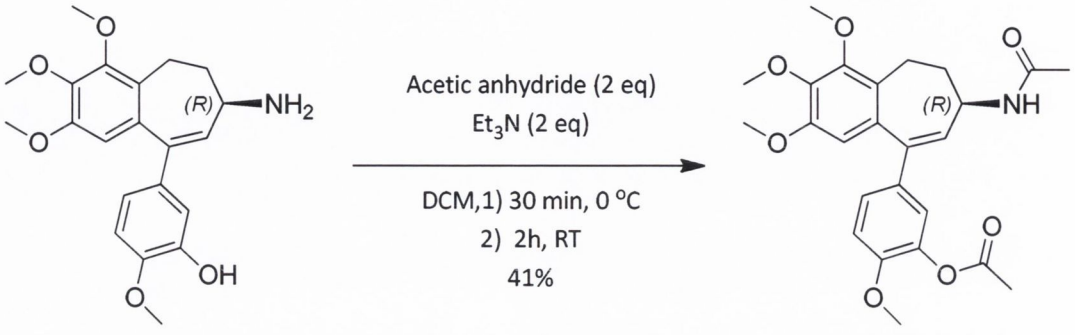

(4.10) **(4.11)**

To a stirred solution of **(4.10)** (0.12 g, 0.32 mmol) in dry DCM (2 mL) under an atmosphere of nitrogen at 0 °C was added acetic anhydride (0.06 mL, 0.65 mmol) and triethylamine (0.09 mL, 0.65 mmol). After 30 min, the temperature of the reaction was allowed to increase to ambient. After a further 2 h the reaction was quenched by the addition of water (25 mL). The reaction mixture was then extracted with diethyl ether (3 x 50 mL). The organic fractions were combined, dried over $MgSO_4$, filtered and concentrated *in vacuo.* The resulting residue was then purified by flash column chromatography (stationary phase; silica gel 230-400 mesh, mobile phase; ethyl acetate) to afford **(4.11)** as a yellow oil (0.06 g, 41%).

R_f: 0.24 (ethyl acetate)

$[\alpha]_D^{25}$ = + 113 (*c* = 4, DCM)

^{1}H NMR ($CDCl_3$, 400 MHz) δ_H ppm: 1.95-1.99 (4H, m, 1 x COC$\underline{H}_3$, 1 x C$\underline{H}_2$), 2.30-2.35 (4H, m, 1 x COC$\underline{H}_3$, 1 x C$\underline{H}_2$), 2.42-2.47 (1H, m, C$\underline{H}_2$), 3.01-3.06 (1H, m, C$\underline{H}_2$), 3.69 (3H, s, OC$\underline{H}_3$), 3.85 (3H, s, OC$\underline{H}_3$), 3.90 (3H, s, OC$\underline{H}_3$), 3.92 (3H, s, OC$\underline{H}_3$), 4.29-4.33 (1H, m, C$\underline{H}$NH), 5.90 (CHN$\underline{H}$), 6.03 (1H, d, J = 5.72 Hz, C=C$\underline{H}$), 6.37 (1H, s, Ar$\underline{H}$), 6.90 (1H, d, J = 8.46 Hz, Ar$\underline{H}$), 6.97 (1H, d, J = 2.20, Ar$\underline{H}$), 7.14-7.17 (1H, m, Ar$\underline{H}$)

^{13}C NMR ($CDCl_3$, 400 MHz) δ_c ppm: 20.69 (CO$\underline{C}H_3$), 22.27 ($\underline{C}H_2$), 23.43 (CO$\underline{C}H_3$), 41.76 ($\underline{C}H_2$), 47.93 ($\underline{C}$HNH), 55.94 (O$\underline{C}H_3$), 56.06 (O$\underline{C}H_3$), 60.86 (O$\underline{C}H_3$), 61.55 (O$\underline{C}H_3$), 109.07 (Ar$\underline{C}$H), 111.95 (Ar$\underline{C}$H), 122.56 (Ar$\underline{C}$H), 126.38 (Ar$\underline{C}$H), 127.36 ($\underline{Q}$C) 129.71 (C=$\underline{C}$H), 134.18 ($\underline{Q}$C), 134.68 ($\underline{Q}$C), 139.37 ($\underline{Q}$C), 139.61 ($\underline{Q}$C), 141.59 ($\underline{Q}$C), 150.59 ($\underline{Q}$C), 150.84 ($\underline{Q}$C), 151.40 ($\underline{Q}$C), 169.10 ($\underline{C}$=O), 169.33 ($\underline{C}$=O)

ν_{MAX} (DCM)/cm^{-1}: 3427.51 (NH), 2934.42, 2853.50, 1766.67 (C=O), 1648.97 (C=O)

HRMS $[M+Na]^+$: calculated 478.1842, found 478.1850, molecular formula ($C_{25}H_{29}NNaO_7$)

7.13.9 Ester hydrolysis: Synthesis of *N*-((*R*,*Z*)-6,7-dihydro-9-(3-hydroxy-4-methoxyphenyl)-2,3,4-trimethoxy-5*H*-benzo[7]annulen-7-yl)acetamide (4.01)

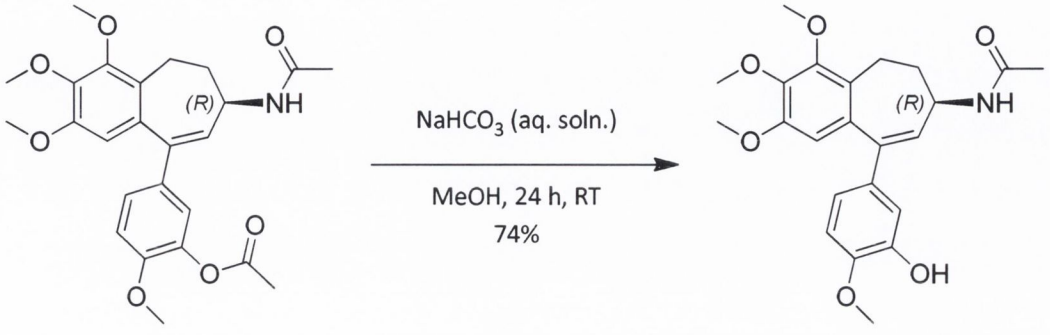

(4.11) **(4.01)**

To a stirred solution of **(4.11)** (0.06 g, 0.13 mmol) in methanol (2 mL) was added saturated sodium bicarbonate aqueous solution (1 mL). After 3 h, the methanol was removed under reduced pressure and the reaction was acidified by the addition of 2 M HCl aqueous solution (10 mL). The reaction mixture was then extracted with diethyl ether (3 x 25 mL). The organic fractions were combined, dried over $MgSO_4$, filtered and concentrated *in vacuo.* The resulting residue was then purified by flash column chromatography (stationary phase; silica gel 230-400 mesh, mobile phase; ethyl acetate) to afford **(4.01)** as a white solid (0.04 g, 74%).

R_f: 0.24 (ethyl acetate)

$[\alpha]_D^{25}$ = + 35.2 (*c* = 2, DCM)

^{1}H NMR ($CDCl_3$, 400 MHz) δ_H ppm: 1.98-2.06 (4H, m, 1 x $COCH_3$, 1 x CH_2), 2.29-2.35 (1H, m, CH_2), 2.46 (1H, s, CH_2), 3.02-3.04 (1H, m, CH_2), 3.69 (3H, s, OCH_3), 3.89 (3H, s, OCH_3), 3.90 (3H, s, OCH_3), 3.93 (3H, s, OCH_3), 4.32 (1H, s, CHNH), 6.07 (C=CH), 6.37 (1H, s, ArH), 6.77 (2H, s, ArH), 6.92 (1H, s, ArH)

^{13}C NMR ($CDCl_3$, 400 MHz) δ_c ppm: 22.20 (CH_2), 22.96 ($COCH_3$), 41.52 (CH_2), 48.51 (CHNH), 55.99 (OCH_3), 56.05 (OCH_3), 60.89 (OCH_3), 61.59 (OCH_3), 109.23 (ArCH), 110.42 (ArCH), 114.42 (ArCH), 119.98 (ArCH), 127.26 (QC), 128.27 (C=CH), 134.58 (QC), 134.99 (QC), 140.66 (QC), 141.56 (QC), 145.37 (QC), 146.44 (QC), 150.77 (QC), 151.34 (QC), 170.51 (C=O)

ν_{MAX} (DCM)/cm^{-1}: 3374.38, 2927.58, 2853.89, 1650.34 (C=O), 1509.18

HRMS $[M+H]^+$: calculated 414.1917, found 414.1909, molecular formula ($C_{23}H_{28}NO_6$)

Melting point: 103-105 °C

7.14 Synthesis of methylene acetamide analogue (S)-N-((9-(3-hydroxy-4-methoxyphenyl)-2,3,4-trimethoxy-6,7-dihydro-5H-benzo[7]annulen-7-yl)methyl)acetamide (4.12)

7.14.1 Nitrile Synthesis: Synthesis of (7*R*)-6,7,8,9-tetrahydro-1,2,3-trimethoxy-5-(methoxymethoxy)-5*H*-benzo[7]annulene-7-carbonitrile (4.14)

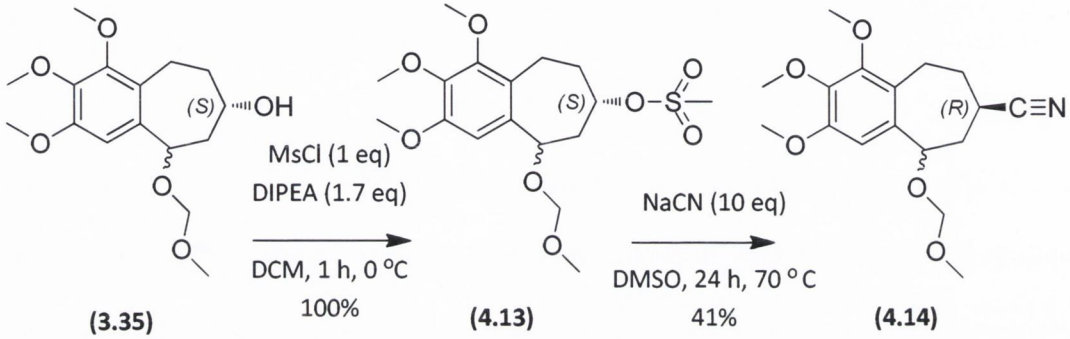

(3.35) **(4.13)** **(4.14)**

To a stirred solution of **(3.35)** (2.99 g, 9.58 mmol) in dry DCM (10 mL) under an atmosphere of nitrogen at 0 °C was added methanesulfonyl chloride (1.26 mL, 16.28 mmol) followed by *N,N*-diisopropylethylamine (2.5 mL, 14.36 mmol). After 1 h, the reaction was quenched by the addition of water (20 mL). The reaction mixture was then extracted with diethyl ether (3 x 25 mL). The organic fractions were combined and dried over $MgSO_4$ and concentrated *in vacuo* to yield the mesylate **(4.13)** as a crude mixture. The mesylate was dissolved in DMSO (10 mL) at room temperature and sodium cyanide (4.96 g, 10.70 mmol) was added to the solution. The reaction was then refluxed at 70 °C for 24 h. The reaction was then quenched by the addition of water (30 mL) and extracted with diethyl ether (3 x 30 mL). The organic fractions were combined, dried over $MgSO_4$, filtered and concentrated under reduced pressure. The product was purified by flash column chromatography (stationary phase; silica gel 230-400 mesh, mobile phase; 4:1, hexane/ethyl acetate) to yield **(4.14)** as a yellow oil (1.27 g, 41% over two steps).

R_f: 0.24 (3:1, hexane/ethyl acetate)

^{1}H NMR ($CDCl_3$, 400 MHz) δ_H ppm: 1.63-1.78 (1H, m, C$\underline{H}_2$), 1.78-1.96 (1H, m, C$\underline{H}_2$), 2.06-2.19 (1H, m, C$\underline{H}_2$), 2.27-2.40 (1H, m, C$\underline{H}_2$), 2.77-2.89 (1H, m, C$\underline{H}_2$), 2.99-3.11 (1H, m, C$\underline{H}_2$), 3.39-3.37 (4H, m, 1 x C$\underline{H}$CN, 1 x OC$\underline{H}_3$), 3.75 (3H, s, OC$\underline{H}_3$), 3.81 (3H, s, OC$\underline{H}_3$), 3.83 (3H, s, OC$\underline{H}_3$), 4.54 (2H, s, OC$\underline{H}_2$OCH$_3$), 4.76 (1H, d, J = 7.60 Hz, C$\underline{H}$OCH$_2$), 6.59 (1H, s, Ar$\underline{H}$)

^{13}C NMR ($CDCl_3$, 400 MHz) δ_c ppm: 22.21 ($\underline{C}H_2$), 28.14 ($\underline{C}HCN$), 31.17 ($\underline{C}H_2$), 36.10 ($\underline{C}H_2$), 55.50 ($O\underline{C}H_3$), 56.00 ($O\underline{C}H_3$), 60.72 ($O\underline{C}H_3$), 61.32 ($O\underline{C}H_3$), 75.37 ($\underline{C}HOCH_2$), 93.93 ($O\underline{C}H_2OCH_3$), 108.73 (Ar$\underline{C}$H), 122.56 ($\underline{C}N$), 135.20 ($\underline{Q}C$), 141.84 ($\underline{Q}C$), 151.06 ($\underline{Q}C$), 151.48 ($\underline{Q}C$)

ν_{MAX} (DCM)/cm^{-1}: 2936.99, 2859.32, 2838.19, 2237.47 (CN), 1599.76

HRMS $[M+Na]^+$: calculated 344.1474, found 344.1465, molecular formula ($C_{17}H_{23}NNaO_5$)

7.14.2 Reduction of nitrile: Synthesis of ((7*R*)-6,7,8,9-tetrahydro-1,2,3-trimethoxy-5-(methoxymethoxy)-5*H*-benzo[7]annulen-7-yl)methanamine (4.15)

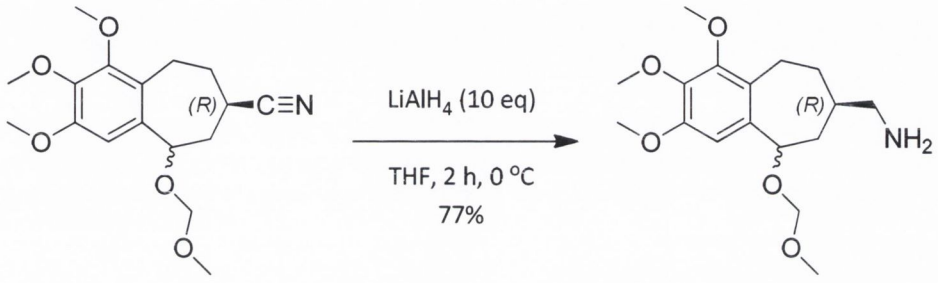

(4.14) **(4.15)**

To a stirred solution of $LiAlH_4$ (0.06 g, 1.56 mmol) under an atmosphere of nitrogen at 0 °C was added a solution of **(4.14)** (0.05 g, 0.16 mmol) dropwise. After 2 h, the reaction mixture was quenched by slowly adding to water (5 mL) at 0 °C. The aqueous layer was then acidified by the addition of 2 M HCl aqueous solution (10 mL) and washed with diethyl ether (3 x 10 mL). The aqueous phase was then basified by the addition of 2.5 M NaOH aqueous solution (20 mL) and extracted with diethyl ether (3 x 50 mL). The organic fractions were combined, dried over $MgSO_4$, filtered and concentrated *in vacuo* to yield **(4.15)** as a colourless oil (0.04 g, 77%).

R_f: 0.06 (3:1, ethyl acetate/methanol)

^1H NMR ($CDCl_3$, 400 MHz) δ_H ppm: 0.83-0.92 (1H, m, major diastereomer, $C\underline{H}_2$), 1.07-1.16 (2H, m, major diastereomer, $C\underline{H}_2$), 1.27-1.52 (2H, m, major and minor diastereomers, $C\underline{H}_2$), 1.80-1.88 (1H, m, minor diastereomer, $C\underline{H}CH_2NH_2$), 1.98-2.03 (3H, m, major and minor diastereomers, 2 x $C\underline{H}_2$, 1 x $C\underline{H}CH_2NH_2$), 2.13-2.31 (2H, major and minor diastereomers, $C\underline{H}_2$), 2.58-2.62 (4H, m, major and minor diastereomers, 2 x $C\underline{H}_2$), 2.78-2.84 (1H, m, major diastereomer, $C\underline{H}_2$), 3.06-3.12 (1H, q, J = 7.55 Hz, major diastereomer, $C\underline{H}_2$), 3.30-3.40 (1H, m, minor diastereomer, $C\underline{H}_2$), 3.38 (3H, s, major diastereomer, $O\underline{C}H_3$), 3.45 (3H, s, minor diastereomer, $O\underline{C}H_3$), 3.80 (3H, s, major diastereomer, $O\underline{C}H_3$), 3.81 (3H, s, minor diastereomer, $O\underline{C}H_3$), 3.85 (3H, s, major diastereomer, $O\underline{C}H_3$), 3.88 (9H, s, major and minor diastereomers, 3 x $O\underline{C}H_3$), 4.58 (2H, s, major diastereomer, $O\underline{C}H_2OCH_3$), 4.71

(1H, d, J = 6.80 Hz, minor diastereomer, $OC\underline{H}_2OCH_3$), 4.76-4.83 (2H, m, major and minor diastereomers, 1 x $OC\underline{H}_2OCH_3$, 2 x $C\underline{H}OCH_2$), 6.59 (1H, s, major diastereomer, Ar$\underline{H}$), 6.92 (1H, s, minor diastereomer, Ar$\underline{H}$)

^{13}C NMR ($CDCl_3$, 400 MHz) δ_c ppm: 22.59 ($\underline{C}H_2$), 23.35 ($\underline{C}H_2$), 31.21 ($\underline{C}H_2$), 31.52 ($\underline{C}H_2$), 36.71 ($\underline{C}H_2$), 39.51 ($\underline{C}H_2$), 39.60 ($\underline{C}HCH_2NH_2$), 44.20 ($\underline{C}HCH_2NH_2$), 49.00 (2 x $\underline{C}H_2$), 55.36 ($O\underline{C}H_3$), 55.71 ($O\underline{C}H_3$), 56.01 ($O\underline{C}H_3$), 56.06 ($O\underline{C}H_3$), 60.84 ($O\underline{C}H_3$), 60.86 ($O\underline{C}H_3$), 61.38 (2 x $O\underline{C}H_3$), 75.40 ($\underline{C}HOCH_2$), 77.35 ($\underline{C}HOCH_2$), 93.90 ($O\underline{C}H_2O$), 95.00 ($O\underline{C}H_2O$), 103.47 (Ar$\underline{C}$H). 109.27 (Ar$\underline{C}$H), 125.78 ($\underline{Q}C$), 128.45 ($\underline{Q}C$), 135.90 ($\underline{Q}C$), 138.83 ($\underline{Q}C$), 140.65 ($\underline{Q}C$), 141.69 ($\underline{Q}C$), 150.47 ($\underline{Q}C$), 150.84 ($\underline{Q}C$), 151.24 ($\underline{Q}C$), 151.36 ($\underline{Q}C$)

ν_{MAX} (DCM)/cm^{-1}: 3376.36 (NH), 2932.52, 2848.60, 1665.26, 1599.56

HRMS $[M+H]^+$:calculated 326.1967, found 326.1970, molecular formula ($C_{17}H_{28}NO_5$)

7.14.3 BOC protection of amine: Synthesis of *tert*-butyl ((7*R*)-6,7,8,9-tetrahydro-1,2,3-trimethoxy-5-(methoxymethoxy)-5*H*-benzo[7]annulen-7-yl)methylcarbamate (4.16)

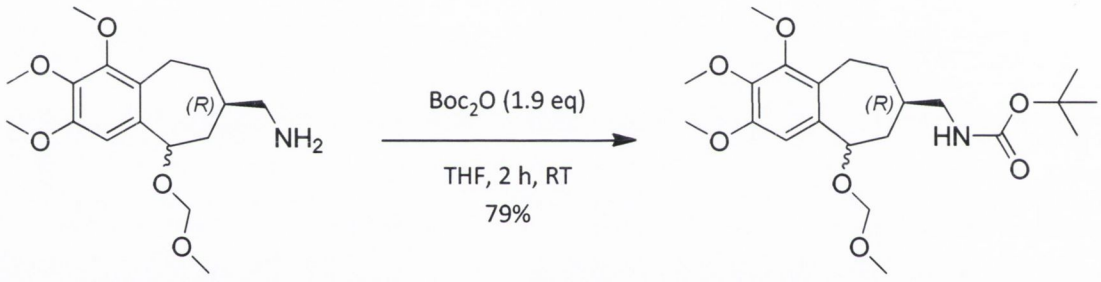

(4.15) **(4.16)**

To a stirred solution of **(4.15)** (0.75 g, 2.30 mmol) in dry THF (3 mL) under an atmosphere of nitrogen at room temperature was added 1 M Di-*tert*-butyl dicarbonate solution (4.41 mL, 4.41 mmol). After 2 h, the reaction was deemed to have gone to completion and the reaction was quenched by the addition of water (10 mL). The reaction was then extracted with diethyl ether (3 x 25 mL). The organic fractions were combined, dried over $MgSO_4$, filtered and concentrated under reduced pressure. The resulting residue was then purified by flash column chromatography (stationary phase; silica gel 230-400 mesh, mobile phase; 4:1, hexane/ethyl acetate) to yield **(4.16)** as a colourless oil (0.77 g, 79%).

R_f: 0.58 (1:1, hexane/ethyl acetate)

^1H NMR ($CDCl_3$, 400 MHz) δ_H ppm: 0.82-0.95 (1H, m, minor diastereomer, $C\underline{H}_2$), 1.08-1.17 (1H, m, major diastereomer, $C\underline{H}_2$), 1.31-1.34 (1H, d, J = 12.1 Hz, minor diastereomer, $C\underline{H}_2$), 1.45 (19H, s,

major and minor diastereomers, 2 x OC($C\underline{H}_3$)$_3$, 1 x $C\underline{H}_2$), 1.92-2.00 (3H, m, major and minor diastereomers, 1 x $C\underline{H}CH_2NH$, 2 x $C\underline{H}_2$), 2.07-2.28 (4H, m, major and minor diastereomers, 3 x $C\underline{H}_2$, 1 x $C\underline{H}CH_2NH$), 2.75-2.82 (1H, m, major diastereomer, $C\underline{H}_2$), 2.99-3.11 (5H, m, major and minor diastereomers, 5 x $C\underline{H}_2$), 3.30-3.38 (1H, m, minor diastereomer, $C\underline{H}_2$), 3.37 (3H, s, major diastereomer, $OC\underline{H}_3$), 3.43 (3H, s, major diastereomer, $OC\underline{H}_3$), 3.79 (3H, s, major diastereomer, $OC\underline{H}_3$), 3.80 (3H, s, minor diastereomer, $OC\underline{H}_3$), 3.84 (3H, s, major diastereomer, $OC\underline{H}_3$), 3.87 (3H, s, minor diastereomer, $OC\underline{H}_3$), 3.87 (3H, s, major diastereomer, $OC\underline{H}_3$), 3.88 (3H, s, minor diastereomer, $OC\underline{H}_3$), 4.56 (2H, s, major diastereomer, $OC\underline{H}_2OCH_3$), 4.69 (1H, d, J = 6.71 Hz, minor diastereomer, $OC\underline{H}_2OCH_3$), 4.72-4.76 (2H, m, major and minor diastereomers, 2 x $C\underline{H}_2$), 4.79 (1H, d, J = 6.71 Hz, minor diastereomer, $OC\underline{H}_2OCH_3$), 6.57 (1H, s, major diastereomer, Ar$\underline{H}$), 6.91 (1H, s, minor diastereomer, Ar$\underline{H}$)

^{13}C NMR ($CDCl_3$, 400 MHz) δ_c ppm: 22.5 ($\underline{C}H_2$), 23.2 ($\underline{C}H_2$), 28.43 ($C(\underline{C}H_3)_3$), 31.11 ($\underline{C}H_2$), 31.62 ($\underline{C}H_2$), 36.53 ($\underline{C}H_2$), 36.79 ($\underline{C}HCH_2NH_2$), 39.33 ($\underline{C}H_2$), 41.06 ($\underline{C}HCH_2NH_2$), 46.97 ($\underline{C}H_2$), 55.37 ($O\underline{C}H_3$), 55.7 ($O\underline{C}H_3$), 56.01 ($O\underline{C}H_3$), 56.05 ($O\underline{C}H_3$), 60.85 ($O\underline{C}H_3$), 61.38 ($O\underline{C}H_3$), 75.22 ($CH_2O\underline{C}H$), 77.3 ($CH_2O\underline{C}H$), 79.07 ($C(\underline{C}H_3)_3$), 79.18 ($\underline{C}(CH_3)_3$), 93.94 ($O\underline{C}H_2O$), 94.99 ($O\underline{C}H_2O$), 103.58 (Ar$\underline{C}$H), 109.39 (Ar$\underline{C}$H), 125.6 (Q$\underline{C}$), 128.3 (Q$\underline{C}$), 135.81 (Q$\underline{C}$), 138.66 (Q$\underline{C}$), 140.72 (Q$\underline{C}$), 141.75 (Q$\underline{C}$), 150.52 (Q$\underline{C}$), 150.87 (Q$\underline{C}$), 151.3 (Q$\underline{C}$), 151.4, (Q$\underline{C}$), 156.02 ($\underline{C}$=O), 156.1 ($\underline{C}$=O)

ν_{MAX} (DCM)/cm^{-1}: 3380.18 (NH), 2930.29, 2852.65, 1701.23 (C=O)

HRMS $[M+Na]^+$: calculated 448.2311, found 448.2386, molecular formula ($C_{22}H_{35}NNaO_7$)

7.14.4 Removal of MOM and oxidation: Synthesis of *tert*-butyl ((*R*)-6,7,8,9-tetrahydro-1,2,3-trimethoxy-5-oxo-5*H*-benzo[7]annulen-7-yl)methylcarbamate (4.18)

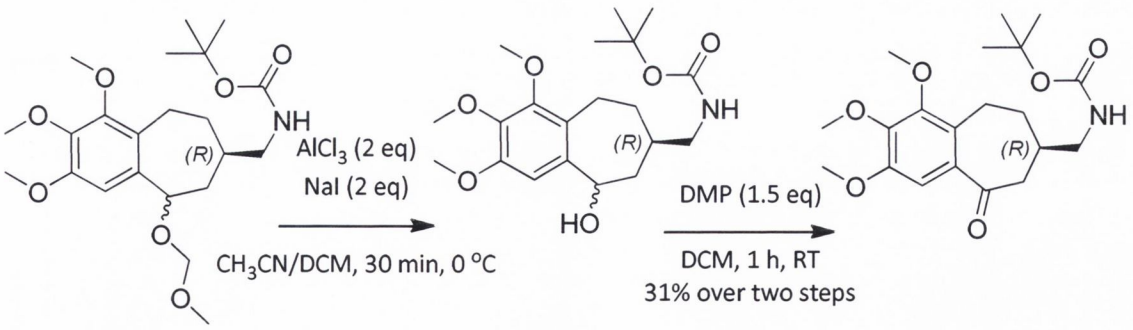

(4.16) **(4.17)** **(4.18)**

To a stirred solution of **(4.16)** (0.58 g, 1.28 mmol) in a mixture of acetonitrile and DCM (2:1; 24 mL) at 0 °C was added aluminium chloride (0.34 g, 2.56 mmol) and sodium iodide (3.8 g, 2.56

mmol). After 30 min, the reaction was quenched by the addition of saturated sodium bicarbonate aqueous solution (50 mL). The reaction was extracted with DCM (3 x 10 mL).To a stirred solution of the combined organic fractions was added Dess-Martin periodinane (0.82 g, 1.92 mmol). After 1 h, the reaction was quenched by the addition of saturated sodium bicarbonate aqueous solution (50 mL) and the reaction was extracted with diethyl ether (3 x 50 mL). The organic fractions were combined, dried over $MgSO_4$, filtered and concentrated *in vacuo*. The resulting residue was then purified by flash column chromatography (stationary phase; silica gel 230-400 mesh, mobile phase; 10:1, hexane/ethyl acetate) to yield **(4.18)** as a yellow oil (0.15 g, 31%).

R_f: 0.17 (3:1, hexane/ethyl acetate)

$[\alpha]_D^{25}$ = - 23.47 (*c* = 7.33, DCM)

^{1}H NMR ($CDCl_3$, 400 MHz) δ_H ppm: 1.46 (10H, s, 1 x C(CH_3)$_3$, 1 x CH_2), 1.95-1.99 (1H, m, CH_2), 2.07-2.19 (1H, m, $CHCH_2$), 2.59-2.65 (1H, m, CH_2), 2.80-2.84 (2H, m, CH_2), 3.01-3.23 (3H, m, CH_2), 3.86 (3H, s, OCH_3), 3.90 (3H, s, OCH_3), 3.95 (3H, s, OCH_3), 7.15 (1H, s, ArH)

^{13}C NMR ($CDCl_3$, 400 MHz) δ_c ppm: 21.92 (CH_2), 27.94 (C(CH_3)$_3$, 29.28 (CH_2), 33.80 ($CHCH_2$), 43.93 (CH_2), 44.50 (CH_2), 55.54 (OCH_3),, 60.45 (OCH_3), 60.85 (OCH_3), 78.99 ($OC(CH_3)_3$), 106.94 (ArCH), 129.40 (QC), 133.56 (QC), 145.43 (QC), 150.57 (QC), 151.14 (QC), 155.57 (C=O)

ν_{MAX} (DCM)/cm^{-1}: 3372.00 (NH), 2973.28, 2932.79, 1711.97 (C=O)

HRMS $[M+Na]^+$: calculated 402.1893, found 402.1862, molecular formula ($C_{20}H_{29}NNaO_6$)

7.14.5 Triflate formation: Synthesis of *tert*-butyl *N*-{[(7R)-2,3,4-trimethoxy-9-(trifluoromethanesulfonyloxy)-6,7-dihydro-5*H*-benzo[7]annulen-7-yl]methyl}carbamate (4.19)

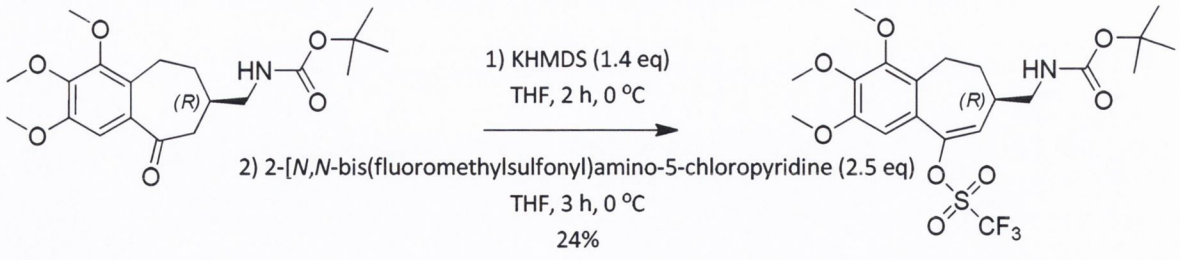

(4.18) **(4.19)**

To a stirred solution of **(4.19)** (0.15 g, 0.40 mmol) in dry THF (2 mL) under an atmosphere of nitrogen at 0 °C was added 0.5 M KHMDS solution in toluene (1.1 mL, 0.55 mmol). After 2 h, a solution of 2-[*N,N*-bis(fluoromethylsulfonyl)amino]-5-chloropyridine (0.39 g, 0.99 mmol) in dry

THF (3 mL) was added dropwise and the reaction was left stirring for a further 3 h. The reaction was then quenched by the addition of water (10 mL) and extracted with diethyl ether (3 x 25 mL). The organic fractions were combined, dried over $MgSO_4$, filtered and concentrated under reduced pressure. The product was purified by flash column chromatography (stationary phase; silica gel 230-400 mesh, mobile phase; 10:1, hexane/ethyl acetate) to yield **(4.19)** as a yellow oil (0.05 g, 24%).

R_f: 0.67 (3:1, hexane/ethyl acetate)

$[\alpha]_D^{25}$ = + 13.44 (*c* = 6.82, DCM)

^{1}H NMR ($CDCl_3$, 400 MHz) δ_H ppm: 1.45 (9H, s, C(C<u>H</u>$_3$)$_3$), 1.81-1.89 (1H, m, C<u>H</u>$_2$), 2.17-2.20 (1H, m, C<u>H</u>$_2$), 2.36-2.38 (1H, m, C<u>H</u>CH$_2$NH), 2.53-2.60 (1H, m, C<u>H</u>$_2$), 2.94-2.99 (1H, m, C<u>H</u>$_2$), 3.20-3.23 (2H, m, C<u>H</u>$_2$), 3.86 (3H, s, OC<u>H</u>$_3$), 3.87 (3H, s, OC<u>H</u>$_3$), 3.94 (3H, s, OC<u>H</u>$_3$), 6.05 (1H, d, J = 5.47 Hz, C=C<u>H</u>), 6.10 (1H, s, N<u>H</u>), 6.82 (1H, s, Ar<u>H</u>)

^{13}C NMR ($CDCl_3$, 400 MHz) δ_c ppm: 22.83 (<u>C</u>H$_2$), 28.32 (C(<u>C</u>H$_3$)$_3$), 36.42 (<u>C</u>H$_2$), 37.48 (<u>C</u>HCH$_2$NH), 44.23 (<u>C</u>H$_2$), 56.01 (O<u>C</u>H$_3$), 60.93 (O<u>C</u>H$_3$), 61.55 (O<u>C</u>H$_3$), 79.74 (<u>C</u>(CH$_3$)$_3$), 105.85 (Ar<u>C</u>H), 116.902 (Q<u>C</u>), 120.09 (Q<u>C</u>), 124.20 (C=<u>C</u>H), 127.77 (Q<u>C</u>), 128.397 (Q<u>C</u>), 143.43 (Q<u>C</u>), 145.69 (Q<u>C</u>), 151.11 (Q<u>C</u>), 151.75 (Q<u>C</u>), 156.06 (Q<u>C</u>)

^{19}F NMR ($CDCl_3$, 400 MHz) δ_c ppm: -74.47

ν_{MAX} (DCM)/cm^{-1}: 3387.04 (NH), 2976.16, 2935.99, 1686.12 (C=O)

HRMS $[M+Na]^+$: calculated 534.1385, found 534.1370, molecular formula ($C_{21}H_{28}F_3NNaO_8S$)

7.14.6 Suzuki coupling: Synthesis of *tert*-butyl *N*-{[(7*R*)-9-{3-[(*tert*-butyldimethylsilyl)oxy]-4-methoxyphenyl}-2,3,4-trimethoxy-6,7-dihydro-5*H*-benzo[7]annulen-7-yl]methyl}carbamate (4.20)

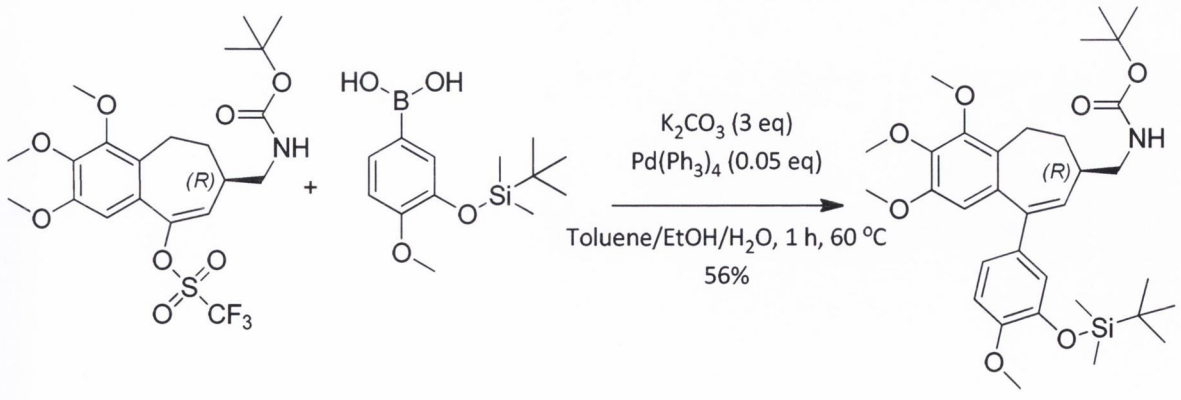

(4.19) **(4.08)** **(4.20)**

To a stirred solution of **(4.19)** (0.06 g, 0.12 mmol) in a mixture of toluene, ethanol and water (5 mL; 3: 1: 1) was added potassium carbonate (0.05 g, 0.35 mmol), (tetrakis(triphenyl)phosphine) palladium (0.01 g, 0.01 mmol) and **(4.08)** (0.04 g, 0.14 mmol). The reaction was heated under reflux to 60 °C for 1 h after which time it was quenched by the addition of water (10 mL). The reaction mixture was then extracted with diethyl ether (3 x 10 mL). The organic fractions were combined, dried over $MgSO_4$, filtered and concentrated *in vacuo.* The resulting residue was then purified by flash column chromatography (stationary phase; silica gel 230-400 mesh, mobile phase; 10:1, hexane/ethyl acetate) to afford **(4.20)** as a yellow resin (0.04 g, 56%).

R_f: 0.51 (3:1, hexane/ethyl acetate)

$[\alpha]_D^{25}$ = + 22.4 (*c* = 3.13, DCM)

^{1}H NMR ($CDCl_3$, 400 MHz) δ_H ppm: 0.16 (6H, d, J = 4.41 Hz, $Si(C\underline{H}_3)_2$), 0.99 (9H, s, $C(C\underline{H}_3)_3$), 1.86-1.88 (1H, m, $C\underline{H}_2$), 2.12-2.24 (2H, m, 1 x $C\underline{H}_2$, 1 x $C\underline{H}CH_2NH$), 2.26-2.32 (1H, m, $C\underline{H}_2$), 3.05-3.09 (1H, m, $C\underline{H}_2$), 3.17-3.20 (1H, m, $C\underline{H}_2$), 3.30-3.32 (1H, m, $C\underline{H}_2$), 3.70 (3H, s, $OC\underline{H}_3$), 3.84 (3H, s, $OC\underline{H}_3$), 3.92 (3H, s, $OC\underline{H}_3$), 3.94 (3H, s, $OC\underline{H}_3$), 6.06 (1H, d, J = 5.83 Hz, C=C$\underline{H}$), 6.37 (1H, s, Ar$\underline{H}$), 6.78-6.81 (2H, s, Ar$\underline{H}$), 6.85-6.87 (1H, s, Ar$\underline{H}$)

^{13}C NMR ($CDCl_3$, 400 MHz) δ_c ppm: -4.53 ($Si(\underline{C}H_3)_2$), 18.47 ($\underline{C}(CH_3)_3$), 23.19 ($\underline{C}H_2$), 25.75 ($C(\underline{C}H_3)_3$), 28.44 ($C(\underline{C}H_3)_3$), 37.83 ($\underline{C}HCH_2NH$), 39.29 ($\underline{C}H_2$), 44.73 ($\underline{C}H_2$), 55.51 ($O\underline{C}H_3$), 55.91 ($O\underline{C}H_3$), 60.89 ($O\underline{C}H_3$), 61.59 ($O\underline{C}H_3$), 79.19 ($\underline{C}(CH_3)_3$), 108.81 (Ar$\underline{C}$H), 111.60 (Ar$\underline{C}$H), 120.67 (Ar$\underline{C}$H), 121.36 (Ar$\underline{C}$H), 128.03 (Q$\underline{C}$), 128.57 (C=$\underline{C}$H), 134.617 (Q$\underline{C}$), 136.06 (Q$\underline{C}$), 141.21 (Q$\underline{C}$), 142.16 (Q$\underline{C}$), 144.58 (Q$\underline{C}$), 150.47 (Q$\underline{C}$), 150.78 (Q$\underline{C}$), 151.02 (Q$\underline{C}$), 156.03 ($\underline{C}$=O)

ν_{MAX} (DCM)/cm^{-1}: 3434.50 (NH), 2961.13, 2931.59, 2857.09, 1645.92 (C=O)

HRMS $[M+Na]^+$: calculated 622.3176, found 622.3192, molecular formula ($C_{33}H_{49}NNaO_7Si$)

7.14.7 Removal of BOC protecting group: Synthesis of [(7*R*)-9-{3-[(*tert*-butyldimethylsilyl)oxy]-4-methoxyphenyl}-2,3,4-trimethoxy-6,7-dihydro-5*H*-benzo[7]annulen-7-yl]methanamine (4.21)

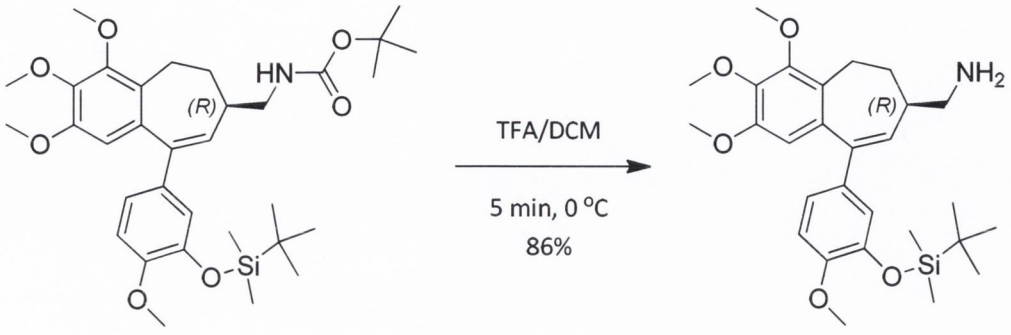

(4.20) **(4.21)**

To stirred solution of **(4.20)** (0.04 g, 0.07 mmol) in dry DCM (0.5 mL) under an atmosphere of nitrogen at 0 °C was added TFA (0.5 mL) dropwise. After 5 min, the volatile organic solvents were removed under reduced pressure and the resulting residue was washed with saturated sodium bicarbonate aqueous solution (5 mL). The aqueous phase was then extracted with diethyl ether (3 x 10 mL). The organic fractions were combined, dried over $MgSO_4$, filtered and concentrated *in vacuo* to afford **(4.21)** as a yellow resin (0.03 g, 86%).

R_f: 0.24 (1:1, ethyl acetate/methanol)

$[\alpha]_D^{25}$ = + 26.67 (*c* = 1.88, DCM)

^{1}H NMR ($CDCl_3$, 400 MHz) δ_H ppm: 0.14 (6H, d, J = 5.19 Hz, Si($C\underline{H}_2$)$_2$), 0.98 (9H, s, C($C\underline{H}_3$)$_3$), 1.27-1.30 (2H, m, $C\underline{H}_2$), 1.80-1.88 (1H, m, $C\underline{H}_2$), 2.12-2.30 (3H, m, 2 x $C\underline{H}_2$, 1 x $C\underline{H}CH_2NH$), 2.87 (2H, s, br, $N\underline{H}_2$), 3.05-3.09 (1H, m, $C\underline{H}_2$), 3.69 (3H, s, $OC\underline{H}_3$), 3.83 (3H, s, $OC\underline{H}_3$), 3.91 (3H, s, $OC\underline{H}_3$), 3.93 (3H, s, $OC\underline{H}_3$), 6.04 (1H, d, J = 5.93 Hz, C=C$\underline{H}$), 6.37 (1H, s, Ar$\underline{H}$), 6.73 (1H, d, J = 2.17 Hz, Ar$\underline{H}$), 6.79 (1H, d, J = 8.37 Hz, Ar$\underline{H}$), 6.93-6.96 (1H, m, Ar$\underline{H}$)

^{13}C NMR ($CDCl_3$, 400 MHz) δ_c ppm: -4.56 (Si($\underline{C}H_3$)$_2$), 23.14 ($\underline{C}H_2$), 25.72 (C($\underline{C}H_3$)$_3$), 29.71 ($\underline{C}H_2$), 30.32 ($\underline{C}$(CH$_3$)$_3$), 39.20 ($\underline{C}H_2$), 55.49 ($O\underline{C}H_3$), 55.88 ($O\underline{C}H_3$), 60.86 ($O\underline{C}H_3$), 61.57 ($O\underline{C}H_3$), 108.86 (Ar$\underline{C}$H), 111.67 (Ar$\underline{C}$H), 120.74 (Ar$\underline{C}$H), 121.33 (Ar$\underline{C}$H), 127.91 ($\underline{Q}C$), 128.04 (C=$\underline{C}$H), 134.53 ($\underline{Q}C$), 136.03 ($\underline{Q}C$), 141.25 ($\underline{Q}C$), 142.62 ($\underline{Q}C$), 144.53 ($\underline{Q}C$), 150.53 ($\underline{Q}C$), 150.74 ($\underline{Q}C$), 151.06 ($\underline{Q}C$)

ν_{MAX} (DCM)/cm^{-1}: 3434.50 (NH), 2930.20, 2855.93, 1678.86, 1570.69

HRMS $[M+H]^+$: calculated 500.2832, found 500.2843, molecular formula ($C_{28}H_{42}NO_5Si$)

7.14.8 Acetylation: Synthesis of *N*-{[(7*R*)-9-{3-[(*tert*-butyldimethylsilyl)oxy]-4-methoxyphenyl}-2,3,4-trimethoxy-6,7-dihydro-5*H*-benzo[7]annulen-7-yl]methyl}acetamide (4.22)

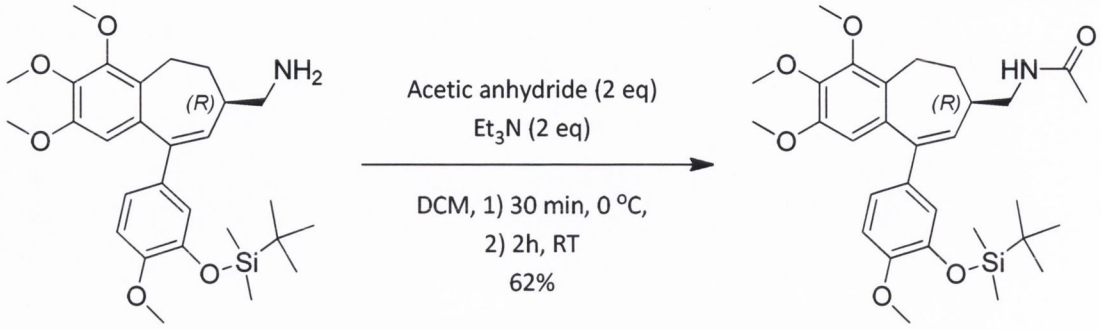

(4.21) **(4.22)**

To a stirred solution of **(4.21)** (0.03 g, 0.06 mmol) in dry DCM (1 mL) under an atmosphere of nitrogen at 0 °C was added acetic anhydride (0.01 mL, 0.12 mmol) and triethylamine (0.02 mL, 0.12 mmol). After 30 min, the temperature of the reaction was allowed to increase to ambient. After a further 2 h, the reaction was quenched by the addition of water (5 mL). The reaction mixture was then extracted with diethyl ether (3 x 5 mL). The organic fractions were combined, dried over $MgSO_4$, filtered and concentrated *in vacuo.* The resulting residue was then purified by flash column chromatography (stationary phase; silica gel 230-400 mesh, mobile phase; ethyl acetate) to afford **(4.22)** as a yellow oil (0.02 g, 62%).

R_f: 0.45 (ethyl acetate)

$[\alpha]_D^{25}$ = + 35.2 (*c* = 0.63, DCM)

^{1}H NMR ($CDCl_3$, 400 MHz) δ_H ppm: 0.16 (6H, d, J = 5.19 Hz, Si($C\underline{H}_2$)$_2$), 0.10 (9H, s, C($C\underline{H}_3$)$_3$), 1.86-1.92 (1H, m, $C\underline{H}_2$), 2.02 (3H, s, CO$C\underline{H}_3$), 2.16-2.24 (2H, m, 1 x $C\underline{H}_2$, 1 x $C\underline{H}CH_2NH$), 2.26-2.35 (1H, m, $C\underline{H}_2$), 3.05-3.10 (1H, m, $C\underline{H}_2$), 3.26-3.32 (1H, m, $C\underline{H}_2$), 3.45-3.50 (1H, m, $C\underline{H}_2$), 3.71 (3H, s, O$C\underline{H}_3$), 3.84 (3H, s, O$C\underline{H}_3$), 3.93 (3H, s, O$C\underline{H}_3$), 3.94 (3H, s, O$C\underline{H}_3$), 5.53 (1H, s, br, N$\underline{H}$), 6.03 (1H, d, J = 6 Hz, C=C$\underline{H}$), 6.38 (1H, s, Ar$\underline{H}$), 6.76 (1H, d, J = 2 Hz, Ar$\underline{H}$), 6.80 (1H, d, J = 8.5 Hz, Ar$\underline{H}$), 6.85 (1H, dd, J_1 = 8.5 Hz, J_2 = 2 Hz, Ar$\underline{H}$)

^{13}C NMR ($CDCl_3$, 400 MHz) δ_c ppm: -4.53 (Si($\underline{C}H_3$)$_2$), 18.47 ($\underline{C}$(CH_3)$_3$), 23.17 ($\underline{C}H_2$), 23.39 (CO$\underline{C}H_3$), 25.74 (C($\underline{C}H_3$)$_3$), 37.38 ($\underline{C}HCH_2NH$), 39.40 ($\underline{C}H_2$), 43.81 ($\underline{C}H_2$), 55.58 (O$\underline{C}H_3$), 55.93 (O$\underline{C}H_3$), 60.89 (O$\underline{C}H_3$), 61.59 (O$\underline{C}H_3$), 108.84 (Ar$\underline{C}H$), 111.67 (Ar$\underline{C}H$), 120.68 (Ar$\underline{C}H$), 121.34 (Ar$\underline{C}H$), 127.97 (Q$\underline{C}$), 128.20 (C=$\underline{C}H$), 134.45 (Q$\underline{C}$), 135.91 (Q$\underline{C}$), 141.29 (Q$\underline{C}$), 142.48 (Q$\underline{C}$), 144.62 (Q$\underline{C}$), 150.58 (Q$\underline{C}$), 150.81 (Q$\underline{C}$), 151.08 (Q$\underline{C}$), 170.16 ($\underline{C}$=O)

ν_{MAX} (DCM)/cm^{-1}: 3412.47 (NH), 298.01, 2854.93, 1649.16 (C=O)

HRMS $[M+H]^+$: calculated 542.2938, found 542.2953, molecular formula ($C_{30}H_{44}NO_6Si$)

7.14.9 Silyl deprotection: Synthesis of *N*-(((*R*,*Z*)-6,7-dihydro-9-(3-hydroxy-4-methoxyphenyl)-2,3,4-trimethoxy-5*H*-benzo[7]annulen-7-yl)methyl)acetamide (4.12)

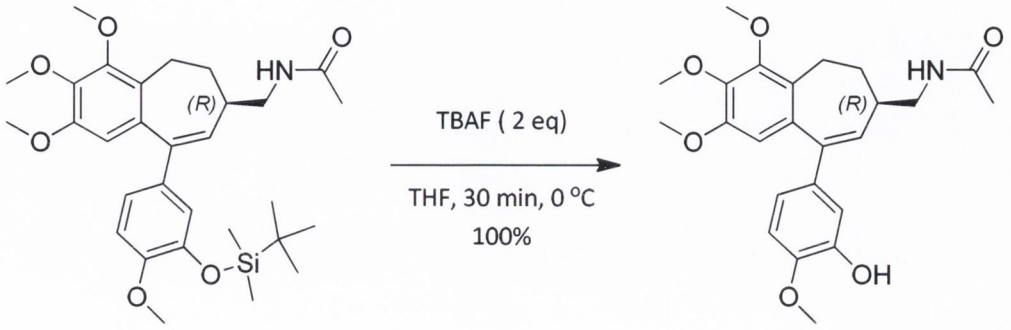

(4.22) **(4.12)**

To a stirred solution of **(4.22)** (0.01 g, 0.02 mmol) in dry THF (1 mL) under an atmosphere of nitrogen at 0 °C was added 1 M TBAF solution in THF (0.04 mL, 0.04 mmol). After 30 min, the THF was blown off in a stream of nitrogen gas and the resulting residue added directly to a silica gel flash column and purified by flash column chromatography (stationary phase; silica gel 230-400 mesh, mobile phase; ethyl acetate) to afford **(4.12)** as a white solid (0.01 g, 100%).

R_f: 0.32 (ethyl acetate)

$[\alpha]_D^{25}$ = + 162 (*c* = 1.11, DCM)

^{1}H NMR ($CDCl_3$, 400 MHz) δ_H ppm: 1.84-1.92 (1H, m, C$\underline{H}_2$), 2.02 (3H, s, COC$\underline{H}_3$), 2.17-2.32 (3H, m, 2 x C$\underline{H}_2$, 1 x C$\underline{H}$CH$_2$NH), 3.05-3.08 (1H, m, C$\underline{H}_2$), 3.29-3.35 (1H, m, C$\underline{H}_2$), 3.40-3.45 (1H, m, C$\underline{H}_2$), 3.72 (3H, s, OC$\underline{H}_3$), 3.92 (3H, s, OC$\underline{H}_3$), 3.93 (3H, s, OC$\underline{H}_3$), 3.95 (3H, s, OC$\underline{H}_3$), 5.54 (1H, s, br, O$\underline{H}$), 6.07 (1H, d, J = 6.01 Hz, C=C$\underline{H}$), 6.39 (1H, s, Ar$\underline{H}$), 6.78 (1H, dd, J_1 = 8.44 Hz, J_2 = 1.86 Hz, Ar$\underline{H}$), 6.82 (1H, d, J = 8.44 Hz, Ar$\underline{H}$), 6.90 (1H, d, J =1.86 Hz, Ar$\underline{H}$)

^{13}C NMR ($CDCl_3$, 400 MHz) δ_c ppm: 23.14 (C$\underline{H}_2$), 23.42 (CO$\underline{C}H_3$), 37.40 (C$\underline{H}$CH$_2$NH), 39.34 (C$\underline{H}_2$), 43.82 (C$\underline{H}_2$), 56.02 (O$\underline{C}H_3$), 56.04 (O$\underline{C}H_3$), 60.89 (O$\underline{C}H_3$), 61.58 (O$\underline{C}H_3$), 108.93 (Ar$\underline{C}$H), 110.33 (Ar$\underline{C}$H), 114.14 (Ar$\underline{C}$H), 119.76 (Ar$\underline{C}$H), 127.99 (Q$\underline{C}$), 128.67 (C=$\underline{C}$H), 135.04 (Q$\underline{C}$), 135.72 (Q$\underline{C}$), 141.36 (Q$\underline{C}$), 142.48 (Q$\underline{C}$), 145.29 (Q$\underline{C}$), 146.18 (Q$\underline{C}$), 150.83 (Q$\underline{C}$), 151.15 (Q$\underline{C}$), 170.26 ($\underline{C}$=O)

ν_{MAX} (DCM)/cm^{-1}: 3349.39, 2923.91, 2851.19, 1652.12 (C=O), 1564.46

HRMS $[M+H]^+$: calculated 428.2073, found 428.2066, molecular formula ($C_{24}H_{30}NO_6$)

Melting point: 85-86 °C

7.15 Synthesis of (R)-enantiomer of C-7 methylene alcohol analogue (R)-5-(7-(hydroxymethyl)-2,3,4-trimethoxy-6,7-dihydro-5H-benzo[7]annulen-9-yl)-2-methoxyphenol

7.15.1 Reduction of nitrile to alcohol: Synthesis of ((7*R*)-6,7,8,9-tetrahydro-1,2,3-trimethoxy-5-(methoxymethoxy)-5*H*-benzo[7]annulen-7-yl)methanol (4.26)

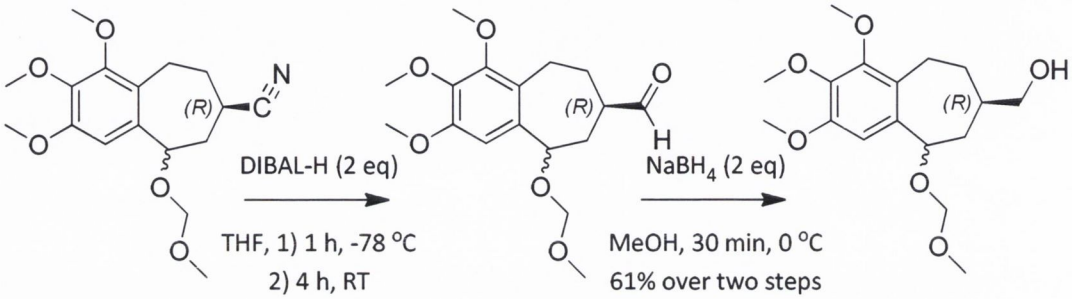

(4.14) **(4.25)** **(4.26)**

To a stirred solution of **(4.14)** (0.08 g, 0.25 mmol) in dry THF (1 mL) under an atmosphere of nitrogen at -78 °C was added 1 M DIBAL-H solution in hexane (0.5 mL, 0.5 mmol) dropwise. After 1 h, the temperature was allowed to increase to ambient. After a further 4 h, the reaction was quenched by the addition of 1 M tartaric acid aqueous solution (5 mL). The reaction mixture was then extracted with diethyl ether (3 x 10 mL). The organic fractions were combined and dried over $MgSO_4$, filtered and concentrated *in vacuo* to yield the aldehyde **(4.25)** as a crude mixture. The aldehyde was dissolved in methanol (5 mL) and the temperature of the reaction reduced to 0 °C. Sodium borohydride (0.02 g, 0.5 mmol) was slowly added to the reaction. After 30 min, the methanol was removed under reduced pressure and the reaction was quenched by the addition of water (5 mL). The reaction was then extracted with diethyl ether (3 x 10 mL). The organic fractions were combined, dried over $MgSO_4$, filtered and concentrated under reduced pressure. The product was purified by flash column chromatography (stationary phase; silica gel 230-400 mesh, mobile phase; 4:1, hexane/ethyl acetate) to yield **(4.26)** as a yellow oil (0.05 g, 61 % over two steps).

R_f: 0.17 (2:1, hexane/ethyl acetate)

^{1}H NMR ($CDCl_3$, 400 MHz) δ_H ppm: 1.49-2.08 (3H, m, 2 x C$\underline{H}_2$, 1 x C$\underline{H}$CH$_2$OH), 2.17-2.36 (2H, m, C$\underline{H}_2$), 2.77-2.89 (1H, m, C$\underline{H}_2$), 3.07-3.17 (1H, m, C$\underline{H}_2$), 3.38 (3H, s, OC$\underline{H}_3$), 3.52 (2H, m, C$\underline{H}_2$OH), 3.80

(3H, s, OC$\underline{H}_3$), 3.85 (3H, s, OC$\underline{H}_3$), 3.88 (3H, s, OC$\underline{H}_3$), 4.58 (2H, s, OC$\underline{H}_2$OCH$_3$), 4.77 (1H, d, J = 6.84 Hz, C$\underline{H}$OCH$_2$), 6.59 (1H, s, Ar$\underline{H}$)

^{13}C NMR ($CDCl_3$, 400 MHz) δ_c ppm: 22.07 ($\underline{C}H_2$), 30.09 ($\underline{C}H_2$), 34.97 ($\underline{C}H_2$), 38.45 ($\underline{C}$HCH$_2$OH), 54.91 (O$\underline{C}$H$_3$), 55.59 (O$\underline{C}$H$_3$), 60.39 (O$\underline{C}$H$_3$), 60.94 (O$\underline{C}$H$_3$), 68.15 ($\underline{C}$H$_2$OH), 76.85 ($\underline{C}$HOCH$_2$), 93.41 (O$\underline{C}$H$_2$OCH$_3$), 108.90 (Ar$\underline{C}$H), 127.96 ($\underline{Q}C$), 135.41 ($\underline{Q}C$), 141.23 ($\underline{Q}C$), 150.02 ($\underline{Q}C$), 150.93 ($\underline{Q}C$)

ν_{MAX} (DCM)/cm^{-1}: 3437.78 (OH), 2930.31, 2852.00, 1720.82, 1599.26

HRMS [M+Na]$^+$: calculated 349.1627, found 349.1633, molecular formula ($C_{17}H_{26}NaO_6$)

7.15.2 Silyl Protection: Synthesis of (((7*R*)-6,7,8,9-tetrahydro-1,2,3-trimethoxy-5-(methoxymethoxy)-5*H*-benzo[7]annulen-7-yl)methoxy)(*tert*-butyl)diphenylsilane (4.27)

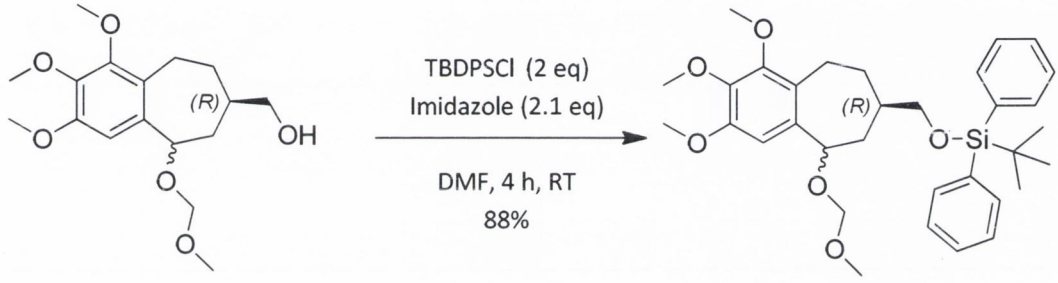

(4.26) **(4.27)**

To a stirred solution of **(4.26)** (0.21 g, 0.64 mmol) and imidazole (0.09 g, 1.35 mmol) in dry DMF (1 mL) under an atmosphere of nitrogen at room temperature was added *tert*-butyldiphenylsilyl chloride (0.33ml, 1.29 mmol). After 4 h, the reaction was quenched by the addition of water (10 mL) and extracted with diethyl ether (3 x 20 mL). The organic fractions were combined, dried over $MgSO_4$, filtered and concentrated under reduced pressure. The product was purified by flash column chromatography (stationary phase; silica gel 230-400 mesh, mobile phase; 20:1, hexane/ethyl acetate) to yield **(4.27)** as a colourless oil (0.32 g, 88%).

R_f: 0.43 (3:1, hexane/ethyl acetate)

^{1}H NMR ($CDCl_3$, 400 MHz) δ_H ppm: 1.12 (9H, s, C(C$\underline{H}_3$)$_3$), 1.46-1.64 (1H, m, C$\underline{H}$CH$_2$OSi), 2.21-2.48 (4H, m, C$\underline{H}_2$), 2.80-2.93 (1H, m, C$\underline{H}_2$), 3.11-3.26 (1H, m, C$\underline{H}_2$), 3.42 (3H, s, OC$\underline{H}_3$), 3.57 (2H, s, C$\underline{H}_2$OSi), 3.85 (3H, s, OC$\underline{H}_3$), 3.90 (3H, s, OC$\underline{H}_3$), 3.94 (3H, s, OC$\underline{H}_3$), 4.64 (2H, s, OC$\underline{H}_2$OCH$_3$), 4.82 (1H, s, C$\underline{H}$OCH$_2$), 6.64 (1H, s, Ar$\underline{H}$), 7.45 (6H, s, Ar$\underline{H}$). 7.73 (4H, s, Ar$\underline{H}$)

^{13}C NMR ($CDCl_3$, 400 MHz) δ_c ppm: 18.89 ($\underline{C}$(CH$_3$)$_3$), 22.30 ($\underline{C}H_2$), 26.45 (C($\underline{C}$H$_3$)$_3$), 30.35 ($\underline{C}H_2$), 35.06 ($\underline{C}H_2$), 38.47 ($\underline{C}$HCH$_2$OSi), 54.85 (O$\underline{C}$H$_3$), 55.59 (O$\underline{C}$H$_3$), 60.42 (O$\underline{C}$H$_3$), 60.95 (O$\underline{C}$H$_3$), 68.90 ($\underline{C}$H$_2$OSi), 77.10 ($\underline{C}$HOCH$_2$), 93.36 (O$\underline{C}$H$_2$OCH$_3$), 109.04 (Ar$\underline{C}$H), 127.19 (4 x Ar$\underline{C}$H), 128.33 ($\underline{Q}C$), 129.13 (2 x

ArCH), 133.42 (4 x QC), 135.20 (4 x ArCH), 135.68 (4 x QC), 141.27 (2 x QC), 149.97 (3 x QC), 151.01 (3 x QC)

ν_{MAX} (DCM)/cm^{-1}: 2930.65, 2856.28, 1598.81, 1494.17

HRMS $[M+Na]^+$: calculated 587.2805, found 587.2816, molecular formula ($C_{33}H_{44}NaO_6Si$)

7.15.3 MOM deprotection and oxidation of alcohol: Synthesis of (7*R*)-7-[(*tert*-butyldiphenylsilyl)oxy]-1,2,3-trimethoxy-6,7,8,9-tetrahydro-5*H*-benzo[7]annulen-5-ol (4.29) and (*R*)-tert-butyldiphenyl((2,3,4-trimethoxy-6,7-dihydro-5*H*-benzo[7]annulen-7-yl)methoxy)silane (4.30)

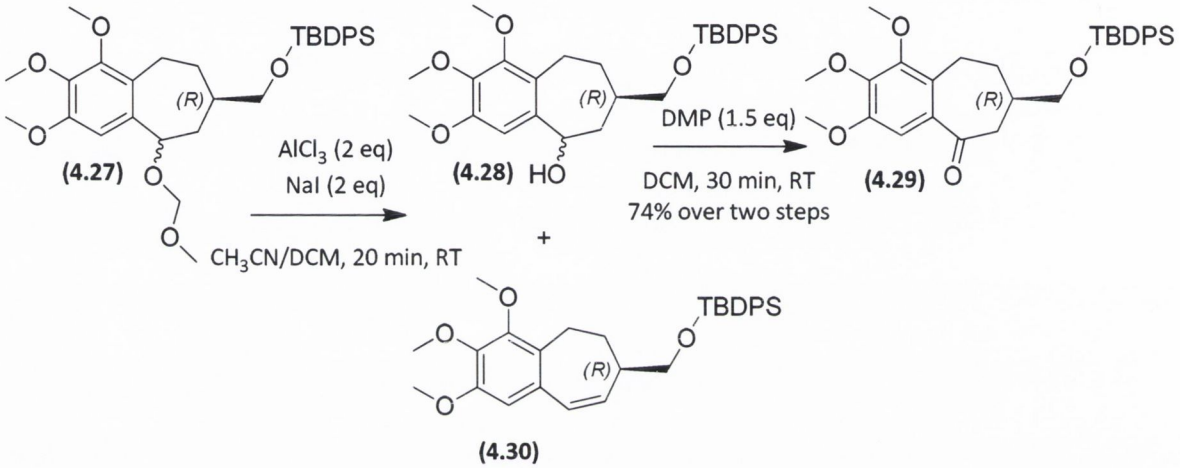

To a stirred solution of **(4.27)** (0.32 g, 0.57mmol) in a mixture of acetonitrile and DCM (2:1, 10 mL) at room temperature was added aluminium chloride (0.15 g, 1.14 mmol) and sodium iodide (0.17 g, 1.14 mmol). After 20 min, the reaction was quenched by the addition of saturated sodium bicarbonate aqueous solution (40 mL). The reaction was then extracted with DCM (3 x 20 mL). To a stirred solution of the combined organic fractions was added Dess-Martin periodinane (0.36 g, 0.85 mmol). After 30 min, the reaction was quenched by the addition of saturated sodium bicarbonate aqueous solution (50 mL) and the reaction was extracted with DCM (3 x 50 mL). The organic fractions were combined, dried over $MgSO_4$, filtered and concentrated under reduced pressure. The products were purified by flash column chromatography (stationary phase; silica gel 230-400 mesh, mobile phase; 10:1, hexane/ethyl acetate) to afford **(4.29)** as a yellow oil (0.22 g, 74% over two steps) and **(4.30)** as a yellow oil (0.07 g, 24%).

(4.29)

R_f: 0.41 (3:1, hexane/ethyl acetate)

$[\alpha]_D^{25}$ = - 2.45 (*c* = 7.33, DCM)

^{1}H NMR ($CDCl_3$, 400 MHz) δ_H ppm: 1.11 (9H, s, C(CH_3)$_3$), 1.70-1.81 (1H, m, CH_2), 1.85-1.98 (1H, m, CH_2), 2.11-2.29 (1H, m, $CHCH_2OSi$), 2.71-2.87 (2H, m, CH_2), 2.92 (1H, d, J = 14.7 Hz, CH_2), 3.19 (1H, d, J = 14.7 Hz, CH_2), 3.60-3.68 (1H, m, CH_2), 3.77-3.85 (1H, m, CH_2), 3.87 (3H, s, OCH_3), 3.92 (3H, s, OCH_3), 3.98 (3H, s, OCH_3), 7.22 (1H, s, ArH), 7.35-7.53 (6H, s, ArH), 7.65-7.81 (4H, s, ArH)

^{13}C NMR ($CDCl_3$, 400 MHz) δ_c ppm: 18.86 (C(CH_3)$_3$), 21.87 (CH_2), 26.43 (C(CH_3)$_3$), 28.06 (CH_2), 35.54 ($CHCH_2OSi$), 43.60 (CH_2), 55.54 (OCH_3), 60.46 (OCH_3), 60.90 (OCH_3), 66.68 ($CHCH_2OSi$), 107.03 (ArCH), 127.28 (4 x ArCH), 129.26 (2 x ArCH), 133.02 (4 x QC), 133.09 (4 x QC), 133.37 (2 x QC), 133.77 (QC), 134.89 (QC), 135.15 (2 x ArCH), 135.17 (2 x ArCH), 141.04 (QC), 145.38 (QC), 150.52 (QC), 151.10 (QC), 202.75 (C=O)

ν_{MAX} (DCM)/cm^{-1}: 2931.54, 2856.81, 1672.13 (C=O), 1589.32

HRMS $[M+Na]^+$: calculated 541.2386, found 541.2339, molecular formula ($C_{31}H_{38}NaO_5Si$)

(4.30)

R_f: 0.52 (3:1, hexane/ethyl acetate)

$[\alpha]_D^{25}$ = + 68.35 (*c* = 7.67, DCM)

^{1}H NMR ($CDCl_3$, 400 MHz) δ_H ppm: 1.10 (9H, s, C(CH_3)$_3$), 1.82-1.85 (1H, m, CH_2), 2.06-2.13 (1H, m, CH_2), 2.71-2.79 (2H, m, 1 x CH_2, 1 x $CHCH_2OSi$), 2.84-2.90 (1H, m, CH_2), 3.59-3.70 (2H, m, CH_2), 3.84 (3H, s, OCH_3), 3.86 (3H, s, OCH_3), 3.91 (3H, s, OCH_3), 5.85 (1H, dd, J_1 = 12 Hz, J_2 = 3.28 Hz, CH=CH), 6.37 (1H, d, J = 12 Hz, CH=CH), 6.54 (1H, s, ArH), 7.40-7.43 (6H, m, ArH), 6.70-7.76 (4H, m, ArH)

^{13}C NMR ($CDCl_3$, 400 MHz) δ_c ppm: 18.88 (C(CH_3)$_3$), 22.79 (CH_2), 26.11 (C(CH_3)$_3$), 30.03 (CH_2), 44.13 ($CHCH_2OSi$), 55.51 (OCH_3), 60.53 (OCH_3), 60.86 (OCH_3), 66.85 (CH_2), 109.67 (ArCH), 127.61 (2 x ArCH), 127.98 (ArCH), 129.16 (2 x ArCH), 129.22 (ArCH), 129.50 (CH=CH), 131.88 (QC), 132.40 (CH=CH), 133.29 (QC), 133.33 (QC), 134.37 (2 x ArCH), 134.72 (QC), 135.59 (2 x ArCH), 140.72 (QC), 150.27 (QC), 150.29 (QC)

ν_{MAX} (DCM)/cm^{-1}: 2957.87, 2857.26, 1591.30, 1569.43

HRMS $[M+Na]^+$: calculated 525.2437, found 525.2438, molecular formula ($C_{31}H_{38}NaO_4Si$)

7.15.4 Preparation of Triflate: Synthesis of (7*R*)-7-{[(*tert*-butyldiphenylsilyl)oxy]methyl}-2,3,4-trimethoxy-6,7-dihydro-5*H*-benzo[7]annulen-9-yl trifluoromethanesulfonate (4.31)

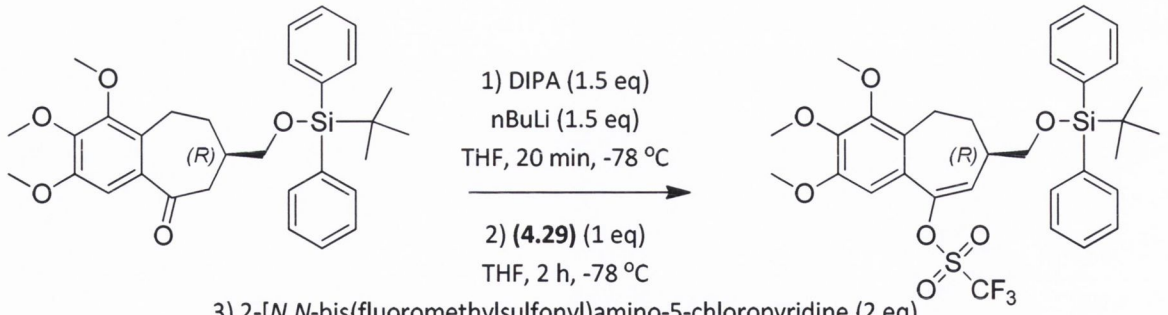

(4.29) **(4.31)**

To a stirred solution of diisopropylamine (0.06 mL, 0.61 mmol) in dry THF (10 mL) at -78 °C under an atmosphere of nitrogen was added 2.5 M *n*-butyllithium solution in hexane (0.24 mL, 0.61 mmol) dropwise. After 20 min, a solution of **(4.29)** (0.21 g, 0.40 mmol) in dry THF (8 mL) was added dropwise. The solution was stirred at -78 °C for 2 h and then a solution of 2-[*N,N*-bis(fluoromethylsulfonyl)amino]-5-chloropyridine (0.32 g, 0.81 mmol) in dry THF (8 mL) was added. The solution was stirred at -78 °C for a further 3 h after which time the reaction was quenched by the addition of saturated sodium chloride aqueous solution (50 mL). The reaction mixture was extracted with diethyl ether (3 x 25 mL). The organic fractions were combined, dried over $MgSO_4$, filtered and concentrated *in vacuo.* The resulting residue was then purified by flash column chromatography (stationary phase; silica gel 230-400 mesh, mobile phase; 10:1, hexane/ethyl acetate) to afford **(4.31)** as a yellow oil (0.15 g, 58%).

R_f: 0.67 (3:1, hexane/ethyl acetate)

$[\alpha]_D^{25}$ = + 46.64 (*c* = 6.82, DCM)

^{1}H NMR ($CDCl_3$, 400 MHz) δ_H ppm: 1.11 (9H, s, C(C$\underline{H}_3$)$_3$), 1.97-2.00 (1H, m, C$\underline{H}_2$), 2.09-2.11 (1H, m, C$\underline{H}_2$), 2.43-2.49 (1H, m, C$\underline{H}$CH$_2$OSi), 2.58-2.63 (1H, m, C$\underline{H}_2$), 2.96-2.99 (1H, m, C$\underline{H}_2$), 3.64-3.72 (2H, m, C$\underline{H}_2$), 3.87 (3H, s, OC$\underline{H}_3$), 3.91 (3H, s, OC$\underline{H}_3$), 3.97 (3H, s, OC$\underline{H}_3$), 6.24 (1H, d, J = 5.08 Hz, C=C$\underline{H}$), 6.88 (1H, s, Ar$\underline{H}$), 7.43-7.44 (6H, m, Ar$\underline{H}$), 7.68-7.70 (4H, m, Ar$\underline{H}$)

^{13}C NMR ($CDCl_3$, 400 MHz) δ_c ppm: 18.81 (C(CH$_3$)$_3$), 22.49 (C$\underline{H}_2$), 26.35 (C(C$\underline{H}_3$)$_3$), 34.38 (C$\underline{H}_2$), 39.01 (C$\underline{H}$CH$_2$OSi), 55.54 (OC$\underline{H}_3$), 60.49 (OC$\underline{H}_3$), 61.09 (OC$\underline{H}_3$), 65.62 (C$\underline{H}_2$), 105.36 (ArC$\underline{H}$), 124.20 (C=C$\underline{H}$), 127.31 (Q$\underline{C}$), 127.53 (4 x ArC$\underline{H}$), 128.13 (Q$\underline{C}$), 129.35 (2 x ArC$\underline{H}$), 132.84 (Q$\underline{C}$), 132.88 (Q$\underline{C}$), 135.14 (4 x ArC$\underline{H}$), 142.84 (Q$\underline{C}$), 144.90 (Q$\underline{C}$), 150.61 (Q$\underline{C}$), 151.21 (Q$\underline{C}$)

^{19}F NMR ($CDCl_3$, 400 MHz) δ_F ppm: -74.47 (3F, s, C$\underline{F}_3$)

ν_{MAX} (DCM)/cm^{-1}: 2930.84, 2855.07, 1592.61, 1566.09, 1417.19

HRMS $[M+H]^+$: calculated 651.206, found 651.2067, molecular formula ($C_{32}H_{38}F_3O_7SSi$)

7.15.5 Suzuki Coupling: Synthesis of *tert*-butyl(5-[{7*R*)-7-{[(*tert*-butyldiphenylsilyl)oxy]methyl}-2,3,4-trimethoxy-6,7-dihydro-5*H*-benzo[7]annulen-9-yl]-2-methoxyphenoxy)dimethylsilane (4.32)

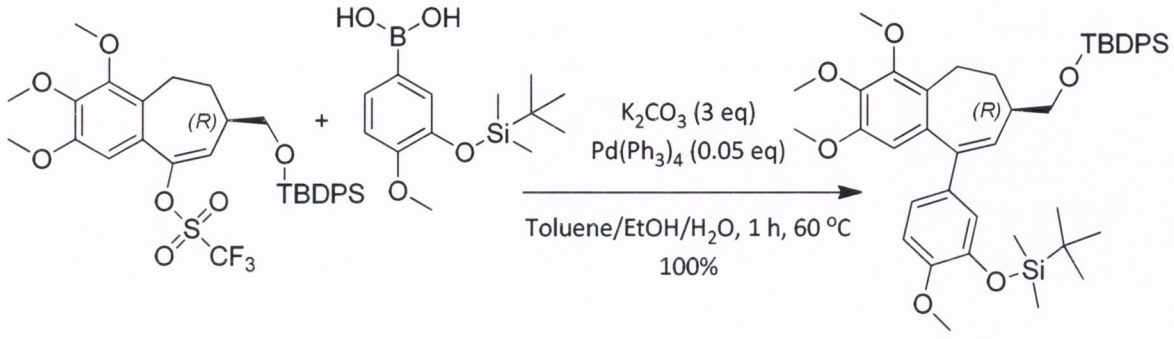

(4.31) **(4.08)** **(4.32)**

To a stirred solution of **(4.31)** (0.14 g, 0.22 mmol) in a mixture of toluene, ethanol and water (5 mL; 3: 1: 1) was added potassium carbonate (0.09 g, 0.65 mmol), (tetrakis(triphenyl)phosphine) palladium (0.01 g, 0.01 mmol) and **(4.08)** (0.07 g, 0.26 mmol). The reaction was heated under reflux at 60 °C for 1 h after which time it was quenched by the addition of water (50 mL). The reaction mixture was extracted with diethyl ether (3 x 50 mL). The organic fractions were combined, dried over $MgSO_4$, filtered and concentrated *in vacuo.* The resulting residue was then purified by flash column chromatography (stationary phase; silica gel 230-400 mesh, mobile phase; 10:1, hexane/ethyl acetate) to yield **(4.32)** as a yellow oil (0.17 g, 100%).

R_f: 0.76 (3:1, hexane/ethyl acetate)

$[\alpha]_D^{25}$ = + 40 (*c* = 8.5, DCM)

^{1}H NMR ($CDCl_3$, 400 MHz) δ_H ppm: 0.20 (6H, d, J = 5.61 Hz, Si(C$\underline{H}_3$)$_2$), 1.04 (9H, s, C(C$\underline{H}_3$)$_3$), 1.12 (9H, s, C(C$\underline{H}_3$)$_3$), 2.00-2.02 (1H, m, C$\underline{H}_2$), 2.15-2.18 (1H, m, C$\underline{H}_2$), 2.25-2.34 (2H, m, 1 x C$\underline{H}_2$, 1 x C$\underline{H}$CH$_2$OSi), 3.08-3.12 (1H, m, C$\underline{H}_2$), 3.75-3.78 (5H, m, 1 x OC$\underline{H}_3$), 1 x C$\underline{H}_2$), 3.87 (3H, s, OC$\underline{H}_3$), 3.95 (3H, s, OC$\underline{H}_3$), 3.98 (3H, s, OC$\underline{H}_3$), 6.29 (1H, d, J = 5.95 Hz, C=C$\underline{H}$), 6.44 (1H, s, Ar$\underline{H}$), 6.92-6.88 (3H, m, Ar$\underline{H}$), 7.39-7.47 (6H, m, Ar$\underline{H}$), 7.71-7.74 (4H, m, Ar$\underline{H}$)

^{13}C NMR ($CDCl_3$, 400 MHz) δ_c ppm: -4.97 (Si($\underline{C}H_3$)$_2$), -4.93 (Si($\underline{C}H_3$)$_2$), 18.03 ($\underline{C}$(CH$_3$)$_3$), 18.89 ($\underline{C}$(CH$_3$)$_3$), 22.87 ($\underline{C}$H$_2$), 25.33 (C($\underline{C}$H$_3$)$_3$), 26.13 (C($\underline{C}$H$_3$)$_3$), 37.60 ($\underline{C}$H$_2$), 39.27 ($\underline{C}$HCH$_2$OSi), 55.10 (O$\underline{C}$H$_3$), 55.48 (O$\underline{C}$H$_3$), 60.48 (O$\underline{C}$H$_3$), 61.17 (O$\underline{C}$H$_3$), 66.37 ($\underline{C}$H$_2$), 108.44 (Ar$\underline{C}$H), 111.19 (Ar$\underline{C}$H), 120.22 (Ar$\underline{C}$H), 121.03 (Ar$\underline{C}$H), 127.20 (2 x Ar$\underline{C}$H), 127.23 (2 x Ar$\underline{C}$H), 127.89 ($\underline{Q}$C), 128.89 (C=$\underline{C}$H), 129.14 (Ar$\underline{C}$H), 129.16 (Ar$\underline{C}$H), 133.32 ($\underline{Q}$C), 133.34 ($\underline{Q}$C), 134.71 ($\underline{Q}$C), 135.20 (4 x Ar$\underline{C}$H), 136.03 ($\underline{Q}$C), 140.54 ($\underline{Q}$C), 140.58 ($\underline{Q}$C), 144.15 ($\underline{Q}$C), 149.87 ($\underline{Q}$C), 150.31 ($\underline{Q}$C), 150.46 ($\underline{Q}$C)

ν_{MAX} (DCM)/cm^{-1}: 2931.19, 2857.14, 1595.87, 1571.08, 1508.50

HRMS $[M+Na]^+$: calculated 761.367, found 761.3615, molecular formula ($C_{44}H_{58}NaO_6Si_2$)

5.15.6 Removal of silyl protecting groups: Synthesis of 5-((*R*,*Z*)-6,7-dihydro-7-(hydroxymethyl)-2,3,4-trimethoxy-5*H*-benzo[7]annulen-9-yl)-2-methoxyphenol (4.23)

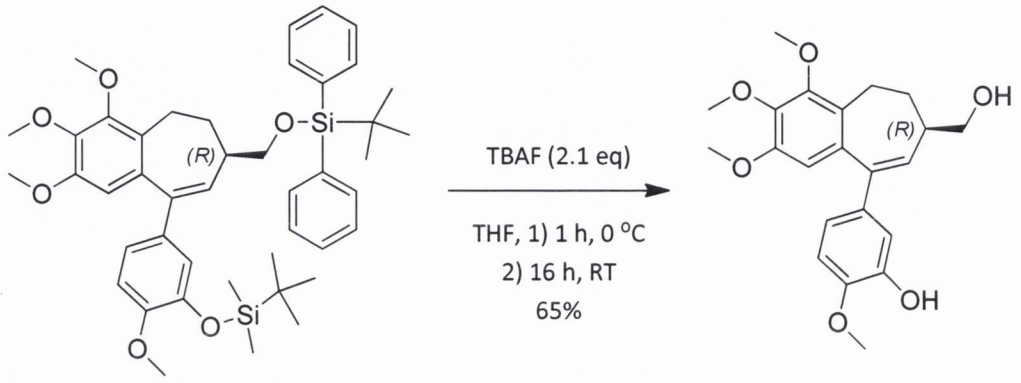

(4.32) **(4.23)**

To a stirred solution of **(4.32)** (0.15 g, 0.20 mmol) in dry THF (5 mL) under an atmosphere of nitrogen at 0 °C was added 1 M TBAF solution in THF (0.43 mL, 0.43 mmol). After 1 h, the temperature was allowed to increase to ambient. After a further 16 h, the THF was removed by blowing with a stream of nitrogen gas and the resulting residue was added directly to a silica gel flash column and purified by flash column chromatography (stationary phase; silica gel 230-400 mesh, mobile phase; 1:1, hexane/ethyl acetate) to afford **(4.23)** as a white solid (0.05 g, 65%).

R_f: 0.28 (1:1, hexane/ethyl acetate)

$[\alpha]_D^{25}$ = + 102.4 (*c* = 3.13, DCM)

^{1}H NMR ($CDCl_3$, 400 MHz) δ_H ppm: 1.88-1.92 (1H, m, C$\underline{H}_2$), 2.16-2.29 (3H, m, 2 x C$\underline{H}_2$, 1 x C$\underline{H}$CH$_2$OH), 3.05-3.10 (1H, m, C$\underline{H}_2$), 3.63-3.70 (5H, m, 1 x C$\underline{H}_2$, 1 x OC$\underline{H}_3$), 3.91 (3H, s, OC$\underline{H}_3$), 3.92 (3H, s, OC$\underline{H}_3$), 3.93 (3H, s, OC$\underline{H}_3$), 5.72 (1H, s, br, O$\underline{H}$), 6.18 (1H, d, J = 6.09 Hz, C=C$\underline{H}$), 6.40 (1H, s, Ar$\underline{H}$), 6.77-6.81 (2H, m, Ar$\underline{H}$), 6.93 (1H, s, Ar$\underline{H}$)

^{13}C NMR ($CDCl_3$, 400 MHz) δ_c ppm: 22.67 (C$\underline{H}_2$), 37.38 (C$\underline{H}_2$), 39.45 (C$\underline{H}$CH$_2$OH), 55.55 (2 x OC$\underline{H}_3$), 60.44 (OC$\underline{H}_3$), 61.14 (OC$\underline{H}_3$), 65.91 (C$\underline{H}_2$), 108.44 (Ar$\underline{C}$H), 109.84 (Ar$\underline{C}$H), 113.80 (Ar$\underline{C}$H), 119.27 (Ar$\underline{C}$H), 127.66 (Q$\underline{C}$), 128.37 (C=$\underline{C}$H), 134.87 (Q$\underline{C}$), 135.58 (Q$\underline{C}$), 140.72 (Q$\underline{C}$), 141.49 (Q$\underline{C}$), 144.79 (Q$\underline{C}$), 145.62 (Q$\underline{C}$), 150.31 (Q$\underline{C}$), 150.57 (Q$\underline{C}$)

ν_{MAX} (DCM)/cm^{-1}: 3420.98 (OH), 2933.63, 2851.31, 1580.94

HRMS $[M+H]^+$: calculated 387.1808, found 387.1834, molecular formula ($C_{22}H_{27}O_6$)

Melting point: 91-93 °C

7.16 Synthesis of (S)-enantiomer of C-7 methylene alcohol analogue (S)-5-(7-(hydroxymethyl)-2,3,4-trimethoxy-6,7-dihydro-5H-benzo[7]annulen-9-yl)-2-methoxyphenol (4.24)

7.16.1 Nitrile Synthesis: Synthesis of (7*S*)-6,7,8,9-tetrahydro-1,2,3-trimethoxy-5-(methoxymethoxy)-5*H*-benzo[7]annulene-7-carbonitrile (4.35)

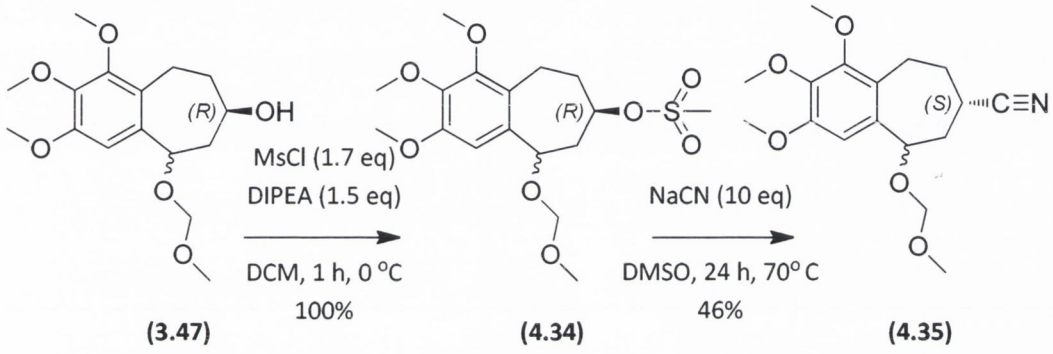

To a stirred solution of **(3.47)** (2.22 g, 7.11 mmol) in dry DCM (10 mL) under an atmosphere of nitrogen at 0 °C was added methanesulfonyl chloride (0.94 mL, 12.08 mmol) followed by *N,N*-diisopropylethylamine (1.86 mL, 10.66 mmol). After 1 h, the reaction was quenched by the addition of water (20 mL). The reaction mixture was extracted with diethyl ether (3 x 25 mL). The organic fractions were combined and dried over $MgSO_4$, filtered and concentrated *in vacuo* to afford the mesylate **(4.34)** as a crude mixture. The mesylate was dissolved in DMSO (10 mL) at room temperature and sodium cyanide (3.48 g, 71.07 mmol) was added to the solution. The reaction was then refluxed at 70 °C for 24 h. The reaction was then quenched by the addition of water (30 mL) and extracted with diethyl ether (3 x 30 mL). The organic fractions were combined, dried over $MgSO_4$, filtered and concentrated under reduced pressure. The product was purified by flash column chromatography (stationary phase; silica gel 230-400 mesh, mobile phase; 4:1, hexane/ethyl acetate) to afford **(4.35)** as a white oil (1.04 g, 46% over two steps).

R_f: 0.24 (3:1, hexane/ethyl acetate)

^{1}H NMR ($CDCl_3$, 400 MHz) δ_H ppm: 1.65-1.77 (2H, m, major and minor diastereomers, C$\underline{H}_2$), 2.02-2.08 (2H, m, major and minor diastereomers, C$\underline{H}_2$), 2.17-2.21 (2H, m, major and minor

diastereomers, C$\underline{H}_2$), 2.30-2.47 (3H, m, major and minor diastereomers, C$\underline{H}_2$), 2.84-2.90 (1H, m, major diastereomer, C$\underline{H}_2$), 3.01-3.14 (2H, m, major and minor diastereomers, 1 x C$\underline{H}$CN, 1 x C$\underline{H}_2$), 3.34-3.39 (5H, m, major and minor diastereomers, 1 x C$\underline{H}$CN, 1x C$\underline{H}_2$, 1 x OC$\underline{H}_3$), 3.44 (3H, s, minor diastereomer, OC$\underline{H}_3$), 3.81 (3H, s, major diastereomer, OC$\underline{H}_3$), 3.82 (3H, s, minor diastereomer, OC$\underline{H}_3$), 3.86 (3H, s, major diastereomer, OC$\underline{H}_3$), 3.87 (3H, s, minor diastereomer, OC$\underline{H}_3$), 3.88 (3H, s, major diastereomer, OC$\underline{H}_3$), 3.89 (3H, s, minor diastereomer, OC$\underline{H}_3$), 4.56 (2H, s, major diastereomer, OC$\underline{H}_2$OCH$_3$), 4.67-4.61 (4H, s, major and minor diastereomers, 1 x OC$\underline{H}_2$OCH$_3$, 2 x C$\underline{H}$OCH$_2$), 6.62 (1H, s, major diastereomer, Ar$\underline{H}$), 6.83 (1H, s, minor diastereomer, Ar$\underline{H}$)

^{13}C NMR ($CDCl_3$, 400 MHz) δ_c ppm: 22.27 (C$\underline{H}_2$), 22.51 (C$\underline{H}_2$), 28.17 (C$\underline{H}$CN), 30.42 (C$\underline{H}$CN), 30.57 (C$\underline{H}_2$), 31.15 (C$\underline{H}_2$), 36.12 (C$\underline{H}_2$), 36.94 (C$\underline{H}_2$), 55.59 (OC$\underline{H}_3$), 55.82 (OC$\underline{H}_3$), 56.06 (2 x OC$\underline{H}_3$), 60.83 (2 x OC$\underline{H}_3$), 61.41 (2 x OC$\underline{H}_3$), 74.62 (C$\underline{H}$OCH$_2$), 75.42 (C$\underline{H}$OCH$_2$), 93.93 (OC$\underline{H}_2$OCH$_3$), 94.72 (OC$\underline{H}_2$OCH$_3$), 105.11 (ArC$\underline{H}$), 108.78 (ArC$\underline{H}$), 121.93 (Q$\underline{C}$), 122.66 (Q$\underline{C}$), 124.54 (Q$\underline{C}$), 126.52 (Q$\underline{C}$), 135.15 (Q$\underline{C}$), 136.83 (Q$\underline{C}$), 141.30 (Q$\underline{C}$), 141.89 (Q$\underline{C}$), 151.09 (Q$\underline{C}$), 151.18 (Q$\underline{C}$), 151.54 (Q$\underline{C}$), 151.63 (Q$\underline{C}$)

ν_{MAX} (DCM)/cm^{-1}: 3535.26, 2936.73, 2837.44, 2238.08 (CN), 1599.54

HRMS $[M+Na]^+$: calculated 344.1474, found 344.1485, molecular formula ($C_{17}H_{23}NNaO_5$)

7.16.2 Reduction of nitrile to alcohol: Synthesis of ((7*S*)-6,7,8,9-tetrahydro-1,2,3-trimethoxy-5-(methoxymethoxy)-5*H*-benzo[7]annulen-7-yl)methanol (4.37)

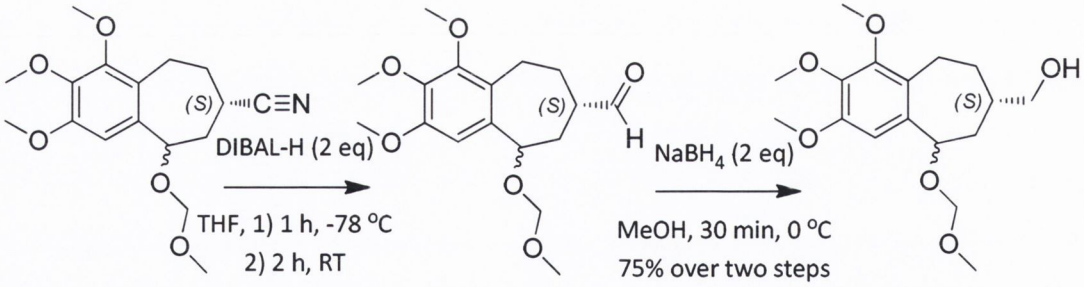

(4.35) **(4.36)** **(4.37)**

To a stirred solution of **(4.35)** (1.1 g, 3.42 mmol) in dry THF (10 mL) under an atmosphere of nitrogen at -78 °C was added 1 M DIBAL-H solution in hexane (6.85 mL, 6.85 mmol) dropwise. After 1 h, the temperature was allowed to increase to ambient. After a further 2 h the reaction was quenched by the addition of 1 M tartaric acid aqueous solution (50 mL). The reaction mixture was then extracted with diethyl ether (3 x 75 mL). The organic fractions were combined, dried over $MgSO_4$, filtered and concentrated *in vacuo* to afford the aldehyde intermediate **(4.36)** as a

crude mixture. The aldehyde was dissolved in methanol (10 mL) and the temperature of the reaction reduced to 0 °C. Sodium borohydride (0.26 g, 6.85 mmol) was slowly added to the reaction. After 30 min the methanol was removed under reduced pressure and the reaction was quenched by the addition of water (50 mL). The reaction was then extracted with diethyl ether (3 x 75 mL). The organic fractions were combined, dried over $MgSO_4$, filtered and concentrated under reduced pressure. The product was purified by flash column chromatography (stationary phase; silica gel 230-400 mesh, mobile phase; 4:1, hexane/ethyl acetate) to yield **(4.37)** as a white oil (0.84 g, 75 % over two steps).

R_f: 0.17 (2:1, hexane/ethyl acetate)

^{1}H NMR ($CDCl_3$, 400 MHz) δ_H ppm: 0.87-0.97 (1H, m, minor diastereomer, C$\underline{H}_2$), 1.12-1.41 (2H, m, minor diastereomer, C$\underline{H}_2$), 1.49-1.56 (1H, m, major diastereomer, C$\underline{H}_2$), 1.76 (2H, s, br, O$\underline{H}$), 2.02-2.06 (3H, m, major and minor diastereomers, 1 x C$\underline{H}_2$, 1 x C$\underline{H}$CH$_2$OH), 2.19-2.32 (4H, m, major and minor diastereomers, 3 x C$\underline{H}_2$, 1 x C$\underline{H}$CH$_2$OH), 2.79-2.84 (1H, m, major diastereomer, C$\underline{H}_2$), 3.08-3.13 (1H, m, major diastereomer, C$\underline{H}_2$), 3.32-3.38 (4H, m, major and minor diastereomers, 1 x C$\underline{H}_2$, 1 x OC$\underline{H}_3$), 3.44 (3H, s, minor diastereomer, OC$\underline{H}_3$), 3.46-3.55 (4H, m, major and minor diastereomers, C$\underline{H}_2$OH), 3.80 (3H, s, major diastereomer, OC$\underline{H}_3$), 3.85 (3H, s, minor diastereomer, OC$\underline{H}_3$), 3.88 (9H, s, major and minor diastereomers, OC$\underline{H}_3$), 4.58 (2H, s, major diastereomer, OC$\underline{H}_2$OCH$_3$), 4.70-4.83 (4H, m, major and minor diastereomers, 1 x C$\underline{H}_2$, 2 x C$\underline{H}$OCH$_2$) 6.59 (1H, s, major diastereomer, Ar$\underline{H}$), 6.93 (1H, s, minor diastereomer, Ar$\underline{H}$)

^{13}C NMR ($CDCl_3$, 400 MHz) δ_c ppm: 22.53 (C$\underline{H}_2$), 23.22 (C$\underline{H}_2$), 30.06 (C$\underline{H}_2$), 30.56 (C$\underline{H}_2$), 35.44 (C$\underline{H}_2$), 38.27 (C$\underline{H}_2$), 38.90 (C$\underline{H}$CH$_2$OH), 43.38 (C$\underline{H}$CH$_2$OH), 55.37 (OC$\underline{H}_3$), 55.71 (OC$\underline{H}_3$), 56.01 (OC$\underline{H}_3$), 56.05 (OC$\underline{H}_3$), 60.85 (2 x OC$\underline{H}_3$), 61.40 (2 x OC$\underline{H}_3$), 68.29 (C$\underline{H}_2$), 68.58 (C$\underline{H}_2$), 75.33 (C$\underline{H}$OCH$_2$), 77.40 (C$\underline{H}$OCH$_2$), 93.87 (C$\underline{H}_2$), 94.93 (C$\underline{H}_2$), 103.59 (Ar$\underline{C}$H), 109.38 (Ar$\underline{C}$H), 125.72 (Q$\underline{C}$), 128.42 (Q$\underline{C}$), 135.88 (Q$\underline{C}$), 138.79 (Q$\underline{C}$), 140.66 (Q$\underline{C}$), 141.69 (Q$\underline{C}$), 150.48 (Q$\underline{C}$), 150.85 (Q$\underline{C}$), 151.24 (Q$\underline{C}$), 151.38 (Q$\underline{C}$)

ν_{MAX} (DCM)/cm^{-1}: 3437.78 (OH),2930.31, 2852.00, 1720.82, 1588.26

HRMS $[M+Na]^+$: calculated 349.1627, found 349.1631, molecular formula ($C_{17}H_{26}NaO_6$)

7.16.3 Silyl Protection: Synthesis of (((7*R*)-6,7,8,9-tetrahydro-1,2,3-trimethoxy-5-(methoxymethoxy)-5*H*-benzo[7]annulen-7-yl)methoxy)(*tert*-butyl)diphenylsilane (4.38)

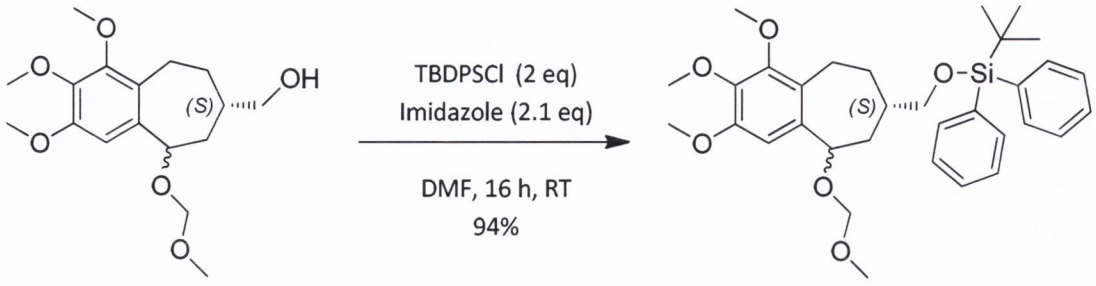

(4.37) **(4.38)**

To a stirred solution of **(4.37)** (0.45 g, 1.38 mmol) and imidazole (0.20 g, 2.90 mmol) in dry DMF (1 mL) under an atmosphere of nitrogen at room temperature was added *tert*-butyldiphenylsilyl chloride (0.72 ml, 2.76 mmol). After 16 h, the reaction was quenched by the addition of water (10 mL) and extracted with diethyl ether (3 x 20 mL). The organic fractions were combined, dried over $MgSO_4$, filtered and concentrated under reduced pressure. The product was purified by flash column chromatography (stationary phase; silica gel 230-400 mesh, mobile phase; 20:1, hexane/ethyl acetate) to afford **(4.38)** as a colourless oil (0.73 g, 94%).

R_f: 0.43 (3:1, hexane/ethyl acetate)

^{1}H NMR ($CDCl_3$, 400 MHz) δ_H ppm: 0.87-0.93 (1H, m, major diastereomer, C$\underline{H}_2$), , 1.09 (18H, s, C(C$\underline{H}_3$)$_3$), 1.14-1.25 (1H, m, minor diastereomer, C$\underline{H}_2$), 1.28-1.41 (1H, m, minor diastereomer, C$\underline{H}_2$), 1.50-1.56 (1H, m, major diastereomer, C$\underline{H}_2$), 2.03-2.11 (3H, m, major and minor diastereomers, 2 x C$\underline{H}_2$, 1 x C$\underline{H}$CH$_2$), 2.26-2.38 (4H, m, major and minor diastereomers, 3 x C$\underline{H}_2$, 1 x C$\underline{H}$CH$_2$), 2.83-2.86 (1H, m, major diastereomer, C$\underline{H}_2$), 3.11-3.17 (1H, m, major diastereomer, C$\underline{H}_2$), 3.34-3.40 (1H, m, minor diastereomer, C$\underline{H}_2$), 3.41 (3H, s, major diastereomer, OC$\underline{H}_3$), 3.43-3.47 (2H, m, minor diastereomer, C$\underline{H}_2$), 3.48 (3H, s, minor diastereomer, OC$\underline{H}_3$), 3.51-3.54 (3H, m, major and minor diastereomers, 2 x C$\underline{H}_2$), 3.82 (3H, s, major diastereomer, OC$\underline{H}_3$), 3.83 (3H, s, minor diastereomer, OC$\underline{H}_3$), 3.88 (3H, s, major diastereomer, OC$\underline{H}_3$), 3.91 (3H, s, minor diastereomer, OC$\underline{H}_3$), 3.92 (9H, s, minor and major diastereomers, OC$\underline{H}_3$), 4.60-4.64 (2H, m, major diastereomer, OC$\underline{H}_2$OCH$_3$), 4.75-4.87 (4H, m, major and minor diastereomers, 1 x OC$\underline{H}_2$OCH$_3$, 2 x CHOC$\underline{H}_2$), 6.61 (1H, s, major diastereomer, Ar$\underline{H}$), 6.97 (1H, s, minor diastereomer, Ar$\underline{H}$), 7.39-7.47 (12H, m, major and minor diastereomers, Ar$\underline{H}$), (1H, s, major diastereomer, Ar$\underline{H}$), 7.70-7.71 (8H, m, major and minor diastereomers, Ar$\underline{H}$)

^{13}C NMR ($CDCl_3$, 400 MHz) δ_c ppm: 19.30 ($\underline{C}(CH_3)_3$), 19.34 ($\underline{C}(CH_3)_3$), 22.73 ($\underline{CH_2}$), 23.43 ($\underline{CH_2}$), 26.87 ($C(\underline{CH_3})_3$), 26.90 ($C(\underline{CH_3})_3$), 30.08 ($\underline{CH_2}$), 30.78 ($\underline{CH_2}$), 35.50 ($\underline{CH_2}$), 38.53 ($\underline{CH_2}$), 38.90 ($\underline{CH}$), 43.69 ($\underline{CH}$), 55.31 ($O\underline{CH_3}$), 55.65 ($O\underline{CH_3}$), 56.01 ($O\underline{CH_3}$), 56.06 ($O\underline{CH_3}$), 60.89 ($O\underline{CH_3}$), 60.90 ($O\underline{CH_3}$), 61.41 (2 x $O\underline{CH_3}$), 68.89 ($\underline{CH_2}$), 69.34 ($\underline{CH_2}$), 75.43 ($\underline{CH}$), 76.77 ($\underline{CH}$), 93.83 ($\underline{CH_2}$), 94.93 ($\underline{CH_2}$), 103.42 (4 x Ar$\underline{CH}$), 109.49 (4 x Ar$\underline{CH}$), 125.80 ($\underline{QC}$), 127.63 (Ar$\underline{CH}$), 127.67 (Ar$\underline{CH}$), 128.76 ($\underline{QC}$), 129.57 (2 x Ar$\underline{CH}$), 129.62 (2 x Ar$\underline{CH}$), 133.76 (2 x $\underline{QC}$), 133.89 ($\underline{QC}$), 133.91 ($\underline{QC}$), 135.61 (4 x Ar$\underline{CH}$), 135.65 (4 x Ar$\underline{CH}$), 136.12 ($\underline{QC}$), 139.12 ($\underline{QC}$), 140.62 ($\underline{QC}$), 141.71 ($\underline{QC}$), 150.41 ($\underline{QC}$), 150.90 ($\underline{QC}$), 151.23 ($\underline{QC}$), 151.44 ($\underline{QC}$)

ν_{MAX} (DCM)/cm^{-1}: 2931.39, 2857.01, 1599.03

HRMS $[M+Na]^+$: calculated 587.2805, found 587.2886, molecular formula ($C_{33}H_{44}NaO_6Si$)

7.16.4 MOM deprotection and oxidation of alcohol: Synthesis of (*S*)-7-(((*tert*-butyldiphenylsilyl)oxy)methyl)-1,2,3-trimethoxy-6,7,8,9-tetrahydro-5*H*-benzo[7]annulen-5-one (4.40)

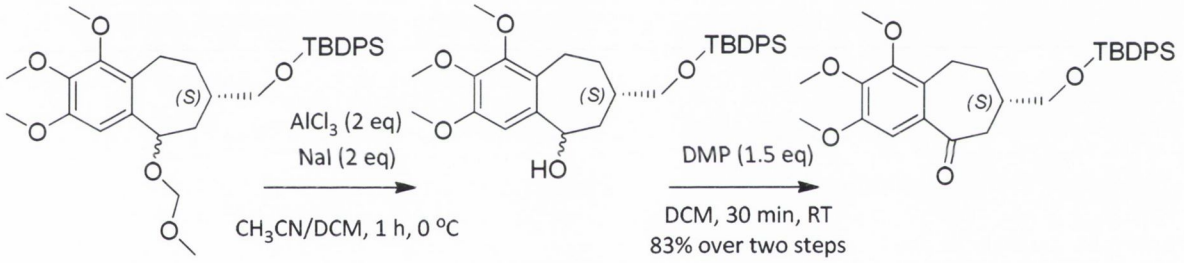

(4.38) **(4.39)** **(4.40)**

To a stirred solution of **(4.38)** (0.73 g, 1.33 mmol) in a mixture of acetonitrile and DCM (2:1; 10 mL) at 0 °C was added aluminium chloride (0.35 g, 2.65 mmol) and sodium iodide (0.40 g, 2.65 mmol). After 1 h, the reaction was quenched by the addition of saturated sodium bicarbonate aqueous solution (50 mL). The reaction was extracted with DCM (3 x 20 mL). To a stirred solution of the combined organic fractions was added Dess-Martin periodinane (0.36 g, 0.85 mmol). After 1 h the reaction was quenched by the addition of saturated sodium bicarbonate aqueous solution (50 mL) and the reaction was extracted with diethyl ether (3 x 50 mL). The organic fractions were combined, dried over $MgSO_4$, filtered and concentrated under reduced pressure. The product was purified by flash column chromatography (stationary phase; silica gel 230-400 mesh, mobile phase; 10:1, hexane/ethyl acetate) to afford **(4.40)** as a yellow oil (0.57 g, 83% over two steps).

$[\alpha]_D^{25}$ = + 0.75 (*c* = 2.14, DCM)

All other data as previously described.

7.16.5 Silyl deprotection: Synthesis of (*S*)-6,7,8,9-tetrahydro-7-(hydroxymethyl)-1,2,3-trimethoxybenzo[7]annulen-5-one (4.41)

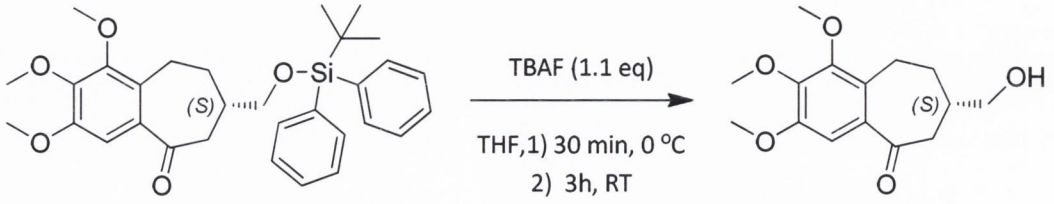

(4.40) **(4.41)**

To a stirred solution of **(4.40)** (0.57 g, 1.10 mmol) in dry THF (5 mL) under an atmosphere of nitrogen at 0 °C was added 1 M TBAF solution (1.21 mL, 1.21 mmol). After 30 min, the temperature of the reaction was allowed to increase to ambient. After a further 3 h, the THF was blown off in a stream of nitrogen gas and the resulting residue added directly to a silica gel flash column and purified by flash column chromatography (stationary phase; silica gel 230-400 mesh, mobile phase; 1:1, hexane/ethyl acetate) to afford **(4.41)** as a yellow oil (0.28 g, 91%).

$[\alpha]_D^{25}$ = + 6.17 (*c* = 17.5, DCM)

All other data as previously described.

7.16.6 Organolithium C-ring coupling: Synthesis of [(7*S*)-9-{3-[(*tert*-butyldimethylsilyl)oxy]-4-methoxyphenyl}-2,3,4-trimethoxy-6,7-dihydro-5*H*-benzo[7]annulen-7-yl]methanol (4.42)

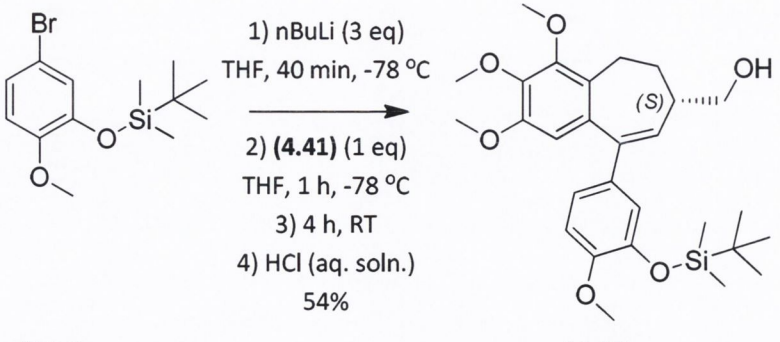

(2.14) **(4.42)**

To a stirred solution of **(2.14)** (0.95 g, 3 mmol) in dry THF (10 mL) at -78 °C under an atmosphere of nitrogen was added 2.5 M nBuLi solution in hexane (1.20 mL, 3 mmol) dropwise. After 40 min, a solution of **(4.41)** (0.28 g, 1 mmol) in dry THF (5 mL) was added to the reaction dropwise. After 1 h, the temperature of the reaction was allowed to increase to ambient. After a further 4 h, the reaction was quenched by the addition of 2 M HCl aqueous solution (25 mL) and was extracted with diethyl ether (3 x 50 mL). The organic fractions were combined, dried over $MgSO_4$, filtered and concentrated under reduced pressure. The product was purified by flash column chromatography (stationary phase; silica gel 230-400 mesh, mobile phase; 4:1, hexane/ethyl acetate) to afford **(4.42)** as a yellow oil (0.27 g, 54%).

$[\alpha]_D^{25}$ = - 49.56 (*c* = 9, DCM)

All other data as previously described.

7.16.7 Silyl deprotection: Synthesis of 5-((*S*,*Z*)-6,7-dihydro-7-(hydroxymethyl)-2,3,4-trimethoxy-5*H*-benzo[7]annulen-9-yl)-2-methoxyphenol (4.24)

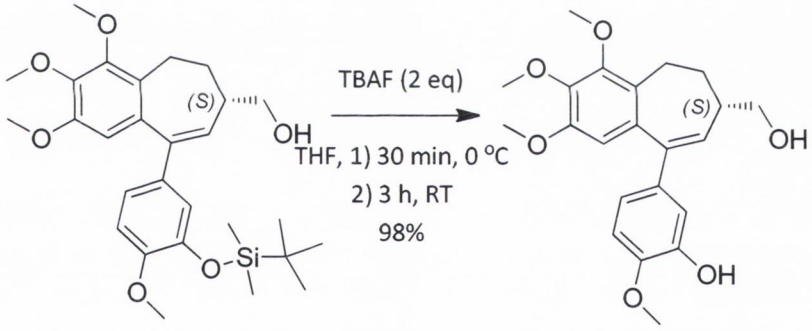

(4.42) **(4.24)**

To a stirred solution of **(4.42)** (0.03 g, 0.06 mmol) in dry THF (1 mL) under an atmosphere of nitrogen at 0 °C was added 1 M TBAF solution in THF (0.12 mL, 0.12 mmol). After 30 min, the temperature of the reaction was allowed to increase to ambient. After a further 3 h, the THF was blown off in a stream of nitrogen gas and the resulting residue added directly to a silica gel flash column and purified by flash column chromatography (stationary phase; silica gel 230-400 mesh, mobile phase; 1:1, hexane/ethyl acetate) to afford **(4.24)** as a white solid (0.03 g, 98%).

$[\alpha]_D^{25}$ = - 71.4 (*c* = 0.48, DCM)

All other data as previously described.

7.17 Synthesis of (R)-enantiomer of C-7 carboxylic acid: Synthesis of (R)-9-(3-hydroxy-4-methoxyphenyl)-2,3,4-trimethoxy-6,7-dihydro-5H-benzo[7]annulene-7-carboxylic acid (4.43)

7.17.1 Removal of silyl protecting group: Synthesis of (*R*)-6,7,8,9-tetrahydro-7-(hydroxymethyl)-1,2,3-trimethoxybenzo[7]annulen-5-one (4.45)

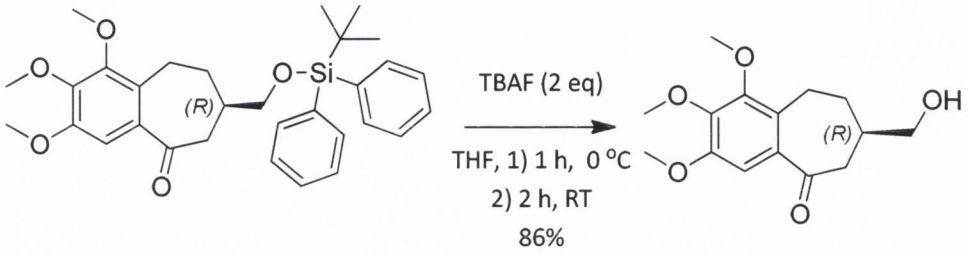

(4.29) **(4.45)**

To a stirred solution of **(4.29)** (0.6 g, 1.16 mmol) in dry THF (5 mL) under an atmosphere of nitrogen at 0 °C was added 1 M TBAF solution in THF (2.3 mL, 2.31 mmol) dropwise. After 1 h, the temperature of the reaction was allowed to increase to ambient. After a further 2 h, the reaction was quenched by the addition of water (25 mL) and extracted with diethyl ether (3 x 30 mL). The organic fractions were combined, dried over $MgSO_4$, filtered and concentrated under reduced pressure. The product was purified by flash column chromatography (stationary phase; silica gel 230-400 mesh, mobile phase; 1:1, hexane/ethyl acetate) to yield **(4.45)** as a clear resin (0.28 g, 86%).

R_f: 0.10 (3:1, hexane/ethyl acetate)

$[\alpha]_D^{25}$ = - 12.10 (*c* = 3.63, DCM)

^{1}H NMR ($CDCl_3$, 400 MHz) δ_H ppm: 1.50-1.61 (1H, m, C$\underline{H}_2$), 1.89-2.01 (1H, m, C$\underline{H}_2$), 2.07-2.18 (1H, m, C$\underline{H}$CH$_2$OH), 2.65-2.74 (1H, m, C$\underline{H}_2$), 2.83-2.94 (1H, m, C$\underline{H}_2$), 3.03-3.12 (1H, m, C$\underline{H}_2$), 2.47-3.58 (1H, m, CHC$\underline{H}_2$OH), 3.58-3.65 (1H, m, C$\underline{H}$CH$_2$OH), 3.82 (3H, s, OC$\underline{H}_3$), 3.87 (3H, s, OC$\underline{H}_3$), 3.91 (3H, s, OC$\underline{H}_3$), 7.14 (Ar$\underline{H}$)

^{13}C NMR ($CDCl_3$, 400 MHz) δ_c ppm: 22.03 (C$\underline{H}_2$), 28.05 (C$\underline{H}_2$), 35.92 (C$\underline{H}$CH$_2$OH), 43.14 (C$\underline{H}_2$), 55.50 (OC$\underline{H}_3$), 60.42 (OC$\underline{H}_3$), 60.83 (OC$\underline{H}_3$), 65.44 (C$\underline{H}_2$OH), 106.94 (Ar$\underline{C}$H), 129.72 (Q$\underline{C}$), 133.56 (Q$\underline{C}$), 145.40 (Q$\underline{C}$), 150.53 (Q$\underline{C}$), 151.05 (Q$\underline{C}$), 202.78 ($\underline{C}$=O)

ν_{MAX} (DCM)/cm^{-1}: 3434.95, 2923.51, 2852.90, 1651.05 (C=O)

HRMS $[M+Na]^+$: calculated 303.1208, found 303.1232, molecular formula ($C_{15}H_{20}NaO_5$)

7.17.2 Organolithium C-Ring Coupling: Synthesis of [(7*R*)-9-{3-[(*tert*-butyldimethylsilyl)oxy]-4-methoxyphenyl}-2,3,4-trimethoxy-6,7-dihydro-5*H*-benzo[7]annulen-7-yl]methanol (4.46)

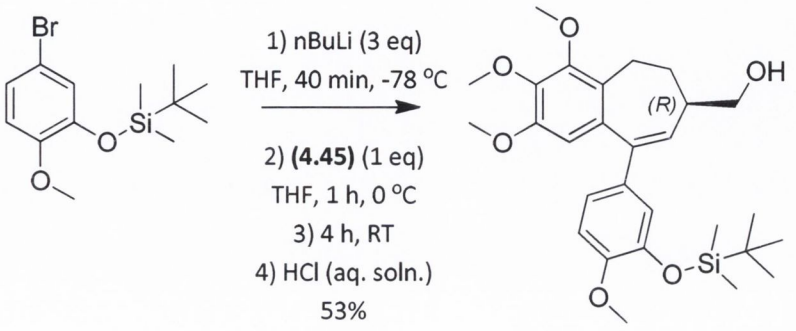

(2.14) **(4.46)**

To a stirred solution of **(2.14)** (1.15 g, 3.64 mmol) in dry THF (10 mL) at -78 °C under an atmosphere of nitrogen was added 2.5 M nBuLi solution in hexane (1.46 mL, 3.64 mmol) dropwise. After 40 min, a solution of **(4.45)** (0.34 g, 1.21 mmol) in dry THF (5 mL) was added to the reaction dropwise. After 1 h, the reaction was allowed to increase to ambient and remained stirring for a further 4 h. The reaction was then quenched by the addition of 2 M HCl aqueous solution (25 mL) and was extracted with diethyl ether (3 x 50 mL). The organic fractions were combined, dried over $MgSO_4$, filtered and concentrated under reduced pressure. The product was purified by flash column chromatography (stationary phase; silica gel 230-400 mesh, mobile phase; 4:1, hexane/ethyl acetate) to yield **(4.46)** as a yellow oil (0.32 g, 53%).

R_f: 0.29 (3:1, hexane/ethyl acetate)

$[\alpha]_D^{25}$ = + 47.26 (*c* = 14.71, DCM)

^{1}H NMR ($CDCl_3$, 400 MHz) δ_H ppm: 0.15 (6H, d, J = 4.56 Hz, Si($C\underline{H}_3$)$_2$), 0.99 (9H, s, C($C\underline{H}_3$)$_3$), 1.86-1.98 (1H, m, $C\underline{H}_2$), 2.13-2.41 (3H, m, 1 x $C\underline{H}CH_2OH$, 2 x $C\underline{H}_2$), 3.04-3.13 (1H, m, $C\underline{H}_2$), 3.70 (5H, s, 1 x $OC\underline{H}_3$), 1 x $C\underline{H}_2OH$), 3.83 (3H, s, $OC\underline{H}_3$), 3.92 (3H, s, $OC\underline{H}_3$), 3.94 (3H, s, $OC\underline{H}_3$), 6.15 (1H, d, J = 6.21 Hz, C=C$\underline{H}$), 6.38 (1H, s, Ar$\underline{H}$), 6.78-6.82 (2H, m, Ar$\underline{H}$), 6.88-6.90 (1H, m, Ar$\underline{H}$)

^{13}C NMR ($CDCl_3$, 400 MHz) δ_c ppm: -4.99 (Si($\underline{C}H_3$)$_2$), 18.00 ($\underline{C}$(CH_3)$_3$), 22.69 ($\underline{C}H_2$), 25.28 (C($\underline{C}H_3$)$_3$), 37.46 ($\underline{C}H_2$), 39.49 ($\underline{C}HCH_2OH$), 50.04 ($O\underline{C}H_3$), 55.44 ($O\underline{C}H_3$), 60.44 ($O\underline{C}H_3$), 61.15 ($O\underline{C}H_3$), 65.94 ($\underline{C}H_2OH$), 108.34 (Ar$\underline{C}H$), 111.12 (Ar$\underline{C}H$), 120.23 (Ar$\underline{C}H$), 120.90 (Ar$\underline{C}H$), 127.62 (Ar$\underline{C}H$), 127.82 (C=$\underline{C}H$), 134.30 (Q$\underline{C}$), 135.77 (Q$\underline{C}$), 140.68 (Q$\underline{C}$), 141.58 (Q$\underline{C}$), 144.08 (Q$\underline{C}$), 149.95 (Q$\underline{C}$), 150.30 (Q$\underline{C}$), 150.52 (Q$\underline{C}$)

ν_{MAX} (DCM)/cm^{-1}: 3400.95, 2927.16, 2854.27, 1596.17, 1571.47

HRMS $[M+H]^+$: calculated 501.2672, found 501.2668, molecular formula ($C_{28}H_{41}O_6Si$)

7.17.3 Oxidation of alcohol to carboxylic acid attempt A: Attempted synthesis of (7*R*)-9-{3-[(*tert*-butyldimethylsilyl)oxy]-4-methoxyphenyl}-2,3,4-trimethoxy-6,7-dihydro-5*H*-benzo[7]annulene-7-carboxylic acid (4.47)

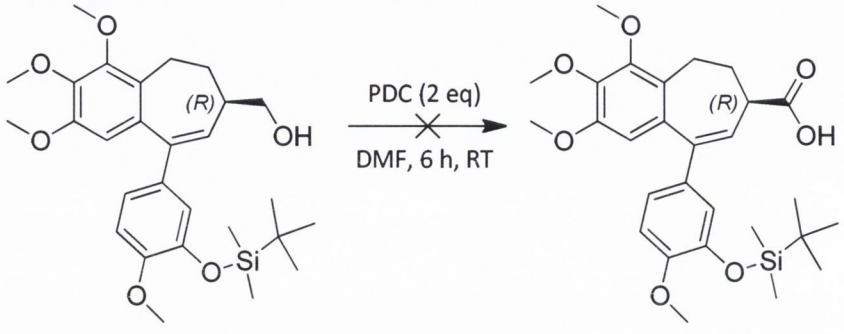

(4.46) **(4.47)**

To a stirred solution of **(4.46)** (0.02 g, 0.04 mmol) in DMF (1 mL) at room temperature was added pyridinium dichromate (0.03 g, 0.08 mmol). After 6 h the reaction was quenched by the addition of 2 M HCl aqueous solution (10 mL) and extracted with diethyl ether (3 x 10 mL). The organic fraction was found to contain a complex mixture of compounds by TLC analysis and was not purified further.

7.17.4 Oxidation of alcohol to carboxylic acid attempt B: Attempted synthesis of (7*R*)-9-{3-[(*tert*-butyldimethylsilyl)oxy]-4-methoxyphenyl}-2,3,4-trimethoxy-6,7-dihydro-5*H*-benzo[7]annulene-7-carboxylic acid (4.47)

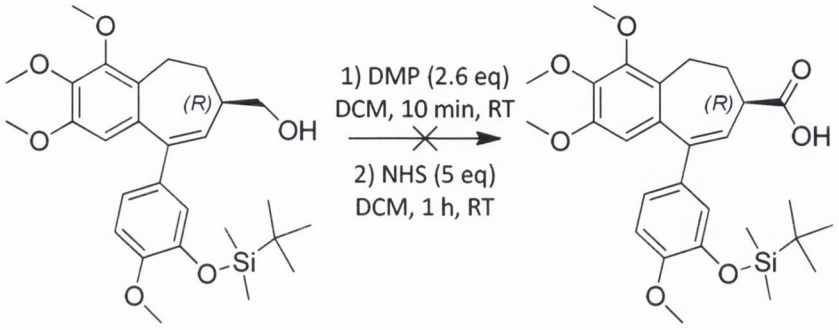

(4.46) **(4.47)**

To a stirred solution of **(4.46)** (0.02 g, 0.04 mmol) in DCM (1 mL) at room temperature was added Dess-Martin periodinane (0.04 g, 0.10 mmol). After 10 min, *N*-hydroxysuccinimide (0.02 g, 0.20 mmol) was added. After 1 h, 2.5 M NaOH aqueous solution (10 mL) was added and the aqueous phase washed with diethyl ether (3 x 15 mL). The ethereal extracts were then reacidified with 2 M HCl aqueous solution (30 mL) and extracted with diethyl ether (3 x 20 mL). The organic fractions were combined, dried over $MgSO_4$ and concentrated *in vacuo* to afford a yellow oil. The crude product was analysed by NMR and found not to be the product of interest. The product was thus not characterised further.

7.17.5 Oxidation of alcohol to aldehyde: Synthesis of (7*R*)-9-{3-[(*tert*-butyldimethylsilyl)oxy]-4-methoxyphenyl}-2,3,4-trimethoxy-6,7-dihydro-5*H*-benzo[7]annulene-7-carbaldehyde (4.48)

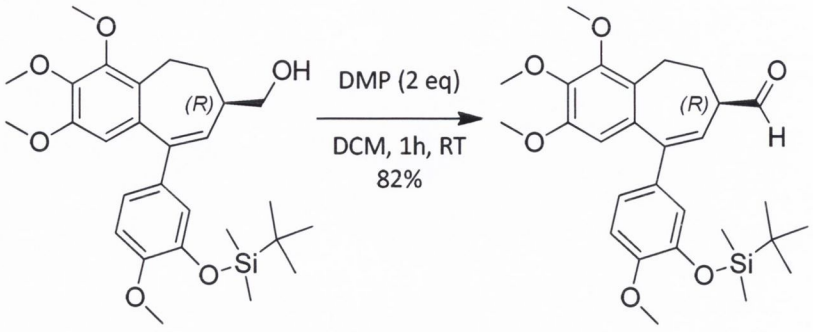

(4.46) **(4.48)**

To a stirred solution of **(4.46)** (0.11 g, 0.22 mmol) in DCM (5 mL) at room temperature was added Dess-Martin periodinane (.19 g, 0.44 mmol). After 1 h, the reaction was quenched by the addition of saturated sodium bicarbonate solution (10 mL). The reaction was extracted with diethyl ether (3 x 20 mL). The organic fractions were combined, dried over $MgSO_4$, filtered and concentrated under reduced pressure. The product was purified by flash column chromatography (stationary phase; silica gel 230-400 mesh, mobile phase; 10:1, hexane/ethyl acetate) to yield **(4.48)** as a yellow oil (0.09 g, 82%).

R_f: 0.38 (4:1, hexane/ethyl acetate)

$[\alpha]_D^{25}$ = 0.00 (*c* = 4.74, DCM)

^{1}H NMR ($CDCl_3$, 400 MHz) δ_H ppm: 0.17 (6H, d, J = 4.56 Hz, Si($C\underline{H}_3$)$_2$), 1.00 (9H, s, C($C\underline{H}_3$)$_3$), 2.40-2.56 (3H, m, $C\underline{H}_2$), 2.88-2.98 (2H, m, 1 x $C\underline{H}$CHO, 1 x $C\underline{H}_2$), 3.70 (3H, s, O$\underline{Me}$,), 3.85 (3H, s, O$C\underline{H}_3$), 3.94 (3H, s, O$C\underline{H}_3$), 3.95 (3H, s, O$C\underline{H}_3$), 6.39 (1H, s, Ar$\underline{H}$), 6.46 (1H, d, J = 7.32 Hz, C=C$\underline{H}$), 6.81-6.85 (2H, m, Ar$\underline{H}$), 6.92 (1H, dd, J_1 =8.03 Hz, J_2 = 2.01 Hz, Ar$\underline{H}$), 9.61 (1H, s, C$\underline{H}$O)

^{13}C NMR ($CDCl_3$, 400 MHz) δ_c ppm: -4.53 (Si($\underline{C}H_3$)$_2$), 18.47 ($\underline{C}$(CH_3)$_3$), 22.69 ($\underline{C}H_2$), 25.73 (C($\underline{C}H_3$)$_3$), 36.77 ($\underline{C}H_2$), 49.81 ($\underline{C}$HCHO), 55.50 (O$\underline{C}H_3$), 55.91 (O$\underline{C}H_3$), 60.89 (O$\underline{C}H_3$), 61.55 (O$\underline{C}H_3$), 109.00 (Ar$\underline{C}$H), 111.61 (Ar$\underline{C}$H), 120.76 (Ar$\underline{C}$H), 121.26 (C=$\underline{C}$H), 121.59 (Ar$\underline{C}$H), 127.92 ($\underline{Q}$C), 134.12 ($\underline{Q}$C), 135.12 ($\underline{Q}$C), 141.66 ($\underline{Q}$C), 143.79 ($\underline{Q}$C), 144.67 ($\underline{Q}$C), 150.84 ($\underline{Q}$C), 150.99 ($\underline{Q}$C), 151.42 ($\underline{Q}$C), 202.16 ($\underline{C}$HO)

ν_{MAX} (DCM)/cm^{-1}: 2929.88, 2856.44, 1726.69 (C=O), 1597.31, 1572.54

HRMS $[M+H]^+$: calculated 499.2516, found 499.2520, molecular formula ($C_{28}H_{39}O_6Si$)

5.17.6 Attempted aldehyde oxidation A: Attempted synthesis of (7*R*)-9-{3-[(*tert*-butyldimethylsilyl)oxy]-4-methoxyphenyl}-2,3,4-trimethoxy-6,7-dihydro-5*H*-benzo[7]annulene-7-carboxylic acid (4.47)

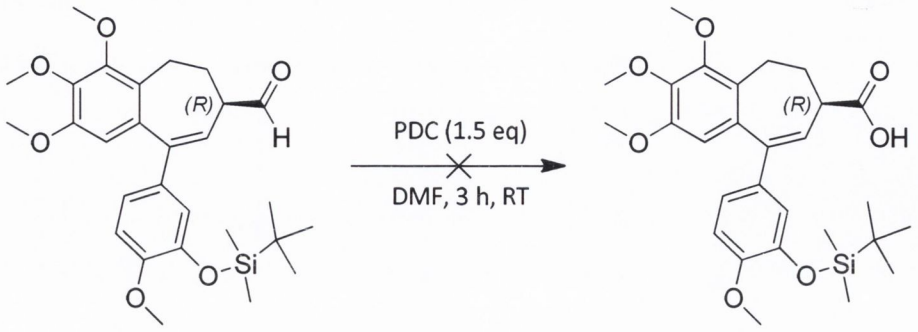

(4.48) **(4.47)**

To a stirred solution of **(4.48)** (0.01 g, 0.02 mmol) in DMF (1 mL) at room temperature was added pyridinium dichromate (0.01 g, 0.03 mmol). After 3 h, the reaction was quenched by the addition of 2 M HCl aqueous solution (10 mL) and extracted with diethyl ether (3 x 10 mL). The organic fraction was found to contain a complex mixture of compounds by TLC analysis and was not purified further.

5.17.7 Aldehyde oxidation attempt B: Synthesis of (7*R*)-9-{3-[(*tert*-butyldimethylsilyl)oxy]-4-methoxyphenyl}-2,3,4-trimethoxy-6,7-dihydro-5*H*-benzo[7]annulene-7-carboxylic acid (4.47)

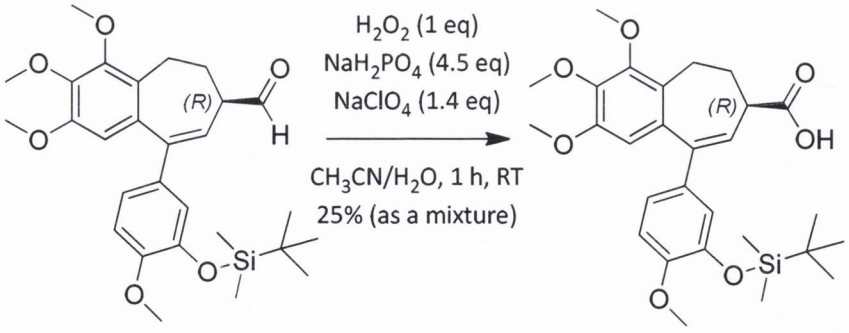

(4.48) **(4.47)**

To a stirred solution of **(4.48)** (0.08 g, 0.16 mmol) in acetonitrile and water (1:1; 1 mL) was added 30% hydrogen peroxide solution in water (0.02 mL, 0. 17 mmol) and NaH_2PO_4 (0.1 g, 0.7 mmol).

Sodium chlorite (0.03 g, 0.22 mmol) in water (0.5 mL) was then added dropwise to the reaction. After 1 h, the reaction was quenched by the addition of 2 M HCl aqueous solution (5 mL). The reaction was extracted with diethyl ether (3 x 10 mL). The organic fractions were combined, dried over $MgSO_4$, filtered and concentrated under reduced pressure. The product was purified by flash column chromatography (stationary phase; silica gel 230-400 mesh, mobile phase; 5:95, methanol/ethyl acetate) to afford a mixture containing **(4.47)** as the major constituent as a yellow resin (0.02 g, 25%). The product was not purified further.

R_f: 0.14 (3:1, hexane/ethyl acetate

ν_{MAX} (DCM)/cm^{-1}: 3434.16 (OH), 2924.29, 2852.93, 1701.96 (C=O), 1643.04

HRMS $[M+H]^+$: calculated 515.2465, found 515.2490, molecular formula ($C_{28}H_{39}O_7Si$)

7.17.8 Aldehyde oxidation attempt C: Attempted Synthesis of (7*R*)-9-{3-[(*tert*-butyldimethylsilyl)oxy]-4-methoxyphenyl}-2,3,4-trimethoxy-6,7-dihydro-5*H*-benzo[7]annulene-7-carboxylic acid (4.47)

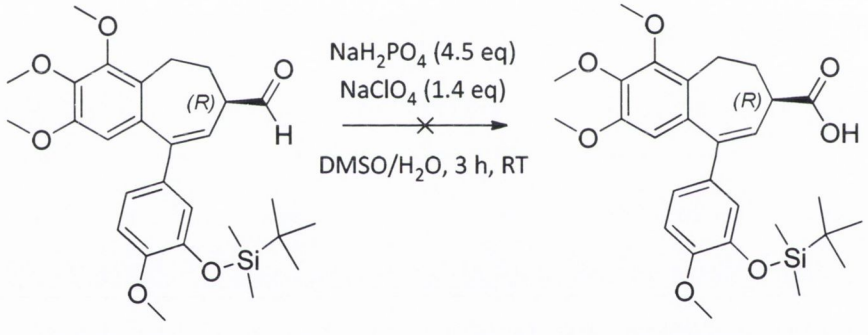

(4.48) **(4.47)**

To a stirred solution of **(4.48)** (0.1 g, 0.19 mmol) in DMSO and water (1:1; 1 mL) was added NaH_2PO_4 (0.12 g, 0.87 mmol). Sodium chlorite (0.03 g, 0.27 mmol) in water (0.5 mL) was then added dropwise to the reaction. After 3 h the reaction was analysed by TLC. Due to the formation of a side-product with very similar R_f value, the product of interest was not isolated.

7.17.9 Aldehyde oxidation attempt D: Alternative synthesis of (7*R*)-9-{3-[(*tert*-butyldimethylsilyl)oxy]-4-methoxyphenyl}-2,3,4-trimethoxy-6,7-dihydro-5*H*-benzo[7]annulene-7-carboxylic acid (4.47)

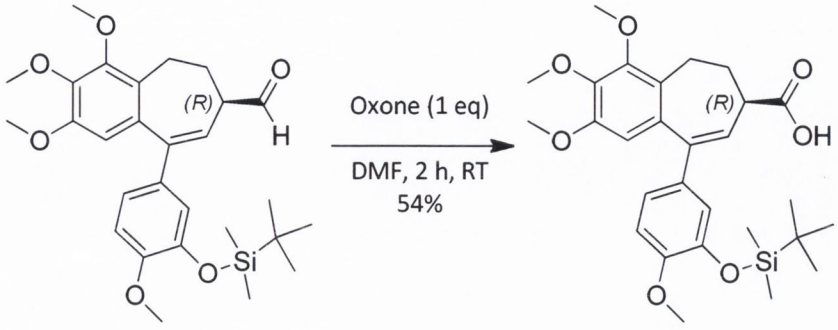

(4.48) **(4.47)**

To a stirred solution of **(4.48)** (0.09 g, 0.17 mmol) in DMF (2 mL) was added oxone (0.11 g, 0.17 mmol). After 2 h, the reaction was quenched by the addition of water (10 mL) and extracted with diethyl ether (3 x 10 mL). The organic fractions were combined, dried over $MgSO_4$, filtered and concentrated under reduced pressure. The product was purified by flash column chromatography (stationary phase; silica gel 230-400 mesh, mobile phase; 5:95, methanol/ethyl acetate) to yield **(4.47)** as a yellow resin (0.05 g, 54%).

R_f: 0.14 (3:1, hexane/ethyl acetate)

$[\alpha]_D^{25}$ = + 0.59 (*c* = 3.33, DCM)

^{1}H NMR ($CDCl_3$, 400 MHz) δ_H ppm: 0.16 (6H, d, J = 6.85 Hz, Si($C\underline{H}_3$)$_2$), 1.00 (9H, s, C($C\underline{H}_3$)$_3$), 2.41-2.56 (3H, m, 2 x $C\underline{H}_2$), 2.90-2.98 (2H, m, 1 x $C\underline{H}CO_2H$, 1 x $C\underline{H}_2$), 3.71 (3H, s, $OC\underline{H}_3$), 3.84 (3H, s, $OC\underline{H}_3$), 3.95 (6H, s, 2 x $OC\underline{H}_3$), 6.39 (1H, s, Ar$\underline{H}$), 6.47 (1H, d, J = 6.48 Hz, C=C$\underline{H}$), 6.80 (1H, d, J = 2.18 Hz, Ar$\underline{H}$), 6.81 (1H, d, J = 8.46 Hz, Ar$\underline{H}$), 6.90 (1H, dd, J_1 = 8.46 Hz, J_2 = 2.18 Hz, Ar$\underline{H}$)

^{13}C NMR ($CDCl_3$, 400 MHz) δ_c ppm: -5.00 (Si($\underline{C}H_3$)$_2$), 18.00 ($\underline{C}$(CH_3)$_3$), 22.39 ($\underline{C}H_2$), 25.28 (C($\underline{C}H_3$)$_3$), 39.00 ($\underline{C}H_2$), 42.31 ($\underline{C}HCO_2H$), 55.04 ($O\underline{C}H_3$), 55.62 ($O\underline{C}H_3$), 60.44 ($O\underline{C}H_3$), 61.16 ($O\underline{C}H_3$), 108.33 (Ar$\underline{C}H$), 111.15 (Ar$\underline{C}H$), 120.33 (Ar$\underline{C}H$), 121.04 (Ar$\underline{C}H$), 122.72 (C=$\underline{C}H$), 126.79 ($\underline{Q}C$), 133.65 ($\underline{Q}C$), 134.98 ($\underline{Q}C$), 140.98 ($\underline{Q}C$), 141.48 ($\underline{Q}C$), 144.11 ($\underline{Q}C$), 150.20 ($\underline{Q}C$), 150.43 ($\underline{Q}C$), 150.85 ($\underline{Q}C$), 179.67 ($\underline{C}O_2H$)

ν_{MAX} (DCM)/cm^{-1}: 3434.16 (OH), 2924.29, 2852.93, 1701.96 (C=O), 1643.04

HRMS $[M+H]^+$: calculated 515.2465, found 515.2443, molecular formula ($C_{28}H_{39}O_7Si$)

7.17.10 Silyl deprotection: Synthesis of (*R,Z*)-6,7-dihydro-9-(3-hydroxy-4-methoxyphenyl)-2,3,4-trimethoxy-5*H*-benzo[7]annulene-7-carboxylic acid (4.43)

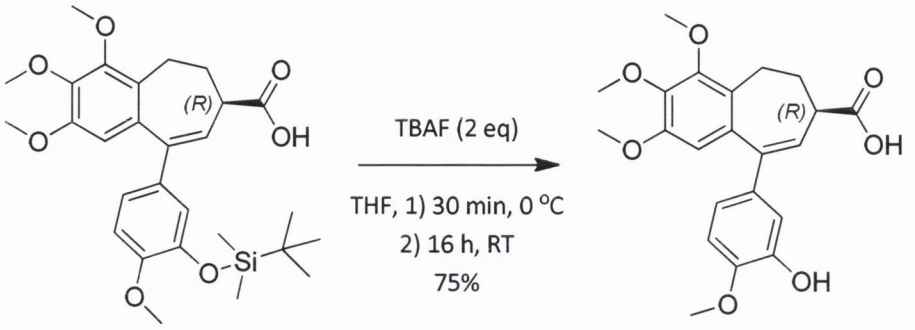

(4.47) **(4.43)**

To a stirred solution of **(4.47)** (0.05 g, 0.10 mmol) in dry THF (1 mL) under an atmosphere of nitrogen at 0 °C was added 1 M TBAF solution in THF (0.19 mL, 0.19 mmol). After 30 min, the temperature of the reaction was allowed to increase to ambient. After a further 16 h, the THF was removed by blowing with a stream of nitrogen gas and the resulting residue added directly to a silica gel flash column and purified by flash column chromatography (stationary phase; silica gel 230-400 mesh, mobile phase; 1:1, hexane/ethyl acetate) to afford **(4.43)** as a white solid (0.03 g, 75%).

R_f: 0.63 (50:50:1, hexane/ethyl acetate/formic acid)

$[\alpha]_D^{25}$ = - 4.40 (*c* = 1.36, DCM)

^{1}H NMR ($CDCl_3$, 400 MHz) δ_H ppm: 2.27-2.39 (2H, m, C$\underline{H}_2$), 2.49-2.60 (1H, m, C$\underline{H}_2$), 2.99-3.05 (1H, m, C$\underline{H}$COOH), 3.11-3.16 (1H, m, C$\underline{H}_2$), 3.72 (3H, s, OC$\underline{H}_3$), 3.93 (3H, s, OC$\underline{H}_3$), 3.94 (3H, s, OC$\underline{H}_3$), 3.96 (3H, s, OC$\underline{H}_3$), 6.40 (1H, s, Ar$\underline{H}$), 6.51 (1H, d, J = 6.66 Hz, C=C$\underline{H}$), 6.82 (1H, d, J = 8.46 Hz, Ar$\underline{H}$), 6.86 (1H, dd, J_1 = 8.46 Hz, J_2 = 2.05 Hz, Ar$\underline{H}$), 6.93 (1H, d, J = 2.05 Hz, Ar$\underline{H}$)

^{13}C NMR ($CDCl_3$, 400 MHz) δ_c ppm: 22.81 (C$\underline{H}_2$), 39.34 (C$\underline{H}_2$), 42.72 (C$\underline{H}$COOH), 56.02 (OC$\underline{H}_3$), 56.06 (OC$\underline{H}_3$), 60.90 (OC$\underline{H}_3$), 61.61 (OC$\underline{H}_3$), 108.91 (Ar$\underline{C}$H), 110.32 (Ar$\underline{C}$H), 114.37 (Ar$\underline{C}$H), 119.90 (Ar$\underline{C}$H), 123.50 (C=$\underline{C}$H), 127.28 (Q$\underline{C}$), 134.70 (Q$\underline{C}$), 135.22 (Q$\underline{C}$), 141.54 (Q$\underline{C}$), 141.99 (Q$\underline{C}$), 145.29 (Q$\underline{C}$), 146.31 (Q$\underline{C}$), 150.92 (Q$\underline{C}$), 151.41 (Q$\underline{C}$), 180.43 ($\underline{C}$OOH)

ν_{MAX} (DCM)/cm^{-1}: 3420.98 (OH), 3416.16 (OH), 2932.79, 2854.23, 1706.92 (C=O), 1582.25

HRMS $[M+Na]^+$: calculated 423.142, found 423.1422, molecular formula ($C_{22}H_{24}NaO_7$)

Melting point: 134-136 °C

7.18 Synthesis of (S)-enantiomer of C-7 carboxylic acid: Synthesis of (S)-9-(3-hydroxy-4-methoxyphenyl)-2,3,4-trimethoxy-6,7-dihydro-5H-benzo[7]annulene-7-carboxylic acid (4.44)

7.18.1 Two step oxidation of alcohol to carboxylic acid: Synthesis (7*S*)-9-{3-[(*tert*-butyldimethylsilyl)oxy]-4-methoxyphenyl}-2,3,4-trimethoxy-6,7-dihydro-5*H*-benzo[7]annulene-7-carboxylic acid (4.50)

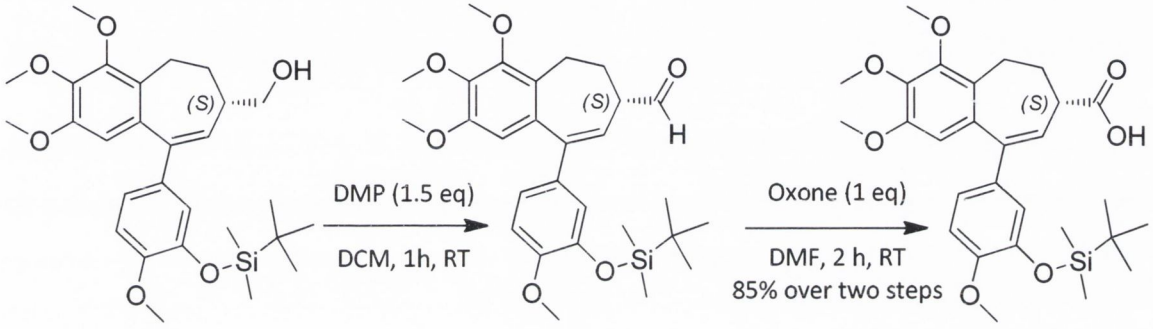

(4.42) **(4.49)** **(4.50)**

To a stirred solution of **(4.42)** (0.15 g, 0.30 mmol) in DCM (5 mL) at room temperature was added Dess-Martin periodinane (0.19 g, 0.45 mmol). After 1 h, the reaction was quenched by the addition of saturated sodium bicarbonate aqueous solution (10 mL). The reaction was extracted with diethyl ether (3 x 20 mL). The organic fractions were combined, dried over $MgSO_4$, filtered and concentrated under reduced pressure. To a stirred solution of the resulting residue reconstituted in DMF (2 mL) was added oxone (0.18 g, 0.30 mmol). After 2 h, the reaction was quenched by the addition of water (10 mL) and extracted with diethyl ether (3 x 10 mL). The organic fractions were combined, dried over $MgSO_4$, filtered and concentrated under reduced pressure. The product was purified by flash column chromatography (stationary phase; silica gel 230-400 mesh, mobile phase; 5:95, methanol/ethyl acetate) to afford **(4.50)** as a yellow resin (0.13 g, 85%).

$[\alpha]_D^{25}$ = - 29.54 (*c* = 8.13, DCM)

All other data as previously described.

7.18.2 Silyl deprotection: Synthesis of (*S*,*Z*)-6,7-dihydro-9-(3-hydroxy-4-methoxyphenyl)-2,3,4-trimethoxy-5*H*-benzo[7]annulene-7-carboxylic acid (4.44)

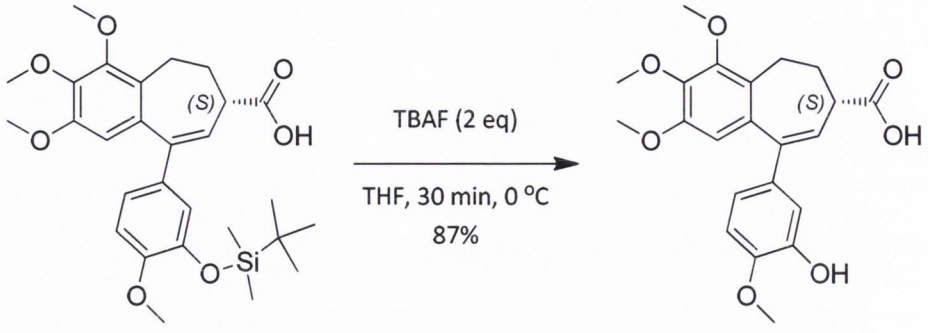

(4.50) **(4.44)**

To a stirred solution of **(4.50)** (0.12 g, 0.23 mmol) in dry THF (2 mL) under an atmosphere of nitrogen at 0 °C was added 1 M TBAF solution in THF (0.47 mL, 0.47 mmol). After 30 min, the THF was blown off in a stream of nitrogen gas and the resulting residue added directly to a silica gel flash column and purified by flash column chromatography (stationary phase; silica gel 230-400 mesh, mobile phase; ethyl acetate) to afford **(4.44)** as an off-white solid (0.08 g, 87%).

$[\alpha]_D^{25}$ = - 40.83 (*c* = 1.71, DCM)

All other data as previously described.

7.19 Attempted synthesis of hydroxamic acid designed-multiple ligand: Attempted synthesis of (R)-N-hydroxy-9-(3-hydroxy-4-methoxyphenyl)-2,3,4-trimethoxy-6,7-dihydro-5H-benzo[7]annulene-7-carboxamide (5.05)

7.19.1 PFP ester formation: Synthesis of (7*R*)-9-{3-[(*tert*-butyldimethylsilyl)oxy]-4-methoxyphenyl}-2,3,4-trimethoxy-6,7-dihydro-5*H*-benzo[7]annulene-7-carboxylate (5.06)

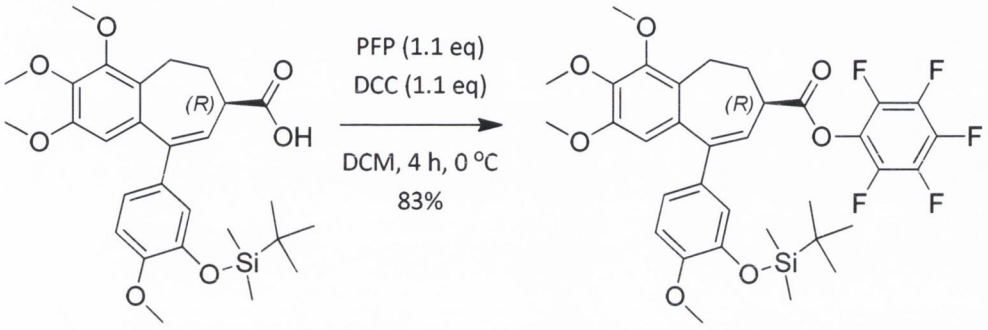

(4.47) **(5.06)**

To a stirred solution of **(4.47)** (0.08 g, 0.16 mmol) and pentafluorophenol (0.03 g, 0.17 mmol) in dry DCM (1 mL) under an atmosphere of nitrogen at 0 °C was added a solution of DCC (0.04 g, 0.17 mmol) in dry DCM (0.5 mL). After 4 h, the reaction was quenched by the addition of water (5 mL) and the reaction extracted with diethyl ether (3 x 10 mL). The organic fractions were combined, dried over $MgSO_4$, filtered and concentrated *in vacuo*. The resulting residue was then purified by flash column chromatography (stationary phase; silica gel 230-400 mesh, mobile phase; 20:1, hexane/ethyl acetate) to yield **(5.06)** as a colourless resin (0.09 g, 83%).

R_f: 0.66 (3:1, hexane/ethyl acetate)

$[\alpha]_D^{25}$ = + 13 (*c* = 4, DCM)

^{1}H NMR ($CDCl_3$, 400 MHz) δ_H ppm: 0.17 (6H, d, J = 6.04 Hz, Si($C\underline{H}_3$)$_2$, 1.00 (9H, s, C($C\underline{H}_3$)$_3$), 2.41-2.46 (1H, m, $C\underline{H}_2$), 2.51-2.54 (1H, m, $C\underline{H}_2$), 2.66-2.71 (1H, m, $C\underline{H}_2$), 3.18-3.23 (1H, m, $C\underline{H}_2$), 3.34-3.37 (1H, m, $C\underline{H}$COO), 3.73 (3H, s, O$C\underline{H}_3$), 3.86 (3H, s, O$C\underline{H}_3$), 3.97 (3H, s, O$C\underline{H}_3$), 3.98 (3H, s, O$C\underline{H}_3$), 6.43 (1H, s, Ar$\underline{H}$), 6.51 (1H, d, J = 6.67 Hz, C=C$\underline{H}$), 6.83-6.85 (2H, m, 2 x Ar$\underline{H}$), 6.92 (1H, dd, J_1 = 8.39 Hz, J_2 = 2.14 Hz, Ar$\underline{H}$)

^{13}C NMR ($CDCl_3$, 400 MHz) δ_c ppm: -4.58 (Si($\underline{C}H_3$)$_2$), -4.54 (Si($\underline{C}H_3$)$_2$), 18.46 ($\underline{C}$(CH$_3$)$_3$), 22.79 ($\underline{C}H_2$), 25.71 (C($\underline{C}H_3$)$_3$), 39.44 ($\underline{C}H_2$), 42.47 ($\underline{C}$HCOO), 55.52 (O$\underline{C}H_3$), 55.96 (O$\underline{C}H_3$), 60.89 (O$\underline{C}H_3$), 61.62 (O$\underline{C}H_3$), 108.88 (Ar$\underline{C}$H), 111.65 (Ar$\underline{C}$H), 120.79 (Ar$\underline{C}$H), 121.46 (C=$\underline{C}$H), 121.63 (Ar$\underline{C}$H), 125.18 ($\underline{Q}C$), 126.98 ($\underline{Q}C$), 133.71 ($\underline{Q}C$), 135.03 ($\underline{Q}C$), 136.61 ($\underline{Q}C$), 139.14 ($\underline{Q}C$), 139.94 ($\underline{Q}C$), 141.71 ($\underline{Q}C$), 142.44 ($\underline{Q}C$), 143.02 ($\underline{Q}C$), 144.72 ($\underline{Q}C$), 150.96 ($\underline{Q}C$), 150.99 ($\underline{Q}C$), 151.55 ($\underline{Q}C$), 171.02 ($\underline{C}$=O)

^{19}F NMR ($CDCl_3$, 400 MHz) δ_F ppm: -162.95- -162.71 (2F, m, Ar$\underline{F}$), -158.54- -158.42 (1F, m, Ar$\underline{F}$), 153.44 (2F, d, J = 19.24 Hz, Ar$\underline{F}$)

ν_{MAX} (DCM)/cm^{-1}: 2926.61, 2855.04, 1785.96 (C=O), 1644.80

HRMS [M+Na]$^+$: calculated 703.2126, found 703.2122, molecular formula ($C_{34}H_{37}F_5NaO_7Si$)

7.19.2 Hydroxamic acid synthesis: Synthesis of (7*R*)-9-{3-[(*tert*-butyldimethylsilyl)oxy]-4-methoxyphenyl}-*N*-hydroxy-2,3,4-trimethoxy-6,7-dihydro-5*H*-benzo[7]annulene-7-carboxamide (5.07)

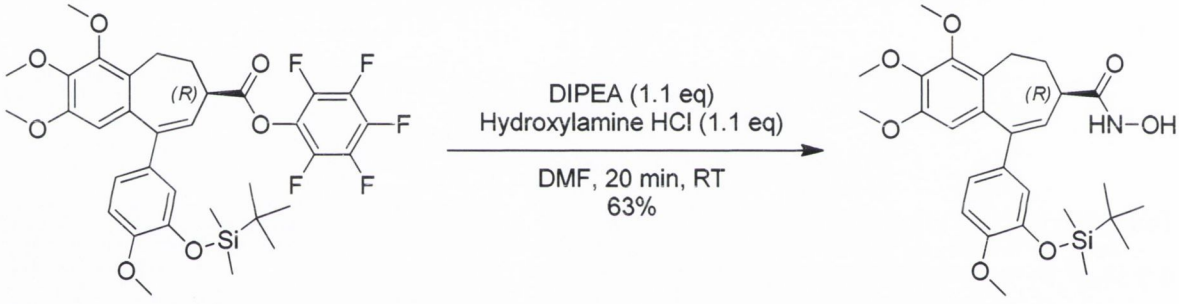

(5.06) **(5.07)**

To a stirred solution of **(5.06)** (0.08 g, 0.12 mmol) in DMF (1 mL) was added DIPEA (0.02 mL, 0.13 mmol) and hydroxylamine HCl (0.01 g, 0.13 mmol) at room temperature. After 20 min, the reaction was quenched by the addition of 0.2 M aqueous HCl aqueous solution (5 mL) and the reaction extracted with diethyl ether (3 x 10 mL). The organic fractions were combined, dried over $MgSO_4$, filtered and concentrated *in vacuo*. The resulting residue was then purified by flash column chromatography (stationary phase; silica gel 230-400 mesh, mobile phase; 50:50:1, hexane/ethyl acetate/formic acid) to afford **(5.07)** as a colourless resin (0.04 g, 63%).

R_f: 0.25 (50:50:1, hexane/ethyl acetate/formic acid)

HRMS [M+Na]$^+$: calculated 552.2393, found 552.2377, molecular formula ($C_{28}H_{39}NNaO_7Si$)

7.20 Attempted synthesis of ether containing hydroxamic acid compound: Attempted synthesis of (R)-2-((9-(3-amino-4-methoxyphenyl)-2,3,4-trimethoxy-6,7-dihydro-5H-benzo[7]annulen-7-yl)methoxy)-N-hydroxyacetamide (5.08)

7.20.1 Suzuki coupling of aniline C-ring and triflate: Synthesis of *tert*-butyl *N*-{5-[(7*R*)-7-{[(*tert*-butyldiphenylsilyl)oxy]methyl}-2,3,4-trimethoxy-6,7-dihydro-5*H*-benzo[7]annulen-9-yl]-2-methoxyphenyl}carbamate (5.09)

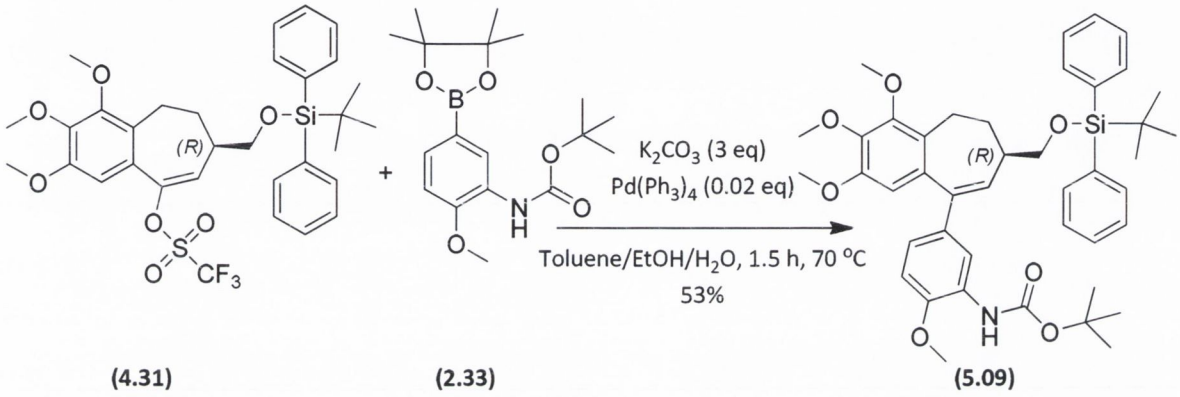

(4.31) **(2.33)** **(5.09)**

To a stirred solution of **(4.31)** (0.22 g, 0.34 mmol) in a mixture of toluene, ethanol and water (10 mL; 3: 1: 1) was added potassium carbonate (0.14 g, 1.02 mmol), (tetrakis(triphenyl)phosphine) palladium (0.02 g, 0.02 mmol) and **(2.33)** (0.18 g, 0.51 mmol). The reaction was heated under reflux at 70 °C for 1.5 h after which time it was quenched by the addition of water (50 mL). The reaction mixture was extracted with diethyl ether (3 x 50 mL). The organic fractions were combined, dried over $MgSO_4$, filtered and concentrated *in vacuo.* The resulting residue was then purified by flash column chromatography (stationary phase; silica gel 230-400 mesh, mobile phase; 10:1, hexane/ethyl acetate) to yield **(5.09)** as an impure yellow oil (0.13 g, 53%). The crude product was not characterised further.

R_f: 0.41 (5:1, hexane/ethyl acetate)

HRMS $[M+Na]^+$: calculated 746.3489, found 746.3459, molecular formula ($C_{43}H_{53}NNaO_7Si$)

7.20.2 Silyl deprotection: Synthesis of *tert*-butyl 5-((*R*,*Z*)-6,7-dihydro-7-(hydroxymethyl)-2,3,4-trimethoxy-5*H*-benzo[7]annulen-9-yl)-2-methoxyphenylcarbamate (5.10)

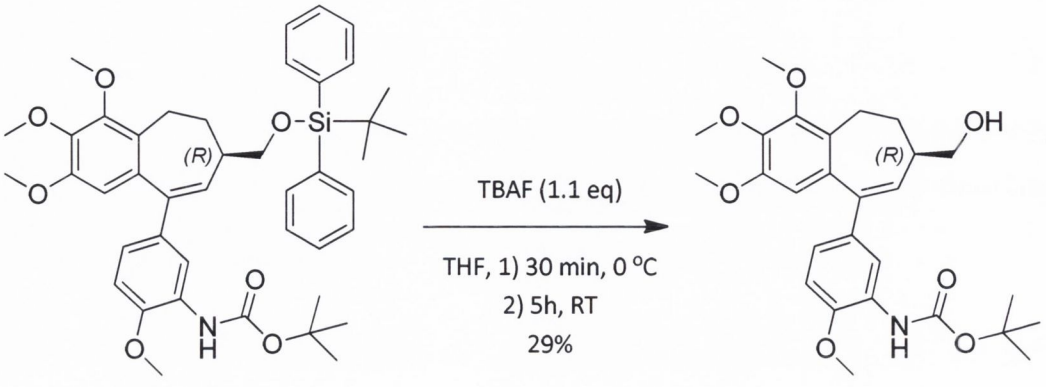

(5.09) **(5.10)**

To a stirred solution of **(5.09)** (0.1 g, 0.14 mmol) in dry THF (1 mL) under an atmosphere of nitrogen at 0 °C was added 1 M TBAF solution in THF (0.15 mL, 0.15 mmol). After 30 min, the temperature of the reaction was allowed to increase to ambient. After a further 5 h, the THF was blown off in a stream of nitrogen gas and the resulting residue added directly to a silica gel flash column and purified by flash column chromatography (stationary phase; silica gel 230-400 mesh, mobile phase; 1:1, hexane/ethyl acetate) to afford **(5.10)** as a yellow oil (0.02 g, 29%).

R_f: 0.21 (2:1, hexane/ethyl acetate)

$[\alpha]_D^{25}$ = + 25.2 (*c* = 1.11, DCM)

^{1}H NMR ($CDCl_3$, 400 MHz) δ_H ppm: 1.53 (9H, s, C(C$\underline{H}_3$)$_3$), 1.91-1.94 (1H, m, C$\underline{H}_2$), 2.17-2.36 (3H, m, 2 x C$\underline{H}_2$, C$\underline{H}$CH$_2$OH), 3.06-3.11 (1H, m, C$\underline{H}_2$), 3.67-3.80 (5H, m, 1 x OC$\underline{H}_3$, 1 x C$\underline{H}_2$), 3.90 (3H, s, OC$\underline{H}_3$), 3.93 (3H, s, OC$\underline{H}_3$), 3.95 (3H, s, OC$\underline{H}_3$), 6.22 (1H, d, J = 6.21, C=C$\underline{H}$), 6.41 (1H, s, Ar$\underline{H}$), 6.76-6.82 (2H, m, Ar$\underline{H}$), 7.08 (1H, s, O$\underline{H}$), 8.16 (1H, s, Ar$\underline{H}$)

^{13}C NMR ($CDCl_3$, 400 MHz) δ_c ppm: 23.23 (C$\underline{H}_2$), 29.72 (C(C$\underline{H}_3$)$_3$), 37.95 (C$\underline{H}_2$), 40.06 (C$\underline{H}$CH$_2$OH), 55.77 (OC$\underline{H}_3$), 56.08 (OC$\underline{H}_3$), 60.88 (OC$\underline{H}_3$), 61.58 (OC$\underline{H}_3$), 66.36 (C$\underline{H}_2$), 109.01 (Ar$\underline{C}$H), 109.45 (Ar$\underline{C}$H), 117.56 (Ar$\underline{C}$H), 122.49 (Ar$\underline{C}$H), 127.83 (Q$\underline{C}$), 128.20 (Q$\underline{C}$), 128.71 (C=$\underline{C}$H), 134.82 (Q$\underline{C}$), 136.26 (Q$\underline{C}$), 141.17 (Q$\underline{C}$), 142.22 (Q$\underline{C}$), 147.10 (Q$\underline{C}$), 150.78 (Q$\underline{C}$), 151.03 (Q$\underline{C}$), 152.80 (Q$\underline{C}$)

ν_{MAX} (DCM)/cm^{-1}: 3434.07 (OH), 2931.78, 1726.83, 1588.84

HRMS $[M+Na]^+$: calculated 508.2311, found 508.2320, molecular formula ($C_{27}H_{35}NNaO_7$)

7.20.3 Attempted alkylation: Attempted synthesis of *tert*-butyl 5-((*R*,*Z*)-7-(((ethoxycarbonyl)methoxy)methyl)-6,7-dihydro-2,3,4-trimethoxy-5*H*-benzo[7]annulen-9-yl)-2-methoxyphenylcarbamate (5.11) and formation of side product *tert*-butyl 5-((*R*,*Z*)-7-((2-bromoacetoyloxy)methyl)-6,7-dihydro-2,3,4-trimethoxy-5*H*-benzo[7]annulen-9-yl)-2-methoxyphenylcarbamate (5.12)

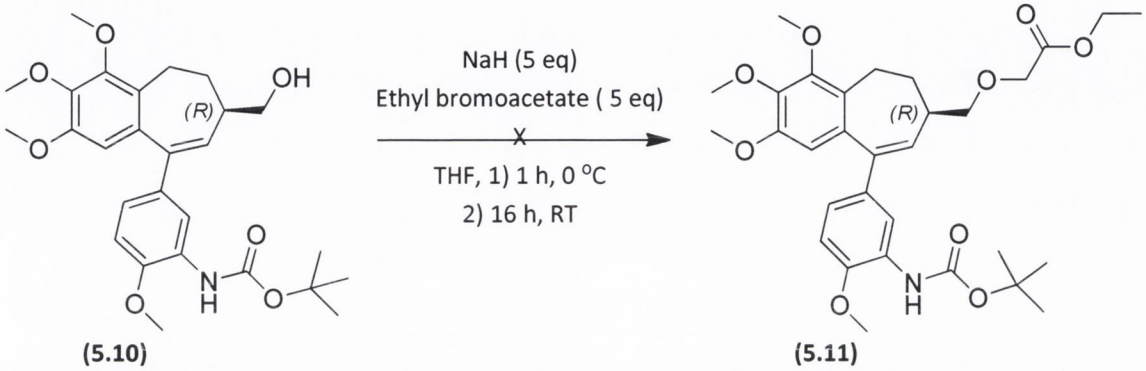

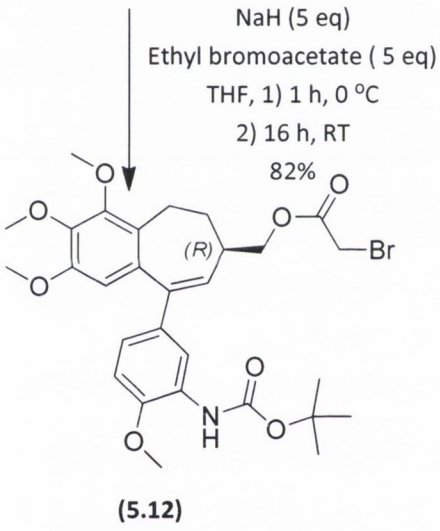

To a stirred solution of **(5.10)** (0.02 g, 0.04 mmol) in dry THF (1 mL) under an atmosphere of nitrogen at 0 °C was added ethyl bromoacetate (0.02 mL, 0.21 mmol) followed by sodium hydride (60%) dispersion in mineral oil (8mg, 0.21 mmol). After 1h, the temperature of the reaction was allowed to reach ambient. After a further 16 h, the reaction was quenched by pouring into ice-water (10 mL) and the aqueous mixture was extracted with diethyl ether (3 x 10 mL). The organic fractions were combined, dried over $MgSO_4$, filtered and concentrated *in vacuo.* The resulting residue was then purified by flash column chromatography (stationary phase; silica gel 230-400 mesh, mobile phase; 4:1 hexane/ethyl acetate) to afford **(5.12)** as a yellow oil (0.02 g, 82%).

R_f: 0.26 (3:1, hexane/ethyl acetate)

^{1}H NMR ($CDCl_3$, 400 MHz) δ_H ppm: 1.53 (9H, s, C(CH_3)$_3$), 1.92-2.00 (1H, m, CH_2), 2.18-2.26 (1H, m, CH_2), 2.29-2.36 (1H, m, CH_2), 2.39-2.45 (1H, m, $CHCH_2O$), 3.08-3.12 (1H, m, CH_2), 3.72 (3H, s, OCH_3), 3.90 (3H, s, OCH_3), 3.91-3.92 (2H, m, CH_2), 3.93 (3H, s, OCH_3), 3.95 (3H, s, OCH_3), 4.19-4.24 (1H, m, CH_2), 4.25-4.32 (1H, m, CH_2), 6.14 (1H, d, J = 6.21 Hz, C=CH), 6.41 (1H, s, ArH), 6.79 (2H, s, ArH), 7.08 (1H, s, ArH), 8.18 (1H, s, NH)

^{13}C NMR ($CDCl_3$, 400 MHz) δ_c ppm: 23.13 (CH_2), 25.94 (CH_2), 28.38 (C(CH_3)$_3$), 36.50 ($CHCH_2O$), 38.14 (CH_2), 55.77 (OCH_3), 56.07 (OCH_3), 60.87 (OCH_3), 61.56 (OCH_3), 69.08 (CH_2), 77.24 (C(CH_3)$_3$, 109.08 (ArCH), 109.46 (ArCH), 117.72 (ArCH), 122.41 (ArCH), 126.32 (QC), 127.87 (QC), 127.32 (C=CH), 127.92 (QC), 135.93 (QC), 137.90 (QC), 141.40 (QC), 142.47 (QC), 147.20 (QC), 150.81 (QC), 167.49 (QC), 170.7 (QC)

ν_{MAX} (DCM)/cm^{-1}: 3435.78, 2928.07, 1728.98, 1589.14, 1481.45

HRMS $[M+H]^+$: calculated 628.1522, found 628.1577, molecular formula ($C_{29}H_{36}BrNNaO_8$)

7.21 Synthesis of hydroxamic acid DML: Synthesis of (R)-N-hydroxy-2-(9-(3-hydroxy-4-methoxyphenyl)-2,3,4-trimethoxy-6,7-dihydro-5H-benzo[7]annulen-7-yl)acetamide (5.13)

7.21.1 Nitrile Synthesis: Synthesis of 2-((7*R*)-6,7,8,9-tetrahydro-1,2,3-trimethoxy-5-(methoxymethoxy)-5*H*-benzo[7]annulen-7-yl)acetonitrile (5.15)

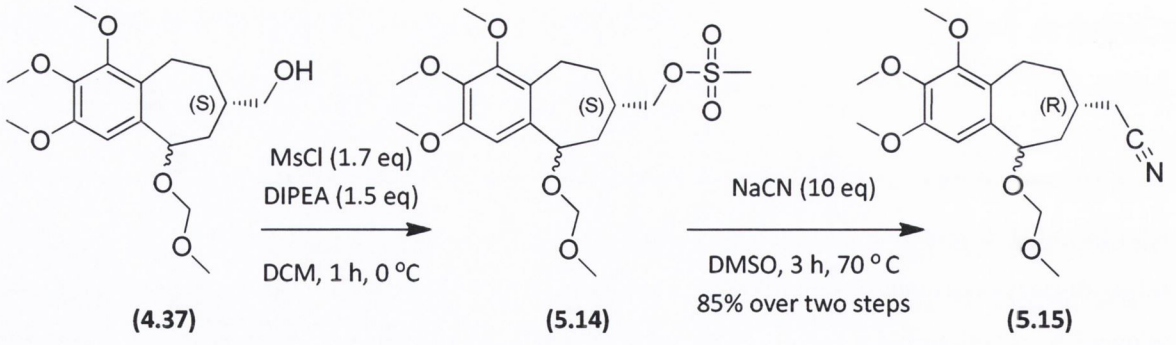

(4.37) **(5.14)** **(5.15)**

To a stirred solution of **(4.37)** (0.84 g, 2.57 mmol) in dry DCM (10 mL) under an atmosphere of nitrogen at 0 °C was added methanesulfonyl chloride (0.34 mL, 4.38 mmol) followed by *N,N*-diisopropylethylamine (0.67 mL, 3.86 mmol). After 1 h, the reaction was quenched by the addition of water (20 mL). The reaction mixture was extracted with diethyl ether (3 x 25 mL). The organic fractions were combined, dried over $MgSO_4$, filtered and concentrated *in vacuo* to afford the

mesylate **(5.14)** as a crude mixture. The mesylate was dissolved in DMSO (10 mL) at room temperature and sodium cyanide (1.26 g, 25.73 mmol) was added to the solution. The reaction was then refluxed at 70 °C for 3 h. The reaction was then quenched by the addition of water (30 mL) and extracted with diethyl ether (3 x 30 mL). The organic fractions were combined, dried over $MgSO_4$, filtered and concentrated under reduced pressure. The product was purified by flash column chromatography (stationary phase; silica gel 230-400 mesh, mobile phase; 4:1, hexane/ethyl acetate) to afford **(5.15)** as a colourless oil (0.73 g, 85% over two steps).

R_f: 0.52 (3:1, hexane/ethyl acetate)

^{1}H NMR ($CDCl_3$, 400 MHz) δ_H ppm: 1.04-1.11 (1H, m, minor diastereomer, C$\underline{H}_2$), 1.24-1.28 (1H, m, major diastereomer, C$\underline{H}_2$), 1.51-1.53 (1H, m, minor diastereomer, C$\underline{H}_2$), 1.59-1.63 (1H, m, major diastereomer, C$\underline{H}_2$), 2.03-2.06 (2H, m, major and minor diastereomers, C$\underline{H}_2$), 2.18-2.33 (6H, m, major and minor diastereomers, 5 x C$\underline{H}_2$, 1 x C$\underline{H}$CH$_2$CN), 2.55 (1H, m, major diastereomer, C$\underline{H}$CH$_2$CN), 2.77-2.81 (1H, m, major diastereomer, C$\underline{H}_2$), 3.12-3.16 (1H, m, major diastereomer, C$\underline{H}_2$), 3.32-3.37 (4H, m, major and minor diastereomers, 1 x C$\underline{H}_2$, 1 x OC$\underline{H}_3$), 3.42 (3H, s, minor diastereomer, OC$\underline{H}_3$), 3.78 (3H, s, major diastereomer, OC$\underline{H}_3$), 3.79 (3H, s, minor diastereomer, OC$\underline{H}_3$), 3.83 (3H, s, major diastereomer, OC$\underline{H}_3$), 3.86 (9H, s, major and minor diastereomers, OC$\underline{H}_3$), 4.52-4.55 (2H, m, major diastereomer, OC$\underline{H}_2$OCH$_3$), 4.68-4.78 (4H, m, major and minor diastereomers, 1 x OC$\underline{H}_2$OCH$_3$, 2 x C$\underline{H}$OCH$_2$O), 6.54 (1H, s, major diastereomer, Ar$\underline{H}$), 6.89 (1H, s, minor diastereomer, Ar$\underline{H}$)

^{13}C NMR ($CDCl_3$, 400 MHz) δ_c ppm: 22.23 (C$\underline{H}_2$), 22.65 (C$\underline{H}_2$), 25.03 (C$\underline{H}_2$), 25.27 (C$\underline{H}_2$), 32.75 (C$\underline{H}_2$), 33.15 (C$\underline{H}$CH$_2$CN), 33.49 (C$\underline{H}_2$), 37.13 (C$\underline{H}$CH$_2$CN), 38.06 (C$\underline{H}_2$), 40.61 (C$\underline{H}_2$), 55.26 (OC$\underline{H}_3$), 55.59 (OC$\underline{H}_3$), 55.88 (OC$\underline{H}_3$), 55.93 (2 x OC$\underline{H}_3$), 60.63 (OC$\underline{H}_3$), 60.65 (OC$\underline{H}_3$), 61.21 (OC$\underline{H}_3$), 74.46 (C$\underline{H}$OCH$_2$O), 76.85 (C$\underline{H}$OCH$_2$O), 93.67 (OC$\underline{H}_2$OCH$_3$), 94.85 (OC$\underline{H}_2$OCH$_3$), 103.67 (Ar$\underline{C}$H), 109.68 (Ar$\underline{C}$H), 118.23 (Q$\underline{C}$), 118.53 (Q$\underline{C}$), 124.71 (Q$\underline{C}$), 127.71 (Q$\underline{C}$), 134.94 (Q$\underline{C}$), 137.83 (Q$\underline{C}$), 140.77 (Q$\underline{C}$), 141.83 (Q$\underline{C}$), 150.55 (Q$\underline{C}$), 150.78 (Q$\underline{C}$), 151.32 (Q$\underline{C}$), 151.38 (Q$\underline{C}$)

ν_{MAX} (DCM)/cm^{-1}: 3608.21, 2933.29, 2840.52, 2244.22 (CN), 1599.32, 1582.04

HRMS $[M+Na]^+$: calculated 358.163, found 358.1628, molecular formula ($C_{18}H_{25}NNaO_5$)

7.21.2 Nitrile reduction: Synthesis of 2-((7*R*)-6,7,8,9-tetrahydro-1,2,3-trimethoxy-5-(methoxymethoxy)-5*H*-benzo[7]annulen-7-yl)ethanol (5.17)

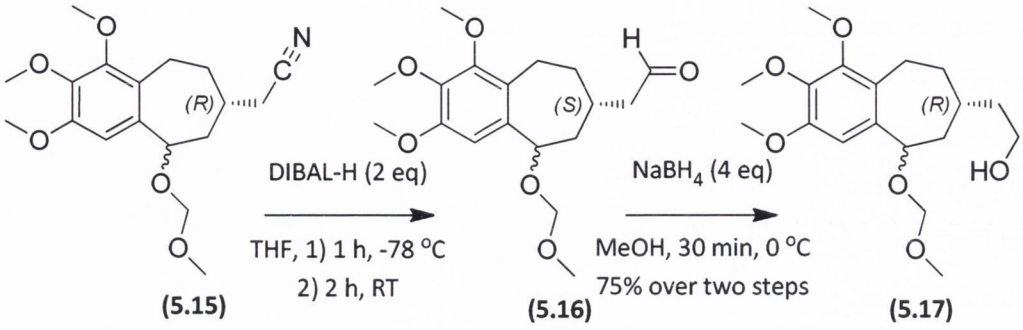

(5.15) **(5.16)** **(5.17)**

To a stirred solution of **(5.15)** (0.73 g, 2.18 mmol) in dry THF (10 mL) under an atmosphere of nitrogen at -78 °C was added 1 M DIBAL-H solution in hexane (4.36 mL, 4.36 mmol) dropwise. After 1 h, the temperature was allowed to increase to ambient. After a further 2 h, the reaction was quenched by the addition of 1 M tartaric acid aqueous solution (50 mL). The reaction mixture was then extracted with diethyl ether (3 x 75 mL). The organic fractions were combined, dried over $MgSO_4$, filtered and concentrated *in vacuo* to afford the aldehyde intermediate **(5.16)** as a crude mixture. The aldehyde was dissolved in methanol (10 mL) and the temperature of the reaction reduced to 0 °C. Sodium borohydride (0.25 g, 6.6 mmol) was slowly added to the reaction. After 30 min, the methanol was removed under reduced pressure and the reaction was quenched by the addition of water (50 mL). The reaction was then extracted with diethyl ether (3 x 75 mL). The organic fractions were combined, dried over $MgSO_4$, filtered and concentrated under reduced pressure. The product was purified by flash column chromatography (stationary phase; silica gel 230-400 mesh, mobile phase; 4:1, hexane/ethyl acetate) to yield **(5.17)** as a colourless oil (0.56 g, 75 % over two steps).

R_f: 0.14 (2:1, hexane/ethyl acetate)

^{1}H NMR ($CDCl_3$, 400 MHz) δ_H ppm: 0.83-0.89 (1H, m, minor diastereomer, C$\underline{H}_2$), 1.10-1.18 (1H, m, major diastereomer, C$\underline{H}_2$), 1.29-1.35 (1H, m, minor diastereomer, C$\underline{H}_2$), 1.46-1.54 (5H, m, major and minor diastereomers, C$\underline{H}_2$), 1.91-1.97 (3H, m, major and minor diastereomers, 1 x C$\underline{H}$C$_2$H$_4$OH, 2 x C$\underline{H}_2$), 2.04-2.27 (4H, m, major and minor diastereomers, 1 x C$\underline{H}$C$_2$H$_4$OH, 3 x C$\underline{H}_2$), 2.76-2.82 (1H, m, major diastereomer, C$\underline{H}_2$), 2.99-3.00 (1H, m, major diastereomer, C$\underline{H}_2$), 3.25-3.30 (1H, m, minor diastereomer, C$\underline{H}_2$), 3.36 (3H, s, major diastereomer, OC$\underline{H}_3$), 3.42 (3H, s, minor diastereomer, OC$\underline{H}_3$), 3.68-3.71 (4H, m, major and minor diastereomers, CH$_2$C$\underline{H}_2$OH), 3.77 (3H, s, major diastereomer, OC$\underline{H}_3$), 3.79 (3H, s, minor diastereomer, OC$\underline{H}_3$), 3.83 (3H, s, major diastereomer,

$OC\underline{H}_3$), 3.87 (9H, s, major and minor diastereomers, $OC\underline{H}_3$), 4.56 (2H, s, major diastereomer, $OC\underline{H}_2OCH_3$), 4.67-4.80 (4H, m, major and minor diastereomers, 1 x $C\underline{H}_2$, 2 x $C\underline{H}OCH_2O$), 6.57 (1H, s, major diastereomer, Ar$\underline{H}$), 6.89 (1H, s, minor diastereomer, Ar$\underline{H}$)

^{13}C NMR ($CDCl_3$, 400 MHz) δ_c ppm: 22.73 ($\underline{C}H_2$), 23.63 ($\underline{C}H_2$), 32.53 ($\underline{C}HC_2H_4OH$), 33.61 ($\underline{C}H_2$), 34.00 ($\underline{C}H_2$), 37.12 ($\underline{C}HC_2H_4OH$), 39.06 ($\underline{C}H_2$), 40.23 ($\underline{C}H_2$), 40.45 ($\underline{C}H_2$), 41.97 ($\underline{C}H_2$), 55.36 ($O\underline{C}H_3$), 55.65 ($O\underline{C}H_3$), 55.97 ($O\underline{C}H_3$), 56.02 ($O\underline{C}H_3$), 60.18 ($\underline{C}H_2$), 60.55 ($\underline{C}H_2$), 60.81 ($O\underline{C}H_3$), 60.83 ($O\underline{C}H_3$), 61.35 (2 x $O\underline{C}H_3$), 75.52 ($\underline{C}HOCH_2O$), 77.45 ($\underline{C}HOCH_2O$), 93.98 ($O\underline{C}H_2OCH_3$), 94.99 ($O\underline{C}H_2OCH_3$), 103.37 (Ar$\underline{C}H$), 109.09 (Ar$\underline{C}H$), 125.75 ($\underline{Q}C$), 128.44 ($\underline{Q}C$), 136.00 ($\underline{Q}C$), 138.89 ($\underline{Q}C$), 140.57 ($\underline{Q}C$), 141.61 ($\underline{Q}C$), 150.45 ($\underline{Q}C$), 150.75 ($\underline{Q}C$), 151.19, ($\underline{Q}C$), 151.26 ($\underline{Q}C$)

ν_{MAX} (DCM)/cm^{-1}: 3428.23 (OH), 2927.14, 2852.12, 1599.47, 1583.34

HRMS $[M+Na]^+$: calculated 363.1784, found 363.1786, molecular formula ($C_{18}H_{28}NaO_6$)

7.21.3 Silyl Protection: Synthesis of (2-((7*R*)-6,7,8,9-tetrahydro-1,2,3-trimethoxy-5-(methoxymethoxy)-5*H*-benzo[7]annulen-7-yl)ethoxy)(*tert*-butyl)diphenylsilane (5.18)

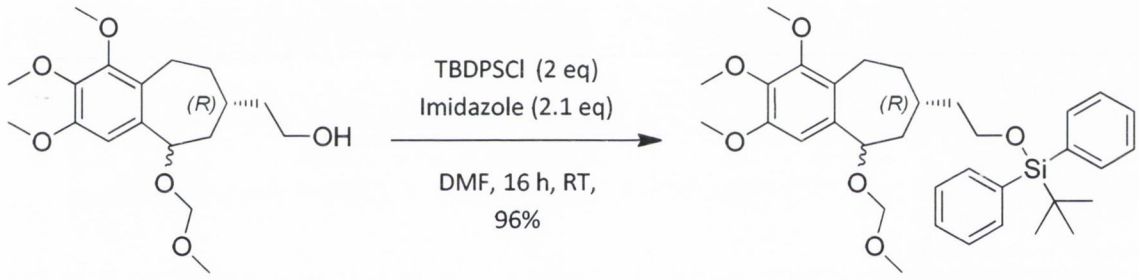

(5.17) **(5.18)**

To a stirred solution of **(5.17)** (0.56 g, 1.65 mmol) and imidazole (0.24 g, 3.45 mmol) in dry DMF (10 mL) under an atmosphere of nitrogen at room temperature was added *tert*-butyldiphenylsilyl chloride (0.86 ml, 3.29 mmol). After 16 h, the reaction was quenched by the addition of water (50 mL) and extracted with diethyl ether (3 x 50 mL). The organic fractions were combined, dried over $MgSO_4$, filtered and concentrated under reduced pressure. The product was purified by flash column chromatography (stationary phase; silica gel 230-400 mesh, mobile phase; 20:1, hexane/ethyl acetate) to afford **(5.18)** as a colourless oil (0.92 g, 96%).

R_f: 0.54 (3:1, hexane/ethyl acetate)

^1H NMR ($CDCl_3$, 400 MHz) δ_H ppm: 0.82-0.98 (1H, m, minor diastereomer, $C\underline{H}_2$), 1.07 (9H, s, major diastereomer, $C(C\underline{H}_3)_3$), 1.09 (9H, s, minor diastereomer, $C(C\underline{H}_3)_3$), 1.22-1.38 (1H, m, major diastereomer, $C\underline{H}_2$), 1.45-1.62 (3H, m, major and minor diastereomers, $C\underline{H}_2$), 1.85-1.88 (1H, m,

minor diastereomer, C<u>H</u>$_2$), 2.08-2.11 (4H, m, major and minor diastereomers, 1 x C<u>H</u>C$_2$H$_4$OSi, 3 x C<u>H</u>$_2$), 2.21-2.28 (2H, m, major and minor diastereomers, 1 x C<u>H</u>$_2$, C<u>H</u>C$_2$H$_4$OSi), 2.78-2.84 (1H, m, major diastereomer, C<u>H</u>$_2$), 2.96 (1H, m, major diastereomer, C<u>H</u>$_2$), 3.24-3.28 (1H, m, minor diastereomer, C<u>H</u>$_2$), 3.87 (3H, s, major diastereomer, OC<u>H</u>$_3$), 3.44 (3H, s, minor diastereomer, OC<u>H</u>$_3$), 3.73-3.77 (4H, m, C<u>H</u>$_2$), 3.80 (3H, s, major diastereomer, OC<u>H</u>$_3$), 3.81 (3H, s, minor diastereomer, OC<u>H</u>$_3$), 3.86 (3H, s, major diastereomer, OC<u>H</u>$_3$), 3.89 (9H, s, major and minor diastereomers, OC<u>H</u>$_3$), 4.59 (2H, s, major diastereomer, OC<u>H</u>$_2$OCH$_3$), 4.70-4.81 (4H, m, major and minor diastereomers, 1 x C<u>H</u>$_2$, 2 x C<u>H</u>OCH$_2$O), 6.60 (1H, s, major diastereomer, Ar<u>H</u>), 6.92 (1H, s, minor diastereomer, Ar<u>H</u>), 7.39-7.45 (12H, m, major and minor diastereomers, Ar<u>H</u>), 7.69-7.70 (8H, m, major and minor diastereomers, Ar<u>H</u>)

^{13}C NMR ($CDCl_3$, 400 MHz) δ_c ppm: 18.76 (2 x <u>C</u>(CH$_3$)$_3$), 22.23 (<u>C</u>H$_2$), 23.23 (<u>C</u>H$_2$), 26.41 (2 x C(<u>C</u>H$_3$)$_3$), 32.01 (<u>C</u>HC$_2$H$_4$OSi), 33.14 (<u>C</u>H$_2$), 33.35 (<u>C</u>H$_2$), 36.79 (<u>C</u>HC$_2$H$_4$OSi), 38.66 (<u>C</u>H$_2$), 39.51 (<u>C</u>H$_2$), 39.85 (<u>C</u>H$_2$), 41.51 (<u>C</u>H$_2$), 54.88 (O<u>C</u>H$_3$), 55.21 (O<u>C</u>H$_3$), 55.54 (O<u>C</u>H$_3$), 55.58 (O<u>C</u>H$_3$), 60.41 (2 x O<u>C</u>H$_3$), 60.94 (2 x O<u>C</u>H$_3$)), 61.06 (<u>C</u>H$_2$), 61.46 (<u>C</u>H$_2$), 74.98 (<u>C</u>HOCH$_2$O), 76.79 (<u>C</u>HOCH$_2$O), 93.47 (O<u>C</u>H$_2$OCH$_3$), 94.45 (O<u>C</u>H$_2$OCH$_3$), 102.85 (Ar<u>C</u>H), 108.30 (Ar<u>C</u>H), 125.48 (<u>Q</u>C), 127.16 (4 x Ar<u>C</u>H), 127.19 (4 x Ar<u>C</u>H), 129.09 (2 x Ar<u>C</u>H), 129.14 (2 x Ar<u>C</u>H), 133.51 (<u>Q</u>C), 133.59 (<u>Q</u>C), 135.10 (4 x Ar<u>C</u>H), 135.13 (4 x Ar<u>C</u>H), 135.80 (<u>Q</u>C), 138.50 (<u>Q</u>C), 140.10 (<u>Q</u>C), 141.07 (<u>Q</u>C), 149.99 (<u>Q</u>C), 150.31 (<u>Q</u>C), 150.71 (<u>Q</u>C), 150.81 (<u>Q</u>C)

ν_{MAX} (DCM)/cm^{-1}: 3332.15, 2931.75, 2857.05, 1673.72, 1589.74

HRMS [M+Na]$^+$: calculated 601.2961, found 601.2967, molecular formula ($C_{34}H_{46}NaO_6Si$)

7.21.4 MOM deprotection and oxidation of alcohol: Synthesis of (7*R*)-7-{2-[(*tert*-butyldiphenylsilyl)oxy]ethyl}-1,2,3-trimethoxy-6,7,8,9-tetrahydro-5*H*-benzo[7]annulen-5-one (5.20)

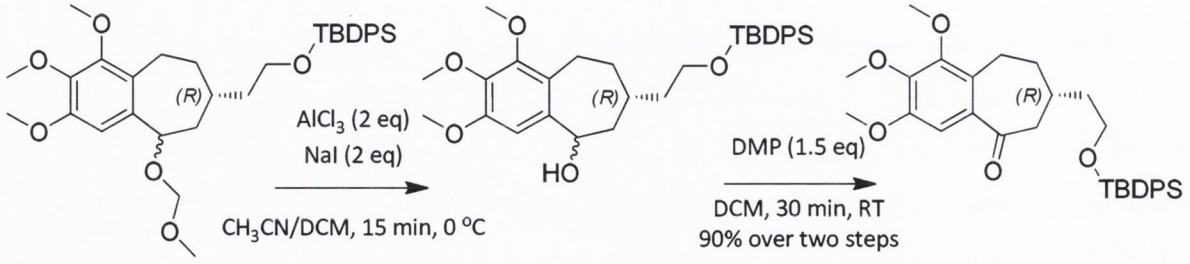

(5.18) **(5.19)** **(5.20)**

To a stirred solution of **(5.18)** (0.92 g, 1.59 mmol) in a mixture of acetonitrile and DCM (2:1; 10 mL) at 0 °C was added aluminium chloride (0.42 g, 3.18 mmol) and sodium iodide (0.48 g, 3.18 mmol). After 15 min, the reaction was quenched by the addition of saturated sodium bicarbonate aqueous solution (50 mL). The reaction was extracted with DCM (3 x 20 mL). To a stirred solution of the combined organic fractions was added Dess-Martin periodinane (1.01 g, 2.38 mmol). After 30 min, the reaction was quenched by the addition of saturated sodium bicarbonate aqueous solution (50 mL) and the reaction was extracted with diethyl ether (3 x 50 mL). The organic fractions were combined, dried over $MgSO_4$, filtered and concentrated under reduced pressure. The product was purified by flash column chromatography (stationary phase; silica gel 230-400 mesh, mobile phase; 10:1, hexane/ethyl acetate) to afford **(5.20)** as a colourless oil (0.76 g, 90% over two steps).

R_f: 0.43 (3:1, hexane/ethyl acetate)

$[\alpha]_D^{25}$ = - 2.85 (*c* = 12.63, DCM)

^{1}H NMR ($CDCl_3$, 400 MHz) δ_H ppm: (9H, s, C(CH_3)$_3$), 1.50 (1H, m, CH_2), 160-1.73 (2H, m, CH_2), 1.94-1.97 (1H, m, CH_2), 2.29 (CHC$_2$H$_5$OSi), 2.55-2.61 (1H, m, CH_2), 2.79-2.88 (2H, m, CH_2), 3.05-3.09 (1H, m, CH_2), 3.73-3.76 (CH_2OSi), 3.86 (3H, s, OCH_3), 3.90 (3H, s, OCH_3), 3.96 (3H, s, OCH_3), 7.16 (1H, s, ArH), 7.39-7.45 (6H, m, ArH), 7.66-7.68 (4H, m, ArH)

^{13}C NMR ($CDCl_3$, 400 MHz) δ_c ppm: 18.75 (C(CH$_3$)$_3$), 22.20 (CH_2), 26.40 (C(CH_3)$_3$), 29.67 (CHC$_2$H$_5$OSi), 31.82 (CH_2), 37.72 (CH_2), 46.32 (CH_2), 55.53 (OCH_3), 60.45 (OCH_3), 60.83 (OCH_3), 61.21 (CH_2), 106.82 (ArCH), 127.22 (4 x ArCH), 129.19 (2 x ArCH), 129.63 (QC), 133.34 (QC), 133.92 (QC), 135.08 (4 x ArCH), 145.21 (QC), 150.52 (QC), 151.03 (QC), 202.82 (C=O)

ν_{MAX} (DCM)/cm^{-1}: 2931.70, 2856.99, 1673.59 (C=O), 1589.73

HRMS $[M+Na]^+$: calculated 555.2543, found 555.2543, molecular formula ($C_{32}H_{40}NaO_5Si$)

7.21.5 Silyl deprotection: Synthesis of (*R*)-6,7,8,9-tetrahydro-7-(2-hydroxyethyl)-1,2,3-trimethoxybenzo[7]annulen-5-one (5.21)

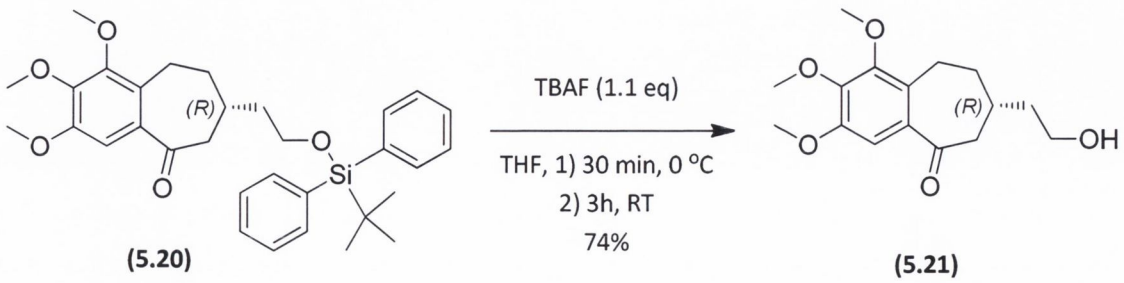

(5.20) **(5.21)**

To a stirred solution of **(5.20)** (0.76 g, 1.43 mmol) in dry THF (5 mL) under an atmosphere of nitrogen at 0 °C was added 1 M TBAF solution in THF (1.57 mL, 1.57 mmol). After 30 min, the temperature of the reaction was allowed to increase to ambient. After 3 h, the THF was blown off in a stream of nitrogen gas and the resulting residue added directly to a silica gel flash column and purified by flash column chromatography (stationary phase; silica gel 230-400 mesh, mobile phase; 1:1, hexane/ethyl acetate) to afford **(5.21)** as a yellow oil (0.31 g, 74%).

R_f: 0.08 (2:1, hexane/ethyl acetate)

$[\alpha]_D^{25}$ = + 4 (*c* = 8.5, DCM)

^{1}H NMR ($CDCl_3$, 400 MHz) δ_H ppm: 1.48 (1H, m, C<u>H</u>$_2$), 1.62-1.63 (2H, m, C<u>H</u>$_2$), 1.98-2.03 (1H, m, C<u>H</u>$_2$), 2.11 (1H, m, C<u>H</u>C$_2$H$_4$OH), 2.57-2.63 (1H, m, C<u>H</u>$_2$), 2.80-2.90 (2H, m, C<u>H</u>$_2$), 3.01-3.05 (1H, m, C<u>H</u>$_2$), 3.69 (2H, m, C<u>H</u>$_2$), 3.82 (3H, s, OC<u>H</u>$_3$), 3.86 (3H, s, OC<u>H</u>$_3$), 3.91 (3H, s, OC<u>H</u>$_3$), 7.12 (Ar<u>H</u>)

^{13}C NMR ($CDCl_3$, 400 MHz) δ_c ppm: 22.70 (<u>C</u>H$_2$), 30.15 (<u>C</u>HC$_2$H$_4$OH), 32.42 (<u>C</u>H$_2$), 38.37 (<u>C</u>H$_2$), 46.56 (<u>C</u>H$_2$), 55.95 (O<u>C</u>H$_3$), 60.33 (<u>C</u>H$_2$), 60.86 (O<u>C</u>H$_3$), 61.26 (O<u>C</u>H$_3$), 107.34 (Ar<u>C</u>H), 130.24 (<u>Q</u>C), 134.14 (<u>Q</u>C), 145.75 (<u>Q</u>C), 150.96 (<u>Q</u>C), 151.48 (<u>Q</u>C), 203.22 (<u>C</u>=O)

ν_{MAX} (DCM)/cm^{-1}: 3422.79 (OH), 2933.35, 1668.82 (C=O), 1589.31

HRMS $[M+Na]^+$: calculated 317.1365, found 317.1368, molecular formula ($C_{16}H_{22}NaO_5$)

7.21.6 Organolithium C-Ring Coupling: Synthesis of 2-[(7*R*)-9-{3-[(*tert*-butyldimethylsilyl)oxy]-4-methoxyphenyl}-2,3,4-trimethoxy-6,7-dihydro-5*H*-benzo[7]annulen-7-yl]ethan-1-ol (5.21)

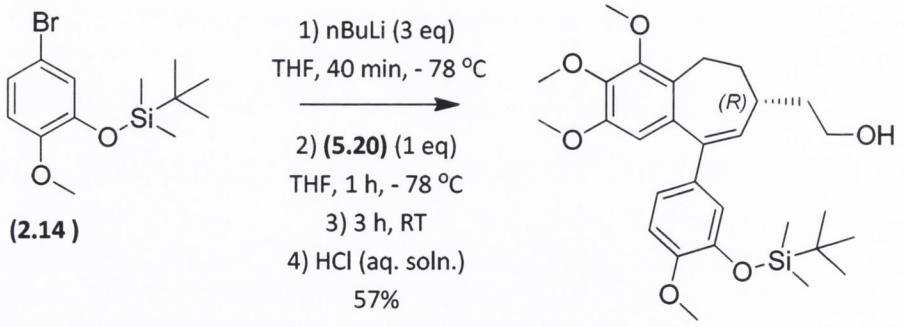

(2.14) **(5.21)**

To a stirred solution of **(2.14)** (1 g, 3.16 mmol) in dry THF (10 mL) at -78 °C under an atmosphere of nitrogen was added 2.5 M nBuLi solution in hexane (1.26 mL, 3.16 mmol) dropwise. After 40 min, a solution of **(5.21)** (0.31 g, 1.05 mmol) in dry THF (5 mL) was added to the reaction dropwise. After 1 h, the reaction was allowed to increase to ambient. After a further 3 h, the

reaction was quenched by the addition of 2 M HCl aqueous solution (25 mL) and was extracted with diethyl ether (3 x 50 mL). The organic fractions were combined, dried over $MgSO_4$, filtered and concentrated under reduced pressure. The product was purified by flash column chromatography (stationary phase; silica gel 230-400 mesh, mobile phase; 4:1, hexane/ethyl acetate) to afford **(5.21)** as a yellow oil (0.31 g, 57%).

R_f: 0.31 (2:1, hexane/ethyl acetate)

$[\alpha]_D^{25}$ = - 41.94 (*c* = 5.53, DCM)

^{1}H NMR ($CDCl_3$, 400 MHz) δ_H ppm: 0.15 (6H, d, J = 5.67 Hz, Si($C\underline{H}_3$)$_2$), 0.99 (9H, s, C($C\underline{H}_3$)$_3$), 1.67-1.70 (1H, m, $C\underline{H}_2$), 1.77-1.90 (2H, m, $C\underline{H}_2$), 2.05-2.09 (1H, m, $C\underline{H}C_2H_5OH$), 2.19-2.29 (2H, m, $C\underline{H}_2$), 3.03-3.05 (1H, m, $C\underline{H}_2$), 3.69 (5H, s, 1 x $OC\underline{H}_3$, 1 x $C\underline{H}_2$), 3.82 (3H, s, $OC\underline{H}_3$), 3.91 (3H, s, $OC\underline{H}_3$), 3.93 (3H, s, $OC\underline{H}_3$), 6.03 (1H, d, J = 6.07 Hz, C=C$\underline{H}$), 6.37 (1H, s, Ar$\underline{H}$), 6.76-6.85 (3H, m, Ar$\underline{H}$)

^{13}C NMR ($CDCl_3$, 400 MHz) δ_c ppm: -5.00 (Si($\underline{C}H_3$)$_2$), -4.98 (Si($\underline{C}H_3$)$_2$), 18.00 ($\underline{C}$(CH_3)$_3$), 23.07 ($\underline{C}H_2$), 25.28 (C($\underline{C}H_3$)$_3$), 33.16 ($\underline{C}HC_2H_4OH$), 37.96 ($\underline{C}H_2$), 41.63 ($\underline{C}H_2$), 55.06 ($O\underline{C}H_3$), 55.41 ($O\underline{C}H_3$), 60.42 ($O\underline{C}H_3$), 61.13 ($O\underline{C}H_3$), 61.17 ($\underline{C}H_2$), 108.34 (Ar$\underline{C}$H), 111.16 (Ar$\underline{C}$H), 120.20 (Ar$\underline{C}$H), 120.84 (Ar$\underline{C}$H), 127.76 (Q$\underline{C}$), 131.17 (C=$\underline{C}$H), 134.41 (Q$\underline{C}$), 135.81 (Q$\underline{C}$), 140.62 (Q$\underline{C}$), 140.70 (Q$\underline{C}$), 144.08 (Q$\underline{C}$), 149.89 (Q$\underline{C}$), 150.27 (Q$\underline{C}$), 150.45 (Q$\underline{C}$)

ν_{MAX} (DCM)/cm^{-1}: 3412.73, 2930.30, 2856.45, 1596.72

HRMS $[M+Na]^+$: calculated 537.2648, found 537.2678, molecular formula ($C_{29}H_{42}NaO_6Si$)

7.21.7 Silyl deprotection: Synthesis of 5-((*R*,*Z*)-6,7-dihydro-7-(2-hydroxyethyl)-2,3,4-trimethoxy-5*H*-benzo[7]annulen-9-yl)-2-methoxyphenol (5.22)

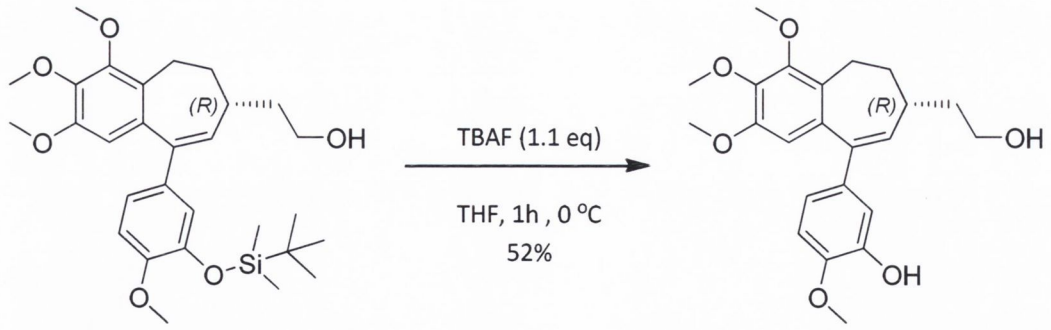

(5.21) **(5.22)**

To a stirred solution of **(5.21)** (0.04 g, 0.08 mmol) in dry THF (1 mL) under an atmosphere of nitrogen at 0 °C was added 1 M TBAF solution in THF (0.09 mL, 0.09 mmol). After 1 h, the THF was blown off in a stream of nitrogen gas and the resulting residue added directly to a silica gel flash

column and purified by flash column chromatography (stationary phase; silica gel 230-400 mesh, mobile phase; 1:1, hexane/ethyl acetate) to afford **(5.22)** as a white solid (0.02 g, 52%).

R_f: 0.45 (1:1, hexane/ethyl acetate)

$[\alpha]_D^{25}$ = - 95.7 (*c* = 0.61, DCM)

^{1}H NMR ($CDCl_3$, 400 MHz) δ_H ppm: 1.62-1.71 (1H, m, C<u>H</u>$_2$), 1.77-1.80 (1H, m, C<u>H</u>$_2$), 1.82-1.90 (1H, m, C<u>H</u>$_2$), 2.07-2.13 (1H, m, C<u>H</u>C$_2$H$_4$OH), 2.16-2.31 (2H, m, C<u>H</u>$_2$), 3.03-3.05 (1H, m, C<u>H</u>$_2$), 3.71 (5H, m, 1 x C<u>H</u>$_2$, 1 x OC<u>H</u>$_3$), 3.91 (6H, s, OC<u>H</u>$_3$), 3.94 (3H, s, OC<u>H</u>$_3$), 6.06 (1H, d, J = 5.82 Hz, C=C<u>H</u>), 6.39 (1H, s, Ar<u>H</u>), 6.76-6.81 (2H, m, Ar<u>H</u>), 6.91 (1H, s, Ar<u>H</u>)

^{13}C NMR ($CDCl_3$, 400 MHz) δ_c ppm: 23.04 (<u>C</u>H$_2$), 33.15 (<u>C</u>HC$_2$H$_4$OH), 37.92 (<u>C</u>H$_2$), 41.58 (<u>C</u>H$_2$), 55.53 (2 x O<u>C</u>H$_3$), 60.43 (O<u>C</u>H$_3$), 61.13 (O<u>C</u>H$_3$), 61.24 (<u>C</u>H$_2$), 108.42 (Ar<u>C</u>H), 109.81 (Ar<u>C</u>H), 113.71 (Ar<u>C</u>H), 119.25 (Ar<u>C</u>H), 125.44 (Q<u>C</u>), 127.79 (Q<u>C</u>), 131.57 (C=<u>C</u>H), 134.99 (Q<u>C</u>), 135.62 (Q<u>C</u>), 140.70 (Q<u>C</u>), 144.78 (Q<u>C</u>), 145.54 (Q<u>C</u>), 150.30 (Q<u>C</u>), 150.52 (Q<u>C</u>)

ν_{MAX} (DCM)/cm^{-1}: 3406.33 (OH), 2929.14, 2850.04, 1580.55, 1508.57

HRMS $[M+Na]^+$: calculated 423.1784, found 423.1818, molecular formula ($C_{23}H_{28}NaO_6$)

Melting point: 75-76 °C

7.21.8 Two step oxidation of alcohol to carboxylic acid: Synthesis of 2-[(7*R*)-9-{3-[(*tert*-butyldimethylsilyl)oxy]-4methoxyphenyl}-2,3,4-trimethoxy-6,7-dihydro-5*H*-benzo[7]annulen-7-yl]acetic acid (5.24)

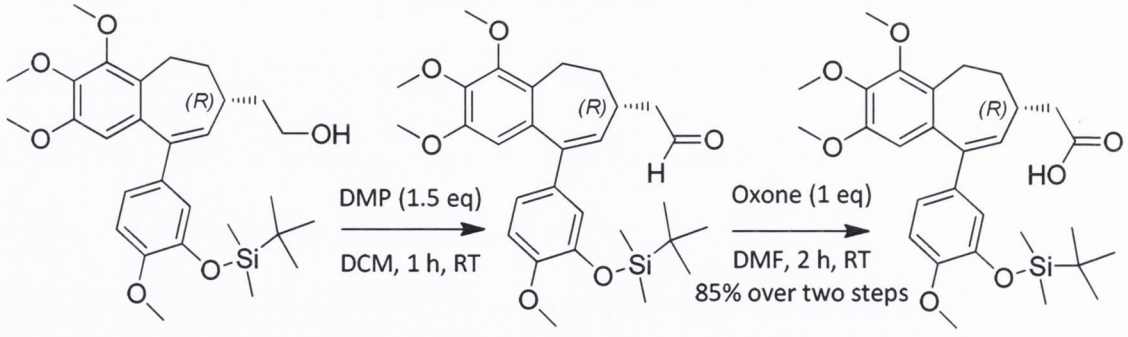

(5.21) **(5.23)** **(5.24)**

To a stirred solution of **(5.21)** (0.16 g, 0.31 mmol) in DCM (5 mL) at room temperature was added Dess-Martin periodinane (0.20 g, 0.47 mmol). After 1 h, the reaction was quenched by the addition of saturated sodium bicarbonate aqueous solution (10 mL). The reaction was extracted with diethyl ether (3 x 20 mL). The organic fractions were combined, dried over $MgSO_4$, filtered and concentrated under reduced pressure. To a stirred solution of the resulting residue

reconstituted in DMF (2 mL) was added oxone (0.19 g, 0.31 mmol). After 2 h, the reaction was quenched by the addition of water (10 mL) and extracted with diethyl ether (3 x 10 mL). The organic fractions were combined, dried over $MgSO_4$, filtered and concentrated under reduced pressure. The product was purified by flash column chromatography (stationary phase; silica gel 230-400 mesh, mobile phase; 5:95, methanol/ethyl acetate) to afford **(5.24)** as a yellow resin (0.14 g, 85%).

R_f: 0.32 (66:33:1, hexane/ethyl acetate/formic acid)

$[\alpha]_D^{25}$ = - 51.81 (*c* = 3.59, DCM)

^{1}H NMR ($CDCl_3$, 400 MHz) δ_H ppm: 0.16 (6H, d, J = 5.67 Hz, (Si(C<u>H</u>$_3$)$_2$), 0.99 (9H, s, C(C<u>H</u>$_3$)$_3$), 1.93-1.97 (1H, m, C<u>H</u>$_2$), 2.26-2.37 (2H, m, C<u>H</u>$_2$), 2.44-2.52 (2H, m, 1 x C<u>H</u>CH$_2$COOH, 1 x C<u>H</u>$_2$), 2.55-2.59 (1H, m, C<u>H</u>$_2$), 3.06-3.07 (1H, m, C<u>H</u>$_2$), 3.70 (3H, s, OC<u>H</u>$_3$), 3.84 (3H, s, OC<u>H</u>$_3$), 3.93 (3H, s, OC<u>H</u>$_3$), 3.94 (3H, s, OC<u>H</u>$_3$), 6.06 (1H, d, J = 5.61 Hz, C=C<u>H</u>), 6.77 (1H, d, J = 1.96 Hz, Ar<u>H</u>), 6.80 (1H, d, J = 8.38 Hz, Ar<u>H</u>), 6.87 (1H, dd, J_1 = 8.38 Hz, J_2 = 1.96 Hz, Ar<u>H</u>)

^{13}C NMR ($CDCl_3$, 400 MHz) δ_c ppm: -4.56 (Si(<u>C</u>H$_3$)$_2$), -4.54 (Si(<u>C</u>H$_3$)$_2$), 18.46 (<u>C</u>(CH$_3$)$_3$), 23.39 (<u>C</u>H$_2$), 25.74 (C(<u>C</u>H$_3$)$_3$), 33.81 (<u>C</u>HCH$_2$COOH), 39.54 (<u>C</u>H$_2$), 41.65 (<u>C</u>H$_2$), 55.56 (O<u>C</u>H$_3$), 55.90 (O<u>C</u>H$_3$) 60.89 (O<u>C</u>H$_3$), 61.61 (O<u>C</u>H$_3$), 108.95 (Ar<u>C</u>H), 111.68 (Ar<u>C</u>H), 120.81 (Ar<u>C</u>H), 121.40 (Ar<u>C</u>H), 127.82 (<u>C</u>), 129.43 (C=<u>C</u>H), 134.65 (<u>C</u>), 135.92 (<u>C</u>), 141.25 (<u>C</u>), 141.49 (<u>C</u>), 144.58 (<u>C</u>), 150.50 (<u>C</u>), 150.79 (<u>C</u>), 151.08 (<u>C</u>), 178.61 (<u>C</u>OOH)

ν_{MAX} (DCM)/cm^{-1}: 2954.62, 2931.23, 2856.55, 1707.96 (C=O), 1598.03, 1571.42

HRMS $[M+Na]^+$: calculated 551.2441, found 551.2396, molecular formula ($C_{29}H_{40}NaO_7Si$)

7.21.9 Silyl deprotection: Synthesis 2-((*R*,*Z*)-6,7-dihydro-9-(3-hydroxy-4-methoxyphenyl)-2,3,4-trimethoxy-5*H*-benzo[7]annulen-7-yl)acetic acid (5.25)

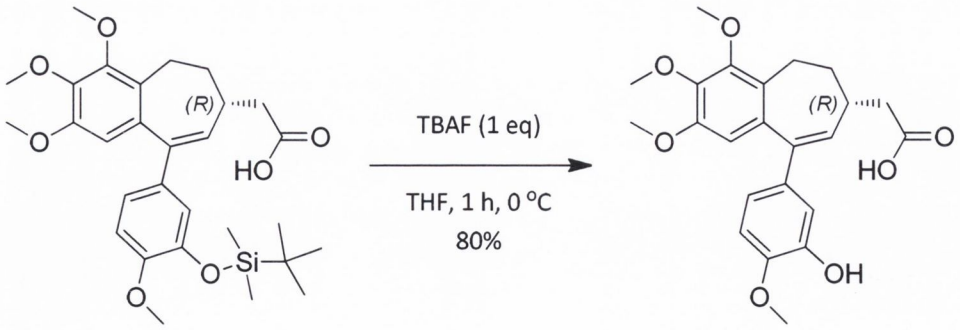

(5.24) **(5.25)**

To a stirred solution of **(5.24)** (0.03 g, 0.06 mmol) in dry THF (1 mL) under an atmosphere of nitrogen at 0 °C was added 1 M TBAF solution in THF (0.09 mL, 0.09 mmol). After 1 h, the THF was blown off in a stream of nitrogen gas and the resulting residue washed with water and extracted with diethyl ether (3 x 10 mL). The organic fractions were combined, dried over $MgSO_4$, filtered and concentrated under reduced pressure. The product was purified by flash column chromatography (stationary phase; silica gel 230-400 mesh, mobile phase; 1:9, methanol/ethyl acetate) to afford **(5.25)** as an off white solid (0.02 g, 80%).

R_f: 0.28 (50:50:1, hexane/ethyl acetate/formic acid)

$[\alpha]_D^{25}$ = - 40 (*c* = 1, DCM)

^{1}H NMR ($CDCl_3$, 400 MHz) δ_H ppm: 1.92-1.96 (1H, m, C$\underline{H}_2$), 2.20-2.35 (2H, m, C$\underline{H}_2$), 2.45-2.47 (2H, m, 1 x C$\underline{H}_2$, 1 x C$\underline{H}$CH$_2$COOH), 2.54-2.58 (1H, m, C$\underline{H}_2$), 3.06-3.06 (1H, m, C$\underline{H}_2$), 3.71 (3H, s, OC$\underline{H}_3$), 3.92 (6H, s, OC$\underline{H}_3$), 3.94 (3H, s, OC$\underline{H}_3$), 5.60 (1H, s, br, O$\underline{H}$), 6.09 (1H, d, J =4.36 Hz, C=C$\underline{H}$), 6.40 (1H, s, Ar$\underline{H}$), 6.80 (2H, s, Ar$\underline{H}$), 6.90 (1H, s, Ar$\underline{H}$)

^{13}C NMR ($CDCl_3$, 400 MHz) δ_c ppm: 22.88 (C$\underline{H}_2$), 33.31 (C$\underline{H}$CH$_2$COOH), 38.92 (C$\underline{H}_2$), 41.10 (C$\underline{H}_2$), 55.55 (2 x OC$\underline{H}_3$), 60.44 (OC$\underline{H}_3$), 61.15 (OC$\underline{H}_3$), 108.54 (ArC$\underline{H}$), 109.80 (ArC$\underline{H}$), 113.80 (ArC$\underline{H}$), 119.40 (ArC$\underline{H}$), 127.35 (Q$\underline{C}$), 129.41 (C=C$\underline{H}$), 134.76 (Q$\underline{C}$), 135.31 (Q$\underline{C}$), 140.82 (Q$\underline{C}$), 140.95 (Q$\underline{C}$), 144.74 (Q$\underline{C}$), 145.61 (Q$\underline{C}$), 150.32 (Q$\underline{C}$), 150.67 (Q$\underline{C}$), 177.34 ($\underline{C}$OOH)

ν_{MAX} (DCM)/cm^{-1}: 2921.18, 2852.21, 1707.44 (C=O), 1508.50

HRMS $[M+Na]^+$: calculated 437.1576, found 437.1613, molecular formula ($C_{23}H_{26}NaO_7$)

Melting point: 122-123 °C

7.21.10 PFP ester formation: Synthesis of 2-[(7*R*)-9-{3-[(*tert*-butyldimethylsilyl)oxy]-4-methoxyphenyl}-2,3,4-trimethoxy-6,7-dihydro-5*H*-benzo[7]annulen-7-yl]acetate (5.26)

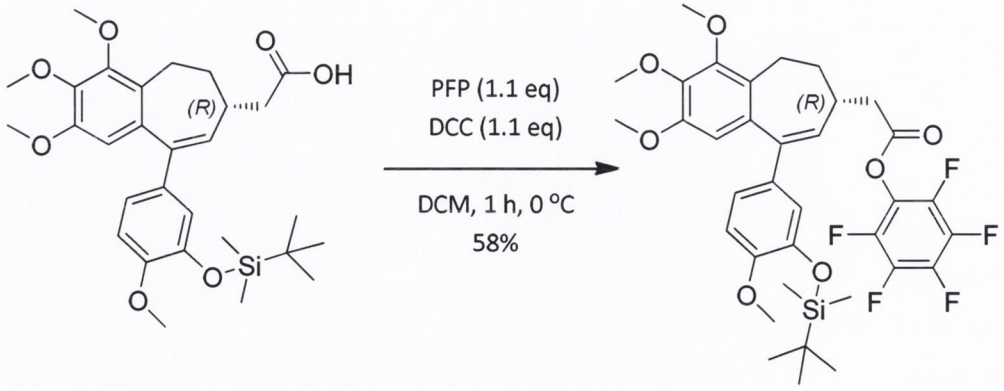

(5.24) **(5.26)**

To a stirred solution of **(5.24)** (0.08 g, 0.15 mmol) and pentafluorophenol (0.03 g, 0.17 mmol) in dry DCM (1 mL) under an atmosphere of nitrogen at 0 °C was added a solution of DCC (0.03 g, 0.17 mmol) in dry DCM (0.5 mL). After 1 h, the DCM was removed under reduced pressure and the resulting residue was added directly to a flash column and purified by flash column chromatography (stationary phase; silica gel 230-400 mesh, mobile phase; 20:1, hexane/ethyl acetate) to yield **(5.26)** as a yellow oil (0.06 g, 58%).

R_f: 0.63 (3:1, hexane/ethyl acetate)

$[\alpha]_D^{25}$ = - 37.2 (*c* = 3.33, DCM)

^{1}H NMR ($CDCl_3$, 400 MHz) δ_H ppm: 0.16 (6H, d, J = 7.59, Si($C\underline{H}_3$)$_2$), 1.00 (9H, s, C($C\underline{H}_3$)$_3$), 2.01-2.07 (1H, m, $C\underline{H}_2$), 2.31-2.36 (2H, m, $C\underline{H}_2$), 2.61-2.69 (1H, m, $C\underline{H}_2$), 2.75-2.80 (1H, m, $C\underline{H}_2$), 2.85-2.90 (1H, m, $C\underline{H}_2$), 3.10-3.12 (1H, m, $C\underline{H}_2$), 3.71 (3H, s, $OC\underline{H}_3$), 3.84 (3H, s, $OC\underline{H}_3$), 3.94 (3H, s, $OC\underline{H}_3$), 3.95 (3H, s, $OC\underline{H}_3$), 6.08 (1H, d, J = 6.16 Hz, C=C$\underline{H}$), 6.40 (1H, s, Ar$\underline{H}$), 6.81-6.86 (3H, s, Ar$\underline{H}$)

^{13}C NMR ($CDCl_3$, 400 MHz) δ_c ppm: -4.64 (Si($\underline{C}H_3$), -4.59 (Si($\underline{C}H_3$), 18.42 ($\underline{C}$(CH_3)$_3$), 23.32 ($\underline{C}H_2$), 25.68 (C($\underline{C}H_3$)$_3$), 34.12 ($\underline{C}$HCH$_2$CO), 38.80 ($\underline{C}H_2$), 41.60 ($\underline{C}H_2$), 55.51 ($O\underline{C}H_3$), 55.92 ($O\underline{C}H_3$), 60.88 ($O\underline{C}H_3$), 61.59 ($O\underline{C}H_3$), 108.95 (Ar$\underline{C}$H), 111.63 (Ar$\underline{C}$H), 120.73 (Ar$\underline{C}$H), 121.49 (Ar$\underline{C}$H), 127.63 (Q$\underline{C}$), 128.11 (C=$\underline{C}$H), 134.46 (Q$\underline{C}$), 135.85 (Q$\underline{C}$), 136.59 (Q$\underline{C}$), 139.14 (Q$\underline{C}$), 139.88 (Q$\underline{C}$), 141.38 (Q$\underline{C}$), 142.28 (Q$\underline{C}$), 142.46 (Q$\underline{C}$), 144.64 (Q$\underline{C}$), 150.62 (Q$\underline{C}$), 150.86 (Q$\underline{C}$), 151.23 (Q$\underline{C}$), 168.47 ($\underline{C}$=O)

^{19}F NMR ($CDCl_3$, 400 MHz) δ_F ppm: -162.77 (2F, t, J = 19.89 Hz, Ar$\underline{F}$), -158.54 (1F, t, J = 21.69 Hz, Ar$\underline{F}$), -153.03 (2F, d, J = 20.11 Hz, Ar$\underline{F}$)

ν_{MAX} (DCM)/cm^{-1}: 3318.48, 2931.22, 2856.42, 2119.16, 1789.83 (C=O), 1520.73

HRMS $[M+Na]^+$: calculated 717.2283, found 717.2294, molecular formula ($C_{35}H_{39}F_5NaO_7Si$)

7.21.11 Hydroxamic acid synthesis: Synthesis of 2-[(7*R*)-9-{3-[(*tert*-butyldimethylsilyl)oxy]-4-methoxyphenyl}-2,3,4-trimethoxy-6,7-dihydro-5*H*-benzo[7]annulen-7-yl]-*N*-hydroxyacetamide (5.27)

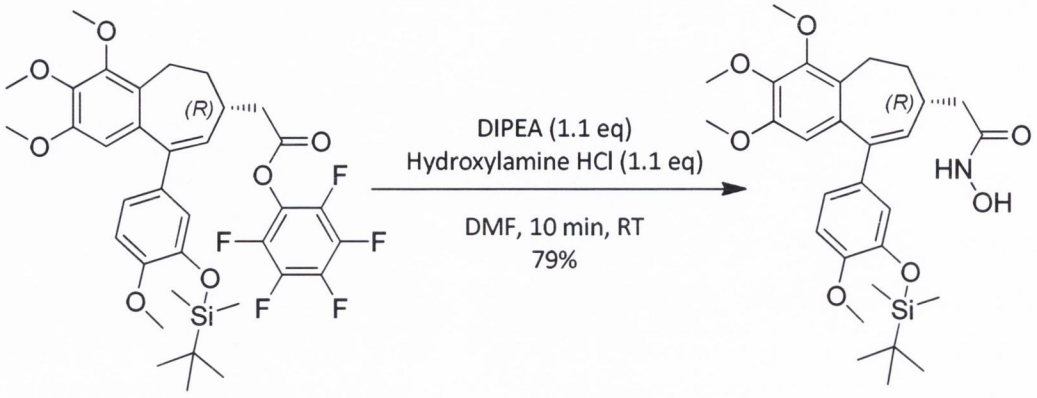

(5.26) **(5.27)**

To a stirred solution of **(5.26)** (0.06 g, 0.07 mmol) in DMF (2 mL) was added DIPEA (0.02 mL, 0.09 mmol) and hydroxylamine HCl (6 mg, 0.09 mmol) at room temperature. After 10 min, the reaction was quenched by the addition of 0.2 M HCl aqueous solution (5 mL) and the reaction was extracted with diethyl ether (3 x 10 mL). The organic fractions were combined, dried over $MgSO_4$, filtered and concentrated *in vacuo*. The resulting residue was then purified by flash column chromatography (stationary phase; silica gel 230-400 mesh, mobile phase; 50:50:1, hexane/ethyl acetate/formic acid) to afford **(5.27)** as a yellow resin (0.03 g, 79%).

R_f: 0.15 (50:50:1, hexane/ethyl acetate/formic acid)

$[\alpha]_D^{25}$ = - 73.5 (*c* = 0.95, DCM)

^{1}H NMR ($CDCl_3$, 400 MHz) δ_H ppm: 0.15 (6H, d, J = 5.92 Hz, Si($C\underline{H}_3$)$_2$), 0.98 (9H, s, C($C\underline{H}_3$)$_3$), 1.28-1.32 (2H, m, $C\underline{H}_2$), 1.87 (1H, s, br, $C\underline{H}_2$), 2.26-2.32 (2H, m, $C\underline{H}_2$), 2.35-2.47 (1H, m, $C\underline{H}CH_2CO$), 3.01 (1H, m, $C\underline{H}_2$), 3.69 (3H, s, $OC\underline{H}_3$), 3.82 (3H, s, $OC\underline{H}_3$), 3.91 (3H, s, $OC\underline{H}_3$), 3.93 (3H, s, $OC\underline{H}_3$), 6.00 (1H, s, C=C$\underline{H}$), 6.72 (1H, s, Ar$\underline{H}$), 6.80-6.87 (2H, s, Ar$\underline{H}$)

^{13}C NMR ($CDCl_3$, 400 MHz) δ_c ppm: -5.01 (Si($\underline{C}H_3$)$_2$), 17.99 ($\underline{C}$(CH$_3$)$_3$), 22.87 ($\underline{C}H_2$), 25.27 (C($\underline{C}H_3$)$_3$), 29.25 ($\underline{C}H_2$), 33.56 ($\underline{C}HCH_2CO$), 41.20 ($\underline{C}H_2$), 55.06 ($O\underline{C}H_3$), 55.45 ($O\underline{C}H_3$), 60.45 ($O\underline{C}H_3$), 61.18 ($O\underline{C}H_3$), 108.52 (Ar$\underline{C}$H), 111.19 (Ar$\underline{C}$H), 120.35 (Ar$\underline{C}$H), 120.99 (Ar$\underline{C}$H), 127.31 ($\underline{Q}C$), 128.48 (C=$\underline{C}$H), 129.31 ($\underline{Q}C$), 133.96 ($\underline{Q}C$), 135.36 ($\underline{Q}C$), 140.82 ($\underline{Q}C$), 141.48 ($\underline{Q}C$), 144.04 ($\underline{Q}C$), 150.09 ($\underline{Q}C$), 150.27 ($\underline{Q}C$), 150.64 ($\underline{Q}C$)

ν_{MAX} (DCM)/cm^{-1}: 3418.74, 2928.54, 2855.25, 1660.92 (C=O), 1594.10

HRMS $[M+Na]^+$: calculated 566.255, found 566.2554, molecular formula ($C_{29}H_{41}NNaO_7Si$)

7.21.12 Silyl deprotection: Synthesis of 2-((*R*,*Z*)-6,7-dihydro-9-(3-hydroxy-4-methoxyphenyl)-2,3,4-trimethoxy-5*H*-benzo[7]annulen-7-yl)-*N*-hydroxyacetamide (5.13)

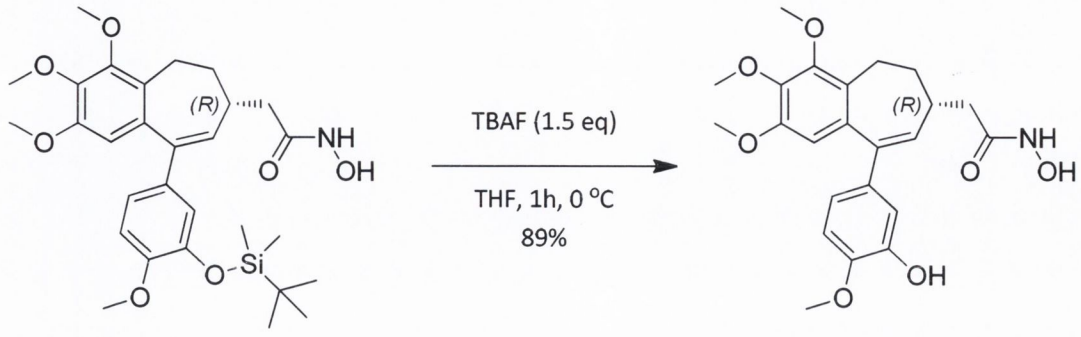

(5.26) **(5.13)**

To a stirred solution of **(5.26)** (0.03 g, 0.06 mmol) in dry THF (1 mL) under an atmosphere of nitrogen at 0 °C was added 1 M TBAF solution in THF (0.06 mL, 0.06 mmol). After 1 h, the THF was blown off in a stream of nitrogen gas and the resulting residue washed with water (5 mL) and extracted with diethyl ether (3 x 10 mL). The organic fractions were combined, dried over $MgSO_4$, filtered and concentrated under reduced pressure. The product was purified by flash column chromatography (stationary phase; silica gel 230-400 mesh, mobile phase; 50:50:1, hexane/ethyl acetate/formic acid) to afford **(5.13)** as an off-white solid (15 mg, 89%).

R_f: 0.13 (66:33:1, ethyl acetate/hexane/formic acid)

$[\alpha]_D^{25}$: - 61.2 (*c* = 0.56, DCM)

^{1}H NMR (CD_3OD, 400 MHz) δ_H ppm: 1.81-1.88 (1H, m, C$\underline{H}_2$), 2.11-2.16 (1H, m, C$\underline{H}_2$), 2.19-2.27 (3H, m, C$\underline{H}_2$), 2.31-2.37 (1H, m, C$\underline{H}$CH$_2$CO), 2.99-3.05 (1H, m, C$\underline{H}_2$), 3.63 (3H, s, OC$\underline{H}_3$), 3.83 (6H, s, OC$\underline{H}_3$), 3.85 (3H, s, OC$\underline{H}_3$), 6.04 (1H, d, J = 6.10 Hz, C=C$\underline{H}$), 6.35 (1H, s, Ar$\underline{H}$), 6.66-6.72 (2H, m, Ar$\underline{H}$), 6.84 (1H, d, J = 8.55 Hz, Ar$\underline{H}$)

^{13}C NMR (CD_3OD, 400 MHz) δ_c ppm: 22.98 ($\underline{C}H_2$), 34.43 ($\underline{C}HCH_2CO$), 37.79 ($\underline{C}H_2$), 41.27 ($\underline{C}H_2$), 54.96 (O$\underline{C}H_3$), 55.00 (O$\underline{C}H_3$), 59.81 (O$\underline{C}H_3$), 60.63 (O$\underline{C}H_3$), 108.89 (Ar$\underline{C}H$), 110.96 (Ar$\underline{C}H$), 114.62 (Ar$\underline{C}H$), 119.17 (Ar$\underline{C}H$), 127.78 (Q$\underline{C}$), 129.01 (C=$\underline{C}H$), 134.70 (Q$\underline{C}$), 136.29 (Q$\underline{C}$), 141.17 (Q$\underline{C}$), 141.62 (Q$\underline{C}$), 145.8 (Q$\underline{C}$), 147.25 (Q$\underline{C}$), 150.66 (Q$\underline{C}$), 151.15 (Q$\underline{C}$), 162.90 ($\underline{C}$=O)

ν_{MAX} (DCM)/cm^{-1}: 3314.58, 2933.07, 2851.68, 1830.77, 1660.04 (C=O), 1596.74

HRMS $[M+Na]^+$: calculated 452.1685, found 452.1684, molecular formula ($C_{23}H_{27}NNaO_7$)

Melting point: 104-106 °C

8 References

1. Chari RV. Targeted delivery of chemotherapeutics: tumor-activated prodrug therapy. *Advanced Drug Delivery Reviews*. 1998;31(1–2):89-104.

2. Kavallaris M. Microtubules and resistance to tubulin-binding agents. *Nature Reviews Cancer*. 2010;10(3):194-204.

3. Dumontet C, Jordan MA. Microtubule-binding agents: a dynamic field of cancer therapeutics. *Nature Reviews Drug Discovery*. 2010;9(10):790-803.

4. Lambert JM. Drug-conjugated monoclonal antibodies for the treatment of cancer. *Current Opinion in Pharmacology*. 2005;5(5):543-9.

5. Vlahov IR, Wang Y, Kleindl PJ, Leamon CP. Design and regioselective synthesis of a new generation of targeted chemotherapeutics. Part II: Folic acid conjugates of tubulysins and their hydrazides. *Bioorganic & Medicinal Chemistry Letters*. 2008;18(16):4558-61.

6. Kupchan SM, Komoda Y, Court WA, Thomas GJ, Smith RM, Karim A, et al. Tumor inhibitors. LXXIII. Maytansine, a novel antileukemic ansa macrolide from Maytenus ovatus. *Journal of the American Chemical Society*. 1972;94(4):1354-6.

7. Oroudjev E, Lopus M, Wilson L, Audette C, Provenzano C, Erickson H, et al. Maytansinoid-Antibody Conjugates Induce Mitotic Arrest by Suppressing Microtubule Dynamic Instability. *Molecular Cancer Therapeutics*. 2010;9(10):2700-13.

8. Lopus M. Antibody-DM1 conjugates as cancer therapeutics. *Cancer Letters*. 2011;307(2):113-8.

9. Chari RVJ, Martell BA, Gross JL, Cook SB, Shah SA, Blättler WA, et al. Immunoconjugates Containing Novel Maytansinoids: Promising Anticancer Drugs. *Cancer Research*. 1992;52(1):127-31.

10. Lambert JM. Antibody-maytansinoid conjugates as anticancer therapeutics: Proving their benefit. *Human Antibodies*. 2007;16(1-2):5-8.

11. Thorpe PE. Vascular targeting agents as cancer therapeutics. *Clinical Cancer Research*. 2004;10(2):415-27.

12. Yusuf RZ, Duan Z, Lamendola DE, Penson RT, Seiden MV. Paclitaxel resistance: molecular mechanisms and pharmacologic manipulation. *Current Cancer Drug Targets*. 2003;3(1):1-19.

13. Argiris A, Duffy AG, Kummar S, Simone NL, Arai Y, Kim SW, et al. Early Tumor Progression Associated with Enhanced EGFR Signaling with Bortezomib, Cetuximab, and Radiotherapy for Head and Neck Cancer. *Clinical Cancer Research*. 2011;17(17):5755-64.

14. Guillemard V, Uri Saragovi H. Prodrug chemotherapeutics bypass p-glycoprotein resistance and kill tumors in vivo with high efficacy and target-dependent selectivity. *Oncogene*. 2004;23(20):3613-21.

15. Teicher BA, Chari RVJ. Antibody Conjugate Therapeutics: Challenges and Potential. *Clinical Cancer Research*. 2011;17(20):6389-97.

16. Christiansen J, Rajasekaran AK. Biological impediments to monoclonal antibody-based cancer immunotherapy. *Molecular Cancer Therapeutics*. 2004;3(11):1493-501.

17. Francisco JA, Cerveny CG, Meyer DL, Mixan BJ, Klussman K, Chace DF, et al. cAC10-vcMMAE, an anti-CD30-monomethyl auristatin E conjugate with potent and selective antitumor activity. *Blood*. 2003;102(4):1458-65.

18. Ducry L, Stump B. Antibody–Drug Conjugates: Linking Cytotoxic Payloads to Monoclonal Antibodies. *Bioconjugate Chemistry*. 2009;21(1):5-13.

19. Webb S. Pharma interest surges in antibody drug conjugates. *Nature Biotechnology*. 2011;29(4):297-8.

20. Goldenberg DM. Monoclonal antibodies in cancer detection and therapy. *The American Journal of Medicine*. 1993;94(3):297-312.

21. Wu X, Ojima I. Tumor specific novel taxoid-monoclonal antibody conjugates. *Current Medicinal Chemistry*. 2004;11(4):429-38.

22. Widdison WC, Wilhelm SD, Cavanagh EE, Whiteman KR, Leece BA, Kovtun Y, et al. Semisynthetic Maytansine Analogues for the Targeted Treatment of Cancer. *Journal of Medicinal Chemistry*. 2006;49(14):4392-408.

23. Hamblett KJ, Senter PD, Chace DF, Sun MM, Lenox J, Cerveny CG, et al. Effects of drug loading on the antitumor activity of a monoclonal antibody drug conjugate. *Clinical Cancer Research*. 2004;10(20):7063-70.

24. Tijink BM, Buter J, de Bree R, Giaccone G, Lang MS, Staab A, et al. A phase I dose escalation study with anti-CD44v6 bivatuzumab mertansine in patients with incurable squamous cell carcinoma of the head and neck or esophagus. *Clinical Cancer Research*. 2006;12(20 Pt 1):6064-72.

25. Ravi V.J C. Targeted delivery of chemotherapeutics: tumor-activated prodrug therapy. *Advanced Drug Delivery Reviews*. 1998;31(1–2):89-104.

26. Garanger E, Boturyn D, Dumy P. Tumor targeting with RGD peptide ligands-design of new molecular conjugates for imaging and therapy of cancers. *Anti-Cancer Agents in Medicinal Chemistry*. 2007;7(5):552-8.

27. Yokota T, Milenic DE, Whitlow M, Schlom J. Rapid tumor penetration of a single-chain Fv and comparison with other immunoglobulin forms. *Cancer Research*. 1992;52(12):3402-8.

28. Adams GP, Schier R, Marshall K, Wolf EJ, McCall AM, Marks JD, et al. Increased affinity leads to improved selective tumor delivery of single-chain Fv antibodies. *Cancer Research*. 1998;58(3):485-90.

29. Kim KM, McDonagh CF, Westendorf L, Brown LL, Sussman D, Feist T, et al. Anti-CD30 diabody-drug conjugates with potent antitumor activity. *Molecular Cancer Therapeutics*. 2008;7(8):2486-97.

30. Junutula JR, Flagella KM, Graham RA, Parsons KL, Ha E, Raab H, et al. Engineered Thio-Trastuzumab-DM1 Conjugate with an Improved Therapeutic Index to Target Human Epidermal Growth Factor Receptor 2–Positive Breast Cancer. *Clinical Cancer Research*. 2010;16(19):4769-78.

31. Braun S, Schlimok G, Heumos I, Schaller G, Riethdorf L, Riethmuller G, et al. ErbB2 overexpression on occult metastatic cells in bone marrow predicts poor clinical outcome of stage I-III breast cancer patients. *Cancer Research*. 2001;61(5):1890-5.

32. Junutula JR, Raab H, Clark S, Bhakta S, Leipold DD, Weir S, et al. Site-specific conjugation of a cytotoxic drug to an antibody improves the therapeutic index. *Nature Biotechnology*. 2008;26(8):925-32.

33. Schrama D, Reisfeld RA, Becker JC. Antibody targeted drugs as cancer therapeutics. *Nature Reviews Drug Discovery*. 2006;5(2):147-59.

34. Erickson HK, Park PU, Widdison WC, Kovtun YV, Garrett LM, Hoffman K, et al. Antibody-maytansinoid conjugates are activated in targeted cancer cells by lysosomal degradation and linker-dependent intracellular processing. *Cancer Research*. 2006;66(8):4426-33.

35. Lopus M, Oroudjev E, Wilson L, Wilhelm S, Widdison W, Chari R, et al. Maytansine and Cellular Metabolites of Antibody-Maytansinoid Conjugates Strongly Suppress Microtubule Dynamics by Binding to Microtubules. *Molecular Cancer Therapeutics*. 2010;9(10):2689-99.

36. Kovtun YV, Audette CA, Ye Y, Xie H, Ruberti MF, Phinney SJ, et al. Antibody-drug conjugates designed to eradicate tumors with homogeneous and heterogeneous expression of the target antigen. *Cancer Research*. 2006;66(6):3214-21.

37. Kovtun YV, Goldmacher VS. Cell killing by antibody–drug conjugates. *Cancer Letters*. 2007;255(2):232-40.

38. Ikeda H, Hideshima T, Fulciniti M, Lutz RJ, Yasui H, Okawa Y, et al. The Monoclonal Antibody nBT062 Conjugated to Cytotoxic Maytansinoids Has Selective Cytotoxicity Against CD138-Positive Multiple Myeloma Cells In vitro and In vivo. *Clinical Cancer Research*. 2009;15(12):4028-37.

39. Lutz RJ, Whiteman KR. Antibody-maytansinoid conjugates for the treatment of myeloma. *Mabs*. 2009;1(6):548-51.

40. Beck A, Senter P, Chari R. World Antibody Drug Conjugate Summit Europe: February 21-23, 2011; Frankfurt, Germany. *Mabs*. 2011;3(4):331-7.

41. Polson AG, Calemine-Fenaux J, Chan P, Chang W, Christensen E, Clark S, et al. Antibody-drug conjugates for the treatment of non-Hodgkin's lymphoma: target and linker-drug selection. *Cancer Research*. 2009;69(6):2358-64.

42. Ma DS, Hopf CE, Malewicz AD, Donovan GP, Senter PD, Goeckeler WF, et al. Potent antitumor activity of an auristatin-conjugated, fully human monoclonal antibody to prostate-specific membrane antigen. *Clinical Cancer Research*. 2006;12(8):2591-6.

43. Podgorski I, Sloane BF. Cathepsin B and its role(s) in cancer progression. *Biochemical Society symposium*. 2003;(70):263-76.

44. Doronina SO, Toki BE, Torgov MY, Mendelsohn BA, Cerveny CG, Chace DF, et al. Development of potent monoclonal antibody auristatin conjugates for cancer therapy. *Nature Biotechnology*. 2003;21(7):778.

45. Wahl AF, Klussman K, Thompson JD, Chen JH, Francisco LV, Risdon G, et al. The anti-CD30 monoclonal antibody SGN-30 promotes growth arrest and DNA fragmentation in vitro and affects antitumor activity in models of Hodgkin's disease. *Cancer Research*. 2002;62(13):3736-42.

46. Doronina SO, Mendelsohn BA, Bovee TD, Cerveny CG, Alley SC, Meyer DL, et al. Enhanced Activity of Monomethylauristatin F through Monoclonal Antibody Delivery: Effects of Linker Technology on Efficacy and Toxicity. *Bioconjugate Chemistry*. 2005;17(1):114-24.

47. Kovtun YV, Audette CA, Mayo MF, Jones GE, Doherty H, Maloney EK, et al. Antibody-maytansinoid conjugates designed to bypass multidrug resistance. *Cancer Research*. 2010;70(6):2528-37.

48. Zhao RY, Wilhelm SD, Audette C, Jones G, Leece BA, Lazar AC, et al. Synthesis and Evaluation of Hydrophilic Linkers for Antibody–Maytansinoid Conjugates. *Journal of Medicinal Chemistry*. 2011;54(10):3606-23.

49. Jeffrey SC, Andreyka JB, Bernhardt SX, Kissler KM, Kline T, Lenox JS, et al. Development and Properties of β-Glucuronide Linkers for Monoclonal Antibody−Drug Conjugates. *Bioconjugate Chemistry*. 2006;17(3):831-40.

50. Albin N, Massaad L, Toussaint C, Mathieu MC, Morizet J, Parise O, et al. Main drug-metabolizing enzyme systems in human breast tumors and peritumoral tissues. *Cancer Research*. 1993;53(15):3541-6.

51. Gilbert CW, McGowan EB, Seery GB, Black KS, Pegram MD. Targeted prodrug treatment of HER-2-positive breast tumor cells using trastuzumab and paclitaxel linked by A-Z-CINN™ Linker. *Journal of Experimental Therapeutics & Oncology*. 2003;3(1):27-35.

52. Ojima I, Geng X, Wu X, Qu C, Borella CP, Xie H, et al. Tumor-specific novel taxoid-monoclonal antibody conjugates. *Journal of Medicinal Chemistry*. 2002;45(26):5620-3.

53. Polson AG, Williams M, Gray AM, Fuji RN, Poon KA, McBride J, et al. Anti-CD22-MCC-DM1: an antibody-drug conjugate with a stable linker for the treatment of non-Hodgkin's lymphoma. *Leukemia*. 2010;24(9):1566-73.

54. Law CL, Cerveny CG, Gordon KA, Klussman K, Mixan BJ, Chace DF, et al. Efficient elimination of B-lineage lymphomas by anti-CD20-auristatin conjugates. *Clinical Cancer Research*. 2004;10(23):7842-51.

55. Yazawa N, Hamaguchi Y, Poe JC, Tedder TF. Immunotherapy using unconjugated CD19 monoclonal antibodies in animal models for B lymphocyte malignancies and autoimmune disease. *Proceedings of the National Academy of Sciences of the United States of America*. 2005;102(42):15178-83.

56. Gerber HP, Kung-Sutherland M, Stone I, Morris-Tilden C, Miyamoto J, McCormick R, et al. Potent antitumor activity of the anti-CD19 auristatin antibody drug conjugate hBU12-vcMMAE against rituximab-sensitive and -resistant lymphomas. *Blood*. 2009;113(18):4352-61.

57. Polson AG, Yu SF, Elkins K, Zheng B, Clark S, Ingle GS, et al. Antibody-drug conjugates targeted to CD79 for the treatment of non-Hodgkin lymphoma. *Blood*. 2007;110(2):616-23.

58. Dornan D, Bennett F, Chen Y, Dennis M, Eaton D, Elkins K, et al. Therapeutic potential of an anti-CD79b antibody-drug conjugate, anti-CD79b-vc-MMAE, for the treatment of non-Hodgkin lymphoma. *Blood*. 2009;114(13):2721-9.

59. Zheng B, Fuji RN, Elkins K, Yu S-F, Fuh FK, Chuh J, et al. In vivo effects of targeting CD79b with antibodies and antibody-drug conjugates. *Molecular Cancer Therapeutics*. 2009;8(10):2937-46.

60. Ab O, Bartle LM, Rui L, Coccia J, Johnson HA, Whiteman KR, et al. Abstract 4576: IMGN853, an anti-Folate Receptor I antibody-maytansinoid conjugate for targeted cancer therapy. *Cancer Research*. 2011;71(8 Supplement):4576.

61. Katz J, Janik JE, Younes A. Brentuximab Vedotin (SGN-35). *Clinical Cancer Research*. 2011;17(20):6428-36.

62. Liu C, Tadayoni BM, Bourret LA, Mattocks KM, Derr SM, Widdison WC, et al. Eradication of large colon tumor xenografts by targeted delivery of maytansinoids. *Proceedings of the National Academy of Sciences*. 1996;93(16):8618-23.

63. Tolcher AW, Ochoa L, Hammond LA, Patnaik A, Edwards T, Takimoto C, et al. Cantuzumab Mertansine, a Maytansinoid Immunoconjugate Directed to the CanAg Antigen: A Phase I, Pharmacokinetic, and Biologic Correlative Study. *Journal of Clinical Oncology*. 2003;21(2):211-22.

64. Robak T, Robak P, Smolewski P. TRU-016, a humanized anti-CD37 IgG fusion protein for the potential treatment of B-cell malignancies. *Current opinion in investigational drugs*. 2009;10(12):1383-90.

65. Park PU, Yi Y, Li M, Chicklas S, Lai KC, Mayo MF, et al. Abstract 2830: Antibody and linker selection for the anti-CD37 antibody-maytansinoid conjugate IMGN529 for the treatment of B-cell malignancies. *Cancer Research*. 2011;71(8 Supplement):2830.

66. Ireton RC, Chen J. EphA2 Receptor Tyrosine Kinase as a Promising Target for Cancer Therapeutics. *Current Cancer Drug Targets*. 2005;5(3):149-57.

67. Ogawa K, Pasqualini R, Lindberg RA, Kain R, Freeman AL, Pasquale EB. The ephrin-A1 ligand and its receptor, EphA2, are expressed during tumor neovascularization. *Oncogene*. 2000;19(52):6043.

68. Lee J-W, Stone RL, Lee SJ, Nam EJ, Roh J-W, Nick AM, et al. EphA2 Targeted Chemotherapy Using an Antibody Drug Conjugate in Endometrial Carcinoma. *Clinical Cancer Research*. 2010;16(9):2562-70.

69. Junttila T, Li G, Parsons K, Phillips G, Sliwkowski M. Trastuzumab-DM1 (T-DM1) retains all the mechanisms of action of trastuzumab and efficiently inhibits growth of lapatinib insensitive breast cancer. *Breast Cancer Research and Treatment*. 2011;128(2):347-56.

70. Mathew J, Perez EA. Trastuzumab emtansine in human epidermal growth factor receptor 2-positive breast cancer: a review. *Current Opinion in Oncology*. 2011;23(6):594-600.

71. Younes A, Yasothan U, Kirkpatrick P. Brentuximab vedotin. *Nature Reviews Drug Discovery*. 2012;11(1):19-20.

72. Oflazoglu E, Kissler KM, Sievers EL, Grewal IS, Gerber H-P. Combination of the anti-CD30-auristatin-E antibody-drug conjugate (SGN-35) with chemotherapy improves antitumour activity in Hodgkin lymphoma. *British Journal of Haematology*. 2008;142(1):69-73.

73. Blanc V, Bousseau A, Caron A, Carrez C, Lutz RJ, Lambert JM. SAR3419: an anti-CD19-Maytansinoid Immunoconjugate for the treatment of B-cell malignancies. *Clinical Cancer Research*. 2011;17(20):6448-58.

74. Sanofi-Aventis. An Open Label Non-Randomized Phase 2 Study Evaluating SAR3419, an Anti-CD19 Antibody - Maytansine Conjugate, Administered as Single Agent by Intravenous Infusion to Patients With Relapsed or Refractory CD19+ Diffuse Large B-Cell Lymphoma. ClinicalTrials.gov [Internet]. Bethesda (MD): National Library of Medicine (US). 2000- [cited 2012 May 12]. Available from: http://www.clinicaltrials.gov/ct2/show/NCT01472887?term=SAR3419&rank=1 NLM Identifier: NCT01472887].

75. MedImmune LLC. Study of MEDI-547 to Evaluate the Safety, Tolerability, and Biologic Activity of IV Administration in Subjects With Relapsed or Refractory Solid Tumors. ClinicalTrials.gov [Internet]. Bethesda (MD): National Library of Medicine (US). 2000- [cited 2012 Feb 23]. Available from: http://clinicaltrials.gov/ct2/show/NCT00796055?intr=%22MEDI-547%22&rank=1 NLM Identifier: NCT00796055].

76. Oflazoglu E, Stone IJ, Gordon K, Wood CG, Repasky EA, Grewal IS, et al. Potent Anticarcinoma Activity of the Humanized Anti-CD70 Antibody h1F6 Conjugated to the Tubulin Inhibitor Auristatin via an Uncleavable Linker. *Clinical Cancer Research*. 2008;14(19):6171-80.

77. Ricart AD. Immunoconjugates Against Solid Tumors: Mind the Gap. *Clinical pharmacology and therapeutics*. 2011;89(4):513-23.

78. Bagnato JD, Eilers AL, Horton RA, Grissom CB. Synthesis and characterization of a cobalamin-colchicine conjugate as a novel tumor-targeted cytotoxin. *Journal of Organic Chemistry*. 2004;69(26):8987-96.

79. Russell-Jones G, McTavish K, McEwan J, Rice J, Nowotnik D. Vitamin-mediated targeting as a potential mechanism to increase drug uptake by tumours. *Journal of inorganic biochemistry*. 2004;98(10):1625-33.

80. Chen S, Zhao X, Chen J, Chen J, Kuznetsova L, Wong SS, et al. Mechanism-Based Tumor-Targeting Drug Delivery System. Validation of Efficient Vitamin Receptor-Mediated Endocytosis and Drug Release. *Bioconjugate Chemistry*. 2010;21(5):979-87.

81. Vlahov IR, Vite GD, Kleindl PJ, Wang Y, Santhapuram HKR, You F, et al. Regioselective synthesis of folate receptor-targeted agents derived from epothilone analogs and folic acid. *Bioorganic & Medicinal Chemistry Letters*. 2010;20(15):4578-81.

82. Lee JW, Lu JY, Low PS, Fuchs PL. Synthesis and Evaluation of Taxol–Folic Acid Conjugates as Targeted Antineoplastics. *Bioorganic & Medicinal Chemistry*. 2002;10(7):2397-414.

83. Dosio F, Arpicco S, Stella B, Brusa P, Cattel L. Folate-mediated targeting of albumin conjugates of paclitaxel obtained through a heterogeneous phase system. *International Journal of Pharmaceutics*. 2009;382(1–2):117-23.

84. Leamon CP, Reddy JA, Vlahov IR, Kleindl PJ, Vetzel M, Westrick E. Synthesis and Biological Evaluation of EC140: A Novel Folate-Targeted Vinca Alkaloid Conjugate. *Bioconjugate Chemistry*. 2006;17(5):1226-32.

85. Vlahov IR, Santhapuram HKR, Kleindl PJ, Howard SJ, Stanford KM, Leamon CP. Design and regioselective synthesis of a new generation of targeted chemotherapeutics. Part 1: EC145, a folic acid conjugate of desacetylvinblastine monohydrazide. *Bioorganic & Medicinal Chemistry Letters*. 2006;16(19):5093-6.

86. Vlahov IR, Santhapuram HKR, Wang Y, Kleindl PJ, You F, Howard SJ, et al. An Assembly Concept for the Consecutive Introduction of Unsymmetrical Disulfide Bonds: Synthesis of a Releasable Multidrug Conjugate of Folic Acid. *The Journal of Organic Chemistry*. 2007;72(16):5968-72.

87. Leamon CP, Reddy JA, Vetzel M, Dorton R, Westrick E, Parker N, et al. Folate targeting enables durable and specific antitumor responses from a therapeutically null tubulysin B analogue. *Cancer Research*. 2008;68(23):9839-44.

88. Reddy JA, Westrick E, Santhapuram HK, Howard SJ, Miller ML, Vetzel M, et al. Folate receptor-specific antitumor activity of EC131, a folate-maytansinoid conjugate. *Cancer Research*. 2007;67(13):6376-82.

89. Nakagawa-Goto K, Yamada K, Nakamura S, Chen T-H, Chiang P-C, Bastow KF, et al. Antitumor agents. 258. Syntheses and evaluation of dietary antioxidant—taxoid conjugates as novel cytotoxic agents. *Bioorganic & Medicinal Chemistry Letters*. 2007;17(18):5204-9.

90. Sauer LA, Dauchy RT. The effect of omega-6 and omega-3 fatty acids on 3H-thymidine incorporation in hepatoma 7288CTC perfused in situ. *British Journal of Cancer*. 1992;66(2):297-303.

91. Sauer LA, Dauchy RT, Blask DE. Mechanism for the antitumor and anticachectic effects of n-3 fatty acids. *Cancer Research*. 2000;60(18):5289-95.

92. Bradley MO, Webb NL, Anthony FH, Devanesan P, Witman PA, Hemamalini S, et al. Tumor targeting by covalent conjugation of a natural fatty acid to paclitaxel. *Clinical Cancer Research*. 2001;7(10):3229-38.

93. Wolff AC, Donehower RC, Carducci MK, Carducci MA, Brahmer JR, Zabelina Y, et al. Phase I study of docosahexaenoic acid-paclitaxel: a taxane-fatty acid conjugate with a unique pharmacology and toxicity profile. *Clinical Cancer Research*. 2003;9(10 Pt 1):3589-97.

94. Jones R, Hawkins R, Eatock M, Ferry D, Eskens F, Wilke H, et al. A phase II open-label study of DHA-paclitaxel (Taxoprexin) by 2-h intravenous infusion in previously untreated patients with locally advanced or metastatic gastric or oesophageal adenocarcinoma. *Cancer Chemotherapy and Pharmacology*. 2008;61(3):435-41.

95. Bedikian AY, DeConti RC, Conry R, Agarwala S, Papadopoulos N, Kim KB, et al. Phase 3 study of docosahexaenoic acid–paclitaxel versus dacarbazine in patients with metastatic malignant melanoma. *Annals of Oncology*. 2011;22(4):787-93.

96. Ke X-Y, Zhao B-J, Zhao X, Wang Y, Huang Y, Chen X-M, et al. The therapeutic efficacy of conjugated linoleic acid - Paclitaxel on glioma in the rat. *Biomaterials*. 2010;31(22):5855-64.

97. Kuznetsova L, Chen J, Sun L, Wu X, Pepe A, Veith JM, et al. Syntheses and evaluation of novel fatty acid-second-generation taxoid conjugates as promising anticancer agents. *Bioorganic and Medicinal Chemistry Letters*. 2006;16(4):974-7.

98. Pignatello R, Paolino D, Pantò V, Pistarà V, Calvagno MG, Russo D, et al. Lipoamino Acid Prodrugs of Paclitaxel: Synthesis and Cytotoxicity Evaluation on Human Anaplastic Thyroid Carcinoma Cells. *Current Cancer Drug Targets*. 2009;9(2):202-13.

99. Sharifi N, Hamel E, Lill MA, Risbood P, Kane CT, Jr., Hossain MT, et al. A bifunctional colchicinoid that binds to the androgen receptor. *Molecular Cancer Therapeutics*. 2007;6(8):2328-36.

100. Liu C, Strobl JS, Bane S, Schilling JK, McCracken M, Chatterjee SK, et al. Design, Synthesis, and Bioactivities of Steroid-Linked Taxol Analogues as Potential Targeted Drugs for Prostate and Breast Cancer. *Journal of Natural Products*. 2003;67(2):152-9.

101. Shen H, Hu D, Du J, Wang X, Liu Y, Wang Y, et al. Paclitaxel–octreotide conjugates in tumor growth inhibition of A549 human non-small cell lung cancer xenografted into nude mice. *European Journal of Pharmacology*. 2008;601(1–3):23-9.

102. Papotti M, Croce S, Bello M, Bongiovanni M, Allia E, Schindler M, et al. Expression of somatostatin receptor types 2, 3 and 5 in biopsies and surgical specimens of human lung tumours. Correlation with preoperative octreotide scintigraphy. *Virchows Archiv : an international journal of pathology*. 2001;439(6):787-97.

103. Sun ML, Wei JM, Wang XW, Li L, Wang P, Li M, et al. Paclitaxel-octreotide conjugates inhibit growth of human non-small cell lung cancer cells in vitro. *Experimental oncology*. 2007;29(3):186-91.

104. Sundaram S, Durairaj C, Kadam R, Kompella UB. Luteinizing hormone-releasing hormone receptor–targeted deslorelin-docetaxel conjugate enhances efficacy of docetaxel in prostate cancer therapy. *Molecular Cancer Therapeutics*. 2009;8(6):1655-65.

105. Pribylova M, Dvorakova M, Hanusova V, Nemethova I, Skalova L, Vanek T. Paclitaxel conjugation with the analog of the gonadotropin-releasing hormone as a targeting moiety. *International Journal of Pharmaceutics*. 2011;415(1–2):175-80.

106. Kumar SK, Williams SA, Isaacs JT, Denmeade SR, Khan SR. Modulating paclitaxel bioavailability for targeting prostate cancer. *Bioorganic & Medicinal Chemistry*. 2007;15(14):4973-84.

107. Régina A, Demeule M, Ché C, Lavallée I, Poirier J, Gabathuler R, et al. Antitumour activity of ANG1005, a conjugate between paclitaxel and the new brain delivery vector Angiopep-2. *British Journal of Pharmacology*. 2008;155(2):185-97.

108. Thomas F, Taskar K, Rudraraju V, Goda S, Thorsheim H, Gaasch J, et al. Uptake of ANG1005, A Novel Paclitaxel Derivative, Through the Blood-Brain Barrier into Brain and Experimental Brain Metastases of Breast Cancer. *Pharmaceutical Research*. 2009;26(11):2486-94.

109. Demeule M, Currie JC, Bertrand Y, Che C, Nguyen T, Regina A, et al. Involvement of the low-density lipoprotein receptor-related protein in the transcytosis of the brain delivery vector angiopep-2. *Journal of neurochemistry*. 2008;106(4):1534-44.

110. Yamada R, Kostova MB, Anchoori RK, Xu S, Neamati N, Khan S. Biological evaluation of Paclitaxel-peptide conjugates as a model for MMP2-targeted drug delivery. *Cancer Biology & Therapy*. 2010;9(3):192-203.

111. Li P, Jiang S, Pero SC, Oligino L, Krag DN, Michejda CJ, et al. Design and synthesis of paclitaxel conjugated with an ErbB2-recognizing peptide, EC-1. *Biopolymers*. 2007;87(4):225-30.

112. Dechantsreiter MA, Planker E, Matha B, Lohof E, Holzemann G, Jonczyk A, et al. N-Methylated Cyclic RGD Peptides as Highly Active and Selective αVβ3 Integrin Antagonists. *Journal of Medicinal Chemistry*. 1999;42(16):3033-40.

113. Chen X, Plasencia C, Hou Y, Neamati N. Synthesis and Biological Evaluation of Dimeric RGD Peptide–Paclitaxel Conjugate as a Model for Integrin-Targeted Drug Delivery. *Journal of Medicinal Chemistry*. 2005;48(4):1098-106.

114. Cao Q, Li Z-B, Chen K, Wu Z, He L, Neamati N, et al. Evaluation of biodistribution and anti-tumor effect of a dimeric RGD peptide–paclitaxel conjugate in mice with breast cancer. *European Journal of Nuclear Medicine & Molecular Imaging*. 2008;35(8):1489-98.

115. Ryppa C, Mann-Steinberg H, Biniossek ML, Satchi-Fainaro R, Kratz F. In vitro and in vivo evaluation of a paclitaxel conjugate with the divalent peptide E-[c(RGDfK)2] that targets integrin alpha v beta 3. *International Journal of Pharmaceutics*. 2009;368(1-2):89-97.

116. Li S, Gray BP, McGuire MJ, Brown KC. Synthesis and biological evaluation of a peptide–paclitaxel conjugate which targets the integrin αvβ6. *Bioorganic & Medicinal Chemistry*. 2011;19(18):5480-9.

117. Hariri G, Yan H, Wang H, Han Z, Hallahan DE. Radiation-guided drug delivery to mouse models of lung cancer. *Clinical Cancer Research*. 2010;16(20):4968-77.

118. Safavy A, Raisch KP, Matusiak D, Bhatnagar S, Helson L. Single-Drug Multiligand Conjugates: Synthesis and Preliminary Cytotoxicity Evaluation of a Paclitaxel–Dipeptide "Scorpion" Molecule. *Bioconjugate Chemistry*. 2006;17(3):565-70.

119. Hohla F, Schally AV. Targeting gastrin releasing peptide receptors: New options for the therapy and diagnosis of cancer. *Cell Cycle*. 2010;9(9):1738-41.

120. Ndungu JM, Lu YJ, Zhu S, Yang C, Wang X, Chen G, et al. Targeted Delivery of Paclitaxel to Tumor Cells: Synthesis and in Vitro Evaluation. *Journal of Medicinal Chemistry*. 2010;53(8):3127-32.

121. Kasthuri RS, Taubman MB, Mackman N. Role of tissue factor in cancer. *Journal of Clinical Oncology*. 2009;27(29):4834-8.

122. Matsumura Y, Maeda H. A new concept for macromolecular therapeutics in cancer chemotherapy: mechanism of tumoritropic accumulation of proteins and the antitumor agent smancs. *Cancer Research*. 1986;46(12 Pt 1):6387-92.

123. Greish K. Enhanced permeability and retention of macromolecular drugs in solid tumors: A royal gate for targeted anticancer nanomedicines. *Journal of Drug Targeting*. 2007;15(7/8):457-64.

124. Maeda H. Tumor-Selective Delivery of Macromolecular Drugs via the EPR Effect: Background and Future Prospects. *Bioconjugate Chemistry*. 2010;21(5):797-802.

125. Gradishar WJ. Albumin-bound paclitaxel: a next-generation taxane. *Expert Opinion on pharmacotherapy*. 2006;7(8):1041-53.

126. Altundag K, Bulut N, Dizdar O, Harputluoglu H. Albumin-Bound Paclitaxel, ABI-007 May Show Better Efficacy than Paclitaxel in Basal-Like Breast Cancers: Association Between Caveolin-1 Expression and ABI-007. *Breast Cancer Research and Treatment*. 2006;100(3):329-30.

127. Altundag K, Dede DS, Purnak T. Albumin-bound paclitaxel (ABI-007; Abraxane) in the management of basal-like breast carcinoma. *Journal of Clinical Pathology*. 2007;60(8):958.

128. Petrelli F, Borgonovo K, Barni S. Targeted delivery for breast cancer therapy: the history of nanoparticle-albumin-bound paclitaxel. *Expert Opinion on pharmacotherapy*. 2010;11(8):1413-32.

129. Dosio F, Arpicco S, Brusa P, Stella B, Cattel L. Poly(ethylene glycol)–human serum albumin–paclitaxel conjugates: preparation, characterization and pharmacokinetics. *Journal of Controlled Release*. 2001;76(1–2):107-17.

130. Chipman SD, Oldham FB, Pezzoni G, Singer JW. Biological and clinical characterization of paclitaxel poliglumex (PPX, CT-2103), a macromolecular polymer-drug conjugate. *International Journal of Nanomedicine*. 2006;1(4):375-83.

131. Shaffer S, Baker-Lee C, Kennedy J, Lai M, de Vries P, Buhler K, et al. In vitro and in vivo metabolism of paclitaxel poliglumex: identification of metabolites and active proteases. *Cancer Chemotherapy and Pharmacology*. 2007;59(4):537-48.

132. Singer JW. Paclitaxel poliglumex (XYOTAX™, CT-2103): A macromolecular taxane. *Journal of Controlled Release*. 2005;109(1–3):120-6.

133. Boddy AV, Plummer ER, Todd R, Sludden J, Griffin M, Robson L, et al. A Phase I and Pharmacokinetic Study of Paclitaxel Poliglumex (XYOTAX), Investigating Both 3-Weekly and 2-Weekly Schedules. *Clinical Cancer Research*. 2005;11(21):7834-40.

134. Paz-ares L, Ross H, O'Brien M, Riviere A, Gatzemeier U, Von Pawel J, et al. Phase III trial comparing paclitaxel poliglumex vs docetaxel in the second-line treatment of non-small-cell lung cancer. *The British Journal of Cancer*. 2008;98(10):1608-13.

135. Van S, Das SK, Wang X, Feng Z, Jin Y, Hou Z, et al. Synthesis, characterization, and biological evaluation of poly(L-gamma-glutamyl-glutamine)- paclitaxel nanoconjugate. *International Journal of Nanomedicine*. 2010;5:825-37.

136. Wang X, Zhao G, Van S, Jiang N, Yu L, Vera D, et al. Pharmacokinetics and tissue distribution of PGG-paclitaxel, a novel macromolecular formulation of paclitaxel, in nu/nu mice bearing NCI-460 lung cancer xenografts. *Cancer Chemotherapy and Pharmacology*. 2010;65(3):515-26.

137. Feng Z, Zhao G, Yu L, Gough D, Howell SB. Preclinical efficacy studies of a novel nanoparticle-based formulation of paclitaxel that out-performs Abraxane. *Cancer Chemotherapy and Pharmacology*. 2010;65(5):923-30.

138. Xie Z, Guan H, Chen X, Lu C, Chen L, Hu X, et al. A novel polymer–paclitaxel conjugate based on amphiphilic triblock copolymer. *Journal of Controlled Release*. 2007;117(2):210-6.

139. Zhang X, Li Y, Chen X, Wang X, Xu X, Liang Q, et al. Synthesis and characterization of the paclitaxel/MPEG-PLA block copolymer conjugate. *Biomaterials*. 2005;26(14):2121-8.

140. Rodrigues PCA, Scheuermann K, Stockmar C, Maier G, Fiebig HH, Unger C, et al. Synthesis and In vitro efficacy of acid-Sensitive poly(ethylene glycol) paclitaxel conjugates. *Bioorganic & Medicinal Chemistry Letters*. 2003;13(3):355-60.

141. Cavallaro G, Licciardi M, Caliceti P, Salmaso S, Giammona G. Synthesis, physico-chemical and biological characterization of a paclitaxel macromolecular prodrug. *European Journal of Pharmaceutics and Biopharmaceutics*. 2004;58(1):151-9.

142. Kakinoki A, Kaneo Y, Tanaka T, Hosokawa Y. Synthesis and Evaluation of Water-Soluble Poly(vinyl alcohol)–paclitaxel Conjugate as a Macromolecular Prodrug. *Biological & Pharmaceutical Bulletin*. 2008;31(5):963-9.

143. Wang Y, Xin D, Liu K, Xiang J. Heparin–Paclitaxel Conjugates Using Mixed Anhydride as Intermediate: Synthesis, Influence of Polymer Structure on Drug Release, Anticoagulant Activity and In Vitro Efficiency. *Pharmaceutical Research*. 2009;26(4):785-93.

144. Wang Y, Xin D, Liu K, Zhu M, Xiang J. Heparin–Paclitaxel Conjugates as Drug Delivery System: Synthesis, Self-Assembly Property, Drug Release, and Antitumor Activity. *Bioconjugate Chemistry*. 2009;20(12):2214-21.

145. Sugahara S-i, Kajiki M, Kuriyama H, Kobayashi T-r. Paclitaxel Delivery Systems: The Use of Amino Acid Linkers in the Conjugation of Paclitaxel with Carboxymethyldextran to Create Prodrugs. *Biological & Pharmaceutical Bulletin*. 2002;25(5):632-41.

146. Sugahara S-i, Kajiki M, Kuriyama H, Kobayashi T-r. Complete regression of xenografted human carcinomas by a paclitaxel–carboxymethyl dextran conjugate (AZ10992). *Journal of Controlled Release*. 2007;117(1):40-50.

147. Sugahara S-i, Kajiki M, Kuriyama H, Kobayashi T-r. Carrier Effects on Antitumor Activity and Neurotoxicity of AZ10992, a Paclitaxel–Carboxymethyl Dextran Conjugate, in a Mouse Model. *Biological & Pharmaceutical Bulletin*. 2008;31(2):223-30.

148. Thanou M, Verhoef JC, Junginger HE. Oral drug absorption enhancement by chitosan and its derivatives. *Advanced Drug Delivery Reviews*. 2001;52(2):117-26.

149. Lee E, Lee J, Lee I-H, Yu M, Kim H, Chae SY, et al. Conjugated Chitosan as a Novel Platform for Oral Delivery of Paclitaxel. *Journal of Medicinal Chemistry*. 2008;51(20):6442-9.

150. Lee E, Kim H, Lee I-H, Jon S. In vivo antitumor effects of chitosan-conjugated docetaxel after oral administration. *Journal of Controlled Release*. 2009;140(2):79-85.

151. Jun YJ, Min JH, Ji DE, Yoo JH, Kim JH, Lee HJ, et al. A micellar prodrug of paclitaxel conjugated to cyclotriphosphazene. *Bioorganic & Medicinal Chemistry Letters*. 2008;18(24):6410-3.

152. Lim J, Lo ST, Hill S, Pavan GM, Sun X, Simanek EE. Antitumor activity and molecular dynamics simulations of paclitaxel-laden triazine dendrimers. *Molecular Pharmaceutics*. 2012;9(3):404-12.

153. Lo S-T, Stern S, Clogston JD, Zheng J, Adiseshaiah PP, Dobrovolskaia M, et al. Biological Assessment of Triazine Dendrimer: Toxicological Profiles, Solution Behavior, Biodistribution, Drug Release and Efficacy in a PEGylated, Paclitaxel Construct. *Molecular Pharmaceutics*. 2010;7(4):993-1006.

154. Lim J, Chouai A, Lo S-T, Liu W, Sun X, Simanek EE. Design, Synthesis, Characterization, and Biological Evaluation of Triazine Dendrimers Bearing Paclitaxel Using Ester and Ester/Disulfide Linkages. *Bioconjugate Chemistry*. 2009;20(11):2154-61.

155. Floyd WC, Datta GK, Imamura S, Kieler-Ferguson HM, Jerger K, Patterson AW, et al. Chemotherapeutic Evaluation of a Synthetic Tubulysin Analogue–Dendrimer Conjugate in C26 Tumor Bearing Mice. *ChemMedChem*. 2011;6(1):49-53.

156. Khandare JJ, Jayant S, Singh A, Chandna P, Wang Y, Vorsa N, et al. Dendrimer Versus Linear Conjugate: Influence of Polymeric Architecture on the Delivery and Anticancer Effect of Paclitaxel. *Bioconjugate Chemistry*. 2006;17(6):1464-72.

157. Miller K, Erez R, Segal E, Shabat D, Satchi-Fainaro R. Targeting Bone Metastases with a Bispecific Anticancer and Antiangiogenic Polymer–Alendronate–Taxane Conjugate. *Angewandte Chemie International Edition*. 2009;48(16):2949-54.

158. Miller K, Eldar-Boock A, Polyak D, Segal E, Benayoun L, Shaked Y, et al. Antiangiogenic Antitumor Activity of HPMA Copolymer–Paclitaxel–Alendronate Conjugate on Breast Cancer Bone Metastasis Mouse Model. *Molecular Pharmaceutics*. 2011;8(4):1052-62.

159. Clementi C, Miller K, Mero A, Satchi-Fainaro R, Pasut G. Dendritic Poly(ethylene glycol) Bearing Paclitaxel and Alendronate for Targeting Bone Neoplasms. *Molecular Pharmaceutics*. 2011;8(4):1063-72.

160. Rosato A, Banzato A, De Luca G, Renier D, Bettella F, Pagano C, et al. HYTAD1-p20: A new paclitaxel-hyaluronic acid hydrosoluble bioconjugate for treatment of superficial bladder cancer. *Urologic Oncology: Seminars and Original Investigations*. 2006;24(3):207-15.

161. Almond A. Hyaluronan. *Cellular and molecular life sciences : CMLS*. 2007;64(13):1591-6.

162. Banzato A, Rondina M, Meléndez-Alafort L, Zangoni E, Nadali A, Renier D, et al. Biodistribution imaging of a paclitaxel-hyaluronan bioconjugate. *Nuclear Medicine and Biology*. 2009;36(5):525-33.

163. De Stefano I, Battaglia A, Zannoni G, Prisco M, Fattorossi A, Travaglia D, et al. Hyaluronic acid–paclitaxel: effects of intraperitoneal administration against CD44(+) human ovarian cancer xenografts. *Cancer Chemotherapy and Pharmacology*. 2011;68(1):107-16.

164. Auzenne E, Ghosh SC, Khodadadian M, Rivera B, Farquhar D, Price RE, et al. Hyaluronic acid-paclitaxel: antitumor efficacy against CD44(+) human ovarian carcinoma xenografts. *Neoplasia*. 2007;9(6):479-86.

165. Galer CE, Sano D, Ghosh SC, Hah JH, Auzenne E, Hamir AN, et al. Hyaluronic acid–paclitaxel conjugate inhibits growth of human squamous cell carcinomas of the head and neck via a hyaluronic acid-mediated mechanism. *Oral Oncology*. 2011;47(11):1039-47.

166. Xin D, Wang Y, Xiang J. The Use of Amino Acid Linkers in the Conjugation of Paclitaxel with Hyaluronic Acid as Drug Delivery System: Synthesis, Self-Assembled Property, Drug Release, and <i>In Vitro</i> Efficiency. *Pharmaceutical Research*. 2010;27(2):380-9.

167. Eldar-Boock A, Miller K, Sanchis J, Lupu R, Vicent MJ, Satchi-Fainaro R. Integrin-assisted drug delivery of nano-scaled polymer therapeutics bearing paclitaxel. *Biomaterials*. 2011;32(15):3862-74.

168. Ito Y, Kobayashi T, Kimura T, Matsuura N, Wakasugi E, Takeda T, et al. Investigation of the oxytocin receptor expression in human breast cancer tissue using newly established monoclonal antibodies. *Endocrinology*. 1996;137(2):773-9.

169. Cavallaro G, Maniscalco L, Campisi M, Schillaci D, Giammona G. Synthesis, characterization and in vitro cytotoxicity studies of a macromolecular conjugate of paclitaxel bearing oxytocin as targeting moiety. *European Journal of Pharmaceutics and Biopharmaceutics*. 2007;66(2):182-92.

170. Johansson EMV, Dubois J, Darbre T, Reymond J-L. Glycopeptide dendrimer colchicine conjugates targeting cancer cells. *Bioorganic & Medicinal Chemistry*. 2010;18(17):6589-97.

171. Lagnoux D, Darbre T, Schmitz ML, Reymond JL. Inhibition of mitosis by glycopeptide dendrimer conjugates of colchicine. *Chemistry-a European Journal*. 2005;11(13):3941-50.

172. Moktan S, Ryppa C, Kratz F, Raucher D. A thermally responsive biopolymer conjugated to an acid-sensitive derivative of paclitaxel stabilizes microtubules, arrests cell cycle, and induces apoptosis. *Investigational New Drugs*. 2012;30(1):236-48.

173. Chun C, Lee SM, Kim SY, Yang HK, Song S-C. Thermosensitive poly(organophosphazene)–paclitaxel conjugate gels for antitumor applications. *Biomaterials*. 2009;30(12):2349-60.

174. Erez R, Segal E, Miller K, Satchi-Fainaro R, Shabat D. Enhanced cytotoxicity of a polymer–drug conjugate with triple payload of paclitaxel. *Bioorganic & Medicinal Chemistry*. 2009;17(13):4327-35.

175. Etrych Ts, Šírová M, Starovoytova L, Říhová B, Ulbrich K. HPMA Copolymer Conjugates of Paclitaxel and Docetaxel with pH-Controlled Drug Release. *Molecular Pharmaceutics*. 2010;7(4):1015-26.

176. Tong R, Yala L, Fan TM, Cheng J. The formulation of aptamer-coated paclitaxel–polylactide nanoconjugates and their targeting to cancer cells. *Biomaterials*. 2010;31(11):3043-53.

177. Shan L, Cui S, Du C, Wan S, Qian Z, Achilefu S, et al. A paclitaxel-conjugated adenovirus vector for targeted drug delivery for tumor therapy. *Biomaterials*. 2012;33(1):146-62.

178. Li H-J, Everts M, Pereboeva L, Komarova S, Idan A, Curiel DT, et al. Adenovirus Tumor Targeting and Hepatic Untargeting by a Coxsackie/Adenovirus Receptor Ectodomain Anti–Carcinoembryonic Antigen Bispecific Adapter. *Cancer Research*. 2007;67(11):5354-61.

179. Bouvier E, Thirot S, Schmidt F, Monneret C. A new paclitaxel prodrug for use in ADEPT strategy. *Organic & Biomolecular Chemistry*. 2003;1(19).

180. Alaoui AE, Saha N, Schmidt F, Monneret C, Florent J-C. New Taxol® (paclitaxel) prodrugs designed for ADEPT and PMT strategies in cancer chemotherapy. *Bioorganic & Medicinal Chemistry*. 2006;14(14):5012-9.

181. Liu D-Z, Sinchaikul S, Reddy PVG, Chang M-Y, Chen S-T. Synthesis of 2′-paclitaxel methyl 2-glucopyranosyl succinate for specific targeted delivery to cancer cells. *Bioorganic & Medicinal Chemistry Letters*. 2007;17(3):617-20.

182. Lin Y-S, Tungpradit R, Sinchaikul S, An F-M, Liu D-Z, Phutrakul S, et al. Targeting the Delivery of Glycan-Based Paclitaxel Prodrugs to Cancer Cells via Glucose Transporters. *Journal of Medicinal Chemistry*. 2008;51(23):7428-41.

183. Aspland SE, Ballatore C, Castillo R, Desharnais J, Eustaquio T, Goelet P, et al. Kinase-mediated trapping of bi-functional conjugates of paclitaxel or vinblastine with thymidine in cancer cells. *Bioorganic & Medicinal Chemistry Letters*. 2006;16(19):5194-8.

184. Skwarczynski M, Noguchi M, Hirota S, Sohma Y, Kimura T, Hayashi Y, et al. Development of first photoresponsive prodrug of paclitaxel. *Bioorganic & Medicinal Chemistry Letters*. 2006;16(17):4492-6.

185. Noguchi M, Skwarczynski M, Prakash H, Hirota S, Kimura T, Hayashi Y, et al. Development of novel water-soluble photocleavable protective group and its application for design of photoresponsive paclitaxel prodrugs. *Bioorganic & Medicinal Chemistry*. 2008;16(10):5389-97.

186. Damen EWP, Nevalainen TJ, van den Bergh TJM, de Groot FMH, Scheeren HW. Synthesis of novel paclitaxel prodrugs designed for bioreductive activation in hypoxic tumour tissue. *Bioorganic & Medicinal Chemistry*. 2002;10(1):71-7.

187. Shah R. The Design and Synthesis of Novel Inhibitors of Tubulin Polymerisation [PhD thesis]. Dublin: University of Dublin, Trinity College Dublin; 2002.

188. Hudson G. Design, Synthesis and Evaluation of Novel Tumour Vasculature-targeting agents [PhD thesis]. Dublin: University of Dublin, Trinity College; 2006.

189. Liotta D, Arbiser J, Short JW, Saindane M. Simple, inexpensive procedure for the large-scale production of alkyl quinones. *The Journal of Organic Chemistry*. 1983;48(17):2932-3.

190. Clayden J, Greeves N, Warren S, Wothers P. Organic Chemistry. Oxford: Oxford University Press; 2001.

191. Carter R, Hodgetts K, McKenna J, Magnus P, Wren S. Studies on the Stereoselective Synthesis of the Marine Antitumor Agent Eleutherobin. *Tetrahedron*. 2000;56(26):4367-82.

192. Dess DB, Martin JC. Readily accessible 12-I-5 oxidant for the conversion of primary and secondary alcohols to aldehydes and ketones. *The Journal of Organic Chemistry*. 1983;48(22):4155-6.

193. Meyer SD, Schreiber SL. Acceleration of the Dess-Martin Oxidation by Water. *The Journal of Organic Chemistry*. 1994;59(24):7549-52.

194. Hui Bing L, Yu Yuan X. Regioselective Oxidation of Phenols to o-Quinones with Dess-Martin Periodinane (DMP). *Chinese chemical letters*. 2003;14:555-6.

195. Rautio J, Kumpulainen H, Heimbach T, Oliyai R, Oh D, Järvinen T, et al. Prodrugs: design and clinical applications. *Nature Reviews Drug Discovery*. 2008;7(3):255-70.

196. Yuan H, Li N, Lai Y. Evaluation of in Vitro Models for Screening Alkaline Phosphatase-Mediated Bioconversion of Phosphate Ester Prodrugs. *Drug Metabolism and Disposition*. 2009;37(7):1443-7.

197. Fleisher D, Bong R, Stewart BH. Improved oral drug delivery: solubility limitations overcome by the use of prodrugs. *Advanced Drug Delivery Reviews*. 1996;19(2):115-30.

198. Perry CM, McTavish D. Estramustine phosphate sodium. A review of its pharmacodynamic and pharmacokinetic properties, and therapeutic efficacy in prostate cancer. *Drugs & aging*. 1995;7(1):49-74.

199. Rose WC, Basler GA, Trail PA, Saulnier M, Crosswell AR, Casazza AM. Preclinical antitumor activity of a soluble etoposide analog, BMY-40481-30. *Investigational New Drugs*. 1990;8 Suppl 1:S25-32.

200. Ueda Y, Mikkilineni AB, Knipe JO, Rose WC, Casazza AM, Vyas DM. Novel water soluble phosphate prodrugs of taxol® possessing in vivo antitumor activity. *Bioorganic & Medicinal Chemistry Letters*. 1993;3(8):1761-6.

201. Pettit GR, Singh SB, Boyd MR, Hamel E, Pettit RK, Schmidt JM, et al. Antineoplastic Agents. 291. Isolation and Synthesis of Combretastatins A-4, A-5, and A-6. *Journal of Medicinal Chemistry*. 1995;38(10):1666-72.

202. Pettit GR, Grealish MP, Jung MK, Hamel E, Pettit RK, Chapuis JC, et al. Antineoplastic Agents. 465. Structural Modification of Resveratrol: Sodium Resverastatin Phosphate1. *Journal of Medicinal Chemistry*. 2002;45(12):2534-42.

203. Miyaura N, Suzuki A. Palladium-Catalyzed Cross-Coupling Reactions of Organoboron Compounds. *Chemical Reviews*. 1995;95(7):2457-83.

204. Wuts PGM, Greene TW. Greene's protective groups in organic synthesis. 4th ed. New York; Chichester: Wiley-Interscience; 2007.

205. Kitagawa K, Inoue A, Shinokubo H, Oshima K. Halogen–Magnesium Exchange via Trialkylmagnesates for the Preparation of Aryl- and Alkenylmagnesium Reagents. *Angewandte Chemie International Edition*. 2000;39(14):2481-3.

206. Song J, Tan Z, Yee N, inventors; Boehringer Ingelheim Pharmaceuticals, Inc. (Ridgefield, CT), assignee. Preparation of aryl intermediates. United States patent US 7,022,883. 2006 April 4.

207. Ishiyama T, Murata M, Miyaura N. Palladium(0)-Catalyzed Cross-Coupling Reaction of Alkoxydiboron with Haloarenes: A Direct Procedure for Arylboronic Esters. *The Journal of Organic Chemistry*. 1995;60(23):7508-10.

208. Pereira S, Srebnik M. A study of hydroboration of alkenes and alkynes with pinacolborane catalyzed by transition metals. *Tetrahedron Letters*. 1996;37(19):3283-6.

209. Giroux A, Han Y, Prasit P. One pot biaryl synthesis via in situ boronate formation. *Tetrahedron Letters*. 1997;38(22):3841-4.

210. Prokopiou E. Preclinical Evaluation of Novel Tumour Vasculature Disrupting Agents [PhD thesis]. Dublin: University of Dublin, Trinity College Dublin; 2012.

211. Lin HL, Chiou SH, Wu CW, Lin WB, Chen LH, Yang YP, et al. Combretastatin A4-induced differential cytotoxicity and reduced metastatic ability by inhibition of AKT function in human gastric cancer cells. *The Journal of pharmacology and experimental therapeutics*. 2007;323(1):365-73.

212. Nihei Y, Suzuki M, Okano A, Tsuji T, Akiyama Y, Tsuruo T, et al. Evaluation of antivascular and antimitotic effects of tubulin binding agents in solid tumor therapy. *Japanese journal of cancer research : Gann*. 1999;90(12):1387-95.

213. Breen EC. The Design, Synthesis and Preliminary Evaluation of Prodrugs and Hybrid Drugs with Tubulin Polymerisation Inhibitory Activity and Anti-Proliferative Activity [PhD thesis]. Dublin: University of Dublin, Trinity College; 2012.

214. Rentsch KM. The importance of stereoselective determination of drugs in the clinical laboratory. *Journal of Biochemical and Biophysical Methods*. 2002;54(1–3):1-9.

215. Caner H, Groner E, Levy L, Agranat I. Trends in the development of chiral drugs. *Drug Discovery Today*. 2004;9(3):105-10.

216. Agranat I, Wainschtein SR. The strategy of enantiomer patents of drugs. *Drug Discovery Today*. 2010;15(5–6):163-70.

217. Ariëns EJ. Stereochemistry, a basis for sophisticated nonsense in pharmacokinetics and clinical pharmacology. *European Journal of Clinical Pharmacology*. 1984;26(6):663-8.

218. Takahashi H, Echizen H. Pharmacogenetics of warfarin elimination and its clinical implications. *Clinical Pharmacokinetics*. 2001;40(8):587-603.

219. Mehvar R, Reynolds JM, Robinson MA, Longstreth JA. Enantioselective kinetics of verapamil and norverapamil in isolated perfused rat livers. *Pharmaceutical Research*. 1994;11(12):1815-9.

220. Islam MR, Mahdi JG, Bowen ID. Pharmacological importance of stereochemical resolution of enantiomeric drugs. *Drug safety : an international journal of medical toxicology and drug experience*. 1997;17(3):149-65.

221. Agranat I, Caner H, Caldwell J. Putting chirality to work: the strategy of chiral switches. *Nature Reviews Drug Discovery*. 2002;1(10):753.

222. Rang HP, Dale MM, Ritter JM, Moore PK. Pharmacology. 5th ed. Edinburgh Churchill Livingstone; 2003.

223. Röhss K, Hasselgren G, Hedenström H. Effect of Esomeprazole 40 mg vs Omeprazole 40 mg on 24-Hour Intragastric pH in Patients with Symptoms of Gastroesophageal Reflux Disease. *Digestive Diseases and Sciences*. 2002;47(5):954-8.

224. Morrissey I, Hoshino K, Sato K, Yoshida A, Hayakawa I, Bures MG, et al. Mechanism of differential activities of ofloxacin enantiomers. *Antimicrobial agents and chemotherapy*. 1996;40(8):1775-84.

225. Marez D, Legrand M, Sabbagh N, Lo Guidice JM, Spire C, Lafitte JJ, et al. Polymorphism of the cytochrome P450 CYP2D6 gene in a European population: characterization of 48 mutations and 53 alleles, their frequencies and evolution. *Pharmacogenetics*. 1997;7(3):193-202.

226. Kristensen K, Christensen CB, Christrup LL. The mu1, mu2, delta, kappa opioid receptor binding profiles of methadone stereoisomers and morphine. *Life Sciences*. 1995;56(2):PL45-50.

227. White PF, Ham J, Way WL, Trevor AJ. Pharmacology of ketamine isomers in surgical patients. *Anesthesiology*. 1980;52(3):231-9.

228. Schuttler J, Stanski DR, White PF, Trevor AJ, Horai Y, Verotta D, et al. Pharmacodynamic modeling of the EEG effects of ketamine and its enantiomers in man. *Journal of pharmacokinetics and biopharmaceutics*. 1987;15(3):241-53.

229. Yatagai M, Ohnuki T. Asymmetric reduction of functionalized ketones with a sodium borohydride-(L)-tartaric acid system. *Journal of the Chemical Society, Perkin Transactions 1*. 1990;0(6):1826-8.

230. Midland MM, McLoughlin JI, Gabriel J. Asymmetric reductions of prochiral ketones with B-3-pinanyl-9-borabicyclo[3.3.1]nonane (Alpine-Borane) at elevated pressures. *The Journal of Organic Chemistry*. 1989;54(1):159-65.

231. Noyori R, Ohkuma T, Kitamura M, Takaya H, Sayo N, Kumobayashi H, et al. Asymmetric hydrogenation of .beta.-keto carboxylic esters. A practical, purely chemical access to .beta.-hydroxy esters in high enantiomeric purity. *Journal of the American Chemical Society*. 1987;109(19):5856-8.

232. Davies HG, Green RH, Kelly DR, Roberts SM. Biotransformations in Preparative Organic Chemistry. The Use of Isolated Enzymes and Whole Cell Systems in Synthesis. London: Academic Press; 1989.

233. Noyori R, Ohkuma T. Asymmetric Catalysis by Architectural and Functional Molecular Engineering: Practical Chemo- and Stereoselective Hydrogenation of Ketones. *Angewandte Chemie International Edition*. 2001;40(1):40-73.

234. Palmer MJ, Wills M. Asymmetric transfer hydrogenation of CO and CN bonds. *Tetrahedron: Asymmetry*. 1999;10(11):2045-61.

235. Mashima K, Kusano K-h, Sato N, Matsumura Y-i, Nozaki K, Kumobayashi H, et al. Cationic BINAP-Ru(II) Halide Complexes: Highly Efficient Catalysts for Stereoselective Asymmetric Hydrogenation of .alpha.- and .beta.-Functionalized Ketones. *The Journal of Organic Chemistry*. 1994;59(11):3064-76.

236. Corey EJ, Bakshi RK, Shibata S. Highly enantioselective borane reduction of ketones catalyzed by chiral oxazaborolidines. Mechanism and synthetic implications. *Journal of the American Chemical Society*. 1987;109(18):5551-3.

237. Corey EJ, Bakshi RK, Shibata S, Chen CP, Singh VK. A stable and easily prepared catalyst for the enantioselective reduction of ketones-Applications to multistep synthesis. *Journal of the American Chemical Society*. 1987;109(25):7925-6.

238. Corey EJ, Shibata S, Bakshi RK. An efficient and catalytically enantioselective route to (S)-(-)-phenyloxirane. *Journal of Organic Chemistry*. 1988;53(12):2861-3.

239. Wallbaum S, Martens J. Asymmetric syntheses with chiral oxazaborolidines. *Tetrahedron-Asymmetry*. 1992;3(12):1475-504.

240. North M. The Baker's Yeast Reduction of Keto-Esters in Organic Solvents: A One Week Research Project for Undergraduate Students. *Journal of Chemical Education*. 1998;75(5):630-null.

241. North M. Baker's yeast reduction of β-keto esters in petrol. *Tetrahedron Letters*. 1996;37(10):1699-702.

242. Jayasinghe LY, Kodituwakku D, Smallridge AJ, Trewhella MA. The Use of Organic Solvent Systems in the Yeast Mediated Reduction of Ethyl Acetoacetate. *Bulletin of the Chemical Society of Japan*. 1994;67(9):2528-31.

243. Athanasiou N, Smallridge AJ, Trewhella MA. Baker's yeast mediated reduction of [beta]-keto esters and [beta]-keto amides in an organic solvent system. *Journal of Molecular Catalysis B: Enzymatic*. 2001;11(4-6):893-6.

244. Medson C, Smallridge AJ, Trewhella MA. The stereoselective preparation of [beta]-hydroxy esters using a yeast reduction in an organic solvent. *Tetrahedron: Asymmetry*. 1997;8(7):1049-54.

245. Parker D. NMR determination of enantiomeric purity. *Chemical Reviews*. 1991;91(7):1441-57.

246. Dale JA, Dull DL, Mosher HS. .alpha.-Methoxy-.alpha.-trifluoromethylphenylacetic acid, a versatile reagent for the determination of enantiomeric composition of alcohols and amines. *The Journal of Organic Chemistry*. 1969;34(9):2543-9.

247. Ohtani I, Kusumi T, Kashman Y, Kakisawa H. High-field FT NMR application of Mosher's method. The absolute configurations of marine terpenoids. *Journal of the American Chemical Society*. 1991;113(11):4092-6.

248. Corey EJ, Link JO. A new chiral catalyst for the enantioselective synthesis of secondary alcohols and deuterated primary alcohols by carbonyl reduction. *Tetrahedron Letters*. 1989;30(46):6275-8.

249. Kawanami Y, Murao S, Ohga T, Kobayashi N. Practical enantioselective reduction of ketones using oxazaborolidine catalyst generated in situ from chiral lactam alcohol and borane. *Tetrahedron*. 2003;59(42):8411-4.

250. Deloux L, Srebnik M. Asymmetric boron-catalyzed reactions. *Chemical Reviews*. 1993;93(2):763-84.

251. Corey EJ, Gras J-L, Ulrich P. A new general method for protection of the hydroxyl function. *Tetrahedron Letters*. 1976;17(11):809-12.

252. Corey EJ, Shirahama H, Yamamoto H, Terashima S, Venkateswarlu A, Schaaf TK. Stereospecific total synthesis of prostaglandins E3 and F3.alpha. *Journal of the American Chemical Society*. 1971;93(6):1490-1.

253. Walsh JJ. The synthesis of cyclocholamide macrocycles with tunable cavity sizes [Phd thesis]. Dublin: University of Dublin, Trinity College; 1994.

254. Gras J-L, Chang Y, Guerin A. Lithium Bromide-Assisted Protection of Primary and Secondary Alcohols as Methoxymethyl Ethers using Dimethoxymethane. *Synthesis*. 1985;1985(01):74-5.

255. Sharma GVM, Reddy KL, Sree Lakshmi P, Radha Krishna P. An efficient protocol for the preparation of MOM ethers and their deprotection using zirconium(IV) chloride. *Tetrahedron Letters*. 2004;45(50):9229-32.

256. Hanessian S, Delorme D, Dufresne Y. Mild cleavage of methoxymethyl (MOM) ethers with trimethylsilyl bromide. *Tetrahedron Letters*. 1984;25(24):2515-8.

257. Moher ED, Grieco PA, Collins JL. (R)-(+)- and (S)-(-)-5-Ethyl-5-methyl-1,3-dioxolane-2,4-dione reagents for the direct preparation of .alpha.-hydroxy-.alpha.-methylbutyrate esters: assignment of the absolute configuration of the .alpha.-acetoxy-.alpha.-methylbutyrate ester side chain of quassimarin via total synthesis. *The Journal of Organic Chemistry*. 1993;58(15):3789-90.

258. Node M, Kajimoto T, Nishide K, Fujita E, Fuji K. Hard Acid and Soft Nucleophile Systems. Part 13. Aluminum Chloride-Sodium Iodide-Acetonitrile System : A Very Mild Reagent for Selective Dealkylation (Commemoration Issue Dedicated to Professor Shigeo Tanimoto On the Occation of His Retirement). *Bulletin of the Institute for Chemical Research, Kyoto University*. 1992;70(3):308 - 17.

259. Maruyama H, Hiraoka T. A stereocontrolled synthesis of thienamycin from 6-aminopenicillanic acid. *The Journal of Organic Chemistry*. 1986;51(3):399-402.

260. Dijkstra G, Kruizinga WH, Kellogg RM. An assessment of the causes of the "cesium effect". *The Journal of Organic Chemistry*. 1987;52(19):4230-4.

261. Wegge T, Schwarz S, Seitz G. A new and efficient synthetic route to enantiopure (+)-anatoxin-a from (-)-cocaine hydrochloride. *Tetrahedron: Asymmetry*. 2000;11(6):1405-10.

262. Enders D, Backes M. First asymmetric synthesis of both enantiomers of Tropional® and their olfactory evaluation. *Tetrahedron: Asymmetry*. 2004;15(11):1813-7.

263. Corey EJ, Schmidt G. Useful procedures for the oxidation of alcohols involving pyridinium dichromate in approtic media. *Tetrahedron Letters*. 1979;20(5):399-402.

264. Mazitschek R, Mülbaier M, Giannis A. IBX-Mediated Oxidation of Primary Alcohols and Aldehydes To Form Carboxylic Acids. *Angewandte Chemie International Edition*. 2002;41(21):4059-61.

265. Dalcanale E, Montanari F. Selective oxidation of aldehydes to carboxylic acids with sodium chlorite-hydrogen peroxide. *The Journal of Organic Chemistry*. 1986;51(4):567-9.

266. Raach A, Reiser O. Sodium Chlorite-Hydrogen Peroxide — A Mild and Selective Reagent for the Oxidation of Aldehydes to Carboxylic Acids. *Journal für praktische Chemie*. 2000;342(6):605-8.

267. Travis BR, Sivakumar M, Hollist GO, Borhan B. Facile Oxidation of Aldehydes to Acids and Esters with Oxone. *Organic Letters*. 2003;5(7):1031-4.

268. Breen EC, Walsh JJ. Tubulin-targeting agents in hybrid drugs. *Current Medicinal Chemistry*. 2010;17(7):609-39.

269. Wickström M, Larsson R, Nygren P, Gullbo J. Aminopeptidase N (CD13) as a target for cancer chemotherapy. *Cancer Science*. 2011;102(3):501-8.

270. Mina-Osorio P. The moonlighting enzyme CD13: old and new functions to target. *Trends in Molecular Medicine*. 2008;14(8):361-71.

271. Pasqualini R, Koivunen E, Kain R, Lahdenranta J, Sakamoto M, Stryhn A, et al. Aminopeptidase N Is a Receptor for Tumor-homing Peptides and a Target for Inhibiting Angiogenesis. *Cancer Research*. 2000;60(3):722-7.

272. Bhagwat SV, Lahdenranta J, Giordano R, Arap W, Pasqualini R, Shapiro LH. CD13/APN is activated by angiogenic signals and is essential for capillary tube formation. *Blood*. 2001;97(3):652-9.

273. Martinez JM, Prieto I, Ramirez MJ, Cueva C, Alba F, Ramirez M. Aminopeptidase activities in breast cancer tissue. *Clinical chemistry*. 1999;45(10):1797-802.

274. Surowiak P, Drag M, Materna V, Suchocki S, Grzywa R, Spaczynski M, et al. Expression of aminopeptidase N/CD13 in human ovarian cancers. *International journal of gynecological cancer*. 2006;16(5):1783-8.

275. Hashida H, Takabayashi A, Kanai M, Adachi M, Kondo K, Kohno N, et al. Aminopeptidase N is involved in cell motility and angiogenesis: its clinical significance in human colon cancer. *Gastroenterology*. 2002;122(2):376-86.

276. Kehlen A, Lendeckel U, Dralle H, Langner J, Hoang-Vu C. Biological significance of aminopeptidase N/CD13 in thyroid carcinomas. *Cancer Research*. 2003;63(23):8500-6.

277. Umezawa H, Aoyagi T, Suda H. Ubenimex, an inhibitor of aminopeptidase B, produced by actinomycetes. *The Journal of antibiotics*. 1976;29:97-9.

278. Krige D, Needham LA, Bawden LJ, Flores N, Farmer H, Miles LEC, et al. CHR-2797: An Antiproliferative Aminopeptidase Inhibitor that Leads to Amino Acid Deprivation in Human Leukemic Cells. *Cancer Research*. 2008;68(16):6669-79.

279. Sakuraya M, Tamura J, Itoh K, Kubota K, Naruse T. Aminopeptidase inhibitor ubenimex inhibits the growth of leukaemic cell lines and myeloma cells through its cytotoxicity. *The Journal of international medical research*. 2000;28(5):214-21.

280. Shim JS, Kim JH, Cho HY, Yum YN, Kim SH, Park HJ, et al. Irreversible inhibition of CD13/aminopeptidase N by the antiangiogenic agent curcumin. *Chemistry & biology*. 2003;10(8):695-704.

281. Zhang X, Fang H, Zhang J, Yuan Y, Xu W. Recent advance in aminopeptidase N (APN/CD13) inhibitor research. *Current Medicinal Chemistry*. 2011;18(32):5011-21.

282. Iguchi K, Nakano T, Usui S, Hirano K. Incadronate inhibits aminopeptidase N expression in prostatic PC-3 cells. *Cancer Letters*. 2006;237(2):223-33.

283. Lipinski CA. Drug-like properties and the causes of poor solubility and poor permeability. *Journal of Pharmacological and Toxicological Methods*. 2000;44(1):235-49.

284. Flipo M, Beghyn T, Charton J, Leroux VA, Deprez BP, Deprez-Poulain RF. A library of novel hydroxamic acids targeting the metallo-protease family: Design, parallel synthesis and screening. *Bioorganic & Medicinal Chemistry*. 2007;15(1):63-76.

285. Wermuth CG. The practice of medicinal chemistry. London: Academic; 2008.

286. Scatena R. Prinomastat, a hydroxamate-based matrix metalloproteinase inhibitor. A novel pharmacological approach for tissue remodelling-related diseases. *Expert Opinion on Investigational Drugs*. 2000;9(9):2159-65.

287. Hemmings FJ, Farhan M, Rowland J, Banken L, Jain R. Tolerability and pharmacokinetics of the collagenase-selective inhibitor Trocade™ in patients with rheumatoid arthritis. *Rheumatology*. 2001;40(5):537-43.

288. Marks PA. Discovery and development of SAHA as an anticancer agent. *Oncogene*. 2007;26(9):1351-6.

289. Wang X, Jing F, Zhu H, Fang H, Zhang J, Xu W. Activity screening and structure–activity relationship of the hit compounds targeting APN/CD13. *Fundamental & Clinical Pharmacology*. 2011;25(2):217-28.

290. Inagaki Y, Tang W, Zhang L, Du G, Xu W, Kokudo N. Novel aminopeptidase N (APN/CD13) inhibitor 24F can suppress invasion of hepatocellular carcinoma cells as well as angiogenesis. *Bioscience trends*. 2010;4(2):56-60.

291. Melzig MF, Bormann H. Betulinic acid inhibits aminopeptidase N activity. *Planta Med*. 1998;64(7):655-7.

292. Mosmann T. Rapid colorimetric assay for cellular growth and survival: application to proliferation and cytotoxicity assays. *Journal of immunological methods*. 1983;65(1-2):55-63.

9 Appendix A

Stack GD, Walsh JJ. Optimising the delivery of tubulin targeting agents through antibody conjugation. *Pharmaceutical Research*. 2012;29(11):2972-84

Optimising the Delivery of Tubulin Targeting Agents through Antibody Conjugation

Gary D. Stack & John J. Walsh

Pharmaceutical Research
An Official Journal of the American Association of Pharmaceutical Scientists

ISSN 0724-8741

Pharm Res
DOI 10.1007/s11095-012-0810-9

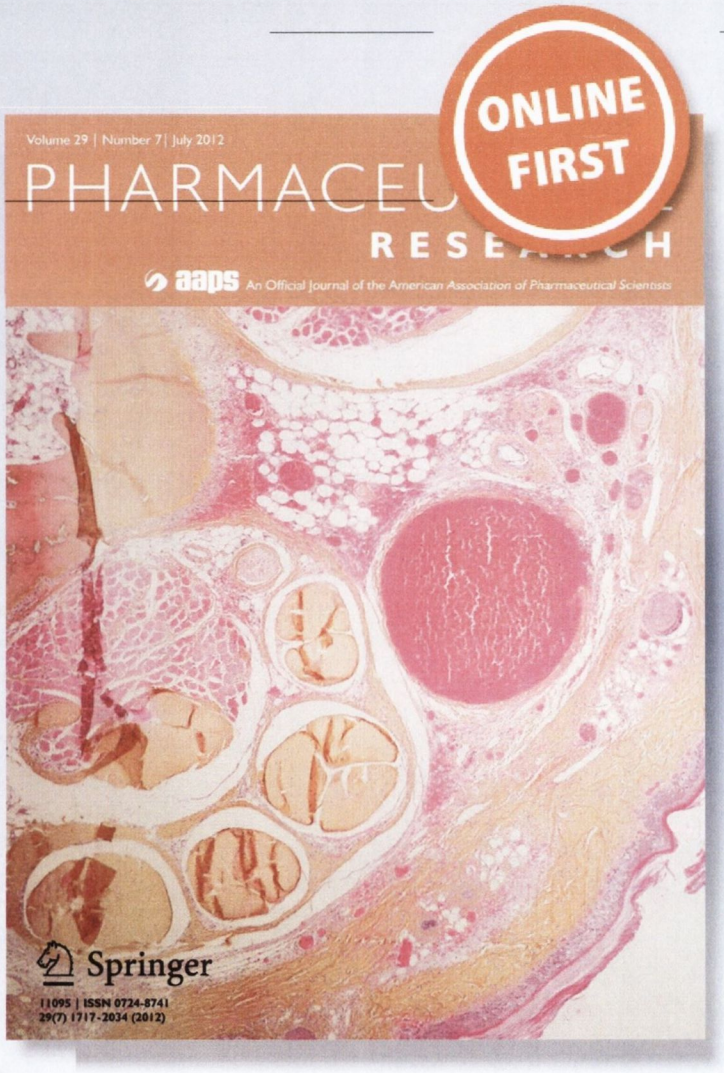

Springer

Your article is protected by copyright and all rights are held exclusively by Springer Science+Business Media, LLC. This e-offprint is for personal use only and shall not be self-archived in electronic repositories. If you wish to self-archive your work, please use the accepted author's version for posting to your own website or your institution's repository. You may further deposit the accepted author's version on a funder's repository at a funder's request, provided it is not made publicly available until 12 months after publication.



Author's personal copy

Pharm Res
DOI 10.1007/s11095-012-0810-9

EXPERT REVIEW

Optimising the Delivery of Tubulin Targeting Agents through Antibody Conjugation

Gary D. Stack • John J. Walsh

Received: 2 March 2012 / Accepted: 11 June 2012
© Springer Science+Business Media, LLC 2012

ABSTRACT Despite their side effect profile, there currently remains a heavy reliance on traditional cytotoxics and particularly tubulin targeting agents in cancer chemotherapy. To address this concern, significant progress has been made in the selective delivery of drugs to the tumour site. This review will examine the published data in support of the hypothesis that forming antibody conjugates of tubulin targeting agents is an effective approach towards their more effective delivery to the tumour site. Particular emphasis will be placed on the diversity of concepts under investigation, the efficacy of resultant conjugates, evidence of decreased resistance and the side effect profiles of the conjugates.

KEY WORDS antibody-drug conjugates · anticancer · resistance · tubulin targeting agents · tumour targeting

ABBREVIATIONS

ADC	antibody-drug conjugate
ALCL	anaplastic large cell lymphoma
BMPEO	*bis*-maleimido-trioxyethylene glycol
DM	drug maytansinoid
EGFR	epidermal growth factor receptor
HER2	human epidermal growth factor receptor 2
IgG	immunoglobulin G
mAb	monoclonal antibody
MC	maleimidocaproyl
MDR-1	multidrug resistance protein-1
MMAE	monomethyl auristatin E
MMAF	monomethyl auristatin F
MTD	maximum tolerated dose
PAB	*p*-aminobenzyloxy carbonyl
PABC	*p*-aminobenzyl carbonyl
PEG	polyethylene glycol
PSMA	prostate specific membrane antigen
Siglec	sialic acid binding Ig-like lectins
SMCC	succinimidyl trans-4-(maleimidylmethyl) cyclohexane-1-carboxylate
SPDB	*N*-succinimidyl-3-(2-pyridylthio) propionate
SPP	*N*-succinimidyl 4-(2-pyridyldithio) pentanoate
vc	valine-citrulline

G. D. Stack • J. J. Walsh (✉)
School of Pharmacy and Pharmaceutical Sciences
Trinity College Dublin
Dublin 2, Ireland
e-mail: jjwalsh@tcd.ie

Published online: 10 July 2012

INTRODUCTION

Cancer patients with metastases typically present with approximately 10^{12} tumour cells and it has been established that greater than 99% of these need to be killed in order to achieve complete remission (1). Despite the emergence of novel treatments for malignancy, conventional chemotherapeutics and tubulin targeting agents in particular remain a cornerstone in many cancer treatment regimens. The major difficulty with these chemotherapeutic agents is that in order to reach that target of 99% cancer cell death, unacceptable toxicities are inevitable. Thus, there remains a significant challenge to develop new therapies that are suitably toxic to cancer cells while leaving normal cells relatively unscathed. The rationale behind the utilisation of antibody conjugation to achieve enhanced delivery of existing cytotoxics to the tumour site is two-fold. Firstly, by masking the toxicity of the drug until it reaches the active site, a lower incidence of side effects is expected. And secondly, by enhancing the specificity of the cytotoxic agent for the desired target cells greater efficacy may be attainable.

Author's personal copy

In this review the disparate antibody based methodologies utilised to optimise the delivery of tubulin targeting agents to the tumour site which have been published throughout the last ten years will be explored and critically appraised in terms of efficacy, therapeutic window and ability to overcome drug resistance.

Tubulin Targeting Agents

Microtubules, which are the target of tubulin binding agents, consist of α and β tubulin heterodimers. They are hollow tubes approximately 25 nm in diameter that are involved in various cellular functions, most notably cell movement, intracellular transport and cell division (2). Microtubule dynamics are very tightly regulated both spatially and temporally (3). At the onset of mitosis in particular there are striking changes in the microtubule network in which the disassembly of microtubules is proceeded by the formation of a new network of spindle microtubules (3). Tubulin targeting agents are known to bind to one of three main binding sites on the β-tubulin subunit: the vinca domain, the colcichine binding site and the paclitaxel site (3). Once bound, these agents act as either microtubule-stabilising or microtubule-destabilising agents interfering with mitosis and leading to cell death. One reason that cancer cells are particularly sensitive to these drugs compared with normal cells is that many cancer cells divide much more rapidly than normal cells offering many more opportunities for tubulin binding agents to disrupt mitosis and cause cell death. Hundreds of compounds have been observed to arrest mitosis by interacting with microtubules. It has been shown that they act by potently suppressing microtubule dynamics (4).

Tubulin binding agents are principally natural product or natural product derived small molecule inhibitors that have diverse structural classes and origins. Lead compounds for these agents include substances derived from bacteria, plants, marine sponges and molluscs (2).

Two of the most clinically pertinent classes of tubulin binding agents are the taxanes and the vinca alkaloids. The vinca alkaloids were first identified over 50 years ago while the taxanes where first identified over 40 years ago, but yet both classes of agents still find significant utility in the first line treatment of many solid tumours and haematological malignancies (4,5).

Other tubulin targeting agents that have been evaluated for anticancer activity include the colchinoids and the epothilones (3). In more recent years, tubulin binding agents that display cytotoxicities many orders of magnitude greater than clinically used agents have been developed. New taxoids have been developed that demonstrate approximately 100-fold greater cytotoxicity than the parent compounds (6). The tubulysins isolated from various myxobacterial species are one such class of potent tubulin binding agents and demonstrate IC_{50} values 20- to 1000-fold lower than many clinically used tubulin binding agents (7). The maytansinoids are another such class of compound. The lead molecule of this class, maytansine is an ansa macrolide first isolated from the Ethiopian shrub *Maytenus ovatus* by Kupchan *et al.* (8). Maytansine causes depolymerisation of microtubules and displays almost 100-fold higher cytotoxicity than the vinca alkaloids (9). Synthetic analogues of maytansine referred to as drug maytansinoids (DMs) have subsequently been developed which were found to possess 100- to 1000-fold greater activity than existing cytotoxic agents in the clinic (10,11). DM1 (*N*-methyl-*N*-[3-mercapto-1-oxopropyl]-L-alanine ester of maytansinol) is an example of one such maytansinoid which has been shown to be effective against a wide range of tumour cells with IC_{50} values in the range of 10–100 pM (12).

Dolastatin-10 is another highly potent inhibitor of microtubule assembly and tubulin polymerisation and is a non-competitive inhibitor of the binding of vinblastine to tubulin (6). Synthetic analogues of dolastatin-10 known as auristatins are potent tubulin inhibitors with cytotoxicities 50- to 200-fold greater than the vinca alkaloids (6).

Despite the promise of tubulin binding agents as cancer therapeutic agents, there are a number of significant disadvantages to their use. Paclitaxel for example, while remaining one of the most clinically important agents currently in use, suffers from dose-limiting toxicity and multidrug resistance (5). The action of efflux pumps such as multidrug resistance protein-1 (MDR-1), which actively pumps paclitaxel from resistant cells, is known to cause subtherapeutic intracellular drug concentrations. Resistance is also known to occur due to changes in β-tubulin or apoptotic and mitosis checkpoint proteins (13). In order to overcome these difficulties various attempts have been made to specifically target tumour cells through the molecular conjugation of antibodies to existing tubulin targeting agents. By selectively delivering existing cytotoxic agents to tumour cells the hope is that more potent cytotoxicity to target cells may be achieved while simultaneously reducing systemic toxicity associated with these agents.

ANTIBODY-DRUG CONJUGATES

In early antibody evaluation, a number of antibodies were produced that bound very specifically to various tumour cell surface antigens. However, in many cases such binding was insufficient to affect tumour growth (6). Two of the most effective monoclonal antibodies for the treatment of cancer currently licensed by the FDA are trastuzumab for breast cancer and cetuximab for colorectal tumours and squamous cell carcinoma of the head and neck, yet both these agents

Author's personal copy

offer only modest single agent activity (6,14). One way to take advantage of the selectivity of monoclonal antibodies for various cell specific antigens is to utilise molecular conjugation to attach a non-selective cytotoxic agent to a monoclonal antibody selective for tumour specific antigens. Various concepts along this theme have been explored but the most common approach involves the monoclonal antibody acting as a vector to the tumour cell, facilitating internalisation and downstream processing to liberate the cytotoxic effector molecule within the cell (6). This has led some commentators to refer to drug-antibody conjugates as tumour-activated prodrugs (6).

Antibody conjugation is considered to be one of the most promising approaches to increasing the anti-tumour activity of antibodies while simultaneously reducing the systemic toxicity of existing cytotoxics such as tubulin targeting agents (15). The various advantages and disadvantages of antibody-drug conjugates (ADCs) are summarised in Table I.

Despite early promise, the emergence of clinically successful drug-antibody conjugates has been somewhat slow due to the difficulties involved in successfully formulating these agents in presentations that can overcome the pharmacokinetic and pharmacodynamic impediments of these relatively large molecules. Durcy *et al.* (20) framed the characteristics of an ideal antibody-drug conjugate along five distinct headings:

1. *Circulation:* The antibody should be stable in circulation and should not have cytotoxic activity until intracellular release of the active drug.
2. *Antigen binding:* The monoclonal antibody should retain its high binding affinity for its intended target despite molecular conjugation to the cytotoxic agent.
3. *Internalisation:* A sufficient intracellular concentration of the ADC should be obtained to exact cell death. This can be challenging if the antigen is expressed only in limited numbers.
4. *Drug release:* Once internalisation has occurred, release of the cytotoxic agent should be timely and efficient.
5. *Drug action:* The drugs utilised in the ADC should be capable of causing cell death at subnanomolar concentrations.

The three constituent parts of an ADC are the antibody, the cytotoxic drug molecule and the linker connecting them as illustrated schematically in Fig. 1.

It has been suggested that early ADCs failed because of inappropriate drug selection, non-specific antibody selection and use of linkers that were not stable (21). Another difficulty with ADCs is that only a tiny fraction of administered ADC reaches the tumour site (6). Consequently, the cytotoxic agent used needs to be much more potent than currently used clinical agents. Thus, it became apparent that optimisation of each of these three variables was required in order to maximise the potential of ADCs.

Drug Characteristics

Although antibodies often display high specificity for the tumour, most of them are not potent enough to be clinically efficacious. Imaging studies with radiolabelled antibodies have shown that the peak concentration of antibodies deposited at the tumour site was of the order of 0.01% of the injected dose per gram of tumour at 24 h (22). Therefore the cytotoxicity of the drug in an ADC must be several-fold higher than conventional anti-cancer drugs (6). It has been suggested that the cytotoxicity of the drug used in an ADC must be at the IC_{50} level of 10–100 pM. Since paclitaxel displays an IC_{50} of the order of 10 nM in a number of cell lines it has been suggested that it is not suitable for this approach (23).

The *in vitro* cytotoxicity (IC_{50} values) of the maytansinoids and auristatins are even lower than the concentration of antibodies found to accumulate at the tumour site, making them suitable candidates for ADC synthesis. For this reason

Table I Advantages and Disadvantages of Antibody-Drug Conjugates

Advantages	Disadvantages
Targeted binding specific for tumour antigen	Requires that tumour be tested for expression of target antigen
Highly potent agents can be selectively delivered to target cells	Molecular target may have some normal tissue expression
Wide therapeutic index	Linker may not be stable leading to premature cytotoxic agent release
Prolonged circulation half-life	Antibody may not reach target in sufficient concentration to be lethal
Stable in circulation	Antigen expression could be heterogeneous especially in solid tumours (17)
Decreased adverse effects	ADC must cross the vascular endothelium and circumvent the interstitial pressure within the solid tumour (18)
Bystander killing effect of endothelial cells and stromal cells essential to tumour growth	Antibody may itself be immunogenic
Reduced MDR-1 mediated resistance compared to systemic administration of the respective drug (16)	Masking of the target antigen with monoclonal antibody devoid of its cytotoxic payload in ADCs with poor stability (19)

Author's personal copy

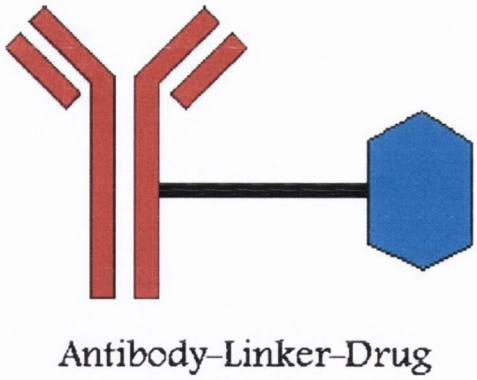

Fig. 1 Schematic of an antibody-drug conjugate.

the maytansinoid DM1 [$N^{2'}$-deacetyl-$N^{2'}$-(3-mercapto-1-oxopropyl)-maytansine] has become one of the most widely utilised tubulin targeting agents in the synthesis of ADCs (24).

To take advantage of the long plasma half-life of IgG antibodies necessary to achieve maximal deposition at tumour sites the drug must be non-toxic in conjugated form, a requirement which both the maytansinoids and auristatins possess (6). Furthermore, these cytotoxic agents are readily linkable to an appropriate antibody and sufficiently water soluble and stable on storage (10).

Drug loading is another critical factor determining the therapeutic characteristics of an ADC (25). A series of conjugates of the anti-CD30 monoclonal antibody cAC10 linked to either 2, 4 or 8 monomethyl auristatin E (MMAE) molecules were synthesised (25). Although the *in vitro* toxicity of the resultant conjugates was directly dependent on the drug loading, *in vivo* the antitumour activity of the 4 MMAE antibody was comparable with the 8 MMAE containing conjugate while the maximum tolerated dose of the 4 MMAE containing conjugate was found to be double that of the 8 MMAE containing conjugate (25). It has also been demonstrated for other conjugates that the *in vivo* activity drops off significantly when less than three cytotoxic drug molecules per antibody are used while an upper limit is often imposed by the solubility characteristics of the resulting conjugate (12).

Antibody Characteristics

The cell surface antigen which the antibody recognises is typically a glycoprotein, a carbohydrate, an oncoprotein, a growth factor receptor or a hormone receptor(1). The factors that need be considered in selecting an appropriate antibody target for the synthesis of an ADC include (1):

1. Degree of target expression on tumour cells compared to normal tissues.
2. Affinity of antibody for target.
3. Efficiency of internalisation following antibody bindin
4. Homogeneity of target expression on all target cells.
5. Degree of target shedding into circulation.

Many early monoclonal antibodies investigated as poter tial drugs lacked specificity. Some of these agents bound t antigens expressed on a wide variety of normal cells tha were merely upregulated in various tumours. Cross reactivity of the antibodies with normal tissues is thus utmost concern when designing any ADC (1). One suc conjugate associated with poor target antigen selection bivatuzumab mertansine (26). This conjugate consists of th monoclonal antibody bivatuzumab covalently conjugated t the maytansinoid DM1. Bivatuzumab is a humanise monoclonal antibody (BIWA 4) that binds selectively t CD44v6. This cell surface antigen is highly and homoge nously expressed on squamous cell carcinoma of the hea and neck, oesophagus, lung, cervix and vulva (26). Its ex pression was also found in some normal tissues such as ski keratinocytes, squamous epithelium of the cervix, epithel um of the cornea and epithelium of the tonsils (26). Tijink *al.* (26) evaluated this agent in patients with incurable squa mous cell carcinoma of the head, neck or oesophagus. In th study, seven patients were administered a total of 23 week doses of bivatuzumab mertansine. Following completion the study, one patient at 100 mg/m^2 and one at 120 mg/m experienced stable disease during the treatment phase bu also suffered severe skin toxicity in the form of desquamatio At the maximum dose level achieved, 140 mg/m^2, one patie developed toxic epidermal necrolysis after two infusions an died. It was concluded that expression of CD44v6 was n specific enough for tumour cells to allow the formulation of safe antibody-based therapy and the development of th agent was discontinued.

Immunogenicity of antibodies is another issue whic must be considered. Antibodies that are used in the co struction of ADCs need to be humanised to avoid th potential of generating an immune response in the patie upon administration which further complicates the synthes of these agents (1).

Being large molecular weight biomolecules, antibodi display certain physicochemical properties that are unfa ourable to the crossing of biological barriers, thereby som what limiting their scope for *in vivo* applications (27). T affect solid tumours, ADCs must cross the vascular end thelium and circumvent the interstitial pressure within th solid tumour (27). Also, expression of target antigens can b heterogeneous throughout the tumour (27). Therefore, th pharmacodynamics of the large immunoglobulin containin ADC may impede its ability to penetrate deep into soli tumours which are often poorly vascularised (1). Smalle recombinant monoclonal antibody structures such as sing chain antibodies and diabodies have been shown t

Author's personal copy

penetrate into the tumour with greater efficiency than the parent antibodies (28). However, these smaller molecules are more rapidly cleared from the plasma resulting in shorter half-lives (29). In fact overall tumour accumulation of diabodies is found to be more than two-fold less than that achieved for corresponding IgG (15).

Modification of the structure of the monoclonal antibodies used in ADCs has also been attempted. An engineered thio-trastuzumab-DM1 conjugate has been developed (30) which possesses two free cysteine residues to facilitate the attachment of two molecules of DM1 to each thio-trastuzumab molecule *via* a non-reducible *bis*-maleimido-trioxyethylene glycol (BMPEO) linker. Trastuzumab is a recombinant human anti-epidermal growth factor receptor 2 (HER2) monoclonal antibody. HER2 is a receptor tyrosine kinase found to be overexpressed on the surface of breast cancer cells in ~30% of newly diagnosed patients and is found to be associated with a poor prognosis. Furthermore, 60–70% of breast cancer cell bone metastases overexpress HER2 (31). The conjugate retained similar *in vitro* cell proliferation inhibitory activity and HER2 binding properties to the conventional trastuzumab-succinimidyl trans-4-(maleimidylmethyl) cyclohexane-1-carboxylate-DM1 (trastuzumab-SMCC-DM1). Furthermore, the conjugate showed improved efficacy over the conventional trastuzumab-DM1 at DM1 equivalent doses and retained efficacy at equivalent antibody doses. The thio-trastuzumab conjugate also displayed a greater than two-fold reduction in toxicity in a safety study in rats compared with the conventional ADC. It is thought that this was due to the lower drug loading per antibody and the improved stability of the linker unit in circulation (30).

Previous experiments utilising these thio-mAbs led to the development of thio-anti-MUC16-maleimidocaproyl-valine-citrulline-*p*-aminobenzyl-carbonate-MMAE (thio-anti-MUC16-MC-vc-PABC-MMAE) (32). This conjugate contained a derivatised humanised anti-MUC16 monoclonal antibody engineered to contain two free thiol groups to which MMAE was conjugated *via* a MC-vc-PABC linker. The conjugate synthesised was found to be as efficacious as a conventional conjugate in a MUC16 ovarian cancer xenograft model in mice. Moreover, it was tolerated at higher doses in rats and cynomolgus monkeys than the same conjugate prepared by conventional approaches suggesting the potential of this strategy in the synthesis of more therapeutically favourable ADCs (32).

Linker Unit Selection

For an antibody-drug conjugate to be effective the chemotherapeutic agent should remain non-toxic as part of the conjugate while in circulation but should be readily liberated on internalisation into the target cell (19). Thus, the choice of linker is of paramount importance in the synthesis of an ADC with a favourable therapeutic index. Several strategies have been employed to maximise the stability of ADCs in circulation while allowing for selective release of the tubulin binding agent at the desired target. Acid labile hydrazone linkers were among the early approaches to be considered however, in more recent times conjugates containing disulfide linkages, peptide based linkages and thioester linker units have found favour due to their greater stability in circulation. The advantages and disadvantages of each of these methodologies and others will thus be discussed in turn together with examples of how these technologies have been utilised to facilitate the selective delivery of the parent ADC to the tumour site.

Acid-Labile Linkers

Early linkers evaluated include various acid-labile hydrazone linkers that utilised the acidic environment of endosomes for cleavage (19). Linkages such as those containing hydrazones have relatively short half-lives that can be significantly less than the expected circulating half-life of the ADC. This can present toxicity issues especially in the case of high potency cytotoxics such as MMAE (19).

Drugs linked to monoclonal antibodies *via* acid-labile linkers have been found to undergo approximately 50% drug release within 2 days upon incubation in human serum (19). Peptide and disulfide containing linkers were subsequently adjudged to be superior to these acid sensitive linkers due to the selectivity of cleavage of these linker types for the tumour intracellular environment (33).

Disulfide-Containing Linkers

Disulfide containing linkers are very commonly employed in the synthesis of ADCs due to their stability at physiological pH (10). While this linker unit is thermodynamically very stable, it is kinetically labile in the presence of sulfhydryl containing functional groups (24). For example, as the concentration of glutathione, a sulfhydryl containing molecule, is 1000-fold higher within cells than in the circulation preferential intracellular drug release of conjugates containing this linker unit has been achieved (10,24).

The relative strength of the disulfide bond in various maytansinoid-antibody conjugates can be manipulated to achieve maximum stability in circulation while allowing for efficient cleavage inside the target cell (24). This is achieved by the introduction of methyl substituents on the carbon atoms geminal to the disulfide link conferring varying degrees of steric hindrance (24). Those conjugates where the methyl groups were located on the maytansinoid side of the disulfide bond were found to have superior activity *in vivo* than those with the methyl groups located on the antibody

Author's personal copy

side of the disulfide bridge despite the fact that both conjugates have identical stability in terms of the fate of the disulfide bridge (12).

The humanised monoclonal antibody, huC242, has been used in a series of experiments to synthesise conjugates with maytansinoids in order to explore the effect of the linker group on the activity of resultant conjugates (34). This antibody binds to the CanAg antigen expressed on colorectal, pancreatic and certain non-small cell lung cancer cells (34). Conjugates of huC242 and the maytansinoids DM4 and DM1 containing a cleavable disulfide linkage huC242-*N*-succinimidyl-3-(2-pyridylthio) propionate-DM4 (huC242-SPDB-DM4) (Fig. 2) and a non-cleavable thioether linkage (huC242-SMCC-DM1) (Fig. 3) were synthesised and evaluated *in vitro* and *in vivo* (34). It was found that both conjugates displayed comparable activity *in vitro* though huC242-SPDB-DM4 was significantly more active in multiple xenograft tumour models. It was concluded that both conjugates are efficiently degraded by lysosomes to release the free maytansinoid molecule together with a number of cytotoxic metabolites. It has been suggested that the enhanced activity of the disulfide containing conjugate is related to the formation of the potent metabolite, S-methyl-DM4, following lysosomal reduction of the disulfide bond. Lopus *et al.* showed that such maytansine derivatives are themselves potent microtubule poisons, interacting with microtubules as efficiently as, or more efficiently than, the parent molecules (35).

In further experiments conducted by Kovtun *et al.* (36,37), it was observed that huC242-DM1 conjugates with non-cleavable linkers such as SMCC (Fig. 3) had similar *in vitro* activity to disulfide containing *N*-succinimidyl 4-(2-pyridyldithio) pentanoate (SPP) linked conjugates (Fig. 4) but were not as active *in vivo*. Considerable evidence suggests that a bystander killing of neighbouring cells is responsible for this disparity (36). It was found that conjugates coupled *via* a reducible disulfide linker unit were capable of this effect while similarly potent conjugates linked *via* a non-reducible thioester bond were not. It has been suggested that this mechanism may overcome various barriers to the even

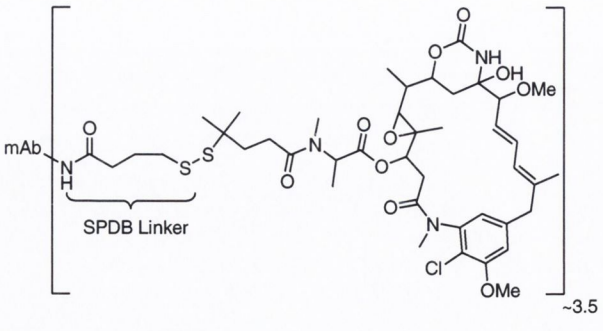

Fig. 2 mAb- SPDB-DM4.

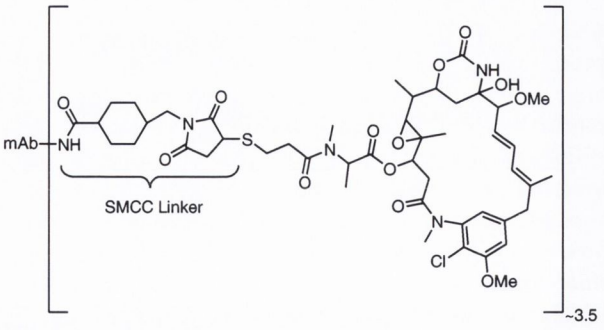

Fig. 3 mAb-SMCC-DM1.

distribution of maytansinoid effector molecules to all cells within a tumour. However, it should be noted that in the case of a number of other maytansinoid-antibody conjugates such as trastuzumab linked to DM1, it was the SMCC linked conjugate which was the most effective (12) (Fig. 3).

In preclinical studies, the monoclonal antibody, nBT062 was conjugated to DM1 and DM4 using different linker technologies. nBT062-SMCC-DM1, nBT062-SPP-DM1 and nBT062-SPDB-DM4 were then evaluated *in vitro* and *in vivo* against multiple myeloma cell lines (38). It was found that nBT062-SPDB-DM4 was the most efficacious of the conjugates *in vivo*, demonstrating target dependent antitumour activity. Bystander killing in the presence of CD138-positive cells observed *in vitro* was hypothesised to be particularly important for BT062 activity *in vivo* causing the death of tumour cells that heterogeneously express CD138 and disrupting the tumour microenvironment (39). The structure of nBT062-SPDB-DM4, designated BT062 consists of a murine/human IgG4 chimeric form of B-B4 (nBT062) targeting CD138 conjugated to DM4 *via* a disulfide linkage (Fig. 2). Phase I clinical trials are currently underway evaluating the safety, tolerability, pharmacokinetics and efficacy of BT062 in patients with CD138-positive multiple myeloma (39). BT062 is also at an advanced stage of preclinical development for the treatment of a number of CD138-positive solid tumours (40).

Polson *et al.* (41) systematically examined potential antigenic targets and drug linker combinations in an attempt to develop the most clinically relevant ADC for the treatment of non-Hodgkin's lymphoma. The antibodies used targeted the antigens CD19, CD20, CD21, CD22, CD72, CD79b, and CD180, all of which are found to be highly expressed on non-Hodgkin's lymphoma cells. The disulfide linker containing maytansinoid derivative SPP-DM1 (Fig. 4) and the non-cleavable thioether derivative SMCC-DM1 (Fig. 3) were variously conjugated to the different antibodies. Similarly, the cathepsin B substrate containing MC-vc-PABC-MMAE and the non-cleavable MC-MMAE were also conjugated to the various antibodies. It was found that the ADCs with cleavable linkers mediated efficacy *via* all these

Author's personal copy

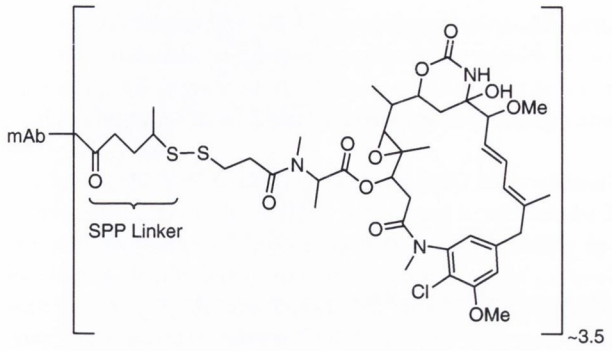

Fig. 4 huC242-SPP-DM1.

targets whereas the ADCs with non-cleavable linkers were only effective when conjugated with anti-CD22 and anti-CD79b. It was also found that those conjugates containing uncleavable linkers showed reduced toxicity *in vivo*. It was suggested that the reason for the broad applicability of the cleavable disulfide linker containing ADCs is that extracellular cleavage to release the cytotoxic agent occurs following antigen binding and it is the free drug that crosses the cell membrane to exert its effect passively, whereas internalisation and intracellular metabolism is necessary to enable release of the cytotoxic agent in the case of ADCs with a non-cleavable linker.

Peptide Linker Units

Ma *et al.* (42) synthesised a conjugate by combining a prostate specific membrane antigen (PSMA) monoclonal antibody and MMAE *via* a valine-citrulline linkage (Fig. 6). This linkage was designed to maintain serum stability while maximising intracellular drug release by human cathepsin B (42). Cathepsin B is a lysosomal exocarboxydipeptidase which is often found to be upregulated in tumour cells particularly during tumour progression (43). *In vitro*, the conjugate potently eliminated all PSMA-positive cell lines with IC_{50} values ranging from 65 to 210 pM whereas these concentrations had no effect on PSMA-negative cells. In fact, the conjugates demonstrated nearly 1000-fold selectivity compared with an isotype control conjugate. *In vivo* efficacy was shown in a mouse xenograft model of androgen independent prostate cancer cell line, C4-2. Each of the two regimens tested were effective in increasing median survival and decreasing serum PSMA in a dose dependent fashion. Overall, a 40% cure rate was observed in animals with established tumours following treatment with a 6 mg/kg regimen. Furthermore, no apparent toxicity was observed with this regimen which may permit the use of even more intense regimens resulting in further improvements in antitumour activity (42).

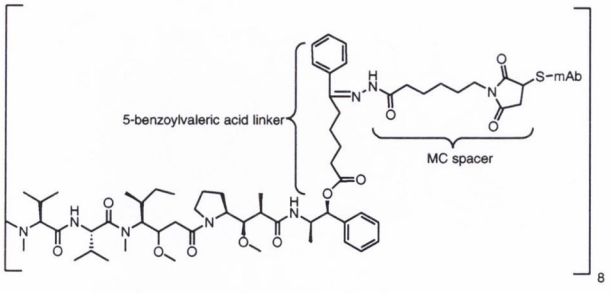

Fig. 5 mAb-AEBV.

Auristatin E and the related compound MMAE were conjugated to the chimeric monoclonal antibodies cBR96 (specific for the Lewis Y antigen on carcinomas) and cAC10 (specific to CD30 on haematological malignancies) (44) using three distinct linker methodologies. CD30 has limited expression in normal tissues but is widely expressed in Hodgkin's disease, non-Hodgkin's lymphoma, multiple myeloma and cutaneous T-cell lymphoma (45). Firstly, conjugates containing the 5-benzoylvaleric acid ester of auristatin E were synthesised (Fig. 5). Secondly, conjugates consisting of the dipeptide valine-citrulline attached to MMAE *via* the self-immolative *p*-aminobenzyl carbonyl (PABC) spacer unit were synthesised. Finally, conjugates consisting of the dipeptide lysine-phenylalanine attached to MMAE *via* the same *p*-aminobenzyl carbonyl spacer were prepared (Fig. 6). All three conjugates also contained a maleimidocaproyl (MC) spacer group. It was found that the peptide linker containing conjugates were much more stable in buffers and plasma than the hydrazone linker conjugates. The mAb-val-cit-MMAE conjugates also demonstrated greater *in vitro* specificity and lower *in vivo* toxicity than corresponding hydrazone containing conjugates. In tumour xenograft models, the peptide linked conjugates induced tumour regression and cures with therapeutic indices as high as 60-fold (i.e. 1/60th of the maximum tolerated dose of cAC10-Val-Cit-MMAE was shown to achieve therapeutic efficacy in a CD30 positive anaplastic large cell lymphoma (ALCL) tumour model).

Alternative Linker Units

In an attempt to further increase the therapeutic window of cAC10-maleimidocaproyl-valine-citrulline-*p*-aminobenzyloxycarbonyl-monomethyl auristatin F conjugate (cAC10-MC-vc-PABC-MMAF), a series of alternate linker units were investigated (46). One conjugate containing a noncleavable

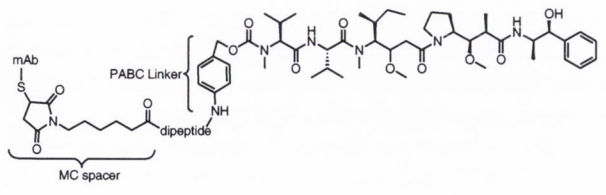

Fig. 6 mAb-Val-Cit-MMAE and mAb-Phe-Lys-MMAE (where dipeptide = valine-citrulline and phenylalanine and lysine respectively).

Author's personal copy

maleimidocaproyl linker unit (Fig. 7) was shown to have similar activity *in vitro* and *in vivo* but could be administered at 3-fold higher doses than cAC10-MC-vc-PABC-MMAF.

Novel linker mechanisms have also been investigated in ADCs with a view to evading multidrug resistance mechanisms such as the overexpression of the transporter MDR-1. In one such study conducted by Kovtun *et al.* (47) a DM1-antibody conjugate using a maleimidyl-based hydrophilic linker, PEG_4Mal, was shown to overcome MDR-1 mediated multidrug resistance *in vitro* and eradicate human MDR-1 xenograft tumours *in vivo*. Following uptake into cells, it was found that conjugates with the PEG_4Mal linker (Fig. 8) were transformed to cytotoxic conjugates that were better retained by MDR-1 expressing cells than metabolites of a similar conjugates with a SMCC linker (Fig. 3).

Even with relatively hydrophilic cytotoxic agents such as DM1 and DM4 conjugated to antibodies *via* the somewhat hydrophobic linkers SPDB and SMCC, only conjugates with 4-5 drug molecules per antibody could be synthesised. When conjugates with higher maytansinoid loads were attempted the resultant conjugates tended to aggregate and precipitate (48). In an attempt to increase the drug antibody ratio without causing aggregation or affecting the binding affinity of the resultant conjugate, a number of different hydrophilic linkers containing either a negatively charged sulfonate group or a hydrophilic, uncharged PEG group were synthesised (48). An important advantage of the conjugates containing these more hydrophilic linkers is their potential to overcome multidrug resistance. Incorporation of the sulfonate group both in cleavable and non-cleavable linkers was found to be associated with enhanced activity of B38.1-DM1 conjugates against MDR cell lines. B38.1-DM1 conjugates consisting of a PEG_4 linker were also observed to display enhanced activity *in vitro* against MDR cell lines. Incorporation of the sulfonate group or the PEG_4 group into non-reducible linkers in DM1 and DM4 conjugates of huC242 also resulted in approximately 100-fold greater cytotoxicity against both COLO 205 and COLO 205/MDR cells. *In vivo*, the B38.1-DM1 and B38.1-DM4 conjugates prepared with sulfonate or PEG containing linkers demonstrated enhanced antitumour activity against the COLO205MDR xenograft model in mice.

A β-glucuronic acid based linker was also utilised for the synthesis of a number of maytansinoid conjugates in which

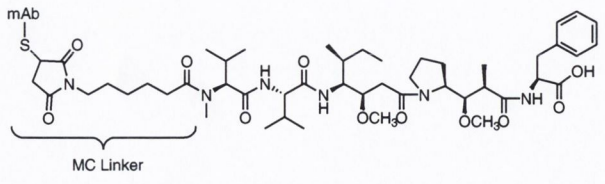

Fig. 7 mAb–mcMMAF.

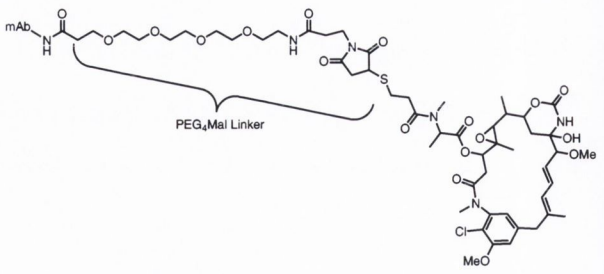

Fig. 8 mAb–PEG_4Mal–DM1.

hydrolysis by the lysosomal enzyme β-glucuronidase releases the active drug. MMAE and MMAF were conjugated to the monoclonal antibodies c1F6 (anti-CD70) and cAC10 (anti-CD30) *via* a novel glucuronic acid linker (Fig. 9) (49). It has been shown that β-glucuronidase is abundantly present within lysosomes and is overexpressed in some tumour types while extracellular enzyme activity is low (50). The resulting conjugates were found to be highly stable in plasma, well tolerated at high doses and efficacious both *in vitro* and *in vivo*.

Trastuzumab was chemically linked to paclitaxel *via* a novel A-Z-CINN linker resulting in an ADC with the potential for light accelerated release of paclitaxel at the tumour site (51). *In vivo*, in HER2 positive BT-474 mammary tumour cells in mice, the conjugate showed enhanced antitumour activity following 5 min light exposure (light from a halogen bulb delivered through a fiber optic probe) adjacent to the tumour and was also found to cause more rapid and extensive reduction in tumour volume than a 10-fold higher concentration of free paclitaxel and free trastuzumab administered to the mice (51).

Antibody-Drug Conjugates in Preclinical Development

The novel taxoid SB-T-12136 was variously linked to three murine monoclonal antibodies against the human epidermal growth factor receptor (EGFR) (23,52). The antibodies KS-61, KS-77 and KS-78 were linked to SB-T-12136 *via* a 4-

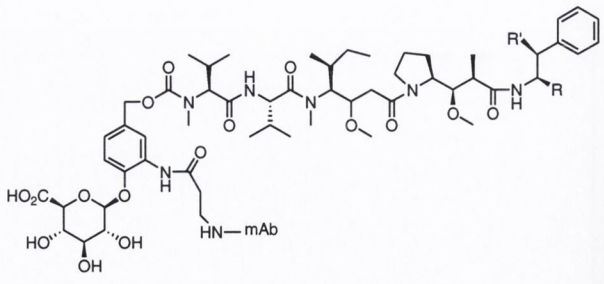

Fig. 9 MMAE/MMAF-glucuronic acid linker-antibody conjugate (where R = Me and R′ = OH for MMAE while R = COOH and R′ = H for MMAF).

Author's personal copy

thiopentanoyl linker (Fig. 10). These conjugates were shown to possess remarkable target-specific antitumour activity *in vivo* against EGFR-expressing A431 tumour xenografts in mice resulting in complete inhibition of tumour growth without any noticeable toxicity.

Anti-CD22-SMCC-DM1 is another ADC in preclinical development. It consists of DM1 conjugated to a humanised antibody that targets CD22, a siglec (sialic acid binding Ig-like lectins) family lectin expressed predominantly on mature B-cells (53). It was found that most non-Hodgkin's lymphoma patients express CD22 and this conjugate was shown to inhibit the proliferation of several non-Hodgkin's lymphoma cell lines *in vitro* and also induced complete regression of tumours in xenograft mouse models. It was well tolerated by cynomolgus monkeys and significantly decreased circulating B-cells as well as follicle size and germinal centre formation in lymphoid organs. It has been suggested that the low levels of expression of CD22 should not limit the scope of this conjugate as some cell lines with very low levels of CD22 expression were sensitive to these agents (53).

Chimeric anti-CD20 antibody, rituximab, has already found use in the clinic in the treatment of certain B-cell lymphomas, most notably Hodgkin's lymphoma (54). The specific binding of rituximab and the anti-CD20 antibody IF5 for CD20 positive B-lymphoma cells both offer the potential for the synthesis of an effective ADC (54). Conjugates of these antibodies linked to MMAE *via* a valine-citrulline linker were synthesised by Law *et al.* (54). These conjugates were shown to be selectively toxic to CD20 positive B-cell lymphoma cell lines *in vitro* with IC_{50} values of between 50 ng/ml and 1 μg/ml. Furthermore, rituximab-vc-MMAE showed antitumour efficacy in human lymphoma CD20 positive tumour xenograft models in mice at doses where rituximab was ineffective.

While CD20 immunotherapy adequately depletes mature B-cells, it does not deplete pre-B cells or immature B cells, some B cell subpopulations, plasma cells or their malignant counterparts (55). Because CD19 is expressed earlier in B cell development it offers the potential to target lymphoblastic leukaemias and lymphomas (55). Therefore, a humanised anti-CD19 antibody (hBU12) was conjugated to MMAE *via* a valine-citrulline linker to yield hBu12-vc-MMAE (56). This conjugate was shown to exhibit potent cell killing against rituximab sensitive and resistant non-Hodgkin's lymphoma cell lines *in vitro*. Furthermore, high rates of durable tumour growth suppression were observed in mice implanted with these tumours. Further examples of ADCs containing tubulin targeting agents currently in preclinical development are shown in Table II.

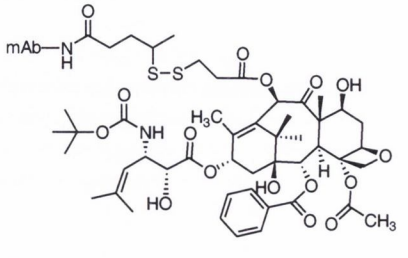

Fig. 10 SB-T-12136-mAb conjugates.

Antibody-Drug Conjugates Undergoing Clinical Evaluation

Brentuximab vedotin is now approved for the treatment of CD30-positive hematologic malignancies (61) while trastuzumab emtansine is in phase III for HER2-positive breast cancer (21). A number of other promising ADCs are undergoing phase I/II evaluation at present (Table III). Of these, C242-DM1 was among the first maytansinoid-antibody conjugates synthesised. C242 recognises CanAg (MUC1), a mucin type glycoprotein expressed on the surface of human colorectal cancer cells. It was shown to be effective in mice xenograft models with complete tumour regression observed (62). This agent subsequently progressed to clinical evaluation as cantuzumab mertansine (huC242-DM1) in which the antibody was humanised. Cantuzumab mertansine consists of up to four molecules of mertansine conjugated to each antibody. The drug showed considerable tumour localisation without inducing severe haematological toxicity in patients with pancreatic and colorectal cancers (63).

Another agent that has shown great potential in preclinical testing is huC242-DM4 (12). Treatment of mice with a single dose of huC242-DM4 resulted in complete regression of tumour xenografts at a dose well below the maximum tolerated dose while equivalent doses of free maytansinoid and a DM4 conjugate with a non-binding antibody had no effect on tumour growth in this model (12). *In vivo* distribution experiments in mice have shown that 1000-fold greater accumulation of maytansinoid at the tumour site can be achieved compared with non-conjugated maytansinoids after 24–28 h. This conjugate contains a disulfide linkage and has an increased stability under physiological conditions. It was found to have a half-life of 7.7 d in mice *versus* ~2 d for cantuzumab mertansine, and is now undergoing phase I clinical evaluation (6).

CD37 also represents an attractive target for an antibody-maytansinoid ADC due to its high expression in B-cell malignancies such as non-Hodgkin's lymphoma and chronic lymphocytic leukaemia and its limited expression in normal tissues (64). Furthermore, anti-CD37 antibodies have been shown to possess intrinsic anti-tumour activity and therefore offer the potential for the synthesis of a dual acting ADC (64). The humanised anti-CD37 monoclonal antibody K7153A was thus conjugated to DM1 using either the hindered disulfide

Author's personal copy

Table II Antibody-Drug Conjugates in Preclinical Development

Antibody-drug conjugate	Target antigen	Cytotoxic agent	Linker used	Anticancer activity/Stage of development	References
Anti-CD79b-SMCC-DM1	Anti-CD79b	DM1	SMCC	*In vitro* activity against non-Hodgkin's lymphoma cell lines Effective *in vivo* in follicular, mantle cell and Burkitt's lymphoma	(57)
Anti-CD79b-MC-MMAF	Anti-CD79b	DM1	MC	*In vitro* activity against non-Hodgkin's lymphoma cell lines Effective *in vivo* in follicular, mantle cell and Burkitt's lymphoma	(57)
Anti-CD79b-vc-MMAE	Anti-CD79b thiomab	MMAE	Vc	*In vitro* and *in vivo* activity against non-Hodgkin's lymphoma cell lines	(58)
Anti-huCD79b (SN8)-MCC-DM1	Humanised anti-CD79b antibody	DM1	SMCC	Caused complete regression of Burkitt's, follicular, and mantle cell lymphoma xenograft tumours	(59)
IMGN853	Anti-folate antibody M9346A	DM4	sulfo-SPDM	Selective cytotoxicity *in vitro* and *in vivo* for FR+ cells, efficacy in MDR-1-positve tumours	(60)

containing SPP linker or the non-cleavable SMCC linker. It was found that the K17153A-SMCC-DM1 (designated IMGN529) was more active against lymphoma cells both *in vitro* and *in vivo* against SU-DHL-4 subcutaneous xenograft tumours. This agent is currently undergoing phase I clinical trials in patients with relapsed or refractory non-Hodgkin's lymphoma (65).

The conjugate MEDI-547 (1C1-mcMMAF) consists of a fully human monoclonal antibody against murine and human EphA2 (1C1) attached to MMAF *via* a stable maleimidocaproyl linker (Fig. 7). The EphA2 receptor is a subtype of the erythropoietin producing hepatoma receptor that is overexpressed in tumours of the breast, prostate, lung, colon and in glioblastoma multiforme (66). It has also been reported that the EphA2 receptor is upregulated in the neovasculature of tumours, which may contribute to the activity associated with agents targeting this receptor (67). *In vivo* experiments in mouse orthotopic xenograft models resulted in 86% to 88% growth inhibition in the orthotopic Hec-1A and Ishikawa models following treatment with this agent. The mice treated with this ADC also had a lower incidence of metastasis than controls and this effect was observed without overt signs of toxicity (68). This agent was subsequently evaluated in phase I clinical trials however the outcome of these studies have yet to be reported.

Table III Antibody-Drug Conjugates Under Clinical Investigation

Antibody-drug Conjugate	Target; Indications	Clinical Stage	References
Brentuximab vedotin (SGN-35; Brentuximab-MC-VC-MMAE)	CD30; hematologic malignancies, Hodgkin's lymphoma	FDA approved	(71)
Trastuzumab emtansine (Trastuzumab-SMCC-DM1)	HER2-positive breast cancer	Phase III	(21)
Lorvotuzumab mertansine (IMGN901; HuN901-SPP-DM1)	CD56; Merkel cell cancer, small cell lung cancer, multiple myeloma ovarian cancer	Phase II	(10)
Glembatumumab vedotin (CDX-011; CDX-011-MC-VC-MMAE)	Glycoprotein NMB; melanoma, breast cancer	Phase II	(21)
SAR3419 (huB4-SPDB-DM4)	CD19; B cell lymphoma	Phase I and II	(73,74)
IMGN388 (Antibody-SPDB-DM4)	Integrin; antivascular/solid tumours	Phase I	(17)
BIIB-015 (Antibody-SPDB-DM4)	Cripto; solid tumours	Phase I	(17)
BT-062 (Anti-CD138-SPDB-DM4)	CD138; multiple myeloma	Phase I and II	(39)
BAY 79-4620 (3ee9-MMAE)	CAIX (MN); solid tumours	Phase I	(17)
MEDI-547 (1C1-MC-MMAF)	EphA2; ovarian cancer, solid tumours	Phase I	(75)
SGN-75 (SGN-70-MC-VC-MMAF)	CD70; renal cell carcinoma, non-Hodgkin's lymphoma	Phase I	(76)
SAR566658 (huDS6-DM4)	CA6; ovarian, cervical, breast cancers	Phase I	(17)
PSMA-ADC (anti-PSMA-MMAE)	PSMA; prostate cancer	Phase I	(77)
MLN2704 (MLN591-DM1)	PSMA; prostate cancer	Phase II	(6)
IMGN529 (Antibody-SMCC-DM1)	Anti-CD37	Phase I	(65)
AVE9633 (Antibody-DM4)	Anti-CD33 antibody (huMy9); acute myeloid leukaemia	Phase I	(10)

Author's personal copy

Trastuzumab emtansine is currently undergoing a number of phase III clinical trials in patients with HER-positive metastatic breast cancer (21). It consists of the anti-HER2 monoclonal antibody trastuzumab conjugated to an average of 3.5 molecules of the maytansinoid DM1 *via* a nonreducible SMCC thioether linkage (Fig. 3). It has been shown that trastuzumab emtansine retains the mechanism of action of unconjugated trastuzumab and is active against lapatinib resistant cell lines and tumours (69). It was also effective in patients for whom trastuzumab alone was found to be inadequate (12). Trastuzumab emtansine's systemic side effects are significantly minimised due to its targeted delivery to HER2 positive cells. Two phase II studies comparing trastuzumab-DM1 with trastuzumab plus docetaxel showed improved tolerability and at least equivalent efficacy. Two phase III randomised trials are currently underway for refractory and HER2-positive breast cancer (70).

In August 2011, brentuximab vedotin (cAC10-vc-MMAE, SGN-35) was approved by the FDA for the treatment of patients with Hodgkin's lymphoma and systemic ALCL (71). To date, the only other ADC to have made it to the clinic is Wyeth's Mylotarg® (gentuzumab ozogamicin) which received FDA approval in 2000 for the treatment of acute myeloid leukaemia. However, it was voluntarily withdrawn after follow up studies raised concern about its safety and clinical efficacy (21). Brentuximab vedotin is a conjugate of the chimeric monoclonal antibody cAC10 directed against CD30 covalently coupled to MMAE. The valine-citrulline peptide linker unit connecting the two components is subject to cleavage by lysosomal enzymes following internalisation into target cells (Fig. 6). The tumour necrosis factor receptor family member CD30 is highly expressed on the cell surfaces of Hodgkin's disease, ALCL and a subset of non-Hodgkin's lymphomas but has only limited expression on healthy tissues. Brentuximab vedotin potently interferes with the growth of CD30-positive haematological tumours including Hodgkin's lymphoma and ALCL (72). It has been suggested that the *in vivo* efficacy of brentuximab vedotin might be mediated, in part, by the diffusion of free MMAE from the target cells resulting in a bystander effect that kills the normal supporting cells in close proximity to malignant cells (61).

CONCLUSIONS

A vast array of delivery strategies are currently being evaluated for the more selective targeting of tubulin binding agents to the tumour site. Encouragingly, many of these methodologies are resulting in agents with improved tumour targeting, enhanced pharmacokinetic characteristics and greater efficacy. The licensing of brentuximab vedotin in particular marks significant progress towards the synthesis of targeted conjugate molecules and away from non-specific small molecule tubulin inhibitors with their associated toxicities. Many of the obstacles associated with early ADCs have been overcome and new generation ADCs are demonstrating greater tumour specificity and enhanced potency. Lessons have undoubtedly been learned from the failed development of bivatuzumab mertansine and much greater care has been taken in selecting antigen targets with limited physiological expression. Optimisation of the cytotoxic payload has resulted in a high level of utilisation of the tubulin targeting auristatins and maytansinoids due to their high potency and ease of conjugation. In particular, the selection of more appropriate linker groups has facilitated the synthesis of conjugates which are more stable in circulation, more selectively cytotoxic for their intended targets and ultimately more efficacious. However, it should be clear from the vast array of linker methodologies used that different malignancies and different ADCs benefit from different linker units and it is still necessary to evaluate the most appropriate linker for each specific therapeutic indication. The sheer number of ADCs at an advanced stage of clinical evaluation suggests that we are on the cusp of a revolution in the immunological treatment of malignancy. Therefore, it would appear that antibody conjugation is certainly a viable methodology for the synthesis of tubulin targeting agents with improved tumour selectivity, lower incidences of resistance and side effects and superior therapeutic efficacy than currently used clinical agents.

ACKNOWLEDGMENTS AND DISCLOSURES

The authors would like to acknowledge funding from the Irish Council for Science Engineering and Technology (IRCSET) and Enterprise Ireland.

REFERENCES

1. Chari RV. Targeted delivery of chemotherapeutics: tumor-activated prodrug therapy. Adv Drug Deliv Rev. 1998;31(1–2):89–104.
2. Kavallaris M. Microtubules and resistance to tubulin-binding agents. Nat Rev Cancer. 2010;10(3):194–204.
3. Jordan MA, Wilson L. Microtubules as a target for anticancer drugs. Nat Rev Cancer. 2004;4(4):253–65.
4. Dumontet C, Jordan MA. Microtubule-binding agents: a dynamic field of cancer therapeutics. Nat Rev Drug Discov. 2010;9(10):790–803.
5. Kavallaris M, Verrills NM, Hill BT. Anticancer therapy with novel tubulin-interacting drugs. Drug Resist Updat. 2001;4(6):392–401.
6. Lambert JM. Drug-conjugated monoclonal antibodies for the treatment of cancer. Curr Opin Pharmacol. 2005;5(5):543–9.
7. Vlahov IR, Wang Y, Kleindl PJ, Leamon CP. Design and regioselective synthesis of a new generation of targeted chemotherapeutics. Part II: Folic acid conjugates of tubulysins and their hydrazides. Bioorg Med Chem Lett. 2008;18(16):4558–61.
8. Kupchan SM, Komoda Y, Court WA, Thomas GJ, Smith RM, Karim A, *et al.* Tumor inhibitors. LXXIII. Maytansine, a novel

Author's personal copy

antileukemic ansa macrolide from Maytenus ovatus. J Am Chem Soc. 1972;94(4):1354–6.
9. Oroudjev E, Lopus M, Wilson L, Audette C, Provenzano C, Erickson H, *et al.* Maytansinoid-antibody conjugates induce mitotic arrest by suppressing microtubule dynamic instability. Mol Cancer Ther. 2010;9(10):2700–13.
10. Lopus M. Antibody-DM1 conjugates as cancer therapeutics. Cancer Lett. 2011;307(2):113–8.
11. Chari RVJ, Martell BA, Gross JL, Cook SB, Shah SA, Blättler WA, *et al.* Immunoconjugates containing novel maytansinoids: promising anticancer drugs. Cancer Res. 1992;52(1):127–31.
12. Lambert JM. Antibody-maytansinoid conjugates as anticancer therapeutics: Proving their benefit. Hum Antibodies. 2007;16(1–2):5–8.
13. Yusuf RZ, Duan Z, Lamendola DE, Penson RT, Seiden MV. Paclitaxel resistance: molecular mechanisms and pharmacologic manipulation. Curr Cancer Drug Targets. 2003;3(1):1–19.
14. Argiris A, Duffy AG, Kummar S, Simone NL, Arai Y, Kim SW, *et al.* Early tumor progression associated with enhanced EGFR signaling with bortezomib, cetuximab, and radiotherapy for head and neck cancer. Clin Cancer Res. 2011;17(17):5755–64.
15. Kim KM, McDonagh CF, Westendorf L, Brown LL, Sussman D, Feist T, *et al.* Anti-CD30 diabody-drug conjugates with potent antitumor activity. Mol Cancer Ther. 2008;7(8):2486–97.
16. Guillemard V, Uri Saragovi H. Prodrug chemotherapeutics bypass p-glycoprotein resistance and kill tumors *in vivo* with high efficacy and target-dependent selectivity. Oncogene. 2004;23(20):3613–21.
17. Teicher BA, Chari RVJ. Antibody conjugate therapeutics: challenges and potential. Clin Cancer Res. 2011;17(20):6389–97.
18. Christiansen J, Rajasekaran AK. Biological impediments to monoclonal antibody-based cancer immunotherapy. Mol Cancer Ther. 2004;3(11):1493–501.
19. Francisco JA, Cerveny CG, Meyer DL, Mixan BJ, Klussman K, Chace DF, *et al.* cAC10-vcMMAE, an anti-CD30-monomethyl auristatin E conjugate with potent and selective antitumor activity. Blood. 2003;102(4):1458–65.
20. Ducry L, Stump B. Antibody−drug conjugates: linking cytotoxic payloads to monoclonal antibodies. Bioconjug Chem. 2009;21(1):5–13.
21. Webb S. Pharma interest surges in antibody drug conjugates. Nat Biotechnol. 2011;29(4):297–8.
22. Goldenberg DM. Monoclonal antibodies in cancer detection and therapy. Am J Med. 1993;94(3):297–312.
23. Wu X, Ojima I. Tumor specific novel taxoid-monoclonal antibody conjugates. Curr Med Chem. 2004;11(4):429–38.
24. Widdison WC, Wilhelm SD, Cavanagh EE, Whiteman KR, Leece BA, Kovtun Y, *et al.* Semisynthetic maytansine analogues for the targeted treatment of cancer. J Med Chem. 2006;49(14):4392–408.
25. Hamblett KJ, Senter PD, Chace DF, Sun MM, Lenox J, Cerveny CG, *et al.* Effects of drug loading on the antitumor activity of a monoclonal antibody drug conjugate. Clin Cancer Res. 2004;10(20):7063–70.
26. Tijink BM, Buter J, de Bree R, Giaccone G, Lang MS, Staab A, *et al.* A phase I dose escalation study with anti-CD44v6 bivatuzumab mertansine in patients with incurable squamous cell carcinoma of the head and neck or esophagus. Clin Cancer Res. 2006;12(20 Pt 1):6064–72.
27. Garanger E, Boturyn D, Dumy P. Tumor targeting with RGD peptide ligands-design of new molecular conjugates for imaging and therapy of cancers. Anticancer Agents Med Chem. 2007;7(5):552–8.
28. Yokota T, Milenic DE, Whitlow M, Schlom J. Rapid tumor penetration of a single-chain Fv and comparison with other immunoglobulin forms. Cancer Res. 1992;52(12):3402–8.
29. Adams GP, Schier R, Marshall K, Wolf EJ, McCall AM, Marks JD, *et al.* Increased affinity leads to improved selective tumor delivery of single-chain Fv antibodies. Cancer Res. 1998;58(3):485–90.
30. Junutula JR, Flagella KM, Graham RA, Parsons KL, Ha E, Raab H, *et al.* Engineered thio-trastuzumab-DM1 conjugate with an improved therapeutic index to target human epidermal growth factor receptor 2–positive breast cancer. Clin Cancer Res. 2010;16(19):4769–78.
31. Braun S, Schlimok G, Heumos I, Schaller G, Riethdorf L, Riethmuller G, *et al.* ErbB2 overexpression on occult metastatic cells in bone marrow predicts poor clinical outcome of stage I-III breast cancer patients. Cancer Res. 2001;61(5):1890–5.
32. Junutula JR, Raab H, Clark S, Bhakta S, Leipold DD, Weir S, *et al.* Site-specific conjugation of a cytotoxic drug to an antibody improves the therapeutic index. Nat Biotech. 2008;26(8):925–32.
33. Schrama D, Reisfeld RA, Becker JC. Antibody targeted drugs as cancer therapeutics. Nat Rev Drug Discov. 2006;5(2):147–59.
34. Erickson HK, Park PU, Widdison WC, Kovtun YV, Garrett LM, Hoffman K, *et al.* Antibody-maytansinoid conjugates are activated in targeted cancer cells by lysosomal degradation and linker-dependent intracellular processing. Cancer Res. 2006;66(8):4426–33.
35. Lopus M, Oroudjev E, Wilson L, Wilhelm S, Widdison W, Chari R, *et al.* Maytansine and cellular metabolites of antibody-maytansinoid conjugates strongly suppress microtubule dynamics by binding to microtubules. Mol Cancer Ther. 2010;9(10):2689–99.
36. Kovtun YV, Audette CA, Ye Y, Xie H, Ruberti MF, Phinney SJ, *et al.* Antibody-drug conjugates designed to eradicate tumors with homogeneous and heterogeneous expression of the target antigen. Cancer Res. 2006;66(6):3214–21.
37. Kovtun YV, Goldmacher VS. Cell killing by antibody–drug conjugates. Cancer Lett. 2007;255(2):232–40.
38. Ikeda H, Hideshima T, Fulciniti M, Lutz RJ, Yasui H, Okawa Y, *et al.* The monoclonal antibody nBT062 conjugated to cytotoxic maytansinoids has selective cytotoxicity against CD138-positive multiple myeloma cells *in vitro* and *in vivo*. Clin Cancer Res. 2009;15(12):4028–37.
39. Lutz RJ, Whiteman KR. Antibody-maytansinoid conjugates for the treatment of myeloma. Mabs. 2009;1(6):548–51.
40. Beck A, Senter P, Chari R. World antibody drug conjugate Summit Europe: February 21-23, 2011; Frankfurt, Germany. Mabs. 2011;3(4):331–7.
41. Polson AG, Calemine-Fenaux J, Chan P, Chang W, Christensen E, Clark S, *et al.* Antibody-drug conjugates for the treatment of non-Hodgkin's lymphoma: target and linker-drug selection. Cancer Res. 2009;69(6):2358–64.
42. Ma DS, Hopf CE, Malewicz AD, Donovan GP, Senter PD, Goeckeler WF, *et al.* Potent antitumor activity of an auristatin-conjugated, fully human monoclonal antibody to prostate-specific membrane antigen. Clin Cancer Res. 2006;12(8):2591–6.
43. Podgorski I, Sloane BF. Cathepsin B and its role(s) in cancer progression. Biochem Soc Symp. 2003;70:263–76.
44. Doronina SO, Toki BE, Torgov MY, Mendelsohn BA, Cerveny CG, Chace DF, *et al.* Development of potent monoclonal antibody auristatin conjugates for cancer therapy. Nat Biotechnol. 2003;21(7):778.
45. Wahl AF, Klussman K, Thompson JD, Chen JH, Francisco LV, Risdon G, *et al.* The anti-CD30 monoclonal antibody SGN-30 promotes growth arrest and DNA fragmentation *in vitro* and affects antitumor activity in models of Hodgkin's disease. Cancer Res. 2002;62(13):3736–42.
46. Doronina SO, Mendelsohn BA, Bovee TD, Cerveny CG, Alley SC, Meyer DL, *et al.* Enhanced activity of monomethylauristatin f through monoclonal antibody delivery: effects of linker technology on efficacy and toxicity. Bioconjug Chem. 2005;17(1):114–24.
47. Kovtun YV, Audette CA, Mayo MF, Jones GE, Doherty H, Maloney EK, *et al.* Antibody-maytansinoid conjugates designed to bypass multidrug resistance. Cancer Res. 2010;70(6):2528–37.

Author's personal copy

48. Zhao RY, Wilhelm SD, Audette C, Jones G, Leece BA, Lazar AC, *et al.* Synthesis and evaluation of hydrophilic linkers for antibody–maytansinoid conjugates. J Med Chem. 2011;54(10):3606–23.
49. Jeffrey SC, Andreyka JB, Bernhardt SX, Kissler KM, Kline T, Lenox JS, *et al.* Development and properties of β-glucuronide linkers for monoclonal antibody−drug conjugates. Bioconjug Chem. 2006;17(3):831–40.
50. Albin N, Massaad L, Toussaint C, Mathieu MC, Morizet J, Parise O, *et al.* Main drug-metabolizing enzyme systems in human breast tumors and peritumoral tissues. Cancer Res. 1993;53(15):3541–6.
51. Gilbert CW, McGowan EB, Seery GB, Black KS, Pegram MD. Targeted prodrug treatment of HER-2-positive breast tumor cells using trastuzumab and paclitaxel linked by A-Z-CINN™ Linker. J Exp Ther Oncol. 2003;3(1):27–35.
52. Ojima I, Geng X, Wu X, Qu C, Borella CP, Xie H, *et al.* Tumor-specific novel taxoid-monoclonal antibody conjugates. J Med Chem. 2002;45(26):5620–3.
53. Polson AG, Williams M, Gray AM, Fuji RN, Poon KA, McBride J, *et al.* Anti-CD22-MCC-DM1: an antibody-drug conjugate with a stable linker for the treatment of non-Hodgkin's lymphoma. Leukemia. 2010;24(9):1566–73.
54. Law CL, Cerveny CG, Gordon KA, Klussman K, Mixan BJ, Chace DF, *et al.* Efficient elimination of B-lineage lymphomas by anti-CD20-auristatin conjugates. Clin Cancer Res. 2004;10(23):7842–51.
55. Yazawa N, Hamaguchi Y, Poe JC, Tedder TF. Immunotherapy using unconjugated CD19 monoclonal antibodies in animal models for B lymphocyte malignancies and autoimmune disease. Proc Natl Acad Sci USA. 2005;102(42):15178–83.
56. Gerber HP, Kung-Sutherland M, Stone I, Morris-Tilden C, Miyamoto J, McCormick R, *et al.* Potent antitumor activity of the anti-CD19 auristatin antibody drug conjugate hBU12-vcMMAE against rituximab-sensitive and -resistant lymphomas. Blood. 2009;113(18):4352–61.
57. Polson AG, Yu SF, Elkins K, Zheng B, Clark S, Ingle GS, *et al.* Antibody-drug conjugates targeted to CD79 for the treatment of non-Hodgkin lymphoma. Blood. 2007;110(2):616–23.
58. Dornan D, Bennett F, Chen Y, Dennis M, Eaton D, Elkins K, *et al.* Therapeutic potential of an anti-CD79b antibody-drug conjugate, anti-CD79b-vc-MMAE, for the treatment of non-Hodgkin lymphoma. Blood. 2009;114(13):2721–9.
59. Zheng B, Fuji RN, Elkins K, Yu S-F, Fuh FK, Chuh J, *et al. In vivo* effects of targeting CD79b with antibodies and antibody-drug conjugates. Mol Cancer Ther. 2009;8(10):2937–46.
60. Ab O, Bartle LM, Rui L, Coccia J, Johnson HA, Whiteman KR, *et al.* Abstract 4576: IMGN853, an anti-Folate Receptor I antibody-maytansinoid conjugate for targeted cancer therapy. Cancer Res. 2011;71(8 Supplement):4576.
61. Katz J, Janik JE, Younes A. Brentuximab vedotin (SGN-35). Clin Cancer Res. 2011;17(20):6428–36.
62. Liu C, Tadayoni BM, Bourret LA, Mattocks KM, Derr SM, Widdison WC, *et al.* Eradication of large colon tumor xenografts by targeted delivery of maytansinoids. Proc Natl Acad Sci USA. 1996;93(16):8618–23.
63. Tolcher AW, Ochoa L, Hammond LA, Patnaik A, Edwards T, Takimoto C, *et al.* Cantuzumab mertansine, a maytansinoid immunoconjugate directed to the CanAg Antigen: a Phase I, pharmacokinetic, and biologic correlative study. J Clin Oncol. 2003;21(2):211–22.
64. Robak T, Robak P, Smolewski P. TRU-016, a humanized anti-CD37 IgG fusion protein for the potential treatment of B-cell malignancies. Curr Opin Investig Drugs. 2009;10(12):1383–90.
65. Park PU, Yi Y, Li M, Chicklas S, Lai KC, Mayo MF, *et al.* Abstract 2830: antibody and linker selection for the anti-CD37 antibody-maytansinoid conjugate IMGN529 for the treatment of B-cell malignancies. Cancer Res. 2011;71(8 Supplement):2830.
66. Ireton RC, Chen J. EphA2 receptor tyrosine kinase as a promising target for cancer therapeutics. Curr Cancer Drug Targets. 2005;5(3):149–57.
67. Ogawa K, Pasqualini R, Lindberg RA, Kain R, Freeman AL, Pasquale EB. The ephrin-A1 ligand and its receptor, EphA2, are expressed during tumor neovascularization. Oncogene. 2000;19(52):6043.
68. Lee J-W, Stone RL, Lee SJ, Nam EJ, Roh J-W, Nick AM, *et al.* EphA2 targeted chemotherapy using an antibody drug conjugate in endometrial carcinoma. Clin Cancer Res. 2010;16(9):2562–70.
69. Junttila T, Li G, Parsons K, Phillips G, Sliwkowski M. Trastuzumab-DM1 (T-DM1) retains all the mechanisms of action of trastuzumab and efficiently inhibits growth of lapatinib insensitive breast cancer. Breast Cancer Res Treat. 2011;128(2):347–56.
70. Mathew J, Perez EA. Trastuzumab emtansine in human epidermal growth factor receptor 2-positive breast cancer: a review. Curr Opin Oncol. 2011;23(6):594–600.
71. Younes A, Yasothan U, Kirkpatrick P. Brentuximab vedotin. Nat Rev Drug Discov. 2012;11(1):19–20.
72. Oflazoglu E, Kissler KM, Sievers EL, Grewal IS, Gerber H-P. Combination of the anti-CD30-auristatin-E antibody-drug conjugate (SGN-35) with chemotherapy improves antitumour activity in Hodgkin lymphoma. Br J Haematol. 2008;142(1):69–73.
73. Blanc V, Bousseau A, Caron A, Carrez C, Lutz RJ, Lambert JM. SAR3419: an anti-CD19-Maytansinoid Immunoconjugate for the treatment of B-cell malignancies. Clin Cancer Res. 2011;17(20):6448–58.
74. Sanofi-Aventis. An Open Label Non-Randomized Phase 2 Study Evaluating SAR3419, an Anti-CD19 Antibody - Maytansine Conjugate, Administered as Single Agent by Intravenous Infusion to Patients With Relapsed or Refractory CD19+ Diffuse Large B-Cell Lymphoma. ClinicalTrials.gov [Internet]. Bethesda (MD): National Library of Medicine (US). 2000- [cited 12 May 02]. Available from: http://www.clinicaltrials.gov/ct2/show/NCT01472887?term=SAR3419&rank=1 NLM Identifier: NCT01472887].
75. MedImmune LLC. Study of MEDI-547 to Evaluate the Safety, Tolerability, and Biologic Activity of IV Administration in Subjects With Relapsed or Refractory Solid Tumors. In: ClinicalTrials.gov [Internet]. Bethesda (MD): National Library of Medicine (US). 2000- [cited 12 Feb 23]. Available from: http://clinicaltrials.gov/ct2/show/NCT00796055?intr=%22MEDI-547%22&rank=1 NLM Identifier: NCT00796055.
76. Oflazoglu E, Stone IJ, Gordon K, Wood CG, Repasky EA, Grewal IS, *et al.* Potent anticarcinoma activity of the humanized anti-CD70 antibody h1F6 conjugated to the tubulin inhibitor Auristatin via an uncleavable linker. Clin Cancer Res. 2008;14(19):6171–80.
77. Ricart AD. Immunoconjugates against solid tumors: mind the gap. Clin Pharmacol Ther. 2011;89(4):513–23.